ADVANCES IN DIAGNOSIS AND THERAPEUTIC INTERVENTION FOR FOODBORNE PARASITIC DISEASES, VOLUME II

EDITED BY: Wei Cong, Shuai Wang, Ehsan Ahmadpour, Xiao-Xuan Zhang, Nian-Zhang Zhang and Guo-Hua Liu

PUBLISHED IN: Frontiers in Cellular and Infection Microbiology

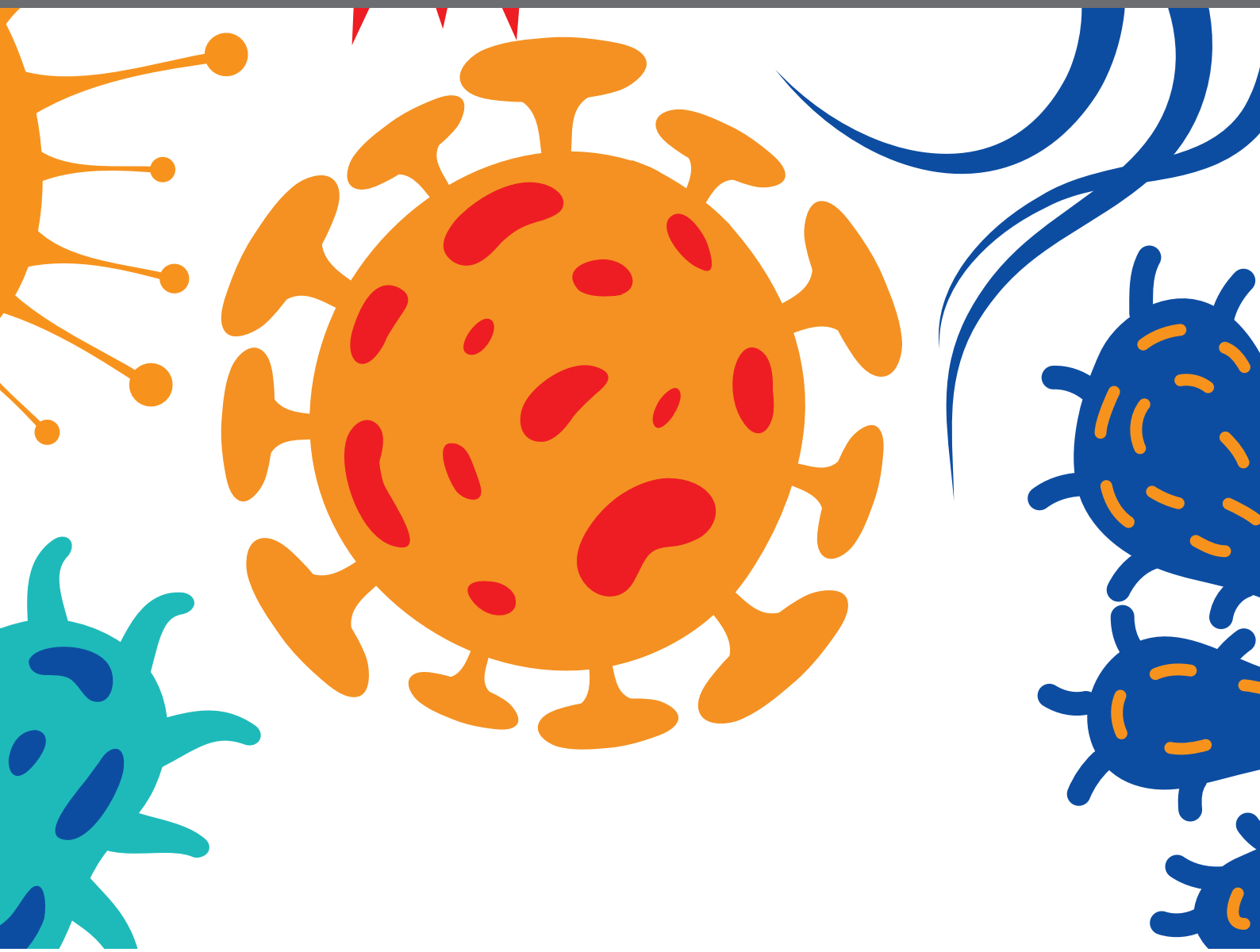

frontiers Research Topics

ISSN 1664-8714
ISBN 978-2-88976-390-0
DOI 10.3389/978-2-88976-390-0

About Frontiers

Frontiers is more than just an open-access publisher of scholarly articles: it is a pioneering approach to the world of academia, radically improving the way scholarly research is managed. The grand vision of Frontiers is a world where all people have an equal opportunity to seek, share and generate knowledge. Frontiers provides immediate and permanent online open access to all its publications, but this alone is not enough to realize our grand goals.

Frontiers Journal Series

The Frontiers Journal Series is a multi-tier and interdisciplinary set of open-access, online journals, promising a paradigm shift from the current review, selection and dissemination processes in academic publishing. All Frontiers journals are driven by researchers for researchers; therefore, they constitute a service to the scholarly community. At the same time, the Frontiers Journal Series operates on a revolutionary invention, the tiered publishing system, initially addressing specific communities of scholars, and gradually climbing up to broader public understanding, thus serving the interests of the lay society, too.

Dedication to Quality

Each Frontiers article is a landmark of the highest quality, thanks to genuinely collaborative interactions between authors and review editors, who include some of the world's best academicians. Research must be certified by peers before entering a stream of knowledge that may eventually reach the public - and shape society; therefore, Frontiers only applies the most rigorous and unbiased reviews.
Frontiers revolutionizes research publishing by freely delivering the most outstanding research, evaluated with no bias from both the academic and social point of view. By applying the most advanced information technologies, Frontiers is catapulting scholarly publishing into a new generation.

What are Frontiers Research Topics?

Frontiers Research Topics are very popular trademarks of the Frontiers Journals Series: they are collections of at least ten articles, all centered on a particular subject. With their unique mix of varied contributions from Original Research to Review Articles, Frontiers Research Topics unify the most influential researchers, the latest key findings and historical advances in a hot research area! Find out more on how to host your own Frontiers Research Topic or contribute to one as an author by contacting the Frontiers Editorial Office: frontiersin.org/about/contact

ADVANCES IN DIAGNOSIS AND THERAPEUTIC INTERVENTION FOR FOODBORNE PARASITIC DISEASES, VOLUME II

Topic Editors:
Wei Cong, Shandong University, Weihai, China
Shuai Wang, Lanzhou Veterinary Research Institute, Chinese Academy of Agricultural Sciences, China
Ehsan Ahmadpour, Tabriz University of Medical Sciences, Iran
Xiao-Xuan Zhang, Qingdao Agricultural University, China
Nian-Zhang Zhang, Lanzhou Veterinary Research Institute, Chinese Academy of Agricultural Sciences, China
Guo-Hua Liu, Hunan Agricultural University, China

Citation: Cong, W., Wang, S., Ahmadpour, E., Zhang, X.-X., Zhang, N.-Z., Liu, G.-H., eds. (2022). Advances in Diagnosis and Therapeutic Intervention for Foodborne Parasitic Diseases, Volume II. Lausanne: Frontiers Media SA.
doi: 10.3389/978-2-88976-390-0

Table of Contents

frontiers in Cellular and Infection Microbiology

ORIGINAL RESEARCH
published: 21 May 2021
doi: 10.3389/fcimb.2021.694957

Von Willebrand Factor Facilitates Intravascular Dissemination of Microsporidia *Encephalitozoon hellem*

Jialing Bao[1,2]*, *Biying Mo*[1,2], *Guozhen An*[1,2], *Jian Luo*[1,2], *Mortimer Poncz*[3], *Guoqing Pan*[1,2], *Tian Li*[1,2] and *Zeyang Zhou*[1,2,4]*

[1] State Key Laboratory of Silkworm Genome Biology, Southwest University, Chongqing, China, [2] Chongqing Key Laboratory of Microsporidia Infection and Control, Southwest University, Chongqing, China, [3] Department of Pediatrics, The Perelman School of Medicine, University of Pennsylvania, Philadelphia, PA, United States, [4] College of Life Sciences, Chongqing Normal University, Chongqing, China

OPEN ACCESS

Edited by:
Wei Cong,
Shandong University, China

Reviewed by:
Majid Pirestani,
Tarbiat Modares University, Iran
Jinshan Xu,
Chongqing Normal University, China
Maria Anete Lallo,
Paulista University, Brazil

***Correspondence:**
Jialing Bao
baojl@swu.edu.cn
Zeyang Zhou
zyzhou@swu.edu.cn

Specialty section:
This article was submitted to Clinical Microbiology, a section of the journal Frontiers in Cellular and Infection Microbiology

Received: *14 April 2021*
Accepted: *04 May 2021*
Published: *21 May 2021*

Citation:
Bao J, Mo B, An G, Luo J, Poncz M, Pan G, Li T and Zhou Z (2021) Von Willebrand Factor Facilitates Intravascular Dissemination of Microsporidia Encephalitozoon hellem. Front. Cell. Infect. Microbiol. 11:694957. doi: 10.3389/fcimb.2021.694957

Microsporidia are a group of spore-forming, fungus-related pathogens that can infect both invertebrates and vertebrates including humans. The primary infection site is usually digestive tract, but systemic infections occur as well and cause damages to organs such as lung, brain, and liver. The systemic spread of microsporidia may be intravascular, requiring attachment and colonization in the presence of shear stress. Von Willebrand Factor (VWF) is a large multimeric intravascular protein and the key attachment sites for platelets and coagulation factors. Here in this study, we investigated the interactions between VWF and microsporidia *Encephalitozoon hellem* (*E. hellem*), and the modulating effects on *E. hellem* after VWF binding. Microfluidic assays showed that *E. hellem* binds to ultra-large VWF strings under shear stress. *In vitro* germination assay and infection assay proved that *E. hellem* significantly increased the rates of germination and infection, and these effects would be reversed by VWF blocking antibody. Mass spectrometry analysis further revealed that VWF-incubation altered various aspects of *E. hellem* including metabolic activity, levels of structural molecules, and protein maturation. Our findings demonstrated that VWF can bind microsporidia in circulation, and modulate its pathogenicity, including promoting germination and infection rate. VWF facilitates microsporidia intravascular spreading and systemic infection.

Keywords: von Willebrand factor, *Encephalitozoon hellem*, microsporidia, intravascular dissemination, infection

INTRODUCTION

Microsporidia are a group of intracellular parasites that have recently been re-classified to fungi (Hirt et al., 1999; Han and Weiss, 2017). The host range of microsporidia is extremely wide, and at least 15 species are human pathogens with the major ones being *Enterocytozoon bieneusi* (*E. bieneusi*), *Encephalitozoon hellem* (*E. hellem*), *Encephalitozoon cuniculi* (*E. cuniculi*) and *Encephalitozoon intestinalis* (*E. intestinalis*) (Weiss, 2001; Valencakova and Danisova, 2019). Microsporidia extrude the polar tube inside-out to inject sporoplasm into the host cells. This

process is called germination and is the key step for infection (Franzen, 2005). Inside the host cell, the sporoplasm proliferates and form more new spores that will further infect surrounding cells (Weber et al., 1993; Meissner et al., 2012). Microsporidia infections could be local and restrained, yet systemic even fatal infections are not rare (Weber et al., 1994; Weiss, 1995; Meissner et al., 2012). Microsporidia spores may disseminate systemically *via* intravascular system (Anderson et al., 2019; Han et al., 2019), however the mechanistic details of dissemination *via* circulatory system have not been fully examined.

In circulatory system, Von Willebrand factor (VWF) mediates the binding and activation of various cells and molecules such as platelets and factor VIII (Sadler, 1998; Yee et al., 2014; Lenting et al., 2015; Dong et al., 2019). Furthermore, the involvements of VWF in pathogen dissemination and inflammation have been reported in multiple settings. During acute infections, such as *Escherichia coli* infection may induce the haemolytic uremic syndrome, triggering the formation of microvascular thrombi mediated by Von Willebrand Factor (VWF) (Zheng and Sadler, 2008; Pillai et al., 2016; Ueda et al., 2017). Studies also revealed that VWF is able to directly bind to *Staphylococcus aureus* in blood under shear stress and promote intravascular infection of the sub-endothelium (Viela et al., 2019). VWF is also found to bind *Streptococcus pneumonia*, promoting pathogen aggregation and attachment to the endothelium surface (Jagau et al., 2019; Viela et al., 2019). In addition, malarial parasitemia caused by *Plasmodium vivax* also involves VWF binding and endothelial activation (Barber et al., 2015). Furthermore in chronic infection conditions, the endothelium damage and related plasma VWF levels increasement are reported. These conditions include carcinomas, chronic parasites infections and human immunodeficiency virus (HIV) infections (Park et al., 2012; van den Dries et al., 2015; Kong et al., 2020), and those individuals are susceptible groups of microsporidia infections.

VWF is a large multidomain protein. The type D domain (VWFD) in D'D3 assembly is not only essential for factor VIII binding but also crucial for multimerization of VWF (Dong et al., 2019). More importantly, VWFD domain is highly conserved in a lot of proteins such as vitellogenin and mucins, and these proteins have been reported to be mediators of pathogen invasion and dissemination in hosts (Sicard et al., 2017; Meng et al., 2018). Based on above facts, it is of great interest to investigate the essential role of VWF in mediating microsporidia dissemination and systemic infections *via* circulatory system.

Here in this study, we used the microsporidia *E. hellem* as a representative infection agent. We utilized various *in vitro* and *in vivo* methods to investigate the interactions between *E. hellem* and VWF. We proved that *E. hellem* spores could directly bind to VWF multimers under shear stress, and the D'D3 domain is essential for the direct interaction. Upon VWF binding, the germination and infection rates of *E. hellem* were significantly increased. Mass spectrometry analysis revealed various biological processes, such as metabolic activities, increased levels of structure molecule levels, and protein maturation of *E. hellem* were affected by VWF interaction. Together, our study is the first to describe key roles of VWF in microsporidia hematogenous dissemination.

MATERIALS AND METHODS

VWF Proteins

Native full-length human VWF, termed FL-VWF, was purchased from Abcam (ab88533, Abcam, USA). Recombinant VWF containing VWFD domain in the partial-length D'D3 assembly (S764-C1130, His-tagged), was expressed and purified from Rosetta (DE3) cells transformed with His-tagged pET32 plasmid (Novagen) containing the target sequence (Robertson et al., 2008). The partial length of D'D3 assembly excluded several cysteines that are essential for disulfide bonding, aiming for better solution of the expressed protein. Yet the recombinant protein was retained in the inclusion bodies thus dissolved in 8 M Urea, 20 mM Tris–Hcl, 0.5 M NaCl, 1mM DTT, 1mM 2-mercaptoethanol at pH 8.0, and then filtered and loaded onto HiTrap™ chelating column (GE Healthcare Life Sciences, USA). Refolding of the bound proteins is achieved by very slowly (0.1 ml/min) wash the column with a liner 8-0M urea gradient, and then eluted by imidazole-containing elution buffer (Duan et al., 2006; Volonte et al., 2011).

E. hellem Microsporidia

E. hellem strain (ATCC 50504/50451) was a gift from Professor Louis Weiss (Albert Einstein College of Medicine, USA). Rabbit kidney cells (RK13, ATCC CCL-37) were cultured in 10% fetal bovine serum (FBS, ThermoFisher) containing Minimum Essential Medium Eagle (MEM, Gibco) with penicillin (100 U/ml)–streptomycin (100 μg/ml) at 5% CO_2. Confluent monolayers were infected with *E. hellem*. The spores were collected from culture media, purified by passing them through a 5 μm size filter (Millipore=) to remove host cells, concentrated by centrifugation, and stored in sterile distilled water at 4°C (Visvesvara et al., 1991). Spores used in these experiments were counted with a hemocytometer (three times/sample) and averaged.

Microfluidic Chamber VWF Binding Assay

FL-VWF protein (20 μg/ml) was perfused through a flow chamber slide (μ-slide I luer, Cat# 80176, Ibidi, Germany), with shear stress of 5 dyn/cm^2 for 2 min with the same concentration of bovine serum albumin (BSA) (Sangon Biotech) used as a control. *E. hellem* spores (10^5/ml) were then perfused through the channel for 1 min. The channels were washed with PBS, and then fixed with 4% paraformaldehyde. The VWF "strings" along the channel were visualized under a fluorescent microscope after incubation with anti-VWF IgG (ab6994, Abcam, USA) followed by Alexa 594-labeled secondary antibody. The *E. hellem* spores were visualized by Calcofluor-white (CFW) (Sigma-Aldrich), a specific dye for chitin on the microsporidia spore surface (Luna et al., 1995).

Recombinant VWF-D'D3 Assembly Binding to *E. hellem* Spore

Recombinant VWF-D'D3 (partial length, containing VWFD) (20 μg/ml) was incubated with *E. hellem* spores (10^7/ml) for 30 min, and then the spores were washed and fixed. The control group was incubated with the same concentration of EGFP (Enhanced Green Fluorescent Protein), also expressed, expressed and purified from *EGFP*-containing pET32 transformed DE3 cells. Direct interaction between VWF-D'D3 and *E. hellem* was observed by fluorescent microscope using anti-VWF IgG (ab6994, Abcam) followed by Alexa 488-labeled secondary antibody, and DAPI (4',6-diamidino-2-phenylindole) (Sigma-Aldrich), respectively.

To further investigate the binding specificity, microfluidic chamber assay was applied. FL-VWF protein (20 μg/ml) was perfused through a flow chamber slide (μ-slide I luer, Cat# 80176, Ibidi, Germany), with shear stress of 5 dyn/cm^2 for 2 min. Next, recombinant VWF-D'D3 (20 μg/ml) pre-incubated *E. hellem* spores (10^5/ml) or same concentration of EGFP protein pre-incubated *E. hellem* spores (10^5/ml) were perfused through the chamber for 1 min. The channels were washed with PBS, and then fixed with 4% paraformaldehyde. The VWF "strings" along the channel were visualized under a fluorescent microscope after incubation with anti-VWF IgG (ab6994, Abcam, USA) followed by Alexa 594–labeled secondary antibody. The *E. hellem* spores were visualized by Calcofluor-white (CFW) (Sigma-Aldrich), and the recombinant VWF-D'D3 was visualized by anti-His antibody (SAB1305538, Sigma-Aldrich, Canada) followed by Alexa 488-labeled secondary antibody.

E. hellem Germination and Infection

Untreated or pre-incubated *E. hellem* spores were subjected to germination, triggered by germination buffer (140 mM NaCl, 5 mM KCl, 1 mM $CaCl_2$, 1 mM $MgCl_2$, pH 9.5) at 37°C for 10 min, and then 5% (v/v, final ratio) H_2O_2 (Sangon Biotech) was added for 5 min (Leitch et al., 1993; He et al., 1996; Pattana Jaroenlak et al., 2020).

For infection assay, human foreskin fibroblast cells (HFF, ATCC CRL-2522) were maintained in Dulbecco's Modified Eagle Medium (DMEM, ThermoFisher Scientific) with penicillin-streptomycin (ThermoFisher Scientific) supplemented with 10% FBS (ThermoFisher Scientific) at 5% CO_2. The *E. hellem* spores were then added to HFF cells (20:1 spores/cells) and co-culture for various time periods. The infection rate of *E. hellem* was assessed by FISH (fluorescence *in situ* hybridization) assay, using Cy3-labeled oligonucleotide probes targeted to species-specific sequences of *E. hellem* 16S rRNA (5'-ACTCTCACACTCACTTCAG-3') to specifically label the proliferating *E. hellem* inside host cells. In brief, *E. hellem* infected HFF cells were fixed, then incubated with hybridization buffer (900 mM NaCl, 20 mM Tris pH 7.5, 0.01% SDS) at 46°C for 12 h. Intracellular *E. hellem* in the host cells was visualized using fluorescently labeled probe (5 pM) under microscopy. The host cells were visualized by DAPI staining. The infection rate was calculated by the ratio of FISH-positive HFF cells over all cells in 20 randomly selected fields.

Label-Free Quantitative Mass Spectrometry

Freshly purified *E. hellem* spores (10^8/ml) were incubated with FL-VWF (20 μg/ml) for 30 min. The spores were then washed with PBS. To extract the total protein, experimental and control spores not exposed to VWF were lysed with 1 ml of SDT-lysis buffer (4% SDS, 0.1 mol/l dithiothreitol, and 0.1 mol/l Tris HCl, pH 7.6) with 10 μl Protease Inhibitor Cocktail (Sangon Biotech) using acid-washed glass beads (diameter: 425–600 μ, Sigma) in a Precellys-24 (Bertin Technologies). Triplicate protein samples were prepared from each experiment, and three experiments were performed. The samples were then subjected to label-free quantitative mass spectrometry.

Statistics

Results of the *E. hellem* germination and infection ratios were compared using paired Student's t-test. Statistical analysis of the mass spectrometry results were conducted using a one-way ANOVA followed by Bonferroni's post-hoc test was used to show significant differences in protein expression. Statistical significances were analyzed and represented with F values, degree of freedom, as well as with P values.

RESULTS

E. hellem Binds to Ultra-Large VWF Under Shear Stress

To investigate whether VWF is essential for hematogenous dissemination of microsporidia, FL-VWF was perfused with *E. hellem* spores through the microfluidic chamber under shear stress. After washing and fixation, VWF strings and *E. hellem* spores were visualized by fluorescent microscopy. As shown in **Figures 1A,B**, *E. hellem* spores specifically attached to the VWF oligomers under shear stress, while no binding to control protein BSA. Also, the shear stress is important for *E. hellem* binding on VWF, for VWF undergoes a conformational transition from a compacted, globular to an extended form (Vergauwe et al., 2014). The inference is proved in **Figure 1C**, showing that when no shear stress presents VWF clumped together and no *E. hellem* binding on it. These results further confirmed the importance of VWF mediating microsporidia dissemination under physiological conditions.

The VWF-D'D3 Assembly Is Key Binding Region for *E. hellem* on VWF

Next, we investigated whether the VWFD domain containing D'D3 assembly is key binding region for *E. hellem*. The purified recombinant VWF-D'D3 assembly (**Figure 2A**) was incubated with *E. hellem* spores, and the binding effect was proved by flow cytometry and fluorescent microscopy analysis (**Figures 2B,C**).

To further confirm the key role of D'D3 assembly in *E. hellem*-VWF binding, recombinant D'D3 assembly was applied to pre-incubate with *E. hellem* and then the spores were perfused with FL-VWF in microfluidic chamber under shear stress. As shown in **Figure 3** that, D'D3 pre-incubation interferes with

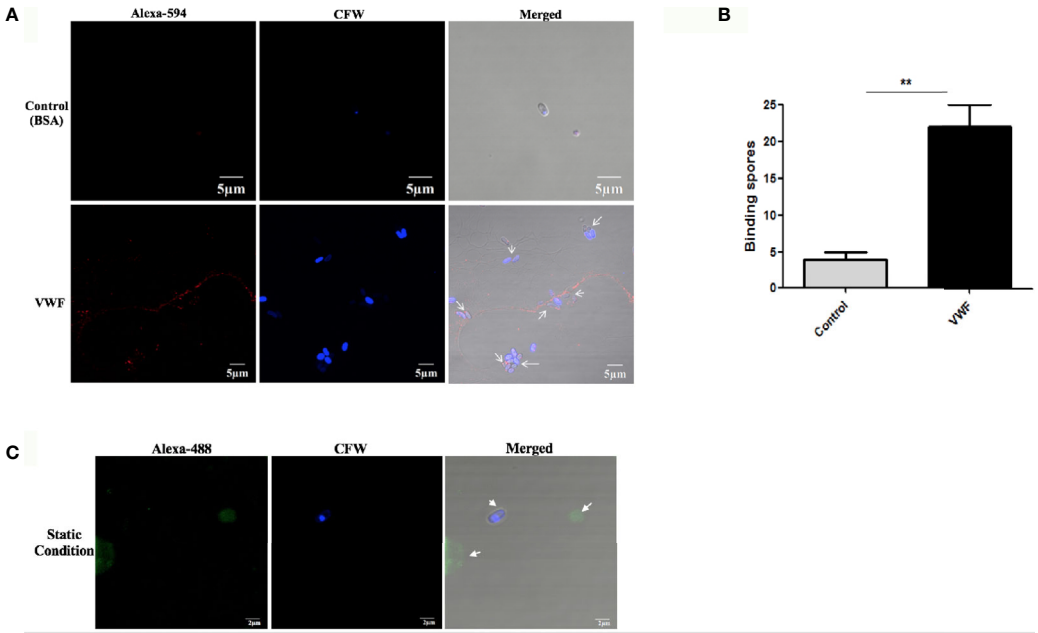

FIGURE 1 | *E. hellem* spores attach to FL-VWF under flow. **(A)** Representative images of control protein (BSA, top) or FL-VWF (bottom), both at 20 μg/ml were perfused through the microfluidic chamber with *E. hellem* spores (10^5 cells/ml) under flow at 5 dyn/cm^2, respectively. The channels were then washed, fixed and stained by Alexa-594-labeled anti-VWF antibody and calcofluor-white (CFW). The fluorescent microscopy analysis showed that the VWF formed ultra large multimers under flow (red), and *E. hellem* spores (blue) attached to the strings of ultra large VWF strings, as pointed out by white arrows in the right figures. (Scale bar = 5 μm). **(B)** The number of binding spores in the channels were calculated, based on three independent studies with 8 random fields for each study ($F(1,23) = 2.25$, $^{**}P < 0.01$). **(C)** Under static conditions with no shear, the FL-VWF clumped and aggregated together (green). The *E. hellem* spores (blue) are not able to bind to clumped VWF.

E. hellem-VWF binding while pre-incubation with un-related protein EGFP had no interference effect. These results indicated that the binding site was pre-occupied by the assembly, and D'D3 assembly is the key binding region for *E. hellem* interaction on VWF.

VWF Binding Promotes *E. hellem* Germination

We next examined whether binding to VWF by microsporidia would influence the biology and potentially influence systemic infection by this organism. We first examined whether binding of spores to VWF influences germination. Freshly purified *E. hellem* spores (10^8/ml) were incubated with FL-VWF for 1 h. Controls were either untreated *E. hellem* spores, spores incubated with VWF together with a blocking anti-human VWF antibody (Abcam, USA), or spores incubated with VWF together with an isotype antibody control. After incubation, *E. hellem* spores from each group were washed with PBS and then subjected to germination accordingly. Under fluorescent microscope, untreated *E. hellem* spores will show blue color due to DAPI staining of their nuclei; while germinated spore will show no color as the sporoplasms with their nuclei had already been extruded. The germination rate was then assessed by calculating the ratio of germinated spores over all spores under the view. Results showed that incubation of the spores with VWF significantly promoted *E. hellem* germination, and this effect was inhibited specifically by blocking anti-VWF antibody (**Figure 4**).

VWF-Bound *E. hellem* Demonstrates Enhanced Host Cell Infectivity

Another potential manner by which VWF may enhance systemic spread of microsporidia infection is by enhancing its ability to infect host cells. We examine this issue by pre-incubating *E. hellem* spores with FL-VWF, while the controls were either untreated *E. hellem* spores or spores treated with BSA. Another control was to pre-germinate the spores to enhance infectivity. The various pre-treated *E. hellem* spores were then co-cultured with HFF cells to allow infection, and then washed and fixed. The proliferating *E. hellem* inside the host cells were visualized by fluorescently labeled FISH probe. The infection rate was calculated by the ratio of FISH-positive HFF cells over total HFF cells. As shown in **Figure 5**, the infectivity of *E. hellem* was significantly increased after FL-VWF incubation, almost to the level of pre-germinated spores.

Mass Spectrometry Analysis of the Impacts of VWF Binding on *E. hellem*

Label-free quantitative mass spectrometry was utilized to analyze the *E. hellem* protein change after VWF incubation. Various

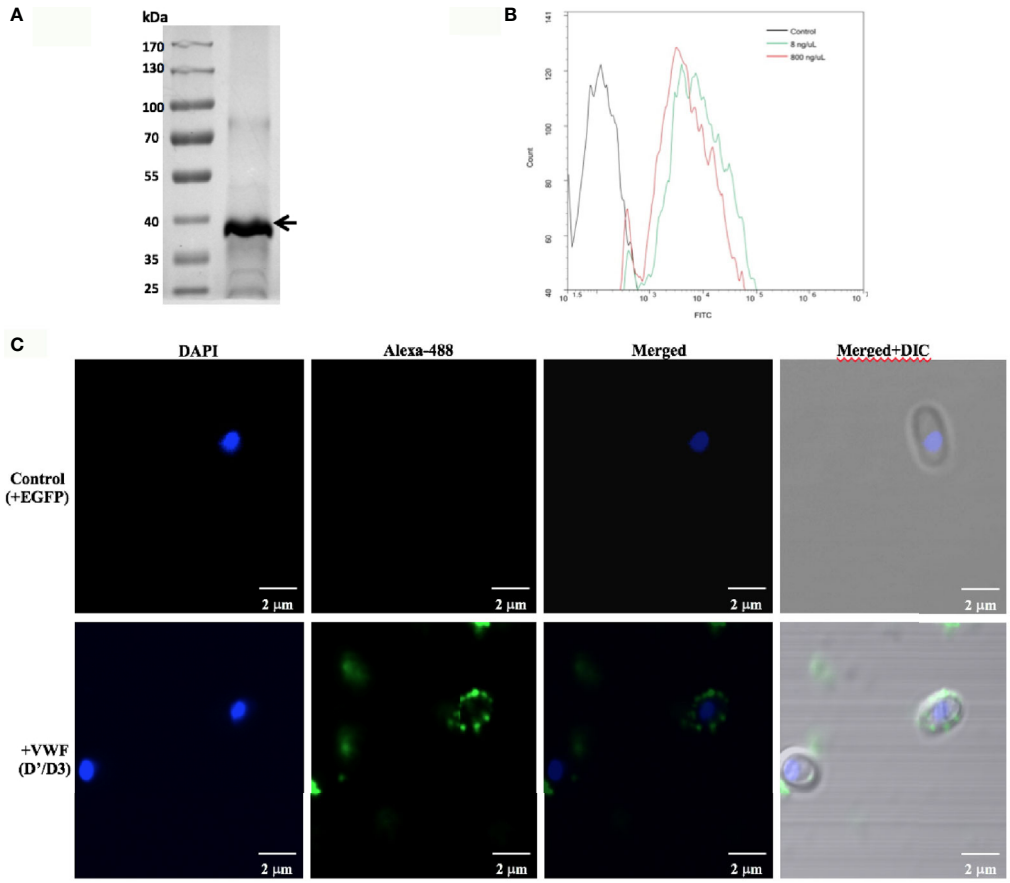

FIGURE 2 | VWF-D'D3 binds to *E. hellem spores*. **(A)** Coomassie staining of recombinant VWF-D'D3. Arrow shows the major protein size at the expected size ~40 kDa. **(B)** Flow cytometry analysis of D'D3 binding to *E. hellem*. *E. hellem* spores (1 × 104 cells) were incubated respectively with, isotype antibody control (in black line), 8 ng/μl recombinant VWF-D' D3 (in green line), and 800 ng/μl recombinant VWF-D'D3 (in red line). The result showed that with the increasing amount of recombinant VWF adding, the fluorescence signal increased as well. **(C)** Representative images of *E. hellem* spores were incubated with either control, recombinant EGFP (top) or VWF-D'D3 (bottom), both at 20 μg/ml for 30 min, then the spores were washed by PBS. After fixation, the direct interaction between VWF (green) and *E. hellem* (blue) was observed by fluorescent microscope (Scale bar = 2 μm).

proteins were significantly increased, including ones involved in metabolic activities, DNA synthesis and intracellular transportation. Changes in the levels of specific proteins of either an increase or a decrease of two fold following FL-VWF binding are shown in **Table 1**. The differentially expressed proteins were further subjected to gene ontology (GO) annotation and enrichment analysis, as shown in **Figure 6**. Various aspects of *E. hellem* are altered after VWF binding, including biological process, molecular function and cellular compartment.

DISCUSSION

Current study is the first to show a direct interaction between plasma protein VWF and the microsporidia, *E. hellem*, and demonstrate that the binding of VWF to *E. hellem* spores significantly enhances their germination and infectivity abilities. Mass spectrometry analysis revealed that various proteins expression levels of *E. hellem* were altered after VWF interaction. For instance, glucose-6-phosphate isomerase, an enzyme involved in glucose metabolism (Kugler and Lakomek, 2000); YOP1, a protein associated with vesicle-mediated transportation and invasion (Viljanen et al., 1991); and aminopeptidase, an enzyme associated with parasitophorous vacuole formation (Lu et al., 2020), were all up-regulated. In the meantime, the translation initiation factor 2B, DNA polymerase, and trehalase, a protease responsible for metabolic process in extreme condition (Zhao et al., 2016), were all significantly down-regulated. These changes together indicate that binding by VWF signals *E. hellem* to slow-down regular DNA and protein synthesis, change the metabolism mode, accelerate vesicle transportation, and other modifications to prepare for germination by the pathogen and invasion of surrounding host cells.

VWF is an essential protein in coagulation and thrombosis, binding to platelet's glycoprotein Ib/IX receptor, to circulating

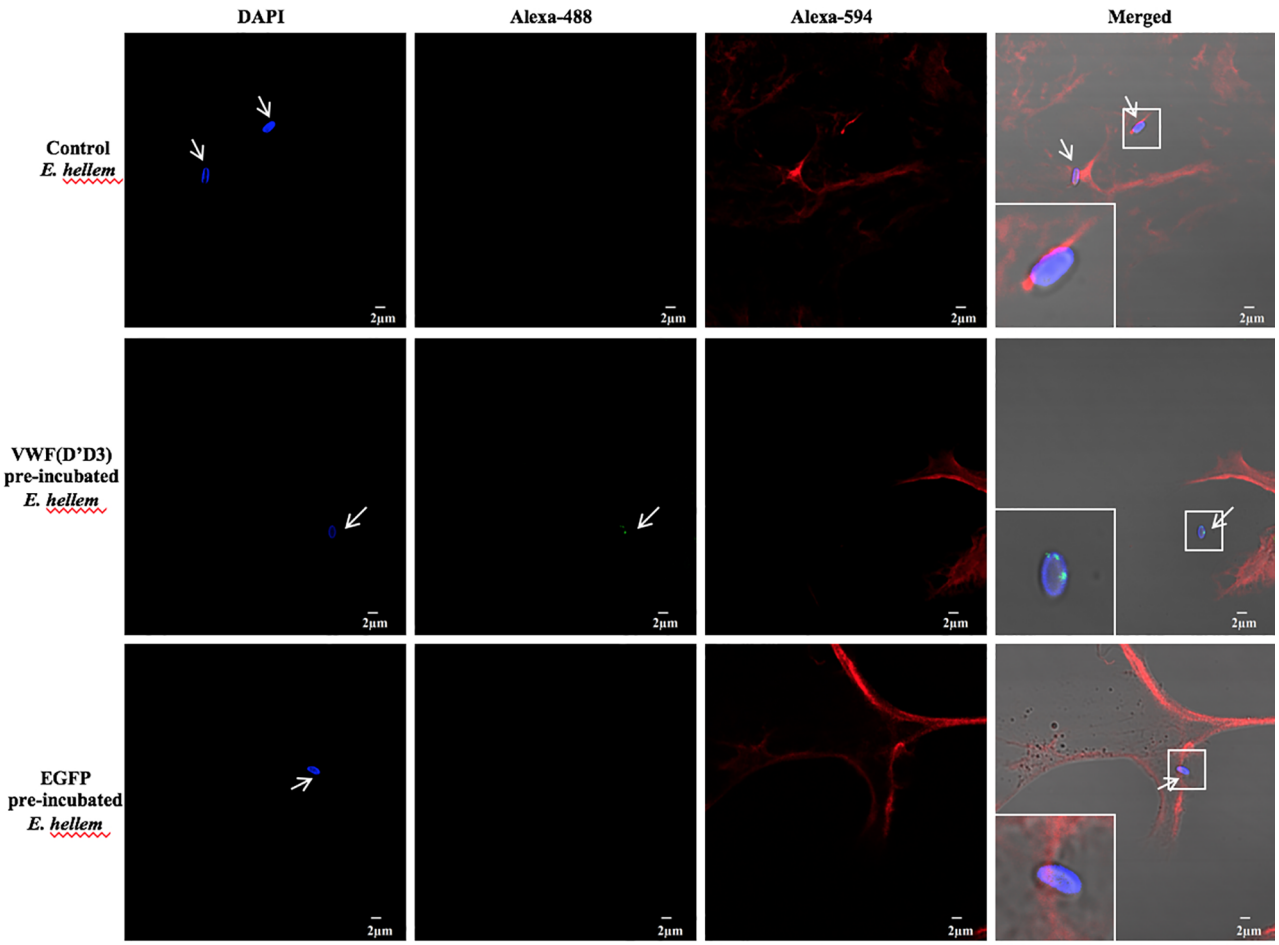

FIGURE 3 | VWF-D'D3 is key binding region for *E. hellem*. In microfluidic chamber, full length VWF (20 μg/ml) was perfused with shear stress of 5 dyn/cm^2 for 2 min. Same concentration (10^5/ml) of either control (un-treated) *E. hellem* spores, VWF-D'D3 pre-incubated *E. hellem* spores, or EGFP pre-incubated *E. hellem* spores were then perfused through. The channels were then washed and fixed. The *E. hellem* spores were visualized by DAPI (blue), and the pre-incubated VWF-D'D3 which has attached to *E. hellem* spores were visualized by anti-His antibody followed by Alexa 488-labeled secondary antibody (green). The VWF oligomers were visualized by anti-VWF antibody followed by Alexa 594-labeled secondary antibody (red). As shown by this immunofluorescence assay, untreated *E. hellem* spores or un-related EGFP treated *E. hellem* spores were both able to attach to the VWF oligomer strings (arrows, and also shown in enlarged views in upper and bottom rows). While VWF-D'D3 pre-incubation occupy the binding site of *E. hellem*, thus the spores could not bind with VWF strings (arrow, and also shown in enlarged view in middle row).

coagulation factor VIII and to exposed subendothelial collagen amongst other ligands (Sadler, 1998). It is known the D'D3 assembly of VWF is important for various ligands binding including coagulation factors FVIII, P-selectin and GpIba, and even some pathogens (Michaux et al., 2006; O'Seaghdha et al., 2006; Madabhushi et al., 2014; Yee et al., 2014). In particular, the D' region (composed of TIL' and E' domains) is especially important for FVIII binding (Shiltagh et al., 2014). Thus in this study, we constructed the recombinant VWF-D'D3 contains full of TIL', E' and most part of D3 (S764-C1130). We aimed to have a construct which retains the full binding abilities but without the residues such as C1142 and C1222 for inter-chain disulfide bonding, so that will get homogenous monomeric protein (Hilbert et al., 2003; Shapiro et al., 2014; Lenting et al., 2015). With this protein, we managed to prove that D'D3 region is the key binding site for *E. hellem* on VWF, thus the occupation by *E. hellem* might interfere with physiologic functions of VWF and any related pathophysiologic processes. It would also be quite interesting to examine whether binding of microsporidia to the D'D3 region of VWF contributes to hemostatic conditions. A case study in a patient with acute myeloblastic leukemia who developed a systemic microsporidia infection also developed disseminate intravascular coagulopathy, consistent with VWF binding to microsporidia interfering with physiologic hemostatic (Yazar et al., 2003). Other reports also are consistent with systemic microsporidia effecting coagulation and thrombosis (Small et al., 2014; Bukreyeva et al., 2017; Pariyakanok et al., 2019).

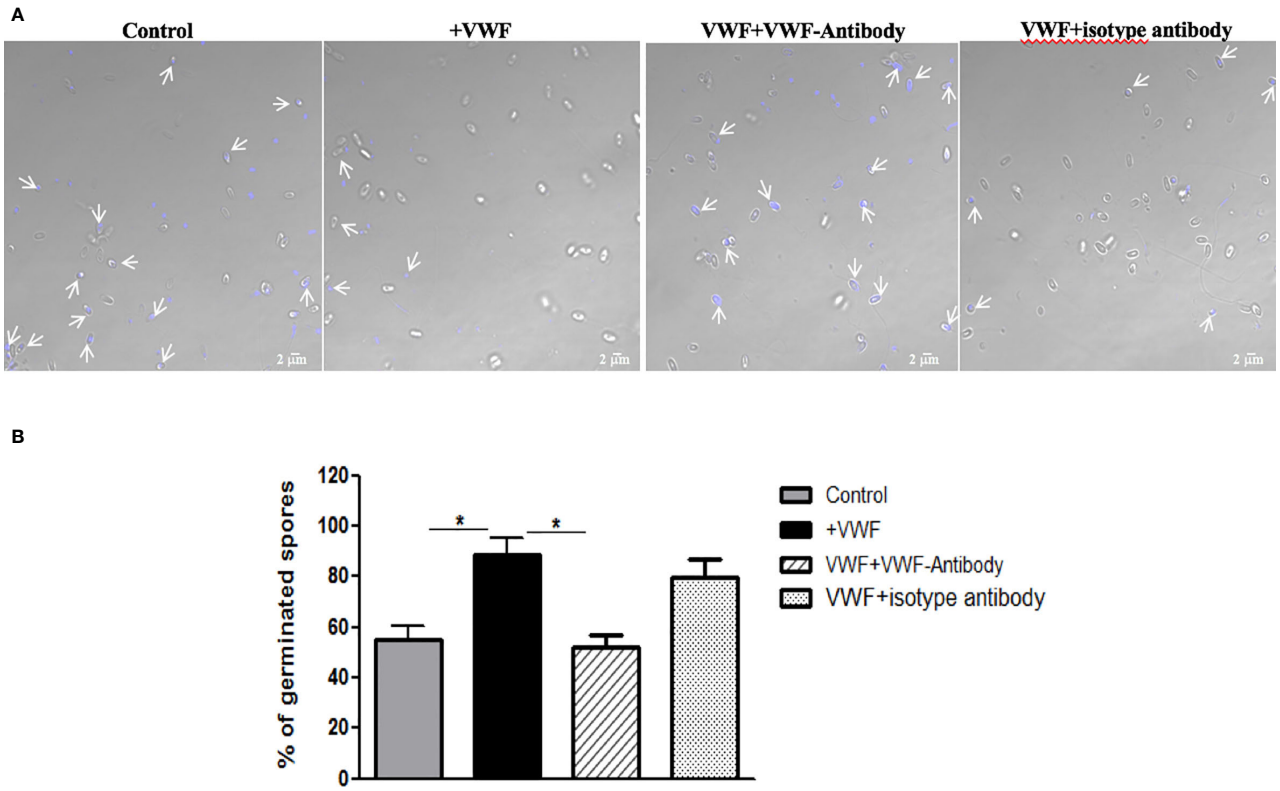

FIGURE 4 | VWF binding promotes *E. hellem* germination. **(A)** Representative images of *E. hellem* germination affected by VWF. The control group *E. hellem* spores were untreated by any protien; The VWF group *E. hellem* spores were incubated with FL-VWF; The VWF + VWF-antibody group *E. hellem* spores were treated by VWF together with anti-VWF antibody; The VWF + isotype antibody group *E. hellem* spores were treated by VWF together with isotype antibody control. All the spores from each group were then stimulated with germination buffer to further trigger germination. The *E. hellem* spores were then stained by DAPI, and un-germinated spores will show blue color (pointed out by arrows). (Scale bar = 5 μm). **(B)** Germination rates were calculated by the ratio of germinated spores over all spores, based on three independent studies with 10 random fields per study. The results showed that VWF treatment significantly promoted *E. hellem* spores' germination ($F(1,29) = 1.89$, $^*P < 0.05$), and this effect was inhibited by VWF specific antibody ($F(1, 29) = 2.09$, $^*P < 0.05$).

Bacterial binding to VWF promotes bacterial settlement, and facilitates the pathogens transmigration and into deeper tissue sites (Steinert et al., 2020). We hypothesized that binding of microsporidia to VWF may also be the underlying mechanism of local and disseminated inflammations. On the other hand, we would not exclude the role of phagocytotic cells facilitating microsporidia spreading, as doing so to other pathogens (Guirado et al., 2013; Delgado Betancourt et al., 2019). However, our preliminary data showed that microsporidia interaction with phagocytes down-regulated the cells' maturation and proper functions such as migration abilities. Thus we hypothesized that microsporidia 'spreading' by the dysfunctional cells may not be as efficient as by shear stress in blood and by binding with VWF for better infection or transmigration to deeper tissues. Furthermore, considering the fact that VWF is a mediator for many other pathogens, such as *S. aureus* dissemination, it will be interesting and important to know whether the interaction with *E. hellem* interferes or facilitates co-infection with other pathogens.

The type D domain (VWFD) is not only presented in the VWF protein but also in many other proteins, such as mucin in the digestive tract (Bukreyeva et al., 2017). Considering the facts that the initial infection site for *E. hellem* may in the digestive tract, it would be important to investigate the interactions between *E. hellem* with those VWD domain containing proteins. In addition, vertical/transovarial transmission is a known feature of microsporidia, especially in invertebrates (Dunn et al., 2001). It has been shown that the VWD D'D3-like domain-containing protein vitellogenin has an essential role in vertical transmission and involves direct binding of pathogens at this domain (Raina et al., 1995; Herren et al., 2013). Thus, it is important to investigate whether VWF facilitates human infecting-microsporidia, such as *E. hellem*, to mediate transovarial transmission or assist in pathogen transmission *via* blood contamination during birthing (Kaneda et al., 1997; Murakami et al., 2012).

In conclusion, the present study revealed that VWF can directly bind the microsporidia *E. hellem*, at least in part, *via* its

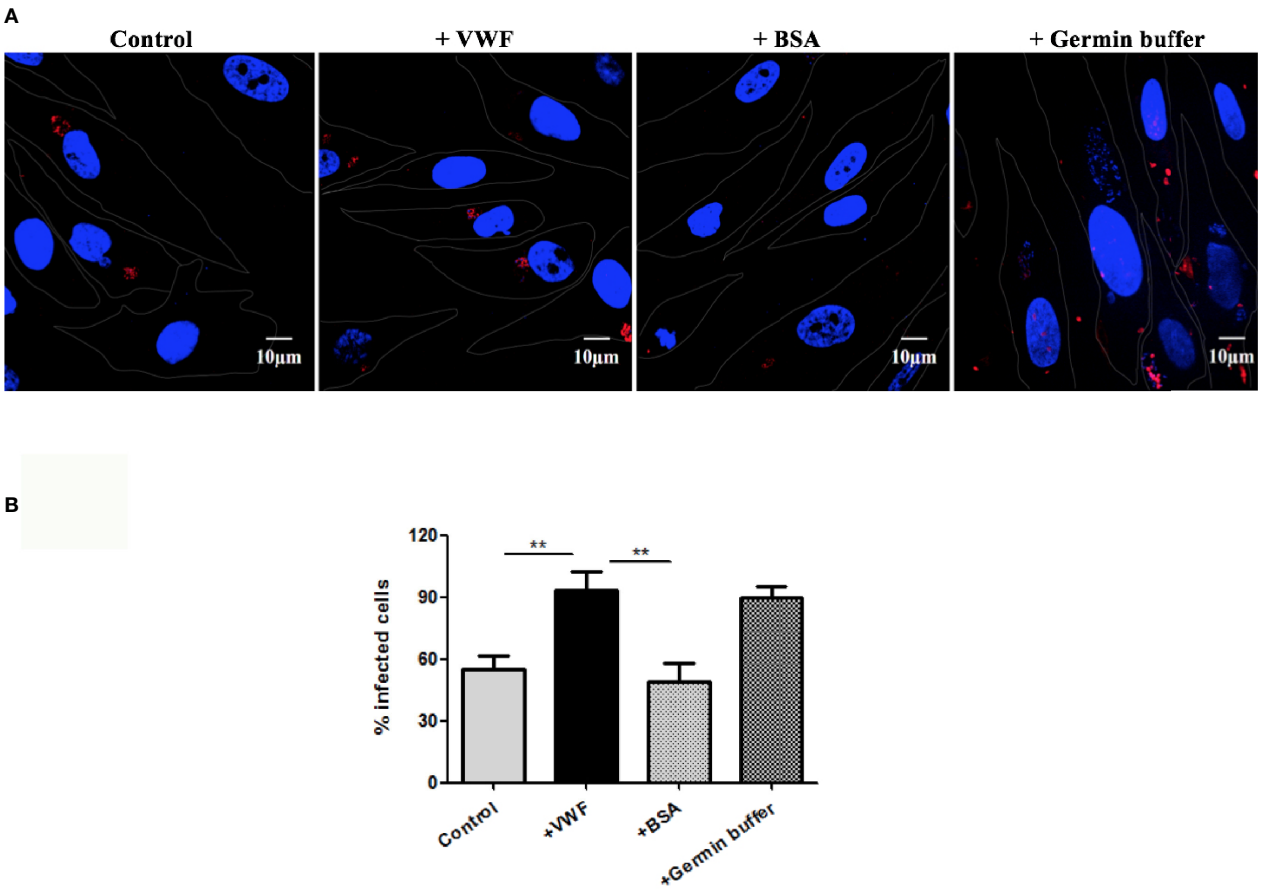

FIGURE 5 | VWF promotes *E. hellem* infection. **(A)** Representative fields of HFF cells exposed to *E. hellem* spores that had undergone no treatment (control) or binding of either FL-VWF or BSA or exposed to germination buffer. The spores were then added to HFF cells and culture for 12 h. The HFF cells outlines were depicted as 'dots' by Adobe Illustrator CS6to the DIC images of the cells. HFF cell nuclei were stained by DAPI (blue), while the infected *E. hellem* was represented by FISH probe (red) (Scale bar = 10 μm). **(B)** Infectivity rate was the ratio of infected HFF cells over all cells, based on three independent studies with 20 random fields per study. The result showed that VWF treatment significantly increased the infection rate of *E. hellem* to host cells ($F(1,59) = 2.42$,**=$P < 0.01$); while the un-related protein treatment of *E. hellem* spores had no effect on the infection ability ($F(1,59) = 1.92$, **$P < 0.01$).

VWD domain. This interaction altered multiple biological aspects of the pathogen that eventually lead to enhanced germination and infectivity. These effects make VWF a candidate for being a key mediator of microsporidia intravascular dissemination, and provide insights into the mechanism(s) by which microsporidia can lead to endocarditis, thrombocytopenia and other systemic manifestations. There have no specific therapeutics for

TABLE 1 | Representatives of ddifferentially expressed proteins of *E. hellem* after VWF incubation.

UniProtKB ID	Protein Name	Unique Peptides	Coverage	Up/Down-regulated
I6UNU1	Glucose-6-phosphate isomerase	55	69.8	Up
I6ULI4	40S ribosomal protein S6	14	38.2	Up
I6TLD3	Protein YOP1	10	33.5	Up
Q5VDH6	Aminopeptidase	2	52.7	Up
I6UEB3	HTH_9 domain containing protein	2	4.8	Up
I6TI03	Trehalase	19	31.2	Down
I6UNA0	Ribosomal protein L14E/L6E/L27E	10	54.7	Down
I6TWX8	V-type proton ATPase subunit a	8	12.1	Down
I6UP05	Translation initiation factor 2B subunit epsilon	3	6.3	Down
I6UM86	DNA polymerase sigma	1	5.4	Down

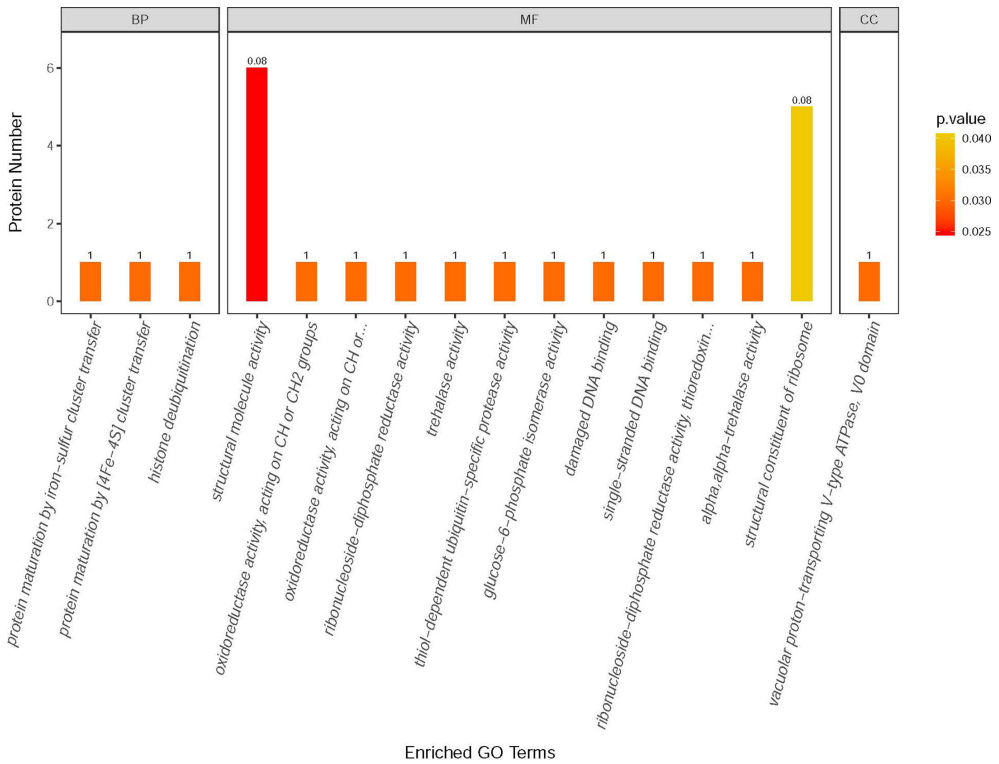

FIGURE 6 | GO annotation and enrichment analysis of differentially expressed proteins in *E. hellem* post-exposure to VWF. The primary Y axis denotes the number of annotated proteins categorized to each GO term. The secondary Y axis represents the percentage of annotated proteins to each GO term in all differential proteins. GO terms are classified into three subcategories, including biological process (BP), molecular function (MF) and cellular compartment (CC). The color gradient represents the p-value; the closer to red, the smaller the p-value. The enriched proteins are categorized and showed on X axis as: 1—Protein maturation by iron-sulfur cluster transfer; 2—Protein maturation by [4Fe–4S] cluster transfer; 3—Histone deubiquitination; 4—Structural molecule activity; 5—Oxidoreductase activity; 6—Oxidoreductase activity, acting on CH2 groups; 7—Ribonucleoside-diphosphate reductase activity; 8—Trehalase activity; 9—Thiol-dependent ubiquitin-specific protease activity; 10—Glucose-6-phosphate isomerise activity; 11—Damage DNA binding; 12—Single-stranded DNA binding; 13—Thioredoxin activity; 14—Alpha trehalase activity; 15—Structural constituent of ribosome; 16—Vacuolar proton-transporting V-type ATPase.

microsporidia. Drugs such as albendazole and fumagillin are either non-specific, not able to eliminate the pathogen, and have toxic side-effects (Didier et al., 2005). Thus, novel treatment strategies for microsporidia are necessary. Based on our findings, preventing the binding of microsporidia to VWF, probably *via* specific antibody neutralizing the binding site, may be an attractive target to prevent microsporidia dissemination and systemic infections.

DATA AVAILABILITY STATEMENT

The raw data supporting the conclusions of this article will be made available by the authors, without undue reservation.

AUTHOR CONTRIBUTIONS

JB designed the study and conducted most the experiments, interpreted the data, and wrote the manuscript. BM, GA, JL, TL and GP assisted in germination and infection experiments and analysis of data. MP contributed to study design and with ZZ contributed in manuscript grammar and language editing. All authors contributed to the article and approved the submitted version.

FUNDING

This work is supported by Fundamental Research Funds for the Central Universities (No. XDJK2020B005) and The National Natural Science Foundation of China (No. 31802141).

ACKNOWLEDGMENTS

We thank Prof. Louis Weiss for providing *E. hellem*; Prof Bing Han for HFF cells. We also appreciate Dr. Timothy Keiffer, Postdoctoral Fellow at Georgia State University, as well as Dr. S. Gaylen Bradley, emeritus dean of Basic Health Sciences, Virginia Commonwealth University, for their contributions in correcting the language in this manuscript.

REFERENCES

Anderson, N. W., Muehlenbachs, A., Arif, S., Bruminhent, J., Deziel, P. J., Razonable, R. R., et al. (2019). A Fatal Case of Disseminated Microsporidiosis Due to Anncaliia Algerae in a Renal and Pancreas Allograft Recipient. *Open Forum Infect. Dis.* 6, ofz285. doi: 10.1093/ofid/ofz285

Barber, B. E., William, T., Grigg, M. J., Parameswaran, U., Piera, K. A., Price, R. N., et al. (2015). Parasite Biomass-Related Inflammation, Endothelial Activation, Microvascular Dysfunction and Disease Severity in Vivax Malaria. *PloS Pathog.* 11, e1004558. doi: 10.1371/journal.ppat.1004558

Bukreyeva, I., Angoulvant, A., Bendib, I., Gagnard, J. C., Bourhis, J. H., Dargere, S., et al. (2017). Enterocytozoon Bieneusi Microsporidiosis in Stem Cell Transplant Recipients Treated With Fumagillin. *Emerging Infect. Dis.* 23, 1039–1041. doi: 10.3201/eid2306.161825

Delgado Betancourt, E., Hamid, B., Fabian, B. T., Klotz, C., Hartmann, S., and Seeber, F. (2019). From Entry to Early Dissemination-Toxoplasma Gondii's Initial Encounter With Its Host. *Front. Cell Infect. Microbiol.* 9, 46. doi: 10.3389/fcimb.2019.00046

Didier, E. S., Maddry, J. A., Brindley, P. J., Stovall, M. E., and Didier, P. J. (2005). Therapeutic Strategies for Human Microsporidia Infections. *Expert Rev. Anti-infective Ther.* 3, 419–434. doi: 10.1586/14787210.3.3.419

Dong, X., Leksa, N. C., Chhabra, E. S., Arndt, J. W., Lu, Q., Knockenhauer, K. E., et al. (2019). The Von Willebrand Factor D'D3 Assembly and Structural Principles for Factor VIII Binding and Concatemer Biogenesis. *Blood* 133, 1523–1533. doi: 10.1182/blood-2018-10-876300

Duan, W., Wang, S., Chen, M., Wang, C., Zhang, L., Liu, J., et al. (2006). Harvest Active Recombinant Rho Kinase From Escherichia Coli. *Biol. Pharm. Bull.* 29, 38–42. doi: 10.1248/bpb.29.38

Dunn, A. M., Terry, R. S., and Smith, J. E. (2001). Transovarial Transmission in the Microsporidia. *Adv. Parasitol.* 48, 57–100. doi: 10.1016/S0065-308X(01)48005-5

Franzen, C. (2005). How Do Microsporidia Invade Cells? *Folia Parasit* 52, 36–40. doi: 10.14411/fp.2005.005

Guirado, E., Schlesinger, L. S., and Kaplan, G. (2013). Macrophages in Tuberculosis: Friend or Foe. *Semin. Immunopathol.* 35, 563–583. doi: 10.1007/s00281-013-0388-2

Han, B., Moretto, M., and Weiss, L. M. (2019). Encephalitozoon: Tissue Culture, Cryopreservation, and Murine Infection. *Curr. Protoc. Microbiol.* 52, e72. doi: 10.1002/cpmc.72

Han, B., and Weiss, L. M. (2017). Microsporidia: Obligate Intracellular Pathogens Within the Fungal Kingdom. *Microbiol. Spectr.* 5 (2), 10. doi: 10.1128/9781555819583.ch5

He, Q., Leitch, G. J., Visvesvara, G. S., and Wallace, S. (1996). Effects of Nifedipine, Metronidazole, and Nitric Oxide Donors on Spore Germination and Cell Culture Infection of the Microsporidia Encephalitozoon Hellem and Encephalitozoon Intestinalis. *Antimicrobial Agents chemotherapy* 40, 179–185. doi: 10.1128/AAC.40.1.179

Herren, J. K., Paredes, J. C., Schupfer, F., and Lemaitre, B. (2013). Vertical Transmission of a Drosophila Endosymbiont Via Cooption of the Yolk Transport and Internalization Machinery. *mBio* 4 (2), e00532–12. doi: 10.1128/mBio.00532-12

Hilbert, L., Jorieux, S., Proulle, V., Favier, R., Goudemand, J., Parquet, A., et al. (2003). Two Novel Mutations, Q1053H and C1060R, Located in the D3 Domain of Von Willebrand Factor, are Responsible for Decreased FVIII-Binding Capacity. *Br. J. Haematol.* 120, 627–632. doi: 10.1046/j.1365-2141.2003.04163.x

Hirt, R. P., Logsdon, J.M.,Jr., Healy, B., Dorey, M. W., Doolittle, W. F., and Embley, T. M. (1999). Microsporidia are Related to Fungi: Evidence From the Largest Subunit of RNA Polymerase II and Other Proteins. *Proc. Natl. Acad. Sci. USA* 96, 580–585. doi: 10.1073/pnas.96.2.580

Jagau, H., Behrens, I. K., Lahme, K., Lorz, G., Koster, R. W., Schneppenheim, R., et al. (2019). Von Willebrand Factor Mediates Pneumococcal Aggregation and Adhesion in Blood Flow. *Front. Microbiol.* 10, 511. doi: 10.3389/fmicb.2019.00511

Kaneda, T., Shiraki, K., Hirano, K., and Nagata, I. (1997). Detection of Maternofetal Transfusion by Placental Alkaline Phosphatase Levels. *J. Pediatr.* 130, 730–735. doi: 10.1016/S0022-3476(97)80014-5

Kong, Q. F., Lv, B., Wang, B., Zhang, X. P., Sun, H. J., and Liu, J. (2020). Association of Von Willebrand Factor (Vwf) Expression With Lymph Node Metastasis and Hemodynamics in Papillary Thyroid Carcinoma. *Eur. Rev. Med. Pharmacol. Sci.* 24, 2564–2571. doi: 10.26355/eurrev_202003_20525

Kugler, W., and Lakomek, M. (2000). Glucose-6-Phosphate Isomerase Deficiency. *Bailliere's Best Pract. Res. Clin. Haematol.* 13, 89–101. doi: 10.1053/beha.1999.0059

Leitch, G. J., He, Q., Wallace, S., and Visvesvara, G. S. (1993). Inhibition of the Spore Polar Filament Extrusion of the Microsporidium, Encephalitozoon Hellem, Isolated From an AIDS Patient. *J. Eukaryot. Microbiol.* 40, 711–717. doi: 10.1111/j.1550-7408.1993.tb04463.x

Lenting, P. J., Christophe, O. D., and Denis, C. V. (2015). Von Willebrand Factor Biosynthesis, Secretion, and Clearance: Connecting the Far Ends. *Blood* 125, 2019–2028. doi: 10.1182/blood-2014-06-528406

Lu, W., Lu, C., Zhang, Q., Cao, S., Zhang, Z., Jia, H., et al. (2020). Localization and Enzyme Kinetics of Aminopeptidase N3 From Toxoplasma Gondii. *Parasitol. Res.* 119, 357–364. doi: 10.1007/s00436-019-06512-6

Luna, V. A., Stewart, B. K., Bergeron, D. L., Clausen, C. R., Plorde, J. J., and Fritsche, T. R. (1995). Use of the Fluorochrome Calcofluor White in the Screening of Stool Specimens for Spores of Microsporidia. *Am. J. Clin. Pathol.* 103, 656–659. doi: 10.1093/ajcp/103.5.656

Madabhushi, S. R., Zhang, C., Kelkar, A., Dayananda, K. M., and Neelamegham, S. (2014). Platelet Gpiba Binding to Von Willebrand Factor Under Fluid Shear: Contributions of the D'D3-Domain, A1-Domain Flanking Peptide and O-Linked Glycans. *J. Am. Heart Assoc.* 3, e001420. doi: 10.1161/JAHA.114.001420

Meissner, E. G., Bennett, J. E., Qvarnstrom, Y., da Silva, A., Chu, E. Y., Tsokos, M., et al. (2012). Disseminated Microsporidiosis in an Immunosuppressed Patient. *Emerging Infect. Dis.* 18, 1155–1158. doi: 10.3201/eid1807.120047

Meng, X. Z., Luo, B., Tang, X. Y., He, Q., Xiong, T. R., Fang, Z. Y., et al. (2018). Pathological Analysis of Silkworm Infected by Two Microsporidia Nosema Bombycis CQ1 and Vairimorpha Necatrix BM. *J. Invertebr. Pathol.* 153, 75–84. doi: 10.1016/j.jip.2017.12.005

Michaux, G., Pullen, T. J., Haberichter, S. L., and Cutler, D. F. (2006). P-Selectin Binds to the D '-D3 Domains of Von Willebrand Factor in Weibel-Palade Bodies. *Blood* 107, 3922–3924. doi: 10.1182/blood-2005-09-3635

Murakami, J., Nagata, I., Iitsuka, T., Okamoto, M., Kaji, S., Hoshika, T., et al. (2012). Risk Factors for Mother-to-Child Transmission of Hepatitis C Virus: Maternal High Viral Load and Fetal Exposure in the Birth Canal. *Hepatology Res. Off. J. Japan Soc. Hepatology* 42, 648–657. doi: 10.1111/j.1872-034X.2012.00968.x

O'Seaghdha, M., van Schooten, C. J., Kerrigan, S. W., Emsley, J., Silverman, G. J., Cox, D., et al. (2006). Staphylococcus Aureus Protein a Binding to Von Willebrand Factor A1 Domain is Mediated by Conserved Igg Binding Regions. *FEBS J.* 273, 4831–4841. doi: 10.1111/j.1742-4658.2006.05482.x

Pariyakanok, L., Satitpitakul, V., Laksanaphuk, P., Ratanawongphaibul, K., Putaporntip, C., and Jongwutiwes, S. (2019). Stromal Keratitis With Endophthalmitis Caused by Vittaforma Corneae in an Immunocompetent Patient: A Case Report. *Ocul. Immunol. Inflamm.* 27, 826–828. doi: 10.1080/09273948.2018.1455875

Park, G. S., Ireland, K. F., Opoka, R. O., and John, C. C. (2012). Evidence of Endothelial Activation in Asymptomatic Plasmodium Falciparum Parasitemia and Effect of Blood Group on Levels of Von Willebrand Factor in Malaria. *J. Pediatr. Infect. Dis. Soc.* 1, 16–25. doi: 10.1093/jpids/pis010

Pattana Jaroenlak, M. C., Davydov, A., Sall, J., Usmani, M., Liang, F.-X., Ekiert, D. C., et al. (2020). 3-Dimensional Organization and Dynamics of the Microsporidian Polar Tube Invasion Machinery. *bioRxiv* 2020, 04.03.024240. doi: 10.1371/journal.ppat.1008738

Pillai, V. G., Bao, J., Zander, C. B., McDaniel, J. K., Chetty, P. S., Seeholzer, S. H., et al. (2016). Human Neutrophil Peptides Inhibit Cleavage of Von Willebrand Factor by ADAMTS13: A Potential Link of Inflammation to TTP. *Blood* 128, 110–119. doi: 10.1182/blood-2015-12-688747

Raina, S. K., Das, S., Rai, M. M., and Khurad, A. M. (1995). Transovarial Transmission of Nosema Locustae (Microsporida: Nosematidae) in the Migratory Locust Locusta Migratoria Migratorioides. *Parasitol. Res.* 81, 38–44. doi: 10.1007/BF00932415

Robertson, P. D., Warren, E. M., Zhang, H., Friedman, D. B., Lary, J. W., Cole, J. L., et al. (2008). Domain Architecture and Biochemical Characterization of

Vertebrate Mcm10. *J. Biol. Chem.* 283, 3338–3348. doi: 10.1074/jbc.M706267200

Sadler, J. E. (1998). Biochemistry and Genetics of Von Willebrand Factor. *Annu. Rev. Biochem.* 67, 395–424. doi: 10.1146/annurev.biochem.67.1.395

Shapiro, S. E., Nowak, A. A., Wooding, C., Birdsey, G., Laffan, M. A., and McKinnon, T. A. (2014). The Von Willebrand Factor Predicted Unpaired Cysteines are Essential for Secretion. *J. Thromb. haemostasis JTH* 12, 246–254. doi: 10.1111/jth.12466

Shiltagh, N., Kirkpatrick, J., Cabrita, L. D., McKinnon, T. A., Thalassinos, K., Tuddenham, E. G., et al. (2014). Solution Structure of the Major Factor VIII Binding Region on Von Willebrand Factor. *Blood* 123, 4143–4151. doi: 10.1182/blood-2013-07-517086

Sicard, J. F., Le Bihan, G., Vogeleer, P., Jacques, M., and Harel, J. (2017). Interactions of Intestinal Bacteria With Components of the Intestinal Mucus. *Front. Cell Infect. Microbiol.* 7, 387. doi: 10.3389/fcimb.2017.00387

Small, H. J., Meyer, G. R., Stentiford, G. D., Dunham, J. S., Bateman, K., and Shields, J. D. (2014). Ameson Metacarcini Sp. Nov. (Microsporidia) Infecting the Muscles of Dungeness Crabs Metacarcinus Magister From British Columbia, Canada. *Dis. Aquat. Org.* 110, 213–225. doi: 10.3354/dao02754

Steinert, M., Ramming, I., and Bergmann, S. (2020). Impact of Von Willebrand Factor on Bacterial Pathogenesis. *Front. Med.* 7, 543. doi: 10.3389/fmed.2020.00543

Ueda, Y., Mohammed, I., Song, D., Gullipalli, D., Zhou, L., Sato, S., et al. (2017). Murine Systemic Thrombophilia and Hemolytic Uremic Syndrome From a Factor H Point Mutation. *Blood* 129, 1184–1196. doi: 10.1182/blood-2016-07-728253

Valencakova, A., and Danisova, O. (2019). Molecular Characterization of New Genotypes Enterocytozoon Bieneusi in Slovakia. *Acta Trop.* 191, 217–220. doi: 10.1016/j.actatropica.2018.12.031

van den Dries, L. W. J., Gruters, R. A., Hovels-van der Borden, S. B. C., Kruip, M. J. H. A., de Maat, M. P. M., van Gorp, E. C. M., et al. (2015). Von Willebrand Factor is Elevated in HIV Patients With a History of Thrombosis. *Front. Microbiol.* 6, 190. doi: 10.3389/fmicb.2015.00180

Vergauwe, R. M., Uji-i, H., De Ceunynck, K., Vermant, J., Vanhoorelbeke, K., and Hofkens, J. (2014). Shear-Stress-Induced Conformational Changes of Von Willebrand Factor in a Water-Glycerol Mixture Observed With Single Molecule Microscopy. *J. Phys. Chem. B* 118, 5660–5669. doi: 10.1021/jp5022664

Viela, F., Prystopiuk, V., Leprince, A., Mahillon, J., Speziale, P., Pietrocola, G., et al. (2019). Binding of Staphylococcus Aureus Protein a to Von Willebrand Factor is Regulated by Mechanical Force. *mBio* 10 (2), e00555–19. doi: 10.1128/mBio.00555-19

Viljanen, J., Lounatmaa, K., and Makela, P. H. (1991). Expression of the Virulence Plasmid-Determined Protein YOP1 and Hela Cell Invasiveness of Yersinia Enterocolitica O:3. *Contributions to Microbiol. Immunol.* 12, 176–181.

Visvesvara, G. S., Leitch, G. J., Moura, H., Wallace, S., Weber, R., and Bryan, R. T. (1991). Culture, Electron Microscopy, and Immunoblot Studies on a Microsporidian Parasite Isolated From the Urine of a Patient With AIDS. *J. Protozoology* 38, 105S–111S.

Volonte, F., Piubelli, L., and Pollegioni, L. (2011). Optimizing HIV-1 Protease Production in Escherichia Coli as Fusion Protein. *Microb. Cell Fact* 10, 53. doi: 10.1186/1475-2859-10-53

Weber, R., Bryan, R. T., Schwartz, D. A., and Owen, R. L. (1994). Human Microsporidial Infections. *Clin. Microbiol. Rev.* 7, 426–461. doi: 10.1128/CMR.7.4.426

Weber, R., Kuster, H., Visvesvara, G. S., Bryan, R. T., Schwartz, D. A., and Luthy, R. (1993). Disseminated Microsporidiosis Due to Encephalitozoon Hellem: Pulmonary Colonization, Microhematuria, and Mild Conjunctivitis in a Patient With AIDS. *Clin. Infect. Dis. an Off. Publ. Infect. Dis. Soc. America* 17, 415–419. doi: 10.1093/clinids/17.3.415

Weiss, L. M. (1995). and Now Microsporidiosis. *Ann. Internal Med.* 123, 954–956. doi: 10.7326/0003-4819-123-12-199512150-00012

Weiss, L. M. (2001). Microsporidia: Emerging Pathogenic Protists. *Acta Trop.* 78, 89–102. doi: 10.1016/S0001-706X(00)00178-9

Yazar, S., Eser, B., Yalcin, S., Sahin, I., and Koc, A. N. (2003). A Case of Pulmonary Microsporidiasis in an Acute Myeloblastic Leukemia (AML) - M3 Patient. *Yonsei Med. J.* 44, 146–149. doi: 10.3349/ymj.2003.44.1.146

Yee, A., Gildersleeve, R. D., Gu, S., Kretz, C. A., McGee, B. M., Carr, K. M., et al. (2014). A Von Willebrand Factor Fragment Containing the D'D3 Domains is Sufficient to Stabilize Coagulation Factor VIII in Mice. *Blood* 124, 445–452. doi: 10.1182/blood-2013-11-540534

Zhao, L., Yang, M., Shen, Q., Liu, X., Shi, Z., Wang, S., et al. (2016). Functional Characterization of Three Trehalase Genes Regulating the Chitin Metabolism Pathway in Rice Brown Planthopper Using RNA Interference. *Sci. Rep.* 6, 27841. doi: 10.1038/srep27841

Zheng, X. L., and Sadler, J. E. (2008). Pathogenesis of Thrombotic Microangiopathies. *Annu. Rev. Pathol.* 3, 249–277. doi: 10.1146/annurev.pathmechdis.3.121806.154311

Conflict of Interest: The authors declare that the research was conducted in the absence of any commercial or financial relationships that could be construed as a potential conflict of interest.

frontiers in Cellular and Infection Microbiology

ORIGINAL RESEARCH
published: 16 June 2021
doi: 10.3389/fcimb.2021.699239

Characterizing the Xenoma of *Vairimorpha necatrix* Provides Insights Into the Most Efficient Mode of Microsporidian Proliferation

Tian Li[1,2*†], *Zhuoya Fang*[1,2†], *Qiang He*[1,2], *Chunxia Wang*[1,2], *Xianzhi Meng*[1,2], *Bin Yu*[1,2] *and Zeyang Zhou*[1,2,3*]

[1] State Key Laboratory of Silkworm Genome Biology, Southwest University, Chongqing, China, [2] Chongqing Key Laboratory of Microsporidia Infection and Control, Southwest University, Chongqing, China, [3] College of Life Science, Chongqing Normal University, Chongqing, China

OPEN ACCESS

Edited by:
Xiao-Xuan Zhang,
Qingdao Agricultural University,
China

Reviewed by:
Yongqi Shao,
Zhejiang University, China
Jinshan Xu,
Chongqing Normal University, China
Edilson Rodrigues Matos,
Federal Government of Brazil, Brazil

***Correspondence:**
Tian Li
lit@swu.edu.cn
Zeyang Zhou
zyzhou@swu.edu.cn

†These authors have contributed equally to this work

Specialty section:
This article was submitted to Clinical Microbiology, a section of the journal Frontiers in Cellular and Infection Microbiology

Received: 23 April 2021
Accepted: 28 May 2021
Published: 16 June 2021

Citation:
Li T, Fang Z, He Q, Wang C, Meng X, Yu B and Zhou Z (2021) Characterizing the Xenoma of Vairimorpha necatrix Provides Insights Into the Most Efficient Mode of Microsporidian Proliferation. Front. Cell. Infect. Microbiol. 11:699239. doi: 10.3389/fcimb.2021.699239

Microsporidia are a group of obligated intracellular parasites that can infect nearly all vertebrates and invertebrates, including humans and economic animals. Microsporidian *Vairimorpha necatrix* is a natural pathogen of multiple insects and can massively proliferate by making tumor-like xenoma in host tissue. However, little is known about the subcellular structures of this xenoma and the proliferation features of the pathogens inside. Here, we characterized the *V. necatrix* xenoma produced in muscle cells of silkworm midgut. In result, the whitish xenoma was initially observed on the 12th day post infection on the outer surface of the midgut and later became larger and numerous. The observation by scanning electronic microscopy showed that the xenoma is mostly elliptical and spindle with dense pathogen-containing protrusions and spores on the surface, which were likely shedding off the xenoma through exocytosis and could be an infection source of other tissues. Demonstrated with transmission electron microscopy and fluorescent staining, the xenoma was enveloped by a monolayer membrane, and full of vesicle structures, mitochondria, and endoplasmic reticulum around parasites in development, suggesting that high level of energy and nutrients were produced to support the massive proliferation of the parasites. Multiple hypertrophic nuclei were found in one single xenoma, indicating that the cyst was probably formed by fusion of multiple muscle cells. Observed by fluorescence *in situ* hybridization, pathogens in the xenoma were in merongony, sporogony, and octosporogony, and mature stages. And mature spores were pushed to the center while vegetative pathogens were in the surface layer of the xenoma. The *V. necatrix* meront usually contained two to three nuclei, and sporont contained two nuclei and was wrapped by a thick membrane with high electron density. The *V. necatrix* sporogony produces two types of spores, the ordinary dikaryotic spore and unicellular octospores, the latter of which were smaller in size and packed in a sporophorous vesicle. In summary, *V. necatrix* xenoma is a specialized cyst likely formed by fusion of multiple muscle cells and provides high concentration of energy and nutrients with increased number of mitochondria and endoplasmic reticulum for the massive proliferation of pathogens inside.

Keywords: microsporidia, *Vairimorpha necatrix*, xenoma, subcellular structure, proliferation

INTRODUCTION

Microsporidia are obligate intracellular parasites and composed of at least 200 genera and 1,400 species (Fayer and Santin-Duran, 2014). Microsporidia can infect nearly all animals, including humans and economically important animals like silkworm, bee, shrimp, crab, and fish (Franzen and Müller, 1999; Joseph et al., 2006). The life cycle of microsporidia can be generally divided into three phases, the initially infective phase, proliferative phase, and sporogonic phase (Cali et al., 2005; Joseph et al., 2005). The first phase is the only stage that exists outside of the host cells, while the latter two phases must be inside host cells (Han and Weiss, 2017).

Different microsporidia species lead to varieties of symptoms and proliferate in divergent patterns. Most microsporidian infections usually cause no obvious tissue lesions, especially for those that can be vertically transmitted, while some species like *Vairimorpha necatrix*, *Glugea arabica*, *Vavraia lutzomyiae*, and *Potaspora morhaphis* can produce xenoma, which is a cyst full of pathogens and presents in many infected insects and aquatic animals (Lom and Dykova, 2005; Matos et al., 2006; Casal et al., 2008; Meng et al., 2018). In infected tissues, microsporidia and host cells interact and form a well-organize xenoparasitic complex, which was finally named "xenoma" by Weissenberg in 1949 (Lom and Dykova, 2005). The *G. arabica* could infect the intestinal wall of the marine teleost *Epinephelus polyphekadion* and produce spherical blackish xenomas (Azevedo et al., 2016). It was found that the xenoma of *Abelspora portucalensis* was scattered in the hepatopancreas of the common foreshore crab and more often observed at the edges of this organ. Most xenomas are formed by fusion of host cells and consist of hypertrophic cells (Azevedo, 1987). A real xenoma was pointed out to be a swollen host cell and surrounded by collagen fibers produced by the host (Cali and Takvorian, 1999). In a xenoma, host nucleus undergoes amitosis to form many small nuclei, and host organelles increase significantly, including mitochondria and endoplasmic reticulum (ER) (Cali et al., 2012).

Microsporidian *V. necatrix* was originally isolated from *Pseudaletia unipuncta* (Kramer, 1965; Pilley, 1976), and is primarily a pathogen of phytophagous Lepidoptera, including at least 36 insects (Maddox et al., 1981). *V. necatrix* is considered to be a potential insecticides for its wide host rang and high virulence (Down et al., 2004). We obtained a *V. necatrix* isolate, named *V. necatrix* BM, from the naturally infected silkworm (Liu et al., 2012; Luo et al., 2014). The infected silkworm presented typical symptoms similar to pébrine disease that caused by *Nosema bombycis*. The silkworm midgut, fat body, and testis were seriously infected, and silk gland and malpighian tubes were slightly infected, while the ovary could not be infected, suggesting that *V. necatrix* cannot be transovarially transmitted in silkworm (Meng et al., 2018). In particular, some xenomas containing massive pathogens were produced on the midgut, manifesting the importance of xenoma for the proliferation of *V. necatrix*. We have characterized the morphology of *V. necatrix* xenoma in our previous work (Meng et al., 2018). However, little is known about its subcellular features, as well as the development of parasites inside. Here, we dissected the *V. necatrix* xenoma by taking advantage of the microsporidia-silkworm system. Silkworm *Bombyx mori* is an ideal model to study lepidopteran insects and their pathogens.

MATERIALS AND METHODS

Preparation of *V. necatrix* BM Spores

V. necatrix BM was isolated from the infected silkworm in Shandong Province, China. The fresh *V. necatrix* BM spores were purified from infected silkworms as described earlier (Liu et al., 2012). After removing the intestinal and puparium from the infected silkworm pupa, tissues were ground in sterilized distilled water using a mortar. The lapping liquid was filtered using cotton to remove tissue fragments and collect the effluent liquid, which was centrifuged at 5,000 rpm for 5 min at 4°C. After removing supernatant, the precipitate was washed with sterilized distilled water for three times, and resuspended with sterilized distilled water. The resuspended spores were counted with hemocytometer and stored at −80°C.

Silkworm Infection

The eggs of silkworm *B. mori* Dazao were obtained from the State Key Laboratory of Silkworm Genome Biology, Southwest University, China. Silkworms in third instar were orally inoculated with 10^5 V. *necatrix* BM spores per larva, and then reared to pupa stage. The infection was observed by dissecting analysis of the larvae in late fifth instar. Silkworm tissues were fixed with 1 ml of 2.5% glutaraldehyde and 4% poly-formaldehyde. Pathogen load in the tissues was then counted under ordinary optical microscope.

Scanning Electron Microscopy (SEM) Assay

The SEM assay was performed referring to (Schottelius et al., 2000). Xenomas were fixed with 2.5% glutaraldehyde and 1% osmium tetroxide, and dehydrated with gradient ethanol (30, 40, 50, 60, 70, 80, 90, and 96%) for 10 min each, and 100% ethanol for two times for 15 min each. Then, the samples were dehydrated with gradient tert-butyl alcohol (50, 75, and 100%), and tert-butyl alcohol: acetonitrile (2:1 and 1:1), followed by absolute acetonitrile for 10 min each. Finally, the dried samples were coated with gold and observed using SEM S-3000N.

Paraffin Sections and Confocal Observations

Silkworm midgut and xenoma were fixed in 4% paraformaldehyde and 0.1% glutaraldehyde and embedded in paraffin wax. The samples were then cut into 5 μm slices and placed on the slides. After deparaffinization and hydration, sections of the slides were stained with hematoxylin and eosin (HE) (Fischer et al., 2008). The other sections of the slides were incubated with DAPI and Fluorescent Brightener 28 (Sigma) at 37°C for 15 min. The slides were then washed for three times with 0.01M PBS buffer (pH 7.2) and suspended with Fluoromount™ Aqueous Mounting Medium (Sigma) and

mounted with a cover glass. Finally, the slides were observed and photographed using an OLYMPUS Biological Confocal Laser Scanning Microscope FV1200.

Staining the Nucleus, Mitochondria, and ER of Xenoma

Xenomas were fixed in 4% paraformaldehyde, decolorized with 6% H_2O_2 in ethanol for 2 h, and washed four times (10 min each) with 0.01 M PBS buffer (pH 7.2). The fixed samples were then incubated with DAPI, Mito-Tracker Red, and ER-Tracker Red at 37°C for 30 min to stain the nucleus, mitochondria, and ER, respectively. After washing four times (5 min each) with 0.01 M PBS buffer (pH 7.2), the slides were suspended using Fluoromount™ Aqueous Mounting Medium (Sigma) and mounted with a cover glass. The slides were finally observed and photographed using an OLYMPUS Biological Confocal Laser Scanning Microscope FV1200.

Fluorescence *In Situ* Hybridization (FISH)

Xenomas were fixed in 4% paraformaldehyde, decolorized with 6% H_2O_2 in ethanol for 2 h, washed for four times (10 min each) with 0.01M PBS buffer (pH 7.2). The samples were then incubated with DAPI at 37°C for 30 min to stain the nuclei. After washing four times (5 min each) in 0.01 M PBS buffer (pH 7.2), the slides were suspended with Fluoromount™ Aqueous Mounting Medium (Sigma) and mounted with a cover glass. Based on the 16S rRNA sequence of *V. necatrix* BM, a DNA probe, VnLSU-V1-Cy3 (5'-Cy3-GTATTCTATTACGACCTTC-3'), was designed using Primer3 software (http://fokker.wi.mit.edu/primer3/) and checked the specificity using the Ribosomal Database Project II "probe match" analysis tool (Gottlieb et al., 2006). Besides, the probe specificity was experimentally verified in silkworm BmE cells infected by *V. necatrix* and *N. bombycis*, the latter of which was labeled with a multiclonal antibody as described in (Song et al., 2020). Stained samples were wholly mounted and viewed under an OLYMPUS Biological Confocal Laser Scanning Microscope FV1200.

Transmission Electron Microscope (TEM)

TEM was performed as previously described (Wu et al., 2010) with slight modifications. Xenomas were fixed with 2.5% glutaraldehyde for 2 h, and washed four times (15 min each) with 0.1 M PBS buffer (pH 7.2), then fixed for 2 h with 1% osmium tetroxide and washed for four times (15 min each) with 0.1 M PBS buffer (pH 7.2). Subsequently, the samples were dehydrated two times with gradient ethanol and 100% acetone, infiltrated with gradient Epon812 (SPI, USA) resin, buried with 100% resin, and aggregated for 48 h at 70°C. Ultrathin sections were made using a LEICA EM UC7 ultra microtome. The sections were stained with 3% uranyl acetate for 20 min, followed by lead citrate for 15 min. The dyed sections were rinsed for six times with distilled H_2O, naturally dried, and then photographed with a JEM-1400 Plus TEM under 80 kv acceleration voltage.

RESULTS

The Development of the Xenoma

The midgut is the main digestive organ of silkworm, and also the first organ infected by microsporidia. Silkworms orally inoculated in the third instar showed no obvious xenoma in 11 days post infection (dpi) (**Figure 1A**). On the 12th dpi, a few of xenomas were observed on the posterior of midgut. On the 13th dpi, the midgut showed a heavier infection and became whitish on the posterior, suggesting that a large number of little xenomas were forming. Subsequently, the xenomas grew larger, and the intestinal enlargement became evident on the 16th dpi. The anatomy showed that a large number of xenomas formed on the posterior of the midgut (**Figures 1B, C**). This particular parasitic pattern is known as an xenoma in many aquatic animals infected by microsporidia. The *V. necatrix* xenoma is spherical in shape and 1 to 5 mm in size (Luo et al., 2014; Meng et al., 2018). Microscopic observations of the xenoma manifested a great many pathogens in different stages and some vesicles each containing eight monocytic spores, the octospores (**Figures 1D, E**).

The Development of the Pathogens in Xenoma

The *V. necatrix* BM in the xenoma was demonstrated by FISH for labeling pathogens in proliferation and DAPI for staining all nuclei. The specificity of the FISH probe and purity of the parasites were firstly verified in silkworm BmE cells infected by *N. bombycis* and *V. necatrix*. In result, the *V. necatrix* was specifically labeled by the probe, while there was no probe sign found in *N. bombycis*, which was instead demonstrated by the specific antibody (**Figure 2A**). As shown in **Figure 2B**, the xenoma was full of parasites in proliferative and mature stages. The meronts were transparent and not visible under DIC, but specifically labeled by FISH and DAPI, which stained the cytosol in red and the nucleus in blue, respectively. The meronts were fusiform in shape and much longer than any other stages for reaching 10 μm in length. The meront nucleus was also much larger, and showed lighter DAPI fluorescence compared with that of the mature spores, indicating that meront chromatins were likely in highly active state. The sporont, clearly stained by FISH and DAPI, were shown oval in shape and 5 μm in length, and became recognizable under DIC for the outer wall being slightly light-reflecting. Large quantities of mature spores were observed in xenoma, especially in the central area. The mature spores could not be labeled by FISH probes for being coated with thick spore wall but showed strong DAPI signals, which manifested condensed nuclei. Mature spores displayed high refractivity and clear outline under DIC so that they were easily recognized under light microscopy. Moreover, some germinated and empty spores were also observed under DIC, which showed no FISH and DAPI signals, suggesting that autoinfection happened inside the xenoma. Besides, the large numbers of germinated spores also indicated that the parasites were in massive reproduction.

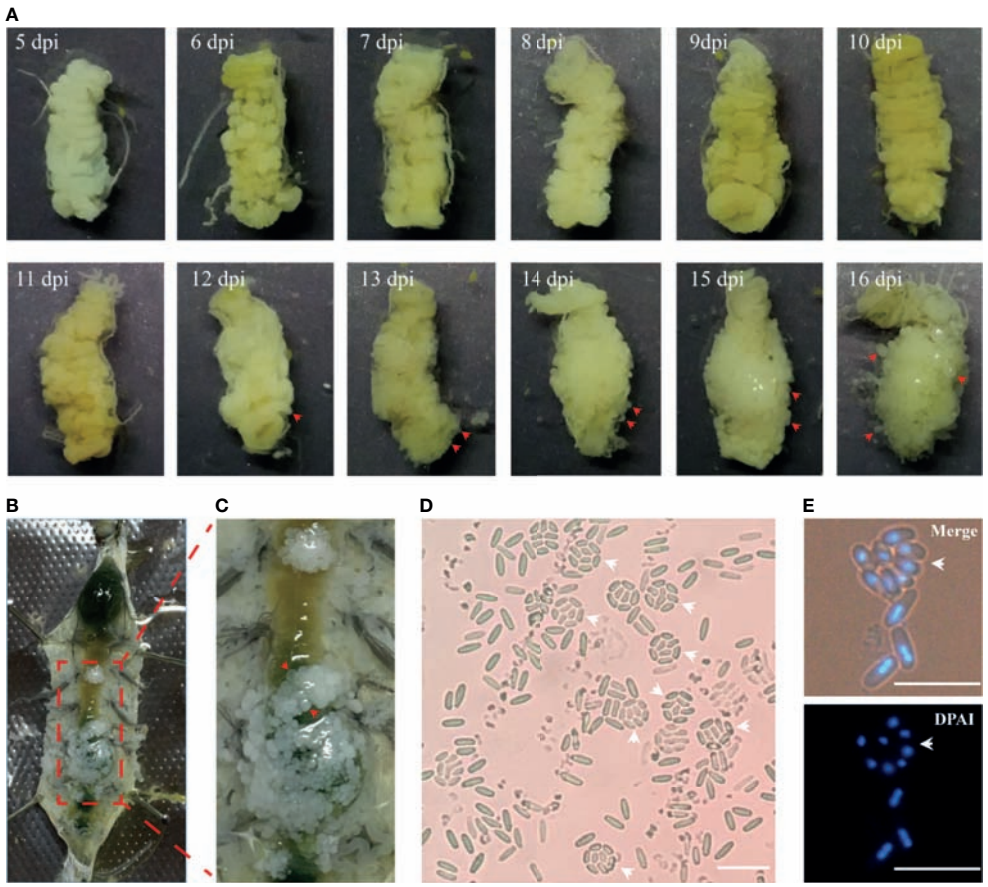

FIGURE 1 | The development of xenoma on the midgut of silkworm infected by *V. necatrix* BM. **(A)** The silkworm midgut from 5 to 16 dpi. The xenomas (arrowhead) could be observed after 12 dpi and were obvious after 13 dpi. The midgut was surround by massive xenomas after 16 dpi; **(B)** The infected silkworm larva was dissected in the 5th instar; **(C)** Massive whitish xenomas (arrowhead) were shown on the outer surface of the infected midgut; **(D, E)** The *V. necatrix* BM in a xenoma produced a large number of meiospores (octospores) contained within a sporophorous vesicle (arrowhead). The bar indicates 10 μm.

The Morphology of the Xenoma

Manifested by the SEM, the xenoma was long oval and spindle in shape (**Figures 3A, B**). The outer surface of the xenoma was covered by highly dense protrusions (**Figures 3C, D**), which were shown to be mature spores by the enlarged views (**Figures 3E, F**). Some spores looked like floating on and adhering to the xenoma surface, and some were partially inlaid in xenoma wall, suggesting that the spores were exiting from the xenoma, and the xenoma could be a source for infecting other tissues. The internal structure was also observed from the broken xenoma using SEM and showed a lot of mature spores embedded in the loose matrices inside (**Figures 3G, H**).

The Organelles in the Xenoma

The *V. necatrix* xenoma is a membrane-encapsulated cystic structure that forms in muscle tissue. However, it is unclear whether there is a host nucleus in the xenoma. In the DAPI stained xenoma, besides a great number of pathogens nuclei, multiple host nuclei were observed (**Figure 4**). These host nuclei were surrounded by massive pathogens and much larger than common nucleus, and apparently hypertrophic deformed and branched and lobed (dash line in **Figure 4**). The multinuclear feature suggested that the xenoma likely produced by fusion of multiple muscle cells.

Microsporidian genomes are compact and reduced, and have lost most genes responsible for the *de novo* synthesis of nucleotides, amino acids, and lipids (Corradi et al., 2010; Heinz et al., 2012; Nakjang et al., 2013). Instead, microsporidia evolved strategies to regulate host pathways for obtaining nutrients from host (Bernal et al., 2016; Han et al., 2020). Massively proliferating in xenoma, the parasites would get large quantities of nutrients from host. Therefore, it is interesting to see what happens to the xenoma mitochondria and endoplasmic reticulum (ER), which are vital organelles in the synthesis of nutrients and energy.

Herein, the mitochondria and ER in the xenoma were stained using Mito-Tracker and ER-Tracker, respectively. In result, the mitochondria were shown in red and mainly appeared and highly aggregated in areas full of meronts but showing less mature spores (**Figure 5A**). The densely aggregated mitochondria showed no distinct outline, instead looked like

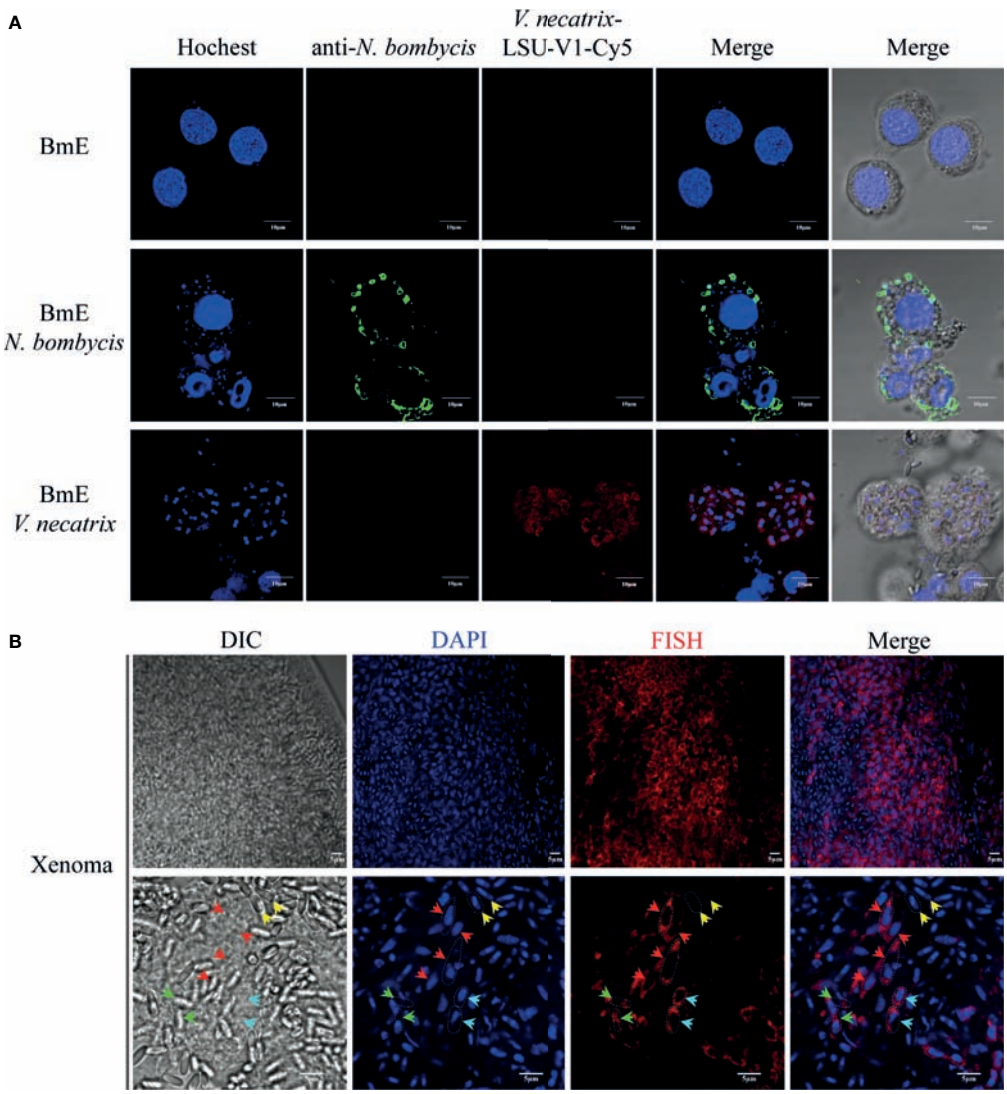

FIGURE 2 | FISH and DAPI staining of *V. necatrix* BM in xenoma. **(A)** The parasite purity was verified by FISH with a probe of *V. necatrix* ribosomal RNA (red) and IFA using an antibody against *N. bombycis* (green) in infected BmE cells, respectively. Bar, 10 μm. **(B)** The nucleus of *V. necatrix* BM in all stages was stained with DAPI (blue). The parasites in development were labeled using FISH with a probe of the ribosomal RNA (red). Red arrowhead, meront; Cyan arrowhead, sporont; Yellow arrowhead, mature spore; Green arrowhead, empty (germinated) spore; Bar, 5 μm.

linking up into a single stretch, suggesting that the replication of mitochondria was significantly increased. Massive mature spores, each with two nuclei, were conspicuous under DIC and DAPI staining, aggregated and formed clusters. The ER was also marked in red by ER-Tracker and densely distributed in the xenoma, and even denser in the locations where pathogens were in proliferation (**Figure 5B**). The high density of mitochondria and ER around the proliferative pathogens suggested that the xenoma likely supplied abundant energy and nutrients for the proliferation of the parasites.

The Subcellular Structures of the Xenoma

The xenoma was analyzed using TEM to observe the ultrastructure of the organelles and pathogens inside. The outer wall of the xenoma was a thin and single-layer membrane for about 100 nm (**Figures 6A–C**). The xenoma interior was full of vesicle structures and pathogens. Pathogens in the early xenoma were nearly in proliferative stages, most of which were merogony (**Figures 6D–F**). The meronts usually contained two to three nuclei, and surrounded by many vesicles in high or low electron density. The mature spores with a thick wall manifested high electron density.

DISCUSSION

V. necatrix can infect a wide range of lepidoptera (Maddox et al., 1981). Besides in silkworm, the proliferative morphology of

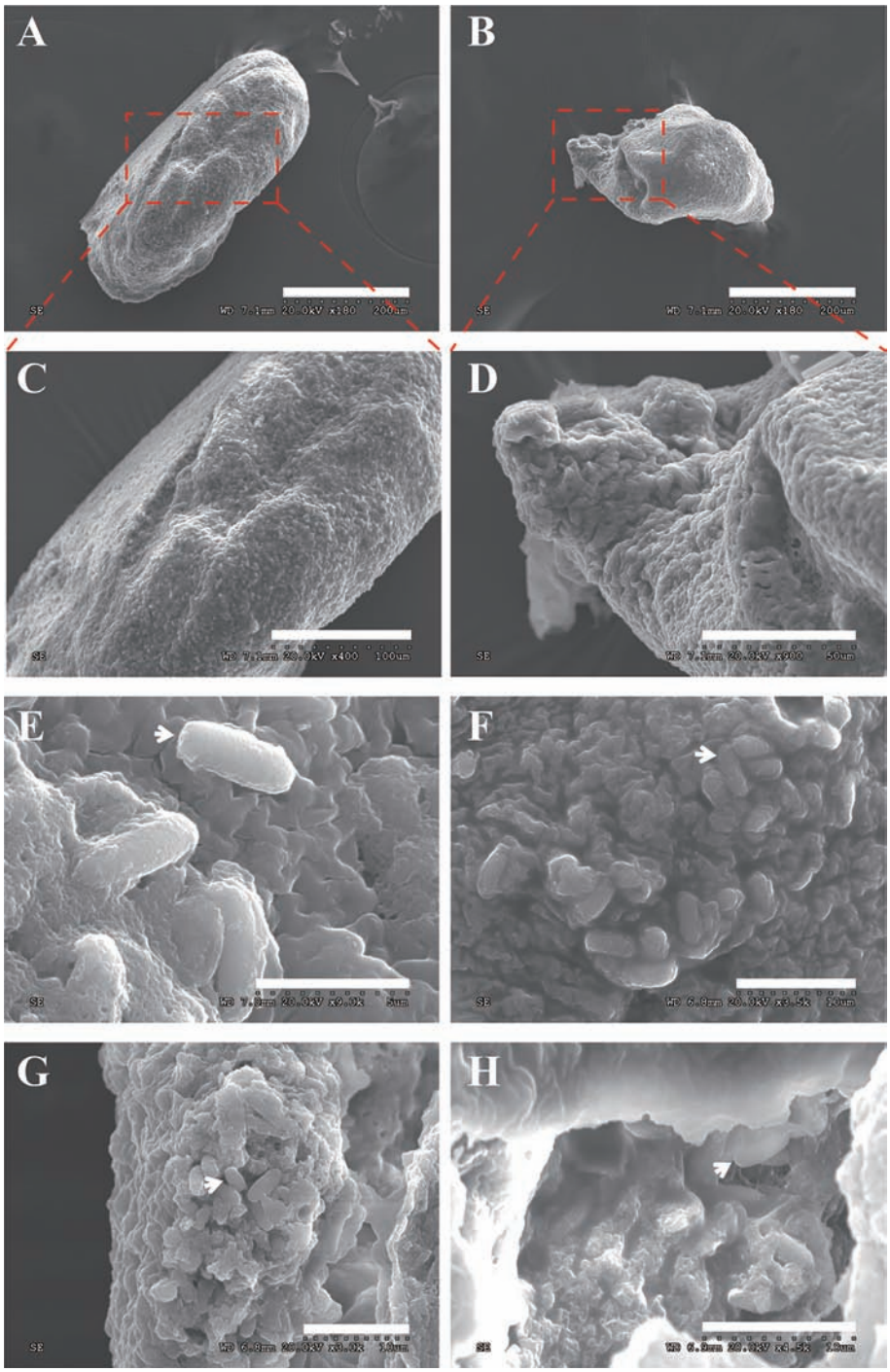

FIGURE 3 | The xenoma observed by SEM. **(A, B)** The elliptical and spindle intact xenoma. **(C, D)** The enlarged graph of the dotted box in panels **(A, B, E)** The mature spores (arrowhead) adhering to the surface of the xenoma, the bar is 50 μm. **(F)** The mature spores inlaid on the surface of the xenoma, the bar is 10 μm. **(G, H)** The mature spores embedded in a transverse xenoma. Bar, 10 μm.

V. necatrix in others lepidopteran insects was also characterized (Maddox et al., 1981; Moore and Brooks, 1992; Luo et al., 2014). A dominant feature of the *V. necatrix* infection is that it can rapidly multiply and quickly kill the host. The maximum spore production of 1×10^{10} spores/g of host was obtained in *Helliothis zea* and *Trichopluisia ni* (Maddox et al., 1981). The spore production and lethal period depend on multiple factors, including the pathogen genotype, host species, temperature,

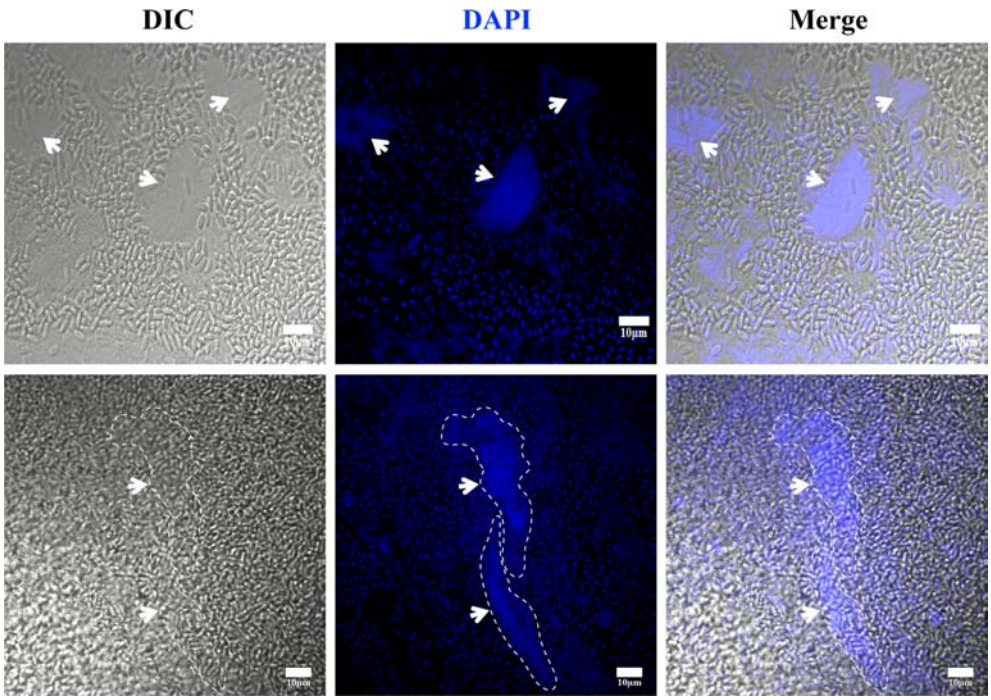

FIGURE 4 | The observation of xenoma nucleus. The nucleus (arrowhead) of xenoma and *V. necatrix* BM were stained with DAPI (blue). The hypertrophied nucleus was labeled with a dashed line. Bar, 10 μm.

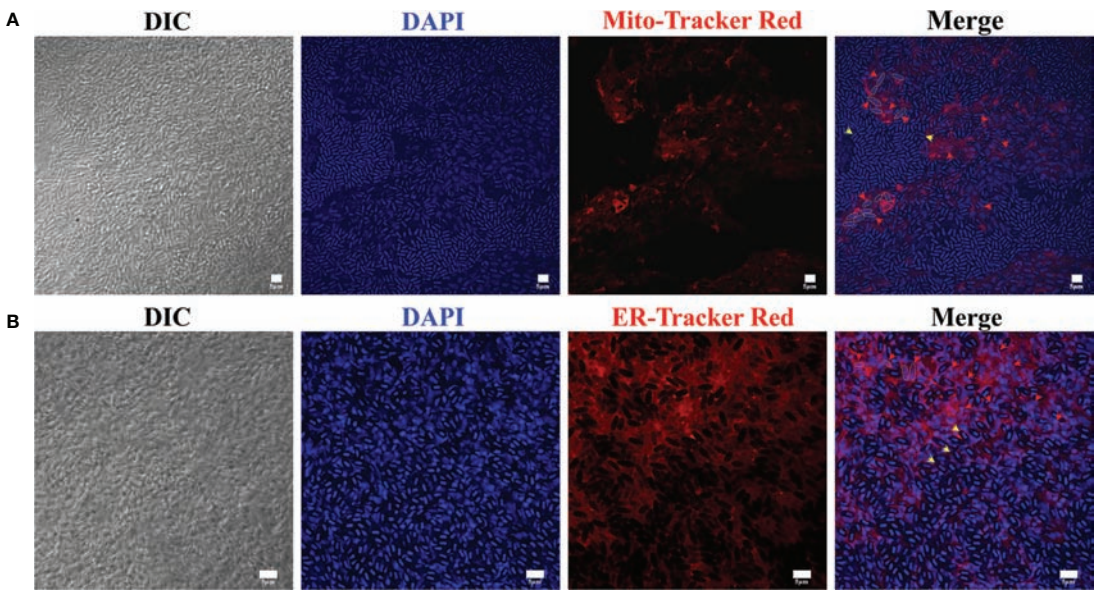

FIGURE 5 | The observation of xenoma mitochondria and endoplasmic reticulum (ER). **(A)** The xenoma was stained with Mito-Tracker Red for labeling mitochondria (red) and DAPI for dying nucleus (blue). **(B)** The xenoma was stained with ER-Tracker Red for labeling ER (red) and DAPI. The nucleus of meronts (red arrowhead) and spores (yellow arrowhead) were stained with DAPI (blue). Bar, 5 μm.

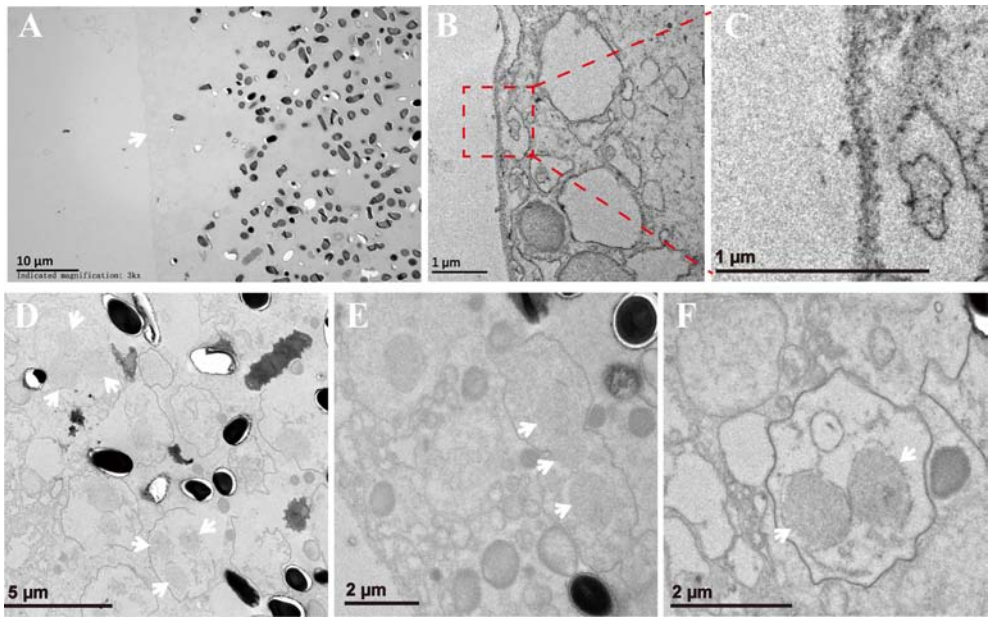

FIGURE 6 | The xenoma observed by TEM. **(A)** The outer wall of xenoma (arrowhead) and *V. necatrix* BM inside. **(B, C)** The magnified outer wall of the xenoma. **(D–F)** The development of *V. necatrix* BM in xenoma. The arrowhead indicates the nuclei of the parasites.

inoculation dosage, and larval instar challenged. When infecting silkworm with a dosage of 1×10^4 V. *necatrix* spores per larva in fourth instar, we obtained an average of 4.52×10^8 spores from a fifth-day pupa (**Supplementary Table 1**, **Supplementary Figure 1**).

The xenoma is a common pathological structure made by some microsporidian species and frequently reported in aquatic animals (Lom and Nilsen, 2003; Lom and Dykova, 2005). The tissue that xenoma produced from is varied in different hosts. In silkworm infected by *V. necatrix*, the xenoma is made from muscle cells and grows on the outer surface of midgut. In *Lophius piscatorius* infected by *Sprague* sp., the xenoma is formed in nerve tissue (Campbell et al., 2013). In *Endoreticulatus eriocheir*-infected crab, the xenoma was found in hepatopancreas (Ding et al., 2016). The xenoma made by *A. portucalensis* was also found in hepatopancreas of the common foreshore crab and contained a great many of cysts consisting of hypertrophic host cells (Azevedo, 1987). The varied locations of the xenoma reflect the tissue preference of different microsporidia. Besides, in the late stage of development, a plurality of small xenomas were formed in a developed (or mature) xenoma, and there were some pinocytotic vesicles in the center of xenoma, which are probably the secondary xenomas formed inside the primary ones (Lom and Dykova, 2005).

The *V. necatrix* in the xenoma presented a binary life cycle, the *Nosema*-like (type species: *N. bombycis*, Nägeli, 1857) and *Thelohania*-like (type species: *T. giardia*, Henneguy and Thelohan, 1892). The *Nosema* presents two nuclei in all stages of the life cycle (Vávra, 1976), while the *Thelohania* develops monokaryotic within a sporophorous vesicle to form octospores (Jouvenaz, 1984). It was reported that the octosporoblastic sporogony occurred primarily at low temperatures (Moore and Brooks, 1992), indicating that the life cycle of some microsporidia can be regulated by temperature.

Wrapped by a host membrane, the intact xenoma provides an environment free of host immune surveillance for that the pathogen antigens cannot be exposed at the surface (Dykova et al., 1980; Canning and Curry, 2005). Moreover, the xenoma contributes to parasite proliferation by generating massive nutrients and energy. The *V. necatrix* xenoma on the silkworm midgut is generated from muscle cells, which were specialized and transformed into a powerful cyst containing multiple hypertrophic nuclei and fully filled with ER and mitochondria around the proliferative parasites. These modified organelles could provide the parasites with much more energy and nutrients (Canning and Curry, 2005). The xenoma nucleus is hypertrophic and branched or lobed. This pathological feature is similar to that of the xenoma produced by fish microsporidia (Lom and Dykova, 2005; Azevedo et al., 2016), however its function and mechanism remain illumination.

V. necatrix and *N. bombycis* are phylogenetically close to each other and natural pathogens infecting silkworm (Liu et al., 2012; Luo et al., 2014). However, both pathogens are quite different in spore morphology and pathology. *V. necatrix* can high-efficiently produce dikaryotic large spores and unicellular small octospores in the xenoma, while *N. bombycis* does not make xenoma and only generates dikaryotic and uniform size spores. On the other hand, *N. bombycis* infects all silkworm tissues, and horizontally and vertically transmit by invading ovary and oocyte. Nevertheless, *V. necatrix* is able to infect nearly all silkworm

tissues except for the ovary so that cannot be vertically transmitted (Meng et al., 2018). These variances are important factors that lead to different virulence and transmissive efficiency between the two parasites.

In summary, the xenoma produced by *V. necatrix* BM is a specialized syncytium with increased mitochondria and ER and hypertrophic nuclei to promote the production of energy and nutrients for the massive the massive proliferation of the parasites inside. Our work provides a clearer view of the xenoma made by *V. necatrix* in silkworm.

DATA AVAILABILITY STATEMENT

The original contributions presented in the study are included in the article/**Supplementary Material**. Further inquiries can be directed to the corresponding authors.

AUTHOR CONTRIBUTIONS

TL and ZZ contributed to conception and design of the study. ZF, QH, CW, XM, and BY contributed to experimental analysis. TL and ZF contributed to data analysis. TL and ZF wrote the first draft of the manuscript. All authors contributed to the article and approved the submitted version.

FUNDING

This work was supported by grants from the National Natural Science Foundation of China (31772678, 31770159, and 31472151), Natural Science Foundation of Chongqing, China (cstc2019yszx- jcyjX0010).

SUPPLEMENTARY MATERIAL

The Supplementary Material for this article can be found online at: https://www.frontiersin.org/articles/10.3389/fcimb.2021.699239/full#supplementary-material

Supplementary Figure 1 | Counting spores with a blood counting chamber. *V. necatrix* BM spores were purified from the fifth-day pupae for counting the spore production. The spores were diluted ×500 and added to the counting chamber. Spores in five middle-sized grids in the four corners and center were counted.

REFERENCES

Azevedo, C. (1987). Fine Structure of the Microsporidan *Abelspora Portucalensis* Gen.N., Sp.N. (Microsporida) Parasite of the Hepatopancreas of *Carcinus Maenas* (Crustacea, Decapoda). *J. Invertebrate Pathol.* 49 (1), 83–92. doi: 10.1016/0022-2011(87)90129-7

Azevedo, C., Abdel-Baki, A. A. S., Rocha, S., Al-Quraishy, S., and Casal, G. (2016). Ultrastructure and Phylogeny of Glugea Arabica N. Sp. (Microsporidia), Infecting the Marine Fish *Epinephelus Polyphekadion* From the Red Sea. *Eur. J. Protistol* 52, 11–21. doi: 10.1016/j.ejop.2015.09.003

Bernal, C. E., Zorro, M. M., Sierra, J., Gilchrist, K., Botero, J. H., Baena, A., et al. (2016). *Encephalitozoon Intestinalis* Inhibits Dendritic Cell Differentiation Through an IL-6-Dependent Mechanism. *Front. Cell Infect. Microbiol.* 6, 4. doi: 10.3389/fcimb.2016.00004

Cali, A., Kent, M., Sanders, J., Pau, C., and Takvorian, P. M. (2012). Development, Ultrastructural Pathology, and Taxonomic Revision of the Microsporidial Genus, Pseudoloma and its Type Species *Pseudoloma Neurophilia*, in Skeletal Muscle and Nervous Tissue of Experimentally Infected Zebrafish *Danio Rerio*. *J. Eukaryotic Microbiol.* 59 (1), 40–48. doi: 10.1111/j.1550-7408.2011.00591.x

Cali, A., and Takvorian, P. M. (1999). "Developmental Morphology and Life Cycles of the Microsporidia" in *The Microsporidia and Microsporidiosis*. (WILEY Blackwell), 85–128.

Cali, A., Weiss, L. M., Takvorian, P. M., Lom, J., Vávra, J., Weiss, L. M., et al. (2005). A Review of the Development of Two Types of Human Skeletal Muscle Infections From Microsporidia Associated With Pathology in Invertebrates and Cold-Blooded Vertebrates. *Folia Parasitol* 52 (1-2), 51–61. doi: 10.14411/fp.2005.007

Campbell, S. E., Williams, T. A., Asim, Y., Soanes, D. M., Paszkiewicz, K. H., and Williams, B. A. P. (2013). The Genome of Spraguea Lophii and the Basis of Host-Microsporidian Interactions. *PloS Genet.* 9 (8), e1003676. doi: 10.1371/journal.pgen.1003676

Canning, E. U., and Curry, A. (2005). *Microgemma Vivaresi* (Microsporidia: Tetramicridae): Host Reaction to Xenomas Induced in Sea Scorpions, *Taurulus Bubalis* (Osteichthyes: Cottidae). *Folia Parasitol (Praha)* 52 (1–2), 95–102. doi: 10.14411/fp.2005.012

Casal, G., Matos, E., Teles-Grilo, M. L., and Azevedo, C. (2008). A New Microsporidian Parasite, Potaspora Morhaphis N. Gen., N. Sp. (Microsporidia) Infecting the Teleostean Fish, *Potamorhaphis Guianensis* From the River Amazon. Morphological, Ultrastructural and Molecular Characterization. *Parasitology* 135 (9), 1053–1064. doi: 10.1017/S0031182008004654

Corradi, N., Pombert, J. F., Farinelli, L., Didier, E. S., and Keeling, P. J. (2010). The Complete Sequence of the Smallest Known Nuclear Genome From the Microsporidian *Encephalitozoon Intestinalis*. *Nat. Commun.* 1, 77. doi: 10.1038/ncomms1082

Ding, Z., Meng, Q., Liu, H., Yuan, S., Zhang, F., Sun, M., et al. (2016). First Case of Hepatopancreatic Necrosis Disease in Pond-Reared Chinese Mitten Crab, *Eriocheir Sinensis*, Associated With Microsporidian. *J. Fish Dis.* 39 (9), 1043–1051. doi: 10.1111/jfd.12437

Down, R. E., Bell, H. A., Kirkbride-Smith, A. E., and Edwards, J. P. (2004). The Pathogenicity of *Vairimorpha Necatrix* (Microspora: Microsporidia) Against the Tomato Moth, *Lacanobia Oleracea* (Lepidoptera: Noctuidae) and its Potential Use for the Control of Lepidopteran Glasshouse Pests. *Pest Manag Sci.* 60 (8), 755–764. doi: 10.1002/ps.872

Dykova, I., Lom, J., and Egusa, S. (1980). Tissue Reaction to Glugea Plecoglossi Infection in its Natural Host, *Plecoglussus Altivelis*. *Folia Parasitol (Praha)* 27 (3), 213–216.

Fayer, R., and Santin-Duran, M. (2014). "Epidemiology of Microsporidia in Human Infections" in *Microsporidia*. (WILEY Blackwell), 135–164.

Franzen, C., and Müller, A. (1999). Molecular Techniques for Detection, Species Differentiation, and Phylogenetic Analysis of Microsporidia. *Clin. Microbiol.* 12 (2), 243–285. doi: 10.1128/CMR.12.2.243

Gottlieb, Y., Ghanim, M., Chiel, E., Gerling, D., Portnoy, V., Steinberg, S., et al. (2006). Identification and Localization of a Rickettsia Sp. In Bemisia Tabaci (Homoptera: Aleyrodidae). *Appl. Environ. Microbiol.* 72 (5), 3646–3652.

Han, Y., Gao, H., Xu, J., Luo, J., Han, B., Bao, J., et al. (2020). Innate and Adaptive Immune Responses Against Microsporidia Infection in Mammals. *Front. Microbiol.* 11, 1468. doi: 10.3389/fmicb.2020.01468

Han, B., and Weiss, L. M. (2017). Microsporidia: Obligate Intracellular Pathogens Within the Fungal Kingdom. *Microbiol. Spectr.* 5 (2), 1–27. doi: 10.1128/microbiolspec.FUNK-0018-2016

Heinz, E., Williams, T. A., Nakjang, S., Noel, C. J., Swan, D. C., Goldberg, A. V., et al. (2012). The Genome of the Obligate Intracellular Parasite *Trachipleistophora Hominis*: New Insights Into Microsporidian Genome Dynamics and Reductive Evolution. *PloS Pathog.* 8 (10), e1002979. doi: 10.1371/journal.ppat.1002979

Henneguy, F., and Thelohan, P. (1892). Myxosporidies parasites des muscles chez quelques crustaces decapodes. *Annales de Micrographie* 4, 617–641.

Joseph, J., Sharma, S., Murthy, S. I., Krishna, P. V., Garg, P., Nutheti, R., et al. (2006). Microsporidial Keratitis in India: 16s rRNA Gene-Based PCR Assay for Diagnosis and Species Identification of Microsporidia in Clinical Samples. *Invest. Ophthalmol. Visual Sci.* 47 (10), 4468. doi: 10.1167/iovs.06-0376

Joseph, J., Vemuganti, G. K., and Sharma, S. (2005). Microsporidia: Emerging Ocular Pathogens. *Indian J. Med. Microbiol.* 23 (2), 80–91. doi: 10.4103/0255-0857.16045

Jouvenaz, D. P. (1984). "Some Protozoa Infecting Fire Ants, Solenopsis Spp," in *Pathogens of Invertebrates: Application in Biological Control and Transmission Mechanisms*. Ed. T. C. Cheng (Boston, MA: Springer US), 195–203.

Kramer, J. P. (1965). Nosema Necatrix Sp. N. And Thelohania Diazoma Sp. N., Microsporidians From the Armyworm *Pseudaletia Unipuncta* (Haworth). *J. Invertebrate Pathol.* 7 (2), 117–121. doi: 10.1016/0022-2011(65)90021-2

Liu, H., Pan, G., Li, T., Huang, W., Luo, B., and Zhou, Z. (2012). Ultrastructure, Chromosomal Karyotype, and Molecular Phylogeny of a New Isolate of Microsporidian Vairimorpha Sp. BM (Microsporidia, Nosematidae) From *Bombyx Mori* in China. *Parasitol Res.* 110 (1), 205–210. doi: 10.1007/s00436-011-2470-9

Lom, J., and Dykova, I. (2005). Microsporidian Xenomas in Fish Seen in Wider Perspective. *Folia Parasitol (Praha)* 52 (1-2), 69–81. doi: 10.14411/fp.2005.010

Lom, J., and Nilsen, F. (2003). Fish Microsporidia: Fine Structural Diversity and Phylogeny. *Int. J. Parasitol* 33 (2), 107–127. doi: 10.1016/s0020-7519(02)00252-7

Luo, B., Liu, H., Pan, G., Li, T., Li, Z., Dang, X., et al. (2014). Morphological and Molecular Studies of *Vairimorpha Necatrix* BM, a New Strain of the Microsporidium *V. Necatrix* (Microsporidia, Burenellidae) Recorded in the Silkworm, *Bombyx Mori*. *Exp. Parasitol* 143, 74–82. doi: 10.1016/j.exppara.2014.05.001

Maddox, J. V., Brooks, W., and Fuxa, J. (1981). "Vairimorpha Necatrix, a Pathogen of Agricultural Pests: Potential for Pest Control" in *Microbial Control of Pests and Plant Diseases*. Ed. H. D. Burges (London: Academic Press), 587–594.

Matos, E., Mendonca, I., and Azevedo, C. (2006). Vavraia Lutzomyiae N. Sp. (Phylum Microspora) Infecting the Sandfly *Lutzomyia Longipalpis* (Psychodidae, Phlebotominae), a Vector of Human Visceral Leishmaniasis. *Eur. J. Protistol* 42 (1), 21–28. doi: 10.1016/j.ejop.2005.09.001

Meng, X. Z., Luo, B., Tang, X. Y., He, Q., Xiong, T. R., Fang, Z. Y., et al. (2018). Pathological Analysis of Silkworm Infected by Two Microsporidia *Nosema Bombycis* CQ1 and *Vairimorpha Necatrix* BM. *J. Invertebr Pathol.* 153, 75–84. doi: 10.1016/j.jip.2017.12.005

Moore, C. B., and Brooks, W. M. (1992). An Ultrastructural Study of *Vairimorpha Necatrix* (Microspora, Microsporida) With Particular Reference to Episporontal Inclusions During Octosporogony. *J. Protozool* 39 (3), 392–398. doi: 10.1111/j.1550-7408.1992.tb01469.x

Nägeli, K. W. (1857). Uber die neue Krankheit der Seidenraupe und verwandte Organismen. *Bot Zeit* 15, 760–761.

Nakjang, S., Williams, T. A., Heinz, E., Watson, A. K., Foster, P. G., Sendra, K. M., et al. (2013). Reduction and Expansion in Microsporidian Genome Evolution: New Insights From Comparative Genomics. *Genome Biol. Evol.* 5 (12), 2285–2303. doi: 10.1093/gbe/evt184

Pilley, B. M. (1976). A New Genus, *Vairimorpha* (Protozoa: Microsporida), for *Nosema Necatrix* Kramer 1965: Pathogenicity and Life Cycle in *Spodoptera Exempta* (Lepidoptera: Noctuidae). *J. Invertebrate Pathol.* 28 (2), 177–183. doi: 10.1016/0022-2011(76)90119-1

Song, Y., Tang, Y., Yang, Q., Li, T., He, Z., Wu, Y., et al. (2020). Proliferation Characteristics of the Intracellular Microsporidian Pathogen *Nosema Bombycis* in Congenitally Infected Embryos. *J. Invertebr Pathol.* 169, 107310. doi: 10.1016/j.jip.2019.107310

Vávra, J. (1976). "Development of the Microsporidia" in *Biology of the Microsporidia*. Eds. L. A. Bulla and T. C. Cheng (Boston, MA: Springer US), 87–109.

Conflict of Interest: The authors declare that the research was conducted in the absence of any commercial or financial relationships that could be construed as a potential conflict of interest.

The reviewer JX declared a shared affiliation, with no collaboration, with one of the authors, ZZ, to the handling editor at the time of review.

frontiers in Cellular and Infection Microbiology

ORIGINAL RESEARCH
published: 26 July 2021
doi: 10.3389/fcimb.2021.711332

Meta-Analysis of the Prevalence of *Echinococcus* in Sheep in China From 1983 to 2020

Yang Gao[1,2†], Wei Wang[3,4†], Chuang Lyu[5,6†], Xin-Yu Wei[4], Yu Chen[4], Quan Zhao[3], Zhi-Guang Ran[2*] and You-Qing Xia[1*]*

[1] The Key Sericultural Laboratory of Agricultural Ministry, College of Biotechnology, Southwest University, Chongqing, China, [2] Research and Development Department, Chongqing Auleon Biological Co., Ltd., Chongqing, China, [3] College of Life Science, Changchun Sci-Tech University, Shuangyang, China, [4] College of Animal Science and Veterinary Medicine, Heilongjiang Bayi Agricultural University, Daqing, China, [5] Animal Health Center, Shandong New Hope Liuhe Group Co., Ltd., Qingdao, China, [6] Animal Health Center, Qingdao Jiazhi Biotechnology Co., Ltd., Qingdao, China

OPEN ACCESS

Edited by:
Wei Cong, Shandong University, Weihai, China

Reviewed by:
Jin Lei Wang, Lanzhou Veterinary Institute (CAAS), China
Mohammad Amin Ghatee, Yasuj University of Medical Sciences, Iran

***Correspondence:**
Quan Zhao
zhaoquan0825@163.com
Zhi-Guang Ran
zhgran@sina.com
You-Qing Xia
xiaqy@swau.cq.cn

[†]*These authors have contributed equally to this work*

Specialty section:
This article was submitted to Clinical Microbiology, a section of the journal Frontiers in Cellular and Infection Microbiology

Received: *18 May 2021*
Accepted: *05 July 2021*
Published: *26 July 2021*

Citation:
Gao Y, Wang W, Lyu C, Wei X-Y, Chen Y, Zhao Q, Ran Z-G and Xia Y-Q (2021) Meta-Analysis of the Prevalence of Echinococcus in Sheep in China From 1983 to 2020. Front. Cell. Infect. Microbiol. 11:711332. doi: 10.3389/fcimb.2021.711332

Echinococcosis is a zoonosis caused by the larval stage of cestode species that belong to the genus *Echinococcus*. The infection of hydatid in sheep is very common in China, especially in the northwestern China. Here, we conducted the first systematic review and meta-analysis of echinococcosis in sheep in China. Six databases (PubMed, ScienceDirect, Baidu Library, CNKI, Wanfang, and VIP Chinese Journal Database) were used to retrieve the literatures on echinococcosis in sheep in China from 1983 to 2020, and 74 studies. The random effects model was used in the "meta" package of the R software and the PFT was chosen for rate conversion. The research data were analyzed through subgroup analysis and univariate meta-regression analysis to reveal the factors that lead to research heterogeneity. The combined prevalence of *Echinococcus* in the selected period was estimated to be 30.9% (192,094/826,406). In the analysis of sampling year, the lowest positive rate was 13.9% (10,296/177,318) after 2011. The highest prevalence of *Echinococcus* was 51.1% (278/531) in the southwestern China. The highest infection rate in sheep was 20.1% (58,344/597,815) in the liver. The analysis based on age showed that the infection rate of elderly sheep was significantly higher than that in younger animals ($P < 0.05$). We also evaluated the effects of different geographic and climatic factors on the prevalence of *Echinococcus* in sheep. The results showed that the prevalence of *Echinococcus* was higher in high altitude, cold, humid, and high rainfall areas. It is necessary to carry out long-term monitoring and control of echinococcosis, cut off the infection route, and reduce the risk of infection in the high risk areas.

Keywords: ***Echinococcus*, sheep, Echinococcosis, meta-analysis, China**

INTRODUCTION

Echinococcosis is a zoonosis caused by the larval stage of cestode species that belong to the genus *Echinococcus* (Villard et al., 2003). The disease is one of the 17 neglected tropical diseases (NTDs) recognized by the World Health Organization (Agudelo Higuita et al., 2016). Echinococcosis is a chronic infection disease in both animals and humans. This disease can take years before being noticed (Ohiolei et al., 2020b). Detection of hydatid infection is common during postmortem

examination of animals and incidentally found in humans (Budke et al., 2013). *Echinococcus* is sometimes asymptomatic during its development stage except a cysts rupture for releasing antigenic material that causes reaction or active cysts located in certain anatomical regions (e.g., joints and eyes), and then exerts pressure on surrounding tissues, thus resulting in pain or discomfort (Budke 2002; Kern et al., 2017).

Generally, the "Ingestion of contaminated food and water" and "direct contact/playing with dogs" are classically mentioned as the sources of human infection and are biologically plausible potential risk factors (Tamarozzi et al., 2019). Humans usually get infections from canines, the infection occurred in sheep directly reflects the endemicity degree and levels of human risk (Rashid et al., 2017). Intermediate hosts accidentally ingesting infective eggs that develop into a metacestode stage in different organs (such as liver, lung, and kidney), leading to echinococcosis. The predators can release infective eggs, which could lead to a contamination for the environment, thus threatening human health (Carmena et al., 2008; Assefa et al., 2015). Echinococcosis was identified as a limiting disease in livestock production, and the infected sheep would cause economic losses to some extent (Wahlers et al., 2012). Recent, a report showed that approximately 30 million livestock were affected by echinococcosis in China. An average of increase of echinococcosis was 7 million per year. Among all infected livestock, sheep occupied approximately 70%, and caused a total economic loss of approximately 1 billion Yuan (RMB) (Yu et al., 2008; Yang et al., 2015).

Notably, it was estimated that a total of one million disability-adjusted life years (DALYs) were caused by echinococcosis globally, out of which 0.40 million were in China (Qian et al., 2017). Additionally, echinococcosis could lead to a loss of US$ 1.92 billion globally per year, China was responsible for US$ 0.66 billion. The annual global livestock production losses associated with echinococcosis were also high, reaching US$ 2.19 billion, of which China occupied a great proportion (Budke et al., 2006; Qian et al., 2017). Sheep can provide meat, milk, and wool for human beings, thus becoming an important livestock in the world. With an increase of human population, the needs of sheep by-products have elevated worldwide (Zhu et al., 2018). China as a big sheep-raising country (Zhao and Zhang, 2019). Thus, it is necessary to estimate the prevalence of *Echinococcus* in sheep in China and identify potential risk factors for providing basic data for researchers. At present, there is no study on the potential risk factors of *Echinococcus* infection in sheep in China. Therefore, a systematic review and meta-analysis were conducted-required to determine the prevalence of *Echinococcus* in sheep in China and to assess potential risk factors (sampling site, region, infection organ, season, detection method, age, geographical location and climate factors, etc.).

MATERIALS AND METHODS

Search Strategy and Selection Criteria

This study has been prepared according to the PRISMA guidelines for the design and analysis of selected qualified studies (**Table S1**) (Moher et al., 2009; Moher et al., 2015). The web of the six literature databases were employed to search for articles that related to the epidemiology of CE in sheep in China, including the China National Knowledge Infrastructure (CNKI), Baidu Library, PubMed, ScienceDirect, VIP Chinese Journal Database, and Wanfang Data. We searched all published papers with regard to CE in sheep from 1983 to December 20, 2020. We used MeSH terms "Echinococcosis", "sheep" and "China", as well as similar terms, such as "Echinococcoses", "*Echinococcus* Infection", "*Echinococcus* Infections", "Infection, *Echinococcus*" "Cystic *Echinocccosis*", "Cystic Echinocccoses", "Echinocccoses, Cystic", "*Echinocccosis*, Cystic", "Hydatidosis", "Hydatidoses", "Cysts, Hydatid", "Cyst, Hydatid", "Hydatid Cysts", "Hydatid Cyst", "Hydatid Disease", "Hydatid Diseases", "*Echinococcus Granulosus* Infection", "*Echinococcus Granulosus* Infections", "*Granulosus* Infection, *Echinococcus*", "*Granulosus* Infections, *Echinococcus*", "Infection, *Echinococcus Granulosus*", and "Infections, *Echinococcus Granulosus*". Boolean operators "AND" and "OR" were used to connect MESH and entry terms. In PubMed, the search formula was ((((((((((((((((((((((("Echinoc occosis"[Mesh]) OR (Echinococcoses)) OR (*Echinococcus* Infection)) OR (*Echinococcus* Infections)) OR (Infection, *Echinococcus*)) OR (Cystic Echinocccosis)) OR (Cystic Echinocccoses)) OR (Echinocccoses, Cystic)) OR (Echinocccosis, Cystic)) OR (Hydatidosis)) OR (Hydatidoses)) OR (Cysts, Hydatid)) OR (Cyst, Hydatid)) OR (Hydatid Cysts)) OR (Hydatid Cyst)) OR (Hydatid Disease)) OR (Hydatid Diseases)) OR (*Echinococcus Granulosus* Infection)) OR (*Echinococcus Granulosus* Infections)) OR (*Granulosus* Infection, *Echinococcus*)) OR (*Granulosus* Infections, *Echinococcus*)) OR (Infection, *Echinococcus Granulosus*)) OR (Infections, *Echinococcus Granulosus*)) AND (((((((("Sheep"[Mesh]) OR (Ovis)) OR (Dall Sheep)) OR (Ovis dalli)) OR (Sheep, Dall)) OR (Sheep, Bighorn)) OR (Sheep, Domestic))) AND ((((((("China"[Mesh]) OR (People's Republic of China)) OR (Mainland China)) OR (Manchuria)) OR (Sinkiang)) OR (Inner Mongolia)). In the Sciencedirect database, we searched for keywords sheep, Hydatid, Echinococcosis, Epidemiology, prevalence, China and the selected article type was research articles. In the four Chinese databases, "sheep" (in Chinese) and "Echinococcosis" (in Chinese) OR "sheep" (in Chinese) and "Hydatidosis" (in Chinese) were used as keywords for advanced search and were set to use synonym expansion or fuzzy search. We restricted the search to review and research articles and conference abstracts.

We adopted the following inclusion criteria: (1) the purpose of the study was to investigate the positive rate of *Echinococcus* in sheep; (2) the study provided the total number of sheep tested and the number of sheep that tested positive; (3) the study had a clear test method; (4) the research location was in China, and a precise sampling area was provided; (5) each sample was from one sheep and could not be mixed. Articles that did not meet these criteria were excluded. In addition, we did not contact the original authors to obtain more information, and unpublished data were not taken into account.

Data Extraction

Three researchers individually used standardized data collection forms to extract the required data for the research. If the

researchers held different views or expressed uncertainty about specific articles, these would be evaluated by a fourth researcher (Y.G., the main reviewer of the meta-analysis). The database was established using Microsoft Excel (version 16.39, Microsoft Corp., Redmond, WA, USA).

The following information was recorded: the first author, the total number of sheep samples examined and the number of positive samples, the year of publication, sampling time and location, the geographic data, the test method, age, gender, season, *Echinococcus* infection organs, *Echinococcus* species, and sample type. Statistical geographic factor data were obtained from the National Meteorological Information Center of China Meteorological Administration, including longitude range, latitude range, annual average rainfall, altitude, average yearly temperature, and average yearly humidity.

Quality Assessment

The quality of the included studies was scored based on the GRADE criteria (Guyatt et al., 2008). The adopted criteria included random sampling, a precise sampling time, a clear detection method, a detailed sampling method, and an analysis containing four or more risk factors.

Each criterion was scored as 1 point. The total score was 5 points if a study met all mentioned criteria. Studies with 5 or 4 points were considered as high quality, studies with a score of 3 or 2 were considered as medium quality, and studies with a score of 1 or 0 were marked as low quality.

Statistical Analysis

The R Studio software version 1.2.5019 ("R core team, R: A language and environment for statistical computing" R core team 2018) was used for data analysis (using the meta package). **Table S2** showed the code in R for this meta-analysis. Before conducting the meta-analysis, we tested four conversion methods to make the data closer to the Normal distribution, namely logarithmic conversion (PLN), logit transformation (PLOGIT), arcsine transformation (PAS), and double-arcsine transformation (PFT). After referring to the research of Wang et al., we chose PFT for rate conversion (Li et al., 2020; Wang et al., 2020). Due to the apparent heterogeneity of the included studies, we chose a random-effects model for meta-analysis. Forest plots were used for the overall assessment of meta-analysis. The funnel plot, trim and fill analysis, and Egger's test were used to assess the publication bias of studies. A sensitivity analysis was conducted, and one study was deleted at a time to check whether any study would have a significant impact on the estimated results. Heterogeneity for studies was calculated by *Cochran-Q*, I^2 statistics, and χ^2 test. A *P-value* < 0.05 and an I^2 statistic with a cut-off of 50% were used to define a statistically significant degree of heterogeneity (Wei et al., 2021).

Subgroup Analysis

In order to further study the potential sources of heterogeneity, the research data subjected to subgroup analysis and univariate meta-regression analysis were used to reveal the factors that led to a research heterogeneity. The boundary division in the subgroup was based on our statistical evaluation results to divide the cut-off value. The survey factors included the year of publication (after 2011 *vs*. before), geographic region (northeastern China *vs*. other regions), age (lamb *vs*. other age groups), gender (ewes *vs*. rams), detection method (ultrasonic test *vs*. other methods), season (autumn *vs*. other three seasons), infected organs (other *vs*. liver, both, lung), *Echinococcus* species (*E. granulosus vs*. *E. multilocularis*), and study quality (low quality *vs*. other levels of quality).

Besides, we assessed the impact of geographic risk factors on the study, including longitude (91-100° *vs*. other longitude ranges), latitude (30-35° *vs*. other longitude ranges), average yearly precipitation (401-1,000 mm *vs*. other precipitation groups), average yearly temperature (-5-0°C *vs*. other temperature ranges), average yearly humidity (61–68% *vs*. other humidity value groups), and altitude (30,001-100,000 dm *vs*. other altitude value groups).

RESULTS

Search Results and Eligible Studies

According to the inclusion and exclusion criteria, a total of 74 studies were used for meta-analysis by searching on six databases (**Figure 1**). 70 of them were from the Chinese database and 4 from the English database. Studies with 4 or 5 scores were considered as high-quality (23 studies), 2 or 3 scores as medium-quality (48 studies), and 0 or 1 score as low-quality research (3 studies; **Table S3**).

Publication Bias and Sensitivity Analysis

The extent of heterogeneity in the selected studies was measured and demonstrated by a forest plot (**Figure 2**). The funnel plot showed that the included studies might have publication biases (**Figure S1**). Meanwhile, the trim and fill analysis indicated a possible publication bias or a small-study effect in our study (**Figure S2**). However, $P < 0.05$ was found by an Egger's test, manifesting that all the included studies may had publication bias (**Figure S3**; **Table S4**). According to the sensitivity tests, the combined prevalence was not significantly affected by any study that was omitted (**Figure S4**). These results validated that our analyses were reasonable and reliable.

Pooling and Heterogeneity Analyses

In the selected studies, ten provinces were included (**Table 1**; **Figure 3**). In the subgroup analysis, we chose "PFT" for rate conversion data (**Table S5**), due to the high degree of heterogeneity in most subgroups, all estimated seroprevalence for each subgroup was calculated using random effect models (**Table 2**).

The prevalence was significantly different in different regions. The southwestern China had the highest prevalence (50.1%), and northeastern China had the lowest prevalence (1.9%). The pooled prevalence of *Echinococcus* in sheep ranged from 1.4% to 78.4% in different provinces (**Figure 3**). In the provinces, Sichuan kept the highest prevalence of 78.4%, and Ningxia was the lowest (1.4%; **Figure 3**).

Our findings showed that the prevalence of *Echinococcus* was higher in studies with sampling site from pasture (39.8%) than

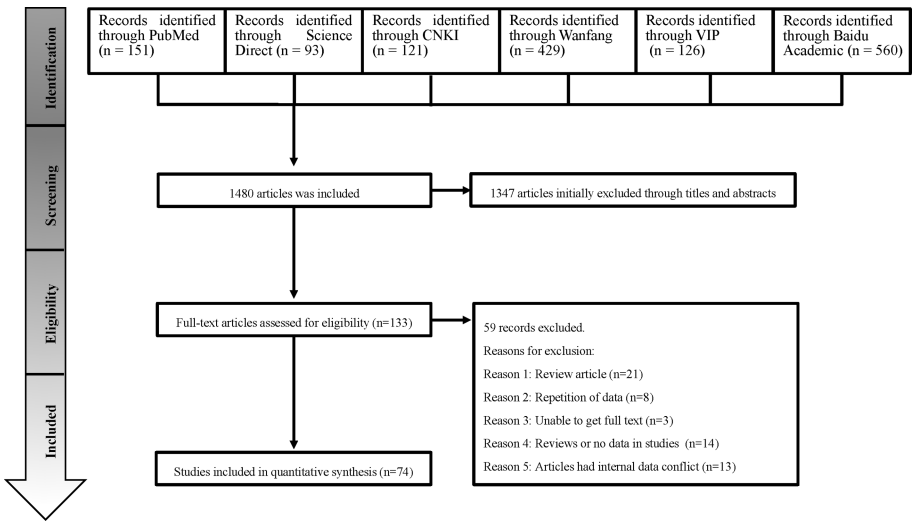

FIGURE 1 | Flow diagram of the search strategies and selection of studies.

slaughterhouse (29.7%). Among these studies, the highest prevalence of *Echinococcus* based on sampling time was 55.9% in 2000 or before, and the lowest prevalence was 13.9% in 2011 or later. The highest detectable rate of *Echinococcus* was 20.1% in samples from liver, and the lowest was 2.5% in other. The prevalence of *Echinococcus* in elderly sheep was the highest (35.9%), and the lowest in young sheep (5.6%; **Table 2**).

Detailed geographical and climatic factors were further analyzed. The results showed that the prevalence of *Echinococcus* at altitude range (3,000-100,000m; 50.7%), rainfall range (401-1,000mm; 43.5%); latitude range (30-35°; 46.9%); longitude range (91-100°; 42.7%); minimum annual mean temperature range (< -5°C; 68.8%); average annual maximum temperature range (0-10°C; 53.0%); temperature range (-5-0°C; 58.7%), and humidity range (61-68; 38.5%) were higher than those in other ranges (**Table S6**).

DISCUSSION

For the first time, we conducted a systematic review and meta-analysis of the infection of *Echinococcus* sheep in China. The statistical results show that season, age, region, infected organization, sampling location, sampling year, article quality and geographic factors (precipitation, temperature and altitude) may be risk factors for sheep infection.

According to the statistics, the combined prevalence of *Echinococcus* in sheep in China was 30.9% (**Figure 2**), which was higher than 12.1% in Africa (Ohiolei et al., 2020a) and 8.8% in Ethiopia (Asmare et al., 2016), in published meta-analysis. Thus, it requires us to pay enough attention and take certain measures to prevent the disease. In regard to the sampling year subgroup, the prevalence of *Echinococcus* in sheep had a significant downward trend, and the combined prevalence after 2011 was the lowest (13.9%, $P < 0.05$; Table 2). In 2012, in accordance with the mission objectives of the "Medium and Long-term Animal Disease Prevention and Control Plan (2012-2020)" issued by China, each region formulated a series of comprehensive prevention and control measures based on the actual situation of echinococcosis in local animals (Zhang, 2016). The measures include immunization of newborn lambs in key areas, deworming of dogs in pastoral areas, and harmless treatment of diseased animal organs in slaughterhouses, etc. The implementation of these measures has played a key role in reducing sheep infections.

Among the included articles, most of the epidemiological investigations were concentrated in the northwestern region (91%; Table 2). The northwestern region was the main breeding area for sheep in China and was also a high-epidemic area for echinococcosis (Han et al., 2019), among which Qinghai province has the highest prevalence rate (**Figure 3**). From the perspective of geographic environment, the altitude subgroup analysis showed a relatively high prevalence of *Echinococcus* among sheep in high altitude areas, such as Qinghai province ($P < 0.05$; **Table S6**). Qinghai province has a plateau continental climate with sufficient sunshine and little precipitation, and the strong wind can provide condition for the spread of insect eggs on the pasture. In addition, the land is vast and rich in animal resources. Many domestic animals and rodents can serve as natural intermediate hosts for echinococcosis, thus providing favorable condition for the spread of the disease (Wen et al., 2019). From the perspective of feeding habits, the local herders are used to raising herding dogs and herding sheep, and often feed the dogs with the organs of dead sheep, causing a large number of infections in dogs (Yang et al., 2015). After an infection, the *Echinococcus* eggs in the dog feces contaminate the pasture and the sheep are infected. This makes a completion of the life cycle of *Echinococcus* in livestock. In addition, several surveys showed that

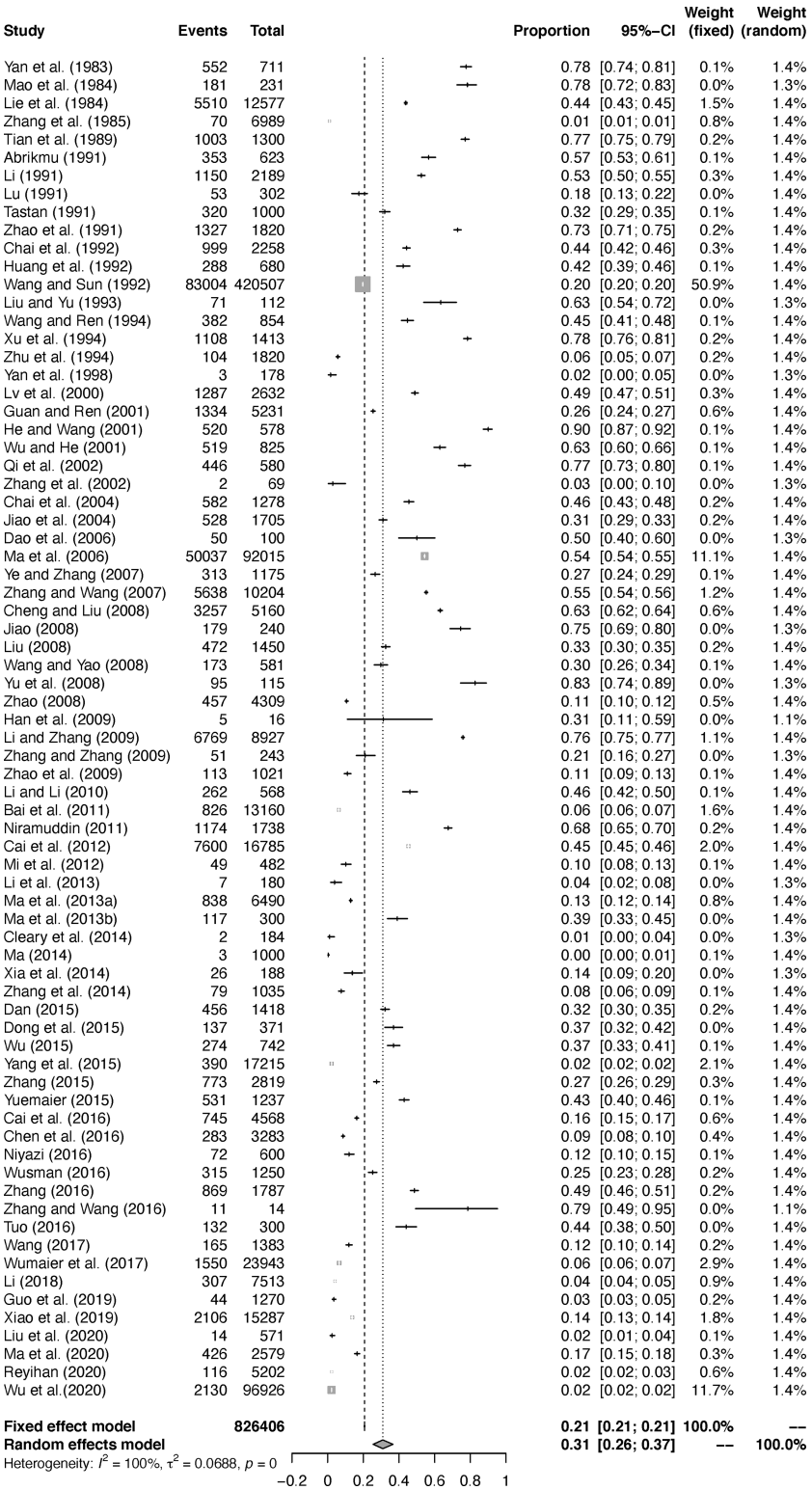

FIGURE 2 | Forest plot of *Echinococcus* prevalence in sheep in China.

TABLE 1 | Studies included in the analysis.

Study ID	Sampling time	Province	Detection method	Total samples	Positive samples	Quality score	Study Quality
Northeast China*							
Yan et al. (1998)	UN*	Liaoning	Anatomical touch detection	178	3	2	Medium
Zhang et al. (2002)	UN	Heilongjiang	Anatomical touch detection	69	2	3	Medium
Northern China*							
Jiao (2008)	UN	Inner Mongolia	UN	240	179	1	Low
Liu et al. (2020)	UN	Beijing	Serological testing	571	14	3	Medium
Northwest China*							
Abrikmu (2020)	UN	Xinjiang	Anatomical touch detection	623	353	2	Medium
Bai et al. (2011)	2007–2009	Gansu	Anatomical touch detection	13,160	826	3	Medium
Cai et al. (2012)	1990–2010	Qinghai	Anatomical touch detection	16,785	7,600	3	Medium
Cai et al. (2016)	UN	Qinghai	Anatomical touch detection	4,568	745	3	Medium
Chai et al. (1992)	1990–1992	Xinjiang	Anatomical touch detection	2,258	999	4	High
Chai et al. (2004)	2000–2002	Xinjiang	Anatomical touch detection	1,278	582	3	Medium
Chen et al. (2016)	2011–2012	Xinjiang	Anatomical touch detection	3,283	283	3	Medium
Cheng and Liu (2008)	1997–2001	Qinghai	Anatomical touch detection	5,160	3,257	3	Medium
Cleary et al. (2014)	2011	Ningxia	Anatomical touch detection	184	2	4	High
Dan (2015)	2004 / 2012–2014	Qinghai	Anatomical touch detection	1,418	456	1	Low
Dao et al. (2006)	UN	Gansu	Anatomical touch detection	100	50	2	Medium
Dong et al. (2015)	2014.07	Xinjiang	Ultrasonic testing	371	137	3	Medium
Guan and Ren (2001)	UN	Qinghai	Anatomical touch detection	5,231	1,334	2	Medium
Guo et al. (2019)	2013.05–2016.05	Xinjiang	Anatomical touch detection	1,270	44	3	Medium
Han et al. (2019)	2007.08–09	Qinghai	Anatomical touch detection	16	5	3	Medium
He and Wang (2001)	2000.06–09	Qinghai	Anatomical touch detection	578	520	3	Medium
Huang et al. (1992)	1991.09	Qinghai	Anatomical touch detection	680	288	3	Medium
Jiao et al. (2004)	2000–2003	Xinjiang	Anatomical touch detection	1,705	528	2	Medium
Li (2009)	2003.02–2008.10	Qinghai	Anatomical touch detection	2,189	1,150	2	Medium
Li (2018)	2016.01–12	Gansu	Anatomical touch detection	7,513	307	5	High
Li and Li (2010)	2009.02–10	Qinghai	Anatomical touch detection	568	262	2	Medium
Li and Zhang (2009)	1984 / 1997 / 2006	Qinghai	Anatomical touch detection	8,927	6,769	3	Medium
Li et al. (2013)	2013	Xinjiang	Ultrasonic testing	180	7	4	High
Lie et al. (1984)	1982.11–12	Qinghai	Anatomical touch detection	12,577	5,510	3	Medium
Liu (2008)	2007.01–08	Qinghai	Anatomical touch detection	1,450	472	4	High
Lu (2015)	2009.03–2009.05	Qinghai	Anatomical touch detection	302	53	2	Medium
Lv et al. (2000)	1999.09–1999.10	Qinghai	Anatomical touch detection	2,632	1,287	2	Medium
Ma (2014)	2012	Qinghai	Anatomical touch detection	1,000	3	4	High
Ma et al. (2006)	1997–2001	Qinghai	Anatomical touch detection	92,015	50,037	3	Medium
Ma et al. (2013a)	2012.10–12	Xinjiang	Anatomical touch detection	6,490	838	3	Medium
Ma et al. (2013b)	2012	Xinjiang	Anatomical touch detection	300	117	3	Medium
Ma et al. (2020)	UN	Xinjiang	Anatomical touch detection	2,579	426	3	Medium
Mi et al. (2012)	2011.09–10	Qinghai	Anatomical touch detection	482	49	4	High
Niramuddin (2011)	2010	Xinjiang	Anatomical touch detection	1,738	1,174	4	High
Niyazi (2016)	2015	Xinjiang	Anatomical touch detection	600	72	4	High
Qi et al. (2002)	1991–1993	Gansu	Serological testing	580	446	3	Medium
Reyihan (2020)	2019	Xinjiang	Anatomical touch detection	5,202	116	3	Medium
Tastan (2011)	2009.07–09	Xinjiang	Anatomical touch detection	1,000	320	5	High
Tian et al. (1989)	UN	Gansu	Anatomical touch detection	1,300	1,003	2	Medium
Tuo (2016)	2016.03–05	Qinghai	Anatomical touch detection	300	132	5	High
Wang (2017)	2016	Xinjiang	Anatomical touch detection & Serological testing	1,383	165	4	High
Wang and Ren (1994)	UN	Gansu	UN	854	382	3	Medium
Wang and Sun (1992)	1980–1987	Xinjiang	Anatomical touch detection	420,507	83,004	2	Medium
Wang and Yao (2008)	2005–2006	Qinghai	Anatomical touch detection	581	173	4	High
Wu (2015)	2014.07	Xinjiang	Ultrasonic testing	742	274	3	Medium
Wu and He (2001)	1989–1991	Qinghai	Anatomical touch detection	825	519	4	High
Wu et al. (2020)	2011–2018	Ningxia	Anatomical touch detection	96,926	2,130	3	Medium
Wumaier et al. (2017)	2012.08–2013.09	Xinjiang	Anatomical touch detection	23,943	1,550	3	Medium
Wusman (2016)	UN	Xinjiang	Anatomical touch detection	1,250	315	2	Medium
Xiao et al. (2019)	2014–2017	Xinjiang	Anatomical touch detection & Serological testing	15,287	2,106	5	High
Xu et al. (1994)	1992–1993	Xinjiang	Anatomical touch detection	1,413	1,108	4	High

(Continued)

TABLE 1 | Continued

Study ID	Sampling time	Province	Detection method	Total samples	Positive samples	Quality score	Study Quality
Yan et al. (1983)	UN	Qinghai	UN	711	552	1	Low
Yang et al. (2015)	2007–2013	Xinjiang	Anatomical touch detection	17,215	390	3	Medium
Ye and Zhang (2007)	2006.09–2006.10	Qinghai	Anatomical touch detection	1,175	313	4	High
Yuemaier (2015)	UN	Xinjiang	Anatomical touch detection	1,237	531	4	High
Yu et al. (2008)	2005.07	Qinghai	Anatomical touch detection	115	95	2	Medium
Zhang (2015)	2011–2015	Xinjiang	Anatomical touch detection	2,819	773	3	Medium
Zhang (2016)	2016	Xinjiang	Serological testing	1,787	869	5	High
Zhang et al. (1985)	UN	Ningxia	Anatomical touch detection	6,989	70	4	High
Zhang and Wang (2007)	1990–2005	Qinghai	Anatomical touch detection	10,204	5,638	5	High
Zhang and Wang (2016)	2015.09–12	Xinjiang	Anatomical touch detection	14	11	4	High
Zhang and Zhang (2009)	2007.08–2008.05	Qinghai	Anatomical touch detection	243	51	3	Medium
Zhang et al. (2014)	2009.08/2010.09	Gansu	Anatomical touch detection	1,035	79	3	Medium
Zhao (2008)	2005–2007	Gansu	Anatomical touch detection	4,309	457	4	High
Zhao et al. (1991)	1990.09–10	Xinjiang	Anatomical touch detection	1,820	1,327	3	Medium
Zhao et al. (2009)	2005.07	Gansu	Anatomical touch detection	1,021	113	3	Medium
Zhu et al. (1994)	1990.02–1992.02	Xinjiang	Anatomical touch detection	1,820	104	2	Medium
Southwest China*							
Liu and Yu (1994)	UN	Xinjiang	UN	112	71	2	Medium
Mao et al. (1984)	1982.11	Sichuan	Anatomical touch detection & Serological testing	231	181	3	Medium
Xia et al. (2014)	UN	Tibet	Anatomical touch detection	188	26	3	Medium

Northeast China: Heilongjiang, Jilin, Liaoning.*
North China: Beijing, Tianjin, Hebei, Shanxi, Inner Mongolia.*
Northwest China: Shaanxi, Gansu, Qinghai, Ningxia, Xinjiang.*
Southwest China: Chongqing, Sichuan, Guizhou, Yunnan, Tibet.*
UN: unclear.*

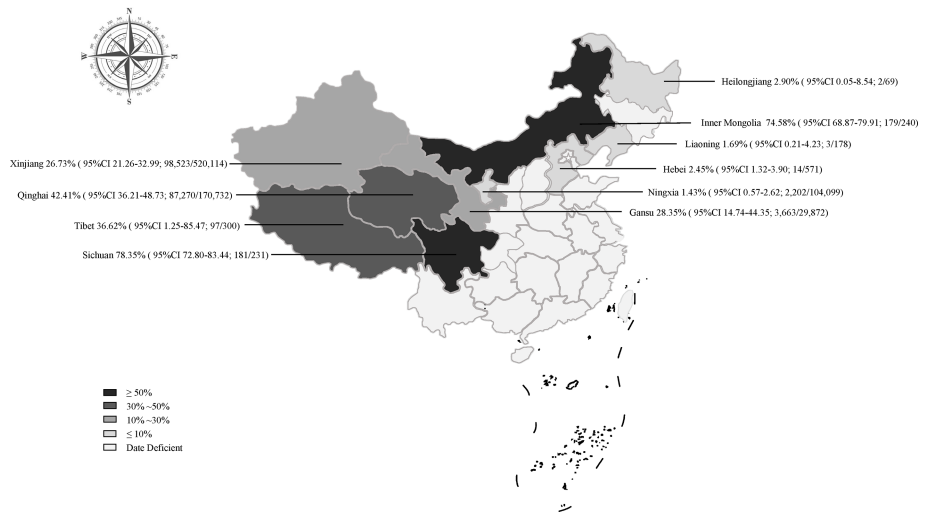

FIGURE 3 | Map of *Echinococcus* prevalence in sheep in China.

the infection rate of *Echinococcus* in dogs, foxes, and rodents in Qinghai province was relatively high (Cai et al., 2016), indicating that the environment in this area was highly contaminated by *Echinococcus* eggs. It also indicated that there was a food chain relationship among the infected animals, which forms the cycle chain of life history (Wen et al., 2019). The production tradition and geographical environment of the local herders have caused a high incidence of *Echinococcus*, bringing a great difficulty to the prevention and control work. It is recommended that the health department in this area strengthen the herders' awareness of

TABLE 2 | The combined prevalence of *Echinococcus* infection in sheep in China.

		No. studies	No. examined	No. positive	% (95% CI*)	Heterogeneity			Univariate meta-regression	
						χ^2	*P*-value	I^2 (%)	*P*-value	Coefficient (95% CI)
Season									0.018	0.209 (0.036 to 0.382)
	Autumn	12	104,273	54,310	44.70% (30.93–58.88)	5,543.24	0.00	99.8		
	Summer	10	8,468	1,778	31.07% (14.95–49.94)	2,235.77	0.00	99.6		
	Winter	4	26,340	1,939	19.48% (10.59–30.26)	265.91	< 0.01	98.9		
	Spring	4	886	186	15.42% (3.65–33.06)	113.17	< 0.01	97.3		
Age*									0.016	-0.309 (-0.560 to -0.057)
	Old sheep	10	2,887	1,203	35.89% (21.38–51.82)	632.93	< 0.01	98.6		
	Adult sheep	27	122,919	55,883	24.67% (14.00–37.20)	27,211.82	0.00	99.9		
	Lamb	8	14,362	411	5.55% (1.56–11.70)	931.52	< 0.01	99.2		
Sampling year									<0.0001	-0.325 (-0.447 to -0.203)
	2000 o rbefore	17	541,354	148,835	55.91% (42.96–68.46)	69106.07	0.00	100		
	2001 to 2010	22	58,989	16,077	33.23% (21.32–46.34)	20,590.54	0.00	99.9		
	2011 or late	23	177,318	10,269	13.86% (9.94–18.3)	9,917.86	0.00	99.8		
Method									0.644	-0.072 (-0.376 to 0.232)
	Serological testing	5	9,855	2,413	28.44% (9.33–52.9)	1,781.97	0.00	99.8		
	Anatomical touch detection	66	814,195	188,501	29.77% (24.09–35.79)	158,630.05	0.00	100		
	Ultrasonic testing	3	1,293	418	23.40% (7.11–45.38)	124.98	< 0.01	98.4		
Region*									0.022	-0.438 (-0.813 to -0.063)
	Southwestern	3	531	278	51.09% (11.51–89.86)	212.49	< 0.01	99.1		
	Northern	2	811	193	31.85% (0.00–99.00)	525.95	< 0.01	99.8		
	Northwestern	67	824,817	191,658	31.23% (25.53–37.23)	160,941.08	0.00	100		
	Northeastern	2	247	5	1.89% (0.42–4.15)	0.49	0.49	0		
Gender									0.885	0.024 (-0.298 to 0.346)
	Ram	3	1,855	1,048	51.55% (32.72–70.16)	24.74	< 0.01	91.9		
	Ewe	6	4,156	2,155	48.86% (30.51–67.36)	635.87	< 0.01	99.2		
Infected organs										
	Liver	34	597,815	58,344	20.10% (15.19–25.51)	40,471.45	0.00	99.9	0.004	-0.246 (-0.415to -0.076)
	Both*	25	154,439	58,206	18.87% (8.92–31.44)	53,576.89	0.00	100		
	lung	29	595,469	58,206	8.23% (4.42–13.05)	51,471.17	0.00	99.9		
	other	7	120,420	2,505	2.50% (0.00–10.62)	8,995.12	0.00	99.9		
Echinococcus species									0.0817	-0.427 (-0.907 to 0.054)
	Echinococcus granulosus	9	15,415	5,306	32.05% (11.49–57.10)	7,626.00	0.00	99.9		
	Echinococcus multilocularis	3	2,175	65	2.99% (0.19–8.74)	68.09	< 0.01	97.1		
Sample type									0.990	0.001 (-0.205 to 0.207)
	Serum	7	14,296	2,666	30.44% 13.85–50.19)	2,934.59	0.00	99.8		
	Organs	71	812,110	189,468	30.52% (24.97–36.37)	158,932.62	0.00	100		
Sampling location									0.016	0.204 (0.038 to 0.370)
	Pasture	18	16,547	4,253	39.82% (21.45–59.78)	9,520.34	0.00	99.8		
	Slaughterhouse	48	699,590	138,966	29.74% (22.60–37.42)	141,267.97	0.00	100		
Quality level									0.034	0.330 (0.026 to 0.633)
	Low	3	2,369	1187	62.05% (27.76–90.63)	494.6	< 0.01	99.6		
	Medium	48	762,128	175,450	31.23% (24.48–38.41)	140,929.80	0.00	100		
	High	23	61,909	15,497	26.63% (16.46–38.23)	196,36.73	0.00	99.9		
	Total	74	826,406	192,094	30.94% (25.51–36.64)					

CI: Confidence interval;*
NA: Not applicable;*
Age: Lamb (< 1 year); Adult sheep (1–6 years old); Old sheep (> 6 years old).*
Both: Mixed liver and lung infection.*

livestock breeding and disease prevention, and regularly feed dogs with anthelmintics and not feed the internal organs of animals in order to cut off the path of infection.

In the seasonal subgroup, the prevalence of *Echinococcus* in sheep was higher in summer and autumn, but the size of data in the subgroup was relatively small. Therefore, we combined geographical factors (temperature, humidity and precipitation subgroups) to specifically analyze the suitable living condition for *Echinococcus* eggs and the impact on the prevalence of *Echinococcus* in sheep. According to the results, the prevalence of sheep was higher in the range of 91-100° longitude and 30-35° latitude and in cold, wet, and rainy areas (**Table S6**). *Echinococcus* eggs were extremely resistant to cold and can maintain vigor in ice and snow. A Swiss study showed that a low temperature may be positively correlated with the infection rate of the intermediate hosts of *Echinococcus* (Burlet et al., 2011). Consistent with our research results. In winter, herders have the habit of using melted ice and snow as drinking water, making ice and snow contaminated by insect eggs the main sources of echinococcosis in humans and animals (Zhao, 2008). The eggs of *Echinococcus* were very sensitive to dryness and high temperature. The infection rate of multilocular echinococcosis in Slovakia was obviously positively correlated with the amount of precipitation. in addition, the seasonal changes can cause stress responses to the animal body. It will affect the prevalence of hydatid disease. For example, in Zurich, the infection rate of *E. multilocularis* in young foxes was highest in winter, 56.75%, and lowest in spring, 13.20% (Li, 2018). We speculate that the geographical and climatic factors may be the risk factors for hydatid infection in sheep, and it is recommended that herders in high-cold and humid areas should pay more attention to the safety of water sources.

Some studies showed that the infection of *Echinococcus* might be related to the age and immunity of livestock (Yang et al., 2015). Therefore, we conducted a subgroup analysis to investigate whether there was a correlation between age and sex of host and *Echinococcus* infection. The subgroup data showed that the highest prevalence rate of *Echinococcus* in elderly sheep was 35.89%, which was much higher than 5.55% of young sheep, and the infection rate was positively correlated with an increase of age ($P < 0.05$; Table 2). Similar results have been found in other studies, showing the prevalence of *Echinococcus* in animals over 5 years old was higher (Cabrera et al., 2003; Azlaf et al., 2006). It is generally believed that with the increase of age, the chance of exposure to pathogens is increased, which makes the infection rate of elderly sheep higher than that of lambs and adult sheep. In the gender subgroup, the prevalence of *Echinococcus* in rams was slightly higher than that of ewes, but no significant difference was observed ($P = 0.88$; Table 2). In the subgroup of infected organs in sheep, it was shown that the *Echinococcus* infection was involved in different organs, with the liver being the most susceptible organ, the highest infection rate was 21.10%. A meta-analysis in Iran showed the same results, with the highest infection rate in the liver of 55% (Mahmoudi et al., 2019). A systematic review of the literature of human cystic *Echinococcus* (CE) indicated that *E. granulosus sensu stricto* metacestodes preferentially developed in the liver (73.4%), and secondly in the lungs (19.6%), with the remainder organs including the brain, spleen, kidney, and heart (Kern et al., 2017). This result can be explained by the fact that the liver and lung were the most important body filters and were the first sites to encounter the migrating parasite larvae, and a few parasites can escape from them and gain access to other organs (Ahmadi and Badi, 2011). From the perspective of the types of hydatid, the infection rate of *E. granulosus* was higher than that of *E. multilocularis*, but only a few articles recorded the types of *Echinococcus*. This may not reflect the true situation.

At present, the investigation of sheep *Echinococcus* is still mainly based on the on-site inspection of the slaughterhouse recommended by OIE. Most of the samples (90%) tested in the study were derived from organs, and a small part (10%) of the samples were serum (**Table 2**). Among them, the anatomical touch method has the highest detection rate, and a small number of them used serology and ultrasound methods. Visceral hydatid cyst inspection can only be performed at the time of livestock slaughter, which has a great limitation. In contrast, the application of serological antibody detection methods is superior to traditional detection methods in sensitivity, specificity, and practicability. Commercial ELISA kits were widely used in a large-scale epidemiological investigation (Siles Lucas et al., 2017), but studies have also shown false negatives and false positives, in addition to low repetition rates (Paul and Stefaniak, 2001; Auer et al., 2009), whereas western blot results showed a better sensitivity (Liance et al., 2000). Imaging techniques are essential for diagnosis, with benefits of relatively inexpensive cost. The portable ultrasound was widely used to diagnose CE liver lesions; X-ray was used for lung cysts (Solomon et al., 2018; Tamarozzi et al., 2018). Ultrasound diagnosis of liver echinococcosis has been employed in China since 1950s. Ultrasound examination is a non-invasive, painless, reproducible, and highly accurate examination method. The diagnostic accuracy rate of ultrasound is as high as 97.2%, and it can be used for an early diagnosis and differential diagnosis of echinococcosis (Zhao, 2008). Therefore, the combination of serological, clinical, and imaging methods is the most suitable diagnostic approach for echinococcosis.

The 74 investigated studies overall were of high quality, among which 23 high-quality studies accounted for 31%, and 48 medium-quality studies accounted for 65% (**Table S3**). The main reason for the loss of scores in low and medium-quality research was that the sampling method was not described in detail or a random sampling. Thus, it is recommended that researchers should record and analyze the actual situation in detail when conducting epidemiological investigations and in-depth excavation, and analysis of the specific causes of sheep infection, in order to provide accurate data for the study of echinococcosis.

This study conducted a comprehensive and detailed analysis of the risk factors for the epidemiology of *Echinococcus* in sheep in China. However, some limitations were also present in this study. First, although we have established a comprehensive search method, omissions may still exist. Secondly, lack of data in some regions, heterogeneity among studies, and insufficient research on certain subgroups (such as the species infected with *Echinococcus* and the gender subgroup of sheep) may affect the results of the

analysis. Despite these limitations, this report has reflected an actual prevalence of echinococcosis in sheep in China.

CONCLUSIONS

In the past three decades, the prevalence of *Echinococcus* in sheep in China has declined. However, the infection of *Echinococcus* in sheep in China is still severe, according to the published data. We comprehensively analyzed various risk factors affecting the prevalence of hydatid cysts and found that the prevalence rate was higher in high-altitude, cold, humid and rainy areas. More attention should be paid to the prevention and control of echinococcosis in the northwestern region that meets the conditions for oocyst survival and is dominated by animal husbandry. Due to a serious effect of echinococcosis on the livestock and poultry breeding industry, and a threat for human health, it is necessary to implement long-term monitoring and control measures for echinococcosis, cut off the path of infection to reduce the risk of human infection.

DATA AVAILABILITY STATEMENT

The original contributions presented in the study are included in the article/**Supplementary Material**. Further inquiries can be directed to the corresponding authors.

AUTHOR CONTRIBUTIONS

Y-QX, Z-GR, and QZ were responsible for the idea and concept of the paper. WW, X-YW, and YC built the database. WW and YG analyzed the data. YG wrote the manuscript. CL critically reviewed and revised the manuscript. All authors contributed to the article and approved the submitted version.

FUNDING

This work was supported by the Key Scientific and Technological Achievements Transformation Project of Jilin Province (20170307016NY). The authors declare that this study received funding from Key Scientific and Technological Achievements Transformation Project of Jilin Province (20170307016NY). The funder had the following involvement in the study: Quan Zhao. Quan Zhao was responsible for the idea and concept of the paper.

SUPPLEMENTARY MATERIAL

The Supplementary Material for this article can be found online at: https://www.frontiersin.org/articles/10.3389/fcimb.2021.711332/full#supplementary-material

REFERENCES

Abrikmu, Y. (2000). Investigation of Hydatid Disease Infection in Sheep Slaughtered in Zhonghuan Road Slaughterhouse in Urumqi. *Rural. Sci. Technol.* 7, 23. doi: 10.19777/j.cnki.issn1002-6193.2000.04.028 (In Chinese).

Agudelo Higuita, N. I., Brunetti, E., and McCloskey, C. (2016). Cystic Echinococcosis. *J. Clin. Microbiol.* 54, 518–523. doi: 10.1128/JCM.02420-15

Ahmadi, N. A., and Badi, F. (2011). Human Hydatidosis in Tehran, Iran: A Retrospective Epidemiological Study of Surgical Cases Between 1999 and 2009 at Two University Medical Centers. *Trop. Biomed.* 28, 450–456.

Asmare, K., Sibhat, B., Abera, M., Haile, A., Degefu, H., Fentie, T., et al. (2016). Systematic Review and Meta-Analysis of Metacestodes Prevalence in Small Ruminants in Ethiopia. *Prev. Vet. Med.* 129, 99–107. doi: 10.1016/j.prevetmed.2016.05.006

Assefa, H., Mulate, B., Nazir, S., and Alemayehu, A. (2015). Cystic Echinococcosis Amongst Small Ruminants and Humans in Central Ethiopia. *Onderstepoort J. Vet. Res.* 82, E1–E7. doi: 10.4102/ojvr.v82i1.949

Auer, H., Stöckl, C., Suhendra, S., and Schneider, R. (2009). Sensitivity and Specificity of New Commercial Tests for the Detection of Specific *Echinococcus* Antibodies. *Wien. Klin. Wochenschr.* 121 (Suppl), 37–41. doi: 10.1007/s00508-009-1233-4

Azlaf, R., and Dakkak, A. (2006). Epidemiological Study of the Cystic Echinococcosis in Morocco. *Vet. Parasitol.* 137, 83–93. doi: 10.1016/j.vetpar.2006.01.003

Bai, T. J., Yang, W. D., Bai, T. X., and Ma, Y. S. (2011). Investigation and Control Measures of Hydatid Infection in Sheep in Tianzhu County. *Anim. Husb. Vet. Med.* 61, 73–75. (In Chinese).

Budke, C. M., Carabin, H., Ndimubanzi, P. C., Nguyen, H., Rainwater, E., Dickey, M., et al. (2013). A Systematic Review of the Literature on Cystic Echinococcosis Frequency Worldwide and its Associated Clinical Manifestations. *Am. J. Trop. Med. Hyg.* 88, 1011–1027. doi: 10.4269/ajtmh.12-0692

Budke, C. M. (2002). WHO/OIE Manual on Echinococcosis in Humans and Animals: A Public Health Problem of Global Concern. J. Eckert, M.A. Gemmell, F.-X. Meslin and Z.S. Pawlowski (Eds.); Office International des Epizooties, Paris, 265 pages, (Euros 40). *Vet. Parasitol.* 104, 357. doi: 10.1016/S0304-4017(01)00631-8

Budke, C. M., Deplazes, P., and Torgerson, P. R. (2006). Global Socioeconomic Impact of Cystic Echinococcosis. *Emerg. Infect. Dis.* 12, 296–303. doi: 10.3201/eid1202.050499

Burlet, P., Deplazes, P., and Hegglin, D. (2011). Age, Season and Spatio-Temporal Factors Affecting the Prevalence of *Echinococcus Multilocularis* and *Taenia Taeniaeformis* in Arvicola Terrestris. *Parasitol. Vectors.* 4, 6. doi: 10.1186/1756-3305-4-6

Cabrera, P. A., Irabedra, P., Orlando, D., Rista, L., Harán, G., Viñals, G., et al. (2003). National Prevalence of Larval Echinococcosis in Sheep in Slaughtering Plants Ovis Aries as an Indicator in Control Programmes in Uruguay. *Acta Trop.* 85, 281–285. doi: 10.1016/s0001-706x(02)00214-0

Cai, H. X., Wang, H., Han, X. M., Ma, X., Liu, Y. F., Liu, P. Y., et al. (2012). Study on the Infection Status and Significance of Different Hosts of *Echinococcus* in Qinghai Plateau. *Chin. J. Endemiol.* 31, 296–300. (In Chinese).

Cai, H. X., Wang, H., Han, X. M., Ma, X., Zhang, J. X., Liu, Y. F., et al. (2016). Investigation on the Prevalence of Hydatidosis in Hainan Tibetan Autonomous Prefecture, Qinghai Province. *J. Pathog. Biol.* 11, 1022–1025. doi: 10.13350/j.cjpb.161115 (In Chinese).

Carmena, D., Sánchez Serrano, L. P., and Barbero Martínez, I. (2008). *Echinococcus Granulosus* Infection in Spain. *Zoonoses. Public Health* 55, 156–165. doi: 10.1111/j.1863-2378.2007.01100.x

Chai, J. J., Jiao, W., Yi, S. L. Y., Chang, Q., Meng, H. B. T., Fu, C., et al. (2004). Epidemic Status of Cystic Echinococcosis in Northern Xinjiang. *Trop. Dis. Parasitol.* 2, 139–143. (In Chinese).

Chai, J. J., Jiao, W., Zhang, W. L., Yi, S. L. Y., Qu, Q., Li, X. L., et al. (1992). Comparative Observation on Infection Characteristics of *Echinococcus Granulosus* in Cattle and Sheep in Different Areas of Xinjiang. *Endemic. Dis. Bull.* 7, 1–7. doi: 10.13215/j.cnki.jbyfkztb.1992.s1.001 (In Chinese).

Cheng, H. P., and Liu, X. R. (2008). Investigation on Infection of Two Types of Hydatid Disease in Plateau Animals in Qingnan Area. *J. High Altitude Med.* 18 (002), 56–58. (In Chinese).

Chen, X. Y., Setiwaldi, Y., and Osman, Y. (2016). Epidemiological Studies on Echinococcosis in Kizilsu Kirgiz Autonomous Prefecture of Xinjiang. *Chin. J. Parasitol. Parasitic. Dis.* 34, 409–413. (In Chinese).

Cleary, E., Barnes, T. S., Xu, Y., Zhao, H., Clements, A. C., Gray, D. J., et al. (2014). Impact of "Grain to Green" Programme on Echinococcosis Infection in Ningxia Hui Autonomous Region of China. *Vet. Parasitol.* 205, 523–531. doi: 10.1016/j.vetpar.2014.08.023

Dan, Z. C. (2015). Analysis on Control Effect of Echinococcosis Among Livestock in Guinan County of Qinghai Province. *Anim. Husb. Feed Sci.* 36, 125–126. doi: 10.16003/j.cnki.issn1672-5190.2015.05.056 (In Chinese).

Dao, J. C., Ge, D., and Wan, D. C. (2006). Epidemiological Investigation of Hydatid Disease in Maqu County, Gannan Prefecture. *China Anim. Health* 9, 34–36. (In Chinese).

Dong, J., Yang, L. F., Zhang, W. B., Li, H. T., Jiang, T., Qi, X. W., et al. (2015). Prevalence Rate of Ovine Hepatic Cystic Echinococcosis in Quaker Wusu Area of Bayinbuluke of Xinjiang 2014. *Chin. J. Epidemiol.* 36, 136–138. (In Chinese).

Guan, G., and Ren, G. J. (2001). Investigation on the Infection of Chickenwood in Cattle and Sheep Slaughtered in Geonangbenbu. *Anim. Inspect. China.* 18, 33–34. (In Chinese).

Guo, B. P., Zhang, Z. Z., Zheng, X. T., Guo, Y. Z., Guo, G., Zhao, L., et al. (2019). Prevalence and Molecular Characterization of *Echinococcus Granulosus* Sensu Stricto in Northern Xinjiang, China. *Korean. J. Parasitol.* 57, 153–159. doi: 10.3347/kjp.2019.57.2.153

Guyatt, G. H., Oxman, A. D., Vist, G. E., Kunz, R., Falck Ytter, Y., Alonso Coello, P., et al. (2008). GRADE: An Emerging Consensus on Rating Quality of Evidence and Strength of Recommendations. *BMJ* 336, 924–926. doi: 10.1136/bmj.39489.470347.AD

Han, X., Jian, Y., Zhang, X., Ma, L., Zhu, W., Cai, Q., et al. (2019). Genetic Characterization of *Echinococcus* Isolates From Various Intermediate Hosts in the Qinghai-Tibetan Plateau Area, China. *Parasitology* 146, 1305–1312. doi: 10.1017/S0031182019000544

Han, X. M., Wang, H., Cai, H. X., Ma, X., Liu, Y. F., Wei, B. H., et al. (2009). Epidemiological Survey on Echinococcosis in Darlag County of Qinghai Province. *Chin. J. Parasitol. Parasitic. Dis.* 27, 22–26. (In Chinese).

He, D. L., and Wang, H. (2001). Epidemiological Evaluation Report of Hydatid Disease in Zeku County, Qinghai Province. *Bull. Dis. Control. Prev. (China)* 16, 36–38. doi: 10.13215/j.cnki.jbyfkztb.2001.04.015 (In Chinese).

Huang, C. G., and Chao, J. T. (1992). About Heimahe and Five Other Villages' Cattle Sheep *Echinococcus* Infections and Hazard Investigation. *Qinghai Husb.* 3, 25–26. (In Chinese).

Jiao, F. R. (2008). Investigation on Epidemic Status of Echinococcosis in Xilinguole League. *Bull. Dis. Control. Prev.* 2, 46–48. doi: 10.13215/j.cnki.jbyfkztb.2008.02.034 (In Chinese).

Jiao, W., Fu, C., Qu, Q., Nu, E. B. K., Xu, S. D., Sun, L. F., et al. (2004). Epidemiological Evaluation on the Efficacy of the Slowly Released Bar of Parziquantel for Dog Use in the Prevention of Cystic Echinococcosis in Human and Sheep. *Chin. J. Zoonoses.* 20, 557–560. (In Chinese).

Kern, P., Menezes da Silva, A., Akhan, O., Müllhaupt, B., Vizcaychipi, K. A., Budke, C., et al. (2017). The Echinococcoses: Diagnosis, Clinical Management and Burden of Disease. *Adv. Parasitol.* 96, 259–369. doi: 10.1016/bs.apar.2016.09.006

Li, Q. Q. (2009). Investigation on *Echinococcus* Infection in Cattle and Sheep in Ulan County. *Chin. Qinghai J. Anim. Vet. Sci.* 39, 3. (In Chinese).

Li, J. F. (2018). Epidemiological Investigation of Sheep Echinococcosis in Yumen City. *Gansu Agr. Univ.* 50, 1–50. (In Chinese).

Li, Y. F., and Li, D. S. (2010). Investigation on Epidemic Situation of Echinococcosis in Haiyan Area. *Anim. Quarantine China* 27, 38. (In Chinese).

Li, X., Ni, H. B., Ren, W. X., Jiang, J., Gong, Q. L., and Zhang, X. X. (2020). Seroprevalence of *Toxoplasma Gondii* in Horses: A Global Systematic Review and Meta-Analysis. *Acta Trop.* 201, 105222. doi: 10.1016/j.actatropica.2019.105222

Li, H. T., Song, T., Duan, X. Y., Qi, X. W., Feng, X. H., Wang, Y. H., et al. (2013). Liver Echinococcosis Screening Report of Population and Flock in Xinjiang and Buxaer Mongolian Autonomous County. *Chin. J. Epidemiol.* 34, 1176–1178. (In Chinese).

Liance, M., Janin, V., Bresson-Hadni, S., Vuitton, D. A., Houin, R., and Piarroux, R. (2000). Immunodiagnosis of *Echinococcus* Infections: Confirmatory Testing and Species Differentiation by a New Commercial Western Blot. *J. Clin. Microbiol.* 38, 3718–3721. doi: 10.1128/JCM.38.10.3718-3721.2000

Lie, T. F., Li, Q. C., Zhou, J. H., and Gongbao, D. J. (1984). Investigation Report on *Echinococcus* Infection in Cattle and Sheep in Gande Area. *Qinghai. J. Anim. Husb. Vet. Med.* 19–21. (In Chinese).

Liu, Y. M. (2008). Investigation of Sheep Hydatid Infection in Chaka District. *Chin. Qinghai J. Anim. Vet. Sci.* 39, 34. (In Chinese).

Liu, K. Y., Guan, C., Liu, Y. H., Fang, S. F., and Cui, P. (2020). Investigation on Sheep Hydatid Infection in Zhangjiakou City. *Chin. Herbiv. Sci.* 40, 89–90. (In Chinese).

Liu, X. T., and Yu, D. J. (1994). Preliminary Investigation of Animal Echinococcosis Infection in Naqu Area. *Chin. J. Parasitol. Parasiti. Dis.* 77. (In Chinese).

Li, L. Z., and Zhang, L. C. (2009). Investigation and Control of Echinococcosis in Tibetan Sheep. Chin. *Anim. Husb. Vet.* 36, 149–150. (In Chinese).

Lu, Y. (2015). Investigation and Control of Sheep Hydatid Disease in Gangcha County. *Contemp. Anim. Husb.* 33, 61–62. (In Chinese).

Lv, C. F., Li, X. Y., Li, S. Y., and Li, X. (2000). Investigation of Hydatid Disease in Sheep in Republic Area. *Chin. Qinghai J. Anim. Vet. Sci.* (In Chinese) 28, 48.

Ma, Y. L. (2014). Screening and Analysis of Hydatid Disease in Hualong County of Qinghai Province in 2012. *Med. Anim. Control.* 30, 577. doi: 10.7629/yxdwfz201405041 (In Chinese).

Ma, L. K., Lin, H. L., Nu, S. L. T., Zuli, H. M. E., Yan, H., Ba, T. L., et al. (2013b). Comprehensive Prevention and Control Measures for Livestock Hydatid Disease in Burqin County. *China Anim. Husb. Vet. Abstracts.* 29, 85–86. (In Chinese).

Ma, L., Shen, X., and He, G. M. (2013a). Investigation and Analysis of Echinococcosis in Sheep in Slaughterhouse in Wusu City, Xinjiang. *Beijing Agr.* 32, 181–182. (In Chinese).

Ma, B., Su, X. Y., Batai, M., and Joe, G. (2020). Epidemiological Investigation of Sheep Hydatid Disease in Some Areas of Bazhou. *Mod. J. Anim. Husb. Vet. Med.* (In Chinese) 49, 45–48.

Ma, S. M., Wang, H., and Li, W. M. (2006). Analysis of Hydatid Disease Data in Qingnan Area From 1997 to 2001. *J. Trop. Med.* 28, 55–57. (In Chinese).

Mahmoudi, S., Mamishi, S., Banar, M., Pourakbari, B., and Keshavarz, H. (2019). Epidemiology of Echinococcosis in Iran: A Systematic Review and Meta-Analysis. *BMC Infect. Dis.* 19 (1), 929. doi: 10.1186/s12879-019-4458-5

Mao, G. H., Weng, J. Y., and Cao, Y. Q. (1984). Investigation on Echinococcosis of Yak and Tibetan Sheep in Shiqu County, Sichuan Province. *J. Vet. Sci. Technol.*, (In Chinese) 31–32. doi: 10.16656/j.issn.1673-4696.1984.01.012

Mi, X. L., Li, D. M., Feng, S. Q., Zhou, Y. Q., and Gao, J. M. (2012). Investigation of Echinococcosis in Cattle and Sheep in Menyuan County. *Qinghai J. Anim. Husb. Vet. Med.* 42, 31–32. (In Chinese).

Moher, D., Liberati, A., Tetzlaff, J., and Altman, D. G. (2009). Preferred Reporting Items for Systematic Reviews and Meta-Analyses: The PRISMA Statement. *PLoS. Med.* 6, e1000097. doi: 10.1371/journal.pmed.1000097

Moher, D., Shamseer, L., Clarke, M., Ghersi, D., Liberati, A., Petticrew, M., et al. (2015). Preferred Reporting Items for Systematic Review and Meta-Analysis Protocols (PRISMA-P) 2015 Statement. *Syst. Rev.* 4, 1. doi: 10.1186/2046-4053-4-1

Niramuddin, A. (2011). Comparative Observation on the Infection Characteristics of Echinococcosis in Sheep and Cattle in Northern and Southern Xinjiang. *Chin. J. Vet. Med.* (In Chinese) 47, 81–82.

Niyazi, A. (2016). Investigation on Echinococcosis Infection of Livestock in Kuqa County, Xinjiang. *Vet. Orienta.* 10, 115–115. (In Chinese).

Ohiolei, J. A., Li, L., Ebhodaghe, F., Yan, H. B., Isaac, C., Bo, X. W., et al. (2020a). Prevalence and Distribution of Echinococcus Spp. In Wild and Domestic Animals Across Africa: A Systematic Review and Meta-Analysis. *Transbound Emerg. Dis.* 67, 2345–2364. doi: 10.1111/tbed.13571

Ohiolei, J. A., Yan, H. B., Li, L., Zhu, G. Q., Muku, R. J., Wu, Y. T., et al. (2020b). Review of Cystic Echinococcosis in Nigeria: A Story of Neglect. *Acta Parasitol.* 65, 1–10. doi: 10.2478/s11686-019-00124-x

Paul, M., and Stefaniak, J. (2001). Comparison of the Dot Immunobinding Assay and Two Enzyme-Linked Immunosorbent Assay Kits for the Diagnosis of Liver Cystic Echinococcosis. *Hepatol. Res.* 21, 14–26. doi: 10.1016/s1386-6346(00)00149-2

Qian, M. B., Abela-Ridder, B., Wu, W. P., and Zhou, X. N. (2017). Combating Echinococcosis in China: Strengthening the Research and Development. *Infect. Dis. Poverty.* 6, 161. doi: 10.1186/s40249-017-0374-3

Qi, Y. Z., Wen, Z. Q., Song, T., and Wang, Y. S. (2002). Epidemiological Investigation of Hydatidosis in Tianzhu Tibetan Autonomous County, Gansu Province. *Endemic. Dis. Bull.* 18, 51–53. (In Chinese).

Rashid, A., Darzi, M. M., Mir, M. S., Dar, L. M., Mir, A., Kashani, S. B., et al. (2017). Prevalence of Ovine Cystic Echinococcosis in Kashmir Valley, North India. *Vet. Parasitol. Reg. Stud. Rep.* 10, 85–89. doi: 10.1016/j.vprsr.2017.08.007

Reyihan, Y. S. F. (2020). Molecular Epidemiological Investigation of Cattle and Sheep Echinococcosis in Parts of Xinjiang. *Tarim. Univ*. 1–51. (In Chinese).

Siles Lucas, M., Casulli, A., Conraths, F. J., and Müller, N. (2017). Laboratory Diagnosis of Echinococcus Spp. In Human Patients and Infected Animals. *Adv. Parasitol.* 96, 159–257. doi: 10.1016/bs.apar.2016.09.003

Solomon, N., Zeyhle, E., Subramanian, K., Fields, P. J., Romig, T., Kern, P., et al. (2018). Cystic Echinococcosis in Turkana, Kenya: 30 Years of Imaging in an Endemic Region. *Acta Trop*. 178, 182–189. doi: 10.1016/j.actatropica.2017.11.006

Tamarozzi, F., Akhan, O., Cretu, C. M., Vutova, K., Akinci, D., Chipeva, R., et al. (2018). Prevalence of Abdominal Cystic Echinococcosis in Rural Bulgaria, Romania, and Turkey: A Cross-Sectional, Ultrasound-Based, Population Study From the HERACLES Project. *Lancet Infect. Dis.* 18, 769–778. doi: 10.1016/S1473-3099(18)30221-4

Tamarozzi, F., Akhan, O., Cretu, C. M., Vutova, K., Fabiani, M., Orsten, S., et al. (2019). Epidemiological Factors Associated With Human Cystic Echinococcosis: A Semi-Structured Questionnaire From a Large Population-Based Ultrasound Cross-Sectional Study in Eastern Europe and Turkey. *Parasitol. Vectors.* 12, 371. doi: 10.1186/s13071-019-3634-1

Tastan, A. (2011). Investigation and Research on the Infection Situation of Cystic Echinococcosis in Sheep in the Surrounding Area of Yining. *Xinjiang Agr. Univ*. 1–40. (In Chinese).

Tian, G. F., Li, Z. H., Liu, J. F., Jia, W. Z., Ye, P. Z., Ming, R. J., et al. (1989). Epidemiological Investigation of Hydatid Disease in Huangcheng Sheep Farm in Gansu Province. *Chin. Vet. Sci.*, 13–16. doi: 10.16656/j.issn.1673-4696.1989.11.008 (In Chinese).

Tuo, J. Z. (2016). Investigation and Control of Hydatid Disease in Sheep. *Chin. Anim. Husb. Vet. Digest.* 32, 121. (In Chinese).

Villard, O., Filisetti, D., Roch-Deries, F., Garweg, J., Flament, J., and Candolfi, E. (2003). Comparison of Enzyme-Linked Immunosorbent Assay, Immunoblotting, and PCR for Diagnosis of Toxoplasmic Chorioretinitis. *J. Clin. Microbiol.* 41, 3537–3541. doi: 10.1128/jcm.41.8.3537-3541.2003

Wahlers, K., Menezes, C. N., Wong, M. L., Zeyhle, E., Ahmed, M. E., Ocaido, M., et al. (2012). Cystic Echinococcosis in Sub-Saharan Africa. *Lancet Infect. Dis.* 12, 871–880. doi: 10.1016/S1473-3099(12)70155-X

Wang, L. M. (2017). Epidemiological Investigation of *Echinococcus* Infection and It's Influences on Sheep in Different Terrains in Akesu Prefecture. *Tarim. Univ*. 1–43. (In Chinese).

Wang, W., Gong, Q. L., Zeng, A., Li, M. H., Zhao, Q., and Ni, H. B. (2020). Prevalence of *Cryptosporidium* in Pigs in China: A Systematic Review and Meta-Analysis. *Transbound Emerg. Dis.* 68 (3), 1400–1413. doi: 10.1111/tbed.13806

Wang, J. G., and Ren, D. Y. (1994). Investigation on Hydatid Infection of Cattle and Sheep in Xiahe County, Gansu Province. *Chin. Vet. Sci. Technol.*, 17–18. doi: 10.16656/j.issn.1673-4696.1994.12.008 (In Chinese).

Wang, F. Y., and Sun, H. S. (1992). Investigation and Analysis of Sheep Echinococcosis in Hami Area. *Meat. Hyg.* 9, 12–13. (In Chinese).

Wang, H. G., and Yao, H. R. (2008). Investigation on *Echinococcus* Infection of Sheep in Zhaba Town of Hualong County. *Chin. Qinghai J. Anima. Vet. Sci.* 38, 44. (In Chinese).

Wei, X. Y., Gong, Q. L., Zeng, A., Wang, W., Wang, Q., and Zhang, X. X. (2021). Seroprevalence and Risk Factors of *Toxoplasma Gondii* Infection in Goats in China From 2010 to 2020: A Systematic Review and Meta-Analysis. *Prev. Vet. Med.* 186:105230. doi: 10.1016/j.prevetmed.2020.105230

Wen, H., Vuitton, L., Tuxun, T., Li, J., Vuitton, D. A., Zhang, W., et al. (2019). Echinococcosis: Advances in the 21st Century. *Clin. Microbiol. Rev.* 32, e00075–e00018. doi: 10.1128/CMR.00075-18

Wu, A. M. (2015). Survey on the Prevalence of Hepatic Cystic Hydatid Disease in Sheep in Emin County, Xinjiang in 2014. *Psychol. Doctor.* 21, 240–241. (In Chinese).

Wu, X. L., Duan, H. J., Qi, R. T., Yan, F., Fu, Y. R., and Ma, T. B. (2020). Evaluation of the Effect of the Integrated Echinococcosis Control Program in Ningxia Hui Autonomous Region From 2011 to 2018. *Chin. J. Schistosomiasis. Control.* 32, 598–604. doi: 10.16250/j.32.1374.2020227 (In Chinese).

Wu, X. H., and He, D. L. (2001). An Epidemiological Investigation on Hydatid Disease in Gonghe County, Qinghai Province. *Bull. Dis. Control. Prev.* 32, 29–31. doi: 10.13215/j.cnki.jbyfkztb.2001.01.012(InChinese

Wumaier, M., Usman, I., Simayi, A., Hou, Y. Y., and Xiao, N. (2017). Investigation and Analysis of Animal *Echinococcus* Infection in Xinjiang Uygur Autonomous Region. *Chin. J. Parasitol. Parasitic. Dis.* 35, 145–149.

Wusman, A. (2016). Detection and Epidemiological Analysis of Aspidistra Spinosa in Livestock Slaughterhouse of Kuqa County. *Chin. Anim. Husb. Vet. Abstracts.* 111. (In Chinese).

Xia, C. Y., Liu, J. Z., Tsering, D., Yuan, Z. J., Gesang, D., Ban, D., et al. (2014). Investigation of Three Finds of Tapeworm Larvae Infections in Tibetan Domestic Animals. *Chin. Vet. Sci.* 44, 1205–1209. doi: 10.16656/j.issn.1673-4696.2014.11.017 (In Chinese).

Xiao, G. L., Zhong, Q., Xie, W. H., and Wang, X. H. (2019). Epidemiological Survey of Sheep Hydatidosis in Kashi Area of Xinjiang From 2014 to 2017. *Chin. Anim. Health Inspection.* 36, 1–5. (In Chinese).

Xu, X. P., Li, X. J., Zhu, H. C., Tao, Y., and Li, Y. X. (1994). Investigation on Current Situation of Hydatid Disease in Shihezi Area. *Shihezi Technol.*, 64–65. (In Chinese).

Yang, S., Wu, W., Tian, T., Zhao, J., Chen, K., Wang, Q., et al. (2015). Prevalence of Cystic Echinococcosis in Slaughtered Sheep as an Indicator to Assess Control Progress in Emin County, Xinjiang, China. *Korean. J. Parasitol.* 53, 355–359. doi: 10.3347/kjp.2015.53.3.355

Yan, Q. L., Wei, M. L., Fan, C. B., Cai, D., and Shi, Y. (1983). Investigation Report on Echinococcosis Infection of Cattle and Sheep in Huangnan Prefecture of Qinghai Province. *Chin. Qinghai J. Anim. Vet. Sci.* 4, 34–36. (In Chinese).

Yan, H. C., Zhou, Z. S., Liu, X. G., and Du, H. (1998). Investigation on Parasite Infection in Sheep Lungs. *Meat. Hyg.* 21, 6. (In Chinese).

Ye, W. X., and Zhang, X. G. (2007). Investigation of Hydatid Infection in Sheep in Minhe County. *Chin. Qinghai J. Anim. Vet. Sci.* 27. (In Chinese).

Yuemaier, T. (2015). Investigation on the Infection Status of Domestic Animal Hydatid Disease in Wushi County, Xinjiang. *Vet. Guide.* 000, 153–153. (In Chinese).

Yu, S. H., Wang, H., Wu, X. H., Ma, X., Liu, P. Y., Liu, Y. F., et al. (2008). Cystic and Alveolar Echinococcosis: An Epidemiological Survey in a Tibetan Population in Southeast Qinghai, China. *Jpn. J. Infect. Dis.* 61, 242–246.

Zhang, X. (2015). Demonstration and Application of Hydatid Detection and Comprehensive Prevention and Control Measures for Hydatid Disease. *Xinjiang Agr. Univ*. 1–49. (In Chinese).

Zhang, R. (2016). Detection of Individual Prevalence of Sheep Hydatid Disease in Wusu City, Xinjiang. *Xinjiang. Agr. Univ*. 1–41. (In Chinese).

Zhang, H. W., Ding, Y. L., and Qiao, T. S. (2002). A Survey on the Parasite System of Sheep in Shuangcheng City, Heilongjiang Province. *Chin. Vet. Sci.* 32, 15–16. (In Chinese).

Zhang, J. X., and Wang, H. (2007). Epidemiological Survey on *Echinococcus* Infection in Animals in Qinghai Province. *Chin. J. Parasitol. Parasitic. Dis.* 24, 350–352. doi: 10.16795/j.cnki.xjxmy.2016.07.008 (In Chinese).

Zhang, L. Y., and Wang, X. F. (2016). Investigation and Research on Endoparasites of Cattle and Sheep in Tuergate Port Area. *Xinjiang Anim. Husb.* 7, 28–30. (In Chinese).

Zhang, K. F., Wu, T. J., and Zhao, Z. Y. (2014). Analysis of Surveillance Results of Hydatid Disease in Minle County From 2009 to 2010. *Fifth Cross-Strait (Qinghai) Featured Agr. Industrialization Forum.* 18, 258–260. (In Chinese).

Zhang, F., Xu, W. P., Wang, H. P., Zhang, Q. H., and Yan, R. L. (1985). Preliminary Investigation on the Epidemiology of Polycephalytaeniasis in Ningxia. *Ningxia Agri Sci. Technol.*, 35–36. (In Chinese).

Zhang, H. C., and Zhang, Y. Q. (2009). Investigation of Hydatid Infection in Dogs and Sheep in Zhugu Township, Menyuan County. *Anim. Husbandry. Vet. Med.* 41, 109. (In Chinese).

Zhao, Y. M. (2008). Epidemiological Study on Hydatid Disease in the Eastern Section of the Qinghai-Tibet Plateau (Gannan Tibetan Autonomous Prefecture). *Gansu. Agr. Univ*. 1–98. (In Chinese).

Zhao, H. J., An, H. H., Wu, D. X., Ro, Z. G. L., Ka, H., Shen, Y., et al. (1991). Investigation of Sheep Hydatid Disease in Yiwu County. *Xinjiang Husb.* 7, 15–17. doi: 10.16795/j.cnki.xjxmy.1991.05.004 (In Chinese).

Zhao, Y. M., Tong, S. X., Jing, T., Zhong, S. G., Cai, X. P., Jing, Z. Z., et al. (2009). Investigation on Echinococcosis in Animals in Gannan Tibetan Autonomous Prefecture. *Chin. J. Parasitol. Parasitic. Dis.* 27, 27–30. (In Chinese).

Zhao, Z. D., and Zhang, L. (2019). Applications of Genome Selection in Sheep Breeding. *Yi Chuan.* 41, 293–303. doi: 10.16288/j.yczz.18-251

Zhu, G. L., Guo, X. H., Liu, Z. Q., Wu, Q. W., and Li, L. F. (1994). Investigation on Hydatid Disease of Sheep in Southern Xinjiang Reclamation Area. *Heilongjiang. Anim. Husb. Vet.*, 26–27. (In Chinese).

Zhu, J., Moawad, A. R., Wang, C. Y., Li, H. F., Ren, J. Y., and Dai, Y. F. (2018). Advances in *In Vitro* Production of Sheep Embryos. *Int. J. Vet. Sci. Med.* 27 (Suppl), S15–S26. doi: 10.1016/j.ijvsm.2018.02.003

Conflict of Interest: YG and Z-GR were employed by Chongqing Auleon Biological Co., Ltd. CL was employed by Shandong New Hope Liuhe Group Co., Ltd., and Qingdao Jiazhi Biotechnology Co., Ltd.

The remaining authors declare that the research was conducted in the absence of any commercial or financial relationships that could be construed as a potential conflict of interest.

Publisher's Note: All claims expressed in this article are solely those of the authors and do not necessarily represent those of their affiliated organizations, or those of the publisher, the editors and the reviewers. Any product that may be evaluated in this article, or claim that may be made by its manufacturer, is not guaranteed or endorsed by the publisher.

frontiers in Cellular and Infection Microbiology

ORIGINAL RESEARCH
published: 03 September 2021
doi: 10.3389/fcimb.2021.730222

Myrislignan Induces Redox Imbalance and Activates Autophagy in *Toxoplasma gondii*

Jili Zhang[1,2], Jia Chen[2], Kun Lv[3], Bing Li[4], Biqing Yan[1], Lei Gai[1], Chaolu Shi[1], Xinnian Wang[1], Hongfei Si[5] and Jiyu Zhang[4]**

[1] Intensive Care Unit, The Affiliated Hospital of Medical School, Ningbo University, Ningbo, China, [2] Ningbo University School of Medicine, Ningbo University, Ningbo, China, [3] Ningbo University School of Business, Ningbo University, Ningbo, China, [4] Lanzhou Institute of Husbandry and Pharmaceutical Sciences, Chinese Academy of Agricultural Sciences, Lanzhou, China, [5] College of Pharmacy, Jinan University, Guangzhou, China

Toxoplasma gondii (T. gondii) is an important health problem in human and animals, and the highlighting side effects of launched therapeutic chemicals cannot be ignored. Thus, it is urgent to develop new drugs to against the infection. Myrislignan originated from nutmeg exhibited excellent anti-*T. gondii* activity *in vitro* and *in vivo*, and was able to destroy mitochondrial function. However, the exact mechanism of action is still unknown. In this study, combining RNAs deep-sequencing analysis and surface plasmon resonance (SPR) analysis, the differentially expressed genes (DEGs) and high affinity proteins suggested that myrislignan may affect the oxidation-reduction process of *T. gondii*. Furthermore, the upregulating ROS activity after myrislignan incubation verified that myrislignan destroyed the oxidant-antioxidant homeostasis of tachyzoites. Transmission electron microscopy (TEM) indicated that myrislignan induced the formation of autophagosome-like double-membrane structure. Moreover, monodansyl cadaverine (MDC) staining and western blot further illustrated autophagosome formation. Myrislignan treatment induced a significant reduction in *T. gondii by* flow cytometry analysis. Together, these findings demonstrated that myrislignan can induce the oxidation-reduction in *T. gondii*, lead to the autophagy, and cause the death of *T. gondii.*

Keywords: myrislignan, *Toxoplasma gondii*, oxidation-reduction process, autophagy, oxidative phosphorylation

OPEN ACCESS

Edited by:
Xiao-Xuan Zhang,
Qingdao Agricultural University, China

Reviewed by:
Feng Tan,
Wenzhou Medical University, China
De-Hua Lai,
Sun Yat-sen University, China

***Correspondence:**
Jiyu Zhang
zhangjiyu@caas.cn
Hongfei Si
shf5162629@163.com

Specialty section:
This article was submitted to Clinical Microbiology, a section of the journal Frontiers in Cellular and Infection Microbiology

Received: *24 June 2021*
Accepted: *17 August 2021*
Published: *03 September 2021*

Citation:
Zhang J, Chen J, Lv K, Li B, Yan B, Gai L, Shi C, Wang X, Si H and Zhang J (2021) Myrislignan Induces Redox Imbalance and Activates Autophagy in Toxoplasma gondii. Front. Cell. Infect. Microbiol. 11:730222. doi: 10.3389/fcimb.2021.730222

INTRODUCTION

Toxoplasma gondii (*T. gondii*) is a kind of parasites that causes widespread zoonotic toxoplasmosis by affecting human health and disrupting animal husbandry. It is a critical public health burden that has caused global concerns (Weiss and Kim, 2013). The general affective symptoms are not obvious in immunocompetent individuals. However, as for immune-compromised individuals, especially in AIDS, *T. gondii* infection often caused serious consequences (Ahmadpour et al., 2014). Furthermore, during pregnancy, *T. gondii* infection through vertical transmission can result in miscarriage, foetal malformations or even death (Fallahi et al., 2018). Currently, pyrimethamine and sulfadiazine are the gold standard therapeutic drugs (Giovati et al., 2018). However, these therapeutic treatments remain dissatisfactory effects because of significant bone marrow toxicity,

drug toxicity and failure to against latent infections. Therefore, novel therapeutic drugs are in urgent need for future intervention strategies.

Constant efforts have been made to seek anti-parasitic drugs against zoonotic parasitic disease, but the novel anti-*T. gondii* drugs with high effectiveness and low toxicity have not yet been launched (Choi and Lee, 2019). It is worth noting that natural products from plants are useful source for developing the anti-*T. gondii* drugs. Myrislignan is a natural product from *Myristica fragrans* Houtt with a wide range of pharmacological activities (Nguyen et al., 2010; Jin et al., 2012; Lu et al., 2017; Yang et al., 2018; Zhang et al., 2019). In the previous study, we have demonstrated that myrislignan could inhibit *T. gondii* replication and invasion in *T. gondii in vitro* without affecting the host cells. Furthermore, myrislignan exposure also induced the surface shrinkage and mitochondrial damage in *T. gondii*. Despite the mitochondrial damage has been further confirmed by the reduced ΔΨm and ATP levels in tachyzoites treated with myrislignan, it is also well worth investigating the mechanism of action of myrislignan against *T. gondii*, thereby highlighting its therapeutic potential in toxoplasmosis. Herein, we illustrated myrislignan may affect the oxidant-antioxidant homeostasis of *T. gondii* and cause autophagy of *T. gondii*, and lead to programmed death of *T. gondii*.

MATERIALS AND METHODS

Cells and Parasites

African green monkey kidney (Vero) cells were cultured in Dulbecco's Modified Eagle's Medium (DMEM) supplemented with 10% (v/v) heat-inactivated foetal bovine serum (FBS), 1% non-essential amino acids (NEAA), 100 U/mL penicillin, 100 μg/mL streptomycin and 1% GlutaMAX at 37°C in a 5% CO_2 atmosphere (Zhang et al., 2019). The *T. gondii* RH stain tachyzoites used in our study were maintained in Vero layers in DMEM contained with 1% FBS, as described previously (Si et al., 2018). All the infection experiments with *T. gondii* were performed under biosafety level 2 (BSL-2) conditions.

Drugs

Myrislignan (batch numbers DST180502-043, Desite Biotechnology Co., Ltd., China) was dissolved in dimethyl sulfoxide (DMSO, Sigma, USA) at a concentration of 4 mg/mL, then diluted in DMEM containing 1% FBS to different concentrations. All drugs were stored at 4°C.

RNA Preparation and Sequencing

T. gondii were isolated from infected Vero cells according to previously described methods. After treatment with different concentrations of myrislignan (32, 50 or 70 μg/mL) in DMEM or without any drug (as parasite control) for 24 h at 37°C, all the samples were washed with cold phosphate-buffered saline (PBS) and immediately stored at -80°C until they were used for RNA isolation. RNA-Seq analysis was based on three biological replicates per experimental group. Total RNA was extracted from *T. gondii* using TRIzol Reagent (Invitrogen, USA) and the concentrations were detected by an Agilent 2100 Bioanalyzer (Agilent RNA 6000 Nano Kit, Agilent Technologies, USA). Sequencing libraries were generated using an Illumina TruSeqTM RNA Sample Preparation Kit (Illumina, San Diego, CA, USA) and sequenced with the HiSeq 2000 System (TruSeq SBS KIT-HS V3, Illumina). RNA isolation, library construction, RNA sequencing, and read alignment were performed by BGI (Shenzhen, China) (He et al., 2019).

The level of gene expression was calculated in units of fragments per kilobase of transcript sequence per million base pairs sequenced (FPKM) of each gene. Differential expression analysis was performed using the DESeq R package. The P-values were adjusted as Q-values using the Benjamini-Hochberg and Storey-Tibshirani correction for multiple testing. As the $|\log2(\text{fold change})| \geq 1$ and Q-values ≤ 0.001, the transcripts were considered differentially expressed. DEGs were subjected to Gene Ontology (GO) (www.geneontology.org/) enrichment and Kyoto Encyclopedia of Genes and Genomes (KEGG) (www.genome.jp/kegg/) analyses, which were performed as described previously (He et al., 2019).

Validation of mRNA Expression

Total RNA from treated and untreated *T. gondii* tachyzoites was extracted as described above, then used to synthesized cDNA. TB Green Premix Ex Taq II (Tli RNaseH Plus) (TaKaRa, Japan) was used to perform quantitative real-time polymerase chain reaction (qRT-PCR) reactions using a QuantStudio 6 Flex Real-Time PCR System (Life Technologies). The qRT-PCR primers used in this study are described in **Supplementary Dataset S1**. α-tubulin was used as an internal standard reference gene. Each sample were carried out in biological triplicates.

Surface Plasmon Resonance (SPR) Experiment

3.74 mg/mL myrislignan in DMSO were spotted in 3D SPRi chips using a BioDot 1520 Array Printer to control the consistency of sample size. No myrislignan in DMSO were spotted in chips as the negative control spot. Freshly released *T. gondii* tachyzoites (1×10^9) were lysed, and the protein concentration was detected with a Thermo Fisher BCA Protein Assay Kit (Number: 23227). The final concentration of the *T. gondii* sample was 200 μg/mL. Protein lysate was flowed through the chip surface to bind the compound on the chip surface, and PBST was also used as the negative control for the measurement of specific signals in oval regions of interest. After *in situ* enzymatic hydrolysis, the kinetic affinity between *T. gondii* peptides and myrislignan was calculated, and the protein or peptides captured on the chip surface were identified by HPLC-MS/MS (Nano Acquity UPLC System, Waters Corp., USA; AB SCIEX TOF/TOF Mass Spectrometry System, AB Sciex Pte. Ltd, USA).

The Reactive Oxygen Species (ROS) Production

Tachyzoites in Vero cells were treated with myrislignan (32 or 70 μg/mL) in DMEM or with no drug (as control) for 8 h, 16 h or 24 h, then fresh tachyzoites (approximately 1×10^6/group) were

extracted and incubated with 10 μM H2DCFDA (DCFH-DA, 2',7'-Dichlorodihydrofluorescein diacetate) probe in DMEM for 20 min at 37°C. All the samples were washed with DMEM twice, and seeded into each well of a 24-well cell culture plate, then the luminescence was detected using a multilabel reader (EnSpire, PerkinElmer, USA) (Chen et al., 2018).

Superoxide Dismutase (SOD) Activity

Fresh tachyzoites (1×10^6 per group) from Vero cells were lysed after incubation with myrislignan (32 or 70 μg/mL) or without drug (control), then centrifuged at 12,000 g for 5 min at 4°C. The supernatant was added to a 96 well plates, and the absorbance of each sample was measured at 450 nm by a total SOD assay kit (WST-8, Beyotime, China) after incubation at 37°C for 30 min in dark (Chen et al., 2018).

Transmission Electron Microscopy (TEM) Analysis

Vero infected with *T. gondii* for 8 h and incubated with 32 or 70 μg/mL myrislignan for 16 h or 24 h, digested with TrypLE Express for 2 min, washed twice with PBS. Then, the cells were processed for TEM, as described previously (Si et al., 2018).

Monodansyl Cadaverine (MDC) Detection

For each sample, tachyzoites in Vero cells were treated with myrislignan (32 or 70 μg/mL) for 16 h in DMEM or with no drug (as a control). After extraction, the fresh tachyzoites were suspended in the MDC solution (100 μM) at 37°C for 60 min, and then washed with PBS, resuspended in 500 μL PBS. The fluorescence in each group was visualized by laser scanning confocal microscopy (ZEISS LSM-800, Jena, German). The experiment was repeated three times (Zhang et al., 2021).

Western Blotting Analysis

After myrislignan (16, 32, 50, 60 or 70 μg/mL) treatment for 16 h, *T. gondii* were lysed with RIPA lysis buffer, all protein samples were separated on 15% urea SDS-polyacrylamide gel electrophoresis and transferred onto 0.22 μm polyvinylidene fluoride (PVDF) membranes (Merck Millipore, US) (Besteiro et al., 2011; Kong-Hap et al., 2013). After blocking, membranes were incubated with the corresponding primary antibodies against TgATG8 (1: 250, presented by researcher Dr. Jia of Harbin Institute of Veterinary Medicine) at 4°C overnight. The membranes were washed with TBST buffer and incubated with horseradish peroxidase-conjugated secondary antibodies (1:2000, Cell Signaling Technology, USA), and chemiluminescent detection was completed with enhanced chemiluminescence Western blot agent (Millipore, Billerica, MA, USA). The protein signals were detected with Amersham Imager 600 system (GE, Boston, MA, USA) and were normalized to the corresponding internal control tubulin to eliminate the variance in total protein (Wang et al., 2010; Lee et al., 2013).

Flow Cytometry Analysis

T. gondii tachyzoites in infected host cells and incubation with myrislignan (32, 50 or 70 μg/mL) for 24 h. Intracellular parasites were collected by passage of host cells, and approximately 1×10^6 tachyzoites were centrifugation at 1,500 g, 15 min at 4°C and washed with PBS. Then, the samples were suspended in 100 μL of binding buffer with 5 μL of annexin V-PE and 5 μL of 7-AAD dye (Becton Dickinson Company, 559763) in the dark for 20 min at 37°C. Double mixtures were analysed by Guava easyCyte flow cytometer (Merck, USA) (Chen et al., 2018). The experiment was repeated three times.

Statistical Analyses

Data comparisons between the control and myrislignan treatment groups in the ROS and SOD tests, flow cytometry assay was statistically analysed by one-way analysis of variance (ANOVA) using SPSS software (SPSS Inc., Chicago, IL, USA). Differences were considered statistically significant at a p value <0.01.

RESULTS

RNA-Seq Data Analysis and Verification

RNA-Seq was used to investigate the gene expression patterns of *T. gondii* treated with myrislignan. To verify the RNA-Seq results, 6 candidate genes were randomly selected and evaluated by qRT-PCR) in this study. The results indicated that the expression levels of DEGs obtained by qRT-PCR were nearly consistent with those obtained by RNA-Seq, demonstrating the validity of the transcriptomic RNA-Seq data (**Figure 1A**).

DEGs analysis was carried out by comparing the gene transcriptional levels in myrislignan-treated *T. gondii* and that in untreated control *T. gondii*, the DEGs in each treatment group in **Table 1**. Venn diagram analysis revealed 63 genes that were differentially co-expressed in myrislignan treated groups (32, 50 or 70 μg/mL) (**Figure 1B**). GO enrichment analysis of DEGs revealed changes in biological processes, molecular functions and cellular components in *T. gondii* after treatment with myrislignan (**Figure 1C**), and the most common GO terms in these categories were "catalytic activity", such as "oxidoreductase activity", "oxidation –reduction process" and "electron transfer activity". KEGG pathway analysis showed that the DEGs were mainly associated with "oxidative phosphorylation", as shown in **Figure 1D**.

Surface Plasmon Resonance (SPR) Analysis

To more precisely identify a target protein, SPR analysis investigated the affinity and interactive effect between myrislignan and the *T. gondii* proteins. A total of 58 *T. gondii* proteins were captured by myrislignan (**Supplementary Dataset S2**). The kinetic affinity between *T. gondii* peptides and myrislignan was calculated. Accordingly, 26 specific binding proteins indicating high affinity with binding scores of greater than 1,000, were selected for the following experiments. According to Gene Ontology (GO) database, the target proteins were further analysed by functional clustering and enrichment. The results of protein classification were shown in **Figure 2A**, the results of molecular function classification were shown in **Figure 2B**, the biological process classification results were

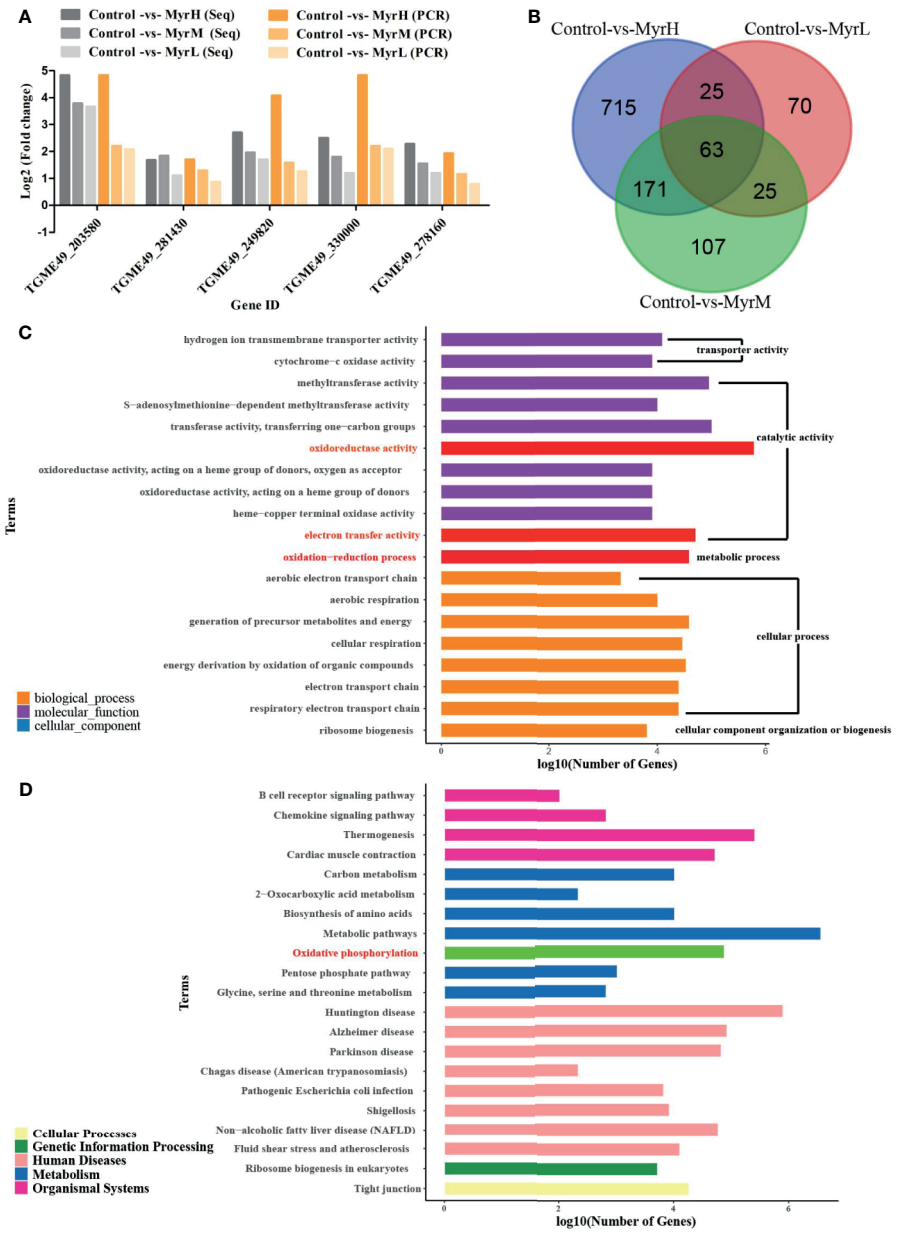

FIGURE 1 | RNA-Seq data analysis and verification. Verification the RNA-Seq data by qRT-PCR **(A)** MyrH (Myrislignan 70 μg/mL); MyrM (Myrislignan 50 μg/mL); MyrL (Myrislignan 32 μg/mL); Venn diagram analysis revealed the DEGs in myrislignan-treated groups (32, 50 or 70 μg/mL) compared with those in the control-treated groups **(B)** GO enrichment analysis of DEGs in *T. gondii* after treatment with myrislignan, DEGs were sorted into three categories: cellular component, biological process and molecular function **(C)** KEGG pathway analysis of RNA-Seq data, among which the x-axis shows the Log10 (number of gene) and the y-axis corresponds to KEGG pathway **(D)**. MyrH (Myrislignan high dose group); MyrM (Myrislignan middle dose group); MyrL (Myrislignan low dose group).

shown in **Figure 2C**, and the cell component classification of the results were shown in **Figure 2D**.

In order to verify and identify new mechanisms of action of myrislignan, RNA-Seq data and SPR-MS data (26 proteins) were compared and combined. We found the DEGs and high affinity proteins were enriched in the oxidation-reduction process (**Figure 2E**). Therefore, myrislignan may play a key role of anti-*T. gondii* activity by affecting the oxidation-reduction process of *T. gondii*.

Myrislignan Induced the Production of SOD and ROS in *T. gondii* Tachyzoites

We investigated whether myrislignan stimulated the increase of ROS production in *T. gondii* tachyzoites. After myrislignan

TABLE 1 | Statistics of number of differentially expressed genes (DEGs).

Compare_group	up	down	total
Control -vs- MyrH	836	138	974
Control -vs- MyrM	309	57	366
Control -vs- MyrL	76	107	183

MyrH (Myrislignan 70 μg/mL); MyrM (Myrislignan 50 μg/mL); MyrL (Myrislignan 32 μg/mL).

incubation, ROS activity was also significantly ($p<0.01$) upregulated (**Figure 3A**). SOD is an important antioxidant produced by parasitic protozoa. It can maintain the stability of the internal environment and prevent the clearance of host immune cells. Therefore, we evaluated the SOD activity of *T. gondii* RH tachyzoites and found that the content of SOD was increased after myrislignan incubation, but did not increase over time (**Figure 3B**).

Myrislignan Induced Autophagy in *T. gondii*

Myrislignan treatment for 16 h caused many autophagic vacuoles to emerge in the cytoplasm, as indicated by the arrows; all of these effects are hallmarks of autophagy (**Figures 4C, E**). In addition, after 24 h of treatment with myrislignan, the cytoplasmic structure and parasitophorous vacuole (PV) membranes of tachyzoites had completely disappeared, and progressive degeneration of the parasites was observed, as shown in (**Figures 4D, F**). However, autophagic vacuoles were not frequently discovered in untreated *T. gondii*. The TEM

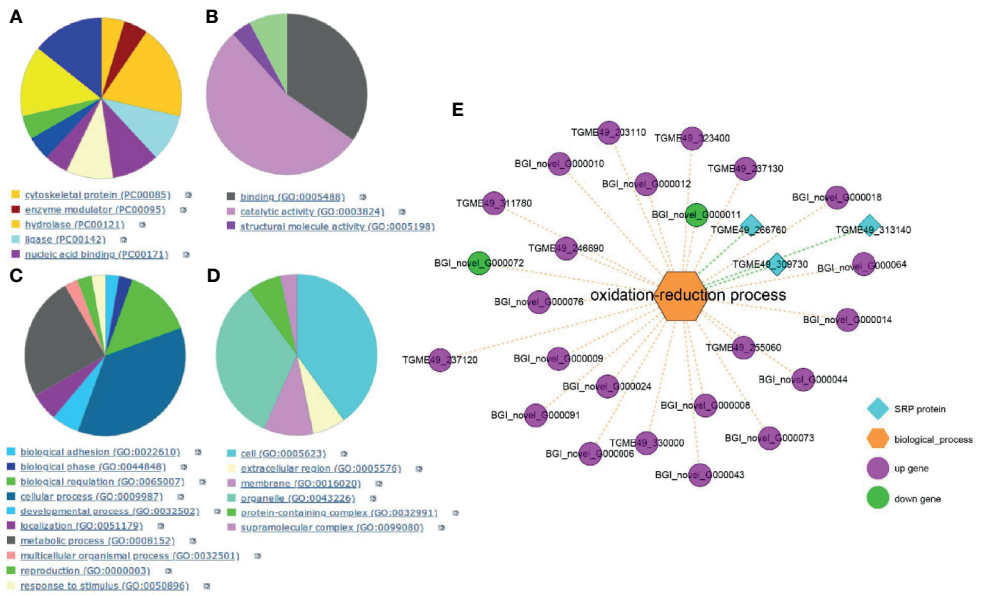

FIGURE 2 | SPR analysis. GO database analysis of the affinity proteins classification in *T. gondii* **(A)**, including categories: molecular function classification **(B)**, biological process **(C)**; cell component **(D)**. Integration of transcriptomics and SPR for target discovery **(E)**.

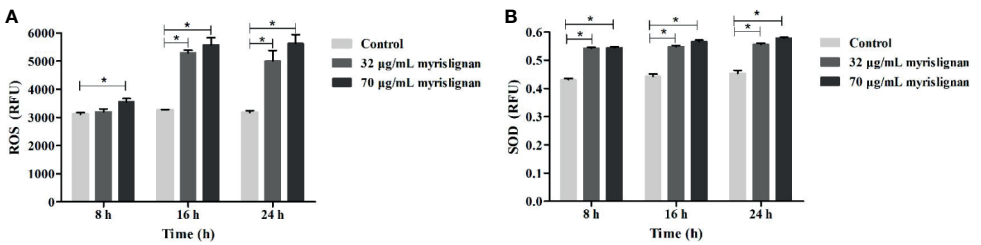

FIGURE 3 | Myrislignan destroyed the oxidation-reduction in *T. gondii* Tachyzoites. Myrislignan induced the increased in ROS of *T. gondii* **(A)**. 1×10^6 tachyzoites were treated with myrislignan (32 or 70 μg/mL) in DMEM or with no drug (as control) for 8 h, 16 h or 24 h, then incubated with 10 μM DCFH-DA probe for 20 min at 37°C, and the luminescence of each sample was detected using a multilabel reader. Myrislignan upregulated SOD activity in *T. gondii* **(B)**, Tachyzoites (1×10^6 per group) were lysed after incubation with myrislignan (32 or 70 μg/mL) or without drug (control), the supernatant was added to a 96 well plates, and the absorbance of each sample was measured at 450 nm by SOD assay kit. *$p < 0.01$ compared with the parasite control.

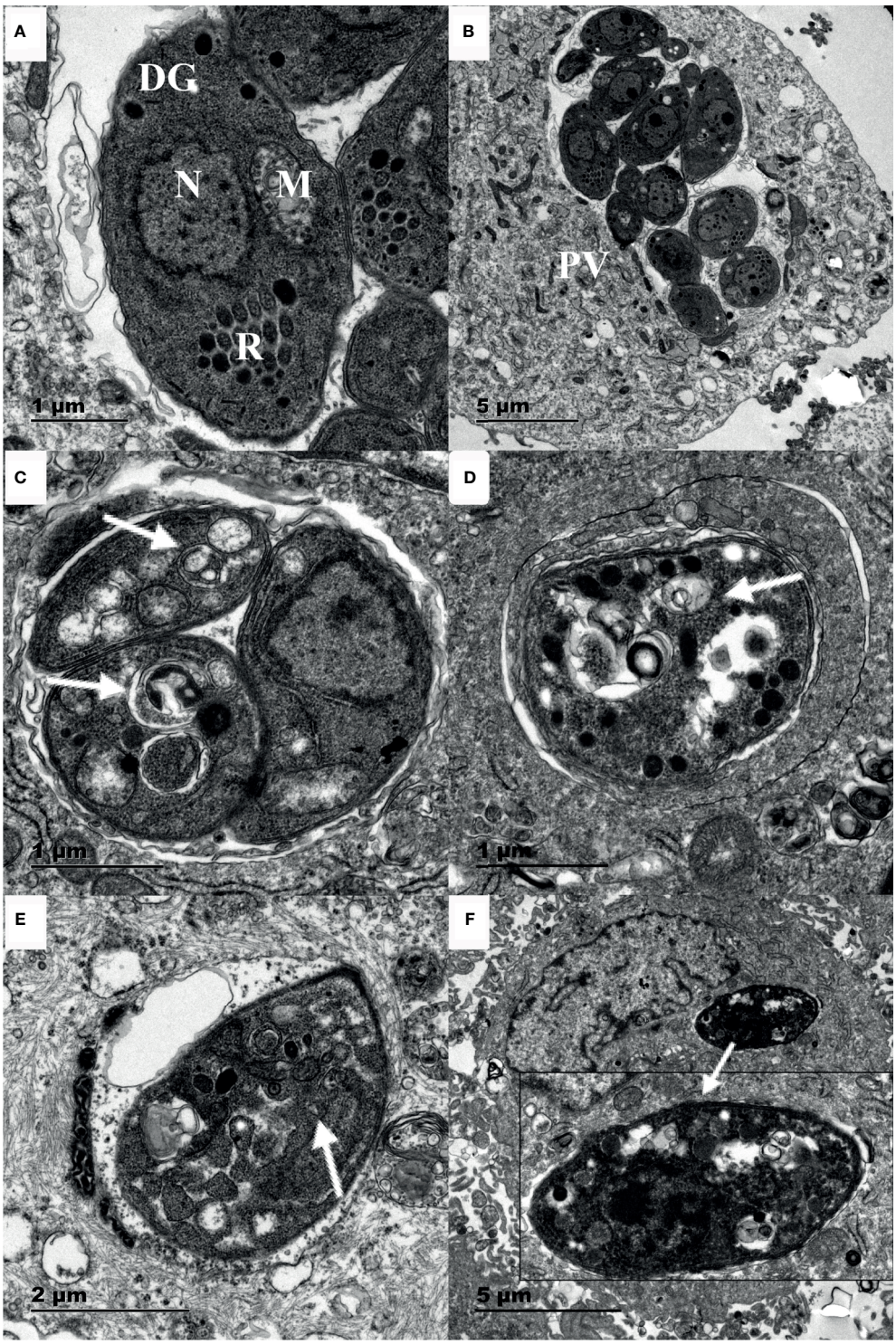

FIGURE 4 | Ultrastructural changes in *T. gondii* tachyzoites after myrislignan. The well-preserved tachyzoite structures were maintained in the control group, including the nucleus (N), rhoptries (R), dense granules (DGs) and mitochondrion (M) **(A, B)**. Myrislignan treatment for 16 h caused many autophagic vacuoles to emerge in the cytoplasm **(C, E)**, as indicated by the arrows. After myrislignan treatment for 24 h, the cytoplasmic structure and parasitophorous vacuole (PV) membranes of tachyzoites had completely disappeared **(F)**. Scale bars: 1 μm **(A, C, D)**; 2 μm **(E)**; 5 μm **(B, F)**.

results confirmed that the untreated parasites displayed a well-preserved intracellular space with typical apicomplexan structural features, including rhoptries (R), dense granules (DGs), a nucleus (N), and a mitochondrion (M) (**Figures 4A, B**). However, confirmation of these structures as autophagosomes will require the generation of specific markers.

To further confirm autophagy in *T. gondii* stimulated by myrislignan, MDC staining was exploited to detect numerous autophagic vacuoles in *T. gondii* after incubation with myrislignan. In MDC staining, myrislignan treatment resulted in obvious fluorescent spot-like structure of *T. gondii*, indicating a large number of autophagic vacuoles (**Figures 5B, C**), while there were no fluorescent dot-like structures in the untreated *T. gondii* (**Figure 5A**), the fluorescence intensity mean value of each group was shown in **Figure 5D**.

Furthermore, the expression of the typical autophagic marker TgATG8-PE was assessed in *T. gondii* in the absence or presence of myrislignan by western blotting analysis. As expected, the results showed that the autophagy marker TgATG8-PE was upregulated after myrislignan treatment in a dose-dependent manner (**Figure 5E**).

Myrislignan Induced Cell Death of Tachyzoites

Furthermore, the cell death of inhibiting extracellular growing tachyzoites after treatment with different concentrations of myrislignan for 24 h was determined by flow cytometry (**Figure 6A**). The different patterns in the Annexin V-PE/7-AAD analysis were used to identify the different *T. gondii* populations where 7-AAD-negative and Annexin V-PE-negative cells were designated as viable tachyzoites. The proportion of viable tachyzoites varied from 88.53% ± 1.31% in control groups to 42.02% ± 1.29%, 26.83% ± 3.29%, 17.22 ± 1.37% in 32, 50 or 70 μg/mL myrislignan treatment groups, respectively. The results showed that myrislignan treatment had a concentration-dependent significant ($p < 0.01$) increase in cell death effect of *T. gondii* tachyzoites (**Figure 6B**).

DISCUSSION

T. gondii is an obligate intracellular pathogen that can infect almost all warm-blooded animals and humans (Ling et al., 2006), causing major health problems. In recent years, people are looking for safe and effective anti-*T. gondii* drugs. Natural products in plants have become an important source of clinical drugs, and some of the new compounds are expected to be the leaders of new drugs (Sepulveda-Arias et al., 2014). Myrislignan is a main active ingredient of nutmeg exhibiting various bioactivities, such as inducing apoptosis and cell cycle arrest in A549 cells (Lu et al., 2017), activating the AMPK enzyme and

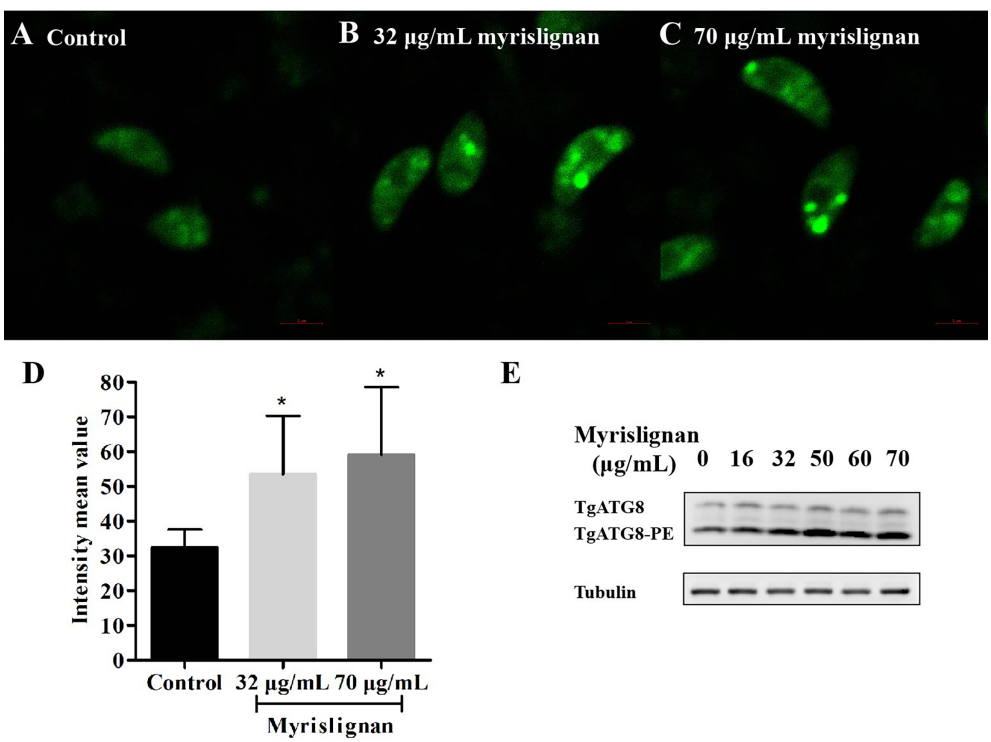

FIGURE 5 | Myrislignan Induced autophagy in *T. gondii*. Myrislignan treatment induced distinct fluorescent dot-like structures corresponding to numerous autophagic vacuoles in *T. gondii* **(B, C)**, while no fluorescent dot-like structures were discovered in the untreated *T. gondii* **(A)**, the fluorescence intensity mean value of each group was shown in **(D)**, *$p < 0.01$ compared with the parasite control. Western blotting analysis showed that TgATG8-PE was upregulated after myrislignan treatment in a dose-dependent manner **(E)**.

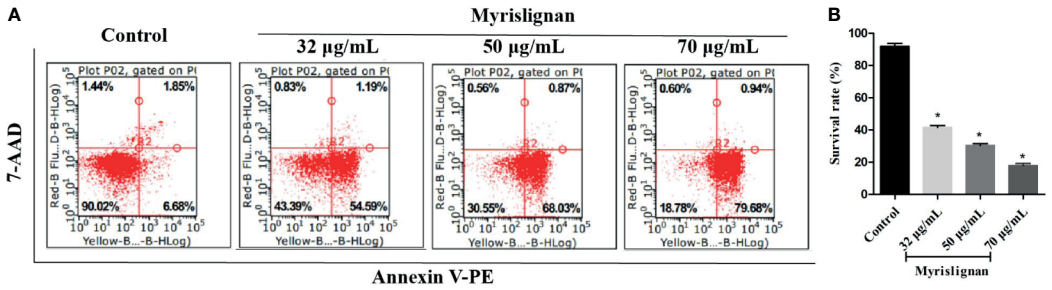

FIGURE 6 | Myrislignan induced cell death of tachyzoites. Myrislignan (32, 50 and 70 μg/mL) treatment induced a decline in the *T. gondii* survival rates of approximately 42.02% ± 1.29%, 26.83% ± 3.29% and 17.22 ± 1.37%, respectively. The survival rate in the control group was approximately 88.53% ± 1.31%. The representative figure is shown in **(A)**. The proportions of *T. gondii* surviving after treatment with myrislignan (32, 50 or 70 μg/mL) for 24 h are shown in **(B)**. *$p < 0.01$ compared with the parasite control.

exerting anti-obesity effect (Nguyen et al., 2010), inhibiting the activation of NF-kB signalling pathway, reducing the inflammatory response of macrophages induced by lipopolysaccharide, and protecting the liver from thioacetamide injury (Jin et al., 2012; Yang et al., 2018). In previous study, myrislignan exerted the anti-*T. gondii* activity by inhibiting its replication and invasion *in vitro*, and reduces the parasite burden in the tissues of infected mice. Our previous findings suggested myrislignan against *T. gondii* might be associated with *T. gondii* mitochondrial function (Zhang et al., 2019). In this study, we also explore the action mechanism of myrislignan against *T. gondii*, and it will provide ideas for the development of new types of anti-*T. gondii* compounds, and contribute to the structural modification and optimization of myrislignan. In agreement with previous work, deep-sequencing analysis of RNAs of *T. gondii* after incubated with myrislignan in different concentrations revealed significant changes in "oxidoreductase activity" and "electron transfer activity" of "catalytic activity" in the DEGs of *T. gondii* by GO enrichment analysis. KEGG pathway analysis showed that the DEGs were mainly associated with "oxidative phosphorylation". Furthermore, combined with SPR analysis, the DEG and high affinity proteins were enriched in the oxidation-reduction process, these indicated that myrislignan may have an anti-*T. gondii* activity by affecting the oxidation-reduction process of *T. gondii*.

In order to verify whether the anti-*Toxoplasma* effect of myrislignan is related to oxidation-reduction process of *T. gondii*, we examined the content of ROS and SOD. ROS is a by-product of aerobic metabolism, including superoxide anion, hydrogen peroxide and hydroxyl radical, which plays an important role in many biological processes (Schieber and Chandel, 2014). SOD is an important reductase widely existing in cells. It can promote the transformation of superoxide anion (O^{2-}) into hydrogen peroxide and oxygen, and is one of the most important antioxidants for parasite protozoa to maintain homeostasis (Miller, 2012; Wang et al., 2018). In *T. gondii*, SOD can not only protect *T. gondii* from oxidative damage, but also participate in the growth process of tachyzoite (Odberg-Ferragut et al., 2000). We investigated that myrislignan strikingly increased the ROS content in tachyzoites with time-dependent manner in 24 h of incubation, indicating the instability of the intracellular redox balance by myrislignan. Furthermore, the SOD activity of RH tachyzoites incubated with myrislignan and found that RH tachyzoites maintained survival by upregulating SOD activity, but did not increase as time. However, the ROS activity induced by myrislignan increased significantly in a time-dependent manner. Therefore, we conceived of the idea that myrislignan may destroy the physiological redox biological signal, thus interfering with the metabolism or proliferation of parasites. Taken together, the significant increase of ROS activity and the abnormal production of SOD indicated that tachyzoites were in an environment of imbalanced internal redox system caused by myrislignan, thus gradually inhibiting the growth of extracellular tachyzoites.

According to our previous study, myrislignan against *T. gondii* might affect *T. gondii* mitochondrial function (Zhang et al., 2019). Mitochondria are not only the main site of ROS production, but also the main target of oxidative damage. Herein, we also indicated myrislignan increased the ROS, destroyed the oxidant-antioxidant homeostasis of tachyzoites, then led to oxidative stress. Taken together, we infer that myrislignan may reduce the mitochondrial membrane potential and ATP level of *T. gondii* and damage mitochondrial function by interfering the redox- antioxidant process of *T. gondii*. In addition, *T. gondii* is different from mammals, it has only one mitochondrion (Melo et al., 2000). The mitochondrial damage may lead to autophagy. Furthermore, in order to explore the effect of redox injury on *T. gondii*, TEM analysis confirmed the presence of autophagy-like structures. Autophagosome is formed by cup-shaped single membrane structure, also known as separation membrane or pre-autophagosome. The maturation of this structure is the conversion of the ATG8 from a diffuse cytosolic form (ATG8) to a lipidated form (ATG8-PE), which associates with the isolated membrane and specially localizes on the inner autophagosome membrane. Thus, ATG8 is a widely used marker for autophagy (Ghosh et al., 2012; Besteiro, 2017). Therefore, we detect the accumulation of TgATG8-PE by western blot analysis on the autophagy of *T. gondii* after incubation with myrislignan (Besteiro et al., 2011; Gao et al., 2014). Myrislignan caused a dose-dependent increase in TgATG8-PE protein levels in *T. gondii*, indicating activation of autophagy. To further confirm that myrislignan induced autophagy, MDC staining was used to stain myrislignan treated *T. gondii*. Abundant autophagic vacuoles appeared in the

cytoplasm of *T. gondii*. Recently, some compounds have been found to cause *T. gondii* death by activating autophagy, such as monensin, the data indicated that autophagy as a potentially important mode of cell death of protozoan parasites in response to drugs (Lavine and Arrizabalaga, 2012). Moreover, myrislignan induced death in *T. gondii* by flow cytometric assessment. Given the results, myrislignan may induce autophagy by damaging the oxidation-reduction process, eventually leading to *T. gondii* death.

In conclusion, our results demonstrated that myrislignan can interfere with the redox homeostasis of the parasites, activate autophagy, and leading to *T. gondii* metabolic disorder and death, but the specific mechanism of action needs to explore.

DATA AVAILABILITY STATEMENT

The datasets presented in this study can be found in online repositories. The names of the repository/repositories and accession number(s) can be found below: NCBI PRJNA753595.

AUTHOR CONTRIBUTIONS

HS and JC revised the manuscript. JYZ directed the project. JLZ supervised the experiments and wrote the manuscript. BL, KL, BY, LG, XW, and CS reviewed the manuscript. All authors contributed to the article and approved the submitted version.

FUNDING

This work was supported by Natural Science Fund of Gansu Provincial Science and Technology Project (20JR10RA023), the Science and Technology Project Fund of Gansu Province-Fundamental Research Innovative Groups (18JR3RA397) and the earmarked fund for the China Agriculture Research System (CARS-37).

ACKNOWLEDGMENTS

We thank Dr. Xingquan Zhu for providing the *T. gondii* RH strain and Dr. Honglin Jia for providing the antibodies against *T. gondii* ATG8 and tubulin.

SUPPLEMENTARY MATERIAL

The Supplementary Material for this article can be found online at: https://www.frontiersin.org/articles/10.3389/fcimb.2021.730222/full#supplementary-material

Supplementary Data Sheet 1 | The qRT-PCR primers used for RNA-seq validation.

Supplementary Data Sheet 2 | The specific binding proteins of *T. gondii* were captured by myrislignan as determined using SPR.

REFERENCES

Ahmadpour, E., Daryani, A., Sharif, M., Sarvi, S., Aarabi, M., Mizani, A., et al. (2014). Toxoplasmosis in Immunocompromised Patients in Iran: A Systematic Review and Meta-Analysis. *J. Infect. Develop. Countries.* 8, 1503–1510. doi: 10.3855/jidc.4796

Besteiro, S. (2017). Autophagy in Apicomplexan Parasites. *Curr. Opin. Microbiol.* 40, 14–20. doi: 10.1016/j.mib.2017.10.008

Besteiro, S., Brooks, C. F., Striepen, B., and Dubremetz, J. F. (2011). Autophagy Protein Atg3 Is Essential for Maintaining Mitochondrial Integrity and for Normal Intracellular Development of *Toxoplasma Gondii* Tachyzoites. *PloS Pathog.* 7, e1002416–437. doi: 10.1371/journal.ppat.1002416

Chen, Q. W., Dong, K., Qin, H. X., Yang, Y. K., He, J. L., Li, J., et al. (2018). The Direct and Indirect Inhibition Effects of Resveratrol Against *Toxoplasma Gondii* Tachyzoites *In Vitro*. *Antimicrob. Agents Chemother.* 63 (3), e01233–e01218. doi: 10.1128/AAC.01233-18

Choi, W. H., and Lee, I. A. (2019). The Mechanism of Action of Ursolic Acid as a Potential Anti-Toxoplasmosis Agent, and Its Immunomodulatory Effects. *Pathogens* (Basel, Switzerland) 8.

Fallahi, S., Rostami, A., Nourollahpour Shiadeh, M., Behniafar, H., and Paktinat, S. (2018). An Updated Literature Review on Maternal-Fetal and Reproductive Disorders of *Toxoplasma Gondii* Infection. *J. Gynecol. Obstetr. Hum. Reprod.* 47, 133–140. doi: 10.1016/j.jogoh.2017.12.003

Gao, D., Zhang, J., Zhao, J., Wen, H., Pan, J., Zhang, S., et al. (2014). Autophagy Activated by *Toxoplasma Gondii* Infection in Turn Facilitates Toxoplasma Gondii Proliferation. *Parasitol. Res.* 113, 2053–2058. doi: 10.1007/s00436-014-3853-5

Ghosh, D., Walton, J. L., Roepe, P. D., and Sinai, A. P.. (2012). Autophagy Is a Cell Death Mechanism in Toxoplasma gondii. *Cell. Microbiol.* 14 (4), 589-607.

Giovati, L., Santinoli, C., Mangia, C., Vismarra, A., Belletti, S., D'Adda, T., et al. (2018). Novel Activity of a Synthetic Decapeptide Against *Toxoplasma Gondii* Tachyzoites. *Front. Microbiol.* 9, 753. doi: 10.3389/fmicb.2018.00753

He, J. J., Ma, J., Wang, J. L., Zhang, F. K., Li, J. X., Zhai, B. T., et al. (2019). Global Transcriptome Profiling of Multiple Porcine Organs Reveals *Toxoplasma Gondii*-Induced Transcriptional Landscapes. *Front. Immunol.* 10, 1531. doi: 10.3389/fimmu.2019.01531

Jin, H., Zhu, Z. G., Yu, P. J., Wang, G. F., Zhang, J. Y., Li, J. R., et al. (2012). Myrislignan Attenuates Lipopolysaccharide-Induced Inflammation Reaction in Murine Macrophage Cells Through Inhibition of NF-kappaB Signalling Pathway Activation. *Phytother. Res.: PTR.* 26, 1320–1326. doi: 10.1002/ptr.3707

Kong-Hap, M. A., Mouammine, A., Daher, W., Berry, L., Lebrun, M., Dubremetz, J. F., et al. (2013). Regulation of ATG8 Membrane Association by ATG4 in the Parasitic Protist *Toxoplasma Gondii*. *Autophagy* 9, 1334–1348. doi: 10.4161/auto.25189

Lavine, M. D., and Arrizabalaga, G. (2012). Analysis of Monensin Sensitivity in *Toxoplasma Gondii* Reveals Autophagy as a Mechanism for Drug Induced Death. *PloS One* 7, e42107. doi: 10.1371/journal.pone.0042107

Lee, Y. J., Song, H. O., Lee, Y. H., Ryu, J. S., and Ahn, M. H. (2013). Proliferation of *Toxoplasma Gondii* Suppresses Host Cell Autophagy. *Korean. J. Parasitol.* 51, 279–287. doi: 10.3347/kjp.2013.51.3.279

Ling, Y. M., Shaw, M. H., Ayala, C., Coppens, I., Taylor, G. A., Ferguson, D. J., et al. (2006). Vacuolar and Plasma Membrane Stripping and Autophagic Elimination of *Toxoplasma Gondii* in Primed Effector Macrophages. *J. Exp. Med.* 203, 2063–2071. doi: 10.1084/jem.20061318

Lu, X., Yang, L., Chen, J., Zhou, J., Tang, X., Zhu, Y., et al. (2017). The Action and Mechanism of Myrislignan on A549 Cells *In Vitro* and *In Vivo*. *J. Natural Medicines* 71, 76–85. doi: 10.1007/s11418-016-1029-6

Melo, E. J., Attias, M., and De Souza, W. (2000). The Single Mitochondrion of Tachyzoites of *Toxoplasma Gondii*. *J. Struct. Biol.* 130, 27–33. doi: 10.1006/jsbi.2000.4228

Miller, A. F. (2012). Superoxide Dismutases: Ancient Enzymes and New Insights. *FEBS Lett.* 586 (5), 585–595. doi: 10.1016/j.febslet.2011.10.048

Nguyen, P. H., Le, T. V., Kang, H. W., Chae, J., Kim, S. K., Kwon, K. I., et al. (2010). AMP-Activated Protein Kinase (AMPK) Activators From Myristica Fragrans (Nutmeg) and Their Anti-Obesity Effect. *Bioorg. Med. Chem. Lett.* 20, 4128–4131. doi: 10.1016/j.bmcl.2010.05.067

Odberg-Ferragut, C., Renault, J. P., Viscogliosi, E., Toursel, C., Briche, I., Engels, A., et al. (2000). Molecular Cloning, Expression Analysis and Iron Metal Cofactor Characterisation of a Superoxide Dismutase From *Toxoplasma Gondii*. *Mol. Biochem. Parasitol.* 106, 121–129. doi: 10.1016/S0166-6851(99)00211-X

Schieber, M., and Chandel, N. S. (2014). ROS Function in Redox Signaling and Oxidative Stress. *Curr. Biol.: CB.* 24, R453–R462. doi: 10.1016/j.cub.2014.03.034

Sepulveda-Arias, J. C., Veloza, L. A., and Mantilla-Muriel, L. E. (2014). Anti-*Toxoplasma* Activity of Natural Products: A Review. *Recent Pat. Antiinfect. Drug Discovery* 9, 186–194. doi: 10.2174/1574891X10666150410120321

Si, H., Xu, C., Zhang, J., Zhang, X., Li, B., Zhou, X., et al. (2018). Licochalcone A: An Effective and Low-Toxicity Compound Against *Toxoplasma Gondii In Vitro* and *In Vivo*. *Int. J. Parasitol.: Drugs Drug Resist.* 8, 238–245. doi: 10.1016/j.ijpddr.2018.02.006

Wang, Y., Branicky, R., Noë, A., and Hekimi, S. (2018). Superoxide Dismutases: Dual Roles in Controlling ROS Damage and Regulating ROS Signaling. *J. Cell Biol.* 217, 1915–1928. doi: 10.1083/jcb.201708007

Wang, Y., Karnataki, A., Parsons, M., Weiss, L. M., and Orlofsky, A. (2010). 3-Methyladenine Blocks *Toxoplasma Gondii* Division Prior to Centrosome Replication. *Mol. Biochem. Parasitol.* 173, 142–153. doi: 10.1016/j.molbiopara.2010.05.020

Weiss, L. M., and Kim, K. (2013). *Toxoplasma Gondii: The Model Apicomplexan—Perspectives and Methods*. *2nd Edn* (Amsterdam: Elsevier).

Yang, X. N., Liu, X. M., Fang, J. H., Zhu, X., Yang, X. W., Xiao, X. R., et al. (2018). Pparα Mediates the Hepatoprotective Effects of Nutmeg. *J. Proteome Res.* 17, 1887–1897. doi: 10.1021/acs.jproteome.7b00901

Zhang, J., Si, H., Li, B., Zhou, X., and Zhang, J. (2019). Myrislignan Exhibits Activities Against *Toxoplasma Gondii* RH Strain by Triggering Mitochondrial Dysfunction. *Front. Microbiol.* 10, 2152. doi: 10.3389/fmicb.2019.02152

Zhang, J., Si, H., Lv, K., Qiu, Y., Sun, J., Bai, Y., et al. (2021). Licarin-B Exhibits Activity Against the Toxoplasma Gondii RH Strain by Damaging Mitochondria and Activating Autophagy. *Front. Cell Dev. Biol.* 9, 684393. doi: 10.3389/fcell.2021.684393

Conflict of Interest: The authors declare that the research was conducted in the absence of any commercial or financial relationships that could be construed as a potential conflict of interest.

Publisher's Note: All claims expressed in this article are solely those of the authors and do not necessarily represent those of their affiliated organizations, or those of the publisher, the editors and the reviewers. Any product that may be evaluated in this article, or claim that may be made by its manufacturer, is not guaranteed or endorsed by the publisher.

frontiers in Cellular and Infection Microbiology

ORIGINAL RESEARCH
published: 06 September 2021
doi: 10.3389/fcimb.2021.713873

Prevalence and Characterization of *Cryptosporidium* Species in Tibetan Antelope (*Pantholops hodgsonii*)

Si-Yuan Qin[1,2†], He-Ting Sun[2†], Chuang Lyu[3,4†], Jun-Hui Zhu[1], Zhen-Jun Wang[1], Tao Ma[1], Quan Zhao[5], Yun-Gang Lan[1*] and Wen-Qi He[1*]*

[1] Key Laboratory of Zoonosis Research, Ministry of Education, College of Veterinary Medicine, Jilin University, Changchun, China, [2] General Monitoring Station for Wildlife-Borne Infectious Diseases, State Forestry and Grass Administration, Shenyang, China, [3] Animal Health Center, Shandong New Hope Liuhe Group Co. Ltd., Qingdao, China, [4] Animal Health Center, Qingdao Jiazhi Biotechnology Co. Ltd., Qingdao, China, [5] College of Life Science, Changchun Sci-Tech University, Shuangyang, China

OPEN ACCESS

Edited by:
Ehsan Ahmadpour, Tabriz University of Medical Sciences, Iran

Reviewed by:
Hongxuan He, Institute of Zoology, Chinese Academy of Sciences (CAS), China
Zhijun Hou, Northeast Forestry University, China
SeyedMousa Motavallihaghi, Hamadan University of Medical Sciences, Iran

***Correspondence:**
Quan Zhao
zhaoquan0825@163.com
Yun-Gang Lan
lanyungang@jlu.edu.cn
Wen-Qi He
hewq@jlu.edu.cn

[†]These authors have contributed equally to this work

Specialty section:
This article was submitted to Clinical Microbiology, a section of the journal Frontiers in Cellular and Infection Microbiology

Received: *24 May 2021*
Accepted: *09 August 2021*
Published: *06 September 2021*

Citation:
Qin S-Y, Sun H-T, Lyu C, Zhu J-H, Wang Z-J, Ma T, Zhao Q, Lan Y-G and He W-Q (2021) Prevalence and Characterization of Cryptosporidium Species in Tibetan Antelope (Pantholops hodgsonii). Front. Cell. Infect. Microbiol. 11:713873. doi: 10.3389/fcimb.2021.713873

Cryptosporidium is an enteric *apicomplexan* parasite, which can infect multiple mammals including livestock and wildlife. Tibetan Antelope (*Pantholops hodgsonii*) is one of the most famous wildlife species, that belongs to the first class protected wild animals in China. However, it has not been known whether Tibetan Antelope is infected with *Cryptosporidium* so far. The objective of the present study was to determine the prevalence and characterization of *Cryptosporidium* species infection in Tibetan Antelope and the corresponding species by using molecular biological method. In the current study, a total of 627 fecal samples were randomly collected from Tibetan Antelope in the Tibet Autonomous Region (2019–2020), and were examined by PCR amplification of the small subunit ribosomal RNA (SSU rRNA) gene. Among 627 samples, 19 (3.03%, 19/627) were examined as *Cryptosporidium*-positive, with 7 (2.33%, 7/300) in females and 12 (3.67%, 12/327) in males. The analysis of SSU rRNA gene sequence suggested that only two *Cryptosporidium* species, namely, *C. xiaoi* and *C. ubiquitum*, were identified in this study. This is the first evidence for an existence of *Cryptosporidium* in Tibetan Antelope. These findings extend the host range for *Cryptosporidium* spp. and also provide important data support for prevention and control of *Cryptosporidium* infection in Tibetan Antelope.

Keywords: *Cryptosporidium*, Tibetan antelope (*Pantholops hodgsonii*), prevalence, characterization, PCR

INTRODUCTION

Cryptosporidium, the causative agent of cryptosporidiosis, causes an intestinal disease in a wide range of hosts worldwide, including wildlife, livestock, and humans. Human infection with *Cryptosporidium* is usually through a close contact with the infected animals or consuming contaminated water or food (Rossignol, 2010). At least 38 species and over 70 genotypes of *Cryptosporidium* can infect humans and animals (Deng et al., 2020). Among them, more than 20 have been considered as zoonotic potential risks, including *C. hominis*, *C. parvum*, *C. meleagridis*, *C. felis*, *C. canis*, *C. cuniculus*, *C. ubiquitum*, *C. viatorum*, *C. muris*, *C. suis*, *C. fayeri*, *C. andersoni*,

C. bovis, *C. scrofarum*, *C. xiaoi*, *C. tyzzeri*, *C. erinaceid*, and *C. horse*, *C. skunk*, and *C. chipmunk* I genotype (Ren et al., 2012; Adamu et al., 2014; Koehler et al., 2014; Kváč et al., 2014; Ma et al., 2014; Qi et al., 2014; Qin et al., 2014; Yang et al., 2014; Galuppi et al., 2015; Lin et al., 2015; Yan et al., 2017; Firoozi et al., 2019; Takaki et al., 2020; Xu et al., 2020). *C. hominis* and *C. parvum* were most frequently found in human. *C. xiaoi* was generally considered as *C. bovis*-like genotype or *C. bovis* when Fayer and Santín identified it as a new species in 2009 based on morphology and molecular methods (Fayer and Santín, 2009).

Since *C. xiaoi* and *C. ubiquitum* were recognized firstly in sheep, many researches were focused on the prevalence of *C. xiaoi* and *C. ubiquitum* in humans and other animals which have closer relationship with the sheep like bovine and cervine. To date, *C. xiaoi* infection in sheep has been reported in many countries, including Ireland, Kuwait, Australia, Norway, Spain, France, Greece, Egypt, Tanzania, Jordan, Poland, Ghana, and Iran (Díaz et al., 2010; Robertson et al., 2010; Yang et al., 2011; Rieux et al., 2013; Mahfouz et al., 2014; Tzanidakis et al., 2014; Parsons et al., 2015; Hijjawi et al., 2016; Mirhashemi et al., 2016; Kaupke et al., 2017; Squire et al., 2017; Majeed et al., 2018; Firoozi et al., 2019). In addition, the pertinent literatures about *C. ubiquitum* infection in sheep were derived from Ireland, Kuwait, Australia, Spain, Greece, Poland, Ghana, Iran, and Algeria (Díaz et al., 2010; Yang et al., 2011; Tzanidakis et al., 2014; Mirhashemi et al., 2016; Kaupke et al., 2017; Squire et al., 2017; Baroudi et al., 2018; Majeed et al., 2018; Firoozi et al., 2019). In China, *C. xiaoi* and *C. ubiquitum* were also found in sheep in Anhui, Xinjiang, Jilin, Inner Mongolia, Ningxia, Shandong, Shanghai, Henan, Qinghai, and Beijing (Mi et al., 2018; Qi et al., 2019), Tibetan sheep in Qinghai (Li et al., 2016), and goat in Guangdong, Hubei, Shandong, Shanghai, Henan, Chongqing, Shaanxi (Mi et al., 2014; Wang et al., 2014; Peng et al., 2016). Interestingly, *C. xiaoi* and *C. ubiquitum* have also been occasionally found in yak (Ma et al., 2014). The infection of *C. xiaoi* and *C. ubiquitum* in hosts is usually asymptomatic. However, the infection occasionally causes diarrhea and weight loss (Santín, 2013). More importantly, *C. xiaoi* is also found in HIV/AIDS patients (Adamu et al., 2014), and *C. ubiquitum*, previously known as the cervine genotype, has been emerging as another major zoonotic species that infects persons (Li et al., 2014), thus posing a risk to public health. Therefore, *C. xiaoi* and *C. ubiquitum* are of public health concern because of its wide geographic distribution and broad host range.

China has abundant biodiversity resources. Tibetan Antelope (*Pantholops hodgsonii*) is one of the most important wild animal species, which is a very important part of the natural ecology in Qinghai-tibet plateau (Peng et al., 2018). In 1981, China had accessed to the convention on international trade about endangered species of wild fauna and flora, in which the Tibetan antelope was classified into appendix I species (http://www.iucnredlist.org/). Since 1988, the Tibetan Antelope was identified as a first-grade state protection of wildlife (http://www.forestry.gov.cn/main/3954/content-1063883.html). However, the information for this pathogen infection in Tibetan Antelope is limited. Importantly, there has been no available information concerning *Cryptosporidium* infection in Tibetan Antelope. Therefore, the objective of the present study was to molecularly determine the prevalence and characterization of *Cryptosporidium* species in Tibetan Antelope in Tibet Autonomous Region, China.

MATERIALS AND METHODS

Specimen Collection

A total of 627 fecal samples of Tibetan Antelope were collected from Nyima County, Shuanghu County, Shenza County, and Baingoin County in Tibet Autonomous Region of China in 2019 and 2020 (**Figure 1**). A fresh fecal sample (approximately 5 g) for each Tibetan Antelope was collected from the ground using sterile gloves after defecation, and then was placed into ice boxes and sent to the laboratory. Tibetan Antelope with horns are males, otherwise, are females. The information regarding sampling time, region, and gender were recorded. This study was approved by the Ethics Committee of Jilin University.

DNA Extraction and PCR Amplification

The fecal samples were diluted with 0.9% normal saline and filtered through 100-mesh stainless steel sieve. The filtrate was centrifuged at 4000 rpm/min for 5 min to enrich *Cryptosporidium* eggs. Genomic DNA was extracted from approximately 200 mg of each stool specimen using the E.Z.N.A.® Stool DNA Kit (Omega Biotek Inc., Norcross, GA, USA) according to the manufacturer's instructions, and then were stored at -20°C prior to a PCR analysis. *Cryptosporidium* prevalence and their species/genotypes were identified by nested PCR amplification of the small subunit ribosomal RNA (SSU

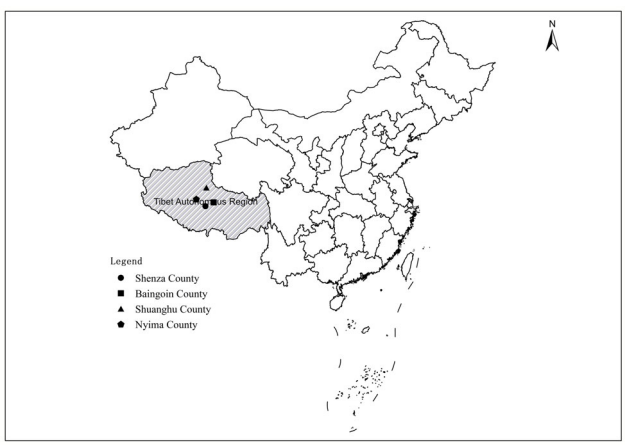

FIGURE 1 | A map of Tibet Autonomous Region, China showing the geographical regions in Nyima County, Shuanghu County, Shenza County, and Baingoin County, in which Tibetan Antelope were sampled.

rRNA) gene, using the primers 18SiCF2 (5′-GACATATCA TTCAAGTTTCTGACC-3′) and 18SiCR2 (5′-CTGAAGG AGTAAGGAACAACC-3′) that amplified a fragment of about 760 bp in length in the first round PCR and the primers 18SiCF1 (5′-CCTATCAGCTTTAGACGGTAGG-3′) and 18SiCR1 (5′-TCTAAGAATTTCACCTCTGACTG-3′) that amplified a fragment of about 590 bp in length in the second round PCR (Qin et al., 2014; Koehler et al., 2018). The positive and negative controls were included in each test. The second PCR products were observed using UV light after electrophoresis at a 1.5% (m/V) agarose gel containing ethidium bromide.

Sequence and Phylogenetic Analyses

The positive PCR products were sent to Sangon Biotech Company (Shanghai, China) for sequencing. The PCR products were sequenced on both strands to guarantee the accuracy of the sequence. A new PCR product was subjected to sequencing when single nucleotide substitution, insertion, or deletion was found in the former sequencing. The alignment and analysis for the SSU rRNA nucleotide sequences and reference sequences were performed using the Clustal X 1.83 program and Basic Local Alignment Search Tool (BLAST) (https://blast.ncbi.nlm.nih.gov), in order to determine the species of *Cryptosporidium*. The phylogenetic trees were reconstructed by MEGA 5.0 software using a neighbor-joining (NJ) method with a Kimura 2-parameter model (1,000 replicates). The representative nucleotide sequences were disposed to GenBank with accession numbers MZ220364 and MZ220365.

Statistical Analysis

To assess the possible risk factors (gender, region, and year) associated with an exposure to *Cryptosporidium* infection in Tibetan Antelope, a multivariable logistic regression analysis was carried out using the PASW Statistics 18.0 (SPSS, Inc., IBM Corporation, Somers, NY) (Zhao et al., 2013). When independent variables were contained in the multivariable logistic regression model, probability (P) value < 0.05 was considered as statistically significant between levels within factors and interactions, and their odd ratio (OR) and 95% confidence interval (CI) were calculated.

RESULTS

Prevalence and Risk Factors of *Cryptosporidium*

In the present study, 19 (3.0%, 95% CI 1.7–4.4) out of 627 Tibetan Antelope fecal samples from Tibet Autonomous Region were tested as *Cryptosporidium*-positive by PCR amplification of the SSU rRNA gene. The prevalence of *Cryptosporidium* infection in Tibetan Antelope was 2.2% (7/322, 95% CI 0.6–3.8) in 2019, and 3.9% (12/305, 95% CI 0.6–3.8) in 2020 (**Table 1**). Male Tibetan Antelope had a higher prevalence (3.7%, 95% CI 1.7–5.7, 12/327) as compared to that of females (2.3%, 95% CI 0.6–4.0, 7/300) (**Table 1**). The prevalence of *Cryptosporidium* in Tibetan Antelope in Nyima County, Shenza County, Shuanghu County, and Baingoin County was 3.8% (7/182, 95% CI 1.1–6.6), 4.8% (10/209, 95% CI 1.9–7.7), 0.9% (1/103, 95% CI 0.0–2.9), and 0.8% (1/133, 95% CI 0.0–2.2), respectively (**Table 1**).

According to multivariable logistic regression, gender, sampling year, and region of Tibetan Antelope were not significant in the logistic regression analysis ($P > 0.05$) and left out of the final model (Hosmer and Lemeshow goodness of fit test $P = 1.00$). Therefore, gender, sampling year, and region of collecting samples were not considered as main risk factor to influence the seroprevalence significantly (**Table 1**).

Distribution and Phylogenetic Analysis of *Cryptosporidium*

In the present study, 19 samples were *Cryptosporidium*-positive tested based on the SSU rRNA gene (**Figure 2**). The analysis of SSU rRNA gene suggested that the samples were *C. xiaoi* (n = 7) and *C. ubiquitum* (n = 12) positive in investigated Tibetan Antelope (**Table 1** and **Figure 3**). *C. ubiquitum* is the predominant *Cryptosporidium* species, which was responsible for 63.2%. *C. xiaoi* was only found in Nyima County (n = 6) and Baingoin County (n = 1) in 2019, and *C. ubiquitum* was only identified in three counties (n = 1 in Nyima County; n = 10 in Shuanghu County; n = 1 in Shenza County) in 2020 (**Table 1**). Moreover, *C. xiaoi* and *C. ubiquitum* were identified in both males (n = 12) and females (n = 7) in present study (**Table 1**). The representative sequences of *C. xiaoi* showed 100% similarity

TABLE 1 | Prevalence and subtypes of *Cryptosporidium* infection in Tibetan Antelope (*Pantholops hodgsonii*) among different related factors.

Factor	Category	No. tested	No. positive	Prevalence(%) (95% CI)	*P* value	OR (95% CI)	Species/genotypes (no.)
Gender	Female	300	7	2.3 (0.6–4.0)	0.333	Reference	*Cryptosporidium ubiquitum* (2); *Cryptosporidium xiaoi* (5)
	Male	327	12	3.7 (1.7–5.7)		1.60 (0.62–4.11)	*Cryptosporidium ubiquitum* (10); *Cryptosporidium xiaoi* (2)
Sampling year	2019	322	7	2.2 (0.6–3.8)	0.205	Reference	*Cryptosporidium xiaoi* (7)
	2020	305	12	3.9 (1.8–6.1)		1.84 (0.72–4.75)	*Cryptosporidium ubiquitum* (12)
Region	Nyima County	182	7	3.8 (1.1–6.6)	0.160	5.28 (0.64–43.44)	*Cryptosporidium ubiquitum* (1); *Cryptosporidium xiaoi* (6)
	Shuanghu County	209	10	4.8 (1.9–7.7)		6.63 (0.84–52.43)	*Cryptosporidium ubiquitum* (10)
	Shenza County	103	1	0.9 (0.0–2.9)		1.29 (0.08–20.94)	*Cryptosporidium ubiquitum* (1)
	Baingoin County	133	1	0.8 (0.0–2.2)		Reference	*Cryptosporidium xiaoi* (1)
Total		627	19	3.0 (1.7–4.4)			*Cryptosporidium ubiquitum* (12); *Cryptosporidium xiaoi* (7)

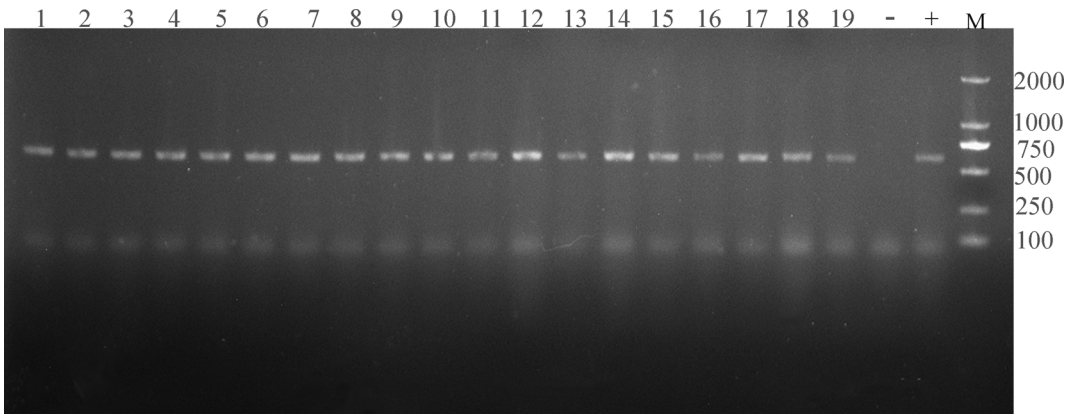

FIGURE 2 | The electropherogram of PCR amplification of SSU rRNA gene of *Cryptosporidium*. Lanes 1–19 represent TA3, TA9, TA12, TA33, TA61, TA94, TA99, TA103, TA203, TA215, TA217, TA220, TA224, TA230, TA231, TA236, TA241, TA258, and TA301, respectively (19 *Cryptosporidium*-positive samples); "-" represents negative control; "+" represents positive control; "M" represents DL2000 DNA marker.

with sequences of *C. xiaoi* (MH049731, KF907825). The representative sequences of *C. ubiquitum* were identical to the sequences of *C. ubiquitum* (MT044147, MK573335).

DISCUSSION

The overall *Cryptosporidium* prevalence was 3.03%, which was significantly lower than that in sheep and goats in Kuwait (9.71%, 54/556) (Majeed et al., 2018), Jordan (10.53%, 12/114) (Hijjawi et al., 2016), Poland (24.78%, 84/339) (Kaupke et al., 2017), Spain (5.9%, 33/58) (Díaz et al., 2018), sheep in Iran (9.1%) (Haghi et al., 2020), goat in Australia (27.2%) (Al-Habsi et al., 2017), and Norwegian sheep in Norway (15%) (Robertson et al., 2010). It is also lower than that in sheep and/or goats in many provinces of China, such as goats in Henan and Chongqing (3.48%, 44/1256) (Wang et al., 2014), Guangdong, Hubei, Shandong, and Shanghai (11.4%, 69/604) (Mi et al., 2014), Tibetan sheep in Qinghai (12.3%, 43/350) (Li et al., 2016), sheep in 10 provinces of China (28.5%, 295/1035) (Mi et al., 2018), but higher than that of sheep in Xinjiang (0.9%, 3/318) (Qi et al., 2019). In the present study, statistical analysis showed that there was no significant difference in *Cryptosporidium* prevalence with several risk factors ($P > 0.05$), suggesting that gender, sampling year, and region may not be crucial factors for *Cryptosporidium* infection in Tibetan Antelope. The difference in *Cryptosporidium* prevalence may be related to sampling position, sensitivity of the employed detection method, sample sizes, susceptibility in different animals, the pollution degree of environment caused by *Cryptosporidium* oocysts, as well as animal husbandry practices.

Cryptosporidium genus consists of more than 108 species/genotypes. To date, *C. ryanae, C. bovis, C. xiaoi, C. parvum, C. andersoni, C. meleagridis, C. baileyi, C. hominis, C. ubiquitum, C. scrofarum, Cryptosporidium cervine* genotype, sheep genotype I, and *Cryptosporidium* rat genotype II have been reported in various sheep worldwide (Wang et al., 2010; Sweeny et al., 2011; Silverlås et al., 2012; Rieux et al., 2013; Koinari et al., 2014; Yang et al., 2014; Koinari et al., 2014; Mirhashemi et al., 2016; Kaupke et al., 2017; Sqquire et al., 2017; Firoozi et al., 2019). However, only *C. xiaoi* and *C. ubiquitum* were identified in Tibetan Antelope in this study, thus suggesting the *C. xiaoi* and *C. ubiquitum* were epidemic in the investigated Tibetan Antelope in Tibet Autonomous Region. Moreover, the sequences of isolates from seven fecal samples carrying *C. xiaoi* shared 100% similarity with isolates from sheep in the Algeria (LC414392) and China (MH049731), goats in Poland (KY055403), and Tibetan sheep in China (KF907825), showing that the sequences of *C. xiaoi* from Tibetan Antelope have a certain correlation with sheep and goat in Algeria, Poland, and China. But the detailed transmission chain of *Cryptosporidium* in Tibetan Antelope should be conducted in-depth study in the future. Similarly, another sequence of the 12 isolates belonging to *C. ubiquitum* showed 100% similarity with an isolate from cattle in the India (MT044147), goats in Algeria (LC414387), and Tibetan sheep in China (MK573335), indicating that the sequences of *C. ubiquitum* from Tibetan Antelope have a connection with cattle, goat, and sheep in India, Algeria, and China. More importantly, *C. ubiquitum* and *C. xiaoi* were also found in other animals and even in HIV/AIDS patients (Adamu et al., 2014; Li et al., 2014). According to relevant literature reports, *C. ubiquitum* was identified as six subtype families (XIIa–XIIf) based on the 60-kDa glycoprotein (gp60) gene (Li et al., 2014). Among them, subtype XIIa of *C. ubiquitum* was found in ruminants worldwide, subtype families XIIb–XIId of *C. ubiquitum* were found in rodents in the United States, and XIIe and XIIf of *C. ubiquitum* were found in rodents in the Slovak Republic (Li et al., 2014). In addition, humans were found to be infected with subtypes XIIa and XIIb–XIId isolates of *C. ubiquitum* (Li et al., 2014). In the investigated regions, the population of Tibetan Antelope lived with other free-range animals on the same prairie, and shared with the same source

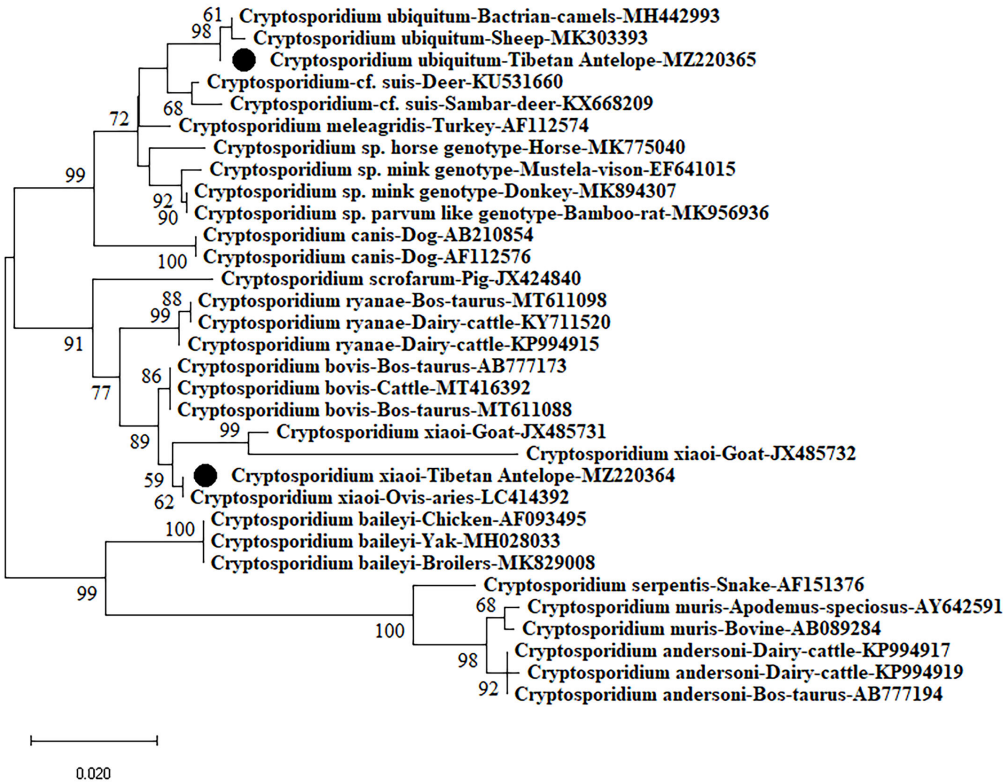

FIGURE 3 | Phylogenetic analyses of *Cryptosporidium* using neighbor-joining (NJ) method (Kimura 2-parameter model). Bootstrap values below 50% are not shown (1,000 replicates). *Cryptosporidium* isolates identified in the present study are indicated by solid circles.

of water, which showing the risk of *Cryptosporidium* transmission between domestic and wild animals. Contacting with sheep infected with *C. ubiquitum* and drinking water contaminated by wildlife infected could be sources of human infections (Li et al., 2014). These findings not only demonstrated that *Cryptosporidium* infection of Tibetan Antelope may result from nearby animals, local herdsmen, or polluted water source, but also suggested that the Tibetan Antelope might be one of the important resources transmitting *Cryptosporidium* to local people and other native animals, including goa, blue sheep, yak, takin, and wapiti.

In addition, the Tibetan Antelope freely lived in high altitude regions, and frequently moved in plenty of space. They can also contact with other animals. Moreover, the shedding of oocysts into environment by Tibetan Antelope becomes the most important resource for a transmission to other animals and humans. As is well-known, *Cryptosporidium* is widely regarded as the pathogen of livestock, poultry, companion animals, and wildlife, posing a threat to public health. Local Tibetan live a herding life for chronically, which result in contacting with wildlife and free-range livestock frequently. Local Tibetan occasionally drink water in the process of grazing. Drinking untreated water contaminated by wildlife might be a potential source of *Cryptosporidium* infecting local Tibetan in Tibet Autonomous Region. Thus, it is very important to take actions for protecting Tibetan Antelope, other free-range animals, and local Tibetan from infecting with *Cryptosporidium* and the infection status of pathogens (not only *Cryptosporidium*) in Tibetan Antelope should continue to be monitored in the future. Further studies will sample more Tibetan Antelope in different regions to determine the dynamics and full profiles of *Cryptosporidium* infection in Tibetan Antelope, to examine the infection status of the local Tibetans with *Cryptosporidium*, and to assess the zoonotic potential of *Cryptosporidium* from Tibetan Antelope.

CONCLUSIONS

This is the first report of *C. xiaoi* and *C. ubiquitum* infection in Tibetan Antelope worldwide. The overall prevalence of *Cryptosporidium* was 3.03%. The results also confirmed that *C. xiaoi* and *C. ubiquitum* were the most common *Cryptosporidium* species in Tibetan Antelope. Furthermore, *C. xiaoi* and *C. ubiquitum*, occasionally found in humans, were also identified in the Tibetan Antelope in this study. These results suggest the transmission of *Cryptosporidium* from Tibetan Antelope to other animals and/or humans should cause enough attention.

DATA AVAILABILITY STATEMENT

The datasets presented in this study can be found in online repositories. The names of the repository/repositories and accession number(s) can be found in the article/supplementary material.

ETHICS STATEMENT

This study was approved by the Ethics Committee of Jilin University.

AUTHOR CONTRIBUTIONS

QZ, Y-GL, and W-QH conceived and designed the study and critically revised the manuscript. S-YQ, H-TS, J-HZ, Z-JW, and TM collected the samples. S-YQ, H-TS, and CL performed the experiments, analyzed the data, and drafted the manuscript. All authors read and approved the final manuscript.

FUNDING

This work was supported by the "Independent research and development project from General Station of Forest and Grassland pest Management, National Forestry and Grassland Administration" (Grant No. LC-3-03), "Special Fund for Forestry Scientific Research in the Public Interest" (Grant No. 201504310), and "National Key Research and Development Program of China" (Grant no. 2017YFD0501706).

REFERENCES

Adamu, H., Petros, B., Zhang, G., Kassa, H., Amer, S., Ye, J., et al. (2014). Distribution and Clinical Manifestations of *Cryptosporidium* Species and Subtypes in HIV/AIDS Patients in Ethiopia. *PloS Negl. Trop. Dis.* 8 (4), e2831. doi: 10.1371/journal.pntd.0002831

Al-Habsi, K., Yang, R., Williams, A., Miller, D., Ryan, U., and Jacobson, C. (2017). Zoonotic *Cryptosporidium* and *Giardia* Shedding by Captured Rangeland Goats. *Vet. Parasitol. Reg Stud. Rep.* 7, 32–35. doi: 10.1016/j.vprsr.2016.11.006

Baroudi, D., Hakem, A., Adamu, H., Amer, S., Khelef, D., Adjou, K., et al. (2018). Zoonotic *Cryptosporidium* Species and Subtypes in Lambs and Goat Kids in Algeria. *Parasitol. Vectors* 11 (1), 582. doi: 10.1186/s13071-018-3172-2

Deng, L., Chai, Y. J., Luo, R., Yang, L. L., Yao, J. X., Zhong, Z. J., et al. (2020). Occurrence and Genetic Characteristics of *Cryptosporidium* Spp. And Enterocytozoon Bieneusi in Pet Red Squirrels (*Sciurus Vulgaris*) in China. *Sci. Rep.* 10, 1026. doi: 10.1038/s41598-020-57896-w

Díaz, P., Quílez, J., Robinson, G., Chalmers, R. M., Díez-Baños, P., and Morrondo, P. (2010). Identification of *Cryptosporidium* Xiaoi in Diarrhoeic Goat Kids (*Capra Hircus*) in Spain. *Vet. Parasitol.* 172, 132–134. doi: 10.1016/j.vetpar.2010.04.029

Díaz, P., Navarro, E., Prieto, A., Pérez-Creo, A., Viña, M., Díaz-Cao, J. M., et al (2018). Cryptosporidium species in post-weaned and adult sheep and goats from N.W. Spain: Public and animal health significance. *Vet. Parasitol.* 254, 1–5. doi: 10.1016/j.vetpar.2018.02.040

Fayer, R., and Santín, M. (2009). Cryptosporidium *Xiaoi* N. Sp. (Apicomplexa: Cryptosporidiidae) in Sheep (*Ovis Aries*). *Vet. Parasitol.* 164, 192–200. doi: 10.1016/j.vetpar.2009.05.011

Firoozi, Z., Sazmand, A., Zahedi, A., Astani, A., Fattahi-Bafghi, A., Kiani-Salmi, N., et al. (2019). Prevalence and Genotyping Identification of *Cryptosporidium* in Adult Ruminants in Central Iran. *Parasitol. Vectors* 12 (1), 510. doi: 10.1186/s13071-019-3759-2

Galuppi, R., Piva, S., Castagnetti, C., Iacono, E., Tanel, S., Pallaver, F., et al. (2015). Epidemiological Survey on *Cryptosporidium* in an Equine Perinatology Unit. *Vet. Parasitol.* 210, 10–18. doi: 10.1016/j.vetpar.2015.03.021

Haghi, M. M., Khorshidvand, Z., Khazaei, S., Foroughi-Parvar, F., Sarmadian, H., Barati, N., et al. (2020). *Cryptosporidium* Animal Species in Iran: A Systematic Review and Meta-Analysis. *Trop. Med. Health* 48, 97. doi: 10.1186/s41182-020-00278-9

Hijjawi, N., Mukbel, R., Yang, R., and Ryan, U. (2016). Genetic Characterization of *Cryptosporidium* in Animal and Human Isolates From Jordan. *Vet. Parasitol.* 228, 116–120. doi: 10.1016/j.vetpar.2016.08.015

Kaupke, A., Michalski, M. M., and Rzeżutka, A. (2017). Diversity of *Cryptosporidium* Species Occurring in Sheep and Goat Breeds Reared in Poland. *Parasitol. Res.* 116, 871–879. doi: 10.1007/s00436-016-5360-3

Koehler, A. V., Wang, T., Haydon, S. R., and Gasser, R. B. (2018). *Cryptosporidium* Viatorum From the Native Australian Swamp Rat Rattus Lutreolus - An Emerging Zoonotic Pathogen? *Int. J. Parasitol. Parasites Wildl* 7, 18–26. doi: 10.1016/j.ijppaw.2018.01.004

Koehler, A. V., Whipp, M. J., Haydon, S. R., and Gasser, R. B. (2014). Cryptosporidium *Cuniculus*–New Records in Human and Kangaroo in Australia. *Parasitol. Vectors* 7, 492. doi: 10.1186/s13071-014-0492-8

Koinari, M., Lymbery, A. J., and Ryan, U. M. (2014). *Cryptosporidium* Species in Sheep and Goats From Papua New Guinea. *Exp. Parasitol.* 141, 134–137. doi: 10.1016/j.exppara.2014.03.021

Kváč, M., Hofmannová, L., Hlásková, L., Květoňová, D., Vítovec, J., McEvoy, J., et al. (2014). Cryptosporidium *Erinacei* N. Sp. (Apicomplexa: Cryptosporidiidae) in Hedgehogs. *Vet. Parasitol.* 201, 9–17. doi: 10.1016/j.vetpar.2014.01.014

Li, P., Cai, J., Cai, M., Wu, W., Li, C., Lei, M., et al. (2016). Distribution of *Cryptosporidium* Species in Tibetan Sheep and Yaks in Qinghai, China. *Vet. Parasitol.* 215, 58–62. doi: 10.1016/j.vetpar.2015.11.009

Lin, Q., Wang, X. Y., Chen, J. W., Ding, L., and Zhao, G. H. (2015). *Cryptosporidium* Suis Infection in Post-Weaned and Adult Pigs in Shaanxi Province, Northwestern China. *Korean J. Parasitol.* 53, 113–117. doi: 10.3347/kjp.2015.53.1.113

Li, N., Xiao, L., Alderisio, K., Elwin, K., Cebelinski, E., Chalmers, R., et al. (2014). Subtyping *Cryptosporidium* Ubiquitum,a Zoonotic Pathogen Emerging in Humans. *Emerg. Infect. Dis.* 20, 217–224. doi: 10.3201/eid2002.121797

Ma, J., Cai, J., Ma, J., Feng, Y., and Xiao, L. (2014). Occurrence and Molecular Characterization of *Cryptosporidium* Spp. In Yaks (*Bos Grunniens*) in China. *Vet. Parasitol.* 202, 113–118. doi: 10.1016/j.vetpar.2014.03.030

Mahfouz, M. E., Mira, N., and Amer, S. (2014). Prevalence and Genotyping of *Cryptosporidium* Spp. In Farm Animals in Egypt. *J. Vet. Med. Sci.* 76, 1569–1575. doi: 10.1292/jvms.14-0272

Majeed, Q. A. H., El-Azazy, O. M. E., Abdou, N. M. I., Al-Aal, Z. A., El-Kabbany, A. I., Tahrani, L. M. A., et al. (2018). Epidemiological Observations on Cryptosporidiosis and Molecular Characterization of *Cryptosporidium* Spp. In Sheep and Goats in Kuwait. *Parasitol. Res.* 117, 1631–1636. doi: 10.1007/s00436-018-5847-1

Mirhashemi, M. E., Zintl, A., Grant, T., Lucy, F., Mulcahy, G., and De Waal, T. (2016). Molecular Epidemiology of *Cryptosporidium* Species in Livestock in Ireland. *Vet. Parasitol.* 216, 18–22. doi: 10.1016/j.vetpar.2015.12.002

Mi, R., Wang, X., Huang, Y., Mu, G., Zhang, Y., Jia, H., et al. (2018). Sheep as a Potential Source of Zoonotic Cryptosporidiosis in China. *Appl. Environ. Microbiol.* 84, e00868–e00818. doi: 10.1128/AEM.00868-18

Mi, R., Wang, X., Huang, Y., Zhou, P., Liu, Y., Chen, Y., et al. (2014). Prevalence and Molecular Characterization of *Cryptosporidium* in Goats Across Four Provincial Level Areas in China. *PLoS One* 9, e111164. doi: 10.1371/journal.pone.0111164

Parsons, M. B., Travis, D., Lonsdorf, E. V., Lipende, I., Roellig, D. M., Collins, A., et al. (2015). Epidemiology and Molecular Characterization of *Cryptosporidium* Spp. In Humans, Wild Primates, and Domesticated Animals in the Greater Gombe Ecosystem, Tanzania. *PloS Negl. Trop. Dis.* 9, e0003529. doi: 10.1371/journal.pntd.0003529

Peng, P., Qin, S. Y., Sun, H. T., Xie, L. H., Chu, D., Geng, H. D., et al. (2018). Prevalence and Prevention and Control Strategy of Caprine Contagious

Pleuropneumonia in Tibetan Antelope in Nagqu Region of Tibet, China. *Chin. J. Wildlife* 39, 972–977. doi: 10.19711/j.cnki.issn2310-1490.20180723.001 (in Chinese)

Peng, X. Q., Tian, G. R., Ren, G. J., Yu, Z. Q., Lok, J. B., Zhang, L. X., et al. (2016). Infection Rate of Giardia Duodenalis, *Cryptosporidium* Spp. And Enterocytozoon Bieneusi in Cashmere, Dairy and Meat Goats in China. *Infect. Genet. Evol.* 41, 26–31. doi: 10.1016/j.meegid.2016.03.021

Qi, M., Huang, L., Wang, R., Xiao, L., Xu, L., Li, J., et al. (2014). Natural Infection of *Cryptosporidium* Muris in Ostriches (*Struthio Camelus*). *Vet. Parasitol.* 205, 518–522. doi: 10.1016/j.vetpar.2014.06.035

Qin, S. Y., Zhang, X. X., Zhao, G. H., Zhou, D. H., Yin, M. Y., Zhao, Q., et al. (2014). First Report of *Cryptosporidium* Spp. In White Yaks in China. *Parasitol. Vectors* 7, 230. doi: 10.1186/1756-3305-7-230

Qi, M., Zhang, Z., Zhao, A., Jing, B., Guan, G., Luo, J., et al. (2019). Distribution and Molecular Characterization of *Cryptosporidium* Spp., Giardia Duodenalis, and *Enterocytozoon Bieneusi* Amongst Grazing Adult Sheep in Xinjiang, China. *Parasitol. Int.* 71, 80–86. doi: 10.1016/j.parint.2019.04.006

Ren, X., Zhao, J., Zhang, L., Ning, C., Jian, F., Wang, R., et al. (2012). Cryptosporidium *Tyzzeri* N. Sp. (Apicomplexa: Cryptosporidiidae) in Domestic Mice (*Mus Musculus*). *Exp. Parasitol.* 130, 274–281. doi: 10.1016/j.exppara.2011.07.012

Rieux, A., Paraud, C., Pors, I., and Chartier, C. (2013). Molecular Characterization of *Cryptosporidium* Spp. In Pre-Weaned Kids in a Dairy Goat Farm in Western France. *Vet. Parasitol.* 192, 268–272. doi: 10.1016/j.vetpar.2012.11.008

Robertson, L. J., Gjerde, B. K., and Furuseth Hansen, E. (2010). The Zoonotic Potential of Giardia and *Cryptosporidium* in Norwegian Sheep: A Longitudinal Investigation of 6 Flocks of Lambs. *Vet. Parasitol.* 171, 140–145. doi: 10.1016/j.vetpar.2010.03.014

Rossignol, J. F. (2010). *Cryptosporidium* and Giardia: Treatment Options and Prospects for New Drugs. *Exp. Parasitol.* 124, 45–53. doi: 10.1016/j.exppara.2009.07.005

Santín, M. (2013). Clinical and Subclinical Infections With *Cryptosporidium* in Animals. *N. Z Vet. J.* 61, 1–10. doi: 10.1080/00480169.2012.731681

Silverlås, C., Mattsson, J. G., Insulander, M., and Lebbad, M. (2012). Zoonotic Transmission of *Cryptosporidium* Meleagridis on an Organic Swedish Farm. *Int. J. Parasitol.* 42, 963–967. doi: 10.1016/j.ijpara.2012.08.008

Squire, S. A., Yang, R., Robertson, I., Ayi, I., and Ryan, U. (2017). Molecular Characterization of *Cryptosporidium* and Giardia in Farmers and Their Ruminant Livestock From the Coastal Savannah Zone of Ghana. *Infect. Genet. Evol.* 55, 236–243. doi: 10.1016/j.meegid.2017.09.025

Sweeny, J. P., Ryan, U. M., Robertson, I. D., Yang, R., Bell, K., and Jacobson, C. (2011). Longitudinal Investigation of Protozoan Parasites in Meat Lamb Farms in Southern Western Australia. *Prev. Vet. Med.* 101, 192–203. doi: 10.1016/j.prevetmed.2011.05.016

Takaki, Y., Takami, Y., Watanabe, T., Nakaya, T., and Murakoshi, F. (2020). Molecular Identification of *Cryptosporidium* Isolates From Ill Exotic Pet Animals in Japan Including a New Subtype in *Cryptosporidium* Fayeri. *Vet. Parasitol. Reg Stud. Rep.* 21, 100430. doi: 10.1016/j.vprsr.2020.100430

Tzanidakis, N., Sotiraki, S., Claerebout, E., Ehsan, A., Voutzourakis, N., Kostopoulou, D., et al. (2014). Occurrence and Molecular Characterization of Giardia Duodenalis and *Cryptosporidium* Spp. In Sheep and Goats Reared Under Dairy Husbandry Systems in Greece. *Parasite* 21, 45. doi: 10.1051/parasite/2014048

Wang, Y., Feng, Y., Cui, B., Jian, F., Ning, C., Wang, R., et al. (2010). Cervine Genotype is the Major *Cryptosporidium* Genotype in Sheep in China. *Parasitol. Res.* 106, 341–347. doi: 10.1007/s00436-009-1664-x

Wang, R., Li, G., Cui, B., Huang, J., Cui, Z., Zhang, S., et al. (2014). Prevalence, Molecular Characterization and Zoonotic Potential of *Cryptosporidium* Spp. In Goats in Henan and Chongqing, China. *Exp. Parasitol.* 142, 11–16. doi: 10.1016/j.exppara.2014.04.001

Xu, N., Liu, H., Jiang, Y. Y., Yin, J. H., Yuan, Z. Y., Shen, Y. J., et al. (2020). First Report of *Cryptosporidium* Viatorum and Cryptosporidium *Occultus* in Humans in China, and of the Unique Novel *C. Viatorum* Subtype XVaA3h. *BMC Infect. Dis.* 20, 16. doi: 10.1186/s12879-019-4693-9

Yan, W., Alderisio, K., Roellig, D. M., Elwin, K., Chalmers, R. M., Yang, F., et al. (2017). Subtype Analysis of Zoonotic Pathogen *Cryptosporidium* Skunk Genotype. *Infect. Genet. Evol.* 55, 20–25. doi: 10.1016/j.meegid.2017.08.023

Yang, R., Fenwick, S., Potter, A., Ng, J., and Ryan, U. (2011). Identification of Novel *Cryptosporidium* Genotypes in Kangaroos From Western Australia. *Vet. Parasitol.* 179, 22–27. doi: 10.1016/j.vetpar.2011.02.011

Yang, R., Jacobson, C., Gardner, G., Carmichael, I., Campbell, A. J., Ng-Hublin, J., et al. (2014). Longitudinal Prevalence, Oocyst Shedding and Molecular Characterisation of *Cryptosporidium* Species in Sheep Across Four States in Australia. *Vet. Parasitol.* 200, 50–58. doi: 10.1016/j.vetpar.2013.11.014

Zhao, G. H., Ren, W. X., Gao, M., Bian, Q. Q., Hu, B., Cong, M. M., et al. (2013). Genotyping *Cryptosporidium* Andersoni in Cattle in Shaanxi Province, Northwestern China. *PLoS One* 8, e60112. doi: 10.1371/journal.pone.0060112

Conflict of Interest: Author CL is employed by Shandong New Hope Liuhe Group Co., Ltd., and Qingdao Jiazhi Biotechnology Co., Ltd.

The remaining authors declare that the research was conducted in the absence of any commercial or financial relationships that could be construed as a potential conflict of interest.

Publisher's Note: All claims expressed in this article are solely those of the authors and do not necessarily represent those of their affiliated organizations, or those of the publisher, the editors and the reviewers. Any product that may be evaluated in this article, or claim that may be made by its manufacturer, is not guaranteed or endorsed by the publisher.

frontiers in Cellular and Infection Microbiology

ORIGINAL RESEARCH
published: 29 September 2021
doi: 10.3389/fcimb.2021.735191

Mucosal Administration of Recombinant Baculovirus Displaying *Toxoplasma gondii* ROP4 Confers Protection Against *T. gondii* Challenge Infection in Mice

*Keon-Woong Yoon[1†], Ki-Back Chu[1†], Hae-Ji Kang[1], Min-Ju Kim[1], Gi-Deok Eom[1], Su-Hwa Lee[2], Eun-Kyung Moon[2] and Fu-Shi Quan[2,3]**

[1] Department of Biomedical Science, Graduate School, Kyung Hee University, Seoul, South Korea, [2] Department of Medical Zoology, School of Medicine, Kyung Hee University, Seoul, South Korea, [3] Medical Research Center for Bioreaction to Reactive Oxygen Species and Biomedical Science Institute, School of Medicine, Graduate School, Kyung Hee University, Seoul, South Korea

Pathogens require physical contact with the mucosal surface of the host organism to initiate infection and as such, vaccines eliciting both mucosal and systemic immune responses would be promising. Studies involving the use of recombinant baculoviruses (rBVs) as mucosal vaccines are severely lacking despite their inherently safe nature, especially against pathogens of global importance such as *Toxoplasma gondii*. Here, we generated rBVs displaying *T. gondii* rhoptry protein 4 (ROP4) and evaluated their protective efficacy in BALB/c mice following immunization *via* intranasal (IN) and oral routes. IN immunization with the ROP4-expressing rBVs elicited higher levels of parasite-specific IgA antibody responses compared to oral immunization. Upon challenge infection with a lethal dose of *T. gondii* ME49, IN immunization elicited significantly higher parasite-specific antibody responses in the mucosal tissues such as intestines, feces, vaginal samples, and brain than oral immunization. Marked increases in IgG and IgA antibody-secreting cell (ASC) responses were observed from intranasally immunized mice. IN immunization elicited significantly enhanced induction of $CD4^+$, $CD8^+$ T cells, and germinal center B (GC B) cell responses from secondary lymphoid organs while limiting the production of the inflammatory cytokines IFN-γ and IL-6 in the brain, all of which contributed to protecting mice against *T. gondii* lethal challenge infection. Our findings suggest that IN delivery of ROP4 rBVs induced better mucosal and systemic immunity against the lethal *T. gondii* challenge infection compared to oral immunization.

Keywords: recombinant baculovirus, ROP4, *Toxoplasma gondii* ME49, vaccine, mucosal immunity

OPEN ACCESS

Edited by:
Wei Cong,
Shandong University, Weihai, China

Reviewed by:
Fatemeh Ghaffarifar,
Tarbiat Modares University, Iran
Camila Figueiredo Pinzan,
University of São Paulo, Brazil

***Correspondence:**
Fu-Shi Quan
fsquan@khu.ac.kr

†These authors have contributed equally to this work

Specialty section:
This article was submitted to Clinical Microbiology, a section of the journal Frontiers in Cellular and Infection Microbiology

Received: *02 July 2021*
Accepted: *14 September 2021*
Published: *29 September 2021*

Citation:
Yoon K-W, Chu K-B, Kang H-J, Kim M-J, Eom G-D, Lee S-H, Moon E-K and Quan F-S (2021) Mucosal Administration of Recombinant Baculovirus Displaying Toxoplasma gondii ROP4 Confers Protection Against T. gondii Challenge Infection in Mice. Front. Cell. Infect. Microbiol. 11:735191. doi: 10.3389/fcimb.2021.735191

INTRODUCTION

A wide array of replicating and non-replicating viral vectors, such as the adenovirus or the vesicular stomatitis virus have been used for vaccine development against a plethora of diseases. Yet, concerns involving their genotoxicity and potential loss of vaccine efficacy due to pre-existing immunity in recipient hosts resulted in a search for alternative options (Robert-Guroff, 2007). Baculoviruses are a family of DNA viruses with inherently safe aspects, which can address the limitations of other viral vectors. For example, because baculoviruses have a narrow specificity range strictly limited to arthropods, their association with diseases in other species has not been reported (Airenne et al., 2013). In line with this notion, neither cytotoxicity nor pathologies were observed in mammalian cells or animal models following baculovirus infection. Moreover, given that baculoviruses are unable to replicate in mammalian cells, the risk of insertional mutagenesis resulting from genomic integration is non-existent (Kwang et al., 2016). Pairing these intrinsic properties with the absence of pre-existing immunity to baculoviruses in humans (Sung et al., 2014), recombinant baculovirus-based vaccines may be a safe and effective alternative. Resultantly, several baculovirus vaccines displaying the target antigens of various pathogens have been documented, which include the circumsporozoite proteins of *Plasmodium* spp. (Yoshida et al., 2003; Strauss et al., 2007), avian influenza virus (Yang et al., 2007), and others. As exemplified above, incorporating baculoviruses to develop an efficacious vaccine against *Toxoplasma gondii* could bring promising results.

T. gondii is an apicomplexan parasite transmitted to humans *via* ingestion of tissue cyst-contaminated food products and is the causative agent of toxoplasmosis (Jones and Dubey, 2012). Currently, approximately a third of the entire world's population is estimated to be infected with *T. gondii* and their persistence can lead to ocular toxoplasmosis, encephalitis, and even birth defects (Montoya and Liesenfeld, 2004). While the ovine toxoplasmosis vaccine Toxovax is commercially available, the use of this live-attenuated vaccine is strictly prohibited in humans due to safety issues (Dubey, 2009). For this reason, developing an efficacious human toxoplasmosis vaccine is urgent. As of current, only a few baculovirus-based toxoplasmosis vaccine studies have been reported. Gene delivery using pseudotyped recombinant baculovirus (rBV) vaccines expressing *T. gondii* SAG1 and MIC3 antigens conferred better protection against *T. gondii* RH strain than DNA vaccines encoding identical antigens (Fang et al., 2010; Fang et al., 2012). While these studies highlighted the potential use of rBV as a toxoplasmosis vaccine design strategy, neither of the two aforementioned studies investigated the vaccine efficacies against *T. gondii* type II clonal lineage which are more frequently associated with human toxoplasmosis (Arranz-Solís et al., 2019). Moreover, the extent of mucosal immunity induced through baculovirus vaccines against *T. gondii* infection remains unreported to date.

The rhoptry proteins (ROP) of *T. gondii* are key components required for successful parasitic invasion of the host cell (Dubremetz, 2007). ROP4 is one such antigen secreted during the parasitic invasion of host cells, which appears to be associated with the vacuole membrane function (Carey et al., 2004). However, their role extends far beyond host cellular intrusion as these have also been documented to be involved in intracellular parasitic proliferation and virulence (El Hajj et al., 2007). Based on these rationales, vaccines expressing the rhoptry proteins as antigens would be effective at restricting parasitic growth and invasion. Previously, we have generated a virus-like particle (VLP) vaccine expressing the ROP4 antigen of *T. gondii* (Kang et al., 2019). However, high production costs and the requirement for extensive downstream purification processes are the main issues of this vaccine platform (Effio and Hubbuch, 2015; Chu and Quan, 2021). Compared to VLPs, rBVs can be rapidly manufactured in large quantities at cheaper production costs, thus enabling these to be suitable vaccine platforms (Kis et al., 2019). Here, we generated rBV vaccines displaying the rhoptry protein 4 (ROP4) antigen and assessed the mucosal immunity induction, as well as their protective efficacy in mice following lethal challenge infection with the type II *T. gondii* ME49 strain. Our findings revealed that rBV vaccines expressing the ROP4 antigen (ROP4-rBV) were effective inducers of mucosal immunity, as indicated by the robust cellular and humoral responses which contributed to protection against a lethal dose of *T. gondii*.

MATERIALS AND METHODS

Animals and Ethics

Six-week-old female BALB/c mice were purchased from NARA Biotech (Seoul, South Korea). Animals were maintained in approved facilities under specific-pathogen-free conditions with easy access to food and water. All animal experiment protocols have been approved and were conducted following the guidelines of the Kyung Hee University IACUC (permit number: KHUASP (SE) 20-648).

Parasite, Cells, and Antibodies

Parasites and cells used in the present study were maintained as previously described (Kang et al., 2020b). *T. gondii* ME49 strain was maintained by serial passage in BALB/c mice and ME49 cysts were isolated from the brains. *Spodoptera frugiperda* (Sf9) cells used for rBV production were cultured in spinner flasks with serum-free SF900II media (Invitrogen, Carlsbad, California, USA) at 27°C, 130–135 rpm. Horseradish peroxidase (HRP)-conjugated goat anti-mouse IgG and IgA secondary antibodies were purchased from Southern Biotech (Birmingham, AL, USA).

Generation of Recombinant Baculovirus

Recombinant baculoviruses were produced following the Bac-to-Bac™ (Thermo Fisher Scientific, Waltham, MA, U.S.) manufacturer's guidelines. Briefly, ROP4 genes were amplified *via* polymerase chain reaction (PCR) and cloned into pFastBac vector. After subsequent transformation into DH10Bac competent cells, bacmid DNA was acquired and transfected into the Sf9 cells as described (Kang et al., 2019). Single plaque purification was performed in the second passage. To quantify the ROP4-rBVs released into the cell culture supernatants, baculovirus plaque assays were performed using the culture supernatants. Endotoxin presence in the recombinant

baculoviruses was checked using Pierce™ Chromogenic Endotoxin Quant Kit (Thermo Fisher Scientific, Waltham, MA, US). To characterize the expression of ROP4 in rBVs, a polyclonal mouse anti-*T. gondii* antibody was used to probe *T. gondii* ROP4 protein in rBVs by ELISA as previously described elsewhere (Welsh, 2011; Lee et al., 2020). Briefly, wells of 96-well plates were coated with serially diluted ROP4 rBVs overnight at 4°C. The wells were incubated with polyclonal mouse anti-*T. gondii* antibody and the secondary HRP-conjugated IgG antibodies. Polyclonal mouse anti-influenza virus antibody was used as a negative control.

Immunization and Challenge Infection

A total of 24 mice were subdivided into 4 groups (n = 6 per group): unimmunized (naïve), unimmunized mice which were challenge-infected (Naïve+Cha), oral immunization (oral), and intranasal immunization (IN). For prime and boost immunizations through the oral and IN routes, 100 µl of ROP4 rBVs ($4.28x10^4$ pfu) were inoculated *via* respective routes at 4 week intervals. Mice were challenge-infected through the oral route with 50 LD_{50} ME49 cysts (2,000 cysts) 4 weeks after boost immunization. All of the mice were monitored daily to record bodyweight changes and survival rates. At 16 days post-infection (dpi), all of the mice were sacrificed for organ sampling and *ex vivo* immunological assay purposes.

Sample Preparation

Blood samples were collected by retro-orbital plexus puncture 3 weeks after each immunization. Mice were sacrificed at 16 dpi for brain and mucosal sample (intestines, feces, and vaginal secretions) acquisition as previously described (Kang et al., 2019). Briefly, feces were collected and normalized by adding 100 µl of PBS per 0.1 g of feces. Vaginal samples were collected by repeatedly washing the vaginal canal with 200 µl of PBS. Duodenums of mice were longitudinally sliced and immersed in 500 µl of PBS. All of the mucosal samples were processed on an individual basis and incubated for 1 hour at 37°C. Samples were centrifuged at 5000 rpm for 10 min to collect supernatants, which were stored at -20°C until use. Brain tissues were individually processed for cyst burden quantification.

Antibody Responses

T. gondii-specific antibody responses from sera, brain, and mucosal tissues were determined using enzyme-linked immunosorbent assay (ELISA) as previously described (Kang et al., 2019). In brief, flat-bottom 96 well immunoplates (SPL Life Sciences, Pocheon, Korea) were coated with 100 µl of sonicated *T. gondii* ME49 dissolved in carbonate coating buffer (4 µg/ml) overnight at 4°C. Plates were blocked with 0.2% gelatin dissolved in 0.1M PBS with 0.05% Tween 20. Sera and mucosal samples diluted in PBS were used as primary antibodies (1:50 sera, 1:100 intestine, 1:20 vaginal, 1:2 fecal sample dilutions). After incubating the wells with the primary antibodies for 1 hour at 37°C, HRP-conjugated goat anti-mouse IgG and IgA (1:2000 dilution in PBS) secondary antibodies were inoculated into the wells and incubated for 1 hour, 37°C. O-phenylenediamine substrate was dissolved in citrate-phosphate buffer (pH 5.0) containing 0.03% H_2O_2 and was used for color development. The optical density at 490 nm was measured using an ELISA reader (EZ Read 400, Biochrom Ltd., Cambridge, UK).

Antibody-Secreting Cell (ASC) Responses

At 16 dpi, spleens and mesenteric lymph nodes (MLN) were collected from sacrificed mice to assess ASC inductions. Single cell suspensions of splenocytes and MLN cells were prepared as previously described (Kang et al., 2019). Briefly, after RBC lysis, splenocytes and MLN cells were seeded (1×10^6 cells/well) into 96 well plates coated with *T. gondii* ME49 (4 µg/ml). After incubating the cells for 5 days at 37°C, 5% CO_2, plates were washed and incubated with HRP-conjugated anti-mouse IgG and IgA antibodies for 1 hour, 37°C. Colorimetric assay was performed using OPD substrate and after stopping the reactions with 2N H_2SO_4, OD_{490} values were measured.

Flow Cytometry Analysis of Immune Cell Populations

Splenocytes and MLN cells were prepared for flow cytometric analysis as previously described (Kang et al., 2020a). Single cell suspensions of splenocytes (1×10^6 cells/mouse) and MLN cells (1×10^5 cells/mouse) were stimulated *ex vivo* with *T. gondii* ME49 antigen (2 µg/mL) at 37°C with 5% CO_2 for 2 hours. After antigen stimulation, cells were stained with the following fluorescent-conjugated antibodies purchased from BD Biosciences (Franklin Lakes, NJ, USA) and Invitrogen (Waltham, MA, USA) for $CD4^+$ T cell, $CD8^+$ T cell, and germinal center B (GC B) cell detection: CD3 (PE-Cy7), CD4 (FITC), CD8 (PE), GL7 (PE), and B220 (FITC). All staining procedures for flow cytometry were performed according to the manufacturer's protocol. Stained cells were acquired using the Accuri C6 flow cytometer and analyzed with the C6 Accuri software (BD Biosciences, Franklin Lakes, NJ, USA).

Inflammatory Cytokine Assays

At 16 dpi, the brain tissues of mice were individually homogenized in 500 µl of PBS. After centrifugation, supernatants were collected for cytokine assay while the pellets were used for brain cyst counting. Pro-inflammatory cytokines IFN-γ and IL-6 were measured from the brain supernatants of *T. gondii*-infected mice using BD OptEIA ELISA kits (BD Biosciences, Franklin Lakes, NJ, USA). All experiments were performed as per manufacturer's instructions and cytokine concentrations were calculated using the generated standard curve.

Parasite Burden

T. gondii ME49 cysts were isolated from the brains and enumerated as previously described (Kang et al., 2019). After centrifuging the brain homogenates, cysts were isolated using Percoll density gradient cell isolation media (BD Biosciences, Franklin Lakes, NJ, USA). Briefly, sedimented pellets were resuspended in 44% Percoll and gently overlaid on top of 67% Percoll media. After centrifugation at 12,100 rpm for 20 min, the layer containing the *T. gondii* cysts was carefully collected and repeatedly washed with PBS. Cysts were mounted on a clean slide glass and counted under the microscope (Leica DMi8, Leica,

Wetzlar, Germany). Cysts were counted from 3 different fields of views per mouse.

Statistical Analysis

All statistical analyses were compared using the GraphPad Prism version 6 software. (San Diego, CA, USA). Data sets were presented as mean ± SD. Statistical significance between the means of groups was determined using One-way ANOVA with Tukey's *post hoc* test or 2-way ANOVA with Bonferroni's *post hoc* test. *P* values (* < 0.05, ** < 0.01, *** < 0.001, **** < 0.0001) were considered statistically significant.

RESULTS

Experimental Schedule and Antibody Responses in Immune Sera

The experiment was performed as illustrated in the vaccine prime-boost scheme (**Figure 1A**). ROP4 in rBVs was characterized by ELISA using polyclonal mouse anti-*T. gondii* antibody (**Figure 1B**). Polyclonal *T. gondii* sera successfully reacted with serially diluted ROP4 rBVs while influenza hemagglutinin (HA1) from A/PR/8/34 showed no reactivity with the anti-*T. gondii* antibody, thereby suggesting that the epitope regions of ROP4 protein in the rBVs were similar to that of *T. gondii*. *T. gondii*-specific antibody responses were measured using the sera acquired from mice following prime and boost immunizations. Enhanced IgG response was observed 4 weeks after prime immunization, regardless of vaccine administration route. IgG antibody induction was further elevated 4 weeks after boost immunization (**Figure 1C**). Contrary to the findings observed for IgG, oral immunization of ROP4-rBVs did not lead to enhanced antibody response after prime immunization. However, a noticeable increase was observed after boost immunization. IgA antibody response profile for IN immunization of ROP4-rBVs was similar to IgG, with a drastic increase in antibody induction being observed after boost immunization (**Figure 1D**). When comparing the two immunization groups, IN-immunized mice elicited greater quantities of IgA than orally immunized mice.

Antibody Responses in Mucosal Samples

To assess the extent of mucosal immunity induction, antibody productions in the mucosal tissues of mice were evaluated. At 16 dpi, compared to unimmunized control, increased IgG and IgA responses were observed from the Naïve+Cha group. Immunizing the mice with ROP4-rBVs resulted in greater quantities of *T. gondii*-specific antibody induction, although significant differences between oral immunization and Naïve+Cha were not observed for IgG (**Figures 2A, D**). Compared to Naïve+Cha, significant increases in fecal IgG and IgA were only observed from IN immunization group (**Figures 2B, E**). Immunizing the mice with the ROP4-rBVs resulted in increased IgG responses in the vaginal samples. However, such increase was only observed from IN-immunized mice for the IgA antibody responses (**Figures 2C, F**). Overall, the highest mucosal antibody responses were observed from the intestines.

Antibody Responses in the Brain

Vaccinating mice with the ROP4-rBVs enabled antibody accumulation in the brains. While the differences in brain IgG responses were comparable for Naïve+Cha and oral immunization group, a marked increase in IgG was observed for IN immunization group (**Figure 3A**). Compared to the naïve control, incremental

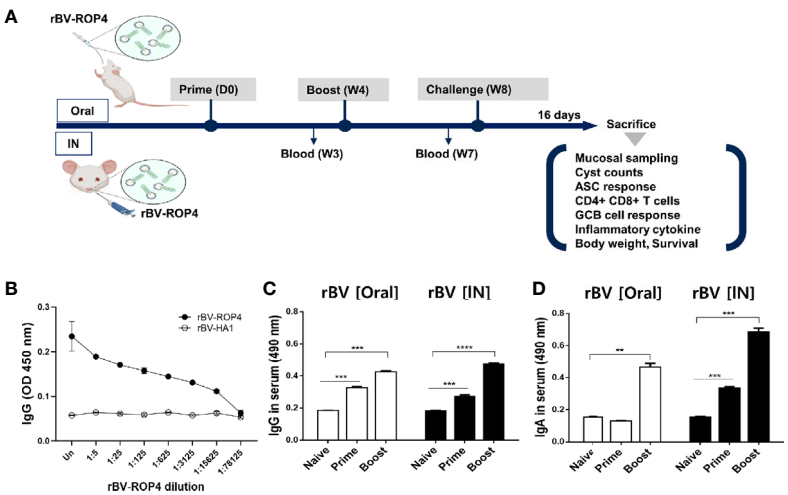

FIGURE 1 | Immunization schematic and *T. gondii* ROP4-specific antibody responses. BALB/c mice were immunized with the ROP4-rBVs vaccine through the oral and intranasal routes with blood collection at regular intervals as scheduled **(A)**. Polyclonal *T. gondii* antibody collected from mice was used to assess ROP4-specificity *via* ELISA **(B)**. Sera were collected 3 weeks after each immunization and *T. gondii* ME49 antigen-specific IgG **(C)** and IgA **(D)** antibody responses were determined by ELISA. Data are presented as mean ± SD and asterisks indicate statistical differences between groups (**$P < 0.01$, ***$P < 0.001$, ****$P < 0.0001$). Images were created with BioRender.com.

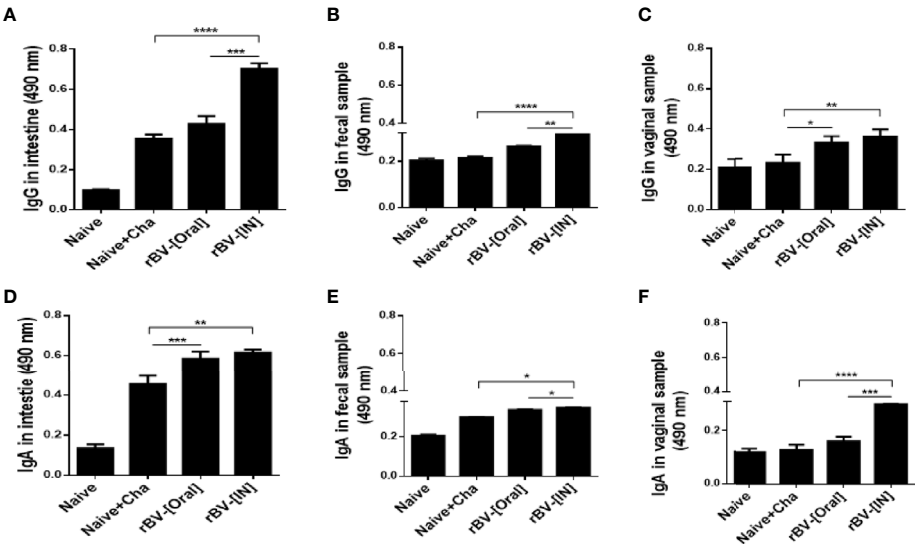

FIGURE 2 | Measurement of enhanced mucosal immune response. *T. gondii*-specific mucosal IgG and IgA responses in the intestines **(A, D)**, feces **(B, E)**, and vaginal samples **(C, F)** were observed using ELISA. Data are presented as mean ± SD and asterisks indicate statistical differences between groups (*$P < 0.05$, **$P < 0.01$, ***$P < 0.001$, ****$P < 0.0001$).

increases in IgA responses were detected for Naïve+Cha and orally immunized mice. However, IN administration of ROP4-rBVs significantly enhanced the induction of IgA responses in the brain (**Figure 3B**).

Oral and IN Vaccination Induces Antibody-Secreting Cell Responses

To determine the antibody-secreting cell response, splenocytes and MLN cells were collected from mice and cultured for 5 days. Differences in IgG and IgA antibody responses were not observed from cultured splenocytes. However, a marked increase in IgG and IgA responses were observed from splenocytes of IN immunization mice (**Figures 4A, B**). Identical findings were also detected from MLN cells as IgG and IgA ASC responses were similar for both Naïve+Cha and oral immunization groups. This was further enhanced by IN immunization with ROP4-rBVs (**Figures 4C, D**).

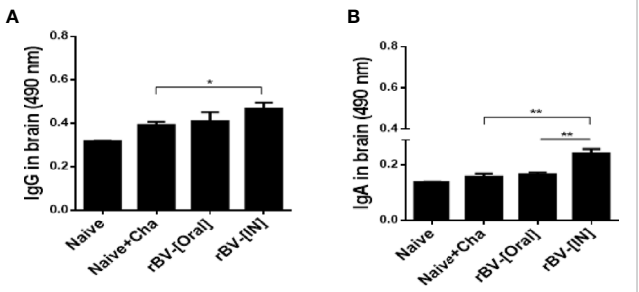

FIGURE 3 | IgG and IgA antibody responses in the brain after *T. gondii* ME49 infection. *T. gondii*-specific IgG **(A)** and IgA **(B)** antibody responses were detected in immunized mice 16 days after challenge infection. Data are presented as mean ± SD and asterisks indicate statistical differences between groups (*$P < 0.05$, **$P < 0.01$).

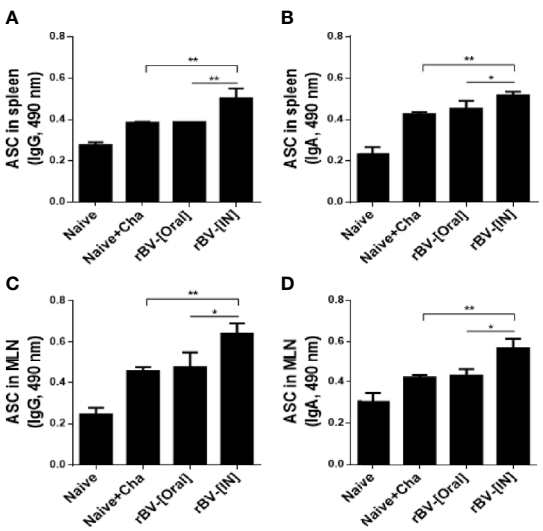

FIGURE 4 | ROP4-rBVs immunization enhances antibody-secreting cell responses. The levels of IgG and IgA antibody-secreting cells were evaluated in spleen and MLN cells. A higher level of *T. gondii*-specific IgG was found in the group of mice immunized with the IN pathway compared to the Naive+Cha group **(A, C)**. The group of mice immunized by the oral route is at a similar level to the Naive+Cha group. The group of mice immunized with the IN route responded significantly to *T. gondii*-specific IgA **(B, D)**. Data are presented as mean ± SD and asterisks indicate statistical differences between groups (*$P < 0.05$, **$P < 0.01$).

Activation of CD4$^+$, CD8$^+$ T cells, and GC B in MLN and Spleen

Flow cytometry was performed to assess the proliferation of CD4 and CD8 T cells, as well as GC B cells in the spleens and MLNs of mice. CD4$^+$ and CD8$^+$ T cell population inductions in the MLN were similar between Naïve+Cha and oral ROP4-rBV immunized mice. However, intranasally administering ROP4-rBVs led to enhanced T cell proliferations (**Figures 5A, B**). GC B cell responses observed from splenocytes were strikingly similar to those of MLN cells. *T. gondii* infection in unimmunized mice elicited marginal GC B cell responses, but this was dramatically elevated upon immunization. Of the two immunization routes, IN route contributed to greater GC B cell response inductions in both spleen and MLN (**Figures 5C, D**).

Pro-Inflammatory Cytokine Responses in the Brain

Brain homogenates of mice were used to assess the production of pro-inflammatory cytokines IFN-γ and IL-6. Challenge-infection with *T. gondii* ME49 in unimmunized mice resulted marked rise in IFN-γ production. While such increases were also observed from the brains of immunized mice, IFN-γ was produced to a significantly lesser extent in these groups (**Figure 6A**). IL-6 levels were comparable between Naïve+Cha and oral immunization groups. However, a stark decrease in IL-6 production was detected from IN immunization groups (**Figure 6B**).

Protective Efficacy of the ROP4-rBV Vaccine

To confirm the protective efficacy of ROP4-rBVs against *T. gondii* ME49 infection, cysts were quantified from the brains of mice under the microscope. More than 6,000 cysts were counted from Naïve+Cha mice, whereas immunized mice underwent a 3-fold reduction in parasite burden (**Figure 7A**). While the cyst counts between the two groups of immunized mice were comparable, bodyweight loss was more apparent in orally immunized mice. At 16 dpi, drastic bodyweight loss exceeding 20% was observed from Naïve+Cha group. Similarly, orally immunized mice also experienced bodyweight reduction approaching the humane intervention point. Yet, IN immunization resulted in 10% bodyweight loss at maximum and retained close to normal bodyweight (**Figure 7B**). Despite the contrasting differences in bodyweight reduction, all of the immunized mice survived (**Figure 7C**). While prolonged survival of immunized mice was highly plausible, all of the mice were sacrificed at 16 dpi to ensure that experiments were carried out on the same day for all groups. These results suggest that the ROP4-rBVs vaccine is more effective when administered *via* IN route.

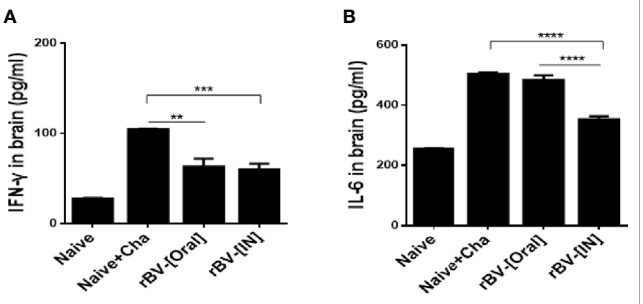

FIGURE 6 | Inhibition of pro-inflammatory cytokines in the brain. Brains of mice were collected 16 days after *T. gondii* challenge infection. The levels of the pro-inflammatory cytokines IFN-γ **(A)** and IL-6 **(B)** were determined in the brain supernatant. Data are presented as mean ± SD and asterisks indicate statistical differences between groups. (**P < 0.01, ***P < 0.001, ****P < 0.0001).

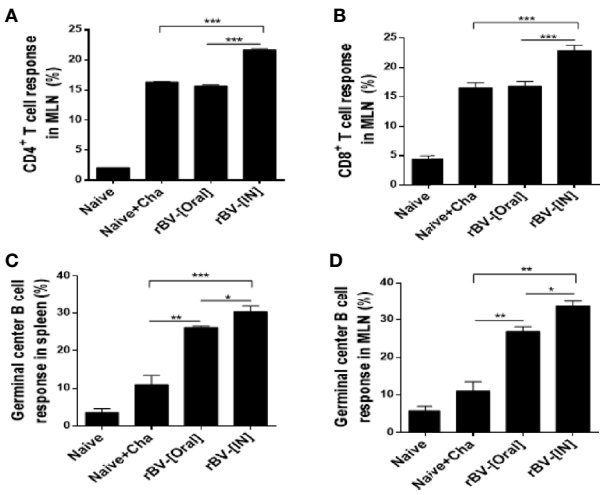

FIGURE 5 | Detection of CD4$^+$ T cell, CD8$^+$ T cell, and GC B cell. Mice were sacrificed at 16 dpi for spleen and MLN acquisition. Single cell suspensions of splenocytes and MLN cells were prepared and analyzed using flow cytometry to confirm proliferation of CD4$^+$ T cell **(A)**, CD8$^+$ T cell **(B)**, and GC B cell **(C)** in MLN. Splenic GC B cell activation was also confirmed using flow cytometry **(D)**. Data are presented as mean ± SD and asterisks denote statistical differences between groups. (*P < 0.05, **P < 0.01, ***P < 0.001).

DISCUSSION

The intestinal epithelium act as the first line of defense against numerous pathogens including *T. gondii* and mounting a robust mucosal immunity can contribute to limiting the parasitic intrusion of the host cells. While the exact function of ROP4 remains unknown, (Carey et al., 2004) have delineated that ROP4 proteins are heavily involved in vacuole membrane function and subsequently undergo phosphorylation in the infected host cells, which may have further implications. Yet, only a handful of immunization studies using this antigen have been conducted to date. The present study investigated the protective efficacy of a recombinant baculovirus vaccine expressing the *T. gondii* ROP4 antigen. Here, we demonstrated that administering this vaccine through the two mucosal routes induced strong mucosal immune responses that protected mice against a lethal dose of *T. gondii* ME49, with intranasal immunization being better of the two immunization routes.

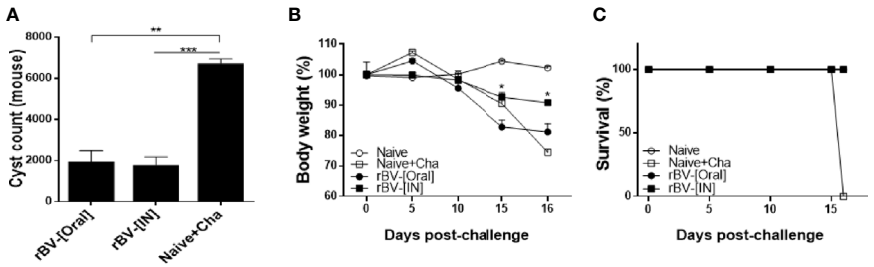

FIGURE 7 | Complete protection against *T. gondii* ME49. Mice were challenge-infected with 50 LD_{50} *T. gondii* ME49 cysts 4 weeks after the final immunization. Mice were sacrificed 16 days post-infection and brain tissues were harvested to isolate and enumerate the cysts **(A)**. Bodyweight changes **(B)** and survival rate **(C)** were monitored daily up to 16 dpi. Data are presented as mean ± SD and asterisks indicate statistical differences between groups. (*$P < 0.05$, **$P < 0.01$, ***$P < 0.001$).

Oral ingestion of *T. gondii* tissue cysts serves as the natural route of *T. gondii* infection, which readily invades the epithelial cells of the small intestines to initiate infection before disseminating to various organs (Dimier-Poisson et al., 2003; Snyder and Denkers, 2020). A robust mucosal immune response, characterized by antibody responses in the intestines, would act as a barrier and limit *T. gondii* transgressions into the epithelial cells. Baculovirus-based vaccines are capable of inducing mucosal immunity against various mucosal pathogens, as demonstrated using the influenza virus and the human papillomavirus (Fragoso-Saavedra and Vega-López, 2020). Consistent with these findings, the ROP4-rBV vaccine generated in this study successfully induced mucosal antibody responses, especially intestinal IgG and IgA which contributed to protection against a lethal dose of *T. gondii* ME49 infection. This result is supported by the GC B cell proliferation observed from splenocytes as well as the MLN, since the GC B cells act as the site for developing antigen-specific antibody responses (Glatman Zaretsky et al., 2012). Also, it is widely regarded that T cell and B cells are activated following the initial phase of *T. gondii* infection and their expressions regulate parasite replication during the chronic phase of its infection (Glatman Zaretsky et al., 2012). In line with this notion, $CD4^+$ and $CD8^+$ T cell proliferation were observed from Naïve+Cha mice in our study, which was comparable to those of orally immunized mice. T cell proliferation occurred to a greater extent in the MLN of IN immunized mice than those of orally immunized group or the control groups, implying that IN immunization of ROP4-rBV conferred better protection against chronic toxoplasmosis. These findings can be attributed to the inherent obstacle associated with oral vaccines. Oral vaccines, when administered through the gastrointestinal (GI) tract, are susceptible to denaturation by the proteolytic enzymes that are present in the highly acidic GI tract environment (Vela Ramirez et al., 2017). Exposure to this harsh environmental condition can weaken the antigenicity of the ROP4-rBVs, which may have resulted in weaker mucosal immunity induction than the IN vaccine immunization.

Pro-inflammatory cytokine milieu in the central nervous system is a prominent feature observed during chronic *T. gondii* infection, and persisting neuroinflammations can lead to neurological and psychiatric disorders (Parlog et al., 2015). In general, a pronounced inflammatory cytokine response is one of the features of type II *T. gondii* strains while these are detected to a lesser extent in the clonal lineage types I and III (Xiao et al., 2011; Innes et al., 2019). Our findings revealed that immunizing the mice with the ROP4-rBVs reduced the production of inflammatory cytokines IFN-γ and IL-6 compared to the unimmunized control group. While ROP4-rBV immunization elicited reduced IFN-γ production in the brains irrespective of immunization routes, differences in immunization routes were noticeable for IL-6 with IN immunization inducing less IL-6 production than the oral immunization group.

Though limited in number, the protective efficacies of *T. gondii* vaccines incorporating the ROP4 antigen have been reported. Several studies have investigated the efficacies of subunit cocktail vaccines comprising ROP4 along with various other antigens such as ROP2, GRA4, SAG1, and MAG1 which significantly reduced the cyst burden in mice challenge-infected with *T. gondii* DX strain, a low-virulent type II strain similar to ME49 (Dziadek et al., 2009; Dziadek et al., 2011; Dziadek et al., 2012; Gatkowska et al., 2018). Our previous study also assessed the efficacies of VLP vaccines displaying ROP4 and ROP13 antigens on the surface (Kang et al., 2019). While different strains of *T. gondii* were used for challenge infection, the cyst burden reductions demonstrated by ROP4-rBVs were comparable to the results of the aforementioned multi-antigenic vaccine studies. Immunization-induced proliferation of $CD4^+$ T cell, $CD8^+$ T cell, and GC B cells in the MLN were consistent with our previous works (Kang et al., 2019).

Noticeable differences in results were observed between the present study and those of our previous studies. Compared to our previous study, discrepancies in mucosal antibody responses were observed which may stem from different vaccine platform usage. The mucosal antibody inductions were much more potent in mice immunized with the ROP4 VLPs than ROP4-rBVs. Notably, while the ROP4-rBVs used in the present study only elicited strong antibody responses in the intestines, ROP4 VLPs from our previous work induced the production of vast quantities of vaginal, urinal, fecal, and intestinal IgG. In many of our previous studies investigating the protective efficacy of *T. gondii* VLP vaccines, unimmunized mice perished around 30 dpi when infected with 450 cysts (Kang et al., 2019; Kang et al.,

2020a; Kang et al., 2021a; Kang et al., 2021b). In the present study, unimmunized mice died by 16 dpi which was attributed to the high infection dose exceeding 450 cysts. Nevertheless, cyst burden reductions, bodyweight changes, and survival data of ROP4-rBVs were strikingly similar to those of ROP4 VLPs, thus confirming the efficacy of the rBV vaccines demonstrated here.

In summary, we demonstrated that oral and intranasal immunization with the ROP4-rBV vaccine elicited mucosal immunity which protected mice from lethal challenge infection with the *T. gondii* ME49. In particular, immunological parameters were induced to a greater extent *via* IN immunization. While additional protective efficacy assessment of the ROP4-rBV vaccines against other clonal lineage types is required, the vaccine design strategy presented here may be well-suited for developing a safe and effective *T. gondii* vaccine.

DATA AVAILABILITY STATEMENT

The original contributions presented in this study are included in the article/supplementary material. Further inquiries can be directed to the corresponding author.

ETHICS STATEMENT

The animal study was reviewed and approved by Kyung Hee University IACUC.

AUTHOR CONTRIBUTIONS

F-SQ conceptualized and designed the experiments. K-WY, K-BC, H-JK, M-JK, G-DE, and S-HL performed the experiment and collected the data. K-WY and H-JK analyzed the data. K-WY and K-BC wrote the manuscript. K-BC, E-KM, and F-SQ performed critical revision of the manuscript. All authors contributed to the article and approved the submitted version.

FUNDING

This research was funded by the National Research Foundation of Korea (NRF) (2018R1A6A1A03025124) and the Ministry of Health & Welfare, Republic of Korea (HV20C0085, HV20C0142).

REFERENCES

Airenne, K. J., Hu, Y. C., Kost, T. A., Smith, R. H., Kotin, R. M., Ono, C., et al. (2013). Baculovirus: An Insect-Derived Vector for Diverse Gene Transfer Applications. *Mol. Ther.* 21 (4), 739–749. doi: 10.1038/mt.2012.286

Arranz-Solís, D., Cordeiro, C., Young, L. H., Dardé, M. L., Commodaro, A. G., Grigg, M. E., et al. (2019). Serotyping of Toxoplasma Gondii Infection Using Peptide Membrane Arrays. *Front. Cell Infect. Microbiol.* 9, 408. doi: 10.3389/fcimb.2019.00408

Carey, K. L., Jongco, A. M., Kim, K., and Ward, G. E. (2004). The Toxoplasma Gondii Rhoptry Protein ROP4 is Secreted Into the Parasitophorous Vacuole and Becomes Phosphorylated in Infected Cells. *Eukaryot Cell* 3 (5), 1320–1330. doi: 10.1128/ec.3.5.1320-1330.2004

Chu, K. B., and Quan, F. S. (2021). Virus-Like Particle Vaccines Against Respiratory Viruses and Protozoan Parasites. *Curr. Top. Microbiol. Immunol.* 433, 77–107. doi: 10.1007/82_2021_232

Dimier-Poisson, I., Aline, F., Mévélec, M. N., Beauvillain, C., Buzoni-Gatel, D., and Bout, D. (2003). Protective Mucosal Th2 Immune Response Against Toxoplasma Gondii by Murine Mesenteric Lymph Node Dendritic Cells. *Infect. Immun.* 71 (9), 5254–5265. doi: 10.1128/iai.71.9.5254-5265.2003

Dubey, J. P. (2009). Toxoplasmosis in Sheep–the Last 20 Years. *Vet. Parasitol* 163 (1-2), 1–14. doi: 10.1016/j.vetpar.2009.02.026

Dubremetz, J. F. (2007). Rhoptries are Major Players in Toxoplasma Gondii Invasion and Host Cell Interaction. *Cell Microbiol.* 9 (4), 841–848. doi: 10.1111/j.1462-5822.2007.00909.x

Dziadek, B., Gatkowska, J., Brzostek, A., Dziadek, J., Dzitko, K., and Dlugonska, H. (2009). Toxoplasma Gondii: The Immunogenic and Protective Efficacy of Recombinant ROP2 and ROP4 Rhoptry Proteins in Murine Experimental Toxoplasmosis. *Exp. Parasitol* 123 (1), 81–89. doi: 10.1016/j.exppara.2009.06.002

Dziadek, B., Gatkowska, J., Brzostek, A., Dziadek, J., Dzitko, K., Grzybowski, M., et al. (2011). Evaluation of Three Recombinant Multi-Antigenic Vaccines Composed of Surface and Secretory Antigens of Toxoplasma Gondii in Murine Models of Experimental Toxoplasmosis. *Vaccine* 29 (4), 821–830. doi: 10.1016/j.vaccine.2010.11.002

Dziadek, B., Gatkowska, J., Grzybowski, M., Dziadek, J., Dzitko, K., and Dlugonska, H. (2012). Toxoplasma Gondii: The Vaccine Potential of Three Trivalent Antigen-Cocktails Composed of Recombinant ROP2, ROP4, GRA4 and SAG1 Proteins Against Chronic Toxoplasmosis in BALB/c Mice. *Exp. Parasitol* 131 (1), 133–138. doi: 10.1016/j.exppara.2012.02.026

Effio, C. L., and Hubbuch, J. (2015). Next Generation Vaccines and Vectors: Designing Downstream Processes for Recombinant Protein-Based Virus-Like Particles. *Biotechnol. J.* 10 (5), 715–727. doi: 10.1002/biot.201400392

El Hajj, H., Lebrun, M., Arold, S. T., Vial, H., Labesse, G., and Dubremetz, J. F. (2007). ROP18 is a Rhoptry Kinase Controlling the Intracellular Proliferation of Toxoplasma Gondii. *PloS Pathog.* 3 (2), e14. doi: 10.1371/journal.ppat.0030014

Fang, R., Feng, H., Hu, M., Khan, M. K., Wang, L., Zhou, Y., et al. (2012). Evaluation of Immune Responses Induced by SAG1 and MIC3 Vaccine Cocktails Against Toxoplasma Gondii. *Vet. Parasitol* 187 (1-2), 140–146. doi: 10.1016/j.vetpar.2011.12.007

Fang, R., Feng, H., Nie, H., Wang, L., Tu, P., Song, Q., et al. (2010). Construction and Immunogenicity of Pseudotype Baculovirus Expressing Toxoplasma Gondii SAG1 Protein in BALB/c Mice Model. *Vaccine* 28 (7), 1803–1807. doi: 10.1016/j.vaccine.2009.12.005

Fragoso-Saavedra, M., and Vega-López, M. A. (2020). Induction of Mucosal Immunity Against Pathogens by Using Recombinant Baculoviral Vectors: Mechanisms, Advantages, and Limitations. *J. Leukoc. Biol.* 108 (3), 835–850. doi: 10.1002/jlb.4mr0320-488r

Gatkowska, J., Wieczorek, M., Dziadek, B., Dzitko, K., Dziadek, J., and Długońska, H. (2018). Assessment of the Antigenic and Neuroprotective Activity of the Subunit Anti-Toxoplasma Vaccine in T. Gondii Experimentally Infected Mice. *Vet. Parasitol* 254, 82–94. doi: 10.1016/j.vetpar.2018.02.043

Glatman Zaretsky, A., Silver, J. S., Siwicki, M., Durham, A., Ware, C. F., and Hunter, C. A. (2012). Infection With Toxoplasma Gondii Alters Lymphotoxin Expression Associated With Changes in Splenic Architecture. *Infect. Immun.* 80 (10), 3602–3610. doi: 10.1128/iai.00333-12

Innes, E. A., Hamilton, C., Garcia, J. L., Chryssafidis, A., and Smith, D. (2019). A One Health Approach to Vaccines Against Toxoplasma Gondii. *Food Waterborne Parasitol* 15:e00053. doi: 10.1016/j.fawpar.2019.e00053

Jones, J. L., and Dubey, J. P. (2012). Foodborne Toxoplasmosis. *Clin. Infect. Dis.* 55 (6), 845–851. doi: 10.1093/cid/cis508

Kang, H. J., Chu, K. B., Kim, M. J., Lee, S. H., Park, H., Jin, H., et al. (2021a). Protective Immunity Induced by CpG ODN-Adjuvanted Virus-Like Particles Containing Toxoplasma Gondii Proteins. *Parasite Immunol.* 43 (1), e12799. doi: 10.1111/pim.12799

Kang, H. J., Chu, K. B., Kim, M. J., Park, H., Jin, H., Lee, S. H., et al. (2020a). Evaluation of CpG-ODN-Adjuvanted Toxoplasma Gondii Virus-Like Particle Vaccine Upon One, Two, and Three Immunizations. *Pharmaceutics* 12 (10), 989. doi: 10.3390/pharmaceutics12100989

Kang, H. J., Chu, K. B., Lee, S. H., Kim, M. J., Park, H., Jin, H., et al. (2020b). Toxoplasma Gondii Virus-Like Particle Vaccination Alleviates Inflammatory Response in the Brain Upon T Gondii Infection. *Parasite Immunol.* 42 (6), e12716. doi: 10.1111/pim.12716

Kang, H. J., Kim, M. J., Chu, K. B., Lee, S. H., Moon, E. K., and Quan, F. S. (2021b). Passive Immunity and Antibody Response Induced by Toxoplasma Gondii VLP Immunization. *Vaccines (Basel)* 9 (5), 425. doi: 10.3390/vaccines9050425

Kang, H. J., Lee, S. H., Kim, M. J., Chu, K. B., Lee, D. H., Chopra, M., et al. (2019). Influenza Virus-Like Particles Presenting Both Toxoplasma Gondii ROP4 and ROP13 Enhance Protection Against T. Gondii Infection. *Pharmaceutics* 11 (7), 342. doi: 10.3390/pharmaceutics11070342

Kis, Z., Shattock, R., Shah, N., and Kontoravdi, C. (2019). Emerging Technologies for Low-Cost, Rapid Vaccine Manufacture. *Biotechnol. J.* 14 (1), e1800376. doi: 10.1002/biot.201800376

Kwang, T. W., Zeng, X., and Wang, S. (2016). Manufacturing of AcMNPV Baculovirus Vectors to Enable Gene Therapy Trials. *Mol. Ther. Methods Clin. Dev.* 3, 15050. doi: 10.1038/mtm.2015.50

Lee, S. H., Kang, H. J., Chu, K. B., Basak, S., Lee, D. H., Moon, E. K., et al. (2020). Protective Immunity Induced by Virus-Like Particle Containing Merozoite Surface Protein 9 of Plasmodium Berghei. *Vaccines (Basel)* 8 (3). doi: 10.3390/vaccines8030428

Montoya, J. G., and Liesenfeld, O. (2004). Toxoplasmosis. *Lancet* 363 (9425), 1965–1976. doi: 10.1016/s0140-6736(04)16412-x

Parlog, A., Schlüter, D., and Dunay, I. R. (2015). Toxoplasma Gondii-Induced Neuronal Alterations. *Parasite Immunol.* 37 (3), 159–170. doi: 10.1111/pim.12157

Robert-Guroff, M. (2007). Replicating and non-Replicating Viral Vectors for Vaccine Development. *Curr. Opin. Biotechnol.* 18 (6), 546–556. doi: 10.1016/j.copbio.2007.10.010

Snyder, L. M., and Denkers, E. Y. (2020). From Initiators to Effectors: Roadmap Through the Intestine During Encounter of Toxoplasma Gondii With the Mucosal Immune System. *Front. Cell Infect. Microbiol.* 10, 614701. doi: 10.3389/fcimb.2020.614701

Strauss, R., Hüser, A., Ni, S., Tuve, S., Kiviat, N., Sow, P. S., et al. (2007). Baculovirus-Based Vaccination Vectors Allow for Efficient Induction of Immune Responses Against Plasmodium Falciparum Circumsporozoite Protein. *Mol. Ther.* 15 (1), 193–202. doi: 10.1038/sj.mt.6300008

Sung, L. Y., Chen, C. L., Lin, S. Y., Li, K. C., Yeh, C. L., Chen, G. Y., et al. (2014). Efficient Gene Delivery Into Cell Lines and Stem Cells Using Baculovirus. *Nat. Protoc.* 9 (8), 1882–1899. doi: 10.1038/nprot.2014.130

Vela Ramirez, J. E., Sharpe, L. A., and Peppas, N. A. (2017). Current State and Challenges in Developing Oral Vaccines. *Adv. Drug Delivery Rev.* 114, 116–131. doi: 10.1016/j.addr.2017.04.008

Welsh, J. P. (2011). *Production of Complex Heterologous Proteins and Protein Assemblies Using E. Coli-Based Cell-Free Protein Synthesis* (Stanford (CA: Stanford University). [dissertation/PhD thesis].

Xiao, J., Jones-Brando, L., Talbot, C. C.Jr., and Yolken, R. H. (2011). Differential Effects of Three Canonical Toxoplasma Strains on Gene Expression in Human Neuroepithelial Cells. *Infect. Immun.* 79 (3), 1363–1373. doi: 10.1128/iai.00947-10

Yang, D. G., Chung, Y. C., Lai, Y. K., Lai, C. W., Liu, H. J., and Hu, Y. C. (2007). Avian Influenza Virus Hemagglutinin Display on Baculovirus Envelope: Cytoplasmic Domain Affects Virus Properties and Vaccine Potential. *Mol. Ther.* 15 (5), 989–996. doi: 10.1038/mt.sj.6300131

Yoshida, S., Kondoh, D., Arai, E., Matsuoka, H., Seki, C., Tanaka, T., et al. (2003). Baculovirus Virions Displaying Plasmodium Berghei Circumsporozoite Protein Protect Mice Against Malaria Sporozoite Infection. *Virology* 316 (1), 161–170. doi: 10.1016/j.virol.2003.08.003

Conflict of Interest: The authors declare that the research was conducted in the absence of any commercial or financial relationships that could be construed as a potential conflict of interest.

Publisher's Note: All claims expressed in this article are solely those of the authors and do not necessarily represent those of their affiliated organizations, or those of the publisher, the editors and the reviewers. Any product that may be evaluated in this article, or claim that may be made by its manufacturer, is not guaranteed or endorsed by the publisher.

frontiers in Cellular and Infection Microbiology

ORIGINAL RESEARCH
published: 29 September 2021
doi: 10.3389/fcimb.2021.747952

The Presence of *Blastocystis* in Tibetan Antelope (*Pantholops hodgsonii*)

Hong-Li Geng[1†], Yu-Zhe Sun[1†], Jing Jiang[2], He-Ting Sun[3], Yuan-Guo Li[4], Si-Yuan Qin[3,4], Zhen-Jun Wang[4], Tao Ma[4], Jun-Hui Zhu[4], Nian-Yu Xue[5] and Hong-Bo Ni[1*]*

[1] College of Veterinary Medicine, Qingdao Agricultural University, Qingdao, China, [2] College of Life Sciences, Changchun Sci-Tech University, Shuangyang, China, [3] General Monitoring Station for Wildlife-Borne Infectious Diseases, State Forestry and Grass Administration, Shenyang, China, [4] Key Laboratory of Zoonosis Research, Ministry of Education, College of Veterinary Medicine, Jilin University, Changchun, China, [5] College of Animal Science and Veterinary Medicine, Heilongjiang Bayi Agricultural University, Daqing, China

OPEN ACCESS

Edited by:
Guo-Hua Liu,
Hunan Agricultural University, China

Reviewed by:
Md Robiul Karim,
Bangabandhu Sheikh Mujibur Rahman Agricultural University, Bangladesh
Zahra Babaei,
Kerman University of Medical Sciences, Iran
Meysam Sharifdini,
Guilan University of Medical Sciences, Iran

***Correspondence:**
Jing Jiang
jiangjingxiaoyao@163.com
Hong-Bo Ni
hongboni@126.com

[†]These authors have contributed equally to this work

Specialty section:
This article was submitted to Clinical Microbiology, a section of the journal Frontiers in Cellular and Infection Microbiology

Received: 27 July 2021
Accepted: 09 September 2021
Published: 29 September 2021

Citation:
Geng H-L, Sun Y-Z, Jiang J, Sun H-T, Li Y-G, Qin S-Y, Wang Z-J, Ma T, Zhu J-H, Xue N-Y and Ni H-B (2021) The Presence of Blastocystis in Tibetan Antelope (Pantholops hodgsonii). Front. Cell. Infect. Microbiol. 11:747952. doi: 10.3389/fcimb.2021.747952

Blastocystis is a protozoan that parasitizes the intestines. A number of hosts of *Blastocystis* have been found, including human and animals. However, there has been no research on the prevalence of *Blastocystis* in Tibetan antelope. Here, a molecular test was performed using 627 Tibetan antelope fecal samples collected on Tibet in China from 2019 to 2020. The result showed that 30 (4.8%) samples were *Blastocystis* positive. The highest prevalence of *Blastocystis* was in Shuanghu County (25/209, 12.0%), followed by Shenza County (2/103, 1.9%), Nyima County (3/182, 1.6%), and Baigoin County (0/133, 0.0%). In addition, logistic regression analysis showed that the gender, sampling year, and area of Tibetan antelope were risk factors for *Blastocystis* prevalence. Three subtypes (ST10, ST13, and ST14) of *Blastocystis* were found in Tibetan antelope through a subtype sequence analysis, and ST13 was identified to be the dominant subtype. This is the first investigation for the infection of *Blastocystis* in Tibetan antelope. Collectively, the data in this study have expanded the host range of *Blastocystis* and provided basic information for the distribution of *Blastocystis* subtypes, which could support the prevention of *Blastocystis* infection in wild animals.

Keywords: *Blastocystis*, prevalence, subtypes, Tibetan antelope (*Pantholops hodgsonii*), PCR

INTRODUCTION

Blastocystis is a protozoan that parasitizes the intestines (Jiménez et al., 2019; Paik et al., 2019). It can infect a variety of hosts, such as mammals, amphibians, birds, and insects (Zhu et al., 2020). *Blastocystis* is transmitted through the fecal–oral route or water and food between susceptible hosts (Asghari et al., 2019; Deng et al., 2019). Hosts infected with *Blastocystis* could develop clinical signs, e.g., diarrhea, abdominal pain, and vomiting. Immunocompromised individuals are more susceptible to *Blastocystis* (Wang et al., 2018a; Paik et al., 2019).

Blastocystis was first isolated from animal feces in 1911 (Alexeieff, 1911). Since then, more and more animals and humans, such as cattle, deer, sheep, and goats, were identified to be the hosts of *Blastocystis* (**Table 1**). In China, *Blastocystis* was first reported in children in 1990 (Li et al., 1990). A large number of investigations regarding *Blastocystis* prevalence in different hosts were performed previously (Song et al.,

TABLE 1 | Subtypes and prevalence of *Blastocystis* sp. detected from the ruminants worldwide (2010–2021).

Host	No. tested	No. positive	Prevalence (%)	Location	Subtypes (STs) identified	Reference
Sheep	832	50	6.00%	China	ST5, ST10, ST14	Li et al., 2018
Sheep	109	6	5.50%	China	ST1, ST5, ST10, ST14	Wang et al., 2018a
Sheep	100	32	32.00%	Iran	ST3, ST5, ST7, ST14	Salehi et al., 2021
Goat	781	2	0.30%	China	ST1	Li et al., 2018
Goat	236	73	30.90%	Malaysia	ST1, ST3, ST6, ST7	Tan et al., 2013
Goat	400	3	0.75%	Nepal	NA	Ghimire and Bhattarai, 2019
Goat	38	36	94.70%	Thailand	ST10, ST12, ST14	Udonsom et al., 2018
Goat	789	458	58.00%	China	ST1, ST3, ST4, ST5	Song et al., 2017
Cattle	147	14	9.52%	China	ST3, ST10, ST14	Wang et al., 2018a
Cattle	22	5	22.70%	UAE	ST10	AbuOdeh et al., 2019
Cattle	28	6	21.40%	Brazil	NA	Moura et al., 2018
Cattle	42	21	50.00%	Thailand	ST10, ST12	Udonsom et al., 2018
Cattle	80	9	11.30%	Turkey	ST10, ST14	Aynur et al., 2019
Cattle	526	54	10.30%	China	ST4, ST5, ST10, ST14	Zhu et al., 2017
Cattle	47	9	19.20%	USA	ST10, ST14	Fayer et al., 2012
Cattle	196	19	9.60%	Iran	ST3, ST5, ST6	Badparva et al., 2015
Cattle	31	7	22.60%	England	ST1, ST5, ST10	Alfellani et al., 2013
Cattle	25	20	80.00%	Colombia	ST1, ST3	Ramírez et al., 2014
Cattle	36	15	41.70%	Libya	ST5, ST10, ST14	Alfellani et al., 2013
Cattle	75	25	33.30%	Iran	ST5, ST10	Sharifi et al., 2020
Cattle	29	10	34.50%	Malaysia	NA	Hemalatha et al., 2014
Cattle	40	14	35.00%	Iran	ST10, ST14	Rostami et al., 2020
Cattle	1512	101	6.70%	Korea	ST1,5,10,14	Lee et al., 2018
Cattle	133	72	54.10%	Japan	ST14	Masuda et al., 2018
Cattle	254	161	63.40%	Lebanon	ST1, ST3, ST5, ST10, ST14	Greige et al., 2019
Cattle	110	6	5.40%	Malaysia	NA	Abd et al., 2019
Cattle	1027	278	27.10%	China	ST10	Ren et al., 2019
Cattle	500	47	9.40%	Indonesia	NA	Hastutiek et al., 2019
Cattle	2539	73	2.90%	USA	ST3, ST4, ST5, ST10, ST14	Maloney et al., 2019
Cattle	120	30	25.00%	Malaysia	ST1, ST3, ST4, ST5, ST10, ST14	Kamaruddin et al., 2020
Cattle	108	108	100.00%	Indonesia	ST10	Suwanti et al., 2020
Reindeer	104	7	6.70%	China	ST10, ST13	Wang et al., 2018b
Sika deer	82	12	14.60%	China	ST10, ST14	Wang et al., 2018b
Water deer	125	51	40.80%	Korean	ST4, ST14	Kim et al., 2020
Red deer	48	0	0.00%	China	NA	Wang et al., 2018b
Spotted deer	30	1	3.30%	Bangladesh	ST14	Li et al., 2019
Sika deer	132	60	45.50%	Japan	ST14	Shirozu et al., 2021
White tailed-deer	80	71	88.80%	USA	ST1, ST3, ST4, ST10, ST14, ST21, ST23, ST24, ST25, ST26	Maloney and Santin, 2021

UAE, United Arab Emirates; NA, not available.

2017; Zhao et al., 2017; Wang et al., 2018a; Wang et al., 2018b). So far, the infection of *Blastocystis* has been reported in many animals, including domestic and wild animals (Zhao et al., 2017; Wang et al., 2018a).

To date, approximately 29 proposed *Blastocystis* subtypes have been identified in a large number of literatures (Ma et al., 2020). ST1-9 and ST12 subtypes were identified in humans, while ST10-17 and ST21-28 subtypes were detected in animals (Stensvold and Clark, 2016; Ning et al., 2020; Hublin et al., 2021). Of note, some subtypes were identified in both humans and animals, such as ST1, ST3, and ST5 subtypes (Song et al., 2017; Wang et al., 2018a). ST4 was found in deer (Wang et al., 2018b; Kim et al., 2020; Shirozu et al., 2021), and ST12 was found in yaks in the plateau area (Ren et al., 2019).

Tibetan antelope (*Pantholops hodgsonii*) belongs to genus Pantholops, family Bovidae, order Cetartiodactyla according to the IUCN Red List in 2016 (IUCN SSC Antelope Specialist Group, 2016). Tibetan antelope is one of the most rare and endangered wild animals. There are approximately 100,000 to 150,000 Tibetan antelope in India and China (IUCN SSC Antelope Specialist Group 2016). Tibetan antelope can carry various pathogens, such as *Mycoplasma capricolum* subspecies, *capripneumoniae* (Mccp) (Yu et al., 2012), and *Escherichia coli* (Bai et al., 2016).

However, the existing data indicate that sheep may carry several potential *Blastocystis* subtypes, including ST1, ST3, ST4, ST5, ST6, and ST7 (Tan et al., 2013; Song et al., 2017; Wang et al., 2018a; Salehi et al., 2021). So far, studies on the prevalence and subtype diversity of *Blastocystis* in Tibetan antelope are unknown and the relevant public health impact is still unclear. This study provides important information on the diversity of *Blastocystis* subtypes in Tibetan antelope, and would help determine the role of Tibetan antelope in the transmission of *Blastocystis* to humans and other animals.

MATERIALS AND METHODS

Specimen Collection

From August 2019 to September 2020, the feces of 627 wild Tibetan antelope was collected in four areas in Tibet (**Table 2** and **Figure 1**). This study randomly observed Tibetan antelope in the field. Fresh fecal samples were put into a PE glove immediately after defecation onto the ground, and then were placed into ice boxes and transported to the laboratory. This study was approved by the Ethics Committee of Jilin University. Appropriate permission was obtained from the General Monitoring Station for Wildlife-Borne Infectious Diseases, State Forestry and Grass Administration.

DNA Extraction and PCR Amplification

Genomic DNA was extracted using the E.Z.N.A.® Stool DNA Kit (Omega Biotek Inc., Norcross, GA, USA) according to the manufacturer's instructions and stored at −20°C until PCR amplification. SSU rRNA gene was the target for PCR analysis using primers RD5 (5′-ATCTGGTTGATCCTGCCAGT-3′) and BhRDr (5′-GAGCTTTTTAACTGCAACAACG-3′) as described previously to amplify an approximately 600-bp region (Scicluna et al., 2006). Positive and negative controls were included in each test. PCR products were observed using UV light after electrophoresis at a 1.5% agarose gel containing ethidium bromide.

Sequence and Phylogenetic Analyses

The *Blastocystis*-positive PCR products were sent to Sangon Biotech Company (Shanghai, China) for sequencing. The sequence accuracy was confirmed by bidirectional sequencing. The sequencing was re-performed if variation was present in the previous result. Basic Local Alignment Search Tool (BLAST) (http://www.ncbi.nlm.nih.gov/blast/) was employed to compare consensus sequences with the similar sequences on GenBank. The subtypes of *Blastocyst* isolates were determined through the online platform PubMLST (https://pubmlst.org/bigsdb?db=pubmlst_blastocystis_seqdef). The obtained sequences were aligned using ClustalX 1.83 program. The alignment was trimmed using the trimAI v1.2 software (http://trimal.cgenomics.org/downloads) (Li et al., 2019). All positions with

TABLE 2 | Factors in the sampling site of different seasons in tibet.

Season	Longitude	Latitude	Altitude	Temperature	Humidity	Climate
Summer (August)	31°29′	92°04′	4,507 m	9.0°C	68 mm	Plateau alpine climate
Autumn (September)				6.1°C	70 mm	

FIGURE 1 | A map of Tibet Autonomous Region, China, in which Tibetan antelope are sampled.

gaps were eliminated, and 104 unambiguously aligned sites were used for phylogenetic inference. The maximum likelihood (ML) method (Kimura two-parameter model) was employed to reconstruct phylogenetic trees by using MEGA X. Representative nucleotide sequences were submitted to GenBank under accession numbers: MZ444657–MZ444662.

Statistical Analysis

The variation of *Blastocystis* prevalence (y) in Tibetan antelope on the basis of sampling year ($x1$), gender ($x2$), and collecting region ($x3$) was analyzed with χ^2 test using SAS version 9.4 (SAS Institute Inc., USA). In the multivariable regression analysis, each of the variables was independently contained in the binary Logit model. The best model was judged by Fisher's scoring algorithm. All tests were two-sided, and the results were considered statistically significant when $p < 0.05$. To explore the association between *Blastocystis* prevalence and the investigated factors, the odds ratios (ORs) and their 95% confidence intervals (95% CIs) were calculated.

RESULTS

Prevalence of *Blastocystis* sp.

In the present study, 30 out of 627 Tibetan antelope feces were identified to be *Blastocystis* positive (**Figure 2**). The infection rate of *Blastocystis* in Tibetan antelope in 2019 (0.6%, 2/322) was lower than that (9.2%, 28/305) in 2020. The prevalence of *Blastocystis* in different investigated counties ranged from 0% to 12% (**Table 3**). *Blastocystis* were detected in all three counties, except for Baigoin County. The highest prevalence of *Blastocystis* was in Shuanghu County (25/209, 12.0%), followed by Shenza

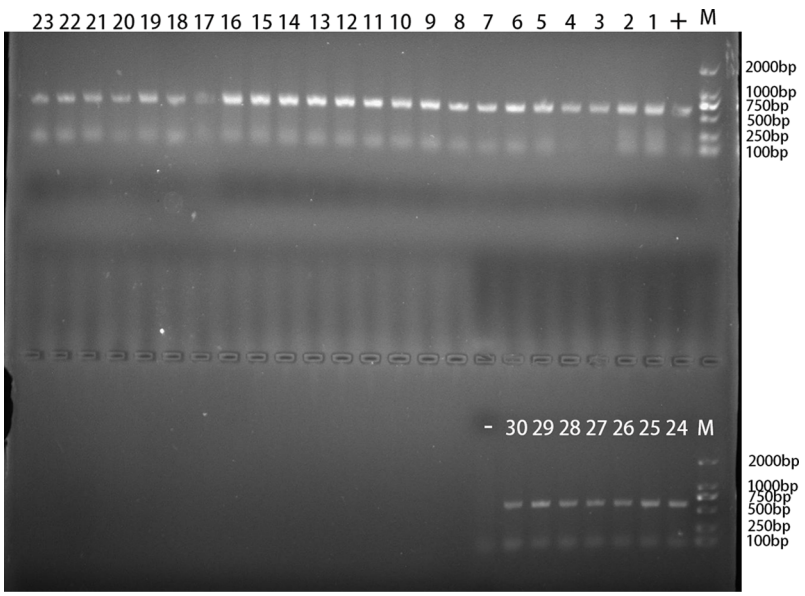

FIGURE 2 | The PCR amplification result of *Blastocystis* rRNA gene. "1–30": 30 positive samples of *Blastocystis* in TA25, TA26, TA72, TA100, TA103, TA105, TA107, TA108, TA111, TA118, TA124, TA128, TA130, TA131, TA147, TA148, TA156, TA157, TA169, TA175, TA214, TA216, TA228, TA230, TA232, TA235, TA238, TA252, TA291, and TA307; "-": negative control; "+": positive control; "M": DL2000 Marker.

TABLE 3 | Occurrence and subtype distribution of *Blastocystis* sp. in tibetan antelope (*Pantholops hodgsonii*).

Factor	Category	No. tested	No. positive	Prevalence (%) (95% CI)	*p*-value	OR (95% CI)	Subtypes (no.)
Gender	Female	300	8	2.7 (0.8–4.5)	0.017	Reference	ST10 (1); ST13 (6); ST14 (1)
	Male	327	22	6.7 (4.0–9.4)		2.63 (1.15–6.00)	ST10 (3); ST13 (18); ST14 (1)
Sampling year	2019	322	2	0.6 (0.0–1.5)	<0.01	Reference	ST13 (2)
	2020	305	28	9.2 (5.9–12.4)		16.17 (3.82–68.50)	ST10 (4); ST13 (22); ST14 (2)
Region	Nyima County	182	3	1.6 (0.0–3.5)	<0.01	Reference	ST13 (3)
	Shuanghu County	209	25	12.0 (7.6–16.4)		8.11 (2.41–27.33)	ST10 (3); ST13 (20); ST14 (2)
	Shenza County	103	2	1.9 (0.0–4.6)		1.18 (0.19–7.19)	ST10 (1); ST13(1)
	Baingoin County	133	0	0.0 (0.0–0.0)		–	–
Total		627	30	4.8 (3.1–6.5)			ST10 (4); ST13 (24); ST14 (2)

County (2/103, 1.9%) and Nyima County (3/182, 1.6%; **Table 3**). The infection rate of *Blastocystis* in Tibetan antelope in females (2.7%, 8/300) was significantly lower than that (6.7%, 22/327) in males ($p = 0.017$).

Risk Factors of *Blastocystis* sp.

To expose gender, sampling year, and collecting region of Tibetan antelope, and *Blastocystis* prevalence, univariate analysis was also conducted in the present study (**Table 3**). A Fisher's scoring method-based positive stepwise logistic regression analysis was performed to estimate the influence of multiple variables on *Blastocystis* infection. Only one variable was found to have effects on the *Blastocystis* infection in the final model, as described by the equation: $y = 1.3138x3 + 0.7097$. Collecting region had a positive impact on the risk of *Blastocystis* infection with the OR of 3.720 (95% CI 2.061–6.715). Nyima County (1.6%, 95% CI 0.0–3.5) was considered to have lower prevalence than Shuanghu County (OR = 8.11, 95% CI 2.41–27.33) and Shenza County (OR = 1.18, 95% CI 0.19–7.19) (**Table 3**).

Distribution and Phylogenetic Analysis of *Blastocystis* Subtypes

Three *Blastocystis* subtypes (ST10, ST13, and ST14) were detected in this study. Among them, the ST13 subtype was found in 24 individuals and was widely distributed in different gender subgroups, sampling years, and collecting regions. In the sampling years, all three *Blastocystis* subtypes appeared in Tibetan antelope in 2020, and only ST13 was found in the Tibetan antelope in 2019 (**Table 3**). In the gender subgroups, although all of the three subtypes appeared in the Tibetan antelope, the infection of ST10 and ST13 in males was higher than that in females. Tibetan antelope in Shuanghu County was found to be infected with three *Blastocystis* subtypes in the regional subgroups. However, only the ST13 subtype was found in the Tibetan antelope in Nyima County (**Table 3**).

The six representative sequences in this study and 49 sequences on GenBank were used to construct a phylogenetic tree. According to the phylogenetic tree analysis, the sequences of the three subtypes (ST10, ST13, and ST14) obtained from this study were clustered with their reference subtypes (**Figure 3**). The sequence of ST10 isolate has 99% homology with that of ST10 isolated from sika deer (MK930358) and sheep (MW850529). The sequence identified as ST13 in this study has a high degree of homology (99%) with the sequence identified in white Kangaroo (MT672637) and reindeer (MH325366). The ST14 sequence has 98% homology with the known reference sequence identified in sheep (MF186707).

DISCUSSION

The overall infection rate of *Blastocystis* in Tibetan antelope was 4.8% (30/627) in Tibet, which was lower than the prevalence of 5.5% (6/109) and 6.0% (50/832) identified in sheep (Wang et al., 2018a; Li et al., 2018) in China and 19.3% (9/150) and 32.0% (32/100) in sheep in Iran (Rostami et al., 2020; Salehi et al., 2021). The difference in the prevalence of *Blastocystis* may be related to the living environment and geographical factors of different countries (Tan, 2008). The infection rate of *Blastocystis* in different species is different. For example, the prevalence of Tibetan antelope in this study and sheep, goats, and cattle in other studies were 4.8% (30/627), 0.75% (3/400) (Ghimire and Bhattarai, 2019), and 14.43% (72/500) (Hastutiek et al., 2019), respectively. The results showed that the prevalence of *Blastocystis* might be related to the sensitivity of animals to *Blastocystis*. Therefore, future research should collect more samples to better understand the population characteristics of *Blastocystis* in Tibetan antelope.

The average temperature in Baingoin County is −17.1°C annually, which is much lower than that of other counties. The survival of *Blastocystis* may be affected by the low-temperature environment in Baingoin County. *Blastocystis* might survive in warm and humid environment (Sari et al., 2021). This is probably the reason why the infection rate of *Blastocystis* in Baingoin County (0.0%, 0/133) was significantly lower than that of the other three counties.

Previous studies have shown that the infection rate of *Blastocystis* in males (4.8%, 25/517) was higher than that in females (3.1%, 9/291) in cattle (Lee et al., 2018) and in sambar (males: 38.2%, 21/55 *vs.* females: 23.3%, 7/30) (Kim et al., 2020). This study also found that the infection rate of *Blastocystis* (6.7%, 22/327) was higher in males than in females (2.7%, 8/300) of Tibetan antelope. This may be due to the fact that males have a wider range of activities than females, and have a relatively higher chance for contacting with cysts.

At present, 29 proposed *Blastocystis* subtypes have been identified (Maloney and Santin, 2021). Among them, ST1, ST3, ST5, ST10, and ST14 subtypes were detected in sheep and goats (Song et al., 2017; Li et al., 2018; Wang et al., 2018a), among which ST10 and ST14 were the most common subtypes (Fayer et al., 2012; Zhao et al., 2017; Hublin et al., 2021). ST10 and ST14 were also detected in Tibetan antelope. However, it is worth noting that ST10 ($n = 4$) and ST14 ($n = 2$) were not common in the samples of Tibetan antelope in this study. On the contrary, ST13 ($n = 24$) represented the infection trend of *Blastocystis* in Tibetan antelope. ST13 subtype is a relatively rare subtype. ST13 has been detected in deer, flying squirrels, kangaroo, monkeys, and other animals (Parkar et al., 2010; Alfellani et al., 2013; Wang et al., 2018b; Li et al., 2019; Xiao et al., 2019). Compared with domestic animals, ST13 may be more common in wild animals. Therefore, the follow-up research should focus on the distribution of *Blastocystis* genotypes in wild animals.

In summary, this is the first report of *Blastocystis* infection in Tibetan antelope in Tibet, China. The total prevalence of *Blastocystis* was 4.11% (30/627). Moreover, ST10, ST13, and ST14 subtypes were found in Tibetan antelope, among which ST13 was the dominant subtype. These results not only expanded the knowledge of hosts of *Blastocystis*, but also provided data for further studies on the distribution of *Blastocystis* subtypes in Tibetan antelope, and also provided data supporting for the prevention of *Blastocystis* infection in wild animals.

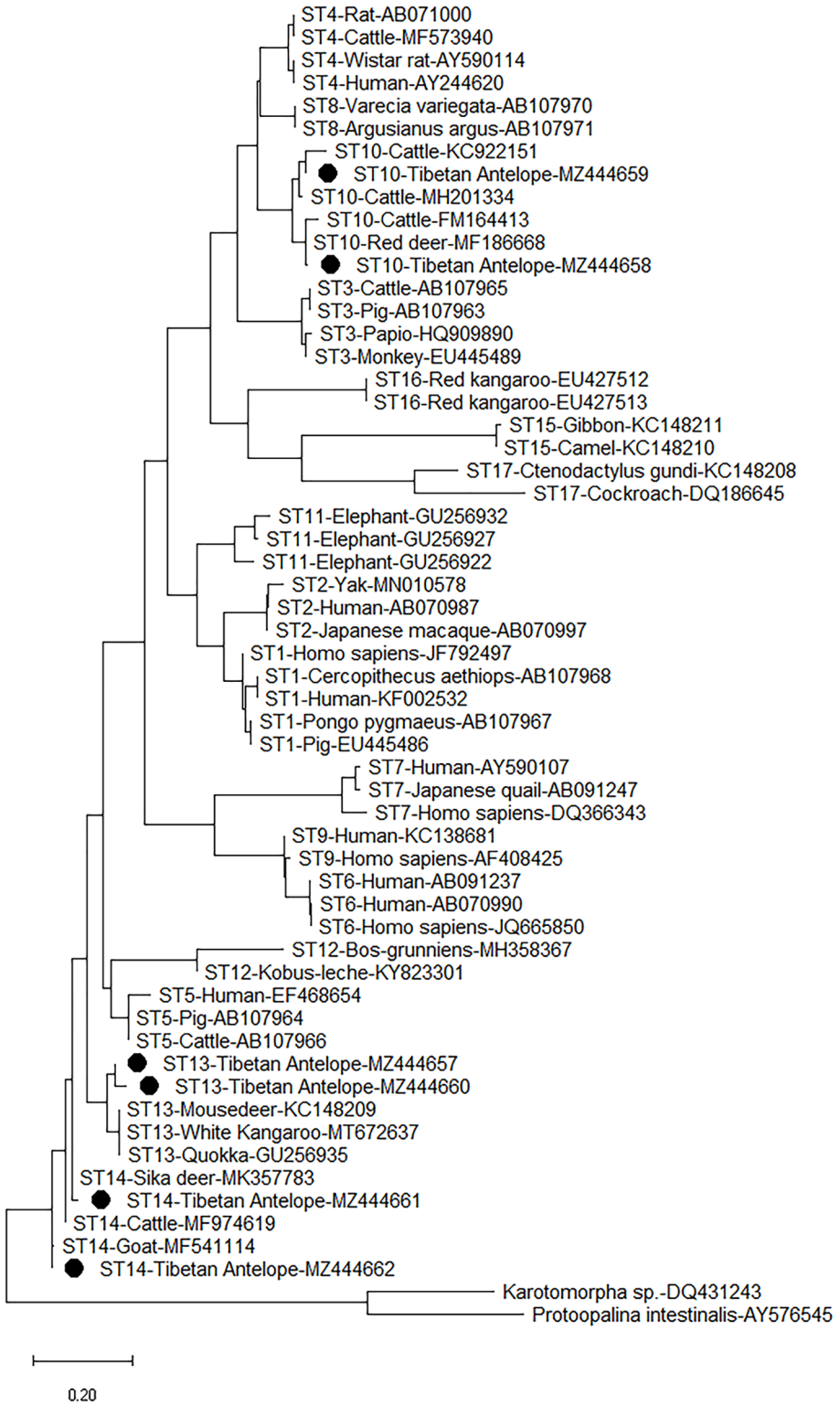

FIGURE 3 | Phylogenetic analyses of *Blastocystis* using (ML) method (Kimura two-parameter model). Bootstrap values below 50% from 1,000 replicates are not shown. *Blastocystis* isolates identified in the present study are indicated by solid circles.

DATA AVAILABILITY STATEMENT

The datasets presented in this study can be found in online repositories. The names of the repository/repositories and accession number(s) can be found in the article/supplementary material.

ETHICS STATEMENT

The animal study was reviewed and approved by the Ethics Committee of Jilin University.

AUTHOR CONTRIBUTIONS

H-BN and JJ conceived and designed the study and critically revised the manuscript. S-YQ, H-TS, J-HZ, Z-JW, and TM collected the samples. H-LG, Y-ZS, Y-GL, and N-YX performed the experiments. H-LG and Y-ZS analyzed the data and drafted the manuscript. All authors contributed to the article and approved the submitted version.

FUNDING

This work was supported by the Research Foundation for Distinguished Scholars of Qingdao Agricultural University (665-1120046).

ACKNOWLEDGMENTS

We thank Dr. Chuang Lyu (Shandong New Hope Liuhe Group Co., Ltd. and Qingdao Jiazhi Biotechnology Co., Ltd., Qingdao, China) for critically revising the manuscript.

REFERENCES

Abd, R. N. A., Yusof, A. M., and Mohammad, M. (2019). Identification of Blastocystis Sp. Infection Form Cattle, Goat and Sheep Isolated From Farms in Pahang, Malaysia. *Int. J. Allied Health Sci.* 3 (3), 810–810.

AbuOdeh, R., Ezzedine, S., Madkour, M., Stensvold, C. R., Samie, A., Nasrallah, G., et al. (2019). Molecular Subtyping of *Blastocystis* From Diverse Animals in the United Arab Emirates. *Protist* 170 (5), 125679. doi: 10.1016/j.protis.2019.125679

Alexeieff, A. (1911). Sur La Nature Des Formations Dites "Kystes De *Trichomonas Intestinalis*". *Comptes Rendus Des. Seances la Sociiti Biologie* 71, 296298.

Alfellani, M. A., Taner-Mulla, D., Jacob, A. S., Imeede, C. A., Yoshikawa, H., Stensvold, C. R., et al. (2013). Genetic Diversity of *Blastocystis* in Livestock and Zoo Animals. *Protist* 164, 497–509. doi: 10.1016/j.protis.2013.05.003

Asghari, A., Sadraei, J., Pirestani, M., and Mohammadpour, I. (2019). First Molecular Identification and Subtype Distribution of Blastocystis Sp. Isolated From Hooded Crows (*Corvus Cornix*) and Pigeons (*Columba Livia*) in Tehran Province, Iran. *Comp. Immunol. Microbiol. Infect. Dis.* 62, 25–30. doi: 10.1016/j.cimid.2018.11.013

Aynur, Z. E., Güçlü, Ö., Yıldız, İ., Aynur, H., Ertabaklar, H., Bozdoğan, B., et al. (2019). Molecular Characterization of *Blastocystis* in Cattle in Turkey. *Parasitol Res.* 118 (3), 1055–1059. doi: 10.1007/s00436-019-06243-8

Badparva, E., Sadraee, J., and Kheirandish, F. (2015). Genetic Diversity of *Blastocystis* Isolated From Cattle in Khorramabad, Iran. *Jundishapur J. Microbiol.* 8 (3), e14810. doi: 10.5812/jjm.14810

Bai, X., Hu, B., Xu, Y., Sun, H., Zhao, A., Ba, P., et al. (2016). Molecular and Phylogenetic Characterization of Non-O157 Shiga Toxin-Producing *Escherichia Coli* Strains in China. *Front. Cell Infect. Microbiol.* 6, 143. doi: 10.3389/fcimb.2016.00143

Deng, L., Chai, Y., Zhou, Z., Liu, H., Zhong, Z., Hu, Y., et al. (2019). Epidemiology of Blastocystis Sp. Infection in China: A Systematic Review. *Parasite* 26, 41. doi: 10.1051/parasite/2019042

Fayer, R., Santin, M., and Macarisin, D. (2012). Detection of Concurrent Infection of Dairy Cattle With *Blastocystis*, *Cryptosporidium*, *Giardia*, and *Enterocytozoon* by Molecular and Microscopic Methods. *Parasitol Res.* 111 (3), 1349–1355. doi: 10.1007/s00436-012-2971-1

Ghimire, T. R., and Bhattarai, N. (2019). A Survey of Gastrointestinal Parasites of Goats in a Goat Market in Kathmandu, Nepal. *J. Parasit. Dis.* 43 (4), 686–695. doi: 10.1007/s12639-019-01148-w

Greige, S., El Safadi, D., Khaled, S., Gantois, N., Baydoun, M., Chemaly, M., et al. (2019). First Report on the Prevalence and Subtype Distribution of Blastocystis Sp. In Dairy Cattle in Lebanon and Assessment of Zoonotic Transmission. *Acta Trop.* 194, 23–29. doi: 10.1016/j.actatropica.2019.02.013

Hastutiek, P., Yuniarti, W. M., Djaeri, M., Lastuti, N. D. R., Suprihati, E., and Suwanti, L. T. (2019). Prevalence and Diversity of Gastrointestinal Protozoa in Madura Cattle at Bangkalan Regency, East Java, Indonesia. *Vet. World* 12 (2), 198–204. doi: 10.14202/vetworld.2019.198-204

Hemalatha, C., Chandrawathani, P., Suresh Kumar, G., Premaalatha, S., Geethamalar, B., Lily Rozita, M. H., et al. (2014). The Diagnosis of Blastocystis Sp. Form Animals-an Emerging Zoonosis. *Malaysian J. Vet. Res.* 5, 15–21.

Hublin, J. S. Y., Maloney, J. G., and Santin, M. (2021). *Blastocystis* in Domesticated and Wild Mammals and Birds. *Res. Vet. Sci.* 135, 260–282. doi: 10.1016/j.rvsc.2020.09.031

Jiménez, P. A., Jaimes, J. E., and Ramírez, J. D. (2019). A Summary of *Blastocystis* Subtypes in North and South America. *Parasit. Vectors* 12 (1), 376. doi: 10.1186/s13071-019-3641-2

Kamaruddin, S. K., Mat, Y. A., and Mohammad, M. (2020). Prevalence and Subtype Distribution of *Blastocystis Sp. In* Cattle From Pahang, Malaysia. *Trop. Biomed.* 37 (1), 127–141.

Kim, K. T., Noh, G., Lee, H., Kim, S. H., Jeong, H., Kim, Y., et al. (2020). Genetic Diversity and Zoonotic Potential of *Blastocystis* in Korean Water Deer, Hydropotes Inermis Argyropus. *Pathogens* 9 (11), 955. doi: 10.3390/pathogens9110955

Lee, H., Lee, S. H., Seo, M. G., Kim, H. Y., Kim, J. W., Lee, Y. R., et al. (2018). Occurrence and Genetic Diversity of *Blastocystis* in Korean Cattle. *Vet. Parasitol.* 258, 70–73. doi: 10.1016/j.vetpar.2018.06.010

Li, J., Karim, M. R., Li, D., Rahaman Sumon, S. M. M., Siddiki, S. H. M. F., Rume, F. I., et al. (2019). Molecular Characterization of Blastocystis Sp. In Captive Wildlife in Bangladesh National Zoo: Non-Human Primates With High Prevalence and Zoonotic Significance. *Int. J. Parasitol Parasites Wildl.* 10, 314–320. doi: 10.1016/j.ijppaw.2019.11.003

Li, W. C., Wang, K., and Gu, Y. (2018). Occurrence of Blastocystis Sp. And *Pentatrichomonas Hominis* in Sheep and Goats in China. *Parasit. Vectors* 11 (1), 93. doi: 10.1186/s13071-018-2671-5

Li, X. M., Zhou, H., Zhong, D. M., and He, J. G. (1990). Diagnosis and Treatment of Two Cases of *Blastocystis Hominis*. *Chin. J. Pediatr.* 28, 8.

Maloney, J. G., Jang, Y., Molokin, A., George, N. S., and Santin, M. (2021). Wide Genetic Diversity of *Blastocystis* in White-Tailed Deer (*Odocoileus Virginianus*) From Maryland, USA. *Microorganisms* 9 (6), 1343. doi: 10.3390/microorganisms9061343

Maloney, J. G., Lombard, J. E., Urie, N. J., Shivley, C. B., and Santin, M. (2019). Zoonotic and Genetically Diverse Subtypes of *Blastocystis* in US Pre-Weaned Dairy Heifer Calves. *Parasitol Res.* 118 (2), 575–582. doi: 10.1007/s00436-018-6149-3

Maloney, J. G., and Santin, M. (2021). Mind the Gap: New Full-Length Sequences of *Blastocystis* Subtypes Generated *via* Oxford Nanopore Minion Sequencing Allow for Comparisons Between Full-Length and Partial Sequences of the Small Subunit of the Ribosomal RNA Gene. *Microorganisms* 9 (5), 997. doi: 10.3390/microorganisms9050997

Ma, L., Qiao, H., Wang, H., Li, S., Zhai, P., Huang, J., et al. (2020). Molecular Prevalence and Subtypes of Blastocystis Sp. In Primates in Northern China. *Transbound Emerg. Dis.* 67 (6), 2789–2796. doi: 10.1111/tbed.13644

Masuda, A., Sumiyoshi, T., Ohtaki, T., and Matsumoto, J. (2018). Prevalence and Molecular Subtyping of *Blastocystis* From Dairy Cattle in Kanagawa, Japan. *Parasitol Int.* 67 (6), 702–705. doi: 10.1016/j.parint.2018.07.005

Moura, R. G. F., Oliveira-Silva, M. B., Pedrosa, A. L., Nascentes, G. A. N., and Cabrine-Santos, M. (2018). Occurrence of Blastocystis Spp. In Domestic Animals in Triângulo Mineiro Area of Brazil. *Rev. Soc. Bras. Med. Trop.* 51 (2), 240–243. doi: 10.1590/0037-8682-0484-2016

Ning, C. Q., Hu, Z. H., Chen, J. H., Ai, L., and Tian, L. G. (2020). Epidemiology of Blastocystis Infection From 1990 to 2019 in China. *Infect. Dis. Poverty* 9 (1), 168. doi: 10.1186/s40249-020-00779-z

Paik, S., Jung, B. Y., Lee, H., Hwang, M. H., Han, J. E., Rhee, M. H., et al. (2019). Molecular Detection and Subtyping of *Blastocystis* in Korean Pigs. *Korean J. Parasitol.* 57 (5), 525–529. doi: 10.3347/kjp.2019.57.5.525

Parkar, U., Traub, R. J., Vitali, S., Elliot, A., Levecke, B., Robertson, I., et al. (2010). Molecular Characterization of *Blastocystis* Isolates From Zoo Animals and Their Animal-Keepers. *Vet. Parasitol.* 169 (1-2), 8–17. doi: 10.1016/j.vetpar.2009.12.032

Ramírez, J. D., Sánchez, L. V., Bautista, D. C., Corredor, A. F., Flórez, A. C., and Stensvold, C. R. (2014). *Blastocystis* Subtypes Detected in Humans and Animals From Colombia. *Infect. Genet. Evol.* 22, 223–228. doi: 10.1016/j.meegid.2013.07.020

Ren, M., Song, J. K., Yang, F., Zou, M., Wang, P. X., Wang, D., et al. (2019). First Genotyping of *Blastocystis* in Yaks From Qinghai Province, Northwestern China. *Parasit. Vectors* 12 (1), 171. doi: 10.1186/s13071-019-3436-5

Rostami, M., Fasihi-Harandi, M., Shafiei, R., Aspatwar, A., Derakhshan, F. K., and Raeghi, S. (2020). Genetic Diversity Analysis of *Blastocystis* Subtypes and Their Distribution Among the Domestic Animals and Pigeons in Northwest of Iran. *Infect. Genet. Evol.* 86:104591. doi: 10.1016/j.meegid.2020.104591

Salehi, R., Rostami, A., Mirjalali, H., Stensvold, C. R., and Haghighi, A. (2021). Genetic Characterization of *Blastocystis* From Poultry, Livestock Animals and Humans in the Southwest Region of Iran-Zoonotic Implications. *Transbound Emerg. Dis.* doi: 10.1111/tbed.14078

Sari, I. P., Audindra, S., Zhafira, A. S., Rahma, A. A., and Wahdini, S. (2021). Nutritional Status of School-Aged Children With Intestinal Parasite Infection in South Jakarta, Indonesia. *Open Access Macedonian J. Med. Sci.* 9 (E), 95–100. doi: 10.3889/oamjms.2021.5711

Scicluna, S. M., Tawari, B., and Clark, C. G. (2006). DNA Barcoding of *Blastocystis*. *Protist* 157 (1), 77–85. doi: 10.1016/j.protis.2005.12.001

Sharifi, Y., Abbasi, F., Shahabi, S., Zaraei, A., Mikaeili, F., and Sarkari, B. (2020). Comparative Genotyping of *Blastocystis* Infecting Cattle and Human in the South of Iran. *Comp. Immunol. Microbiol. Infect. Dis.* 72, 101529. doi: 10.1016/j.cimid.2020.101529

Shirozu, T., Morishita, Y. K., Koketsu, M., and Fukumoto, S. (2021). Molecular Detection of Blastocystis Sp. Subtype 14 in the Yezo Sika Deer (*Cervus Nippon Yesoensis*) in Hokkaido, Japan. *Vet. Parasito*. 100585, 2405–9390. doi: 10.1016/j.vprsr.2021.100585

Song, J. K., Yin, Y. L., Yuan, Y. J., Tang, H., Ren, G. J., Zhang, H. J., et al. (2017). First Genotyping of Blastocystis Sp. In Dairy, Meat, and Cashmere Goats in Northwestern China. *Acta Trop.* 176, 277–282. doi: 10.1016/j.actatropica

Stensvold, C. R., and Clark, C. G. (2016). Current Status of *Blastocystis*: A Personal View. *Parasitol Int.* 65 (6 Pt B), 763–771. doi: 10.1016/j.parint.2016.05.015

Suwanti, L. T., Susana, Y., Hastutiek, P., Suprihati, E., and Lastuti, N. D. R. (2020). *Blastocystis* Spp. Subtype 10 Infected Beef Cattle in Kamal and Socah, Bangkalan, Madura, Indonesia. *Vet. World* 13 (2), 231–237. doi: 10.14202/vetworld.2020.231-237

Tan, K. S. (2008). New Insights on Classification, Identification, and Clinical Relevance of Blastocystis Spp. *Clin. Microbiol. Rev.* 21 (4), 639–665. doi: 10.1128/CMR.00022-08

Tan, T. C., Tan, P. C., Sharma, R., Sugnaseelan, S., and Suresh, K. G. (2013). Genetic Diversity of Caprine *Blastocystis* From Peninsular Malaysia. *Parasitol Res.* 112 (1), 85–89. doi: 10.1007/s00436-012-3107-3

Udonsom, R., Prasertbun, R., Mahittikorn, A., Mori, H., Changbunjong, T., Komalamisra, C., et al. (2018). *Blastocystis* Infection and Subtype Distribution in Humans, Cattle, Goats, and Pigs in Central and Western Thailand. *Infect. Genet. Evol.* 65, 107–111. doi: 10.1016/j.meegid.2018.07.007

Wang, J., Gong, B., Liu, X., Zhao, W., Bu, T., Zhang, W., et al. (2018b). Distribution and Genetic Diversity of Blastocystis Subtypes in Various Mammal and Bird Species in Northeastern China. *Parasit. Vectors* 11 (1), 522. doi: 10.1186/s13071-018-3106-z

Wang, J., Gong, B., Yang, F., Zhang, W., Zheng, Y., and Liu, A. (2018a). Subtype Distribution and Genetic Characterizations of *Blastocystis* in Pigs, Cattle, Sheep and Goats in Northeastern China's Heilongjiang Province. *Infect. Genet. Evol.* 57, 171–176. doi: 10.1016/j.meegid.2017.11.026

Xiao, X., Zhou, S. H., Jiang, N., Tian, D. Z., Zhou, Z. M., Zhang, M., et al. (2019). First Record of *Leptospira* and *Blastocystis* Infections in Captive Flying Squirrels (*Trogopterus Xanthipes*) From Enshi County, China. *Acta Trop.* 197, 105065. doi: 10.1016/j.actatropica.2019.105065

Yu, Z., Wang, T., Sun, H., Xia, Z., Zhang, K., Chu, D., et al. (2012). Contagious Caprine Pleuropneumonia in Endangered Tibetan Antelope, Chin. *Emerg. Infect. Dis.* 19 (12), 2051–2053. doi: 10.3201/eid1912.130067

Zhao, G. H., Hu, X. F., Liu, T. L., Hu, R. S., Yu, Z. Q., Yang, W. B., et al. (2017). Molecular Characterization of Blastocystis Sp. In Captive Wild Animals in Qinling Mountains. *Parasitol Res.* 116 (8), 2327–2333. doi: 10.1007/s00436-017-5506-y

Zhu, W., Tao, W., Gong, B., Yang, H., Li, Y., Song, M., et al. (2017). First Report of *Blastocystis* Infections in Cattle in China. *Vet. Parasitol.* 246, 38–42. doi: 10.1016/j.vetpar.2017.09

Zhu, W., Wei, Z., Li, Q., Lin, Y., Yang, H., and Li, W. (2020). Prevalence and Subtype Diversity of *Blastocystis* in Human and Nonhuman Primates in North China. *Parasitol Res.* 119 (8), 2719–2725. doi: 10.1007/s00436-020-06761-w

Conflict of Interest: The authors declare that the research was conducted in the absence of any commercial or financial relationships that could be construed as a potential conflict of interest.

frontiers in Cellular and Infection Microbiology

ORIGINAL RESEARCH
published: 29 September 2021
doi: 10.3389/fcimb.2021.755715

In Vitro Evaluation of *Lavandula angustifolia* Essential Oil on Anti-*Toxoplasma* Activity

Na Yao[1,2,3†], Jia-Kang He[4†], Ming Pan[1,2,3], Zhao-Feng Hou[1,2,3], Jin-Jun Xu[1,2,3], Yi Yang[5], Jian-Ping Tao[1,2,3] and Si-Yang Huang[1,6]*

[1] Institute of Comparative Medicine, College of Veterinary Medicine, Yangzhou University, Yangzhou, China, [2] Jiangsu Co-Innovation Center for Prevention and Control of Important Animal Infectious Diseases and Zoonosis, Yangzhou University, Yangzhou, China, [3] Jiangsu Key Laboratory of Zoonosis, Yangzhou University, Yangzhou, China, [4] College of Animal Science and Technology, Guangxi University, Nanning, China, [5] College of Animal Sciences, Zhejiang Provincial Key Laboratory of Preventive Veterinary Medicine, Institute of Preventive Veterinary Medicine, Zhejiang University, Hangzhou, China, [6] Joint International Research Laboratory of Agriculture and Agri-Product Safety, The Ministry of Education of China, Yangzhou University, Yangzhou, China

OPEN ACCESS

Edited by:
Wei Cong,
Shandong University, Weihai, China

Reviewed by:
De-Hua Lai,
Sun Yat-sen University, China
Shuai Wang,
Xinxiang Medical University, China

***Correspondence:**
Si-Yang Huang
siyang.huang@hotmail.com

[†]These authors have contributed equally to this work

Specialty section:
This article was submitted to Clinical Microbiology, a section of the journal Frontiers in Cellular and Infection Microbiology

Received: *09 August 2021*
Accepted: *08 September 2021*
Published: *29 September 2021*

Citation:
Yao N, He J-K, Pan M, Hou Z-F, Xu J-J, Yang Y, Tao J-P and Huang S-Y (2021) In Vitro Evaluation of Lavandula angustifolia Essential Oil on Anti-Toxoplasma Activity. Front. Cell. Infect. Microbiol. 11:755715. doi: 10.3389/fcimb.2021.755715

The current methods of treating toxoplasmosis have a number of side effects, and these therapies are only effective against the acute stage of the disease. Thus, development of new low toxicity and efficient anti-*Toxoplasma* drugs is extremely important. Natural products are important sources for screening new drugs; among them, essential oils (EOs) have efficacy in anti-bacterial, anti-inflammatory, anti-insect, and other aspects. In this study, 16 EOs were screened for their anti-*T. gondii* activity. *Lavandula angustifolia* essential oil (*La* EO)was found to have an anti-parasitic effect on *T. gondii*. The cytotoxicity of *La* EO was firstly evaluated using the MTT assay on human foreskin fibroblast (HFF) cells, and then the anti-*T. gondii* activity was evaluated by plaque assay. Finally, the invasion experiment and electron microscope observation were used to study the mechanism of *La* EO in anti-toxoplasma activity. The results indicated that the CC_{50} of *La* EO was 4.48 mg/ml and that *La* EO had activity against *T. gondii* and the inhibition was in a dose-dependent manner under safe concentrations. *La* EO was able to reduce *T. gondii* invasion, which may be due to its detrimental effect on changes of the morphology of tachyzoites. These findings indicated that *La* EO could be a potential drug for treating toxoplasmosis.

Keywords: *Toxoplasma gondii*, natural medicine, *Lavandula angustifolia* essential oil, *in vitro*, treatment

INTRODUCTION

Toxoplasma gondii is a zoonotic parasite found worldwide, which can infect almost all warm-blooded animals and human beings (Chemoh et al., 2013). It can cause severe or even a fatal outcome in immunocompromised individuals, such as organ transplant patients and AIDS patients. Pregnant women who are primarily infected during pregnancy can develop neonatal malformations, miscarriage, chorioretinitis, blindness, intellectual disability, and hydrocephalus in the infected fetus. *T. gondii* propagates sexually in the definitive host cat and excretes infectious

oocysts through feces (Martorelli Di Genova et al., 2019). In addition, *T. gondii* can reproduce without a definitive host because of its special ability of asexual reproduction. All infectious forms (tachyzoites, cysts, and oocysts) can be transmitted through the food chain (Hussain et al., 2017). Its reproductive patterns, routes of transmission, and resistance to the outside environment make it widely distributed.

Controlling toxoplasmosis has been a great challenge because no vaccine is currently available. Nowadays, drugs are widely used to control this disease; sulfonamides are the gold treatment of toxoplasmosis in clinic, especially in combination with pyrimidine (Wei et al., 2015). Although the effect is quite good, the side effects are quite serious, such as myelosuppression and teratogenic problems in early pregnancy (Schmidt et al., 2006). Many people have to give up treatment due to the side effects. The fundamental disadvantage of this combination, even if adverse reactions are not considered, is that it only solves the problem of acute infection, but has no effect on the underlying chronic infection (Mirzaalizadeh et al., 2018). Moreover, the emergence of drug-resistant strains has exacerbated this dilemma.

The difficulty of treating toxoplasmosis has motivated the search for new effective and less toxic anti-*T. gondii* drugs. Natural products have always been an important source of drug discovery and improvement (Newman and Cragg, 2012; Yuan et al., 2017). Most plants, such as those in the large *Lamiaceae* family, are known to be rich in a variety of aromatic oils, many of which have been studied for medicinal purposes (Waller et al., 2017; Bekut et al., 2018; Uritu et al., 2018). After being treated with 200 μg/mL *Lavandula angustifolia* (*La*) EO for 24 hours, all the *Schistosoma japonicum* were killed completely (Mantovani et al., 2013). The accumulation of excessive amyloid beta (Aβ) plague in the hippocampus can cause cognitive impairment, while the aqueous extract of *La* can inhibit amyloid beta (Aβ) accumulation to some extent and has strong free radical scavenging activity, thus improving impaired memory and learning ability (Soheili et al., 2019). *Mentha pulegium* essential oil showed significant anti-*Bacillus subtilis* and anti-*Proteus mirabilis* activity, while *Rosmarinus officinalis* essential oil had an inhibitory effect on *Listeria* monocytogenes, *Bacillus subtilis*, *Escherichia coli*, and *Leishmania spp* (Bakri et al., 2017). In addition, they all have significant antioxidant capacity. *Scutellaria baicalensis* is one of the important ingredients of proprietary Chinese medicine, and its extract has a series of biological functions such as antiviral, antibacterial, liver protection, and so on (Wang et al., 2018). Searching for antiparasitic drugs from natural sources has increased in recent years, and EOs continue to be a major source of biologically active new drugs. Therefore, in this study, a plant extract, *La* EO, was selected to evaluate the *in vitro* inhibitory effect on *T. gondii* and provide a basis for the development of drugs for the treatment of toxoplasmosis.

MATERIALS AND METHODS

Culture of Cells and Parasites

Human foreskin fibroblast (HFF) cells were cultured in Dulbecco's Modified Eagle Medium (DMEM, Gibco™, USA), supplemented with 100 IU/mL penicillin and 100 μg/mL streptomycin (Solarbio, Beijing, China), along with 10% heat-inactivated fetal bovine serum (FBS, Gibco®, USA). The experimental strain of *T. gondii*, GFP-RH, was maintained in HFF cells with 2% heat-inactivated FBS at 37°C and 5% CO_2. To isolate the tachyzoites, heavily infected cells were scraped, and the parasites were released by passing the cells through a 27-gauge needle 3–5 times, and were centrifuged at 3,500 rmp for 10 min to purify tachyzoites. The final centrifugal precipitates were suspended with PBS and then counted using a hemocytometer.

Essential Oils

The 16 EOs used in this experiment were provided by Guangxi University and dissolved in dimethyl sulfoxide (DMSO) in a 1:1 ratio. The solutions were then diluted with DMEM, such that the final concentration of DMSO in the samples used in the experiment was lower than 1.56% v/v. The species number of *Lavandula angustifolia* used in this study is GXCM 2019032.

Cytotoxicity Tests

HFF cells (1×10^5 cells/well) were cultured in 96-well plates at 37°C and 5% CO_2 for 24 h, then the cells were treated with different concentrations of EOs for 24 h. A 1.56% solution of DMSO in DMEM and DMEM containing 10% FBS and 0.01% penicillin-streptomycin was used as the vehicle control. The HFF cells' viability were measured by the MTT (3-[4,5-methylthiazol-2-yl]-2,5-diphenyltetrazolium bromide) colorimetric method according to (Costa et al., 2018). 20 μL of MTT solution (5 mg/mL) was added to each well and allowed to incubate at 37°C with 5% CO2 for 3 h and then 200 μL of DMSO was added to dissolve the formazan crystals. Absorbance was measured at 490 nm using an iMark™ Microplate Absorbance Reader (BioRad, Hercules, CA, USA) and the 50% cytotoxic concentrations (CC_{50}) were calculated using Graph Pad Prism 8.0. The cytotoxicity experiment was performed in triplicate, using three separate plates.

Effect of EOs in *T. gondii* Plaque Assay

In order to make a preliminary identification of the anti-*T. gondii* ability of Eos, 100 tachyzoites of the GFP-RH strain were used to infect HFF monolayers in 6-well plates in DMEM with 2% FBS at 37°C and 5% CO2. 4 hours later, HFF cells were treated with safe concentrations of two different doses of EOs. The non-infected and untreated cells were used as a blank control. HFF cells were washed wish PBS 3 times after 6 or 7 days of culture. The washed product was fixed with methanol for 10 min and stained with 0.1% crystal violet for 30 min. After washing with PBS three times and drying naturally, the plaque formed by tachyzoite infection could be seen and photographed under microscope as previously mentioned (Bai et al., 2018).

Effects of *La* EO on *T. gondii* Infections *In Vitro*

HFF cells were incubated in 24-well plates with 10% FBS in DMEM for 48 h at 37°C in an atmosphere containing 5% CO_2. Then the medium was replaced by DMEM with 2% FBS and 10^4

freshly released tachyzoites of the GFP-RH strain were added to each well. After 4 h, the extracellular parasites were removed and fresh medium containing either different concentrations of *La* EO (6.67mg/ml, 3.34mg/ml, 1.67mg/ml, 0.83mg/ml, 0.42mg/ml), 1.56% DMSO (vehicle control), or 10μg/ml SMZ (positive control) was added to each well. 32 hours later, fluorescence microscope was used to observe and photograph the growth of GFP-RH, and the growth of GFP-RH was statistically analyzed by Image-Pro-Express.

Effect of La EO on the Invasion of *T. gondii*

The invasion experiments were performed according to Augusto et al (Augusto et al., 2018). A 6-well plate of HFF cells was prepared, and 3 ml of 2% FBS in DMEM medium was added to each well. 10^4 GFP-RH and 1.67mg/ml *La* EO were added simultaneously to the wells, allowing the tachyzoites to invade host cells for 20 min, 40 min, or 60 min, respectively. The supernatant was gently absorbed and the cells were fixed with methanol for 10 min, and then washed three times with PBS. After this, 5% BSA/PBS solution was added and blocked for 1 h, then gently washed three times with PBS. Mouse anti-*Toxoplasma* SAG1 monoclonal antibodies (mAb), diluted (1:1000) with a 1% BSA/PBS solution, were added to each well, and incubated at room temperature for 2 h. Then, goat anti-mouse IgG H&L(FITC) secondary antibodies, diluted (1:1000) in 1% BSA/PBS, were added to 6-well plates and incubated at room temperature for 2 h. After washing thrice with PBS, 300 μL of 0.2% Triton X-100 was added, and the mixture was left for 30 min. Cells were then gently washed three times with PBS, and 300 μL of a 5% BSA/PBS solution was added dropwise for a second blocking. The antibodies were added as per the procedure described earlier, this time using goat anti-mouse IgG H&L (Alexa Fluor ® 568) (ab175473) instead of the goat anti-mouse IgG H&L(FITC). Finally, 300 μL of 30% glycerol was added to each well. Five visual fields were randomly selected for observation under the × objective of the fluorescence microscope and the parasites in each field were counted. Three repetitions were performed to increase the accuracy of the experiment.

Tachyzoites that were unable to successfully invade the cells were dyed green by goat anti-mouse IgG H&L(FITC), while all tachyzoites in the field of vision (including the non-invading and successfully invading ones) were stained red by goat anti-mouse IgG H&L (Alexa Fluor ® 568)(ab175473). The difference between the tachyzoites of the two colors is termed as the absolute invasion number of tachyzoites. The ratio of the invasion number to the total number of tachyzoites is termed as the invasion rate of tachyzoites.

Scanning Electron Microscopy Analysis

In order to observe the ultrastructure of the surface of tachyzoites, 10^3 purified tachyzoites were added to each tube, and then treated with1.67mg/ml *La* EO and1.56% DMSO and incubated at 37°C for 8 h respectively. The sample was washed twice with PBS immediately, and the precipitate obtained by centrifugation was fixed overnight with 2.5% glutaraldehyde at room temperature. After gradient dehydration of 30%, 50%, 70%, 80%, 90%, 95%, and 100% ethanol, the critical point drying was carried out. Gold was used as the coating material, and the surface of the sample was sprayed with gold and then observed by scanning electron microscopy.

Statistical Analysis

The Prism 8.0 software was used to analyze all the data. The antiparasitic activity of *La* EO was analyzed by an unpaired *t*-test, while the invasion experimental data are processed by multiple *t*-test, to compare the results of the test groups and those of the control group (**$P < 0.01$, ***$P < 0.001$).

RESULTS

Cytotoxicity of EOs

The cytotoxic potential of EOs on the HFF cell needed to be confirmed before further study. Among 16 EOs, 11 of them showed serious cell cytotoxicity, and only five of them had less cytotoxicity and could be further studied (**Table S1**); the CC_{50} of *La* EO was 4.48mg/ml, as shown in **Figure 1**.

Antiparasitic Activity of *La* EO *In Vitro*

Preliminary plaque assay was used to screen the anti-*T. gondii* activity of EOs. Only *La* EO has anti-*T. gondii* activity (data not shown). From **Figure 2**, we can see that the plaques were smaller and fewer after being treated with two different concentrations of *La* EO, compared to those in the DMSO-treated and untreated groups. *La* EO has anti-*T. gondii* activity under these two safe concentrations. To conform the anti-*T. gondii* activity of *La* EO, gradient concentrations *La* EO were used to treat *T. gondii* infection, and the results showed that the growth of RH could be inhibited within the safe concentrations of *La* EO in a dose-dependent manner (**Figure 3**). **Figure 3** showed the growth of *T. gondii* was significantly reduced at 6.67mg/ml *La* EO treatment (474.7vs1636; 474.7vs1629, P<0.001) when compared to the untreated and 1.56%DMSO treated groups. There was also a significant difference between the 3.34mg/ml *La* EO treatment and control groups (756.3vs1636, 756.3vs1629, P <0.01), which indicated that the inhibition in 3.34mg/ml group is also very good, although the effect was not as good as that in SMZ group (756.3vs 627.3, P(0.0035)>P(0.0005).

Effect of *La* EO on the Invasion of *T. gondii*

As shown in **Figure 4**, in the 3.34mg/ml *La* EO treatment group, the *T. gondii* invasion rates at 20 min, 40 min, and 60 min post-infection were found to be 21.3%, 29.77%, and 39.17%, respectively. For the untreated groups, the invasion was 38.50%, 51.51%, and 67.64%, respectively. It clearly indicated that *La* EO could inhibit the invasion of *T. gondii*, especially in 20- and 40-minutes groups (P <0.001). No change in the invasion rate of *T. gondii* was observed in any group treated with DMSO, across all experiments.

Electron Microscopy Analysis

The SEM results showed that tachyzoites were seriously deformed and shrunk after being treated by *La* EO and no

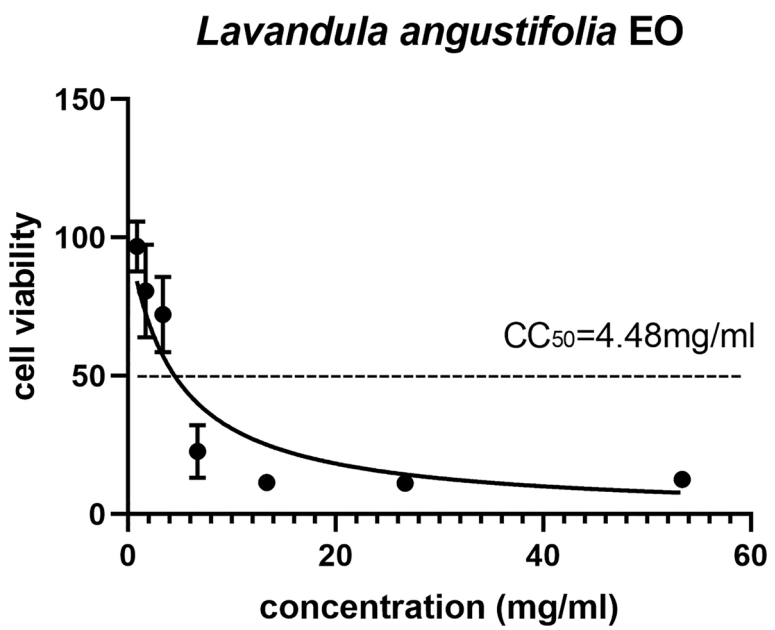

FIGURE 1 | The 50% cytotoxic concentrations (CC50) of *La* EO. Cytotoxicity of La EO on HFF cells. Different concentrations of La EO were treated on HFF cells for 24 h and then Cytotoxicity was evaluated using MTT Assay. All data are presented with error bars and the experiments were performed in triplicate.

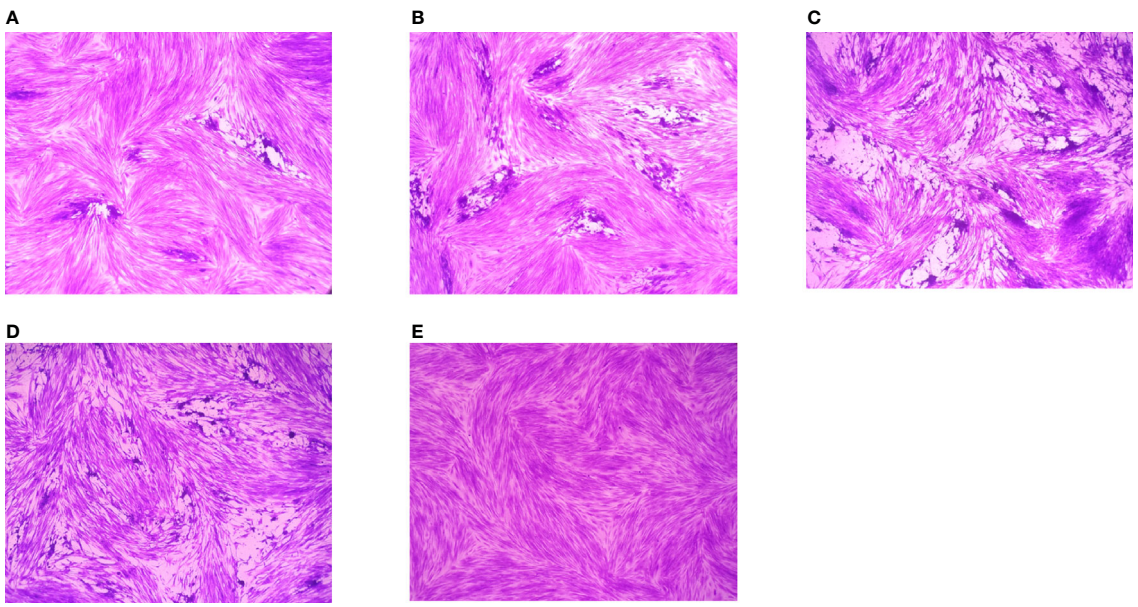

FIGURE 2 | Plaque test for preliminary detection of anti-*T. gondii* activity. Images of *T. gondii* plaque under different concentrations of *La* EO. **(A)** HFF cells were infected by *T. gondii* and treated with 3.34mg/ml *La* EO; **(B)** HFF cells were infected by *T. gondii* and treated with 0.83mg/ml *La* EO; **(C)** HFF cells were infected by *T. gondii* and untreated; **(D)** HFF cells were infected by *T. gondii* and treated with DMSO **(E)** HFF cells were not infected and treated.

longer maintain the crescent shape (**Figure 5A**) compared to no treatent group (**Figure 5C**) and DMSO-treated group (**Figure 5B**). *La* EO greatly changed the morphology and structure of tachyzoites, which seriously affected the movement ability and inhibited the invasion.

DISCUSSION

T. gondii has attained global attention due to its socioeconomic impacts and public health safety hazards, while the therapeutic drugs still have various limitations, such as side effects and drug

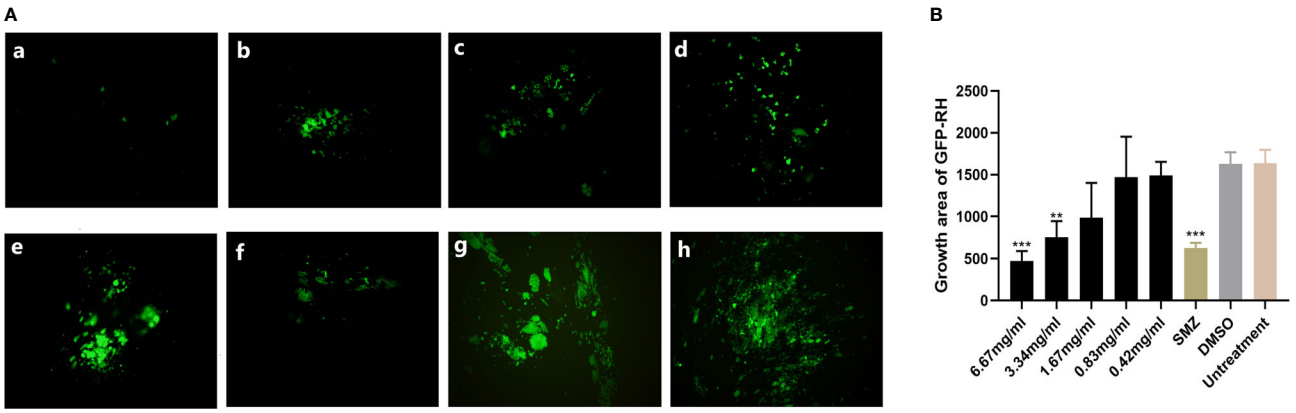

FIGURE 3 | Anti-*T. gondii* activity of *La* EO evaluated by intracellular growth assay. **(A)** Fluorescence area indicates the growth of *T. gondii* during different treatment. (a–e) different concentrations of *La* EO, (a) 6.67mg/ml; (b) 3.34mg/ml; (c) 1.67mg/ml; (d) 0.83mg/ml; (e) 0.42mg/ml; (f) SMZ(10μg/ml); (g) DMSO; (h) no treatment. **(B)** Data analysis based on fluorescence area of RH-GFP. Each bar represents the mean ± SD of three wells per group. **P < 0.01, ***P < 0.001 compared with untreated group. All data are presented as with error bars and the experiments were performed in triplicate.

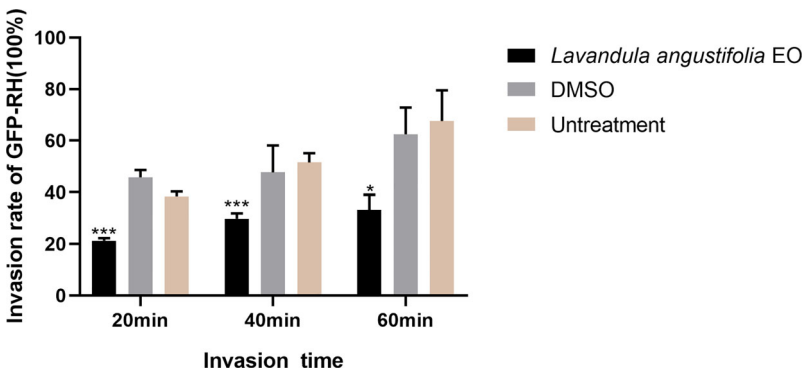

FIGURE 4 | Effect of *La* EO on the invasion of *T. gondiii*. Statistics of *T. gondii* invasion rate using two immunofluorescent dyes after being treated with *La* EO for 20, 40, and 60 minutes, respectively. *P < 0.05, ***P < 0.001 compared with untreated group. All data are presented as with error bars and the experiments were performed in triplicate.

resistance. Research into new anti-*toxoplasma* drugs is still urgent and important. Compared to chemical drugs, the natural drug resources are more abundant, therefore, exploring new drugs from natural products is worthy of consideration and, in fact, this research direction has a strong foundation in reality. For example, vanillin isolated from the pods of tropical plants can significantly improve the survival rate of Swiss-Webster albino infected with *T. gondii* ME49 (Oliveira et al., 2014). Pyrimethamine is the standard treatment drug of *T. gondii*, while the anti-*T. gondii* therapy of eucalyptus extract was superior to that of pyrimethamine in mouse survival rate and cell safety (Mirzaalizadeh et al., 2018). Due to these findings, we focused on *Lavandula angustifolia* from a potential family of Labiatae and tried to find drugs that have the anti-*T. gondii* activity.

According to the *in vitro* results, *La* EO showed higher CC50 than other EOs in HFF cells. Interestingly, *La* EO under concentration of 4.48mg/ml did not significantly reduce the viability in HFF cells. At the same time, *La* EO showed an anti-*T. gondii* activity in a dose-dependent manner in infected HFF cells. *La* EO significantly reduced the plaque sizes and numbers compared to the control groups; these results indicated that *La* EO inhibited the growth of *T. gondii* probably by inhibiting the invasion and intracellular proliferation. Lots of studies showed the effects of different herbal drugs against *T. gondii* infection *in vivo*. In this study we found that *La* EO has significant activity against *T. gondii*, although the main active ingredients were not clear. Our finding supported the idea that natural compounds and traditional herbal medicine are important candidates for searching for new anti-parasite drugs.

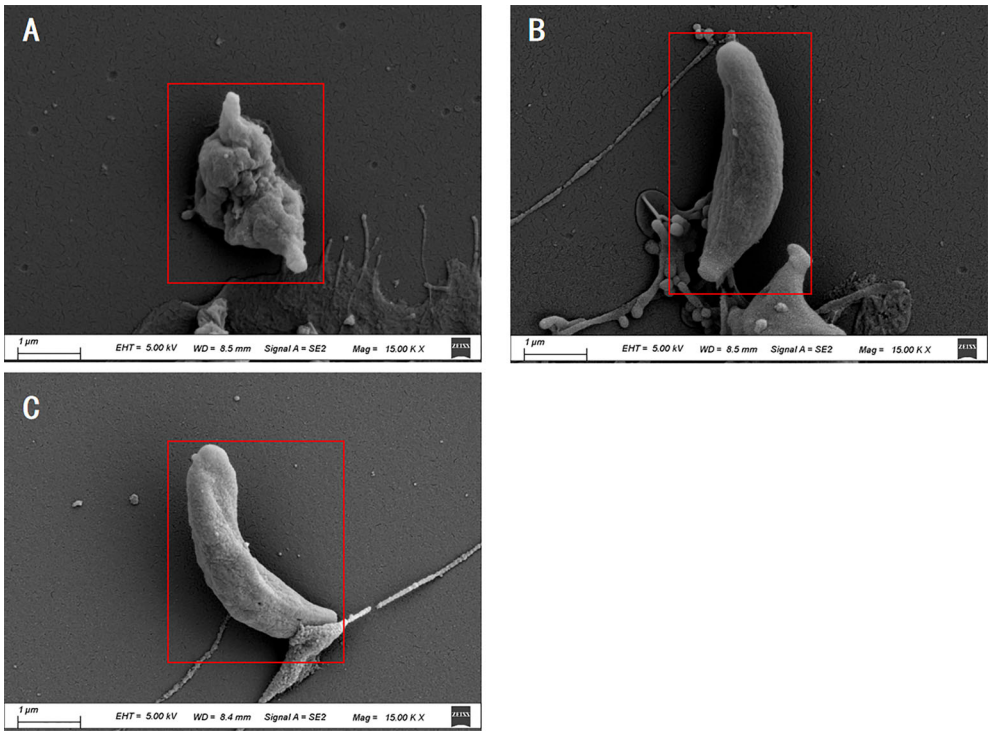

FIGURE 5 | Scanning electron microscopy assay. *T.gondii* were treated with 3.34mg/mL *La* EO **(A)**, DMSO **(B)** or untreated **(C)**. After being treated by *La* EO, the tachyzoites became rough, wrinkled, and sunken compared with untreated tachyzoites, Scale bars: 1µm. The experiments were performed in triplicate.

According to previous reports, the main active ingredients of lavender essential oil are linalool, terpineol, eucalyptus oil, lavender alcohol, and geraniol. (Białoń et al., 2019). Due to the presence of these ingredients, *La* EO is hydrophobic, so it easily penetrates the cell membrane (Ben Hsouna and Hamdi, 2012; Mantovani et al., 2013). Geraniol and terpineol, similar to octopamine (OA), can bind to specific G protein-coupled receptors, thereby affecting the concentration of cAMP and $Ca2^{+}$, and then activate the corresponding kinases to exert their biological activities (Jankowska et al., 2017; Ebadollahi et al., 2020). It is well known that the kinase domain of CDPKs family can be directly regulated by calcium ion (Wernimont et al., 2010). CDPK1 is closely related to the adhesion and invasion of *T. gondii* (Johnson et al., 2012). Therefore, some components of *La* EO may affect the calcium concentration, and then inhibit the function of CDPK1, which causes the invasion to be significantly inhibited by *La* EO (**Figure 4**). Unfortunately, we did not find the OA-like receptors in *T. gondii*; better understanding this pathway will improve the development of new drugs. At the same time, cAMP is also closely related to the invasion of tachyzoites, which is also important for further drug development (Hartmann et al., 2013).

From the electron microscope results, we found that the surface of *T. gondii* tachyzoites became rough, wrinkled, and sunken after being treated by *La* EO compared to the control groups. The ultrastructure of *Toxoplasma* showed that La EO caused serious damage to the membrane of *T. gondii*. This chemical reaction results in a huge depression in the middle of the tachyzoite since the various components of the essential oil itself can damage the permeability of the cell membrane (Mantovani et al., 2013; Essid et al., 2017; Gucwa et al., 2018). The cAMP signal is generally believed to regulate mitochondrial initiation of apoptosis, and apoptosis can be promoted by maintaining a high level of intracellular cAMP (Valsecchi et al., 2013). As mentioned before, the cAMP levels can be increased by some components of EOs (Jankowska et al., 2017). It has been reported that some components of EO can disrupt ion channels, destroy the depolarization of mitochondrial membrane, cause electrolyte leakage, and make mitochondria permeable, thus causing *T. gondii* damage and death (Swamy et al., 2016). We hypothesized that *La* EO interfered with the normal metabolism of *T. gondii*, and the normal morphology cannot be maintained, so that the invasion is inhibited, and then the growth of *T. gondii* was inhibited. However, the accurate mechanism is still not clear and further studies need to be carried out.

CONCLUSION

In summary, natural extracts are important sources for screening new drugs. *La* EO was found to have anti-*Toxoplasma* activity. The inhibitory effect may be due to the influence on the *T. gondii* shape, and then the invasion was inhibited. However, the specific mechanism of action from *La* EO on *T. gondii* is still unclear and warrants further studies.

DATA AVAILABILITY STATEMENT

The original contributions presented in the study are included in the article/**Supplementary Material**. Further inquiries can be directed to the corresponding author.

AUTHOR CONTRIBUTIONS

S-YH and NY conceived and designed the study. NY, J-KH, MP, and Z-FH performed the laboratory analyses. J-JX, YY, and J-PT analyzed the data. All authors critically appraised and interpreted the results. NY drafted the first version of the manuscript. All authors contributed to the article and approved the submitted version.

FUNDING

The sample collection and some experiments were supported by the Outstanding Youth Foundation of Jiangsu Province of China (BK20190046), The China Postdoctoral Science Foundation (2020M671615), the Science and Technology Major Project of Zhejiang Province, China. (No. 2012C12009-2), and the Priority Academic Program Development of Jiangsu Higher Education Institutions (Veterinary Medicine).

SUPPLEMENTARY MATERIAL

The Supplementary Material for this article can be found online at: https://www.frontiersin.org/articles/10.3389/fcimb.2021.755715/full#supplementary-material

REFERENCES

Augusto, L., Martynowicz, J., Staschke, K. A., Wek, R. C., and Sullivan, W. J. Jr. (2018). Effects of PERK Eif2α Kinase Inhibitor Against Toxoplasma Gondii. *Antimicrob. Agents Chemother.* 62, e01442-18. doi: 10.1128/AAC.01442-18

Bai, M. J., Wang, J. L., Elsheikha, H. M., Liang, Q. L., Chen, K., Nie, L. B., et al. (2018). Functional Characterization of Dense Granule Proteins in Toxoplasma Gondii RH Strain Using CRISPR-Cas9 System. *Front. Cell Infect. Microbiol.* 8, 300. doi: 10.3389/fcimb.2018.00300

Bakri, Y., Talbaui, A., Dakka, N., Bouyahya, A., Et-Touys, A., Abrini, J., et al. (2017). Chemical Composition of Mentha Pulegium and Rosmarinus Officinalis Essential Oils and Their Antileishmanial, Antibacterial and Antioxidant Activities. *J. Microb Pathogenesis* 111, 41–9. doi: 10.1016/j.micpath.2017.08.015

Bekut, M., Brkić, S., Kladar, N., Dragović, G., Gavarić, N., and Božin, B. (2018). Potential of Selected Lamiaceae Plants in Anti(Retro)Viral Therapy. *Pharmacol. Res.* 133, 301–314. doi: 10.1016/j.phrs.2017.12.016

Ben Hsouna, A., and Hamdi, N. (2012). Phytochemical Composition and Antimicrobial Activities of the Essential Oils and Organic Extracts From Pelargonium Graveolens Growing in Tunisia. *Lipids Health Dis.* 11, 167. doi: 10.1186/1476-511X-11-167

Białoń, M., Krzyśko-Łupicka, T., Nowakowska-Bogdan, E., and Wieczorek, P. P. (2019). Chemical Composition of Two Different Lavender Essential Oils and Their Effect on Facial Skin Microbiota. *Molecules* 24, 3270. doi: 10.3390/molecules24183270

Chemoh, W., Sawangjaroen, N., Nissapatorn, V., Suwanrath, C., Chandeying, V., Hortiwakul, T., et al. (2013). Toxoplasma Gondii Infection: What Is the Real Situation? *Exp. Parasitol* 135, 685–689. doi: 10.1016/j.exppara.2013.10.001

Costa, S., Cavadas, C., Cavaleiro, C., Salgueiro, L., and Do Céu Sousa, M. (2018). In Vitro Susceptibility of Trypanosoma Brucei Brucei to Selected Essential Oils and Their Major Components. *Exp. Parasitol.* 190, 34–40. doi: 10.1016/j.exppara.2018.05.002

Ebadollahi, A., Ziaee, M., and Palla, F. (2020). Essential Oils Extracted From Different Species of the Lamiaceae Plant Family as Prospective Bioagents Against Several Detrimental Pests. *Molecules* 25, 1556. doi: 10.3390/molecules25071556

Essid, R., Hammami, M., Gharbi, D., Karkouch, I., Hamouda, T. B., Elkahoui, S., et al. (2017). Antifungal Mechanism of the Combination of Cinnamomum Verum and Pelargonium Graveolens Essential Oils With Fluconazole Against Pathogenic Candida Strains. *Appl. Microbiol. Biotechnol.* 101, 6993–7006. doi: 10.1007/s00253-017-8442-y

Gucwa, K., Milewski, S., Dymerski, T., and Szweda, P. (2018). Investigation of the Antifungal Activity and Mode of Action of Thymus Vulgaris, Citrus Limonum, Pelargonium Graveolens, Cinnamomum Cassia, Ocimum Basilicum, and Eugenia Caryophyllus Essential Oils. *Molecules* 23, 1116. doi: 10.3390/molecules23051116

Hartmann, A., Arroyo-Olarte, R. D., Imkeller, K., Hegemann, P., Lucius, R., and Gupta, N. (2013). Optogenetic Modulation of an Adenylate Cyclase in Toxoplasma Gondii Demonstrates a Requirement of the Parasite cAMP for Host-Cell Invasion and Stage Differentiation. *J. Biol. Chem.* 288, 13705–13717. doi: 10.1074/jbc.M113.465583

Hussain, M. A., Stitt, V., Szabo, E. A., and Nelan, B. (2017). Toxoplasma Gondii in the Food Supply. *Pathogens* 6, 21. doi: 10.3390/pathogens6020021

Jankowska, M., Rogalska, J., Wyszkowska, J., and Stankiewicz, M. (2017). Molecular Targets for Components of Essential Oils in the Insect Nervous System-A Review. *Molecules* 23, 34. doi: 10.3390/molecules23010034

Johnson, S. M., Murphy, R. C., Geiger, J. A., Derocher, A. E., Zhang, Z., Ojo, K. K., et al. (2012). Development of Toxoplasma Gondii Calcium-Dependent Protein Kinase 1 (TgCDPK1) Inhibitors With Potent Anti-Toxoplasma Activity. *J. Med. Chem.* 55, 2416–2426. doi: 10.1021/jm201713h

Mantovani, A. L. L., Vieira, G. P. G., Cunha, W. R., Groppo, M., Santos, R. A., Rodrigues, V., et al. (2013). Chemical Composition, Antischistosomal and Cytotoxic Effects of the Essential Oil of Lavandula Angustifolia Grown in Southeastern Brazil. *J. Rev. Bras. Farmacognosia*, 23, 877–884. doi: 10.1590/S0102-695X2013000600004

Martorelli Di Genova, B., Wilson, S. K., Dubey, J. P., and Knoll, L. J. (2019). Intestinal Delta-6-Desaturase Activity Determines Host Range for Toxoplasma Sexual Reproduction. *PloS Biol.* 17, e3000364. doi: 10.1371/journal.pbio.3000364

Mirzaalizadeh, B., Sharif, M., Daryani, A., Ebrahimzadeh, M. A., Zargari, M., Sarvi, S., et al. (2018). Effects of Aloe Vera and Eucalyptus Methanolic Extracts on Experimental Toxoplasmosis In Vitro and In Vivo. *Exp. Parasitol* 192, 6–11. doi: 10.1016/j.exppara.2018.07.010

Newman, D. J., and Cragg, G. M. (2012). Natural Products as Sources of New Drugs Over the 30 Years From 1981 to 2010. *J. Natural Products* 75, 311–335. doi: 10.1021/np200906s

Oliveira, C. B., Meurer, Y. S., Oliveira, M. G., Medeiros, W. M., Silva, F. O., Brito, A. C., et al. (2014). Comparative Study on the Antioxidant and Anti-Toxoplasma Activities of Vanillin and Its Resorcinarene Derivative. *Molecules* 19, 5898–5912. doi: 10.3390/molecules19055898

Schmidt, D. R., Hogh, B., Andersen, O., Hansen, S. H., Dalhoff, K., and Petersen, E. (2006). Treatment of Infants With Congenital Toxoplasmosis: Tolerability and Plasma Concentrations of Sulfadiazine and Pyrimethamine. *Eur. J. Pediatr.* 165, 19–25. doi: 10.1007/s00431-005-1665-4

Soheili, M., and Salami, M. (2019). Lavandula Angustifolia Biological Characteristics: An In Vitro Study. *J. Cell. Physiol.* 234, 16424–16430. doi: 10.1002/jcp.28311

Swamy, M. K., Akhtar, M. S., and Sinniah, U. R. (2016). Antimicrobial Properties of Plant Essential Oils Against Human Pathogens and Their Mode of Action: An Updated Review. *Evid. Based Complement Alternat. Med.* 2016, 3012462. doi: 10.1155/2016/3012462

Uritu, C. M., Mihai, C. T., Stanciu, G. D., Dodi, G., Alexa-Stratulat, T. , Luca, A., et al. (2018). Medicinal Plants of the Family Lamiaceae in Pain Therapy: A Review. *Pain Res. Manag* 2018, 7801543. doi: 10.1155/2018/7801543

Valsecchi, F., Ramos-Espiritu, L. S., Buck, J., Levin, L. R., and Manfredi, G. (2013). cAMP and Mitochondria. *Physiol. (Bethesda)* 28, 199–209. doi: 10.1152/physiol.00004.2013

Waller, S. B., Cleff, M. B., Serra, E. F., Silva, A. L., Gomes, A. D., De Mello, J. R., et al. (2017). Plants From Lamiaceae Family as Source of Antifungal Molecules

in Humane and Veterinary Medicine. *Microb. Pathog.* 104, 232–237. doi: 10.1016/j.micpath.2017.01.050

Wang, Z. L., Wang, S., Kuang, Y., Hu, Z. M., Qiao, X., and Ye, M. (2018). A Comprehensive Review on Phytochemistry, Pharmacology, and Flavonoid Biosynthesis of Scutellaria Baicalensis. *Pharm. Biol.* 56, 465–484. doi: 10.1080/13880209.2018.1492620

Wei, H. X., Wei, S. S., Lindsay, D. S., and Peng, H. J. (2015). A Systematic Review and Meta-Analysis of the Efficacy of Anti-Toxoplasma Gondii Medicines in Humans. *PloS One* 10, e0138204. doi: 10.1371/journal.pone.0138204

Wernimont, A. K., Artz, J. D., Finerty, P. Jr., Lin, Y. H., Amani, M., Allali-Hassani, A., et al. (2010). Structures of Apicomplexan Calcium-Dependent Protein Kinases Reveal Mechanism of Activation by Calcium. *Nat. Struct. Mol. Biol.* 17, 596–601. doi: 10.1038/nsmb.1795

Yuan, R., Hou, Y., Sun, W., Yu, J., Liu, X., Niu, Y., et al. (2017). Natural Products to Prevent Drug Resistance in Cancer Chemotherapy: A Review. *Ann. N. Y. Acad. Sci.* 1401, 19–27. doi: 10.1111/nyas.13387

Conflict of Interest: The authors declare that the research was conducted in the absence of any commercial or financial relationships that could be construed as a potential conflict of interest.

frontiers in Cellular and Infection Microbiology

ORIGINAL RESEARCH
published: 13 October 2021
doi: 10.3389/fcimb.2021.759396

Comparison of Molecular and Parasitological Methods for Diagnosis of Human Trichostrongylosis

Mehdi Pandi[1], *Meysam Sharifdini*[1]*, *Keyhan Ashrafi*[1], *Zahra Atrkar Roushan*[2], *Behnaz Rahmati*[1] *and Nayereh Hajipour*[3]

[1] Department of Medical Parasitology and Mycology, School of Medicine, Guilan University of Medical Sciences, Rasht, Iran, [2] Department of Biostatistics, School of Medicine, Guilan University of Medical Sciences, Rasht, Iran, [3] Department of Microbiology, School of Medicine, Guilan University of Medical Sciences, Rasht, Iran

OPEN ACCESS

Edited by:
Ehsan Ahmadpour, Tabriz University of Medical Sciences, Iran

Reviewed by:
Apichat Vitta, Naresuan University, Thailand
Fabiana De Paula, Hospital das Clinicas da FMUSP, Brazil

***Correspondence:**
Meysam Sharifdini
sharifdini@gums.ac.ir; sharifdini5@gmail.com

Specialty section:
This article was submitted to Clinical Microbiology, a section of the journal Frontiers in Cellular and Infection Microbiology

Received: *16 August 2021*
Accepted: *20 September 2021*
Published: *13 October 2021*

Citation:
Pandi M, Sharifdini M, Ashrafi K, Atrkar Roushan Z, Rahmati B and Hajipour N (2021) Comparison of Molecular and Parasitological Methods for Diagnosis of Human Trichostrongylosis. Front. Cell. Infect. Microbiol. 11:759396. doi: 10.3389/fcimb.2021.759396

Human trichostrongyliasis is a zoonotic disease that is prevalent among rural populations in some countries. This study was performed to evaluate various parasitological methods and polymerase chain reaction (PCR) for the diagnosis of human trichostrongyliasis. A total of 206 fresh stool samples were collected from residents of endemic villages of Northern Iran. All samples were examined using conventional parasitological methods, including wet mount, formalin ethyl acetate concentration (FEAC), agar plate culture (APC), Harada–Mori culture (HMC), and Willis, along with the PCR technique. Among the total of 206 individuals examined, 72 people (35%) were found infected with *Trichostrongylus* species using combined parasitological methods. By considering the combined results of parasitological methods as the diagnostic gold standard, the Willis technique had a sensitivity of 91.7% compared with 52.8% for the APC, 40.3% for the HMC, 37.5% for FEAC, and 5.6% for the wet mount technique. The diagnostic specificity of all the parasitological methods was 100%. Furthermore, the PCR method detected *Trichostrongylus* spp. DNA in 79 fecal samples (38.3%) with a sensitivity of 97.2% and a specificity of 93.3%. According to the current findings, the Willis method was more sensitive than are the other parasitological methods in the diagnosis of human trichostrongyliasis. However, the PCR assay was more sensitive and more reliable in the detection of human trichostrongyliasis in comparison with the parasitological methods.

Keywords: human trichostrongyliasis, wet mount, Harada–Mori culture, Willis, agar plate culture, formalin ethyl acetate concentration, PCR

INTRODUCTION

Nematodes of the genus *Trichostrongylus* are primarily parasites of herbivorous animals with a worldwide distribution. Ruminants are considered the most important reservoir for human trichostrongylosis (Ghadirian and Arfaa, 1975). Human infections associated with *Trichostrongylus* species have been reported sporadically from various countries of the Middle and the Far East, Africa, South America, Europe, and Oceania, with the highest prevalence rates

reported in Iran (Ghadirian and Arfaa, 1975; Cancrini et al., 1982; Boreham et al., 1995; Lattes et al., 2011; Sato et al., 2011; Wall et al., 2011; Phosuk et al., 2013; Watthanakulpanich et al., 2013). In recent decades, a sharply decreasing trend was observed in the prevalence of most human soil-transmitted helminths (STHs) in Iran (Rokni, 2008; Sharifdini et al., 2017b; Sharifdini et al., 2020). However, recent epidemiological studies have demonstrated that trichostrongylosis is still a common helminth infection in humans in some parts of Iran, which results from its ability of zoonotic transmission to humans (Ashrafi et al., 2015; Gholami et al., 2015; Sharifdini et al., 2017a; Sharifdini et al., 2017c; Ashrafi et al., 2020).

Twelve valid species of *Trichostrongylus* have been detected from humans in various areas of the world, nine of which were only reported from Iran (Ghadirian et al., 1974; Ghadirian and Arfaa, 1975; Ghadirian, 1977; Sharifdini et al., 2017a). Within the past decades, in most parts of Iran, the predominant species of *Trichostrongylus* in humans were *Trichostrongylus orientalis* and *Trichostrongylus colubriformis* (Ghadirian and Arfaa, 1975). Agricultural use of night soil as fertilizer was an important reason for the high prevalence of *T. orientalis* in these regions because the transmission of this species primarily occurs from human to human (Ghadirian and Arfaa, 1975). At present, the predominant species is *T. colubriformis* because of its high prevalence in domestic animals and its high zoonotic potential (Gholami et al., 2015; Sharifdini et al., 2017a; Sharifdini et al., 2017c).

The transmission route of human infections is mainly through the ingestion of vegetables contaminated with filariform larvae (Roberts and Janovy, 2012). Although trichostrongylosis is generally considered asymptomatic and the only present finding is low-grade peripheral eosinophilia, heavy infections may be followed by abdominal discomfort, diarrhea, nausea, anorexia, weakness, flatulence, dizziness, generalized fatigue or malaise, and mild anemia (Ghanbarzadeh et al., 2019).

Definitive diagnosis of trichostrongylosis depends on observing the characteristic eggs in stool samples or finding the larva in fecal cultures (Roberts and Janovy, 2012). It should be noted that *Trichostrongylus* eggs may be mistaken with those of hookworms (Sato et al., 2011). Additionally, *Trichostrongylus* larvae are relatively similar to those of hookworms and *Strongyloides stercoralis*, which may be difficult to distinguish clearly (Roberts and Janovy, 2012). Although there are several parasitological methods for the detection of *Trichostrongylus* infection, there are limited studies that show comparisons of their sensitivity and specificity (Najmi et al., 2017; Saraei et al., 2019). Recently, only a few studies applied polymerase chain reaction (PCR)-based techniques for specific detection of *Trichostrongylus* spp. in human fecal samples (Gholami et al., 2015; Sharifdini et al., 2017c; Perandin et al., 2018). However, these studies had small sample sizes and insufficient power to evaluate their efficacy. In this study, we compared several parasitological methods along with conventional PCR for the diagnosis of *Trichostrongylus* infection in human fecal samples.

Abbreviations: FEAC, formalin ethyl acetate concentration; APC, agar plate culture; HMC, Harada–Mori culture; STHs, soil-transmitted helminths; ITS, internal transcribed spacer; PCR, polymerase chain reaction.

METHODS

Study Area and Sample Size Determination

The study area comprises highly endemic villages of trichostrongylosis within the Fouman District in Guilan Province, Northern Iran. The sample size was calculated based on the prevalence of *Trichostrongylus* in the region using the following formula: Z^2 se $(1 - \text{se})/d^2 \times$ prev, where prev is the prevalence of *Trichostrongylus*, se is sensitivity, d is the precision of the estimate, and Z is the standard score corresponding to 1.96. The prevalence rate of *Trichostrongylus* in the study area based on a pilot study and unpublished data was about 36%. For the calculation, a 95% sensitivity and a 5% precision of estimate were used. This gave a sample size of 197. To minimize errors arising from the likelihood of non-compliance, 5% of the sample size was added, giving a final sample size of about 206.

Sample Collection

A total of 206 fresh stool samples were collected from the residents of the villages from June to October 2020. Fecal samples were transferred immediately after collection to the Department of Parasitology and Mycology, Guilan University of Medical Sciences.

Parasitological Methods

All stool samples were examined using the wet mount, formalin ethyl acetate concentration (FEAC), agar plate culture (APC), Harada–Mori culture (HMC), and Willis techniques.

The APC method was applied for the detection of *Trichostrongylus* spp. larvae. In brief, 3–4 g of each fecal sample was placed on nutrient agar culture. After incubation for 3–5 days at room temperature (25–35°C), the plates were examined under a stereomicroscope for the presence of moving larvae or their tracks. In order to collect the larvae, the surface of the positive agar plates was washed out by lukewarm phosphate-buffered saline (PBS) solution. Larvae of *Trichostrongylus* species were identified from other probable intestinal nematodes, such as *S. stercoralis* and hookworms, based on morphological characteristics (Sharifdini et al., 2017a).

In the HMC method, approximately 2 g of each fresh stool sample was smeared on a folded strip of filter paper. After adding up to 5 ml of distilled water into a 15-ml falcon tube, the strip containing the fecal sample was placed into the tube and stored at room temperature for 7 days. Finally, the tube fluid was checked for detection of larvae of *Trichostrongylus* species (Harada and Mori, 1955).

For the sodium chloride flotation technique or the Willis method, about 2–3 g of each fecal sample was diluted in 20 ml of saturated salt solution (NaCl, 1.20 g/ml). The mixture was then filtered through sterile gauze and immediately transferred into a

test tube. Then, a coverslip was placed carefully on top of the tube. After 15 min, the coverslip was lifted off the test tube and deposited on a microscope slide (Willis, 1921).

Molecular Methods

DNA Extraction

For DNA isolation, about 2 g of each stool sample was processed using the sodium chloride flotation technique. Next, the supernatant was washed twice with distilled water, followed by centrifugation at 8,000 × *g* for 5 min to remove the salt. Subsequently, genomic DNA was extracted from the sediment using a commercial DNA extraction kit (Viragene, Tehran, Iran) based on the instructions on the manual and stored at −20°C for PCR amplification.

PCR Amplification

PCR reactions were performed in 20 µl volumes containing 2× red PCR premix (Ampliqon, Odense, Denmark), 20 pmol of each primer, and 3 µl of extracted DNA. The ribosomal DNA internal transcribed spacer 2 (*ITS*2) was amplified using forward primer (Tri-F: 5′-AATGAATTTCTACAGTGTGG-3′) and reverse primer (Tri-R: 5′-CATACATGTCCCTGTTTAAATC-3′), resulting in an amplicon size for *Trichostrongylus* spp. of 211 bp (Mizani et al., 2017). The PCR conditions comprised an initial denaturing step of 95°C for 5 min, followed by 35 cycles of denaturation at 95°C for 45 s, annealing at 54°C for 45 s, and extension at 72°C for 60 s, and a final extension at 72°C for 7 min. Finally, the PCR product was electrophoresed on 1.5% agarose gel and visualized with a UV transilluminator. Later, the PCR products were sent to a domestic sequencing company (Codon Genetic Company, Tehran, Iran) for sequence determination *via* the Sanger method.

To confirm the results of the molecular method, eight positive products—four positive and four negative parasitological stool samples—were selected randomly and sent to a domestic sequencing company (Codon Genetic Company, Tehran, Iran) for sequence determination via the Sanger method. Sequence results were manually edited and analyzed using Chromas (version 2.6) software. The sequences were compared with those submitted to GenBank using the BLAST system (http://www.ncbi.nlm.nih.gov/), and multiple sequence alignment was carried out using the Clustal W method of Bioedit software (version 7.2).

Analytical Sensitivity and Specificity of PCR

To determine the analytical sensitivity of the molecular method, genomic DNA was extracted from 100, 50, 20, 10, 5, and from 1 egg of *Trichostrongylus* spp. using a DNA extraction kit (Viragene, Tehran, Iran) according to the manufacturer's protocol. Subsequently, PCR for these samples was carried out as mentioned above.

The specificity of the PCR method was assessed using extracted DNAs from adult *Necator americanus*, *Taenia saginata*, *Haemonchus contortus*, *Marshallagia marshalli*, *Ostertagia ostertagi*, and *Rhabditis axei*, and also from stool samples infected with *S. stercoralis*, *Fasciola hepatica*, *Dicrocoelium denriticum*, *Cryptosporidium* sp., *Enterocytozoon bieneusi*, *Entamoeba coli*, *Giardia lamblia*, and *Blastocystis hominis*.

Data Analysis

Data were analyzed using SPSS software (version 18, SPSS Inc., Chicago, IL, USA) to determine the diagnostic sensitivity and specificity of the molecular and parasitological methods.

Ethical Approval

This study was reviewed and approved by the Ethics Committees of Guilan University of Medical Sciences, Iran (ref. no. IR.GUMS.REC.1398.434).

RESULTS

Comparison of Parasitological and PCR Methods

Among the total of 206 individuals examined, 72 people (35%) were found infected with *Trichostrongylus* species using combined parasitological methods (**Figure 1**). The detection rates for the wet mount, FEAC, APC, HMC, and Willis techniques solely were 4 (1.9%), 27 (13.1%), 38 (18.4%), 29 (14.1%), and 66 (32%), respectively (**Table 1**). The Willis method, as the most sensitive among the parasitological methods, could detect 4 of the 4 positive cases found using wet mount, 26 of the 27 by FEAC, 27 of the 29 by HMC, and 35 of the 38 by APC. In addition, the Willis technique detected 62, 40, 39, and 31 more samples, which were negative by wet mount, FEAC, HMC, and APC, respectively. Moreover, the other intestinal parasites detected in the current study using parasitological methods were *S. stercoralis* (0.97%), *G. lamblia* (1.4%), *B. hominis* (0.97%), and *F. hepatica* (0.48%).

The PCR method detected *Trichostrongylus* species DNA in 79 out of 206 stool samples (38.3%) (**Figure 2**). All these positive cases were detected using wet mount, FEAC, and HMC. However, PCR failed to detect one APC and two Willis positive cases. Also, the PCR assay detected nine (4.37%) more samples, which were negative using the parasitological methods (**Table 2**). Sequence analysis of 167 bp of the eight randomly selected PCR products revealed that all of them had 100% similarity to *T. colubriformis* in the GenBank reference sequences. All positive isolates were registered in the GenBank database with accession numbers MW680815–MW680822.

Since there is no valid gold standard for the diagnosis of *Trichostrongylus* spp. infections, the combined results of the parasitological methods were considered as the gold standard in this study. Therefore, the diagnostic sensitivity values of the wet mount, HMC, Willis, APC, FEAC, and PCR methods were calculated as 5.6%, 40.3%, 91.7%, 52.8%, 37.5%, and 97.2%, respectively. The diagnostic specificity of all the parasitological methods was 100%, while that of the PCR assay was 93.3%.

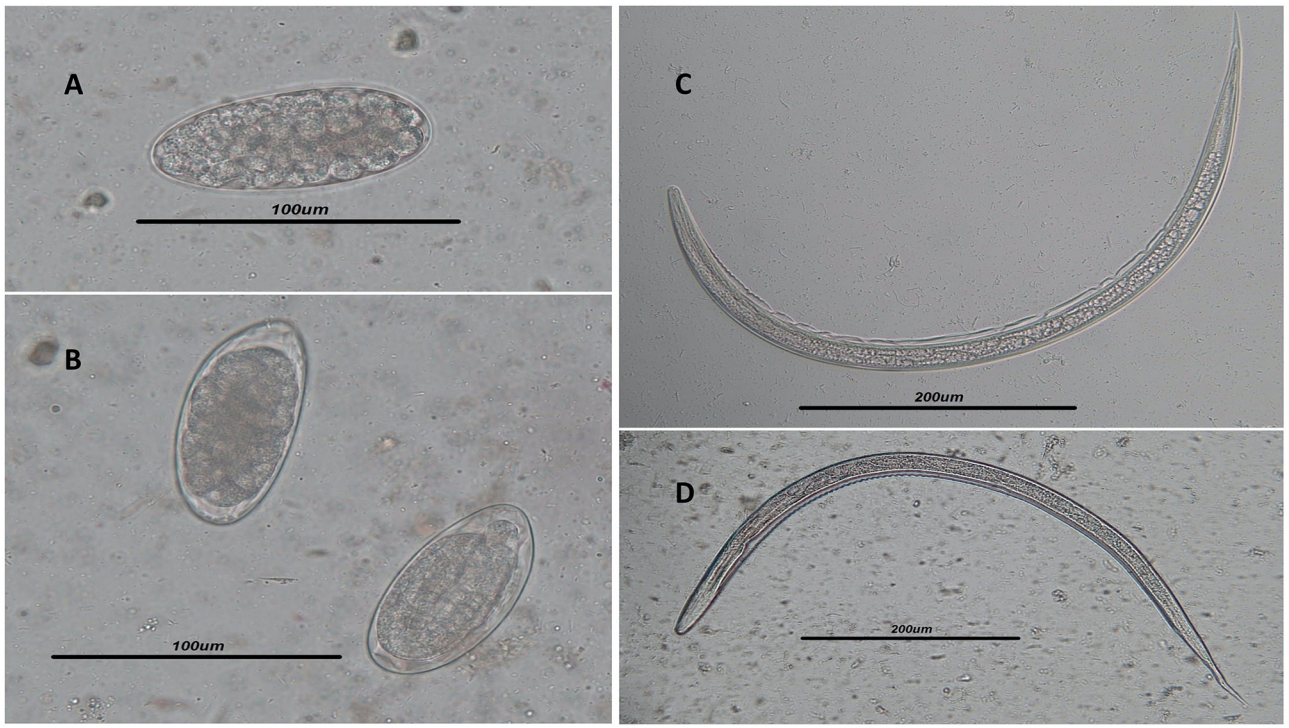

FIGURE 1 | **(A, B)** Light microscope view of *Trichostrongylus* spp. eggs isolated by the Willis technique in the stool samples of infected humans. *Scale bar*, 100 μm. **(C, D)** Filariform larvae of *Trichostrongylus* spp. isolated from agar plate culture. *Scale bar*, 200 μm.

Analytical Sensitivity and Specificity of PCR

The detection limit for the PCR method was DNA of one *Trichostrongylus* spp. egg (**Figure 3**). No amplification was found in the PCR assay from the DNAs extracted from all the above-mentioned intestinal parasites, except *Trichostrongylus* species. The results illustrated that the PCR assay was highly specific for the detection of *Trichostrongylus* spp.

DISCUSSION

Recent epidemiological studies have shown that the prevalence of most human STHs, such as *Ascaris lumbricoides* and hookworms, has decreased sharply in Iran; however, *S. stercoralis* and *Trichostrongylus* species are still being reported in a few parts of the country (Rokni, 2008; Sharifdini et al., 2017a; Sharifdini et al., 2017b; Sharifdini et al., 2020). Utilizing an accurate diagnostic method is one of the most important tools in the effective prevention and control of human trichostrongylosis. Our findings provide important new information on the performance of five types of parasitological methods and the PCR assay for the diagnosis of *Trichostrongylus* infection in humans.

In this study, the Willis technique detected *Trichostrongylus* eggs in 66 of the 206 stool samples with a sensitivity of 91.7% and a specificity of 100%. The sensitivity of the Willis technique for *Trichostrongylus* diagnosis was considerably much higher compared with that of the other parasitological methods. This method diagnosed 100%, 96.3%, 93.1%, and 92.1% of *Trichostrongylus* cases detected using the wet mount, FEAC, HMC, and APC methods, respectively. Also, the Willis technique detected *Trichostrongylus* eggs in 62, 40, 39, and 31 samples, which were scored as negative by wet mount, FEAC, HMC, and APC, respectively. Our results confirmed previous

TABLE 1 | Comparison of the parasitological and molecular methods in the detection of *Trichostrongylus* spp. in fecal samples (n = 206).

	Wet mount	FEAC	APC	HMC	Willis	PCR
Positive (72)	4	27	38	29	66	79
Negative (134)	202	179	168	177	140	127
Sensitivity (%)	5.6	37.5	52.8	40.3	91.7	97.2
Specificity (%)	100	100	100	100	100	93.3

FEAC, formalin ethyl acetate concentration; APC, agar plate culture; HMC, Harada–Mori culture.

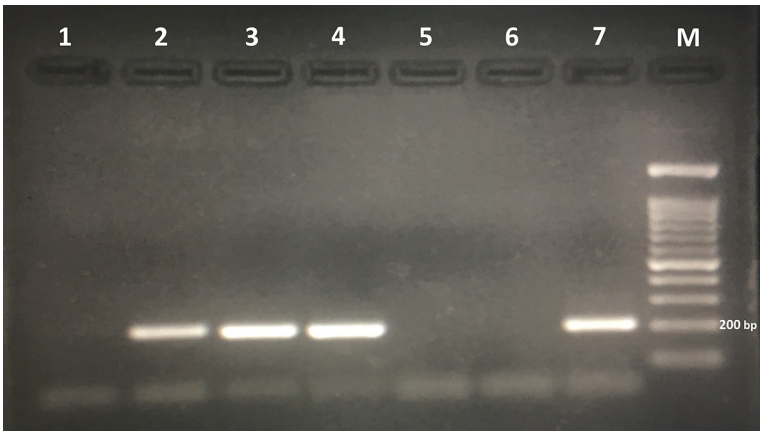

FIGURE 2 | Agarose gel electrophoresis of polymerase chain reaction products amplified with genomic DNA from stool samples. *Lanes 2*, *3*, and *4*: polymerase chain reaction products of stool samples positive for *Trichostrongylus* spp. *Lane 6*: negative control. *Lane 7*: positive control (*Trichostrongylus colubriformis*). *M*, 100-bp DNA marker.

findings that the fecal flotation technique is a highly sensitive diagnostic test for STHs, especially hookworms (Inpankaew et al., 2014; Clarke et al., 2018; Zeleke et al., 2020). On the other hand, this technique is simple and faster, cheaper, and is user-friendly compared to the FEAC, HMC, and APC methods for the diagnosis of trichostrongylosis. Zeleke et al. reported that both the sensitivity and diagnostic accuracy of the fecal flotation technique were 100% for the detection of hookworm infections (Zeleke et al., 2020).

The present study also demonstrated that APC was the second most sensitive parasitological examination, with a sensitivity of 52.8%. Although several studies have confirmed APC as being more sensitive than the other parasitological tests in the diagnosis of *S. stercoralis* infection (Sharifdini et al., 2014; Sharifdini et al., 2015; Mirzaei et al., 2021), its sensitivity was much less than that of the Willis technique for the detection of *Trichostrongylus* eggs in the current study. Additionally, this method is time-consuming, labor-intensive, and requires a well-trained microscopist (Ericsson et al., 2001). In the current study, HMC and FEAC were ranked as the third (40.3%) and fourth (37.5%) most sensitive techniques, respectively. Until now, only two studies have been performed comparing parasitological methods such as APC and FEAC for the diagnosis of human trichostrongylosis. Similar to our results, Najmi et al. reported that APC (88.23%) was more sensitive than FEAC (62.75%) in the diagnosis of human trichostrongyliasis (Najmi et al., 2017). In contrast to our findings, another study showed that the sensitivity of FEAC for the detection of *Trichostrongylus* was higher than that of APC (95.8% *vs.* 90.1%) (Saraei et al., 2019). The observed differences in the sensitivity between the two methods in these studies could be due to the skill variations of technicians.

Our study findings illustrated that the direct wet mount method had very low sensitivity (5.6%) for the diagnosis of trichostrongylosis compared to the other parasitological methods. This is similar to other studies, which demonstrated that the direct wet mount method had a low detection ability for intestinal helminthic infections and may lead to false-negative results (Mengist et al., 2018; Demeke et al., 2021).

PCR-based techniques using the *ITS*2 region of rDNA are considered effective tools for the detection and identification of *Trichostrongylus* species in human fecal samples (Gholami et al., 2015; Sharifdini et al., 2017c; Perandin et al., 2018; Hidalgo et al., 2020). The DNA isolation procedure is a critical step that is helpful in the efficacy of molecular methods. In this study, similar to that in others (Hidalgo et al., 2018; Hidalgo et al., 2020), the processing of stool samples using the flotation technique was applied efficiently for DNA isolation. This method significantly reduced the PCR inhibitory substances in the stool samples, such as bacterial proteases, nucleases, cell debris, and bile acids, and resulted in the improved detection rate of PCR. On the other hand, this isolation method is rapid, labor-effective, and can be applied in the detection of light-intensity infections.

TABLE 2 | Evaluation of the PCR assay in comparison with parasitological methods for the diagnosis of *Trichostrongylus* spp. infection in stool samples (*n* = 206).

Methods		Wet mount		FEAC		APC		HMC		Willis	
		Positive (4)	Negative (202)	Positive (27)	Negative (179)	Positive (38)	Negative (168)	Positive (29)	Negative (177)	Positive (66)	Negative (140)
PCR	Positive (79)	4	75	27	52	37	42	29	50	64	15
	Negative (127)	0	127	0	127	1	126	0	127	2	125

FEAC, formalin ethyl acetate concentration; APC, agar plate culture; HMC, Harada–Mori culture

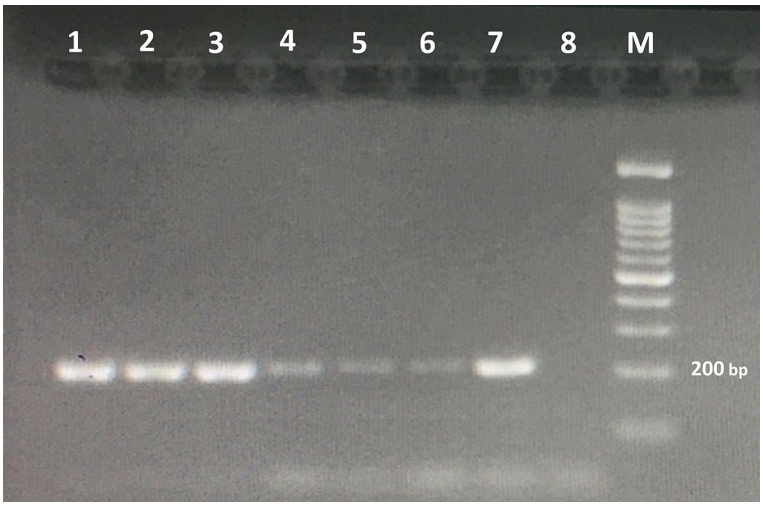

FIGURE 3 | Agarose gel electrophoresis of the PCR products amplified with genomic DNA from stool samples. The PCR products are as follows: *lane 1*, DNA from 100 eggs of *Trichostrongylus* species; *lane 2*, DNA from 50 eggs of *Trichostrongylus* species; *lane 3*, DNA from 20 eggs of *Trichostrongylus* species; *lane 4*, DNA from 10 eggs of *Trichostrongylus* species; *lane 5*, DNA from 5 eggs of *Trichostrongylus* species; *lane 6*, DNA from one egg of *Trichostrongylus* species; *lane 7*, positive control (*Trichostrongylus colubriformis*); *lane 8*: negative control. *M*, 100-bp DNA marker.

The PCR method detected *Trichostrongylus* spp. DNA in 79 fecal samples with a sensitivity of 97.2% and a specificity of 93.3%. Our findings illustrated that this method was more sensitive than are the parasitological methods in the diagnosis of *Trichostrongylus* species infection. It detected all samples that had been detected as positive by the wet mount, FEAC, and HMC methods, but could not detect one APC and two Willis positive cases. In addition, PCR was positive in nine samples (4.37%) that had not been detected by the parasitological methods. This study, for the first time, compared molecular methods with various parasitological examinations for the diagnosis of human trichostrongylosis. However, several studies have shown that PCR-based methods are more sensitive than are conventional parasitological techniques for the detection of intestinal helminthic infections (Sharifdini et al., 2015; Chidambaram et al., 2017).

Our sequence analysis showed that all PCR products, including the negative and positive parasitological samples, were confirmed as *T. colubriformis*. Therefore, based on these negative parasitological samples that were true positives with PCR, the specificity of the PCR assay will be increased. Additionally, the sequence analysis confirmed previous studies showing that *T. colubriformis* are a predominant species in residents of Northern Iran (Gholami et al., 2015; Sharifdini et al., 2017a; Sharifdini et al., 2017c; Ashrafi et al., 2020).

This is the first study evaluating PCR in comparison to various parasitological methods for the detection of *Trichostrongylus* species in fecal samples. Our findings showed that, among the different parasitological methods evaluated, the Willis technique was more sensitive than are the others. While the PCR method is superior to the Willis technique in the detection of positive cases, the Willis technique is simple, rapid, and inexpensive, and only simple technology and equipment are required to propose screening and epidemiological studies. In addition, although PCR is an expensive method, it is not dependent on skilled microscopists and is feasible in detecting infections with low parasite numbers.

DATA AVAILABILITY STATEMENT

The datasets presented in this study can be found in online repositories. The names of the repository/repositories and accession number(s) can be found below: NCBI [accession: MW680815–MW680822].

ETHICS STATEMENT

The studies involving human participants were reviewed and approved by Ref. No. IR.GUMS.REC.1398.434. The patients/participants provided their written informed consent to participate in this study.

AUTHOR CONTRIBUTIONS

MS designed the study. MP collected the samples. MP and BR carried out the parasitological methods. MP, MS, and NH performed the molecular method. MS, ZR, and KA analyzed the data. MS drafted the manuscript. All authors read and approved the final version of the manuscript.

FUNDING

This study has been fnancially supported by Research Deputy of Guilan University of Medical Sciences, with project No. 98072002.

ACKNOWLEDGMENTS

The authors would like to thank all those who have contributed to this research.

REFERENCES

Ashrafi, K., Sharifdini, M., Heidari, Z., Rahmati, B., and Kia, E. B. (2020). Zoonotic Transmission of *Teladorsagia Circumcincta and Trichostrongylus* Species in Guilan Province, Northern Iran: Molecular and Morphological Characterizations. *BMC Infect. Dis.* 20, 28. doi: 10.1186/s12879-020-4762-0

Ashrafi, K., Tahbaz, A., Sharifdini, M., and Mas-Coma, S. (2015). Familial *Trichostrongylus* Infection Misdiagnosed as Acute Fascioliasis. *Emerg. Infect. Dis.* 21, 1869–1870. doi: 10.3201/eid2110.141392

Boreham, R. E., Mccowan, M. J., Ryan, A. E., Allworth, A. M., and Robson, J. M. (1995). Human Trichostrongyliasis in Queensland. *Pathology* 27, 182–185. doi: 10.1080/00313029500169842

Cancrini, G., Boemi, G., Iori, A., and Corselli, A. (1982). Human Infestations by *Trichostrongylus axei, T. capricola and T. vitrinus*: 1st Report in Italy. *Parassitologia* 24, 145–149.

Chidambaram, M., Parija, S. C., Toi, P. C., Mandal, J., Sankaramoorthy, D., George, S., et al. (2017). Evaluation of the Utility of Conventional Polymerase Chain Reaction for Detection and Species Differentiation in Human Hookworm Infections. *Trop. Parasitol.* 7, 111–117. doi: 10.4103/tp.TP_26_17

Clarke, N. E., Llewellyn, S., Traub, R. J., Mccarthy, J., Richardson, A., and Nery, S. V. (2018). Quantitative Polymerase Chain Reaction for Diagnosis of Soil-Transmitted Helminth Infections: A Comparison With a Flotation-Based Technique and an Investigation of Variability in DNA Detection. *Am. J. Trop. Med. Hyg.* 99, 1033. doi: 10.4269/ajtmh.18-0356

Demeke, G., Fenta, A., and Dilnessa, T. (2021). Evaluation of Wet Mount and Concentration Techniques of Stool Examination for Intestinal Parasites Identification at Debre Markos Comprehensive Specialized Hospital, Ethiopia. *Infect. Drug Resistance* 14, 1357–1362. doi: 10.2147/IDR.S307683

Ericsson, C. D., Steffen, R., Siddiqui, A. A., and Berk, S. L. (2001). Diagnosis of *Strongyloides stercoralis* Infection. *Clin. Infect. Dis.* 33, 1040–1047. doi: 10.1086/322707

Ghadirian, E. (1977). Human Infection With *Trichostrongylus lerouxi* (Biocca, Chabaud, and Ghadirian 1974) in Iran. *Am. J. Trop. Med. Hyg.* 26, 1212–1213. doi: 10.4269/ajtmh.1977.26.1212

Ghadirian, E., and Arfaa, F. (1975). Present Status of Trichostrongyliasis in Iran. *Am. J. Trop. Med. Hyg.* 24, 935–941. doi: 10.4269/ajtmh.1975.24.935

Ghadirian, E., Arfaa, F., and Sadighian, A. (1974). Human Infection With *Trichostrongylus capricola* in Iran. *Am. J. Trop. Med. Hyg.* 23, 1002–1003. doi: 10.4269/ajtmh.1974.23.1002

Ghanbarzadeh, L., Saraei, M., Kia, E. B., Amini, F., and Sharifdini, M. (2019). Clinical and Haematological Characteristics of Human Trichostrongyliasis. *J. Helminthol.* 93, 149–153. doi: 10.1017/S0022149X17001225

Gholami, S., Babamahmoodi, F., Abedian, R., Sharif, M., Shahbazi, A., Pagheh, A., et al. (2015). *Trichostrongylus colubriformis*: Possible Most Common Cause of Human Infection in Mazandaran Province, North of Iran. *Iran J. Parasitol.* 10, 110–115.

Harada, Y., and Mori, O. (1955). A New Method for Culturing Hook Worm. *Yonago Acta Med.* 1, 177–179.

Hidalgo, A., Gacitúa, P., Melo, A., Oberg, C., Herrera, C., and Fonseca-Salamanca, F. (2020). First Molecular Characterization of *Trichostrongylus colubriformis* Infection in Rural Patients From Chile. *Acta Parasitol.* 65, 790–795. doi: 10.2478/s11686-020-00206-1

Hidalgo, A., Melo, A., Romero, F., Hidalgo, V., Villanueva, J., and Fonseca-Salamanca, F. (2018). DNA Extraction in *Echinococcus granulosus and Taenia* Spp. Eggs in Dogs Stool Samples Applying Thermal Shock. *Exp. Parasitol.* 186, 10–16. doi: 10.1016/j.exppara.2018.01.016

Inpankaew, T., Schär, F., Khieu, V., Muth, S., Dalsgaard, A., Marti, H., et al. (2014). Simple Fecal Flotation is a Superior Alternative to Guadruple Kato Katz Smear Examination for the Detection of Hookworm Eggs in Human Stool. *PloS Negl. Trop. Dis.* 8, e3313. doi: 10.1371/journal.pntd.0003313

Lattes, S., Ferte, H., Delaunay, P., Depaquit, J., Vassallo, M., Vittier, M., et al. (2011). *Trichostrongylus colubriformis* Nematode Infections in Humans, France. *Emerg. Infect. Dis.* 17, 1301–1302. doi: 10.3201/eid1707.101519

Mengist, H. M., Demeke, G., Zewdie, O., and Belew, A. (2018). Diagnostic Performance of Direct Wet Mount Microscopy in Detecting Intestinal Helminths Among Pregnant Women Attending Ante-Natal Care (ANC) in East Wollega, Oromia, Ethiopia. *BMC Res. Notes* 11, 1–6. doi: 10.1186/s13104-018-3380-z

Mirzaei, L., Ashrafi, K., Roushan, Z. A., Mahmoudi, M. R., Masooleh, I. S., Rahmati, B., et al. (2021). *Strongyloides stercoralis* and Other Intestinal Parasites in Patients Receiving Immunosuppressive Drugs in Northern Iran: A Closer Look at Risk Factors. *Epidemiol. Health* 43, 1-7. doi: 10.4178/epih.e2021009

Mizani, A., Gill, P., Daryani, A., Sarvi, S., Amouei, A., Katrimi, A. B., et al. (2017). A Multiplex Restriction Enzyme-PCR for Unequivocal Identification and Differentiation of *Trichostrongylus* Species in Human Samples. *Acta Trop.* 173, 180–184. doi: 10.1016/j.actatropica.2017.06.001

Najmi, B., Kia, E., Hosseini, M., Mobedi, I., and Kamranrashani, B. (2017). Comparative Efficacy of Nutrient Agar Plate Culture and Formalin Ether Concentration Methods in the Laboratory Diagnosis of Human Trichostrongyliasis. *J. Guilan Univ. Med. Sci.* 25, 57–65.

Perandin, F., Pomari, E., Bonizzi, C., Mistretta, M., Formenti, F., and Bisoffi, Z. (2018). Assessment of Real-Time Polymerase Chain Reaction for the Detection of *Trichostrongylus* spp. DNA From Human Fecal Samples. *Am. J. Trop. Med. Hyg.* 98, 768. doi: 10.4269/ajtmh.17-0733

Phosuk, I., Intapan, P. M., Sanpool, O., Janwan, P., Thanchomnang, T., Sawanyawisuth, K., et al. (2013). Molecular Evidence of *Trichostrongylus colubriformis* and *Trichostrongylus axei* Infections in Humans From Thailand and Lao PDR. *Am. J. Trop. Med. Hyg.* 89, 376–379. doi: 10.4269/ajtmh.13-0113

Roberts, L. S., and Janovy, J. (2012). *Foundations of Parasitology* (New York: McGraw-Hill).

Rokni, M. (2008). The Present Status of Human Helminthic Diseases in Iran. *Ann. Trop. Med. Parasitol.* 102, 283–295. doi: 10.1179/136485908X300805

Saraei, M., Ghanbarzadeh, L., Hajialilo, E., Barghandan, T., Amini, F., and Sharifdini, M. (2019). Comparison of Nutrient Agar Plate Culture and Formalin-Ethyl Acetate Concentration Methods in Diagnosis of Human Trichostrongyliasis. *J. Ardabil. Univ. Med. Sci.* 18, 506–514. doi: 10.29252/jarums.18.4.506

Sato, M., Yoonuan, T., Sanguankiat, S., Nuamtanong, S., Pongvongsa, T., Phimmayoi, I., et al. (2011). Short Report: Human *Trichostrongylus colubriformis* Infection in a Rural Village in Laos. *Am. J. Trop. Med. Hyg.* 84, 52–54. doi: 10.4269/ajtmh.2011.10-0385

Sharifdini, M., Derakhshani, S., Alizadeh, S. A., Ghanbarzadeh, L., Mirjalali, H., Mobedi, I., et al. (2017a). Molecular Identification and Phylogenetic Analysis of Human *Trichostrongylus* Species From an Endemic Area of Iran. *Acta Trop.* 176, 293–299. doi: 10.1016/j.actatropica.2017.07.001

Sharifdini, M., Eshrat Beigom, K., Ashrafi, K., Hosseini, M., Mirhendi, H., Mohebali, M., et al. (2014). An Analysis of Clinical Characteristics of *Strongyloides stercoralis* in 70 Indigenous Patients in Iran. *Iranian J. Parasitol.* 9, 155.

Sharifdini, M., Ghanbarzadeh, L., Barikani, A., and Saraei, M. (2020). Prevalence of Intestinal Parasites Among Rural Inhabitants of Fouman, Guilan Province, Northern Iran With Emphasis on Strongyloides Stercoralis. *Iran J. Parasitol.* 15, 91–100. doi: 10.18502/ijpa.v15i1.2531

Sharifdini, M., Ghanbarzadeh, L., Kouhestani-Maklavani, N., Mirjalali, H., and Saraei, M. (2017b). Prevalence and Molecular Aspects of Human Hookworms in Guilan Province, Northern Iran. *Iranian J. Parasitol.* 12, 374.

Sharifdini, M., Heidari, Z., Hesari, Z., Vatandoost, S., and Kia, E. B. (2017c). Molecular Phylogenetics of *Trichostrongylus* Species (Nematoda: Trichostrongylidae) From Humans of Mazandaran Province, Iran. *Korean J. Parasitol.* 55, 279–285. doi: 10.3347/kjp.2017.55.3.279

Sharifdini, M., Mirhendi, H., Ashrafi, K., Hosseini, M., Mohebali, M., Khodadadi, H., et al. (2015). Comparison of Nested Polymerase Chain Reaction and Real-Time Polymerase Chain Reaction With Parasitological Methods for Detection of *Strongyloides stercoralis* in Human Fecal Samples. *Am. J. Trop. Med. Hyg.* 93, 1285–1291. doi: 10.4269/ajtmh.15-0309

Wall, E. C., Bhatnagar, N., Watson, J., and Doherty, T. (2011). An Unusual Case of Hypereosinophilia and Abdominal Pain: An Outbreak of *Trichostrongylus* Imported From New Zealand. *J. Travel Med.* 18, 59–60. doi: 10.1111/j.1708-8305.2010.00474.x

Watthanakulpanich, D., Pongvongsa, T., Sanguankiat, S., Nuamtanong, S., Maipanich, W., Yoonuan, T., et al. (2013). Prevalence and Clinical Aspects of Human *Trichostrongylus colubriformis* Infection in Lao PDR. *Acta Trop.* 126, 37–42. doi: 10.1016/j.actatropica.2013.01.002

Willis, H. H. (1921). A Simple Levitation Method for the Detection of Hookworm Ova. *Med. J. Aust.* 2, 375–376. doi: 10.5694/j.1326-5377.1921.tb60654.x

Zeleke, A. J., Addisu, A., Derso, A., Tegegne, Y., Birhanie, M., and Sisay, T. (2021). Evaluation of Hookworm Diagnosis Techniques from Patients in Debre Elias and Sanja Districts of the Amhara Region, Ethiopia. *J. Parasitol. Res.* 1–7 doi: 10.1155/2021/6682330

Conflict of Interest: The authors declare that the research was conducted in the absence of any commercial or financial relationships that could be construed as a potential conflict of interest.

frontiers in Cellular and Infection Microbiology

ORIGINAL RESEARCH
published: 18 October 2021
doi: 10.3389/fcimb.2021.779259

Identification of Myoferlin, a Potential Serodiagnostic Antigen of Clonorchiasis, *via* Immunoproteomic Analysis of Sera From Different Infection Periods and Excretory-Secretory Products of *Clonorchis sinensis*

Xiao-Xiao Ma[1,2,3†], *Yang-Yuan Qiu*[2,3†], *Zhi-Guang Chang*[4], *Jun-Feng Gao*[2], *Rui-Ruo Jiang*[5], *Chun-Lin Li*[2], *Chun-Ren Wang*[2] *and Qiao-Cheng Chang*[1,2*]

[1] School of Public Health, Shantou University, Shantou, China, [2] College of Animal Science and Veterinary Medicine, Heilongjiang Bayi Agricultural University, Daqing, China, [3] Key Laboratory of Zoonosis Research, Ministry of Education, Institute of Zoonosis, College of Veterinary Medicine, Jilin University, Changchun, China, [4] The Seventh Affiliated Hospital, Sun Yat-sen University, Shenzhen, China, [5] Institute of NBC Defence, PLA Army, Beijing, China

OPEN ACCESS

Edited by:
Nian-Zhang Zhang,
Lanzhou Veterinary Research Institute (CAAS), China

Reviewed by:
Xi Zhang,
Zhengzhou University, China
Wen-Bin Zheng,
Shanxi Agricultural University, China

***Correspondence:**
Qiao-Cheng Chang
changqiaocheng2001@163.com

[†]These authors have contributed equally to this work and share first authorship

Specialty section:
This article was submitted to Clinical Microbiology, a section of the journal Frontiers in Cellular and Infection Microbiology

Received: 18 September 2021
Accepted: 04 October 2021
Published: 18 October 2021

Citation:
Ma X-X, Qiu Y-Y, Chang Z-G, Gao J-F, Jiang R-R, Li C-L, Wang C-R and Chang Q-C (2021) Identification of Myoferlin, a Potential Serodiagnostic Antigen of Clonorchiasis, via Immunoproteomic Analysis of Sera From Different Infection Periods and Excretory-Secretory Products of Clonorchis sinensis. Front. Cell. Infect. Microbiol. 11:779259. doi: 10.3389/fcimb.2021.779259

Clonorchiasis, which is caused by *Clonorchis sinensis*, is an important foodborne disease worldwide. The excretory-secretory products (ESPs) of *C. sinensis* play important roles in host-parasite interactions by acting as causative agents. In the present study, the ESPs and sera positive for *C. sinensis* were collected to identify proteins specific to the sera of *C. sinensis* (i.e., proteins that do not cross-react with *Fasciola hepatica* and *Schistosoma japonicum*) at different infection periods. Briefly, white Japanese rabbits were artificially infected with *C. sinensis*, and their sera were collected at 7 days post-infection (dpi), 14 dpi, 35 dpi, and 77 dpi. To identify the specific proteins in *C. sinensis*, a co-immunoprecipitation (Co-IP) assay was conducted using shotgun liquid chromatography tandem-mass spectrometry (LC-MS/MS) to pull down the sera roots of *C. sinensis*, *F. hepatica*, and *S. japonicum*. For the annotated proteins, 32, 18, 39, and 35 proteins specific to *C. sinensis* were pulled down by the infected sera at 7, 14, 35, and 77 dpi, respectively. Three proteins, Dynein light chain-1, Dynein light chain-2 and Myoferlin were detected in all infection periods. Of these proteins, myoferlin is known to be overexpressed in several human cancers and could be a promising biomarker and therapeutic target for cancer cases. Accordingly, this protein was selected for further studies. To achieve a better expression, myoferlin was truncated into two parts, Myof1 and Myof2 (1,500 bp and 810 bp), based on the antigenic epitopes provided by bioinformatics. The estimated molecular weight of the recombinant proteins was 57.3 ku (Myof1) and 31.3 ku (Myof2). Further, both Myof1 and Myof2 could be probed by the sera from rabbits infected with *C. sinensis*. No cross-reaction occurred with the positive sera of *S. japonica*, *F. hepatica*, and negative controls. Such findings indicate that

myoferlin may be an important diagnostic antigen present in the ESPs. Overall, the present study provides new insights into proteomic changes between ESPs and hosts in different infection periods by LC-MS/MS. Moreover, myoferlin, as a biomarker, may be used to develop an objective method for future diagnosis of clonorchiasis.

Keywords: *Clonorchis sinensis*, ESPs, Co-IP, myoferlin, diagnosis

INTRODUCTION

Clonorchis sinensis is an important foodborne pathogen that causes clonorchiasis as well as liver and biliary diseases when raw fish with *C. sinensis* metacercariae is consumed (Ju et al., 2009). Juvenile fluke, excysting in the duodenum of the host, migrate to the intrahepatic bile ducts, where they develop into adults and survive for more than one decade. It primarily affects mammals, such as dogs, cats, and humans, and its typical clinical symptoms include jaundice, cholangitis, and biliary obstruction (Qian et al., 2016). Clonorchiasis is also closely related to liver fibrosis, other human hepatobiliary diseases, and cholangiocarcinoma (CCA) (Pak et al., 2017). In 2009, *C. sinensis* was classified as a class I biological carcinogen (Véronique et al., 2009). It is estimated that 15 million people suffer from clonorchiasis, and approximately 200 million people, primarily in East and Southeast Asia, such as China, South Korea, and Vietnam, are at risk of infection (Qian et al., 2016; Tang et al., 2016).

Excretory-secretory products (ESPs), which are released by excretory organs during parasitism, can stimulate the host immune response, play important roles in host-parasite interactions, and provide attractive materials for identifying antigenic candidates and new drug targets (Li et al., 2020). Different sources of worms produce various antigen substances and distinct immune response procedures (Pino et al., 1986). Thus, identifying the proteins in ESPs is crucial for understanding the mechanisms inherent to parasite-induced pathogenesis. The ESPs of *C. sinensis* are highly sensitive and specific antigens for the diagnosis of clonorchiasis (Cho et al., 2020). During the development of *C. sinensis*, complex antigens that can affect the host immune system are secreted. Although the antigenic and pathogenic functions of *C. sinensis* have been investigated for several decades, the components and roles of *C. sinensis* ESPs remain limited (Li et al., 2004). The components of *C. sinensis* ESPs are complex; however, they mainly include 7-8, 26-28, and 34-37 ku proteins, with the range of 26-45 ku playing major roles in the production of antibodies in infected rabbits (Hong et al., 2001; Hong et al., 2002). These antigenic candidates, to a great extent, are yet to be characterized. Therefore, discovering reliable and prognostic markers for clonorchiasis diagnosis is of great importance. The protein components of ESPs in several species, such as *F. gigantica*, *S. japonicum*, *S. mansoni*, and *Paragonimus westermani*, have already been characterized using proteomics approaches based on mass spectrometry (Lee et al., 2006; Guillou et al., 2007; Liu et al., 2009; Huang et al., 2019).

Exploiting proteomic tools can enable the identification of more sensitive and specific serodiagnostic antigens that do not cross-react with other parasites. Hence, in this study, the co-immunoprecipitation (Co-IP) assay was used to pull down three types of serum. The sera of rabbits infected with *C. sinensis* were collected at 7 days post infection (dpi), 14 dpi, 35 dpi, and 77 dpi, and the sera positive for *F. hepatica* and *S. japonicum* were also collected. Immunoprecipitation was assessed and characterized using liquid chromatography-tandem mass spectrometry (LC-MS/MS). The objective of in this study was to identify more sensitive and specific antigenic targets in ESPs, and provide more potential diagnostic antigens for clonorchiasis.

MATERIALS AND METHODS

Parasites and Sera

C. sinensis metacercariae were collected from naturally infected *Pseudorasbora parva* in the endemic area of Qiqihar, Heilongjiang province, China. Muscular tissue was digested with artificial digestive juice (1% pepsin-hydrochloric acid, Aladdin, China). White Japanese rabbits were purchased from Yisi Experimental Animal Technology Corporation (Changchun City, Jilin Province, China). Fecal examination was conducted before selection to exclude any prior infection with *C. sinensis*. This study was approved by the Animal Health, Animal Care, and Use Committee of the Heilongjiang Bayi Agricultural University. Twenty rabbits (8-9-month-old) negative for *C. sinensis* were selected and randomly divided into two groups: control group and *C. sinensis*-infected group (n=10 each). Rabbits in the experimental group were infected orally with 500 viable metacercariae, while rabbits in the control group were mock-inoculated with 0.85% w/v NaCl solution without metacercariae. After 18 days of infection, the feces of rabbits were collected for fecal examination. Blood samples from each animal were collected aseptically into tubes without anticoagulant, and at 7, 14, 35, and 77 dpi, sera were separated by centrifugation and preserved at -80°C for further use. Positive sera for *F. hepatica* and *S. japonicum* were both obtained from artificially infected rabbits. The rabbits were orally infected with 40 viable *F. hepatica* metacercariae, and the sera were obtained at 90 dpi, stored at the College of Animal Science and Veterinary Medicine, Heilongjiang Bayi Agricultural University. After 42 dpi, positive sera of *S. japonicum* were acquired from rabbits, which infected with 1000 ± 10 *S. japonicum* cercariae, the sera were provided by the Laboratory Animal Center of Shanghai Veterinary Research Institute, Chinese Academy of Agriculture Sciences.

Collection and Preparation of *C. sinensis* ESPs

CSESPs were prepared according to standard procedures (Pak et al., 2017). Briefly, *C. sinensis* adults were separated from the bile ducts of infected rabbits, washed three times with PBS (stored at

37°C), and preincubated in Locke's medium (NaCl 8.9 g, KCl 0.42 g, $NaHCO_3$ 0.2 g, and $CaCl_2$ 0.24 g (wt/vol) at 37°C and 5% CO_2 for 1 h. Thereafter, the parasites were transferred to fresh medium and incubated for 48 h; the medium was changed at 6-h intervals. Finally, the collected cultures were centrifuged at 10 000 g for 30 min at 4°C, to obtain the supernatant, filtered (0.22 μm), and stored at -80°C.

Co-IP

The protein A/G plus-agarose immunoprecipitation kit (Santa Cruz Biotechnology, USA) was used for Co-IP according to the manufacturer's instructions. Briefly, 200 μL of serum positive and negative (7, 14, 35, and 77 dpi) for *C. sinensis* was added into tubes; rabbit sera positive for *S. japonicum* and *F. hepatica* were handled in the same manner. Protein A/G plus-agarose beads (30 μL) were added to each tube and incubated overnight at 4°C. The beads were pelleted by centrifugation at 1,000 g for 30 s at 4°C. Five hundred micrograms *C. sinensis* ESPs (500 μg) was precleared by incubation with protein A/G plus-agarose beads, and incubated for 1.5 h at 4°C. The pellet, collected by centrifugation at 1,000 × g for 5 min at 4°C, was washed three times with PBS buffer, and resuspended in 50 μL SDS loading buffer. The samples were then boiled at 100°C for 10 min. Ten microliters of the sample was analyzed by SDS-PAGE, and the remaining 40 μL was stored for mass spectrometry identification.

Trypsin Digestion

The stained protein bands were cut into 1 mm^3 pieces and washed twice with 200 μL of mass spectrometry (MS) water for 10 min. The gels were detained with 50% acetonitrile (ACN) in 50 mM ammonium bicarbonate (ABC), dehydrated by washing with 100% ACN until the gel turned white, and then washed twice with 200 μL of MS water for 10 min/wash. ACN was added to induce dehydration, which occurred until the colloidal particles turned white. Thereafter, they were vacuum dried for 10 min. Proteins on the gels were treated with 200 μL of 10 mM DTT for 1 h at 37°C and subsequently alkylated with 200 μL of 55 mM iodoacetamide (IAM) for 30 min in the dark. The gels were then washed with digested buffer and treated with ACN, as described above. The suspension was washed with the following solutions: MS water (once), ACN (once), MS water (once), and ACN (once) for 10 min/wash, each experiment group was performed three times.

Liquid Chromatography-Tandem Mass Analysis

Peptides were separated by liquid chromatography using an Acclaim Pep Map 100 column and an EASY-Spray column on an EASY-NLC 1,000 system. The flow rate was set to 0.600 μL/min, and gradient elution was performed for 88 min. The gradient was generated using mobile phase A, which comprised of 100% ddH_2O containing 0.1% formic acid, and mobile phase B, which consisted of 100% ACN containing 0.1% formic acid. Label-free mass spectrometry was performed using a QE HF-X mass spectrometer. The scan events were composed of one single full MS scan and a 3 s MS/MS scan dependent on the previous scan data. The spray voltages were set at 3.8 kV, and the heated capillary temperature was 320°C. The parameters of the MS/MS scan were as follows: resolution, 15,000; auto gain control target, under 2×10^4; maximum isolation time, 30 ms; and normalized collision energy, 27%, each experiment group was performed three times.

Data Analysis

Specific proteins were analyzed using Proteome Discoverer 2.4.1.15. Trypsin was employed as the enzyme, which cleaved after all lysine and arginine residues, with up to two missed cleavages allowed. Carbamidomethylating of cysteine was specified as fixed modification, and protein N-terminal acetylation, oxidation of methionine, and pyro-glutamate formation from glutamine were considered as variable modifications for all groups. The raw file of the mass spectrum was identified and analyzed using the commercial software, Max Quant (Thermo Fisher Scientific, Waltham, MA, USA). The precursor ion mass tolerance was set to 15 ppm and the fragment ion mass tolerance was set to 0.02 Da. All data were searched as a single batch with PSM and protein FDR set to 1% using a target decoy approach. The search parameters were as follows: species, *C. sinensis*; dynamic modification, oxidation; mass tolerance of the precursor ion, ± 15 ppm; fragment ion mass tolerance, ± 0.5 Da; and protein false discovery rate (FDR), 0.01. The maximum number of missed cleavages was two. Kyoto Encyclopedia of Genes and Genomes (KEGG) analysis of the proteins of *C. sinensis* was performed to select the most significant pathway and to analyze the relationship between the abundance of specific proteins of different pathways and the different periods of infection.

C. sinensis Myoferlin cDNA Protein Expression

Cloning of cDNAs encoding myoferlin from *C. sinensis* was achieved using the Uniprot database (protein ID H2KUF2). Further, the bioinformatics, including domains, antigen epitopes, and associated interacting proteins, was analyzed. Ultimately, to achieve a better expression of the protein, it was truncated into two parts: Myof1 (aa 160-aa 660) and Myof2 (aa 600-aa 870). The two coding regions of myoferlin were amplified by polymerase chain reaction (PCR) using the following primers: 5'-GGA TCC ACC ATA AAG GAT GTC CGT CA-3' and 5'-CTC GAG CAG ACA ATG ACT CGT AGC TCA T-3' (Cs-Myof1), or 5'-GGA TCC CTA CCA CTA GTA AAA GAG CAC G-3' and 5'-CTC GAG CAC AAC CAA AAG AAC GAT GTC TC-3' (Cs-Myof2), the underline represents restriction enzyme cutting sites (*Bam*HI, GGA TCC and *Xho*I, CTC GAG). The resulting DNA was digested, purified, and ligated into the *Bam*HI and *Xho*I cloning sites of the pET32a plasmid designed for expression. Recombinant plasmids (pET32a-CsMyof1 and pET32a-CsMyof2) were transformed into *E. coli* BL21 (DE3) cells, and positive clones were selected. Following induction with 1 mM IPTG, bacterial cells were harvested and lysed by sonication in PBS buffer. The lysate was centrifuged at 12,000 g for 20 min at 4°C, and the supernatant was collected. The fusion protein was purified by gel cutting, frozen, and melted five

times using liquid nitrogen repeatedly. After centrifugation at 12,000 g for 20 min at 4°C, the supernatant was collected for further use.

Western Blot

The purified recombinant CsMyof1 and CsMyof2 were subjected to SDS-PAGE (12% gel) and transferred to a Hybond-C pure NC membranes (Immobilon-P, 0.45 μm; Millipore). The membranes were subsequently blocked with blocking buffer (5% w/v skim milk in PBS-T buffer) overnight at 4°C. The sera of rabbits infected with *C. sinensis*, *S. japonicum*, *F. hepatica*, and the negative sera were used as primary antibodies at a dilution of 1:200; the sera were incubated with membranes for 2 h at 37°C. Thereafter, the membranes were washed three times with PBS-T buffer for 30 min. Further incubation was performed using goat anti-rabbit IgG antibody conjugated with HRP at a dilution of 1:5,000 in blocking buffer for 1 h. After washing five times with PBS-T buffer, the membranes were treated with a diaminobenzidine substrate solution for 10 min.

RESULTS

Collection of Sera and ESPs

The metacercariae of *C. sinensis* were collected from *Pseudorasbora parva* (**Figure 1A**). Fecal examination and morphological examination of eggs were carried out (**Figure 1B**). The first identification was performed at 19 dpi, and all infections were confirmed at 25 dpi. After the infected rabbits were sacrificed, the worms were detected in their hepatobiliary tract (**Figure 1C**); however, no worms were observed in control rabbits. *C. sinensis* was collected and made into films (**Figure 1D**), which complies with its typical characteristics, such as the branched testicles and S-shaped excretory sac. The model of rabbits infected with *C. sinensis* was successfully established, and sera at different periods of infection (7, 14, 35, and 77 dpi) were collected. Adult C. *sinensis* worms were collected and cultured *in vitro* for 48 h to prepare the ESPs. The majority of proteins among the ESPs ranged in molecular weight from 10 to 170 ku (**Figure S1A**). A total of 334 proteins were obtained, among which 254 annotated proteins were obtained from the *C. sinensis* protein library by BLAST homology comparison and Uniport identification (**Figure S1B**).

LC-MS/MS Analysis and the Identification of Sera Proteins at Different Periods

An immuno-proteomic approach was used to identify the proteins secreted by *C. sinensis*, specifically using infection sera to pull down the *C. sinensis* ESPs that might be involved in host-parasite interactions. The results of the Co-IP assay revealed that the antibodies from serum at the periods of 7, 14, 35, and 77 dpi, could recognize and pull down the specific proteins from *C. sinensis* ESPs, with most proteins ranging in molecular weight from 15 to 170 ku (**Figure 2**). There were 32, 18, 39, and 35 proteins in the first round of differential screening between positive and negative serum samples (**Figure 3A**). The second round of screening was carried out by comparing and analyzing different types of positive sera, including *F. hepatica*, *S. japonicum*, and *C. sinensis*, based on the first screening (**Figure 3B**). According to the LC-MS/MS analysis, the obtained data was compared with the *C. sinensis* protein library to screen the differential proteins in each period. There were 13, 9, 16, and 15 types of proteins specific to the periods of 7, 14, 35, and 77 dpi with *C. sinensis*, respectively (**Tables 1**–**4**). Five proteins could only be detected in the early stage (7 dpi), which may explain their induction of an early response in the host, and three proteins were found to be specifically co-purified

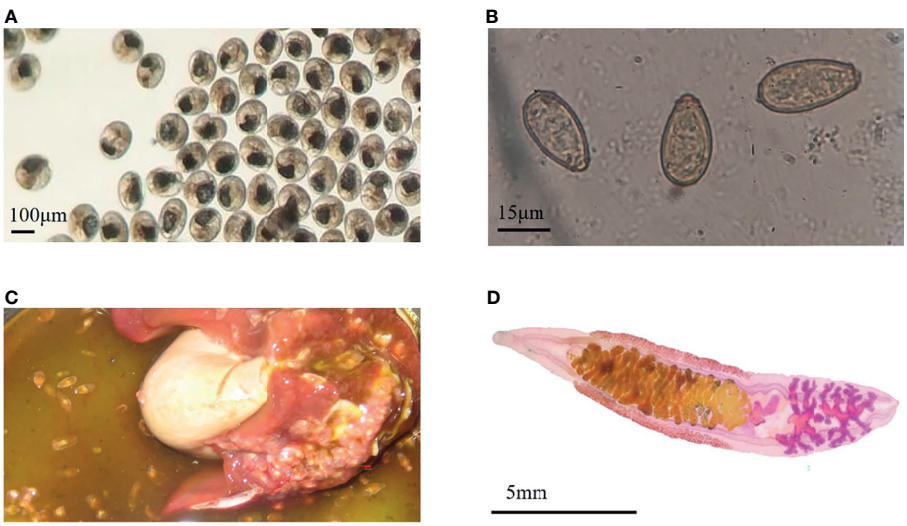

FIGURE 1 | Infection characteristics. **(A)** The Metacercariae of *Clonorchis sinensis* used to infect rabbits. **(B)** *Clonorchis sinensis* eggs observed under an optical microscope. **(C)** Adult worms in the hepatobiliary tract. **(D)** The adult worm collected from the liver of infected rabbit.

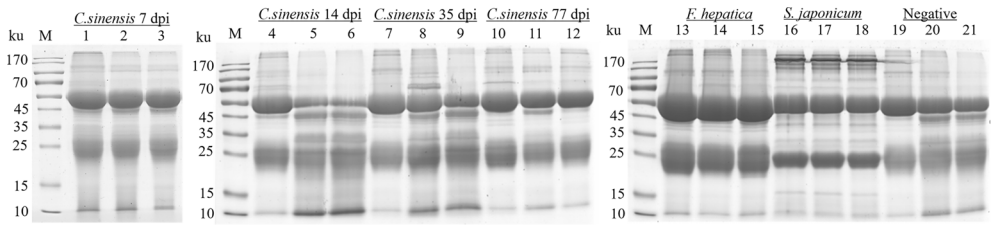

FIGURE 2 | SDS-PAGE analysis of rabbit sera samples of *C. sinensis* at different infection period; *F. hepatica* and *S. japonicum* were co-cultured with the *C. sinensis* ESPs. Lines 1-3: proteins pulled down by rabbit serum at 7 dpi with *C. sinensis*. Lines 4-6: proteins pulled down by rabbit serum at 14 dpi with *C. sinensis*. Lines 7-9: proteins pulled down by rabbit serum at 35 dpi with *C. sinensis*. Lines 10-12: proteins pulled down by rabbit serum at 77 dpi with *C. sinensis*. Lines 13-15: proteins pulled down by *F. hepatica* serum. Lines 16-18: proteins pulled down by *S. japonicum* serum. Lines 19-21: proteins pulled down by rabbit negative serum.

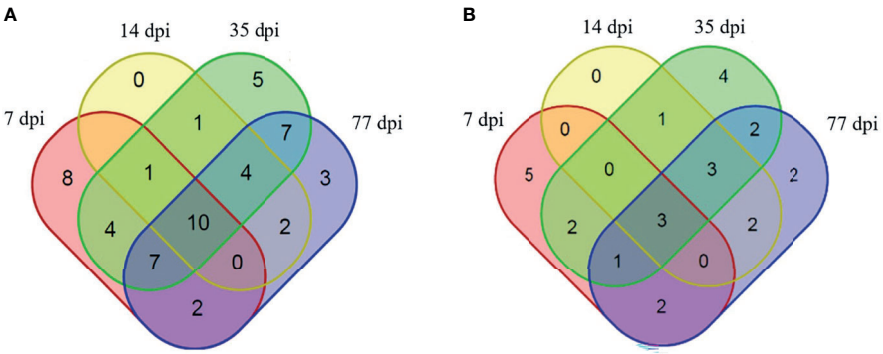

FIGURE 3 | Proteins identified to be binding to rabbit sera at different infection time points. **(A)** Proteins specifically identified to bind to rabbit serum at 7 dpi with *C. sinensis* (pink), 14 dpi (yellow), 35 dpi (green) and 77 dpi (blue), compared with negative serum. **(B)** Proteins specifically identified to bind to rabbit serum at 7 dpi with *C. sinensis* (pink), 14 dpi (yellow), 35 dpi (green), and 77 dpi (blue), compared with *S. japonicum* serum, *F. hepatica* serum, and negative serum.

in all four periods of *C. sinensis* (**Table 5**), including dynein light chain-1, dynein light chain-2, and myoferlin, which were characterized by label-free quantification and functional analysis. These three proteins are involved in body movement and energy metabolism, and were found to display high expression at different stages, thereby providing energy for *C. sinensis*. Myoferlin, an important protein related to tumors, is a member of the ferlin family and is a type II transmembrane protein with a single transmembrane domain at the C terminus.

The Selected Signal Path Based on KEGG

Twenty-seven proteins were detected in *C. sinensis*, but not in *F. hepatica* and *S. japonicum*, where they participate in host-parasite interactions. KEGG analysis revealed that these proteins were

TABLE 1 | *Clonorchis sinensis* excretory and secretory products which were detected by sera of rabbits in 7 dpi.

Accession	Species	Description	Peptides	Unique Peptides	Coverage	MW [ku]	pI
G7YYI1	*C.sinensis*	NADH pyrophosphatase	1	1	5	21.7	5.8
A0A3R7D3C8	*C.sinensis*	Beta-galactosidase	1	1	1	100.9	6.32
G7YV19	*C.sinensis*	Uncharacterized protein	1	1	2	40.8	9.44
G7YFQ8	*C.sinensis*	Cleavage and polyadenylation specificity factor subunit 3	1	1	1	77.9	6.81
A0A3R7FK18	*C.sinensis*	Sorcin	1	1	3	46.7	8.85
A0A3R7CX34	*C.sinensis*	Dynein light chain-1	1	1	8	19.3	5.26
H2KUF2	*C.sinensis*	Myoferlin	1	1	1	105.3	6.02
G7YYI0	*C.sinensis*	NAD (+) kinase	2	2	9	32.5	6.79
A0A3R7GD73	*C.sinensis*	Dynein light chain-2	3	3	38	10.5	8.1
A0A3R7C7M8	*C.sinensis*	ATP synthase subunit alpha	1	1	1	102.9	9.54
G7YYJ7	*C.sinensis*	Acetylornithine deacetylase	2	2	14	29.1	6.13
O96912	*C.sinensis*	Cysteine proteinase	2	2	18	19.8	5.95
G7YFI6	*C.sinensis*	Putative cys1 protein	10	2	6	185.3	7.25

TABLE 2 | *Clonorchis sinensis* excretory and secretory products which were detected by sera of rabbits in 14 dpi.

Accession	Species	Description	Peptides	Unique Peptides	Coverage (%)	MW [ku]	pI
G7YBN0	*C. sinensis*	Charged multivesicular body protein 2A	1	1	2	58.3	9.54
H2KUQ9	*C. sinensis*	Serpin B	1	1	3	37.9	5.2
H2KUG0	*C. sinensis*	Universal stress protein	1	1	8	18.7	6.86
H2KPA8	*C. sinensis*	DNA damage	1	1	5	28	6.14
A0A3R7CX34	*C. sinensis*	Dynein light chain-1	1	1	8	19.3	5.26
H2KUF2	*C. sinensis*	Myoferlin	1	1	1	105.3	6.02
G7YL60	*C. sinensis*	Phospholipid scramblase	1	1	9	16	6.87
A0A3R7GD73	*C. sinensis*	Dynein light chain-2	3	3	38	10.5	8.1
A0A419PK16	*C. sinensis*	Adenosylhomocysteinase	2	2	6	47.7	6.14

TABLE 3 | *Clonorchis sinensis* excretory and secretory products which were detected by sera of rabbits in 35 dpi.

Accession	Species	Description	Peptides	Unique Peptides	Coverage (%)	MW [ku]	pI
G7YJJ5	*C. sinensis*	Transient receptor potential cation channel subfamily M member 2	1	1	1	226.5	6.58
G7YYH0	*C. sinensis*	Phosphomethylpyrimidine synthase	1	1	2	48.9	5.29
G7YG42	*C. sinensis*	16 kDa calcium-binding protein	1	1	7	17.4	4.82
H2KUG0	*C. sinensis*	Universal stress protein	1	1	8	18.7	6.86
A0A3R7FK18	*C. sinensis*	Sorcin	1	1	3	46.7	8.85
H2KPA8	*C. sinensis*	DNA damage-regulated autophagy modulator protein 2	1	1	5	28	6.14
G7YCE6	*C. sinensis*	Ras-related protein Ral-A	1	1	2	66.9	8.72
A0A3R7CX34	*C. sinensis*	Dynein light chain-1	1	1	8	19.3	5.26
H2KUF2	*C. sinensis*	Myoferlin	1	1	1	105.3	6.02
G7YL60	*C. sinensis*	Phospholipid scramblase	1	1	9	16	6.87
A0SWW1	*C. sinensis*	Glutathione peroxidase	2	2	10	19.5	7.44
A0A3R7GD73	*C. sinensis*	Dynein light chain-2	3	3	38	10.5	8.1
G7YVN8	*C. sinensis*	Proactivator polypeptide	1	1	2	70.9	9.1
A0A419PK16	*C. sinensis*	Adenosylhomocysteinase	2	2	6	47.7	6.14
A0A3R7C7M8	*C. sinensis*	ATP synthase subunit alpha	1	1	1	102.9	9.54
G7YFI6	*C. sinensis*	Putative cys1 protein	10	2	6	185.3	7.25

TABLE 4 | *Clonorchis sinensis* excretory and secretory products which were detected by sera of rabbits in 77 dpi.

Accession	Species	Description	Peptides	Unique Peptides	Coverage (%)	MW [ku]	pI
G7YBN0	*C. sinensis*	Charged multivesicular body protein 2A	1	1	2	58.3	9.54
A0A3R7D3C8	*C. sinensis*	Beta-galactosidase	1	1	1	100.9	6.32
G7YYH0	*C. sinensis*	Phosphomethylpyrimidine synthase	1	1	2	48.9	5.29
H2KUQ9	*C. sinensis*	Serpin B	1	1	3	37.9	5.2
G7YG42	*C. sinensis*	16 kDa calcium-binding protein	1	1	7	17.4	4.82
H2KUG0	*C. sinensis*	Universal stress protein	1	1	8	18.7	6.86
A0A3R7FK18	*C. sinensis*	Sorcin	1	1	3	46.7	8.85
H2KPA8	*C. sinensis*	DNA damage-regulated autophagy modulator protein 2	1	1	5	28	6.14
A0A3R7CX34	*C. sinensis*	Dynein light chain-1	1	1	8	19.3	5.26
H2KUF2	*C. sinensis*	Myoferlin	1	1	1	105.3	6.02
B5G4Y2	*C. sinensis*	Aspartic protease	2	2	5	46.6	7.33
G7YL60	*C. sinensis*	Phospholipid scramblase	1	1	9	16	6.87
A0A3R7GD73	*C. sinensis*	Dynein light chain-2	3	3	38	10.5	8.1
H2KTR5	*C. sinensis*	Fibropellin-1	4	1	2	210.4	7.34
O96912	*C. sinensis*	Cysteine proteinase	2	2	18	19.8	5.95

TABLE 5 | *Clonorchis sinensis* excretory and secretory products which were detected by rabbit post-infection in all four periods.

Accession	Species	Description	Peptides	Unique Peptides	Coverage (%)	MW [ku]	pI
A0A3R7CX34	*C. sinensis*	Dynein light chain-1	1	1	8	19.3	5.26
H2KUF2	*C. sinensis*	Myoferlin	1	1	1	105.3	6.02
A0A3R7GD73	*C. sinensis*	Dynein light chain-2	3	3	38	10.5	8.1

mainly involved in oxidative phosphorylation, membrane transport, signal transduction, and metabolism. The abundance of proteins was different in each period of infection; cystoskeleton, oxidative phosphorylation, and mRNA surveillance pathway-related proteins were highly expressed at the early infection stage (7 dpi), and may be involved in early immune evasion (**Figure 4A**). In the middle stage of parasite infection (14 dpi), membrane trafficking related proteins were evidently increased, and may play important roles in providing energy for parasites (**Figure 4B**). NOD-like receptor signaling pathway, glutathione metabolism, and lysosome-related proteins were highly expressed at the late infection stage (35 dpi and 77 dpi); lysosomes secreted by *C. sinensis* can effectively inactivate the proteins released by hosts to protect themselves (**Figures 4C, D**).

Analysis of the Amino Acid Sequence of Myoferlin

Myoferlin has two same domains: protein kinase C conserved region 2 (aa415-aa514, aa655-aa783). Regions with significant homology to the C2 domain have been identified in many proteins. The C2 domain is thought to be involved in calcium-dependent phospholipid binding and membrane-targeting processes, such as subcellular localization. Myoferlin also has two low-complexity domains (domain I, aa254-aa265 and II aa388-aa399) and a transmembrane region (aa887-aa909) (**Figure S2A**). The B cell epitopes of Myoferlin were predicted *via* IEDB (http://tools.iedb.org/), which resulted in ten linear epitopes (**Table S1**) and five discontinuous epitopes (**Table S2**). The predicted scores were all greater than 0.5, which indicated that the protein has a potential for binding antigens. The protein network interactions of myoferlin were also predicted (https://string-db.org/), which resulted in a total of 11 associated proteins (**Figure S2B**). Among these relative proteins, ATPase (ASAN1) is required for the post-translational delivery of tail-anchored proteins to the endoplasmic reticulum. ATPase also recognizes and selectively binds to the transmembrane domain of TA proteins in the cytosol. Vesicle-associated membrane protein 2 (VAMP2), a member of the SNARE family, is the first synaptobrevin studied in synaptic vesicles, and is regarded as a molecule that plays a key role in the process of cell growth, neurotransmission, hormone secretion, and insulin-dependent glucose uptake.

Gene Cloning and Antigenicity Analysis of Recombinant Proteins

To achieve a better expression, myoferlin was truncated into two parts (Myof1 and Myof2) according to the antigenic epitopes provided by bioinformatics. The Myof1 and Myof2 (1,500 bp and 810 bp) genes were amplified using specific oligonucleotide primers (**Figure 5A**) and sub-cloned into the *E. coli* pET32a expression vector. After sub-cloning, the size of the inserted DNA was confirmed by restriction digestion with *Bam*HI and *Xho*I (**Figure 5B**). Subsequently, the cloned Myof1 and Myof2 were successfully expressed in *E. coli* BL21 (DE3) cells. The recombinant proteins were purified by gel cutting and analyzed by SDS-PAGE (**Figure 6A**). The molecular weights of the recombinant proteins were determined to be approximately 60 ku (Myof1) and 31 ku (Myof2). The sera from rabbits infected with *C. sinensis* could be probed at different levels, and the sera positive for *S. japonica*, *F. hepatica*, and from naive rabbit could hardly be probed (**Figure 6B**), which indicates that myoferlin may be a potential antigen for the detection of clonorchiasis.

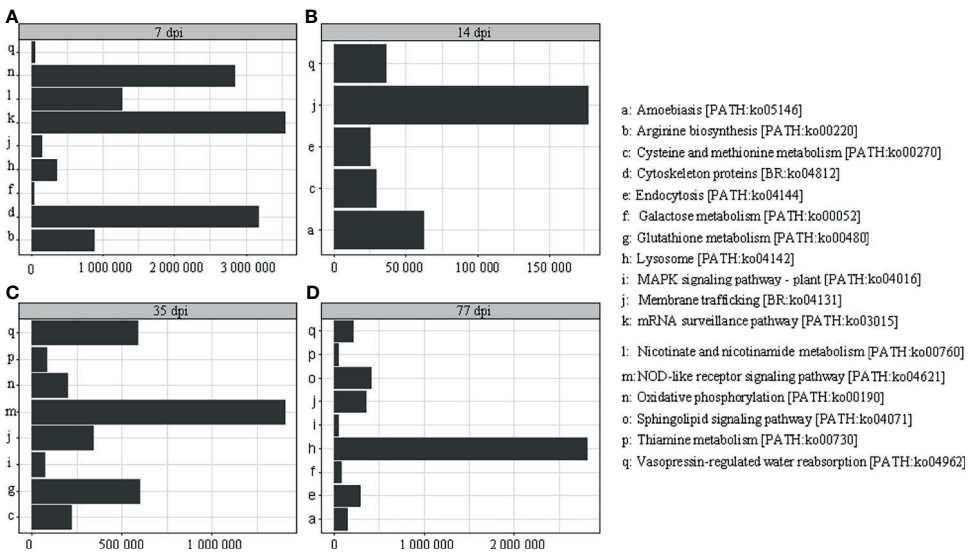

FIGURE 4 | Kyoto Encyclopedia of Genes and Genomes (KEGG) analysis of the different periods after infection; the different periods are displayed on the horizontal axis and the abundance expressed by specific proteins is displayed on the longitudinal axis. **(A)** KEGG analysis of proteins at 7 dpi with *C. sinensis*. **(B)** KEGG analysis of proteins at 14 dpi with *C. sinensis*. **(C)** KEGG analysis of proteins at 35 dpi with *C. sinensis*. **(D)** KEGG analysis of proteins at 77 dpi with *C. sinensis*.

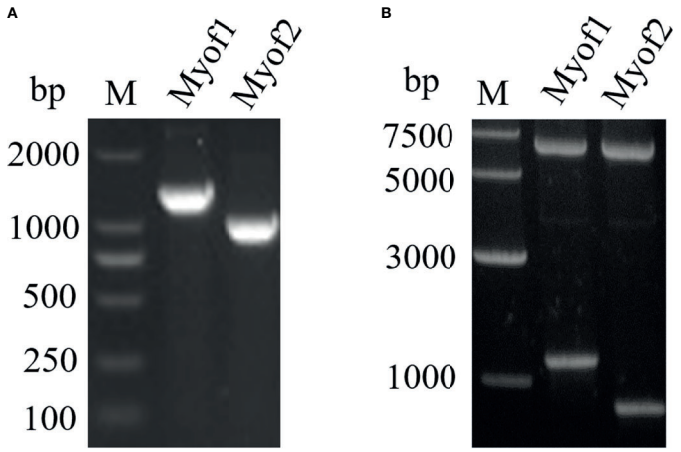

FIGURE 5 | Amplification and cloning of Myof1 and Myof2. **(A)** The amplified genes of Myof1 and Myof2 (1500 bp and 810 bp) using specific oligonucleotide primers. **(B)** Cloning of the coding sequence for Myof1 and Myof2 into the pET32a vector; the inserted DNA was digested with *Bam*HI and *Xho*I.

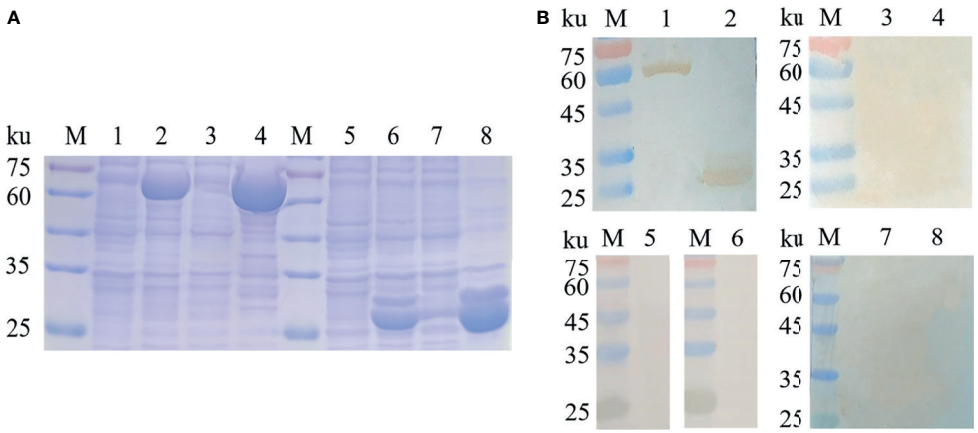

FIGURE 6 | Expression and antigenicity analysis of Myof1 and Myof2. **(A)** The recombinant proteins, Myof1 and Myof2, were subjected to SDS-PAGE (12% gel). M: standard molecular size; Line 1: Un-induced recombinant Myof1-C/BL21; Line 2: Induced recombinant pET-32a-Myof1-C/BL21 with IPTG; Lines 4-5: Supernatant and precipitate of the expression product from the recombinant pET-32a-Myof1 with IPTG induction, respectively. Line 5: Un-induced recombinant Myof2-C/BL21; Line 6: Induced recombinant pET-32a-Myof2-C/BL21 with IPTG; Lines 7-8: Supernatant and precipitate of the expression product from the recombinant pET-32a-Myof2 with IPTG induction, respectively. **(B)** The recombinant proteins reacted with different sera. M: standard molecular size; Lines 1-2: The recombinant proteins, Myof1 and Myof2, incubated with positive sera of the rabbit infected with *C sinensis*; Lines 3-4: Negative serum of rabbit as a control. Lines 5-6: The recombinant proteins, Myof1 and Myof2, incubated with positive sera of the rabbit infected with *S. japonicum*. Lines 7-8: The recombinant proteins, Myof1 and Myof2, incubated with positive sera of the rabbit infected with *F. hepatica*.

DISCUSSION

Clonorchiasis, a foodborne trematodiasis, is an emerging public health problem in China, Korea, and Vietnam (Na et al., 2020). Direct parasite irritation in the bile duct epithelium can cause not only mechanical irritation, but also chemical impairment. Epidemiological and experimental studies have reported that *C. sinensis* infections can induce biliary epithelial hyperplasia, periductal fibrosis, and cystic changes in the ducts, and may also facilitate the development of cholangiocarcinoma (Qian et al., 2016). ESPs, consisting of a complex mixture of proteins, carbohydrates, and lipids, are generally considered to play important roles in host-parasite interactions, including invasion, digestion, detoxification, and immune evasion (Kim et al., 2021). *C. sinensis* continuously releases ESPs (complex mixture of proteins, carbohydrates, lipids, etc.) from the excretory orifice to the outside. Cells exposed to ESPs exert a variety of pathophysiological reactions, including proliferation, apoptosis, destruction of redox homeostasis, and inflammation (Serradell et al., 2007; Kim et al., 2008a). The transcriptomic and proteomic profiles of human cholangiocarcinoma cells treated with ESPs demonstrated that host mRNA was upregulated or downregulated to varying degrees;

upregulated genes were related to tumorigenesis, cell proliferation, and differentiation, while downregulated genes were related to apoptosis (Pak et al., 2014). Identification of proteins in ESPs is thus crucial to our understanding of the mechanisms underlying parasite-induced pathogenesis. Proteomic analysis of *C. sinensis* ESPs revealed that the identified proteins have high immunogenicity and certain specificity, such as detoxifying enzymes, myoglobin proteases, and grain-like growth factors (Mulvenna et al., 2010). Cathepsin F is the major protein in ESPs at 0-3 h, and the main protein of enzymatic proteolytic activity (Kang et al., 2010). ESPs at 0-5 h regulate the proliferation and apoptosis of cholangiocarcinoma cells (Kim et al., 2008b). Cysteine, ESPs at 0-12 h, induce cytotoxicity (Pak et al., 2009). ESPs from *C. sinensis* are directly exposed to the host immune system and are widely used as antigens in serological assays. Further, the antigens of ESPs tend to be superior to those of crude extracts in *C. sinensis* for serodiagnosis of clonorchiasis. Methionine aminopeptidase 2 acid phosphatase, and fructose-1,6-bisphosphatase were found to display high specificity and sensitivity, indicating that they are potential diagnostic antigens (Zheng et al., 2011; Zheng et al., 2013).

Although many studies have revealed the components of ESPs at different periods of *C. sinensis*, few studies have examined the relationship between ESPs and sera at different infection periods. Such finding can not only help us identify the key proteins that interact with sera, but also establish an early diagnosis method for clonorchiasis. Five proteins were found in this study, which were only present in the7 dpi interacting with ESPs. Among them, the cleavage and polyadenylation specificity factor proteins exist widely in many organisms (Shi and Manley, 2015). Most mRNA precursors (pre-mRNAs) are cleaved and polyadenylated at the 3' end prior to their export from the nucleus (Sun et al., 2020). This sequence of events is carefully orchestrated, providing both a tight regulation of cleavage/polyadenylation and the opportunity to select from multiple cleavage sites with various affinities (Gruber and Zavolan, 2019). Switching between these sites can lead to changes in the length and sequence of the 3' UTR of mRNAs, which has many effects on protein expression, mRNA stability, and localization (El Mouali and Balsalobre, 2019). Acetylornithine deacetylase is mainly involved in the ornithine cycle, and the formation of N-acetyl-glutamate from glutamate and acetyl-CoA in a reaction catalyzed by N-acetyl-glutamate synthase (Javid-Majd and Blanchard, 2000). NOD-like receptors are a large family of 22 intracellular proteins in humans that perform a diverse array of cellular functions and play key roles in the regulation of innate immune responses (Lupfer et al., 2020).

To date, ESPs have been known to contain sensitive antigens for the diagnosis of clonorchiasis, and popular antigenic candidates are yet to be characterized in detail. In this study, proteomic and Co-IP assays were used to pull down three types of serum: *C. sinensis*, *F. hepatica*, and *S. japonicum* interacting with the ESPs of *C. sinensis*. Proteins specific to *C. sinensis* were identified by cross-screening using shotgun LC-MS/MS. Due to the limitations of the existing database, only 254 of the 334 proteins were annotated in the total mass spectrum of ESPs. We identified multiple proteins from positive serum samples of *C. sinensis* at different infection periods, and the functions of the identified proteins were classified based on various biological processes. Protein relative pathway analysis revealed that these proteins were mainly involved in oxidative phosphorylation, signal transduction, and metabolism, thereby playing important roles in the interaction between parasites and hosts. Among these proteins, we focused on Myoferlin, one of the three proteins detected in the serum collected at the four infection periods. Myoferlin, which belongs to the ferlin family, is an evolutionarily conserved family of vesicle fusion proteins that is reported to be involved in myoblast fusion, vesicle trafficking, and plasma membrane integrity (Turtoi et al., 2013). Recent studies have shown that myoferlin is overexpressed in several human cancers and enhances tumor progression by regulating migration, invasion, and tumorigenesis (Zhang et al., 2018). Myoferlin is highly involved in oxaliplatin resistance and tumor progression in gastric cancer. The protein could be a promising biomarker and a therapeutic target for cases of oxaliplatin-resistant gastric cancer (Gupta et al., 2021). Studies have shown that myoferlin is also involved in pivotal physiological functions related to numerous cell membranes, such as extracellular secretion, endocytosis, vesicle trafficking, membrane repair, membrane receptor recycling, and secreted protein efflux (Gu et al., 2020).

However, the function of myoferlin in clonorchiasis, especially its effects on detection sensitivity, has received little attention. Thus, we cloned and expressed both Myof1 and Myof2 of the protein to determine their reactogenicity. According to the cross-reactivity analysis results, both Myof1 and Myof2 did not show any cross-reactivity with the sera from *F. hepatica*, *S. japonicum*, and uninfected rabbits. Further, both parts of myoferlin demonstrated a higher degree of specificity to the sera of infected rabbits. Our findings indicate that the immuno-proteomic approaches used in this study could have a significant effect on the identification of serodiagnostic antigens against clonorchiasis. Additionally, myoferlin may be a potential protein for the immunological diagnosis of clonorchiasis.

DATA AVAILABILITY STATEMENT

The datasets presented in this study can be found in online repositories. The names of the repository/repositories and accession number(s) can be found below: http://www.proteomexchange.org/, PXD028236.

ETHICS STATEMENT

The animal study was reviewed and approved by Animal Health, Animal Care and Use Committee of Heilongjiang Bayi Agricultural University.

AUTHOR CONTRIBUTIONS

C-RW and Q-CC designed the project and experiments. X-XM and Y-YQ conducted the experiments. Z-GC and R-RJ analyzed

the data. C-LL and J-FG made the images. X-XM, Y-YQ and Q-CC prepared the manuscript. All authors contributed to the article and approved the submitted version.

FUNDING

This work was supported by the National Natural Science Foundation of China (Grant Nos. 31672399, 81802869 and 32172886), Heilongjiang Postdoctoral Science Foundation (Grant No. LBH-Z19191), and the Heilongjiang Provincial Postdoctoral Natural Science Foundation of China (Grant No. LH2021C071).

ACKNOWLEDGMENTS

We thank Qinglian Biotech Co., Ltd. (Beijing, China) for providing the experimental equipment and commercial database, and the Laboratory Animal Center of Shanghai Veterinary Research Institute, Chinese Academy of Agriculture Sciences for providing the sera positive for *S. japonicum*.

SUPPLEMENTARY MATERIAL

The Supplementary Material for this article can be found online at: https://www.frontiersin.org/articles/10.3389/fcimb.2021.779259/full#supplementary-material

Supplementary Figure 1 | Mass spectrometry analysis of the ESP components. **(A)** SDS-PAGE analysis of the total ESPs of *C. sinensis*. **(B)** Comparative analysis between the identified proteins and *C. sinensis* protein library.

Supplementary Figure 2 | Domains and interacting proteins prediction of myoferlin. **(A)** The domains predetermination of myoferlin. **(B)** The protein network interaction predetermination of myoferlin.

REFERENCES

Cho, P. Y., Lee, J. Y., Kim, T. I., Song, J. H., Hong, S. J., Yoo, W. G., et al. (2020). Serodiagnostic Antigens of Clonorchis Sinensis Identified and Evaluated by High-Throughput Proteogenomics. *PLoS Negl. Trop. Dis.* 14, e0008998. doi: 10.1371/journal.pntd.0008998

El Mouali, Y., and Balsalobre, C. (2019). 3′Untranslated Regions: Regulation at the End of the Road. *Curr. Genet.* 65, 127–131. doi: 10.1007/s00294-018-0877-x

Gruber, A. J., and Zavolan, M. (2019). Alternative Cleavage and Polyadenylation in Health and Disease. *Nat. Rev. Genet.* 20, 599–614. doi: 10.1038/s41576-019-0145-z

Guillou, F., Roger, E., Moné, Y., Rognon, A., Grunau, C., Théron, A., et al. (2007). Excretory-Secretory Proteome of Larval Schistosoma Mansoni and *Echinostoma Caproni*, Two Parasites of Biomphalaria Glabrata. *Mol. Biochem. Parasitol.* 155, 45–56. doi: 10.1016/j.molbiopara.2007.05.009

Gu, H. J., Peng, Y. R., and Chen, Y. H. (2020). An Emerging Therapeutic Approach by Targeting Myoferlin (MYOF) for Malignant Tumors. *Curr. Top. Med. Chem.* 20, 1509–1515. doi: 10.2174/1568026620666200618123436

Gupta, S., Yano, J., Mercier, V., Htwe, H. H., Shin, H. R., Rademaker, G., et al. (2021). Lysosomal Retargeting of Myoferlin Mitigates Membrane Stress to Enable Pancreatic Cancer Growth. *Nat. Cell Biol.* 23, 232–242. doi: 10.1038/s41556-021-00644-7

Hong, S. J., Kim, T. Y., Song, K. Y., Sohn, W. M., and Kang, S. Y. (2001). Antigenic Profile and Localization of Clonorchis Sinensis Proteins in the Course of Infection. *Korean J. Parasitol.* 39, 307–312. doi: 10.3347/kjp.2001.39.4.307

Hong, S. J., Yun Kim, T., Gan, X. X., Shen, L. Y., Sukontason, K., Sukontason, K., et al. (2002). *Clonorchis Sinensis*: Glutathione s-Transferase as a Serodiagnostic Antigen for Detecting Igg and Ige Antibodies. *Exp. Parasitol.* 101, 231–233. doi: 10.1016/s0014-4894(02)00112-1

Huang, S. Y., Yue, D. M., Hou, J. L., Zhang, X. X., Zhang, F. K., Wang, C. R., et al. (2019). Proteomic Analysis of Fasciola Gigantica Excretory and Secretory Products (Fgesps) Interacting With Buffalo Serum of Different Infection Periods by Shotgun LC-MS/MS. *Parasitol Res.* 118, 453–460. doi: 10.1007/s00436-018-6169-z

Javid-Majd, F., and Blanchard, J. S. (2000). Mechanistic Analysis of the ARGE-Encoded N-Acetylornithine Deacetylase. *Biochemistry* 39, 1285–1293. doi: 10.1021/bi992177f

Ju, J. W., Joo, H. N., Lee, M. R., Cho, S. H., Cheun, H. I., Kim, J. Y., et al. (2009). Identification of a Serodiagnostic Antigen, Legumain, by Immunoproteomic Analysis of Excretory-Secretory Products of Clonorchis Sinensis Adult Worms. *Proteomics* 9, 3066–3078. doi: 10.1002/pmic.200700613

Kang, J. M., Bahk, Y. Y., Cho, P. Y., Hong, S. J., Kim, T. S., Sohn, W. M., et al. (2010). A Family of Cathepsin F Cysteine Proteases of Clonorchis Sinensis is the Major Secreted Proteins That are Expressed in the Intestine of the Parasite. *Mol. Biochem. Parasitol.* 170, 7–16. doi: 10.1016/j.molbiopara.2009.11.006

Kim, Y. J., Choi, M. H., Hong, S. T., and Bae, Y. M. (2008a). Proliferative Effects of Excretory/Secretory Products From Clonorchis Sinensis on the Human Epithelial Cell Line HEK293 *via* Regulation of the Transcription Factor E2F1. *Parasitol Res.* 102, 411–417. doi: 10.1007/s00436-007-0778-2

Kim, E. M., Kim, J. S., Choi, M. H., Hong, S. T., and Bae, Y. M. (2008b). Effects of Excretory/Secretory Products From Clonorchis Sinensis and the Carcinogen Dimethylnitrosamine on the Proliferation and Cell Cycle Modulation of Human Epithelial HEK293T Cells. *Korean J. Parasitol.* 46, 127–132. doi: 10.3347/kjp.2008.46.3.127

Kim, J. W., Yi, J., Park, J., Jeong, J. H., Kim, J., Won, J., et al. (2021). Transcriptomic Profiling of Three-Dimensional Cholangiocyte Spheroids Long Term Exposed to Repetitive Clonorchis Sinensis Excretory-Secretory Products. *Parasit Vectors.* 14, 213. doi: 10.1186/s13071-021-04717-2

Lee, E. G., Na, B. K., Bae, Y. A., Kim, S. H., Je, E. Y., Ju, J. W., et al. (2006). Identification of Immunodominant Excretory-Secretory Cysteine Proteases of Adult Paragonimus Westermani by Proteome Analysis. *Proteomics* 6, 1290–1300. doi: 10.1002/pmic.200500399

Li, S., Chen, X., Zhou, J., Xie, Z., Shang, M., He, L., et al. (2020). Amino Acids Serve as an Important Energy Source for Adult Flukes of Clonorchis Sinensis. *PLoS Negl. Trop. Dis.* 14, e0008287. doi: 10.1371/journal.pntd.0008287

Li, S. Y., Chung, B. S., Choi, M. H., and Hong, S. T. (2004). Organ-Specific Antigens of Clonorchis Sinensis. *Korean J. Parasitol.* 42, 169–174. doi: 10.3347/kjp.2004.42.4.169

Liu, F., Cui, S. J., Hu, W., Feng, Z., Wang, Z. Q., and Han, Z. G. (2009). Excretory/Secretory Proteome of the Adult Developmental Stage of Human Blood Fluke, Schistosoma Japonicum. *Mol. Cell Proteomics.* 8, 1236–1251. doi: 10.1074/mcp.M800538-MCP200

Lupfer, C. R., Anand, P. K., Qi, X. P., and Zaki, H. (2020). Editorial: Role of NOD-Like Receptors in Infectious and Immunological Diseases. *Front. Immunol.* 11, 923. doi: 10.3389/fimmu.2020.00923

Mulvenna, J., Sripa, B., Brindley, P. J., Gorman, J., Jones, M. K., Colgrave, M. L., et al. (2010). The Secreted and Surface Proteomes of the Adult Stage of the Carcinogenic Human Liver Fluke Opisthorchis Viverrini. *Proteomics* 10, 1063–1078. doi: 10.1002/pmic.200900393

Na, B. K., Pak, J. H., and Hong, S. J. (2020). *Clonorchis Sinensis* and Clonorchiasis. *Acta Trop.* 203, 105309. doi: 10.1016/j.actatropica.2019.105309

Pak, J. H., Bashir, Q., Kim, I. K., Hong, S. J., Maeng, S., Bahk, Y. Y., et al. (2017). *Clonorchis Sinensis* Excretory-Secretory Products Promote the Migration and Invasion of Cholangiocarcinoma Cells by Activating the Integrin β4-FAK/Src Signaling Pathway. *Mol. Biochem. Parasitol.* 06, 214. doi: 10.1016/j.molbiopara.2017.03.002

Pak, J. H., Kim, I. K., Kim, S. M., Maeng, S., Song, K. J., Na, B. K., et al. (2014). Induction of Cancer-Related MicroRNA Expression Profiling Using Excretory-Secretory Products of Clonorchis Sinensis. *Parasitol Res.* 113, 4447–4455. doi: 10.1007/s00436-014-4127-y

Pak, J. H., Moon, J. H., Hwang, S. J., Cho, S. H., Seo, S. B., and Kim, T. S. (2009). Proteomic Analysis of Differentially Expressed Proteins in Human Cholangiocarcinoma Cells Treated With Clonorchis Sinensis Excretory-Secretory Products. *J. Cell Biochem.* 108, 1376–1388. doi: 10.1002/jcb.22368

Pino, H. S., Petitt, M., Beckstead, J. H., and McKerrow, J. H. (1986). Preparation of Mouse Monoclonal Antibodies and Evidence for a Host Immune Response to the Preacetabular Gland Proteinase of Schistosoma Mansoni Cercariae. *Am. J. Trop. Med. Hyg.* 35, 536–543. doi: 10.4269/ajtmh.1986.35.536

Qian, M. B., Utzinger, J., Keiser, J., and Zhou, X. N. (2016). Clonorchiasis. *Lancet* 387, 800–810. doi: 10.1016/S0140-6736(15)60313-0

Serradell, M. C., Guasconi, L., Cervi, L., Chiapello, L., and Masih, D. T. (2007). Excretory-Secretory Products From Fasciola Hepatica Induce Eosinophil Apoptosis by a Caspase-Dependent Mechanism. *Vet. Immunol. Immunopathol.* 117, 197–208. doi: 10.1016/j.vetimm.2007.03.007

Shi, Y., and Manley, J. L. (2015). The End of the Message: Multiple Protein-RNA Interactions Define the mRNA Polyadenylation Site. *Genes Dev.* 29, 889–897. doi: 10.1101/gad.261974.115

Sun, Y., Hamilton, K., and Tong, L. (2020). Recent Molecular Insights Into Canonical Pre-mRNA 3′-End Processing. *Transcription* 11, 83–96. doi: 10.1080/21541264.2020.1777047

Tang, Z. L., Huang, Y., and Yu, X. B. (2016). Current Status and Perspectives of Clonorchis Sinensis and Clonorchiasis: Epidemiology, Pathogenesis, Omics, Prevention and Control. *Infect. Dis. Poverty.* 5, 71. doi: 10.1186/s40249-016-0166-1

Turtoi, A., Blomme, A., Bellahcène, A., Gilles, C., Hennequière, V., Peixoto, P., et al. (2013). Myoferlin is a Key Regulator of EGFR Activity in Breast Cancer. *Cancer Res.* 73, 5438–5448. doi: 10.1158/0008-5472.CAN-13-1142

Véronique, B., Robert, B., Kurt, S., Yann, G., Béatrice, S., Fatiha, E. G., et al. (2009). A Review of Human Carcinogens-Part B: Biological Agents. *Lancet Oncol.* 10, 321–322. doi: 10.1016/s1470-2045(09)70096-8

Zhang, T., Li, J., He, Y., Yang, F., Hao, Y., Jin, W., et al. (2018). A Small Molecule Targeting Myoferlin Exerts Promising Anti-Tumor Effects on Breast Cancer. *Nat. Commun.* 9, 3726. doi: 10.1038/s41467-018-06179-0

Zheng, M., Hu, K., Liu, W., Hu, X., Hu, F., Huang, L., et al. (2011). Proteomic Analysis of Excretory Secretory Products From Clonorchis Sinensis Adult Worms: Molecular Characterization and Serological Reactivity of a Excretory-Secretory Antigen-Fructose-1,6-Bisphosphatase. *Parasitol Res.* 109, 737–744. doi: 10.1007/s00436-011-2316-5

Zheng, M., Hu, K., Liu, W., Li, H., Chen, J., and Yu, X. (2013). Proteomic Analysis of Different Period Excretory Secretory Products From Clonorchis Sinensis Adult Worms: Molecular Characterization, Immunolocalization, and Serological Reactivity of Two Excretory Secretory Antigens-Methionine Aminopeptidase 2 and Acid Phosphatase. *Parasitol Res.* 112, 1287–1297. doi: 10.1007/s00436-012-3264-4

Conflict of Interest: The authors declare that the research was conducted in the absence of any commercial or financial relationships that could be construed as a potential conflict of interest.

Publisher's Note: All claims expressed in this article are solely those of the authors and do not necessarily represent those of their affiliated organizations, or those of the publisher, the editors and the reviewers. Any product that may be evaluated in this article, or claim that may be made by its manufacturer, is not guaranteed or endorsed by the publisher.

frontiers in Cellular and Infection Microbiology

ORIGINAL RESEARCH
published: 18 October 2021
doi: 10.3389/fcimb.2021.770612

Prevalence of *Cryptosporidium* spp. in Yaks (*Bos grunniens*) in China: A Systematic Review and Meta-Analysis

Hong-Li Geng[1†], Hong-Bo Ni[1†], Jing-Hao Li[2], Jing Jiang[3], Wei Wang[4], Xin-Yu Wei[4], Yuan Zhang[5] and He-Ting Sun[2*]*

[1] College of Veterinary Medicine, Qingdao Agricultural University, Qingdao, China, [2] General Monitoring Station for Wildlife-Borne Infectious Diseases, State forestry and Grass Administration, Shenyang, China, [3] College of Life Sciences, Changchun Sci-Tech University, Shuangyang, China, [4] College of Animal Science and Veterinary Medicine, Heilongjiang Bayi Agricultural University, Daqing, China, [5] College of Animal Science and Technology, Jilin Agricultural University, Changchun, China

OPEN ACCESS

Edited by:
Wei Cong,
Shandong University, Weihai, China

Reviewed by:
Yang Zou,
Lanzhou Veterinary Research Institute (CAAS), China
Hongchao Sun,
Zhejiang Academy of Agricultural Sciences, China

***Correspondence:**
Jing Jiang
jiangjingxiaoyao@163.com
He-Ting Sun
xiaofengsht@163.com

[†]These authors have contributed equally to this work

Specialty section:
This article was submitted to Clinical Microbiology, a section of the journal Frontiers in Cellular and Infection Microbiology

Received: *04 September 2021*
Accepted: *27 September 2021*
Published: *18 October 2021*

Citation:
Geng H-L, Ni H-B, Li J-H, Jiang J, Wang W, Wei X-Y, Zhang Y and Sun H-T (2021) Prevalence of Cryptosporidium spp. in Yaks (Bos grunniens) in China: A Systematic Review and Meta-Analysis. Front. Cell. Infect. Microbiol. 11:770612. doi: 10.3389/fcimb.2021.770612

Cryptosporidium spp., the causative agent of cryptosporidiosis, can infect a variety of hosts. So far, there has been limited information regarding *Cryptosporidium* spp. infection in yaks (*Bos grunniens*). Here, we performed the first systematic review and meta-analysis for *Cryptosporidium* spp. infection in yaks in China. To perform the meta-analysis, five databases (Chinese National Knowledge Infrastructure (CNKI), VIP Chinese journal database, WanFang Data, PubMed, and ScienceDirect) were employed to search for studies related to the prevalence of *Cryptosporidium* spp. in yaks in China. The total number of samples was 8,212, and the pooled *Cryptosporidium* spp. prevalence in yaks was estimated to be 10.52% (1192/8012). The prevalence of *Cryptosporidium* spp. in yaks was 13.54% (1029/5277) and 4.49% (148/2132) in northwestern and southwestern China, respectively. In the sampling year subgroups, the prevalence before 2012 (19.79%; 650/2662) was significantly higher than that after 2012 (6.07%; 437/4476). The prevalence of *Cryptosporidium* spp. in cold seasons (20.55%; 188/794) was higher than that in warm seasons (4.83%; 41/1228). In the age subgroup, the yaks with age < 12 months had a higher prevalence (19.47%; 231/1761) than that in yaks with age ≥12 months (16.63%; 365/2268). Among 12 *Cryptosporidium* spp. species/genotypes, the *C. bovis* had the highest prevalence. Moreover, the effects of geography (latitude, longitude, precipitation, temperature, and altitude) and climate on *Cryptosporidium* spp. infection in yaks were evaluated. Through analyzing the risk factors correlated with the prevalence of *Cryptosporidium* spp., we recommend that effective management measures should be formulated according to the differences of different geographical factors, in order to prevent cryptosporidiosis and reduce economic losses in yaks in China.

Keywords: *Cryptosporidium* spp., yaks, China, meta-analysis, prevalence, zoonosis

INTRODUCTION

Cryptosporidium spp. is an opportunistic protozoan that parasitizes the mucosal epithelial cells of gastrointestinal tract in animals (Wang et al., 2019a). *Cryptosporidium* spp. has a wide range of hosts, including cattle, cats, birds and human (Bhat et al., 2019). The transmission routes for *Cryptosporidium* spp. include a direct contact with infected animals, contaminated water or food, and fecal-oral route (Qin et al., 2014; Ryan et al., 2016; Yildirim et al., 2020). In general, the infection of *Cryptosporidium* spp. in individual was asymptomatic. However, severe symptoms may be induced in immunocompromised individual (Desai, 2020).

The average altitude of yaks' (*Bos grunniens*) habitats is around 3,000 meters above sea level (Lan et al., 2020). The main habitats for yaks are in Tibet municipality, Qinghai Province, Gansu Province, and Sichuan Province (Wang et al., 2019b). Qinghai Province, which was identified to be the largest population of yaks in the world, has approximately 5 million yaks (Wang et al., 2018). So far, 38 species and over 70 genotypes of *Cryptosporidium* spp. have been identified (Deng et al., 2020). Twelve *Cryptosporidium* spp. species/genotypes have been identified in yaks, including *C. bovis*, *C. ryanae*, *C. baileyi*, *C. andersoni*, *C. parvum*, *C. hominis*, *C. canis*, *C. struthionis*, *C. xiaoi*, and *C. ubiquitum* (Ma et al., 2014b; Qi et al., 2015; Wang et al., 2018). More importantly, some of them, such as *C. parvum*, *C. hominis*, and *C. ubiquitum*, were also frequently found in humans (Widmer, 2009; Li et al., 2014; Ryan et al., 2016), and the infection rate is 36.4%, 9.3% and 1.6% (Guy et al., 2021). *Cryptosporidium* may cause fatal persistent diarrhea in infants and people with weakened or immune function and cognitive development, thus representing a public health threat (Xiao et al., 2004). The droppings of yaks that infected with *Cryptosporidium* spp. can be washed away by rain, thus resulting in an influx of *Cryptosporidium* spp. oocysts into the local source of water. The herdsmen and yaks, who live on the plateau, have a high probability to share the source of water. Thus, the yaks infected with *Cryptosporidium* spp. could bring the pathogen to herdsmen through the shared water (Wang et al., 2018). *Cryptosporidium* spp. infection in yaks can cause a loss of appetite, diarrhea, and other symptoms, which leads to a reduced resistance to the disease (Huang et al., 2014; Li et al., 2016a; Gong et al., 2017). The people living on the plateau can obtain various daily necessities (e.g., milk and beef) from yaks. Thus, the yaks are one of the important economic resources for the local people, leading to a direct correlation of yak's health and economy (Mi et al., 2013). So far, there has been no effective drugs or available vaccines for preventing and controlling cryptosporidiosis (Gao, 2012; Ikiroma and Polloc, 2021). The prevention of cryptosporidiosis is an important approach for reducing losses to the breeding industry.

Currently, a systematic evaluation and analysis for cryptosporidiosis in yaks is absent. Thus, it is essential to carry out a systematic evaluation and meta-analysis based on the existing literatures. In this study, our study aim was to analyze the epidemic status of cryptosporidiosis among yaks in China, evaluate and discuss the corresponding risk factors that contribute to *Cryptosporidium* spp. infection in yaks.

Abbreviations: VIP, VIP Chinese Journal Databases; CNKI, China National Knowledge Infrastructure; WanFang, WanFang Databases.

METHODS

Systematic Search Strategy

This paper was prepared according to the PRISMA guidelines for the design and analysis of selected qualified studies (**Table S1**). A literature search was conducted to identify articles published from the inception to January 18, 2021. The aim was to obtain all articles in Chinese and English with topics of *Cryptosporidium* spp. infection in yaks in China. The articles were collected from five databases, including China National Knowledge Infrastructure (CNKI), VIP Chinese Journals Database, Wanfang Data, PubMed, and ScienceDirect. The keywords "yak" and "*Cryptosporidium*" were used for searching on the databases CNKI, VIP Chinese Journals Database, Wanfang Data, and ScienceDirect. The MeSH terms "*Cryptosporidium*", "yak" and "China", and their entry terms, such as "*Bos indicus*", "Zebu", "*Bos taurus*", "Domestic Cow", "Domestic Cows", "*Bos grunniens*", and "*Cryptosporidium*" were used for searching on PubMed. The boolean operators "AND" and "OR" were used to connect MeSH terms and the entry terms, respectively. Finally, the search formula "((*Cryptosporidium*) OR *Cryptosporidiums*) AND ((((((((((yak) OR *Bos indicus*) OR Zebu) OR Zebus) OR *Bos taurus*) OR Cow, Domestic) OR Cows, Domestic) OR Domestic Cow) OR Domestic Cows) OR *Bos grunniens*) OR Yak) OR Yaks)))) AND ((((((China) OR People's Republic of China) OR Mainland China) OR Manchuria) OR Sinkiang) OR Inner Mongolia)" was used for searching on PubMed. The Endnote (X9.2 version) was employed to collate information of obtained articles.

Data Extraction and Exclusions

The inclusion criteria for our systematic review and meta-analysis were as follows: (1) the subjects of the study were limited to yaks; (2) the detection of *Cryptosporidium* spp. was at least carried out by nucleic acid or pathogen detection methods, such as PCR, ELISA or microscopy; (3) the selected articles should contain the information of sample number, positive number, and detection site; (4) the article should contain a full-text with complete data; (5) studies must be designed for a cross-sectional extension; (6) the sample should come from a separate yak (not a mixed sample).

The extracted data included the first author, the year of publication, the province where the study performed, sample collection time, age and gender of yak, detection method, sampling seasons, geographical location (latitude and longitude), relative humidity, annual average temperature, annual precipitation, method type, total number of samples, number of positive samples, and data score. According to the report by Fan and colleagues, the climate of China's plateau is unique, with the warm weather from June to October and the cold weather from November to May (Fan et al., 2011). Therefore, this division method was used to classify seasonal subgroups in this study. Our database was constructed by using Microsoft Excel (version 16.32).

Two reviewers independently extracted and recorded data from each selected research. The differences derived from reviewers or uncertainty about the qualifications of the research were further assessed by another author of this paper.

Quality Assessment

The standardized data collection table was used for data extraction according to the research purpose and inclusion criteria. The article quality was evaluated based on the Grading of Recommendations Assessment reported previously (Guyatt et al., 2008). The scoring criteria of data scoring items were as follows: (1) there was a detailed sampling time-point; (2) there was a specific sampling location; (3) the number of samples was over than 200; and (4) there were more than three risk factors. According to the above scoring criteria, 1 point was given for each item, and the total score of each item was added up to get the total score of the article. The total score was identified to be high quality for 3-4 points, medium quality for 2 points, and low quality for 0-1 points.

Statistical Analyses

The meta package in R software version 4.0.3 ("R core team, R: A language and environment for statistical computing" R core team 2018) was used to analyze the data in this study (Li et al., 2020a). The W-value close to 1 and the *P*-value greater than 0.05 is identified to be close to the Gaussian distribution criterion. The double-arcsine transformation (PFT) method was chosen for data conversion (**Table 1**). The heterogeneity among studies was predicted by Cochran's Q-value (represented by X^2 and *P*-value) and I^2 statistics. Cochran's Q (X^2 and *P*-value) and I^2 statistics were employed to predict the inter-study heterogeneity. The random effect model was chosen for an analysis, according to the heterogeneity of the included articles (Ni et al., 2020). Forest plots were used for a comprehensive analysis. Funnel plot and Egger's test were used to evaluate the publication bias. The stability of the study was evaluated by the trim and filling test, and sensitivity analysis (Wang et al., 2020).

The potential sources of heterogeneity were further studied by subgroup analysis and meta regression analysis. The individual and multivariate model factors were analyzed to determine the factors contributing to the heterogeneity. The survey factors included the sampling year (before 2012 *vs*. after 2012), region (Northwestern China *vs*. Southwestern China), province (Qinghai province *vs*. other provinces), diagnostic method (Immunofluorescence technique (IFA) *vs*. other methods), age (age < 12 months *vs*. age ≥ 12 months), season (cold seasons vs. warm seasons), genotype (*Cryptosporidium bovis vs*. other genotypes), the quality level of the included publications (high quality *vs*. others), longitude (95-100° *vs*. others), latitude (> 35° *vs*. others), altitude (< 95° *vs*. others), average annual precipitation (< 300 mm *vs*. > 300 mm), average annual temperature (< 1°C *vs*. others), average annual humidity (< 55% *vs*. ≥ 55%), altitude (< 3000 m *vs*. > 3000 m), and climate (plateau mountain vs. others).

TABLE 1 | Normal distribution test for the normal rate and the different conversion of the normal rate.

Conversion form	W	*P*
PRAW	0.86549	0.009798
PLN	NaN	NA*
PLOGIT	NaN	NA*
PAS	0.93191	0.1681
PFT	0.93356	0.1808

"PRAW": original rate; "PLN": logarithmic conversion; "PLOGIT": logit transformation; "PAS": arcsine transformation; "PFT": double-arcsine transformation; "NaN": meaningless number; "NA": missing data.*

RESULTS

Search Results

Through searching on five databases, 1,006 relevant articles were screened out for further analyses. According to the selection criteria described in section "2.2", the uncertain articles were excluded by checking the abstracts and/or full-text. Finally, 49 out of 1,006 articles were selected. Among of the selected articles, four were repeated publications, ten were not research objects, one was overview article and letter, and fourteen were removed due to an incomplete or unclear information. Thus, a total of 20 articles were included in this study (**Figure 1**).

Qualification Studies and Publication Bias

Consequently, the included articles covered four provinces. Among the 20 studies, the total number of samples and positive number was 8,212 and 1,192, respectively (**Table 2**). Based on the quality standard, fourteen articles were of high quality (3 or 4 points), five were of medium quality (2 points), and one was of low quality (1 point; **Table 2** and **Table S1**).

In the selected studies, the forest plot measurement demonstrated the degree of heterogeneity (**Figure 2**). According to the funnel chart, we found that the distribution of dots was not completely symmetrical, which might be explained by publication bias or small sample bias (**Figures 3**, **4**). No supplementary study was found by the trim and filling test. The Egger test was used to assess the potential publication bias in the analysis, and the *P*-value greater than 0.05 indicated that no publication bias was present in the data (**Figure 5**). Sensitivity test indicated that the recombined data were not significantly affected by any study that was excluded (**Figure 6**). These results verified rationality and reliability of our analyses.

Results of the Meta-Analysis

From 2001 to 2021, the total prevalence of *Cryptosporidium* spp. in yaks in China was 10.52% (95% CI: 5.64-16.63; **Table 2**). In region group, the higher prevalence was detected in northwestern China (13.54%, 95% CI: 7.10-21.58); than southwestern China (**Table 2**). In the covered four provinces of the meta-analysis, Qinghai province had the highest prevalence of 14.17% (95% CI: 7.34-22.70), and Gansu province and Tibet municipality had the lowest prevalence of 5.98% (95% CI: 2.29-11.12) and 6.03% (95% CI: 4.56-21.34), respectively (**Table 3**). To further identify sources of

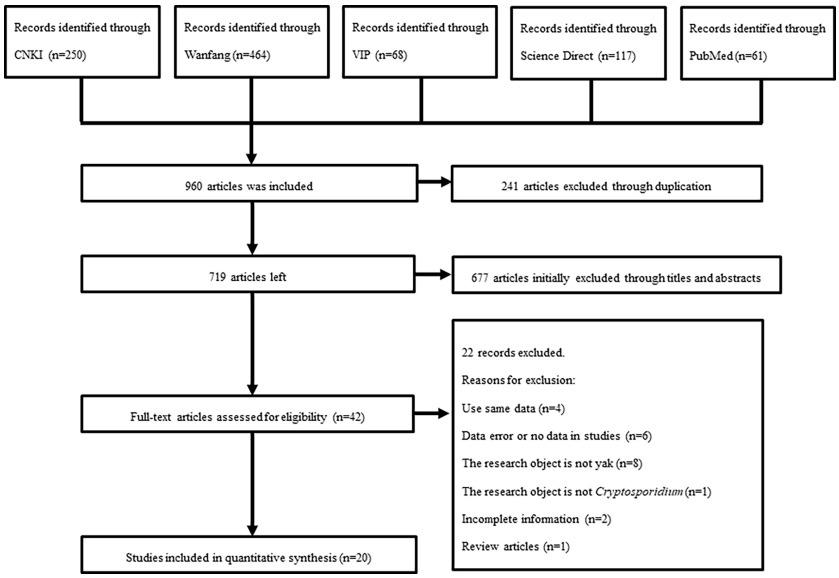

FIGURE 1 | Flow diagram of literature search and selection.

heterogeneity, we analyzed subgroups of season, age, sampling year, detection methods, detailed geographic, and climatic factors. Sampling year was a risk factor for *Cryptosporidium* spp. infection in yaks ($P < 0.05$; **Table 2**). The prevalence of *Cryptosporidium* spp. in yaks before 2012 was 19.47% (95% CI: 10.25-30.56), and 6.07% (95% CI: 1.64-12.91) in yaks after 2012 respectively (**Table 2**). Among 12 *Cryptosporidium* spp. species/genotypes, the *C. bovis* has the highest prevalence (0.34%, 173/4277, 95% CI: 0.16-0.25), followed by *C. andersoni* (0.25%, 100/4277, 95% CI: 0.19-0.32) and *C. parvum* (0.25%, 95% CI: 0.17-0.35; **Table 4**). The prevalence of *C. baileyi*, C. *ubiquitum*, and *C. xiaoi* were the lowest (0.02%, 1/4277, 95%CI: 0.00-0.40; 2/4277, 95%CI: 0.00-0.10; 1/4277, 95%CI: 0.00-0.10; **Table 4**). The information for subgroups analysis of geographical latitude included latitude range (> 35°; 14.68%, 95% CI: 6.19-25.85), longitude range (< 95°; 6.03%, 95% CI: 0.37-16.76), precipitation range (> 300 mm; 12.27%, 95% CI: 6.66-19.24), temperature range (< 1°C; 19.96%, 95% CI: 10.49-31.38), humidity range (≥ 55%; 12.36%, 95% CI: 4.74-22.80), and altitude range (< 3000 m; 13.15%, 95% CI: 5.38-23.60; **Table 5**).

TABLE 2 | Pooled prevalence of *Cryptosporidium* infection in yaks in China.

Variable	Category	No. studies	No. examined	No. positive	% (95% CI*)	Heterogeneity			Univariate meta-regression	
						$\chi 2$	*P*-value	I^2 (%)	*P*-value*	Coefficient (95% CI)
Season	Cold	5	794	188	20.55% (9.76–33.96)	63.24	< 0.01	95.3	0.012	0.331 (0.074 to 0.588)
	Warm	5	1228	41	4.83% (0.12-14.52)	0.14	< 0.01	0.0		
Age	<12 months	11	1761	231	19.47% (10.25–30.56)	241.34	< 0.01	95.9	0.659	0.042 (-0.145 to 0.229)
	≥12 months	6	2268	365	16.63% (7.84-27.84)	191.62	< 0.01	97.4		
Collection	Before 2012	7	2662	650	19.79% (9.34–32.83)	290.71	< 0.01	97.9	0.025	0.214 (0.027 to 0.400)
	After 2012	10	4476	437	6.07% (1.64–12.91)	540.89	< 0.01	98.3		
Method	PCR	12	5443	632	8.80% (3.83–15.45)	588.43	< 0.01	98.1	0.440	-0.088 (-0.312 to 0.136)
	Microscopy	7	1884	206	12.00% (4.04–23.29)	248.58	< 0.01	97.6		
	ELISA	2	1229	369	12.44% (0.00–58.23)	127.99	< 0.01	99.2		
	IFA	3	560	45	6.52% (0.16-18.65)	24.98	< 0.01	92.0		
Region*	Northwestern	15	5277	1029	13.54% (7.10–21.58)	826.49	< 0.01	98.3	0.093	0.160 (-0.026 to 0.346)
	Southwestern	6	2132	148	4.49% (0.60–11.22)	139.93	< 0.01	96.4		
Quality* level	High	14	6951	1056	12.14% (6.00-20.02)	1041.69	< 0.01	98.8	0.426	0.081(-0.118 to 0.280)
	Middle	5	859	123	7.76% (0.16-22.61)	119.43	< 0.01	96.7		
	Low	1	402	13	3.23% (1.70–5.22)	0.00	< 0.01	NA*		
Total		20	8212	1192	10.52% (5.64–16.63)					

CI, Confidence interval; NA*, not applicable; P-value*, P < 0.05 is statistically significant.*
Region: Northwestern China: Qinghai, Gansu; Southwestern China: Sichuan, Tibet.*
Quality : High: 4 or 3 points; Middle: 2 points; Low: 1 point.*

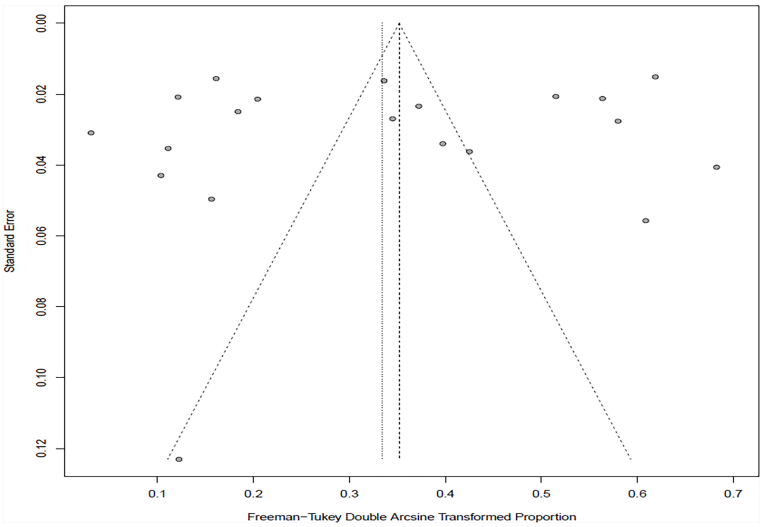

FIGURE 2 | Funnel plot with pseudo 95% confidence interval for publication bias test.

DISCUSSION

Cryptosporidium spp. can cause economic losses in animal husbandry, and bring a great threat to human health (Ouakli et al., 2018; Pumipuntu and Pirate, 2018). Therefore, it is essential to understand the prevalence of *Cryptosporidium* spp. in its hosts. A systematic review and meta-analysis of *Cryptosporidium* spp. prevalence among yaks in China was performed in this study. In 2012 and 2013, China issued the mid to long term animal disease prevention plan (2012-2020) and the National Development Plan for Beef and Mutton Production (2013-2020) to strengthen the prevention and control for animal diseases (Gong et al., 2020; Wei et al., 2021). Therefore, the year "2012" is taken as the cut-off time-point. After an introduction of the above policies, the effective prevention and control measurements might be one reason for the decreased prevalence of *Cryptosporidium* spp. after 2012 (General Office of the State Council, 2012).

In general, *Cryptosporidium* spp. prefers to live in a warm and humid environment, such as southwestern regions (Jagai et al., 2009; Taghipour et al., 2020). However, the prevalence of *Cryptosporidium* spp. in the northwestern regions was reported to be higher than that in the southwestern regions. We found that most of the articles retrieved in the southwestern regions

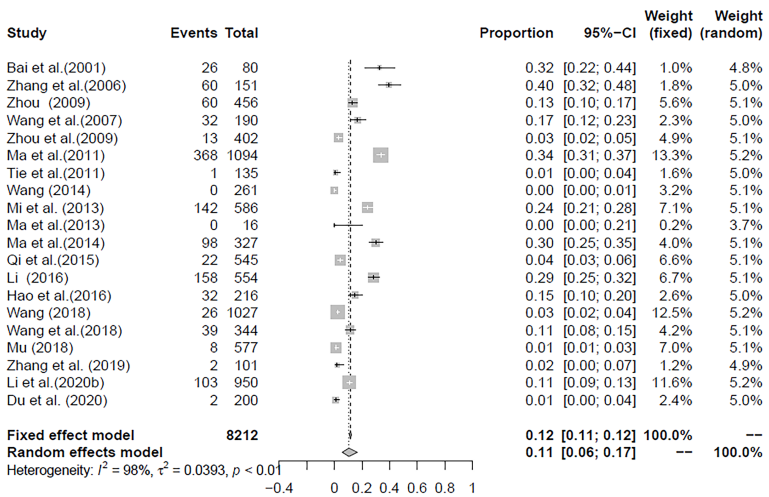

FIGURE 3 | Forest plot of *Cryptosporidium* prevalence in yaks in China.

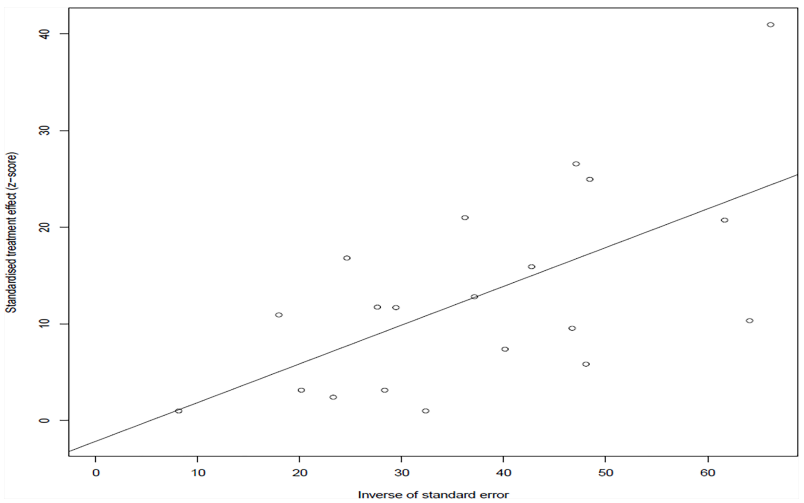

FIGURE 4 | Publication bias of included studies by Egger' test.

were from Qinghai province (**Figure 7**). Qinghai province had a significant effect on the results of northwestern China. Meanwhile, the infection rate of *Cryptosporidium* spp. in Qinghai province was found to be the highest among the analyzed provinces. Several studies showed that the prevalence of *Cryptosporidium* spp. in other animals was also at a high level in Qinghai province. For instance, the prevalence of *Cryptosporidium* spp. is identified to be 22.8% and 39.02% in sheep and goats, respectively (Karanis et al., 2007; Niu and Ma, 2007; Ma et al., 2010; Ma et al., 2013). Some of the water in Qinghai province contains high concentration of *Cryptosporidium* spp. oocysts (Ma et al., 2014a; Ma et al., 2019), and the infected animals were also potential factors inducing water pollution. The oocysts in the environment were difficult to be eliminated, thus resulting in an increased *Cryptosporidium* spp. infection rate in yaks through ingesting contaminated water (Li et al., 2016b; Li et al., 2019). This may lead to an increase of *Cryptosporidium* spp. infection in yaks. Multiple factors, such as climate change, animal husbandry practices, and parasite control measures, may cause various prevalence in different geographic regions (Taghipour et al., 2020). The latitude and longitude of Qinghai province are "31° 36'-99°19'" and "89°35'-103°04'", respectively. At the same time, we found that the areas with latitude > 35° and longitude of 95-100° were also located in Qinghai province, and the infection rate was high (**Table 4**). Qinghai province has a typical continental

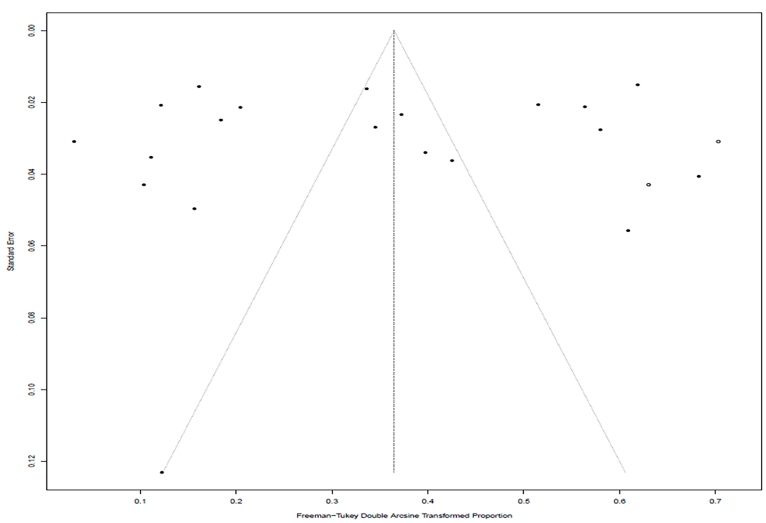

FIGURE 5 | The trim and filling test.

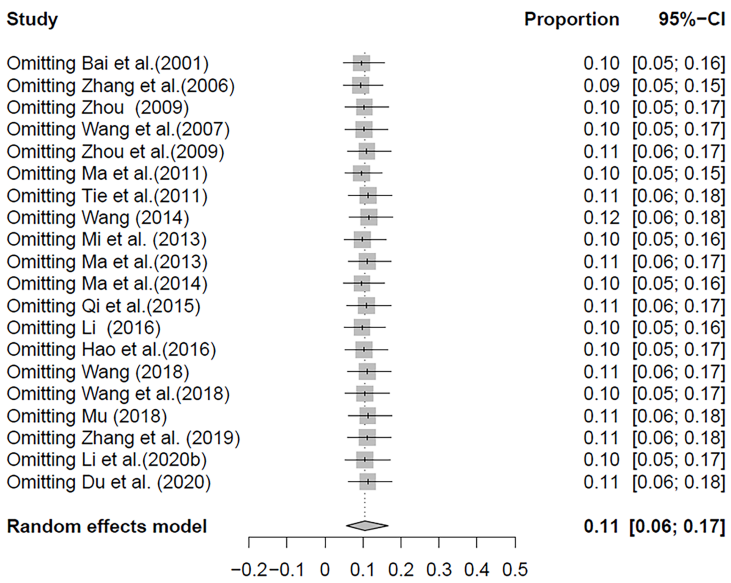

FIGURE 6 | Sensitivity test.

plateau climate (Zhang, 2010) that is high altitude, low temperature, and unpredictable climate (Wei et al., 2015; Zhang et al., 2019). The same characteristics were also observed in our climate subgroup analysis. The prevalence of *Cryptosporidium* spp. in the continental plateau climate was higher than that in other subgroups.

The prevalence of *Cryptosporidium* spp. in yaks < 12 months was higher than that ≥12 months based on our data. The age of sexual maturity of the yak is about 12 months, so the age "12 months" is taken as the cut-off age-point (Wen, 1988). The maternal antibodies obtained from colostrum in young yaks disappear approximately in 2-6 months, therefore, the immunity may decrease and then result in an increased morbidity (Sareyyüpoğlu et al., 2019; Wang et al., 2020). The prevalence of *Cryptosporidium* spp. was slightly lower in the younger yaks.

To date, a total of 12 *Cryptosporidium* spp. species/genotypes were identified in yaks. Among these species/genotypes, *C. parvum*, *C. hominis*, and *C. ubiquitum* were identified in humans, which has caused a widespread concern (Widmer, 2009; Li et al., 2014; Ryan et al., 2016). Interestingly, co-infection of two species/genotypes (*C. ryanae* and *C. bovis* or *C. parvum* and *C. bovis*) was also found in yaks (Mi et al., 2013; Ma et al., 2014b), suggesting that the environment might be contaminated by more than one *Cryptosporidium* spp. species/genotype. The present study found that *C. bovis* had the highest prevalence in the investigated yaks. *C. bovis* is one of the main genotypes that cause cryptosporidiosis in cattle (Wang et al., 2017) and *C. bovis* has been found to be the most prevalent species in pre-weaned calves (Wang et al., 2011; Murakoshi et al., 2012; Zhang et al., 2013). Other studies have also confirmed *C. bovis* was the dominant species in cattle (Mi et al., 2013; Ma et al., 2014b).

In the subgroup of precipitation, the prevalence of *Cryptosporidium* spp. at altitude < 3000 m was higher than that at altitude > 3000 m. Additionally, the temperature was usually high at the low altitude. Previous studies showed that cryptosporidiosis mainly occurred in warm and humid seasons (Lou, 2016). In the subgroups of precipitation and humidity, we found that the prevalence of *Cryptosporidium* spp. in precipitation (> 300 mm) and humidity (> 55%) environment was also high. Thus, our data were in line with previous findings (Taghipour et al., 2020).

The prevalence of *Cryptosporidium* spp. in the cold weather was higher than that in the warm weather, owing to a generally lower temperature on the plateau (Taghipour et al., 2020). Due to the special physiological characteristics of the yak, most of the yaks are grazing in the resource-rich plateau grasslands (Fu et al., 2018). The forage has a low nutrient content in the cold weather, which does not meet the nutrients required by yaks. This causes a loss of body weight and a decreased immunity of yaks, and thus increasing the probability of *Cryptosporidium*

TABLE 3 | Pooled *Cryptosporidium* prevalence in yaks in various provinces.

Provinces	Regions	No. Studies	No. tested	No. positive	Prevalence (%)	95% CI
Qinghai	Northwestern	14	5160	1022	14.17%	7.34-22.70
Sichuan	Southwestern	3	561	33	3.15%	0.00-17.38
Tibet	Southwestern	3	1571	115	6.03%	4.56-21.34
Gansu	Northwestern	1	117	7	5.98%	2.29-11.12

TABLE 4 | The species/genotype of *Cryptosporidium* in yaks was detected by PCR.

Category	No. studies	No. examined	No. positive	% (95% CI*)	Heterogeneity			Univariate meta-regression	
					$\chi 2$	*P*-value	I^2 (%)	*P*-value*	Coefficient (95% CI)
C. ryanae	10	4277	117	0.20% (0.16-0.25)	120.12	< 0.01	92.5	0.104	0.0183 (-0.0037 to 0.0403)
C. bovis	9	4277	173	0.34% (0.28-0.40)	173.36	< 0.01	95.4		
C. baileyi	1	4277	1	0.02% (0.00-0.10)	0.00	< 0.01	NA*		
C. andersoni	6	4277	100	0.25% (0.19-0.32)	144.65	< 0.01	96.5		
C. suis-like	1	4277	2	0.05% (0.00-0.14)	0.00	< 0.01	NA*		
C. parvum	3	4277	34	0.25% (0.17-0.35)	6.99	< 0.01	71.4		
C. hominis	1	4277	4	0.09% (0.02-0.21)	0.00	< 0.01	NA*		
C. canis	1	4277	3	0.07% (0.01-0.18)	0.00	< 0.01	NA*		
C. struthionis	1	4277	5	0.12% (0.03-0.25)	0.00	< 0.01	NA*		
C. ubiquitum	2	4277	2	0.02% (0.00-0.10)	0.00	< 0.01	0.0		
C. xiaoi	1	4277	1	0.02% (0.00-0.10)	0.00	< 0.01	NA*		
C. new genotype	1	4277	2	0.05% (0.00-0.14)	0.00	< 0.01	NA*		

CI, Confidence interval; NA*, not applicable; P-value*, P < 0.05 is statistically significant.*

TABLE 5 | Sub-group analysis of the prevalence of *Cryptosporidium* according to geographic location and climate variables.

Variable	Category	No. studies	No. examined	No. positive	% (95% CI*)	Heterogeneity			Univariate meta-regression	
						$\chi 2$	*P*-value	I^2 (%)	*P*-value*	Coefficient (95% CI)
Latitude	< 30°	3	822	73	10.88% (0.00-39.41)	129.15	< 0.01	98.5	0.576	0.049 (-0.122 to 0.220)
	30-35°	9	2858	354	11.78% (5.62-19.77)	265.95	< 0.01	97.0		
	> 35°	12	3521	681	14.68% (6.19-25.85)	700.44	< 0.01	98.4		
Longitude	< 95°	3	1571	115	6.03% (0.37–16.76)	66.98	< 0.01	97.0	0.356	-0.126 (-0.393 to -0.142)
	95-100°	7	1094	198	14.22% (4.24–28.38)	185.29	< 0.01	96.8		
	> 100°	13	4536	795	13.44% (5.91–23.35)	865.07	< 0.01	98.6		
Precipitation (mm)	< 300	5	445	56	11.48% (6.00-18.27)	12.96	< 0.01	69.1	0.934	-0.007 (-0.182 to 0.167)
	> 300	20	6700	1054	12.27% (6.66-19.24)	1168.48	< 0.01	98.4		
Temperature (°C)	< 1	8	1759	292	19.96% (10.49–31.38)	147.67	< 0.01	95.3	0.178	0.125 (-0.057 to 0.307)
	1-5	11	2565	414	11.09% (4.17-20.58)	418.38	< 0.01	97.6		
	> 5	10	2659	399	11.71% (3.60-23.50)	538.62	< 0.01	98.5		
Humidity	< 55%	12	2868	365	11.09% (6.31-16.94)	194.38	< 0.01	94.3	0.825	-0.019 (-0.187 to 0.149)
	≥ 55%	13	3539	565	12.36% (4.74-22.80)	191.57	< 0.01	95.3		
Altitude (0.1 m)	< 30000	12	3646	677	13.15% (5.38–23.60)	806.97	< 0.01	98.5	0.850	-0.019 (-0.219 to 0.181)
	> 30000	16	3555	433	10.40% (5.32–16.83)	425.07	< 0.01	96.5		
Climate	Plateau mountain climate	18	6995	1158	14.02% (8.15–21.11)	1018.27	< 0.01	98.3	0.055	0.193 (-0.004 to 0.390)
	Temperate continental climate	1	117	7	5.98% (2.29–11.12)	0.00	< 0.01	NA*		
	Subtropical monsoon climate	4	211	12	2.77% (0.00-12.97)	65.08	< 0.01	95.4		

CI, Confidence interval; NA*, not applicable; P-value*, P < 0.05 is statistically significant.*

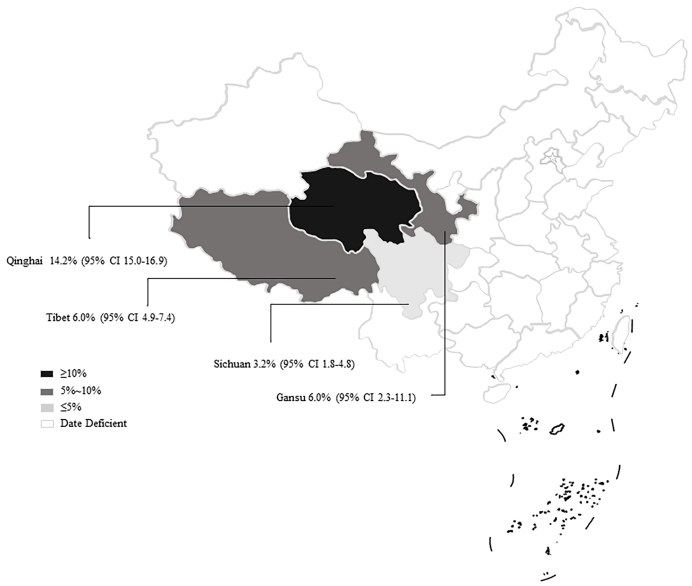

FIGURE 7 | Map of *Cryptosporidium* prevalence in yaks in China.

spp. infection and prevalence. The forage becomes enriched after the end of cold weather. The body weight and resistance of yaks will increase in the warm weather (Zhou et al., 2020). This may be the reason for the lowest prevalence of *Cryptosporidium* spp. observed in the seasons with a lower temperature. Thus, we suggest an increased feed should be provided in time to enhance the resistance of yaks in the cold weather.

In this study, the prevalence of *Cryptosporidium* spp. with Enzyme-linked immunosorbent assay (ELISA) was higher than that with the other three methods in previous reports. ELISA has high specificity and large sample size (Liu et al., 2015; Gong et al., 2020). However, ELISA cannot be used for species typing. In addition, ELISA was rarely used to detect species of parasites (Seema et al., 2014). In this subgroup, there were fewer articles using ELISA to detect *Cryptosporidium* spp., and the lack of data in this subgroup might lead to a higher prevalence than the other groups, thus resulting in unstable results. The advantages of microscope inspection include simple operation, reasonable price, and easy to capture (Taghipour et al., 2020). Microscopic examination can be used to detect intestinal parasitic infection and shows the presence of pathogens and non-pathogenic parasites, but the specific detection of different *Cryptosporidium* spp. species is not reliable (Incani et al., 2017; Taghipour et al., 2020). Microscopy also has a low sensitivity which may lead to false positive (Wang et al., 2020). This may be one reason for the high prevalence. IFA has high sensitivity, specificity, and stability for detection of oocysts. The sensitivity is high for even a low oocyst concentration (Ahmed and Panagiotis, 2018). A cross-reaction with fecal yeast during a longer treatment process is one of disadvantages for IFA (Johnston et al., 2003). PCR allows a simultaneous detection of different parasites in a single reaction, which has a higher sensitivity and easier interpretation (Incani et al., 2017). PCR can be used to detect complete DNA and fragments of parasites, and has become the best method for detecting *Cryptosporidium* spp. (Efrat et al., 2019). Thus, we suggest that the researchers to use the PCR method for detecting *Cryptosporidium* spp. during epidemiological investigations.

In our meta-analysis (n = 20), there are 5 medium-quality articles and 1 low-quality article. The reason for appearance of medium- or low-quality articles was that most studies had a sample size less than 200 and less than 3 risk factors. It is recommended that researchers should take a large sample size, explore more risk factors, clarify the cause of *Cryptosporidium* spp. infection, and provide scientific data and theoretical support for the prevention and control of *Cryptosporidium* spp. infection in yaks.

There were several limitations for our meta-analysis. First, the studies from five databases were limited for obtaining all relevant research data. Second, most of the data were derived from Qinghai province, leading to an uneven data distribution in the northwestern China, and thus affecting the true positive rate. Third, since most of the data show that the yaks are free-range, there is no way to analyze the impact of the feeding mode on *Cryptosporidium* spp. Finally, the available data for this analysis are limited.

CONCLUSIONS

The results of this systematic review and meta-analysis using 20 articles showed that *Cryptosporidium* spp. is common in yaks in China. Different seasons and sampling years had a statistically significant effect on the *Cryptosporidium* spp. infection in yaks. Yaks under 12 months had a higher prevalence of *Cryptosporidium* spp. Thus, the protective measures should be strengthened at this age stage. This study provided basic data for the prevention and

control of cryptosporidiosis in yaks. This may help monitor the prevalence of *Cryptosporidium* spp. in yaks, prevent and control *Cryptosporidium* spp. infection in yaks, in order to reduce the risk of *Cryptosporidium* spp. infection in humans.

DATA AVAILABILITY STATEMENT

The original contributions presented in the study are included in the article/**Supplementary Material**. Further inquiries can be directed to the corresponding authors.

ETHICS STATEMENT

The data regarding the Yaks were collected from five online databases (Chinese National Knowledge Infrastructure (CNKI), VIP Chinese journal database, WanFang Data, PubMed, and ScienceDirect). Written informed consent was obtained from the owners for the participation of their animals in this study.

AUTHOR CONTRIBUTIONS

H-TS, JJ, and H-BN were responsible for the idea and concept of the paper. X-YW and WW built the database. H-LG and WW analyzed the data. H-LG wrote the manuscript. J-HL, JJ, and X-YW critically reviewed and revised the manuscript. All authors contributed to the article and approved the submitted version.

FUNDING

This work was supported by the Wild Animal Disease Monitoring and Early Warning System Maintenance Project (2130211), and the Research Foundation for Distinguished Scholars of Qingdao Agricultural University (665-1120046).

ACKNOWLEDGMENTS

We thank Dr. Chuang Lyu (Shandong New Hope Liuhe Group Co., Ltd. & Qingdao Jiazhi Biotechnology Co., Ltd., Qingdao, China) for critically revising the manuscript.

SUPPLEMENTARY MATERIAL

The Supplementary Material for this article can be found online at: https://www.frontiersin.org/articles/10.3389/fcimb.2021.770612/full#supplementary-material

REFERENCES

Ahmed, S. A., and Panagiotis, K. (2018). Comparison of Current Methods Used to Detect *Cryptosporidium* Oocysts in Stools. *Int. J. Hyg Environ. Health* 221, 743–763. doi: 10.1016/j.ijheh.2018.04.006

Bhat, A. M., Malik, H. U., Wani, N. M., Paul, S., Gupta, S., Dolma, T., et al. (2019). First Report of Cryptosporidium Sp. Infection in Sheep Population of Ladakh, India. *J. Parasit Dis.* 43 (3), 513–516. doi: 10.1007/s12639-019-01119-1

Deng, L., Chai, Y. J., Luo, R., Yang, L. L., Yao, J. X., Zhong, Z. J., et al. (2020). Occurrence and Genetic Characteristics of Cryptosporidium Spp. And *Enterocytozoon Bieneusi* in Pet Red Squirrels (*Sciurus Vulgaris*) in China. *Sci. Rep.* 10 (1), 1026. doi: 10.1038/s41598-020-57896-w

Desai, A. N. (2020). Cryptosporidiosis. *JAMA*. 323, 288. doi: 10.1001/jama.2019.18691

Efrat, G. S., Said, A., Tamar, G., Esther, M., Avi, O., Maya, A., et al. (2019). The Prevalence of *Cryptosporidium* Among Children Hospitalized Because of Gastrointestinal Symptoms and the Efficiency of Diagnostic Methods for *Cryptosporidium*. *Am. J. Trop. Med. Hyg.* 101, 160–163. doi: 10.4269/ajtmh.19-0057

Fan, S. R., Fan, G. Z., Dong, Y. P., and Zhou, D. W. (2011). Discussion on the Division Method of Four Seasons in Qinghai Tibet Plateau. *Plateau Mountain Meteorol Res.* 31, 1–11.

Fu, Y. X., Zhao, Z. F., and Chen, B. L. (2018). Research on Spatial Distribution of Grassland Resources in China. *J. Sci. Technol. Inf.* 16, 68–69.

Gao, M. (2012). Studies on the Species of Bovine Coccidiosis and Genotyping of *Cryptosporidium Andersoni* in Guanzhong Area. *Northwest A&F Univ.* 1, 1–60.

General Office of the State Council (2012). National Medium-and Long-Term Plan for Prevention and Control of Animal Disease-2020). *Heilongjiang J. Anim. Vet. Sci.* 33 (7), 26–30.

Gong, C., Cao, X. F., Deng, L., Li, W., Huang, X. M., Lan, J. C., et al. (2017). Epidemiology of *Cryptosporidium* Infection in Cattle in China: A Review. *Parasite* 24:1. doi: 10.1051/parasite/2017001

Gong, Q. L., Li, J., Li, D., Tian, T., Leng, X., Li, J. M., et al. (2020). Seroprevalence of *Toxoplasma Gondii* in Cattle in China From 2010 to 2019: A Systematic Review and Meta-Analysis. *Acta Trop.* 211, 105439. doi: 10.1016/j.actatropica.2020.105439

Guyatt, G. H., Oxman, A. D., Vist, G. E., Kunz, R., Falck-Ytter, Y., Alonso-Coello, P., et al. (2008). GRADE: An Emerging Consensus on Rating Quality of Evidence and Strength of Recommendations. *BMJ.* 336, 924–926. doi: 10.1136/bmj.39489.470347.AD

Guy, R. A., Yanta, C. A., Muchaal, P. K., Rankin, M. A., Thivierge, K., Lau, R., et al. (2021). Molecular Characterization of *Cryptosporidium* Isolates From Humans in Ontario, Canada. *Parasit Vectors.* 14 (1), 69. doi: 10.1186/s13071-020-04546-9

Huang, J., Yue, D., Qi, M., Wang, R., Zhao, J., Li, J., et al. (2014). Prevalence and Molecular Characterization of Cryptosporidium Spp. And *Giardia Duodenalis* in Dairy Cattle in Ningxia, Northwestern China. *BMC Vet. Res.* 10:292. doi: 10.1186/s12917-014-0292-6

Ikiroma, I. A., and Polloc, K. G. (2021). Influence of Weather and Climate on Cryptosporidiosis-A Review. *Zoonoses Public Health* 68, 285–298. doi: 10.1111/zph.12785

Incani, R. N., Ferrer, E., Hoek, D., Ramak, R., Roelfsema, J., Mughini-Gras, L., et al. (2017). Diagnosis of Intestinal Parasites in a Rural Community of Venezuela: Advantages and Disadvantages of Using Microscopy or RT-PCR. *Acta Trop.* 167, 64–70. doi: 10.1016/j.actatropica.2016.12.014

Jagai, J. S., Castronovo, D. A., Monchak, J., and Naumova, E. N. (2009). Seasonality of Cryptosporidiosis: A Meta-Analysis Approach. *Environ. Res.* 109 (4), 465–478. doi: 10.1016/j.envres.2009.02.008

Johnston, S. P., Ballard, M. M., Beach, M. J., Causer, L., and Wilkins, P. P. (2003). Evaluation of Three Commercial Assays for Detection of *Giardia* and *Cryptosporidium* Organisms in Fecal Specimens. *J. Clin. Microbiol.* 41, 623–626. doi: 10.1128/JCM.41.2.623-626.2003

Karanis, P., Plutzer, J., Halim, N. A., Igor, K., Nagasawa, H., Ongerth, J., et al. (2007). Molecular Characterization of *Cryptosporidium* From Animal Sources in Qinghai Province of China. *Parasitol Res.* 101, 1575–1580. doi: 10.1007/s00436-007-0681-x

Lan, D., Ji, W., Xiong, X., Liang, Q., Yao, W., Mipam, T. D., et al. (2020). Population Genome of the Newly Discovered Jinchuan Yak to Understand its

Adaptive Evolution in Extreme Environments and Generation Mechanism of the Multirib Trait. *Integr. Zool.* 16 (5), 685–695. doi: 10.1111/1749-4877.12484

Li, Z. (2017). Safety Analysis and Potential Hazard Control of Yak Feeding Inputs. *Southwest Minzu Univ.* 2017, 1–110.

Li, P., Cai, J., Cai, M., Wu, W., Li, C., Lei, M., et al. (2016a). Distribution of *Cryptosporidium* Species in Tibetan Sheep and Yaks in Qinghai, China. *Vet. Parasitol.* 215, 58–62. doi: 10.1016/j.vetpar.2015.11.009

Li, K., Li, Z. X., Zeng, Z. B., Li, A. Y., Mehmood, K., Shahzad, M., et al. (2020b). Prevalence and Molecular Characterization of Cryptosporidium Spp. In Yaks (*Bos Grunniens*) in Naqu, China. *Microb. Pathog.* 144, 104190. doi: 10.1016/j.micpath.2020.104190

Li, K., Nader, S. M., Zhang, X., Ray, B. C., Kim, C. Y., Das, A., et al. (2019). Novel Lactate Dehydrogenase Inhibitors With *In Vivo* Efficacy Against *Cryptosporidium Parvum*. *PloS Pathog.* 15, e1007953. doi: 10.1371/journal.ppat.1007953

Li, X., Ni, H. B., Ren, W. X., Jiang, J., Gong, Q. L., and Zhang, X. X. (2020a). Seroprevalence of *Toxoplasma Gondii* in Horses: A Global Systematic Review and Meta-Analysis. *Acta Trop.* 201, 105222. doi: 10.1016/j.actatropica.2019

Liu, Q., Wang, Z. D., Huang, S. Y., and Zhu, X. Q. (2015). Diagnosis of Toxoplasmosis and Typing of *Toxoplasma Gondii*. *Parasit Vectors.* 8, 292. doi: 10.1186/s13071-015-0902-6

Li, F. H., Wang, H. Y., Zhang, Z. J., Li, J. Q., Wang, C. R., Zhao, J. F., et al. (2016b). Prevalence and Molecular Characterization of Cryptosporidium Spp. And *Giardia Duodenalis* in Dairy Cattle in Beijing, China. *Vet. Parasitol.* 219, 61–65. doi: 10.1016/j.vetpar.2016.01.023

Li, N., Xiao, L., Alderisio, K., Elwin, K., Cebelinski, E., Chalmers, R., et al. (2014). Subtyping *Cryptosporidium Ubiquitum*, a Zoonotic Pathogen Emerging in Humans. *Emerg. Infect. Dis.* 20, 217–224. doi: 10.3201/eid2002.121797

Lou, Z. L. (2016). *Epidemiological Investigation and Genotyping of Toxoplasma Gondii, Microsporidium and Cryptosporidium in Cultured Arctic Foxes in Eastern China* (Jilin Agricultural University), 1–67 (in Chinese).

Ma, L. Q., Cai, Q. G., and Lu, Y. (2010). Serological Investigation on Cryptosporidiosis of Lambs in Qinghai Province. *Chin. J. Vet. Med.* 2010, 55–56.

Ma, J. B., Cai, J. Z., Ma, J. W., Feng, Y. Y., and Xiao, L. H. (2014b). Occurrence and Molecular Characterization of Cryptosporidium Spp. In Yaks (*Bos Grunniens*) in China. *Vet. Parasitol.* 202 (3-4), 113–118. doi: 10.1016/j.vetpar.2014.03.030

Ma, L. Q., Sotiriadou, I., Cai, Q. G., Karanis, G., Wang, G. P., Wang, G. H., et al. (2014a). Detection of *Cryptosporidium* and *Giardia* in Agricultural and Water Environments in the Qinghai Area of China by IFA and PCR. *Parasitol Res.* 113, 3177–3184. doi: 10.1007/s00436-014-3979-5

Ma, L. Q., Wang, G. P., Lu, Y., Cai, Q. G., Wang, G. H., Li, X. P., et al. (2013). Molecular Characteristics of *Cryptosporidium* in Qinghai Province. *Chin. Qinghai J. Anim. Vet. Sci.* 2013, 1–3.

Ma, L. Q., Zhang, X. Y., Jian, Y. N., Li, X. P., Wang, G. P., Hu, Y., et al. (2019). Detection of *Cryptosporidium* and *Giardia* in the Slaughterhouse, Sewage and River Waters of the Qinghai Tibetan Plateau Area (QTPA), China. *Parasitol Res.* 118 (7), 2041–2051. doi: 10.1007/s00436-019-06330-w

Mi, R., Wang, X., Li, C., Huang, Y., Zhou, P., Li, Z., et al. (2013). Prevalence and Genetic Characterization of *Cryptosporidium* in Yaks in Qinghai Province of China. *PloS One* 8, e74985. doi: 10.1007/s00436-018-5861-3

Murakoshi, F., Xiao, L., Matsubara, R., Sato, R., Kato, Y., Sasaki, T., et al. (2012). Molecular Characterization of Cryptosporidium Spp. In Grazing Beef Cattle in Japan. *Vet. Parasitol.* 187 (1-2), 123–128. doi: 10.1016/j.vetpar.2011.12.011

Ni, H. B., Gong, Q. L., Zhao, Q., Li, X. Y., and Zhang, X. X. (2020). Prevalence of *Haemophilus Parasuis* "*Glaesserella Parasuis*" in Pigs in China: A Systematic Review and Meta-Analysis. *Prev. Vet. Med.* 182, 105083. doi: 10.1016/j.prevetmed.2020.105083

Niu, X. Y., and Ma, L. Q. (2007). Serological Investigation of Sheep Cryptosporidiosis in Haixi Area of Qinghai Province. *Chin. J. Vet. Med.* 2007, 55–56.

Ouakli, N., Belkhiri, A., de Lucio, A., Köster, P. C., Djoudi, M., Dadda, A., et al. (2018). *Cryptosporidium*-Associated Diarrhoea in Neonatal Calves in Algeria. *Vet. Parasitol Reg. Stud. Rep.* 12, 78–84. doi: 10.1016/j.vprsr.2018.02.005

Pumipuntu, N., and Piratae, S. (2018). Cryptosporidiosis: A Zoonotic Disease Concern. *Vet. World.* 11 (5), 681–686. doi: 10.14202/vetworld.2018.681-686

Qi, M., Cai, J. Z., Wang, R. J., Li, J. Q., Jian, F. C., Huang, J. Y., et al. (2015). Molecular Characterization of Cryptosporidium Spp. And *Giardia Duodenalis* From Yaks in the Central Western Region of China. *BMC Microbiol.* 15, 108. doi: 10.1186/s12866-015-0446-0

Qin, S. Y., Zhang, X. X., Zhao, G. H., Zhou, D. H., Yin, M. Y., Zhao, Q., et al. (2014). First Report of Cryptosporidium Spp. In White Yaks in China. *Parasit Vectors.* 7, 230. doi: 10.1186/1756-3305-7-230

Ryan, U., Zahedi, A., and Paparini, A. (2016). *Cryptosporidium* in Humans and Animals-A One Health Approach to Prophylaxis. *Parasite Immunol.* 38, 535–547. doi: 10.1111/pim.12350

Sareyyüpoğlu, B., Gülyaz, V., Çokçalışkan, C., Ünal, Y., Çökülgen, T., Uzunlu, E., et al. (2019). Effect of FMD Vaccination Schedule of Dams on the Level and Duration of Maternally Derived Antibodies. *Vet. Immunol. Immunopathol.* 217, 109881. doi: 10.1016/j.vetimm.2019.109881

Seema, M., Madhu, S., Uma, C., and Aparna, Y. (2014). Comparison of ELISA and Microscopy for Detection of Cryptosporidium in Stool. *J. Clin. Diagn. Res.* 8, DC07–DC08. doi: 10.7860/JCDR/2014/9713.5088

Taghipour, A., Olfatifar, M., Bahadory, S., Godfrey, S. S., Abdoli, A., Khatami, A., et al. (2020). The Global Prevalence of *Cryptosporidium* Infection in Dogs: A Systematic Review and Meta-Analysis. *Vet. Parasitol.* 281, 109093. doi: 10.1016/j.vetpar.2020.109093

Wang, W., Gong, Q. L., Zeng, A., Li, M. H., Zhao, Q., and Ni, H. B. (2020). Prevalence of *Cryptosporidium* in Pigs in China: A Systematic Review and Meta-Analysis. *Transbound Emerg. Dis.* 68, 1400–1413. doi: 10.1111/tbed.13806

Wang, Y., Shen, Y., Liu, H., Yin, J., Zhang, X. T., Gong, A. Y., et al. (2019a). Induction of Inflammatory Responses in Splenocytes by Exosomes Released From Intestinal Epithelial Cells Following *Cryptosporidium Parvum* Infection. *Infect. Immun.* 87 (4), e00705–e00718. doi: 10.1128/IAI.00705-18

Wang, G. P., Wang, G. H., Li, X. P., Zhang, X. Y., Karanis, G., Jian, Y. N., et al. (2018). Prevalence and Molecular Characterization of Cryptosporidium Spp. And *Giardia Duodenalis* in 1-2-Month-Old Highland Yaks in Qinghai Province, China. *Parasitol Res.* 117, 1793–1800. doi: 10.1007/s00436-018-5861-3

Wang, R., Wang, H., Sun, Y., Zhang, L., Jian, F., Qi, M., et al. (2011). Characteristics of *Cryptosporidium* Transmission in Preweaned Dairy Cattle in Henan, China. *J. Clin. Microbiol.* 9 (3), 1077–1082. doi: 10.1128/JCM.02194-10

Wang, R., Zhao, G., Gong, Y., and Zhang, L. (2017). Advances and Perspectives on the Epidemiology of Bovine *Cryptosporidium* in China in the Past 30 Years. *Front. Microbiol.* 8:1823. doi: 10.3389/fmicb.2017.01823

Wang, K., Zhu, C. Z., Zhao, G. M., Hao, W. M., Tian, W., and Shen, M. Y. (2019b). Breed and Distribution of Yak in China. *Chin. J. Anim. Sci.*, 168–171.

Wei, X. Y., Gong, Q. L., Zeng, A., Wang, W., Wang, Q., and Zhang, X. X. (2021). Seroprevalence and Risk Factors of *Toxoplasma Gondii* Infection in Goats in China From 2010 to 2020: A Systematic Review and Meta-Analysis. *Prev. Vet. Med.* 186, 105230. doi: 10.1016/j.prevetmed.2020

Wei, D., Xu, R., Tenzin, T., Wang, Y., and Wang, Y. (2015). Considerable Methane Uptake by Alpine Grasslands Despite the Cold Climate: In Situ Measurements on the Central Tibetan Platea-2013. *Glob Chang Biol.* 21, 777–788. doi: 10.1111/gcb.12690

Wen, Z. Z. (1988). Investigation on Age Distribution of Yak Population and Analysis of Intraspecies Structure. *J. Domest. Anim. Ecol.* 1988 (02), 16–22+38.

Widmer, G. (2009). Meta-Analysis of a Polymorphic Surface Glycoprotein of the Parasitic Protozoa *Cryptosporidium Parvum* and *Cryptosporidium Hominis*. *Epidemiol. Infect.* 137, 1800–1808. doi: 10.1017/S0950268809990215

Xiao, L., Fayer, R., Ryan, U., and Upton, S. J. (2004). *Cryptosporidium* Taxonomy: Recent Advances and Implications for Public Health. *Clin. Microbiol. Rev.* 17 (1), 72–97. doi: 10.1128/CMR.17.1.72-97.2004

Yildirim, A., Adanir, R., Inci, A., Yukari, B. A., Duzlu, O., Onder, Z., et al. (2020). Prevalence and Genotyping of Bovine *Cryptosporidium* Species in the Mediterranean and Central Anatolia Region of Turkey. *Comp. Immunol. Microbiol. Infect. Dis.* 69, 101425. doi: 10.1016/j.cimid.2020.101425

Zhang, X. H. (2010). SWOT Analysis of Ecotourism Development in Qinghai Province. *J. Landscape Res.* 2, 42–44+48.

Zhang, W., Wang, R., Yang, F., Zhang, L., Cao, J., Zhang, X., et al. (2013). Distribution and Genetic Characterizations of Cryptosporidium Spp. In Pre-Weaned Dairy Calves in Northeastern China's Heilongjiang Province. *PloS One* 8, e54857. doi: 10.1371/journal.pone.0054857

Zhang, Q. X., Zhang, Z. C., Ai, S. T., Wang, X. Q., Zhang, R. Y., and Duan, Z. Y. (2019). *Cryptosporidium* Spp., *Enterocytozoon Bieneusi*, and *Giardia Duodenalis* From Animal Sources in the Qinghai-Tibetan Plateau Area (QTPA) in China. *Comp. Immunol. Microbiol. Infect. Dis.* 67, 101346. doi: 10.1016/j.cimid.2019.101346

Zhou, J., Yue, S., Peng, Q., Wang, L., Wang, Z., and Xue, B. (2020). Metabonomic Responses of Grazing Yak to Different Concentrate Supplementations in Cold Season. *Anim. (Basel)* 10, 1595. doi: 10.3390/ani10091595

Conflict of Interest: The authors declare that the research was conducted in the absence of any commercial or financial relationships that could be construed as a potential conflict of interest.

Publisher's Note: All claims expressed in this article are solely those of the authors and do not necessarily represent those of their affiliated organizations, or those of the publisher, the editors and the reviewers. Any product that may be evaluated in this article, or claim that may be made by its manufacturer, is not guaranteed or endorsed by the publisher.

frontiers in Cellular and Infection Microbiology

ORIGINAL RESEARCH
published: 21 October 2021
doi: 10.3389/fcimb.2021.760400

Detection of Specific IgG-Antibodies Against *Toxoplasma gondii* in the Serum and Milk of Domestic Donkeys During Lactation in China: A Potential Public Health Concern

Long Chen[1], *Zi-Jian Zhao*[2*] *and Qing-Feng Meng*[3*]

[1] Institute of Animal Nutrition and Feed, Jilin Academy of Agricultural Sciences, Gongzhuling, China, [2] Institute of Agro-food Technology, Jilin Academy of Agricultural Sciences, Changchun, China, [3] Technology Center, Changchun Customs, Changchun, China

OPEN ACCESS

Edited by:
Xiao-Xuan Zhang,
Qingdao Agricultural University, China

Reviewed by:
Huanping Guo,
Army Medical University, China
Qing Liu,
Shanxi Agricultural University, China

***Correspondence:**
Zi-Jian Zhao
zhaojaas@163.com
Qing-Feng Meng
mqfboy@163.com

Specialty section:
This article was submitted to Clinical Microbiology, a section of the journal Frontiers in Cellular and Infection Microbiology

Received: 18 August 2021
Accepted: 27 September 2021
Published: 21 October 2021

Citation:
Chen L, Zhao Z-J and Meng Q-F (2021) Detection of Specific IgG-Antibodies Against Toxoplasma gondii in the Serum and Milk of Domestic Donkeys During Lactation in China: A Potential Public Health Concern. Front. Cell. Infect. Microbiol. 11:760400. doi: 10.3389/fcimb.2021.760400

Toxoplasma gondii is a worldwide zoonotic protozoan. Donkeys are often susceptible to many pathological agents, acting as carriers of pathogens for other animal species and humans. However, data on the prevalence of *T. gondii* in donkeys during lactation and on the status of antibodies against *T. gondii* in donkey milk are lacking. A cross-sectional study evaluated the variation of the anti-*T. gondii* antibodies in the blood and milk of domestic donkeys during lactation. A total of 418 domestic donkeys were randomly selected from the Shandong province, eastern China from January 2019 to March 2020. The anti-*T. gondii* antibodies were found in 11.72% (49/418) serum and 9.81% (41/418) milk samples using a commercial ELISA kit, respectively. There was a very high consistency between the serum and milk (Spearman's coefficient = 0.858, p-value < 0.0001 and Kendall's tau = 0.688, p-value < 0.0001), particularly at the 45th to 60th day of lactation. The present results of the statistical analysis showed that the history of abortion (p = 0.026; adjusted OR = 2.20; 95% CI: 1.15–4.20) and cat in the house (p = 0.008; adjusted OR = 2.36; 95% CI: 1.26–4.44) were significantly associated with *T. gondii* infection in the domestic donkeys. This is the first report to detect antibodies against *T. gondii* in donkey milk in China. These results indicate a potential risk of humans contracting the infection through the consumption of raw milk from the naturally infected donkeys.

Keywords: *Toxoplasma gondii*, specific IgG-antibodies, domestic donkeys, sera, milk

INTRODUCTION

Toxoplasmosis is a very important and prevalent foodborne parasitic disease, caused by *Toxoplasma gondii*, infecting all warm-blooded animals including human beings, livestock, birds, and marine mammals (Dubey, 2010). Normally, *T. gondii* infection does not result in obvious clinical symptoms. However, the *T. gondii* infection occurring in pregnant women, organ transplant

patients, and patients with immune deficiency triggers severe clinical symptoms and even death (Montoya and Liesenfeld, 2004). Thus, *T. gondii* infection induces huge damages in both the public health sector and the veterinary field. The infection occurs mainly in three ways: congenital transmission, organ transplant/blood transfusion, and through food and water contaminated by either of the three forms of this parasite (tachyzoite, cysts, and oocysts) (Tenter et al., 2000). Usually, raw or undercooked meat, contaminated milk, and unwashed fruit vegetables can induce this parasitic infection (Pinto-Ferreira et al., 2019). To date, no reports suggest evidence of *T. gondii* infection due to the consumption of donkey's milk, and raw goat's milk has been proven to be associated with the *T. gondii* infection in humans in clinical practice (Camossi et al., 2011).

So far, *T. gondii* has been reported in the milk of various hosts like a goat (Bezerra et al., 2015; Gazzonis et al., 2019), sheep (Iacobucci et al., 2019), cat (Powell et al., 2001), camel (Saad et al., 2018), buffalo (Dehkordi et al., 2013), cow (Koethe et al., 2017), and even lactating women (Azab et al., 1992). Thus, *T. gondii* infection is presumed to occur upon the consumption of either of the milk when consumed raw (Boughattas, 2017). Therefore, there is a necessity of identifying the parasitic contamination in donkey's milk (Martini et al., 2014). However, there is limited information available on the prevalence of *T. gondii* in donkey's milk available worldwide (Haridy et al., 2010; Mancianti et al., 2014; Martini et al., 2014; Perrucci et al., 2021), especially in China, which is one of the world's largest donkey breeding countries.

The consumption of raw milk products has been well-known to pose a very large potential risk, especially in some special groups, such as infants and the aged. Thus, this study aimed to evaluate the prevalence of *T. gondii* in the serum and milk of domestic donkeys during lactation in China. This would provide primary data regarding the prevalence of *T. gondii* in donkey milk in China and add some new data for the safety of the public.

MATERIALS AND METHODS

Ethical Statement

The owners of the donkeys and the local veterinarians were employed to collect the serum and milk from the domestic donkeys. All of the samples were procured with the approval of the owners. All the procedures involving animals were approved by the Animal Care and Ethics Committee of Jilin Academy of Agricultural Sciences.

Sample and Animal Data Collection

A cross-sectional study was carried out in four donkey culturing cities (Jining, Linyi, Rizhao, and Liaocheng) from the Shandong province, eastern China (**Figure 1**). A total of 418 serum and 418 milk samples from the domestic donkeys were randomly collected from January 2019 to March 2020. The blood samples and corresponding milk samples were obtained from each of the donkeys. About 10 ml of blood samples was obtained from the jugular vein of the donkeys using the blood lancet and stored in vacuum tubes without anticoagulant agents. Before collecting the milk samples, the teats were firstly disinfected, and then, about 10 ml of milk samples was collected by milking donkeys by humans and stored in sterile tubes. After transferring the samples to the laboratory, the blood samples were centrifuged at 1,500 *g* for 10 min and then placed at room temperature for 4 h. Finally, the obtained serum was stored at −20°C until further use. For processing the collected milk samples, the fatty components and the somatic cells were removed according to a previous study (Petruzzelli et al., 2013) and then stored at −20°C until further use. For collecting the animal data, the individual data about the age and history of abortion of each donkey, cats in the house, source of water, and source of fodder were obtained from the owners. Moreover, the day of birth of each donkey was set as day 0, and the day of lactation was calculated (Gazzonis et al., 2019).

Laboratory Testing for the *T. gondii* Antibody

To detect the specific IgG-antibodies against *T. gondii* in the collected samples, the available commercial ELISA kit (ID Screen® Toxoplasmosis Indirect MultiSpecies, IDVET, Montpellier) was employed according to the instructions of the manufacturer following the protocol described in the previous study (Gazzonis et al., 2018). The absorbance was measured as the optical density (OD) at 450 nm using a microplate reader (BIO-RAD iMark, United States). The test

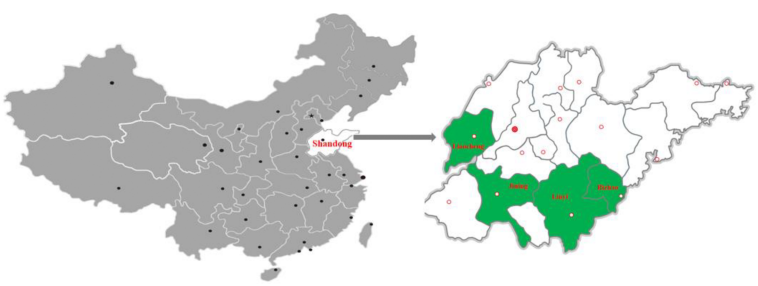

FIGURE 1 | A map of China showing the four cities, Jining, Linyi, Rizhao, and Liaocheng, in Shandong province, eastern China, where the serum and milk samples of the domestic donkeys were collected.

results were calculated according to the formula provided by the manufacturer:

$$S/P\,\% = 100 \times (\text{OD sample} - \text{OD negative control})/(\text{OD positive control} - \text{OD negative control}).$$

The cutoff value for the positive serum samples and milk samples were set at S/P% ≥50% and S/P% ≥21.8%, respectively (Gazzonis et al., 2018).

Statistical Analysis

The statistical analysis was performed using the SPSS 25.0 software package IBM, (Armonk, NY, United States). *p*-values less than 0.05 were considered statistically significant. Spearman and Kendall's rank correlation coefficients analyzed the correspondence between sera and milk results. The logistic regression was used to analyze the association between the *T. gondii* infection and potential risk factors. The multivariate logistic analysis was further performed using the full model, including all the potential risk factors in the analyses.

RESULTS

The *T. gondii* Antibody Detection in the Serum and Milk Samples

In total, 11.72% (49/418) serum samples and 9.81% (41/418) milk samples were found to be positive for the anti-*T. gondii* antibodies, respectively. Comparing the results obtained from the serum and the milk samples, eight positive serum samples were found to have yielded negative results for the correspondent milk samples, while none of the negative serum samples yielded positive correspondent milk samples.

There was a very high consistency between the results on the serum and milk samples (Spearman's coefficient = 0.858, *p*-value < 0.0001 and Kendall's tau = 0.688, *p*-value < 0.0001). The best agreement was obtained from the 46–60 DP (days from parturition), followed by 0–15 DP, while the worst was evident at the second half of the month of lactation (16–30 DP) (**Table 1**). The trend in the antibody level in the serum and milk was explored: the ELISA S/P% values of the serum and milk samples were high in the third phase of lactation (31–45 DP) and the fourth phase of lactation (46–60 DP), respectively. Moreover, both the ELISA S/P % values of the serum and milk samples decreased in the last lactation (>60 DP) (**Figure 2**).

All of the tested domestic donkeys were divided into four age groups. The highest seroprevalence of *T. gondii* in the serum samples was 13.73% for the age group 37–48 months old, and the highest prevalence of *T. gondii* in the milk samples was 11.94% for the age group >48 months old (**Table 2**). In terms of region, Linyi (15.31%) and Rizhao (11.34%) were found to have the highest prevalence of *T. gondii* in the serum and milk samples, respectively (**Table 2**). Considering the sampling time, both the highest prevalence of *T. gondii* in the serum and milk samples were found in winter (16.16% and 14.14, respectively), and the lowest was found in autumn (8.33% and 6.82%. respectively) (**Table 2**). By days from postpartum, the highest prevalence of *T. gondii* in the serum and milk samples were found in the 46–60 DP group (18.67%) and the >60 DP group (15.00%), respectively, but both the lowest prevalence of *T. gondii* in the serum and milk samples were found in the 0–15 DP group (4.29% and 2.86%. respectively) (**Table 2**).

TABLE 1 | The conformance between the lactating donkey's serum and milk samples based on the ELISA S/P% results.

Statistical test	Days from parturition				
	0–15	16–30	31–45	45–60	>60
Kendall's Tau	0.670	0.665	0.683	0.730	0.649
(*p*-value)	(0.000)	(0.000)	(0.000)	(0.000)	(0.000)
Spearman's coefficient	0.852	0.833	0.842	0.888	0.836
(*p*-value)	(0.000)	(0.000)	(0.000)	(0.000)	(0.000)

Risk Factors for *T. gondii* Infection

In the univariate analysis for the serum samples, two variables were found to be associated with the anti-*T. gondii* IgG positivity, including the history of abortion ($p = 0.012$; adjusted OR = 2.17; 95% CI: 1.18–3.96) and cat in the house ($p = 0.002$; adjusted OR = 2.66; 95% CI: 1.45–4.90). Only one variable (cat in the house, $p = 0.038$; adjusted OR = 2.02; 95% CI: 1.04–3.91) was found to be associated with the anti-*T. gondii* IgG positivity in the univariate analysis for the milk samples (**Table 2**). The following multivariate logistic regression showed that the history of abortion ($p = 0.026$; adjusted OR = 2.20; 95% CI: 1.15–4.20) and cat in the house ($p = 0.008$; adjusted OR = 2.36; 95% CI: 1.26–4.44) were independent risk factors for *T. gondii* seropositivity in the domestic donkeys (**Table 3**).

DISCUSSION

Donkey's milk has been used since antiquity mainly for its important medicinal properties as well as nutrient values (Li Q. et al., 2020).

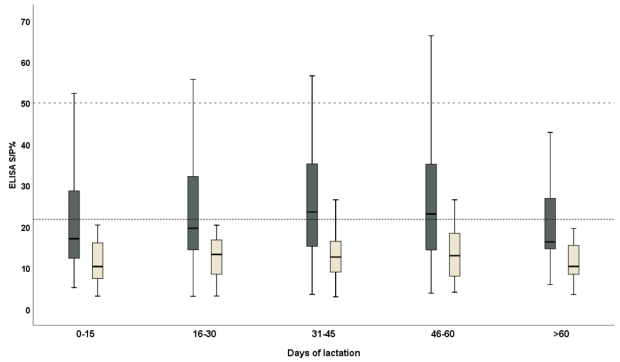

FIGURE 2 | The distribution trend of the ELISA S/P% values of serum (black) and milk (yellow) samples of the domestic donkeys during the lactation. The cutoff values for the anti-*T. gondii* IgG were 50 (dashed line) and 21.8 (dotted line) in the serum and milk samples and were considered positive, respectively.

TABLE 2 | Univariate analysis of the variables associated with *T. gondii* prevalence in the serum and milk samples of the domestic donkeys tested by ELISA.

Variable	No. tested	Serum			Milk		
		Positivity (%)	Odds ratio (95% confidence interval)	*p*-value	Positivity (%)	Odds ratio (95% confidence interval)	*p*-value
Age (Months)							
≦ 24	67	4.48	0.35 (0.09–1.37)	0.130	4.48	0.35 (0.09–1.37)	0.130
25–36	182	13.19	1.12 (0.48–2.63)	0.794	9.89	0.81 (0.33–1.96)	0.639
37–48	102	13.73	1.17 (0.46–2.97)	0.736	11.76	0.98 (0.38–2.55)	0.972
>48	67	11.94	Reference		11.94	Reference	
Region							
Jining	116	9.48	0.91 (0.38–2.21)	0.842	7.76	0.82 (0.32–2.09)	0.672
Linyi	98	15.31	1.58 (0.69–3.62)	0.283	11.22	1.23 (0.50–3.03)	0.658
Rizhao	97	12.37	1.23 (0.52–2.94)	0.638	11.34	1.24 (0.50–3.07)	0.640
Liaocheng	107	10.28	Reference		9.35	Reference	
Sampling time							
Spring	108	11.11	0.65 (0.29–1.45)	0.291	7.41	0.49 (0.19–1.21)	0.122
Summer	79	12.66	0.75 (0.32–1.76)	0.512	12.66	0.88 (0.37–2.10)	0.774
Autumn	132	8.33	0.47 (0.21–1.07)	0.071	6.82	0.44 (0.18–1.07)	0.071
Winter	99	16.16	Reference		14.14	Reference	
History of abortion							
Yes	130	17.69	2.17 (1.18–3.96)	0.012*	12.31	1.48 (0.76–2.87)	0.251
No	288	9.03	Reference		8.68	Reference	
Days from postpartum							
0–15	70	4.29	0.25 (0.05–1.37)	0.111	2.86	0.17 (0.03–1.08)	0.060
16–30	164	14.02	0.92 (0.25–3.41)	0.906	11.59	0.74 (0.20–2.77)	0.658
31–45	89	6.74	0.41 (0.09–1.80)	0.238	6.74	0.41 (0.09–1.80)	0.238
46–60	75	18.67	1.30 (0.34–5.51)	0.704	14.67	0.97 (0.24–3.89)	0.970
>60	20	15.00	Reference		15.00	Reference	
Cats in house							
Yes	115	20.00	2.66 (1.45–4.90)	0.002*	14.78	2.02 (1.04–3.91)	0.038*
No	303	8.58	Reference		7.92	Reference	
Source of Water							
Well	141	10.64	0.71 (0.35–1.45)	0.344	9.22	0.78 (0.36–1.69)	0.781
Tap water	138	10.14	0.67 (0.32–1.39)	0.284	8.70	0.73 (0.33–1.61)	0.438
Well/Tap water	139	14.39	Reference		11.51	Reference	
Source of fodder							
Forage	96	13.54	1.17 (0.57–2.39)	0.676	13.54	1.79 (0.83–3.85)	0.138
Commercial feed	111	9.91	0.82 (0.39–1.73)	0.600	9.91	1.26 (0.57–2.78)	0.576
Forage/Commercial feed	211	11.85	Reference		8.06	Reference	
Total	418	11.72			41	9.81	

**Statistically significant.*

It is endowed with the potent ability to regulate the immune system to postpone senility, making it a potentially functional health food for inhibiting the progression of some diseases, such as triple-negative breast tumors (Li Q. et al., 2020), type 2 diabetes (Li Y. et al., 2020), and atherosclerosis (Tafaro et al., 2007). Moreover, donkey's milk has been recognized as an ideal alternative to human milk because of its total protein and lactose contents, as well as similar fatty acid and protein profiles (Zhang et al., 2021). Owing to these advantages, there has been a booming global demand for the direct consumption of donkey milk. This escalating demand has to be met by simultaneously and chiefly prioritizing the safety of the consumers, especially considering that many consumers often buy donkey milk directly raw from the farms and individual raisers (Boughattas, 2017). The ingestion of unpasteurized milk has been found to have potential risks and sources of *T. gondii* infection for children living in rural areas (Radon et al., 2004). Moreover, consumption of unpasteurized milk also elevates the potential risk factor for toxoplasmosis in females with recurrent pregnancy loss (Rehman et al., 2020). The latest China Statistical Yearbook has reported about 2.53 million donkeys in China in 2018 (Luoyizha et al., 2020). Although several studies have been conducted to detect the prevalence of *T. gondii* infection in the donkeys from the different regions of China (Miao et al., 2013; Yang et al., 2013; Zhang et al., 2017; Cong et al., 2018; Meng et al., 2018), the data regarding the prevalence of *T. gondii* infection in the donkey's milk in China is scarce. This is the first study to estimate the prevalence of the specific IgG-antibodies against *T. gondii* in the milk of the domestic donkeys during lactation in China, which provided important data for controlling and preventing toxoplasmosis in human beings in China.

The present study investigated the anti-*T. gondii* IgG levels during lactation in the serum and milk samples of the domestic donkeys in China and evaluated the information about the dynamics of specific antibody levels both in the serum and milk. About 9.81% (41/418) of milk samples were found to be contaminated with *T. gondii*. Until now, only four studies have

TABLE 3 | Multivariate logistic regression with a full model for the risk factors of *T. gondii* infection in the domestic donkeys in China.

Variable	Odds ratio (95% confidence interval)	*P*-value
Age (months) (≦24 *vs*. >48)	0.45 (0.11–1.88)	0.274
Age (months) (25–36 *vs* >48)	1.60 (0.64–3.99)	0.316
Age (months) (37–48 *vs* >48)	1.27 (0.48–3.35)	0.633
Region (Jining *vs* Liaocheng)	0.83 (0.33–2.11)	0.696
Region (Linyi *vs*. Liaocheng)	2.06 (0.86–4.96)	0.106
Region (Rizhao *vs*. Liaocheng)	1.42 (0.58–3.47)	0.444
Sampling time (Spring *vs*. Winter)	0.69 (0.30–1.57)	0.380
Sampling time (Summer *vs*. Winter)	1.08 (0.43–2.73)	0.866
Sampling time (Autumn *vs*. Winter)	0.38 (0.17–0.89)	0.026
History of abortion	2.20 (1.15–4.20)	0.017
Days from postpartum (0–15 *vs*. >60)	0.17 (0.03–0.96)	0.045
Days from postpartum (16–30 *vs*. >60)	0.79 (0.21–3.01)	0.729
Days from postpartum (31–45 *vs*. >60)	0.43 (0.09–1.91)	0.265
Days from postpartum (46–60 *vs*. >60)	0.99 (0.24–4.03)	0.988
Cat in house	2.36 (1.26–4.44)	0.008
Source of Water (Well *vs*. Well/Tap water)	0.57 (0.27–1.23)	0.152
Source of Water (Tap water *vs*. Well/Tap water)	0.62 (0.29–1.33)	0.217
Source of fodder (Forage *vs*. Forage/ Commercial feed)	1.23 (0.58–2.61)	0.594
Source of fodder (Commercial feed *vs*. Forage/ Commercial feed)	0.71 (0.33–1.55)	0.391

been conducted to explore the contamination status of the milk matrix of donkeys by *T. gondii* globally. In Egypt, the antibodies against *T. gondii* in the milk of a pregnant Egyptian donkey female were detected using an ELISA and reported a contamination rate of 46.3% (Haridy et al., 2010). In Italy, *T. gondii* DNA was detected in three of the six tested milk samples using nest-PCR (Mancianti et al., 2014). In another study conducted in Italy, 4 (22.2%) out of 18 donkeys presented *T. gondii* DNA in milk (Martini et al., 2014). Simultaneously, the milk quality in the positive donkeys showed a significant difference compared to that in the negative donkeys, suggesting that *T. gondii* infection might induce changes in the milk quality. Moreover, the DNA of *T. gondii* was found in the milk of three jennies in all the 19 milk samples collected from central Italy by a nest-PCR (Perrucci et al., 2021). In Europe, raw milk collected from any animal can be sold directly to any people (the producer of milk product, a local milk seller, or final consumers) without any processing except refrigeration between 0 and 4°C (Mancianti et al., 2014). To sum up, donkey's milk should be considered as a potential pathway of *T. gondii* infection in human beings.

The concordance was explored between the serum and milk collected from the different phases of lactation to find the best agreement in the 45–60 days from parturition, followed by the first phase (0–15 days from parturition). However, the phase of lactation was not found to be a risk factor influencing the antibody level both in the serum and milk samples in the present study. Unfortunately, there is limited information about the physiological immunoglobulin levels in the donkey's milk during lactation. Based on the present data, in milk, the IgG level demonstrates a little change among the different phases of lactation and the peak was evident in the fourth phase of lactation (46–60 DP). Likewise, in the serum, the IgG level was high in the fourth phase of lactation; subsequently, it decreased sharply in the last phase of lactation (>60 DP). However, the trends of antibody levels in the milk samples are mostly the same as those in the serum; thus, the IgG trend of milk during lactation might reflect the process of the systemic immunoglobulin production, although more in-depth studies are needed to explain these differences.

As we all know, *T. gondii* is one of the infectious agents causing early embryonic problems such as abortion, stillbirth, mummification, and death (Dubey, 2009). *T. gondii* has been considered a potential factor for reproductive failures in domestic animals worldwide (Nayeri et al., 2021). In this study, the domestic donkeys with a history of abortion have been found to demonstrate a significantly higher *T. gondii* seroprevalence compared to those without a history of abortion (**Table 2**). So, effective control measures and strategies are needed for reducing the rate of abortion in domestic donkeys as well as reducing the economic damage to the livestock industry.

Cats, as the final hosts of this parasite, excrete oocysts *via* their feces infecting the intermediate hosts such as the domestic animals (Dubey, 2004). The presence of cats in the animals' habitat has been strongly associated with the prevalence of the anti-*T. gondii* antibodies (Moreira et al., 2019). In this study, the presence of a cat in the house was found to be a significant risk factor for *T. gondii* seropositivity among these tested domestic donkeys (p = 0.008; adjusted OR = 2.36; 95% CI: 1.26–4.44) (**Table 3**). Moreover, the tested domestic donkeys were collected from the rural areas, thus, the number of feral cats may be certainly large. Therefore, it is important to effectively bar cats out of the donkey's habitat to reduce the incidence of infection.

Exploring the transmission route of toxoplasmosis infection in donkeys can provide important suggestions for preventing and treating toxoplasmosis. Undoubtedly, considering the dietary habits of herbivores, they are most likely to contract the infection by ingesting the oocysts that existed in their environment because feline is the final host of *T. gondii* discharging oocysts into the environment. Furthermore, some external forces such as wind, rain, and surface water can facilitate its diffusions in the environment. Although the source of water and source of fodder were not evaluated as the potential risk factors in the present study, these have been identified as the risk factors associated with *T. gondii* infection in domestic animals, such as cow, goat, sheep, and equids (Dubey et al., 2014; Gazzonis et al., 2019; Moreira et al., 2019). Thus, more future studies should be conducted for detecting the *T. gondii* oocysts in their environment for further assessment of the risk of infection.

In the present study, an available commercial validated ELISA kit was employed to test the serum–milk pairs and an optimal agreement was obtained between the results of the two biological matrices. In this case, it is easier and less expensive to collect the milk samples rather than collecting the serum samples. Moreover, collecting milk is less irritating to the animals. Thus, during the routine disease screening of toxoplasmosis at the individual, herd, and farm levels, this method should be considered for the first round of screening (Schares et al., 2004). However, more studies are needed for supporting the hypothesis of parasite transmission *via* the ingestion of raw milk or dairy products, including molecular diagnosis and biological methods.

Although this is the first study detecting the antibodies against *T. gondii* in donkey milk in China, two main limitations cannot be neglected. Firstly, the serum and milk samples were not respectively collected on a different phase of lactation from the same objects. Thus, the concordance between the serum and milk samples may be affected by some objective factors. Secondly, only serological tests were conducted in the present study. The diagnosis of toxoplasmosis merely based on serological tests is ineffective and insufficient. The serological results require a confirmatory diagnostic method that is based on directly demonstrating the parasite in the tissues or biological fluids by tissue culture or mouse inoculation. Thus, more studies should be conducted to verify the current results, including the isolation of the live organisms and more rigorous and standard sampling schemes.

Given the present results, health instruction from the health authorities must be implemented and distributed to the consumers of the animals' milk. Boiling or pasteurization are recommended procedures for eliminating the risk of transmission of *T. gondii*. In addition, more studies should be carried out to evaluate the quantity and viability of *T. gondii* eliminated in the donkey's milk. There is an immense need for some studies based on natural infections, especially in the rural or some individual farmers because they are habituated to consuming raw donkey milk. Both priority and special concerns should be focused on the most vulnerable consumer groups, including the immunocompromised patients, the aged, and babies with milk allergies. Moreover, heat treatment of the milk is strongly recommended before consumption.

DATA AVAILABILITY STATEMENT

The original contributions presented in the study are included in the article/supplementary material. Further inquiries can be directed to the corresponding authors.

ETHICS STATEMENT

All procedures involving animals were approved by the Animal Care and Ethic Committee of Jilin Academy of Agricultural Sciences. Written informed consent was obtained from the owners for the participation of their animals in this study.

AUTHOR CONTRIBUTIONS

LC: Methodology, formal analysis, and writing—original draft. Z-JZ: Conceptualization, methodology, and writing—review and editing. Q-FM: Conceptualization and writing—review and editing. All authors contributed to the article and approved the submitted version.

FUNDING

This research was supported by Basic Scientific Research Projects of Jilin Academy of Agricultural Sciences (KYJF2021ZR016); the Funding Program for High-Level Scientific and Technological Innovation Talents introduced by scientific research institutes of Jilin province (project no. 2018001); and the 68th General Grant of China Postdoctoral Science Foundation (project no. 2020M681063).

ACKNOWLEDGMENTS

The authors are grateful to the owners of donkeys and to local veterinarians for their help in samples collection.

REFERENCES

Azab, M. E., Kamel, A. M., Makled, K. M., Khattab, H., el-Zayyat, E. A., Abo-Amer, E. A., et al. (1992). Naturally Occurring Toxoplasma Antibodies in Serum and Milk of Lactating Women. *J. Egypt. Soc. Parasitol.* 22, 561–568.

Bezerra, M. J., Kim, P. C., Moraes, É.P., Sá, S. G., Albuquerque, P. P., Silva, J. G., et al. (2015). Detection of *Toxoplasma gondii* in the Milk of Naturally Infected Goats in the Northeast of Brazil. *Transbound Emerg. Dis.* 62, 421–424. doi: 10.1111/tbed.12160

Boughattas, S. (2017). *Toxoplasma* Infection and Milk Consumption: Meta-Analysis of Assumptions and Evidences. *Crit. Rev. Food. Sci. Nutr.* 57, 2924–2933. doi: 10.1080/10408398.2015.1084993

Camossi, L. G., Greca-Júnior, H., Corrêa, A. P., Richini-Pereira, V. B., Silva, R. C., Da Silva, A. V., et al. (2011). Detection of *Toxoplasma gondii* DNA in the Milk of Naturally Infected Ewes. *Vet. Parasitol.* 177, 256–261. doi: 10.1016/j.vetpar.2010.12.007

Cong, W., Chen, L., Shan, X. F., Qian, A. D., and Meng, Q. F. (2018). First Genetic Characterization of *Toxoplasma gondii* Infection in Donkey Meat Slaughtered for Human Consumption in Shandong Province, Eastern China. *Infect. Genet. Evol.* 61, 1–3. doi: 10.1016/j.meegid.2018.03.008

Dehkordi, F. S., Borujeni, M. R., Rahimi, E., and Abdizadeh, R. (2013). Detection of *Toxoplasma gondii* in Raw Caprine, Ovine, Buffalo, Bovine, and Camel Milk Using Cell Cultivation, Cat Bioassay, Capture ELISA, and PCR Methods in Iran. *Foodborne. Pathog. Dis.* 10, 120–125. doi: 10.1089/fpd.2012.1311

Dubey, J. P. (2004). Toxoplasmosis - A Waterborne Zoonosis. *Vet. Parasitol.* 126, 57–72. doi: 10.1016/j.vetpar.2004.09.005

Dubey, J. P. (2009). History of the Discovery of the Life Cycle of *Toxoplasma gondii*. *Int. J. Parasitol.* 39, 877–82. doi: 10.1016/j.ijpara.2009.01.005

Dubey, J. P. (2010). *Toxoplasmosis of Animals and Humans*. Boca Raton, FL: CRC Press.

Dubey, J. P., Ness, S. L., Kwok, O. C., Choudhary, S., Mittel, L. D., and Divers, T. J. (2014). Seropositivity of *Toxoplasma gondii* in Domestic Donkeys (*Equus Asinus*) and Isolation of *T. gondii* From Farm Cats. *Vet. Parasitol.* 199, 18–23. doi: 10.1016/j.vetpar.2013.09.027

Gazzonis, A. L., Zanzani, S. A., Stradiotto, K., Olivieri, E., Villa, L., and Manfredi, M. T. (2018). *Toxoplasma gondii* Antibodies in Bulk Tank Milk Samples of Caprine Dairy Herds. *J. Parasitol.* 104, 560–565. doi: 10.1645/17-44

Gazzonis, A. L., Zanzani, S. A., Villa, L., and Manfredi, M. T. (2019). *Toxoplasma gondii* in Naturally Infected Goats: Monitoring of Specific IgG Levels in Serum and Milk During Lactation and Parasitic DNA Detection in Milk. *Prev. Vet. Med.* 170, 104738. doi: 10.1016/j.prevetmed.2019.104738

Haridy, F. M., Saleh, N. M., Khalil, H. H., and Morsy, T. A. (2010). Anti-*Toxoplasma gondii* Antibodies in Working Donkeys and Donkey's Milk in Greater Cairo, Egypt. J. *Egypt. Soc. Parasitol.* 40, 459–464.

Iacobucci, E., Taus, N. S., Ueti, M. W., Sukhbaatar, L., Bastsukh, Z., Papageorgiou, S., et al. (2019). Detection and Genotypic Characterization of *Toxoplasma gondii* DNA Within the Milk of Mongolian Livestock. *Parasitol. Res.* 118, 2005–2008. doi: 10.1007/s00436-019-06306-w

Koethe, M., Schade, C., Fehlhaber, K., and Ludewig, M. (2017). Survival of *Toxoplasma gondii* Tachyzoites in Simulated Gastric Fluid and Cow's Milk. *Vet. Parasitol.* 233, 111–114. doi: 10.1016/j.vetpar.2016.12.010

Li, Y., Fan, Y., Shaikh, A. S., Wang, Z., Wang, D., and Tan, H. (2020). Dezhou Donkey (*Equus Asinus*) Milk a Potential Treatment Strategy for Type 2 Diabetes. *J. Ethnopharmacol.* 246, 112221. doi: 10.1016/j.jep.2019.112221

Li, Q., Li, M., Zhang, J., Shi, X., Yang, M., Zheng, Y., et al. (2020). Donkey Milk Inhibits Triple-Negative Breast Tumor Progression and Is Associated With Increased Cleaved-Caspase-3 Expression. *Food. Funct.* 11, 3053–3065. doi: 10.1039/C9FO02934F

Luoyizha, W., Wu, X., Zhang, M., Guo, X., Li, H., and Liao, X. (2020). Compared Analysis of Microbial Diversity in Donkey Milk From Xinjiang and Shandong of China Through High-Throughput Sequencing. *Food. Res. Int.* 2137, 109684. doi: 10.1016/j.foodres.2020.109684

Mancianti, F., Nardoni, S., Papini, R., Mugnaini, L., Martini, M., Altomonte, I., et al. (2014). Detection and Genotyping of *Toxoplasma gondii* DNA in the Blood and Milk of Naturally Infected Donkeys (*Equus Asinus*). *Parasitol. Vectors.* 7, 165. doi: 10.1186/1756-3305-7-165

Martini, M., Altomonte, I., Mancianti, F., Nardoni, S., Mugnaini, L., and Salari, F. (2014). A Preliminary Study on the Quality and Safety of Milk in Donkeys Positive for *Toxoplasma gondii*. *Animal.* 8, 1996–1998. doi: 10.1017/S1751731114001980

Meng, Q. F., Li, D., Yao, G. Z., Zou, Y., Cong, W., and Shan, X. F. (2018). Seroprevalence of *Toxoplasma gondii* Infection and Variables Associated With Seropositivity in Donkeys in Eastern China. *Parasite.* 25, 66. doi: 10.1051/parasite/2018066

Miao, Q., Wang, X., She, L. N., Fan, Y. T., Yuan, F. Z., Yang, J. F., et al. (2013). Seroprevalence of *Toxoplasma gondii* in Horses and Donkeys in Yunnan Province, Southwestern China. *Parasitol. Vectors.* 6, 168. doi: 10.1186/1756-3305-6-168

Montoya, J. G., and Liesenfeld, O. (2004). Toxoplasmosis. *Lancet.* 363, 1965–1976. doi: 10.1016/S0140-6736(04)16412-X

Moreira, T. R., Sarturi, C., Stelmachtchuk, F. N., Andersson, E., Norlander, E., de Oliveira, F. L. C., et al. (2019). Prevalence of Antibodies Against *Toxoplasma gondii* and Neospora Spp. In Equids of Western Para, Brazil. *Acta Trop.* 189, 39–45. doi: 10.1016/j.actatropica.2018.09.023

Nayeri, T., Sarvi, S., Moosazadeh, M., and Daryani, A. (2021). Global Prevalence of *Toxoplasma gondii* Infection in the Aborted Fetuses and Ruminants That had an Abortion: A Systematic Review and Meta-Analysis. *Vet. Parasitol.* 290, 109370. doi: 10.1016/j.vetpar.2021.109370

Perrucci, S., Guardone, L., Altomonte, I., Salari, F., Nardoni, S., Martini, M., et al. (2021). Apicomplexan Protozoa Responsible for Reproductive Disorders: Occurrence of DNA in Blood and Milk of Donkeys (*Equus Asinus*) and Minireview of the Related Literature. *Pathogens.* 10, 111. doi: 10.3390/pathogens10020111

Petruzzelli, A., Amagliani, G., Micci, E., Foglini, M., Di Renzo, E., and Brandi, G.. (2011). Prevalence Assessment of Coxiella burnetii and Verocytotoxin-Producing Escherichia coli in Bovine Raw Milk Through Molecular Identification. *Food. Control.* 32, 532–536. doi: 10.1016/j.foodcont.2013.01.041

Pinto-Ferreira, F., Caldart, E. T., Pasquali, A. K. S., Mitsuka-Breganó, R., Freire, R. L., and Navarro, I. T. (2019). Patterns of Transmission and Sources of Infection in Outbreaks of Human Toxoplasmosis. *Emerg. Infect. Dis.* 25, 2177–2182. doi: 10.3201/eid2512.181565

Powell, C. C., Brewer, M., and Lappin, M. R. (2001). Detection of *Toxoplasma gondii* in the Milk of Experimentally Infected Lactating Cats. *Vet. Parasitol.* 102, 29–33. doi: 10.1016/S0304-4017(01)00521-0

Radon, K., Windstetter, D., Eckart, J., Dressel, H., Leitritz, L., Reichert, J., et al. (2004). Farming Exposure in Childhood, Exposure to Markers of Infections and the Development of Atopy in Rural Subjects. *Clin. Exp. Allergy* 34, 1178–1183. doi: 10.1111/j.1365-2222.2004.02005.x

Rehman, F., Shah, M., Ali, A., Ahmad, I., Sarwar, M. T., Rapisarda, A. M. C., et al. (2020). Unpasteurised Milk Consumption as a Potential Risk Factor for Toxoplasmosis in Females With Recurrent Pregnancy Loss. *J. Obstet. Gynaecol.* 40, 1106–1110. doi: 10.1080/01443615.2019.1702630

Saad, N. M., Hussein, A. A. A., and Ewida, R. M. (2018). Occurrence of *Toxoplasma gondii* in Raw Goat, Sheep, and Camel Milk in Upper Egypt. *Vet. World.* 11, 1262–1265. doi: 10.14202/vetworld.2018.1262-1265

Schares, G., Bärwald, A., Staubach, C., Wurm, R., Rauser, M., Conraths, F. J., et al. (2004). Adaptation of a Commercial ELISA for the Detection of Antibodies Against *Neospora Caninum* in Bovine Milk. *Vet. Parasitol.* 120, 55–63. doi: 10.1016/j.vetpar.2003.11.016

Tafaro, A., Magrone, T., Jirillo, F., Martemucci, G., D'Alessandro, A. G., Amati, L., et al. (2007). Immunological Properties of Donkey's Milk: Its Potential Use in the Prevention of Atherosclerosis. *Curr. Pharm. Des.* 13, 3711–3717. doi: 10.2174/138161207783018590

Tenter, A. M. M., Heckeroth, A. R. R., and Weiss, L. M. M. (2000). *Toxoplasma gondii*: From Animals to Humans. *Int. J. Parasitol.* 30, 1217–1258. doi: 10.1016/S0020-7519(00)00124-7

Yang, N., Mu, M. Y., Yuan, G. M., Zhang, G. X., Li, H. K., and He, J. B. (2013). Seroprevalence of *Toxoplasma gondii* in Slaughtered Horses and Donkeys in Liaoning Province, Northeastern China. *Parasitol. Vectors.* 6, 140. doi: 10.1186/1756-3305-6-140

Zhang, X., Jiang, B., Ji, C., Li, H., Yang, L., Jiang, G., et al. (2021). Quantitative Label-Free Proteomic Analysis of Milk Fat Globule Membrane in Donkey and Human Milk. *Front. Nutr.* 8, 670099. doi: 10.3389/fnut.2021.670099

Zhang, X. X., Shi, W., Zhang, N. Z., Shi, K., Li, J. M., Xu, P., et al. (2017). Prevalence and Genetic Characterization of *Toxoplasma gondii* in Donkeys in Northeastern China. *Infect. Genet. Evol.* 54, 455–457. doi: 10.1016/j.meegid.2017.08.008

Conflict of Interest: The authors declare that the research was conducted in the absence of any commercial or financial relationships that could be construed as a potential conflict of interest.

Publisher's Note: All claims expressed in this article are solely those of the authors and do not necessarily represent those of their affiliated organizations, or those of the publisher, the editors and the reviewers. Any product that may be evaluated in this article, or claim that may be made by its manufacturer, is not guaranteed or endorsed by the publisher.

frontiers in Cellular and Infection Microbiology

METHODS
published: 10 November 2021
doi: 10.3389/fcimb.2021.762472

Rapid Detection of *Cysticercus cellulosae* by an Up-Converting Phosphor Technology-Based Lateral-Flow Assay

Dejia Zhang[1†], Yu Qi[1†], Yaxuan Cui[1], Weiyi Song[1], Xinrui Wang[1], Mingyuan Liu[2], Xuepeng Cai[3], Xuenong Luo[3], Xiaolei Liu[2] and Shumin Sun[1,4*]*

[1] College of Animal Science and Technology, Inner Mongolia University for Nationalities, Tongliao, China, [2] Key Laboratory of Zoonosis Research, Ministry of Education, Institute of Zoonosis/College of Veterinary Medicine, Jilin University, Changchun, China, [3] Key Laboratory of Veterinary Parasitology of Gansu Province, State Key Laboratory of Veterinary Etioloical Biology, Lanzhou Veterinary Research Institute, Chinese Academy of Agricuitural Sciences, Lanzhou, China, [4] College of Veterinary Medicine, Yunnan Agricultural University, Kunming, China

OPEN ACCESS

Edited by:
Wei Cong,
Shandong University, Weihai, China

Reviewed by:
Shuai Wang,
Xinxiang Medical University, China
Kabemba Evans Mwape,
University of Zambia, Zambia
Guofeng Cheng,
Tongji University, China

***Correspondence:**
Xiaolei Liu
liuxlei@163.com
Shumin Sun
shums1975@163.com

[†]These authors have contributed equally to this work

Specialty section:
This article was submitted to Clinical Microbiology, a section of the journal Frontiers in Cellular and Infection Microbiology

Received: *22 August 2021*
Accepted: *22 October 2021*
Published: *10 November 2021*

Citation:
Zhang D, Qi Y, Cui Y, Song W, Wang X, Liu M, Cai X, Luo X, Liu X and Sun S (2021) Rapid Detection of Cysticercus cellulosae by an Up-Converting Phosphor Technology-Based Lateral-Flow Assay. Front. Cell. Infect. Microbiol. 11:762472. doi: 10.3389/fcimb.2021.762472

Cysticercosis is a neglected tropical disease caused by the larvae of *Taenia solium* in pigs and humans. The current diagnosis of porcine cysticercosis is difficult, and traditional pathological tests cannot meet the needs of detection. This study established a UPT-LF assay for the detection of *Cysticercus cellulosae*. UCP particles were bound to two antigens, TSOL18 and GP50; samples were captured, and the signal from the UCP particles was converted into a detectable signal for analysis using a biosensor. Compared to ELISA, UPT-LF has higher sensitivity and specificity, with a sensitivity of 93.59% and 97.44%, respectively, in the case of TSOL18 and GP50 antigens and a specificity of 100% for both. Given its rapidness, small volume, high sensitivity and specificity, and good stability and reproducibility, this method could be used in the diagnosis of cysticercosis.

Keywords: ***Taenia solium*, *Cysticercus cellulosae*, antigen, immune diagnosis, UPT-LF**

INTRODUCTION

Cysticercosis is an important zoonotic parasitic disease, which is mainly caused by eating *Taenia solium* larvae by mistake. (Bizhani et al., 2020). This disease is distributed worldwide and is widely prevalent in some relatively backward countries and regions, such as Africa, Asia, and Latin America (Hamamoto et al., 2020). Because some rural areas in relatively backward countries meet the conditions required for the life cycle of Cysticercus, where has poor sanitary conditions, limited or absent meat inspection, low awareness, and inadequate facilities for safe food preparation, which result in accidental ingestion of eggs or larvae containing infective worms and lead to the appearance of cysts in pig muscle or in the human brain and spinal cord, caused serious harm to the economy and human health (Lightowlers et al., 2016; Lightowlers, 2020). From a global perspective, *Cysticercus cellulosae* (*C. cellulosae*) is listed as "one of the Top Ten Foodborne Parasites Harmful to Humans" by the WHO and is also known as "one of the 17 Neglected Tropical Diseases" and "one of the Key Parasitic Diseases Planned and Prevented by the Ministry of Health of the People's Republic of China". Therefore, the diagnosis of *C. cellulosae* is particularly essential

(Tsai et al., 2013). To reduce the global burden of *C. cellulosae*, serologic tests are commonly used in endemic areas to screen for the parasite and control disease progression by using a combination of antigens and antibodies (Gomez-Puerta et al., 2019). Among the currently used methods for detecting cystic larvae, the most effective serological method is enzyme immunoelectrotransfer blot (EITB). Although EITB is the reference standard and has high sensitivity and specificity, it is unsuitable for widespread use or field testing (Garcia et al., 2018; Romo et al., 2020).

TSOL18 is an oncosphere-stage protein with high protective and immunogenic properties, and GP50 is a cystic larval-stage protein with specificity and immunogenicity. Both are regarded as antigens for the early diagnosis of cysticercosis (Gomez-Puerta et al., 2019). In recent years, up-converting phosphor technology-based lateral flow (UPT-LF) has been increasingly used for the detection of parasitic diseases (Corstjens et al., 2014). In this study, up-converting phosphor (UCP) particles were bound to two antigens, TSOL18 and GP50; samples were captured; and the signal from the UCP particles was converted into a detectable signal for analysis using a biosensor (Liu et al., 2016; Yang et al., 2017).

This study has established a convenient, rapid, specific, stable, and environmentally friendly method for the quantitative detection of *C. cellulosae* at a wide range of concentrations to overcome the shortcomings of current detection methods. The simplicity of the procedure allows detection without professional technicians on site, and the method is suitable for large-scale detection as well as rapid on-site detection.

MATERIALS AND METHODS

Materials

UCP nanomaterials (NaYF4:Yb^{3+}, Er^{3+}) were purchased from Shanghai SunLipo NanoTech. Nitrocellulose film and glass fiber were purchased from Millipore Company in the United States. Absorbent paper and viscous backing were purchased from Shanghai Jieyi Biotechnology Company. The plastic shell of the test strip was designed and manufactured by Shenzhen Jincanhua Company. Goat anti-pig IgG was purchased from Beijing Baiaolaibo Technology Co., Ltd., and rabbit anti-goat IgG was purchased from Shanghai Absin Bioscience Inc. The instrument used to read the ELISA results was a full-wavelength enzyme labeling instrument (BioTek Instruments, Inc.). The UPT biosensor (UPT-3A-1200) was purchased from Beijing Hotgen Biotechnology Co., Ltd.

Sample Collection

In this study, positive sera from a pig with *Cysticercus cellulosae* infection were acquired and preserved in the clinical laboratory of the School of Animal Science and Technology, Inner Mongolia University for Nationalities, and sera positive for *Taenia asiatica*, *Toxoplasma gondii*, *Clonorchis sinensis*, and *Trichinella spiralis* were provided by the Institute of Human and Veterinary Diseases, Jilin University.

Enzyme-Linked Immunosorbent Assay

After diluting the target protein (TSOL18 or GP50) to 1 μg/mL with buffer, then 100 μL antigen was added to each well of the 96-well ELISA plate and incubated overnight at 4°C. After the buffer was absorbed in the 96-well enzyme plate, 150 μL PBST buffer was added to each well, was blotted with clean filter papers 5 times to remove the remaining liquid. Blocking buffer containing 150 μL of 1% BSA was added to each well for sealing, and the plate was washed with PBST buffer 5 times after incubation at 37°C for 2 h. The serum to be tested was diluted with 1% BSA and added to a 96-well enzyme reaction plate. One hundred microliters of the tested serum were added per well, and 3 replicates were performed. Uninfected pig serum was used as the negative control serum and washed 5 times after being placed in a 37°C incubator for 1 h. Goat anti-porcine IgG antibodies labeled with horseradish peroxidase were diluted with blocking buffer at a ratio of 1:2000. Then, 100 μL of diluted antibodies was added to each well, and the plate was washed 5 times after being placed in an incubator at 37°C for 1 h. TMB (100 μL) was added to each well, and the plate was incubated for 15 min at room temperature and in the dark. Then, 50 μL of 2 mol/L H_2SO_4 termination solution was added per well, and the reaction was stopped. The absorption value of each pore was detected at a wavelength of 450 nm by ELISA enzyme labeling, and the result was judged. When the value of the sample to be tested was more than 2.1 times the negative control value, it was judged to be positive.

Preparation and Modification of UCP Particles

The UCP particles in this study are based on sodium fluoride (Na F), which is doped with three rare earth metal elements—yttrium (Y), ytterbium (Yb), and erbium (Er)—to form the crystal structure Na YF_4:Yb^{3+}, Er^{3+}, i.e., UCP particles. Although the particles have the unique optical properties of uptransfer luminescence materials, they do not have the ability to bind with biologically active molecules and still need to be processed through surface modification and activation of the particles. This process makes the particles suitable for biological applications. Using ethyl orthosilicate (TEOS), the surface of the UCP particles can be silicified through a series of chemical reactions, resulting in a large number of surface-active groups (Huang Y. et al., 2019). Through these free active groups, UCP particles can be covalently combined with antigens, antibodies, nucleic acids, biotin, and other bioactive molecules to make them biologically active. At the same time, the covalent binding of UCP particles to bioactive molecules makes the binding between the two more secure and ensures that detection is not easily affected by complex samples, laying a solid foundation for the widespread application of UCP-LF detection technology.

Assembly of the UPT-LF Test Card

The absorbent pad, NC membrane, conjugated pad, and sample pad were placed on the adhesive lamination card to make a complete test card, which was cut transversely into 4 mm wide

strips using a high-speed CNC chopping machine, put into a plastic casing, and stored in a dry cabinet for later use. Antigen at a concentration of 0.5 mg/mL and rabbit anti-goat IgG at a concentration of 0.5 mg/mL were then sprayed onto the test strip T and quality control strip C, respectively. The silicified and carboxyl-modified UCP-NPs were centrifuged, and the supernatant was discarded, resuspended in UCP storage buffer, and sonicated 3 times. After vortex sonication, the sample was mixed with 100 μL of buffer (0.01 M phosphate buffer PBS, pH 7.2, containing 1% (w/v) BSA, 10% (w/v) sucrose, and 1% (v/v) Tween-20) and added to the wells of the sample paper. The results were read using an uprotation luminescent biosensor after 15 min of resting. The sensor was used to determine the peak area of detection and the quality control bands, and the detection/quality control band values were used as the final results.

Sensitivity, Specificity, and Stability Test of the UPT-LF Assay

For evaluation of the sensitivity, the sera of all pigs containing *C. cellulosae* were diluted according to a certain proportion and tested using the UPT-LF assay. Several positive sera were detected by UPT-LF to evaluate the specificity, including sera containing *T. asiatica*, *T. gondii*, *C. sinensis*, and *T. spiralis*. The test results (Vt/Vc value) were recorded at several time points and two temperatures (4°C and 25°C) after sample addition was completed. Using the same batch, three test strips were used for positive and negative serum samples. Each sample was tested three times, the results of the test card at different time points were compared with those detected at 15 min, and the relative deviation (δ) was calculated. $\delta < 15\%$ was the acceptable standard.

Data Analysis

The test card was inserted into the UPT-3A-1200 biosensor, the measurement button was pressed, and the test results were obtained in approximately five seconds. The peak areas of the T and C lines were calculated by the special software of the reader, the value was input into Excel, and then the value of the T line was divided by the value of the C line for each test strip. The Vt/Vc value can be used for data analysis.

RESULTS

Detection System of the UPT-LF Assay

The UPT-LF assay system consists of a sample dilutant, a test card, and a biosensor (**Figure 1**). The test card consists of two parts: the outer shell and the internal test strip. The housing consists of an upper and bottom shell. The upper shell has two windows, followed by a sample addition window and a sample scanning window. The test strips are placed in the grooves of the bottom shell. The portable UPT-3A-1200 biosensor has the advantages of simple operation, rapid detection, high sensitivity, and safety, making it an ideal candidate for the detection of *C. cellulosae*.

Sensitivity of the UPT-LF assay

Dilutions of positive serum at a given initial concentration in PBS buffer were detected by UPT-LF assay, and the Vt/Vc value decreased with the increase of the dilution ratio of the tested serum (**Figure 2**). The 1000x dilution was still greater than the UPT-LF assay cutoff value, indicating that the sensitivity of the UPT-LF assay can meet the requirements of rapid detection in the field.

Specificity of the UPT-LF Assay

This study evaluated the specificity of the UPT-LF test using four enzyme-linked immunosorbent assay (ELISA)-confirmed positive serum samples, including *T. asiatica*, *T. gondii*, *C. sinensis*, and *T. spiralis*, as the study subjects. *C. cellulosae*-positive serum samples served as controls, and the UPT-LF test showed good specificity with all other positive serum samples, producing negative results (**Figure 3**).

The Stability of the UPT-LF Assay

The sensitivity and specificity of the test strip stored at 4°C for 24 weeks were 100%, indicating that the test strip could be stored at 4°C for at least 6 months, and the sensitivity and specificity of the test strip stored at room temperature were 100% at 16 weeks. There was no significant difference in the color of the detection line or the control line. From the 18th week, the colors of the T line and C line became lighter, so the test strips could be stored for 16 weeks at room temperature. It is proven that this test strip

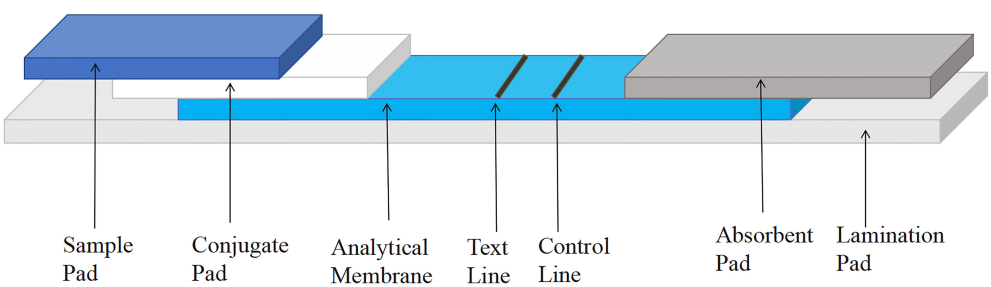

FIGURE 1 | Schematic diagram of the up-converting phosphor technology-based lateral-flow (UPT-LF) strip. The sample flow direction from sample pad, conjugate pad, analytical membrane to the absorbent pad, which all the structures above are on laminating card. The results were obtained by scanning the test card of the UPT-3A-1200 biosensor.

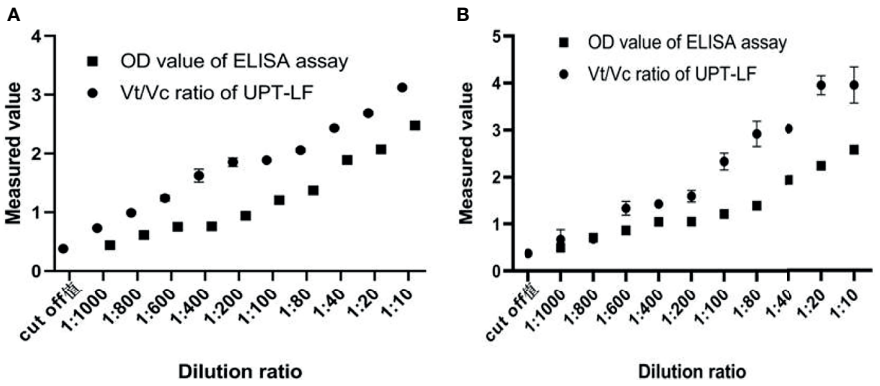

FIGURE 2 | **(A)** TSOL18 and **(B)** GP50, the up-converting phosphor technology-based lateral-flow (UPT-LF) assay is more sensitive than the enzyme-linked immunosorbent assay (ELISA), and the value of Vt/Vc is still higher than that of cut off when diluted 1000 times.

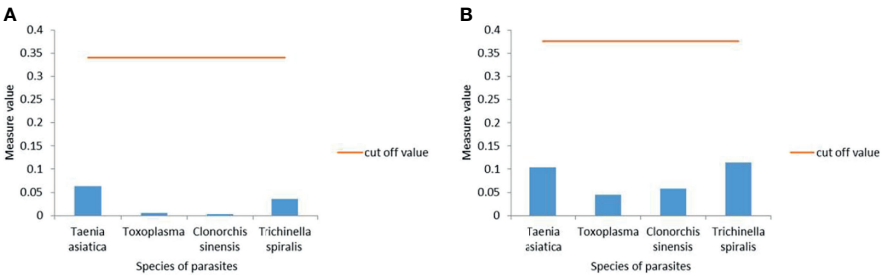

FIGURE 3 | **(A)** TSOL18 and **(B)** GP50, the up-converting phosphor technology-based lateral flow (UPT-LF) assay for detection of *T. asiatica*, *T. gondii*, *C. sinensis*, and *T. spiralis*, showed excellent specificity.

has the characteristics of good stability, strong practicability, easy preservation, and value for market development.

Comparison of the UPT-LF Assay and ELISA

UPT-LF and ELISA were used to detect 78 negative sera. In the case of TSOL18 and GP50 antigens, 72 were negative for both antigens according to ELISA, and 73 and 76 were negative according to UPT-LF, indicating that UPT-LF and ELISA are consistent in detecting *C. cellulosae*. In the case of TSOL18 and GP50 antigens, the sensitivity of UPT-LF was 93.59% and 97.44%, respectively, while the sensitivity of ELISA was 92.31% for both. Compared to the two methods, the UPT-LF can greatly reduce the false positive rate and can be more sensitive to test samples. Therefore, UPT-LF has the advantages of high speed and easy readability, which makes UPT-LF has broad application prospects.

Specifically speaking, the UPT-LF assay has the following advantages over traditional ELISA. First, the surface-modified UCP particles can be freely combined with a wide range of spectra for quantitative and multiplex analyses; the unique energy conversion process of the UCP particles avoids interference from impurities in the detection background; and the phenomenon of uptransfer luminescence is a physical process using infrared light excitation to produce visible light (Zheng et al., 2015; Huang C. et al., 2019). UPT-LF does not involve chemical reactions, is stable, and does not pose any hazards to laboratory operators or the outside environment. Second, the UPT-LF assay demonstrates good sensitivity and specificity and is suitable for screening and large-scale testing of diseases because it can be performed with a small sample volume within a short period of time (Zhu et al., 2021). Finally, the UPT-LF method is easy to use, portable, and can be performed and analyzed in remote and unprotected areas (Wu et al., 2014; Hua et al., 2015). In addition, the UPT-LF assay requires only a biosensor and test strip, which is less expensive and safer. Overall, the UPT-LF method is suitable for field detection of *C. cellulosae*.

In this study, a preliminary UPT-LF assay for the detection of *C. cellulosae* was developed. This test card uses UCP-labeled TSOL18 or GP50 as the antigen and test strips as the solid-phase vehicle for immunoreactivity. This UPT-LF assay has not only high sensitivity and a wide detection range but also good stability. The strips can be stored at 4°C for six months and at

room temperature for four months, indicating that low temperatures are more suitable for storage of the strips and that room temperature or higher temperatures may cause degradation of the antibodies on the conjugated pad or the NC membrane. Using the UPT-LF method, the cystic larvae were significantly distinguished from those of *T. asiatica*, *Toxoplasma*, *C. sinensis*, and *T. spiralis*, indicating high specificity of the test strip.

In conclusion, the UPT-LF assay established in this study provides a safe, reliable, convenient, and rapid method for the quantitative detection of *C. cellulosae*. The preliminary establishment of this diagnostic method will contribute to the further detection of *C. cellulosae* and enhance the screening and diagnosis of *C. cellulosae*, thus contributing to socioeconomic and human health improvement.

DATA AVAILABILITY STATEMENT

The original contributions presented in the study are included in the article/supplementary material. Further inquiries can be directed to the corresponding authors.

ETHICS STATEMENT

The animal study was reviewed and approved by The University of Jilin Animal Care and Use Committee (IZ-2009-08).

AUTHOR CONTRIBUTIONS

SS and XLL conceived and designed the experiments. XW performed the experiments. YC and WS analyzed the data. ML, XC, and XNL. DZ and YQ wrote the manuscript. All authors contributed to the article and approved the submitted version.

FUNDING

This work was supported by the National Key Research and Development Program of China (2017YFD0501300); the National Natural Science Foundation of China (NSFC 32160842,31960707, 31460658); the Natural Science Foundation of Inner Mongolia Autonomous Region (2021MS03037).

ACKNOWLEDGMENTS

All experiments were conducted according to the regulations of the Administration of Affairs Concerning Experimental Animals in China. The procedure of animal experiments was approved by the Institutional Animal Care and Use Committee of Jilin University (IZ-2009-08). Thanks to all authors for their contributions to this article. Written informed consent was obtained from the owners for the participation of their animals in this study.

REFERENCES

Bizhani, N., Hashemi, H. S., Mohammadi, N., Rezael, M., and Rokni, M. B. (2020). Human Cysticercosis in Asia: A Systematic Review and Meta-Analysis. *Iran J. Public Health* 49, 1839–1847. doi: 10.18502/ijph.v49i10.4683

Corstjens, P. L., De Dood, C. J., Kornelis, D., Tjonkonfat, E. M., Alan Wilson, R., Kariuki, T. M., et al. (2014). Tools for Diagnosis, Monitoring and Screening of Schistosoma Infections Utilizing Lateral-Flow Based Assays and Upconverting Phosphor Labels. *Parasitology* 141, 1841–1855. doi: 10.1017/S0031182014000626

Garcia, H. H., O'Neal, S. E., Noh, J., and Handali, S. (2018). Laboratory Diagnosis of Neurocysticercosis (Taenia Solium). *J. Clin. Microbiol.* 56. doi: 10.1128/JCM.00424-18

Gomez-Puerta, L., Vargas-Calla, A., Castillo, Y., Lopez-Urbina, M. T., Dorny, P., Garcia, H. H., et al. (2019). Evaluation of Cross-Reactivity to Taenia Hydatigena and Echinococcus Granulosus in the Enzyme-Linked Immunoelectrotransfer Blot Assay for the Diagnosis of Porcine Cysticercosis. *Parasit. Vectors* 12, 57. doi: 10.1186/s13071-018-3279-5

Hamamoto, F. P., Singh, G., Winkler, A., Carpio, A., and Fleury, A. (2020). Could Differences in Infection Pressure Be Involved in Cysticercosis Heterogeneity? *Trends Parasitol.* 36, 826–834. doi: 10.1016/j.pt.2020.07.003

Huang, C., Wei, Q., Hu, Q., Wen, T., Xue, L., Li, S., et al. (2019). Rapid Detection of Severe Fever With Thrombocytopenia Syndrome Virus (SFTSV) Total Antibodies by Up-Converting Phosphor Technology-Based Lateral-Flow Assay. *Luminescence* 34, 162–167. doi: 10.1002/bio.3588

Huang, Y., Zhang, S., Zheng, Q., Li, Y., Yu, L., Wu, Q., et al. (2019). Development of Up-Converting Phosphor Technology-Based Lateral Flow Assay for Quantitative Detection of Serum PIVKA-II: Inception of a Near-Patient PIVKA-II Detection Tool. *Clin. Chim. Acta* 488, 202–208. doi: 10.1016/j.cca.2018.11.020

Hua, F., Zhang, P., Zhang, F., Zhao, Y., Li, C., Sun, C., et al. (2015). Development and Evaluation of an Up-Converting Phosphor Technology-Based Lateral Flow Assay for Rapid Detection of Francisella Tularensis. *Sci. Rep.* 5, 17178. doi: 10.1038/srep17178

Lightowlers, M. (2020). Diagnosis of Porcine Cysticercosis at Necropsy: When Is Enough, Enough? *Trends Parasitol.* 36, 575–578. doi: 10.1016/j.pt.2020.04.006

Lightowlers, M., Garcia, H., Gauci, C., Donadeu, M., and Abela-ridder, B. (2016). Monitoring the Outcomes of Interventions Against Taenia Solium: Options and Suggestions. *Parasit. Immunol.* 38, 158–169. doi: 10.1111/pim.12291

Liu, X., Zhao, Y., Sun, C., Wang, X., Wang, X., Zhang, P., et al. (2016). Rapid Detection of Abrin in Foods With an Up-Converting Phosphor Technology-Based Lateral Flow Assay. *Sci. Rep.* 6, 34926. doi: 10.1038/srep34926

Romo, M. L., Hernandez, M., Astudillo, O. G., Diego, G., Arana, J. L., Lucas-meza, A., et al. (2020). Diagnostic Value of Glycoprotein Band Patterns of Three Serologic Enzyme-Linked Immunoelectrotransfer Blot Assays for Neurocysticercosis. *Parasitol. Res.* 119, 2521–2529. doi: 10.1007/s00436-020-06750-z

Tsai, I. J., Magdaiena, Z., Nancy, H., Garciarrubio, A., Flores, A. S., Brooks, K. L., et al. (2013). The Genomes of Four Tapeworm Species Reveal Adaptations to Parasitism. *Nature* 496, 57–63. doi: 10.1038/nature12031

Wu, Y., Cen, Y., Huang, L., Qin, R., and Chu, X. (2014). Upconversion Fluorescence Resonance Energy Transfer Biosensor for Sensitive Detection of Human Immunodeficiency Virus Antibodies in Human Serum. *Chem. Commun. (Cambridge England)* 50, 4759–4762. doi: 10.1039/C4CC00569D

Yang, X., Liu, L., Hao, Q., Zou, Q., Zhang, X., Zhang, L., et al. (2017). Development and Evaluation of Up-Converting Phosphor Technology-Based Lateral Flow Assay for Quantitative Detection of NT-proBNP in Blood. *PloS One* 12, e0171376. doi: 10.1371/journal.pone.0171376

Zheng, W., Tu, D., Huang, P., Zhou, S., Chen, Z., and Chen, X. (2015). Time-Resolved Luminescent Biosensing Based on Inorganic Lanthanide-Doped Nanoprobes. *Chem. Commun. (Cambridge. England).* 51, 4129–4143. doi: 10.1039/C4CC10432C

Zhu, F., Zhang, B., and Zhu, L. (2021). An Up-Converting Phosphor Technology-Based Lateral Flow Assay for Rapid Detection of Major Mycotoxins in Feed:

Comparison With Enzyme-Linked Immunosorbent Assay and High-Performance Liquid Chromatography-Tandem Mass Spectrometry. *PloS One* 16, e0250250. doi: 10.1371/journal.pone.0250250

Conflict of Interest: The authors declare that the research was conducted in the absence of any commercial or financial relationships that could be construed as a potential conflict of interest.

Publisher's Note: All claims expressed in this article are solely those of the authors and do not necessarily represent those of their affiliated organizations, or those of the publisher, the editors and the reviewers. Any product that may be evaluated in this article, or claim that may be made by its manufacturer, is not guaranteed or endorsed by the publisher.

frontiers in Cellular and Infection Microbiology

ORIGINAL RESEARCH
published: 22 November 2021
doi: 10.3389/fcimb.2021.793089

Evaluation of *Origanum vulgare* Essential Oil and Its Active Ingredients as Potential Drugs for the Treatment of Toxoplasmosis

Na Yao[1,2,3†], *Qiong Xu*[1,2,3†], *Jia-Kang He*[4], *Ming Pan*[1,2,3], *Zhao-Feng Hou*[1,2,3], *Dan-Dan Liu*[1,2,3], *Jian-Ping Tao*[1,2,3] *and Si-Yang Huang*[1,2,3,5*]

[1] Institute of Comparative Medicine, College of Veterinary Medicine, Yangzhou University, Yangzhou, China, [2] Jiangsu Co-innovation Center for Prevention and Control of Important Animal Infectious Diseases and Zoonosis, Yangzhou, China, [3] Jiangsu Key Laboratory of Zoonosis, Yangzhou, China, [4] College of Animal Science and Technology, Guangxi University, Nanning, China, [5] Joint International Research Laboratory of Agriculture and Agri-Product Safety, the Ministry of Education of China, Yangzhou University, Yangzhou, China

OPEN ACCESS

Edited by:
Wei Cong,
Shandong University, Weihai, China

Reviewed by:
Lan He,
Huazhong Agricultural University, China
Hua Cong,
Shandong University, China

***Correspondence:**
Si-Yang Huang
siyang.huang@hotmail.com

[†]These authors have contributed equally to this work

Specialty section:
This article was submitted to Clinical Microbiology, a section of the journal Frontiers in Cellular and Infection Microbiology

Received: 11 October 2021
Accepted: 27 October 2021
Published: 22 November 2021

Citation:
Yao N, Xu Q, He J-K, Pan M, Hou Z-F, Liu D-D, Tao J-P and Huang S-Y (2021) Evaluation of Origanum vulgare Essential Oil and Its Active Ingredients as Potential Drugs for the Treatment of Toxoplasmosis. Front. Cell. Infect. Microbiol. 11:793089. doi: 10.3389/fcimb.2021.793089

Toxoplasma gondii is a serious hazard to public health and animal husbandry. Due to the current dilemma of treatment of toxoplasmosis, it is urgent to find new anti-*T. gondii* drugs to treat toxoplasmosis. In this study, the anti-*T. gondii* activity of Origanum vulgare essential oil (*Ov* EO) was firstly studied, and then, carvanol (Ca), the main ingredient of *Ov* EO was evaluated using the MTT assay on human foreskin fibroblast (HFF) cells *in vitro*. The cytotoxicity was evaluated using the MTT assay on HFF cells. The CC_{50} of *Ov* EO and Ca was 134.9 and 43.93 μg/ml, respectively. Both of them exhibited anti-parasitic activity, and inhibited the growth of *T. gondii* in a dose-dependent manner. For the inhibition effect, Ca was better than *Ov* EO at the same concentration, the IC_{50} of *Ov* EO and Ca was 16.08 and 7.688 μg/ml, respectively. In addition, treatment with Ca, was found to change the morphology of *T. gondii* tachyzoites and made their shapes curl up. These results showed that Ca was able to inhibit the proliferation of *T. gondii* by reducing invasion, which may be due to its detrimental effect on the mobility of tachyzoites. Our results indicated that Ca could be a potential new and effective drug for treating toxoplasmosis.

Keywords: *Toxoplasma gondii*, natural medicine, *Origanum vulgare* essential oil, carvacrol, *in vitro*

INTRODUCTION

The opportunistic pathogen *Toxoplasma gondii* is a serious hazard to public health and animal husbandry (Chemoh et al., 2013). One-third of the people in the world have been infected by *T. gondii* where tachyzoites, cysts and oocysts are three infectious stages. Human intake of raw meat or water containing *T. gondii* cysts or oocysts can be infectious. In a few cases, direct contact with *T. gondii* tachyzoites between the mucous membrane and the damaged skin can also cause an infection. Cats are intermediate hosts of *T. gondii* and can rule out infectious oocysts. Accidental contact between humans and cat feces is a risk of infection. For most individuals with competent immunity, infection is asymptomatic and the *T. gondii* eventually lies dormant as a tissue cyst. For some people primary infection can cause ocular disease, and in pregnant women, it can lead to

abortion, stillbirth or brain damage in a congenitally infected fetus. Recurrence of chronic infection is a frequent cause of toxoplasmic encephalitis (TE) in an immunosuppressive patient such as advanced HIV infection, neoplastic disease, or in those receiving immunosuppressive therapies (e.g., rituximab).

As *T. gondii* has a wide range of hosts, apart from humans, it also infects many animals, like cattle, sheep, pig and other domestic animals. This causes the economic loss of animal husbandry and the hidden danger of public food hygiene and safety.

The drug treatment of toxoplasmosis can be traced back to the use of sulfonamides in the 1940s. In the 1950s, sulfadiazine combined with pyrimethamine successfully treated toxoplasmosis in mice. It is still the golden treatment for toxoplasmosis today (Wei et al., 2015). However, the side effects and the emergence of drug resistance have undermined the perfection of the treatment regimen (Schmidt et al., 2006). In the case of pregnant women infected with *T. gondii*, spiramycin is a good drug for the treatment of toxoplasmosis because of its low toxicity and it cannot penetrate the placental barrier; however it has no effect on the infected fetus (Desmonts and Couvreur, 1974). Other drugs such as Trimethoprim-sulfamethoxazole, Clindamycin, and Atovaquone also have their own disadvantages (Dunay et al., 2018). Therefore, it is urgent to find new anti-*T. gondii* drugs with high efficiency and low toxicity to treat toxoplasmosis.

Natural products are one of the important sources of drug development (Petrovska, 2012). In the field of cancer treatment alone, from the 1940s to now, 48.6% of the 175 small molecules are natural products or obtained directly from there (Newman and Cragg, 2012). Plants as one of the natural products usually grow outdoors, so they have to resist the infection of disease and the pressure of harsh environment in the process of growing (Weng et al., 2012). In this process of defense, the molecules they produce give plants smell, color and even toxicity (Lietava, 1992). Essential oils are a mixture of these molecules, which are a potential drug reservoir.

Origanum vulgare that is native to the Mediterranean coast, North Africa and West Asia is a perennial herb of the genus Oregon of the *Lamiaceae* family (Elshafie et al., 2017). The *O. vulgare* essential oil (*Ov* EO) has been proven to have certain biological activity (Argyri et al., 2021). At a concentration of 60 μg/ml, *Ov* EO can inhibit the invasion rate of *Cryptosporidium parvum* into Human colon adenocarcinoma (HCT-8) cells by 60% (Gaur et al., 2018). *Ov* EO can also inhibit the growth of *Aeromonas hydrophila*, *Brevibacterium linens*, *Clostridium sporogenes*, *Leuconostoc cremoris*, and *Pseudomonas aeruginosa* (Dorman and Deans, 2000). The crude *Ov* EO can decrease the activity of liver cancer cells (HepG2 cell) in a dose-dependent manner, and the IC50 value was 236 μg/μl (Elshafie et al., 2017). In addition, *Ov* EO also shows excellent anti-inflammatory and antioxidant activities, and also has potential functions in controlling cardiovascular diseases and metabolic syndrome (Leyva-López et al., 2017).

In this study, the anti-*T. gondii* activity of *Ov* EO was firstly studied, and then the inhibited activity of carvanol (Ca), the main ingredient of *Ov* EO, was selected to evaluate *in vitro*.

MATERIALS AND METHODS

Cell Culture and Parasites

T. gondii tachyzoites of the GFP-RH strain, expressing green fluorescence protein were proliferated in human foreskin fibroblast (HFF) cells, cultured in Dulbecco's modified Eagle's medium (DMEM), supplemented with 10% heat-inactivated fetal bovine serum (FBS) at 37°C, in an atmosphere containing 5% CO_2. To isolate the tachyzoites, heavily infected cells were scraped and the parasites were released by passing the cells through a 27-gauge needle, three to five times. Cell debris was removed by passing the mixture through a 3-μm pore membrane filter (Whatman, ThermoFisher, Waltham, MA, USA). Tachyzoites were quantified using a hemocytometer before proceeding to further experiments.

Essential Oil and Chemical Components

The *Ov* EO and Ca used in this experiment was provided by Guangxi University, EO was extracted by steam distillation and dissolved in dimethyl sulfoxide (DMSO) in a 1:1 ratio. Ca was dissolved into a suitable mother liquor with DMSO. The species number of *O. vulgare* used in this study is GXCM 2019023. The solutions were then diluted with DMEM, such that the final concentration of DMSO in the samples used in the experiment was lower than 1.56% v/v.

Cytotoxicity Assay

The cytotoxicity of *Ov* EO and Ca was evaluated in an HFF cell line with a CellTiter 96® AQueous One Solution Cell Proliferation Assay (Promega Corp., Madison, WI, USA), according to the manufacturer's instructions. HFF cells (1×10^5 cells/well) were seeded in 96-well plates and cultured at 37°C, in an atmosphere containing 5% CO_2, for 24 h. The cells were treated with varying concentrations of *Ov* EO (70, 35, 17, 9, and 4 μg/ml), Ca (70, 35, 17, 9, and 4μg/ml) or sulfamethoxazole (SMZ), and a 1.56% solution of DMSO in DMEM was used as the vehicle control. After incubating for 24 h, the HFF cells viability were measured by the MTT (3-[4,5-methylthiazol-2-yl]-2,5-diphenyltetrazolium bromide) colorimetric method according to Costa et al. (2018). Approximately 20 μl of MTT solution (5 mg/ml) was added to each well and allowed to incubate at 37°C with 5% CO_2 for 3 h and then 200 μl of DMSO was added to dissolve the formazan crystals. Absorbance was measured at 490 nm using an iMark™ Microplate Absorbance Reader (BioRad, Hercules, CA, USA). and the 50% cytotoxic concentrations (CC_{50}) were calculated using Graph Pad Prism 8.0. The cytotoxicity experiment was performed in triplicate, using three separate plates.

Anti-*T. gondii* Activity of *Ov* EO and Ca Evaluated by a Plaque Assay

One hundred freshly released GFP-RH tachyzoites were added to HFF monolayers in 6-well plates, in DMEM with 2% FBS. They were incubated at 37°C, in an atmosphere containing 5% CO_2, for 4 h. Then, the extracellular parasites were removed with medium, and fresh medium containing various concentrations of *Ov* EOs, Ca or 1.56% DMSO (vehicle control) were added to each

well. Uninfected and untreated wells were used as blank controls. After 7 days, HFF cells were washed three times with PBS, fixed with methanol for 10 min, and stained with 0.1% crystal violet for 30 min. After washing three times with phosphate buffered saline (PBS) and drying naturally (Huang et al., 2021), the plaques formed by tachyzoites were examined by microscopy.

Anti-*T. gondii* Activity of *Ov* EO Evaluated by an Intracellular Growth Assay

HFF cells were incubated in 24-well plates for 48 h, then the medium was replaced by DMEM with 2% FBS, 100 freshly released GFP-RH tachyzoites were added to each well, and incubated at 37°C in an atmosphere containing 5% CO_2, for 4 h. The medium containing extracellular parasites was removed and fresh medium containing either *Ov* EO (70, 35, 17, 9, and 4 μg/ml) or Ca (17, 9, 4, and 2 μg/ml), 1.56% DMSO (vehicle control), or 10 μg/ml SMZ (positive control) was added to each well. After 32 h, the growth of GFP-RH was observed and photographed under a fluorescence microscope. Growth of GFP-RH was calculated using Image-Pro-Express.

Effect of *Ov* EO and Ca on the Invasion of *T. gondii*

Invasion experiments were performed as described by Augusto et al. (2018). HFF cells was cultured in a 6-well plate, and 3 ml DMEM with 2% FBS was added to each well. Then, 10^4 RH and 17 μg/ml *Ov* EO or *Ca* were added simultaneously to the wells, respectively, incubating for 20, 40, or 60 min. The supernatant was gently removed, cells were fixed with 2 ml methanol for 10 min, washed three times with PBS, blocked by 5% solution of BSA in PBS (BSA/PBS) for 1 h, and washed three times with PBS. This was then incubated with mouse anti-*Toxoplasma* SAG1 monoclonal antibodies (mAb), diluted (1:1,000) with a 1% BSA/PBS solution, at room temperature for 2 h. Then, goat anti-mouse IgG H&L(FITC) secondary antibodies, diluted (1:1,000) in 1% BSA/PBS, were added to 6-well plates and incubated at room temperature for 2 h. After washing thrice with PBS, 300 μl of 0.2% Triton X-100 was added, and the mixture was left for 30 min. Cells were then gently washed three times with PBS, and 300 μl of a 5% BSA/PBS solution was added dropwise for a second blocking. The antibodies were added as per the procedure described earlier, this time using goat anti-mouse IgG H&L (Alexa Fluor ® 568) (ab175473) instead of the goat anti-mouse IgG H&L (FITC). Finally, 300 μl of 30% glycerol was added to each well. Five visual fields were randomly selected for observation under the 40× objective of the fluorescence microscope and the parasites in each field were counted. Three repetitions were performed to increase the accuracy of the experiment. The difference between the tachyzoites of the two colors is termed as the absolute invasion number of tachyzoites. The ratio of the invasion number to the total number of tachyzoites is termed as the invasion rate of tachyzoites.

Assessment of Tachyzoite Ultrastructure Using Scanning Electron Microscopy

To determine differences in the ultrastructure of tachyzoites after treatment, the purified tachyzoites were treated with 17 μg/ml *Ov* EO or Ca, respectively. After being cultured at 37 °C for 4 h, they were washed gently with PBS twice, and fixed overnight with 2.5% glutaraldehyde at room temperature. Gradient dehydration was carried out with 30, 50, 70, 80, 90, 95 and 100% ethanol respectively, and the critical point drying was carried out after dehydration. The tachyzoites were coated with gold (20–30 nm) and observed by scanning electron microscopy.

Statistical Analysis

All data were analyzed using GraphPad Prism 8.0. The anti-parasitic activity of the *Ov* EO and Ca was analyzed using an unpaired *t*-test, while the cell invasion data were processed using multiple *t*-tests, to compare the results of the test groups and those of the control group (*P <0.05, **P <0.01, ***P <0.001).

RESULTS

Cytotoxicity of *Ov* EO and Ca

The cytotoxic potential of *Ov* EO on the host cell was confirmed before the antiparasitic activity study. According to MTT assay result, the concentration that induced 50% HFF cells mortality (CC_{50}) of *Ov* EO was 134.9 μg/ml (**Figure 1**). After the antiparasitic activity of *Ov* EO was confirmed, the cytotoxic potential of Ca was carried out, and the result indicated that the CC_{50} of Ca was 43.93 μg/ml (**Figure 1**).

Antiparasitic Activity of *Ov EO* and Ca *In Vitro*

The anti-*T. gondii* activity of *Ov* EO was preliminarily evaluated by plaque test. As seen in **Figure 2A**, we found that the plaques visible were fewer in number and smaller in size after treatment with 9 or 17 μg/ml *Ov* EO (**Figures 2Aa, b**), as compared to those in the DMSO-treated and untreated groups. These results indicated that *Ov* EO was able to inhibit the growth of RH within safe concentrations. In order to find the effective ingredients in *Ov* EO that have the role of anti-toxoplasma, Ca was evaluated by plaque test. The results indicated that Ca was able to inhibit the growth of RH at 9 or 17 μg/ml (**Figures 2Ae, f**). The results indicated that the growth of *T. gondii* was inhibited by each of the concentrations of *Ov* EO and Ca tested (**Figure 2B**). To confirm and evaluate the effect of *Ov* EO concentration on anti-parasitic activity, five different concentrations were compared using an *in vitro* inhibition assay. The results indicated that the growth of *T. gondii* was inhibited by each of the concentrations of *Ov* EO tested (**Figure 3**), and the inhibition increased in a dose-dependent manner (**Figure 4A**), the IC_{50} of *Ov* EO was 16.08 μg/ml. We could find that the growth of *T. gondii* was significantly reduced after treatment with 70 and 35 μg/ml *Ov* EO (71 *vs.* 1,337; 320 *vs.* 1,337, P <0.001), as compared to the untreated and 1.56% DMSO-treated groups.

To compare the effect between *Ov* EO and Ca on anti-parasitic activity, four different concentrations of Ca were compared using the same assay. The results indicated that the growth of *T. gondii* was inhibited by each of the concentrations of Ca tested (**Figure 3**), and the inhibition also increased in a

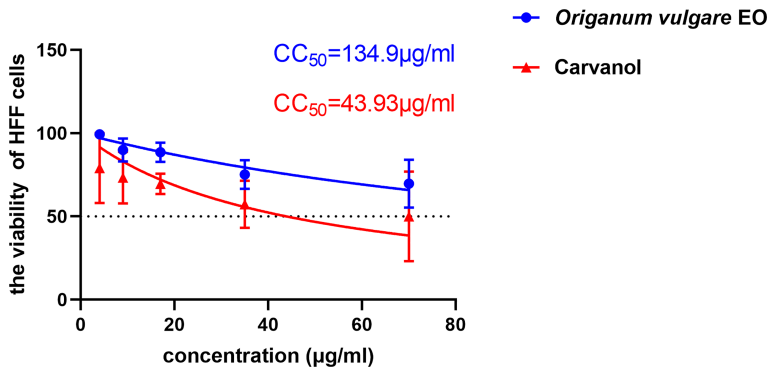

FIGURE 1 | The 50% cytotoxic concentrations (CC_{50}) of *Ov* EO and Ca. Cytotoxicity of *Ov* EO and Ca on HFF cells. Different concentrations of *Ov* EO *and* Ca treat HFF cells for 24 h and then cytotoxicity was evaluated using MTT Assay. All data are presented as with error bars and the experiments were performed in triplicate.

dose-dependent manner (**Figure 4B**), the IC_{50} of Ca was 7.688 μg/ml. Comparing to the untreated group, the growth of *T. gondii* was also significantly reduced in low Ca concentrations treated groups (9 and 4 μg/ml) (606.8 vs 1,337; 980.7 *vs.* 1,337, P <0.05). Both *Ov* EO and Ca inhibited the growth of *T. gondii* in a dose-dependent manner, for the groups treated with 17 μg/ml *Ov* EO and 17 μg/ml Ca, the differences were also significant (692.9 *vs.* 1,337, *P* <0.01; 225.5vs. 1,337, *P* <0.001). For the inhibition effect, Ca was better than *Ov* EO at the same concentration. The inhibition of *T. gondii* was much more significant in the groups treated with 17 μg/ml Ca, than in those treated with SMZ (225.5 *vs.* 1,337, *P* <0.001; 490 *vs.* 1,337, *P* <0.01). There was no significant decrease in untreatment groups after treatment with 1.56% DMSO, which indicated that DMSO had no inhibitory effect on GFP-RH (1,322 vs 1,337). Due to the results of inhibition, we can calculate the IC 50 of *Ov* EO and Ca was 16.08 and 7.688 μg/ml, respectively (**Figure 5**). After statistical analysis, the selectivity index (SI) of *Ov* EO and Ca was 8.389 and 5.714, respectively (**Table 1**). From the comprehensive comparison of safety, the performance of *Ov* EO is better than that of Ca.

Effect of *Ov* EO and Ca on the Invasion of *T. gondii*

As summarized in **Figure 6**, in the 17 μg/ml *Ov* EO treatment group, the *T. gondii* invasion rates at 20, 40, and 60 min post-infection were found to be 17.84, 24.10, and 28.96% respectively (**Figure 6A**). In the untreated group, invasion rates were found to be 38.85, 47.52, and 54.70% respectively at the three time points (**Figure 5A**). The invasion of *T. gondii* was significantly inhibited by *Ov* EO at 40 *min* (24.10% *vs.* 47.52%, *P* <0.01) and 60 min (28.96% *vs.* 54.70%, *P* <0.05). In the 17 μg/ml Ca treatment group, the *T. gondii* invasion rates were 21.09, 27.51, and 32.03% respectively at the three time points (**Figure 6B**), and the control group, invasion rates were found to be 30.52, 51.20, and 57.81% respectively (**Figure 6B**). Compared to the untreated group.

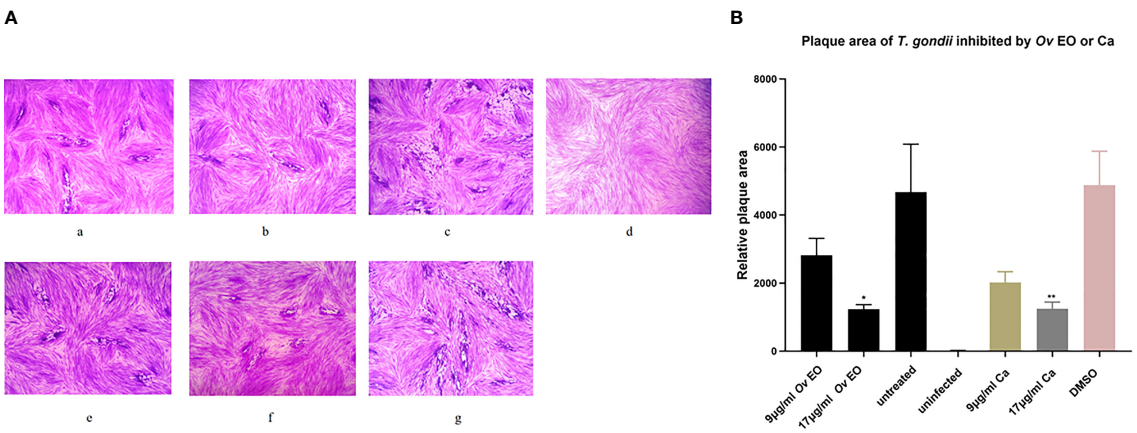

FIGURE 2 | Plaque test for preliminary detection of anti-*T. gondii* activity of *Ov* EO and Ca. **(A)** Images of *T. gondii* plaque under different concentrations of *Ov* EO and Ca. **(B)** Statistical analysis of the images plaque. **(a)** HFF cells were infected by *T. gondii* and treated with 9 μg/ml *Ov* EO; **(b)** HFF cells were infected by *T. gondii* and treated with 17 μg/ml *Ov* EO; **(c)** HFF cells were infected by *T. gondii* and untreated; **(d)** HFF cells were not infected and treated; **(e)** HFF cells were infected by *T. gondii* and treated with 9 μg/ml Ca; **(f)** HFF cells were infected by *T. gondii* and treated with 17 μg/ml Ca; **(g)** HFF cells were infected by *T. gondii* and treated with 1.56% DMSO.

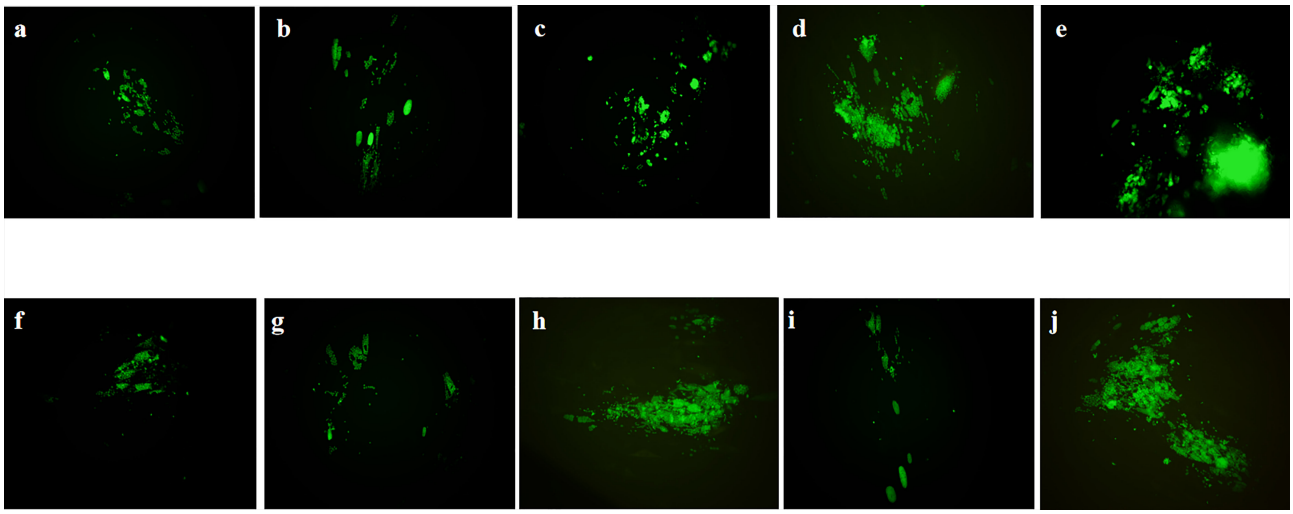

FIGURE 3 | Anti-*T. gondii* activity of *Ov* EO and Ca evaluated by growth assay. Fluorescence area indicates the growth of *T. gondii* during different treatment. **(A–D)** Different concentrations of *Ov* EO, **(A)** 70 μg/ml, **(B)** 35 μg/ml, **(C)** 17 μg/ml, **(D)** 9 μg/ml, and **(E)** no treatment; **(F–H)** Different concentrations of Ca, **(F)** 17 μg/ml, **(G)** 9 μg/ml, **(H)** 4 μg/ml, **(I)** SMZ, and **(J)** DMSO.

Ca significantly reduced the invasion of *T. gondii*, especially after treatment for 40 and 60 min (27.51% *vs.* 51.20%, $P < 0.001$; 32.03% *vs.* 57.81%, $P < 0.05$, **Figure 6B**). The inhibitory effect was observed to increase as the treatment time increased. No change in the invasion rate of *T. gondii* was observed in any group treated with DMSO, across all experiments.

Tachyzoite Ultrastructure Analysis

The Scanning electron microscopy (SEM) results showed that the tachyzoites curled into a head-to-tail shape after the Ca treatment, but the individual was still plump and not shriveled (**Figure 7B**). After treatment with *Ov* EO, the morphology of the tachyzoites changed significantly, the worms were distorted, and showed a certain shriveled state (**Figure 7A**). In comparison, the tachyzoites were normal full crescent-shaped in DMSO treated group (**Figure 7C**) and untreated group (**Figure 7D**).

DISCUSSION

T. gondii is an important zoonotic parasite, which can cause serious consequences after infected different hosts (Elsheikha, 2008; Maldonado and Read, 2017; El Bissati et al., 2018). In the face of the current dilemma of treatment and prevention, it is urgent to explore new drugs to inhibit *T. gondii* and control toxoplasmosis. At present, several reports indicated that plant

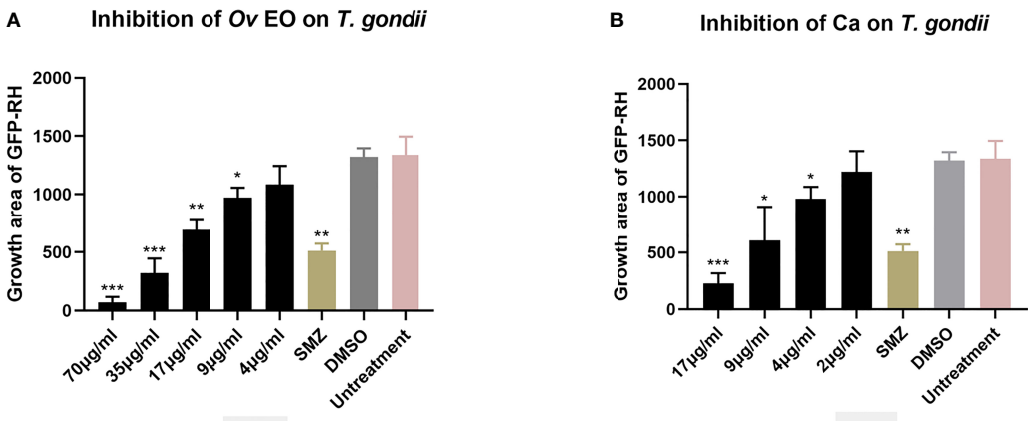

FIGURE 4 | Statistical analysis of the inhibition effect of *Ov* EO and Ca in anti-*T. gondii*. Data analysis based on fluorescence area of GFP-RH. Each bar represents the mean ± SD of three wells per group. $^{*}P < 0.05$, $^{**}P < 0.01$, $^{***}P < 0.001$ compared with untreatment group. **(A)** Anti-*T. gondii* activity of *Ov* EO, and **(B)** Anti-*T. gondii* activity of Ca.

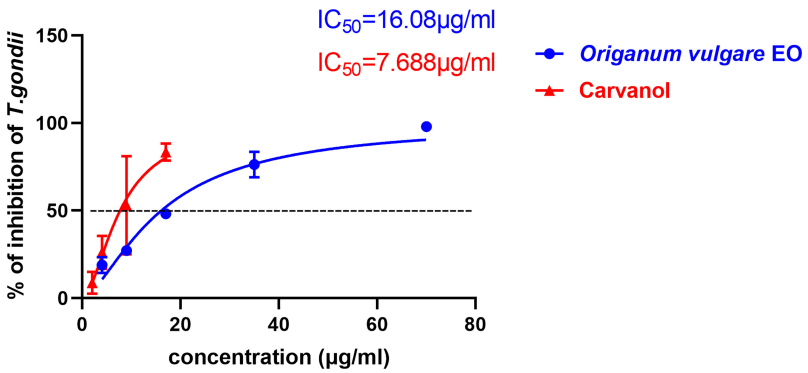

FIGURE 5 | The 50% inhibition concentrations (CC_{50}) of *Ov* EO and Ca. Inhibition of *Ov* EO and Ca to *T. gondii*. Different concentrations of *Ov* EO *and* Ca treated infected HFF cells for 32 h, the growth of GFP-RH was observed and photographed under a fluorescence microscope. Growth of GFP-RH was calculated using Image-Pro-Express. All data are presented as with error bars and the experiments were performed in triplicate.

essential oils had the inhibitory effect on *T. gondii*, in which, *Bunium persicum* (Boiss) EO (Tavakoli Kareshk et al., 2015) and *Thymus broussonetii Boiss* EO (Dahbi et al., 2010) played obvious roles in acute and chronic *T. gondii* infection in mice respectively. *Ov* EO is an important condiment, perfume, cosmetics, incense and preservative, with a long history of application (Diniz do Nascimento et al., 2020). The composition and content of *Ov* EO are affected by many factors, such as the place of production, cultivation conditions, extraction technology, etc. Research data shows that Ca is an important component in *Ov* EO, and its content mainly depends on the place of production, The carvacrol content in *Ov* EO produced in Argentina, Brazil, Greece and China is 26.7–81.92, 73.9, 63.03, and 30.73%, respectively (Leyva-López et al., 2017). This was the reason we chose the Ca study whether it plays an anti-*Toxoplasma* effect in *Ov* EO.

The cytotoxicity of *Ov* EO is related to the extraction method, and its toxicity to different cell lines is also different. The cytotoxicity of methanolic extracted *Ov* EO was more toxic, the CC_{50} of it was 382–374 μg/ml in MCF-7 cells. Chaouki reported that the CC_{50} of *Ov* EO was 5.5, 5.2, and 7.5 μg/ml in breast cancer cells (MCF-7), lung cancer cells (H-460) and central nervous system cancer cells (SF-268), respectively (Chaouki et al., 2010). In our experiment, the CC_{50} of *Ov* EO was 134.9 μg/mL in HFF. It has quite low cytotoxicity, so we can continue to carry out follow-up studies to evaluate its anti-*Toxoplasma* effect. The CC_{50} of Ca was 43.93 μg/ml, which is more toxic than *Ov* EO in HFF cells. Mostly, the active ingredients are more toxic than essential oil mixtures, and the effect will be better. From our results we found that the SI of *Ov* EO and Ca was not very high, which means that the cytotoxic of them are quite high, so further study should be carry on to reduce their cytotoxicity. Gaur et al. (2018) also found that Ca was more toxic than *Ov* EO in HCT-8 cells. In our experiment, Ca showed better anti-*T. gondii* activity than *Ov* EO at same concentration. As a kind of phenol, Ca has a significant repellent effect on many kinds of insects, such as *Aedes albopictus*, *Culex quinquefasciatus*, *Ixodes scapularis*, *Rhipicephalus appendiculatus* and so on (Lima et al., 2019). Moreover, Ca also shows anti-nematode effect on different nematodes such as *Ascaris suum* (Trailović et al., 2015). The main reason is that Ca can inhibit the contraction of muscle cells induced by acetylcholine, thereby inhibiting the muscle contraction of the parasite and affecting its motility (Marjanović et al., 2020). The above speculation is that the mechanism of carvacrol against *T. gondii* is related to the restriction of the motility of the parasite. However, its effect on the stability of calcium ions is also worthy of attention. Carvacrol has a certain regulatory effect on the stability of intracellular calcium ions. Studies have shown that carvacrol can adjust the TRP channels of transient calcium permeation receptor potentials, such as TRPV3, thereby increasing the concentration of calcium ions in the cytoplasm of primary mouse corneal epithelial cells and cultured human corneal epithelial cells (HCE-T cells) (Yamada et al., 2010). As we all know, there is a very important Ser/Thr protein kinase family in *T. gondii*, the CDPK family, whose activity is directly regulated by calcium ions. One family member, CDPK1, is closely related to the adhesion and invasion of *T. gondii*. Therefore, the reason why carvacrol can inhibit *T. gondii* may be achieved by inhibiting the activity of its invasion-related proteins. In our results, Ca did significantly inhibit the invasion rate of tachyzoites on HFF cells.

According to the results of SEM, the tachyzoites curled into a head-to-tail shape after the Ca treatment. Obviously, this obvious morphological change caused damage to the mobility of

TABLE 1 | Anti-*T. gondii* activity and cytotoxic effects of *Ov* EO or Ca.

	CC_{50} (μg/ml) (95% Confidence Intervals)HFF	IC_{50} (μg/ml) (95% Confidence Intervals)*T. gondii*	Selectivity Index (SI) (CC_{50}/IC_{50})
Ov EO	134.9 (102.6–184.9)	16.08 (13.88–18.55)	8.389
Ca	43.93 (26.87–75.07)	7.688 (5.711–10.33)	5.714

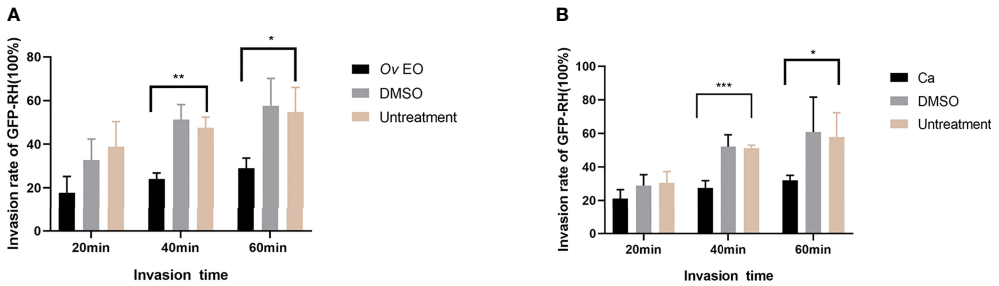

FIGURE 6 | Effect of *Ov* EO on the invasion of *T. gondii*. Statistics of *T. gondii* invasion rate using two immunofluorescent dyes after treated with *Ov* EO **(A)** and Ca **(B)** for 20, 40, 60 min, respectively. $^{*}P < 0.05$, $^{**}P < 0.01$, $^{***}P < 0.001$ compared with untreated group.

tachyzoites, which in turn affected its ability to invade. Studies have shown that carvacrol may induce apoptosis by reducing mitochondrial potential, releasing cytochrome C, activating caspase and carving PARP, thereby inhibiting human metastatic breast cancer cell line (MDA-MB 231) or human non-small cell lung cancer cell line Proliferation (A549) (Suntres et al., 2015). Therefore, the specific mechanism of Ca inhibiting *T. gondii* is not yet fully understood, and further research is needed. After *Ov EO* treatment, the tachyzoites showed severe dehydration and dryness. *Ov EO* is a mixture of different components, including terpenes, aldehydes, alcohols, esters, phenolic, ethers, and ketones and so on (Swamy et al., 2016). Among them, phenol can dehydrate the cells, resulting in the desiccation phenomenon (Samie et al., 2019). In addition, some

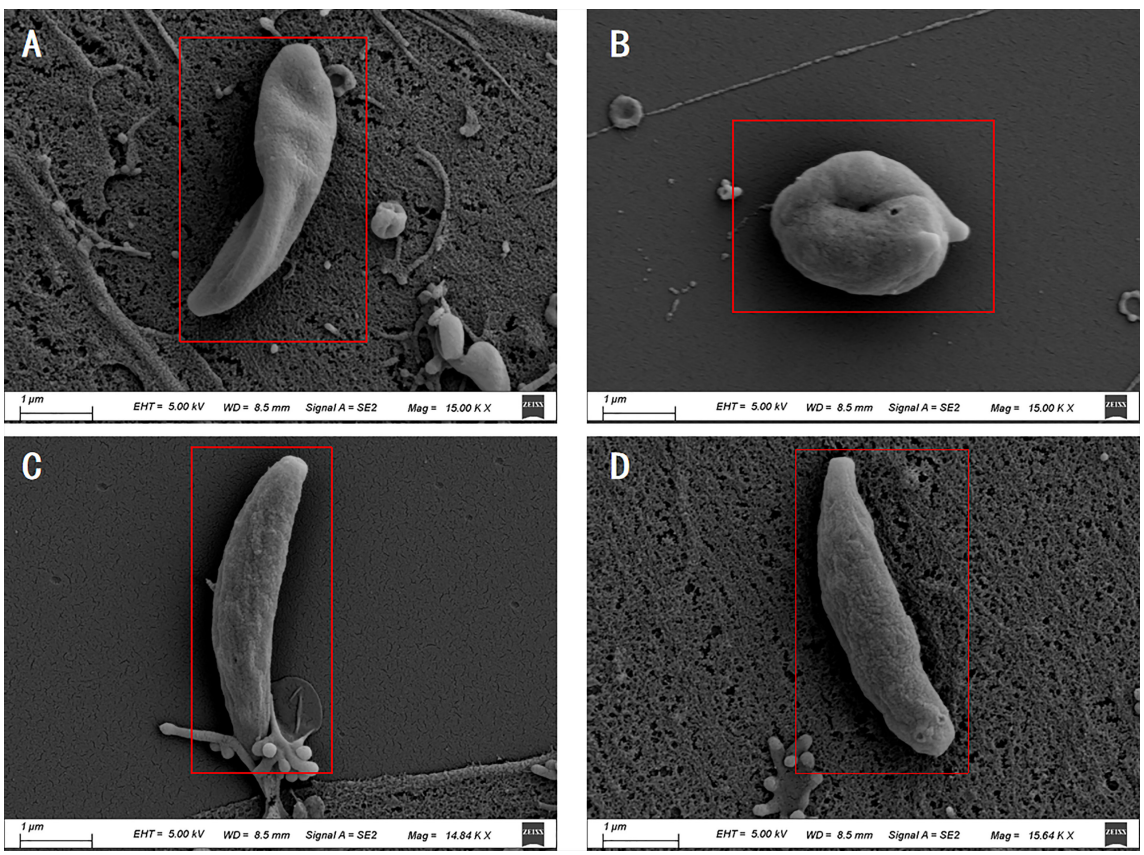

FIGURE 7 | Scanning electron microscopy assay. The *T. gondii* were treated with 17 μg/ml *Ov* EO **(A)**, 17 μg/ml Ca **(B)**, DMSO **(C)** or untreated **(D)**. After treated by *Ov* EO, the tachyzoites became sunken compared with those untreated tachyzoites. Tachyzoites treated with Ca become curled up. Scale bars: 1 μm.

hydrophobic compounds can pass through biological barriers and biological membranes, which may also have anti-*T. gondii* effects (Costa et al., 2018).

CONCLUSION

In this study, we found that *Ov* EO and Ca had obvious anti-*Toxoplasma* effect, which is likely to be achieved by changing the shape of tachyzoites, thereby limiting its movement ability, and then affecting its invasion ability. At the same time, Ca may have other biological functions, which can inhibit the proliferation of *T. gondii*. However, the target molecular and mechanism of action of *Ov* EO on *T. gondii* are still unclear and warrant further studies.

DATA AVAILABILITY STATEMENT

The raw data supporting the conclusions of this article will be made available by the authors, without undue reservation.

AUTHOR CONTRIBUTIONS

S-YH and NY conceived and designed the study. NY, QX, J-KH, MP, and Z-FH performed the laboratory analyses. D-DL and JPT analyzed the data. All authors critically appraised and interpreted the results. NY drafted the first version of the manuscript. All authors provided feedback on the manuscript, and read and approved the final version.

FUNDING

The sample collection and some experiments were supported by the Outstanding Youth Foundation of Jiangsu Province of China (BK20190046), the China Postdoctoral Science Foundation (2020M671615), the Science and Technology Major Project of Zhejiang Province, China. (No. 2012C12009-2), and the Priority Academic Program Development of Jiangsu Higher Education Institutions (Veterinary Medicine).

REFERENCES

Argyri, A. A., Doulgeraki, A. I., Varla, E. G., Bikouli, V. C., Natskoulis, P. I., Haroutounian, S. A., et al. (2021). Evaluation of Plant Origin Essential Oils as Herbal Biocides for the Protection of Caves Belonging to Natural and Cultural Heritage Sites. *Microorganisms* 9, 1836. doi: 10.3390/microorganisms9091836

Augusto, L., Martynowicz, J., Staschke, K. A., Wek, R. C., and Sullivan, W. J. Jr. (2018). Effects of PERK Eif2α Kinase Inhibitor Against Toxoplasma Gondii. *Antimicrob. Agents Chemother.* 62, 1–8.doi: 10.1128/AAC.01442-18.

Chaouki, W., Leger, D. Y., Eljastimi, J., Beneytout, J. L., and Hmamouchi, M. (2010). Antiproliferative Effect of Extracts From Aristolochia Baetica and Origanum Compactum on Human Breast Cancer Cell Line MCF-7. *Pharm. Biol.* 48, 269–274. doi: 10.3109/13880200903096588

Chemoh, W., Sawangjaroen, N., Nissapatorn, V., Suwanrath, C., Chandeying, V., Hortiwakul, T., et al. (2013). Toxoplasma Gondii Infection: What Is the Real Situation? *Exp. Parasitol* 135, 685–689. doi: 10.1016/j.exppara.2013.10.001

Costa, S., Cavadas, C., Cavaleiro, C., Salgueiro, L., and Do Céu Sousa, M. (2018). In Vitro Susceptibility of Trypanosoma Brucei Brucei to Selected Essential Oils and Their Major Components. *Exp. Parasitol* 190, 34–40. doi: 10.1016/j.exppara.2018.05.002

Dahbi, A., Bellete, B., Flori, P., Hssaine, A., Elhachimi, Y., Raberin, H., et al. (2010). The Effect of Essential Oils From Thymus Broussonetii Boiss on Transmission of Toxoplasma Gondii Cysts in Mice. *Parasitol Res.* 107, 55–58. doi: 10.1007/s00436-010-1832-z

Desmonts, G., and Couvreur, J. (1974). Toxoplasmosis in Pregnancy and its Transmission to the Fetus. *Bull. N. Y. Acad. Med.* 50, 146–159. doi: 10.1097/00006254-197409000-00007

Diniz do Nascimento, L., Moraes, A., Costa, K. S. D., Pereira Galúcio, J. M., Taube, P. S., Costa, C. M. L., et al. (2020). Bioactive Natural Compounds and Antioxidant Activity of Essential Oils From Spice Plants: New Findings and Potential Applications. *Biomolecules* 10, 988. doi: 10.3390/biom10070988

Dorman, H. J., and Deans, S. G. (2000). Antimicrobial Agents From Plants: Antibacterial Activity of Plant Volatile Oils. *J. Appl. Microbiol.* 88, 308–316. doi: 10.1046/j.1365-2672.2000.00969.x

Dunay, I. R., Gajurel, K., Dhakal, R., Liesenfeld, O., and Montoya, J. G. (2018). Treatment of Toxoplasmosis: Historical Perspective, Animal Models, and Current Clinical Practice. *Clin. Microbiol. Rev.* 31, e00057–17. doi: 10.1128/CMR.00057-17

El Bissati, K., Levigne, P., Lykins, J., Adlaoui, E. B., Barkat, A., Berraho, A., et al. (2018). Global Initiative for Congenital Toxoplasmosis: An Observational and International Comparative Clinical Analysis. *Emerg. Microbes Infect.* 7, 165. doi: 10.1038/s41426-018-0164-4

Elshafie, H. S., Armentano, M. F., Carmosino, M., Bufo, S. A., De Feo, V., and Camele, I. (2017). Cytotoxic Activity of Origanum Vulgare L. @ on Hepatocellular Carcinoma Cell Line HepG2 and Evaluation of its Biological Activity. *Molecules* 22, 1435. doi: 10.3390/molecules22091435.

Elsheikha, H. M. (2008). Congenital Toxoplasmosis: Priorities for Further Health Promotion Action. *Public Health* 122, 335–353. doi: 10.1016/j.puhe.2007.08.009

Gaur, S., Kuhlenschmidt, T. B., Kuhlenschmidt, M. S., and Andrade, J. E. (2018). Effect of Oregano Essential Oil and Carvacrol on Cryptosporidium Parvum Infectivity in HCT-8 Cells. *Parasitol. Int.* 67, 170–175. doi: 10.1016/j.parint.2017.11.001

Huang, S. Y., Yao, N., He, J. K., Pan, M., Hou, Z. F., Fan, Y. M., et al. (2021). *In Vitro* Anti-Parasitic Activity of Pelargonium X. Asperum Essential Oil Against Toxoplasma Gondii. *Front. Cell Dev. Biol.* 9, 616340. doi: 10.3389/fcell.2021.616340

Leyva-López, N., Gutiérrez-Grijalva, E. P., Vazquez-Olivo, G., and Heredia, J. B. (2017). Essential Oils of Oregano: Biological Activity Beyond Their Antimicrobial Properties. *Molecules* 22, 989. doi: 10.3390/molecules22060989

Lietava, J. (1992). Medicinal Plants in a Middle Paleolithic Grave Shanidar Iv? *J. Ethnopharmacol.* 35, 263–266. doi: 10.1016/0378-8741(92)90023-K

Lima, A. D. S., Landulfo, G. A., and Costa-Junior, L. M. (2019). Repellent Effects of Encapsulated Carvacrol on the Rhipicephalus (Boophilus) Microplus (Acari: Ixodidae). *J. Med. Entomol.* 56, 881–885. doi: 10.1093/jme/tjy240

Maldonado, Y. A., and Read, J. S. (2017). Diagnosis, Treatment, and Prevention of Congenital Toxoplasmosis in the United States. *Pediatrics* 139, e20163860. doi: 10.1542/peds.2016-3860

Marjanović, D. S., Zdravković, N., Milovanović, M., Trailović, J. N., Robertson, A. P., Todorović, Z., et al. (2020). Carvacrol Acts as a Potent Selective Antagonist of Different Types of Nicotinic Acetylcholine Receptors and Enhances the Effect of Monepantel in the Parasitic Nematode Ascaris Suum. *Vet. Parasitol.* 278, 109031. doi: 10.1016/j.vetpar.2020.109031

Newman, D. J., and Cragg, G. M. (2012). Natural Products as Sources of New Drugs Over the 30 Years From 1981 to 2010. *J. Nat. Prod.* 75, 311–335. doi: 10.1021/np200906s

Petrovska, B. B. (2012). Historical Review of Medicinal Plants' Usage. *Pharmacogn. Rev.* 6, 1–5. doi: 10.4103/0973-7847.95849

Samie, S., Trollope, K. M., Joubert, L. M., Makunga, N. P., and Volschenk, H. (2019). The Antifungal and Cryptococcus Neoformans Virulence Attenuating Activity of Pelargonium Sidoides Extracts. *J. Ethnopharmacol.* 235, 122–132. doi: 10.1016/j.jep.2019.02.008

Schmidt, D. R., Hogh, B., Andersen, O., Hansen, S. H., Dalhoff, K., and Petersen, E. (2006). Treatment of Infants With Congenital Toxoplasmosis: Tolerability and

Plasma Concentrations of Sulfadiazine and Pyrimethamine. *Eur. J. Pediatr.* 165, 19–25. doi: 10.1007/s00431-005-1665-4

Suntres, Z. E., Coccimiglio, J., and Alipour, M. (2015). The Bioactivity and Toxicological Actions of Carvacrol. *Crit. Rev. Food Sci. Nutr.* 55, 304–318. doi: 10.1080/10408398.2011.653458

Swamy, M. K., Akhtar, M. S., and Sinniah, U. R. (2016). Antimicrobial Properties of Plant Essential Oils Against Human Pathogens and Their Mode of Action: An Updated Review. *Evid. Based Complement. Alternat. Med.* 2016, 3012462. doi: 10.1155/2016/3012462

Tavakoli Kareshk, A., Keyhani, A., Mahmoudvand, H., Tavakoli Oliaei, R., Asadi, A., Andishmand, M., et al. (2015). Efficacy of the Bunium Persicum (Boiss) Essential Oil Against Acute Toxoplasmosis in Mice Model. *Iran J. Parasitol.* 10, 625–631.

Trailović, S. M., Marjanović, D. S., Nedeljković Trailović, J., Robertson, A. P., and Martin, R. J. (2015). Interaction of Carvacrol With the Ascaris Suum Nicotinic Acetylcholine Receptors and Gamma-Aminobutyric Acid Receptors, Potential Mechanism of Antinematodal Action. *Parasitol. Res.* 114, 3059–3068. doi: 10.1007/s00436-015-4508-x

Wei, H. X., Wei, S. S., Lindsay, D. S., and Peng, H. J. (2015). A Systematic Review and Meta-Analysis of the Efficacy of Anti-Toxoplasma Gondii Medicines in Humans. *PLoS One* 10, e0138204. doi: 10.1371/journal.pone.0138204

Weng, J. K., Philippe, R. N., and Noel, J. P. (2012). The Rise of Chemodiversity in Plants. *Science* 336, 1667–1670. doi: 10.1126/science.1217411

Yamada, T., Ueda, T., Ugawa, S., Ishida, Y., Imayasu, M., Koyama, S., et al. (2010). Functional Expression of Transient Receptor Potential Vanilloid 3 (TRPV3) in Corneal Epithelial Cells: Involvement in Thermosensation and Wound Healing. *Exp. Eye Res.* 90, 121–129. doi: 10.1016/j.exer.2009.09.020

Conflict of Interest: The authors declare that the research was conducted in the absence of any commercial or financial relationships that could be construed as a potential conflict of interest.

Publisher's Note: All claims expressed in this article are solely those of the authors and do not necessarily represent those of their affiliated organizations, or those of the publisher, the editors and the reviewers. Any product that may be evaluated in this article, or claim that may be made by its manufacturer, is not guaranteed or endorsed by the publisher.

frontiers in Cellular and Infection Microbiology

ORIGINAL RESEARCH
published: 25 November 2021
doi: 10.3389/fcimb.2021.783508

Molecular Detection of *Cryptosporidium* spp. and *Enterocytozoon bieneusi* Infection in Wild Rodents From Six Provinces in China

Hong-Bo Ni[1,2,3†], Yu-Zhe Sun[2†], Si-Yuan Qin[4†], Yan-Chun Wang[5], Quan Zhao[1*], Zheng-Yao Sun[2], Miao Zhang[2], Ding Yang[4], Zhi-Hui Feng[4], Zheng-Hao Guan[4], Hong-Yu Qiu[6], Hao-Xian Wang[6], Nian-Yu Xue[6] and He-Ting Sun[4*]*

[1] College of Life Science, Changchun Sci-Tech University, Shuangyang, China, [2] College of Veterinary Medicine, Qingdao Agricultural University, Qingdao, China, [3] State Key Laboratory of Veterinary Etiological Biology, Key Laboratory of Veterinary Parasitology of Gansu Province, Lanzhou Veterinary Research Institute, Chinese Academy of Agricultural Sciences, Lanzhou, China, [4] Center of Prevention and Control Biological Disaster, State Forestry and Grassland Administration, Shenyang, China, [5] Veterinary Department, Muyuan Foods Co.,Ltd., Nanyang, China, [6] College of Animal Science and Veterinary Medicine, Heilongjiang Bayi Agricultural University, Daqing, China

Enterocytozoon (*E.*) *bieneusi* and *Cryptosporidium* spp. are the most important zoonotic enteric pathogens associated with diarrheal diseases in animals and humans. However, it is still not known whether *E. bieneusi* and *Cryptosporidium* spp. are carried by wild rodents in Shanxi, Guangxi, Zhejiang, Shandong, and Inner Mongolia, China. In the present study, a total of 536 feces samples were collected from *Rattus (R.) norvegicus*, *Mus musculus*, *Spermophilus* (*S.*) *dauricus*, and *Lasiopodomys brandti* in six provinces of China, and were detected by PCR amplification of the SSU rRNA gene of *Cryptosporidium* spp. and ITS gene of *E. bieneusi* from June 2017 to November 2020. Among 536 wild rodents, 62 (11.6%) and 18 (3.4%) samples were detected as *E. bieneusi*- and *Cryptosporidium* spp.-positive, respectively. Differential prevalence rates of *E. bieneusi* and *Cryptosporidium* spp. were found in different regions. *E. bieneusi* was more prevalent in *R. norvegicus*, whereas *Cryptosporidium* spp. was more frequently identified in *S. dauricus*. Sequence analysis indicated that three known *Cryptosporidium* species/genotypes (*Cryptosporidium viatorum*, *Cryptosporidium felis*, and *Cryptosporidium* sp. rat genotype II/III) and two uncertain *Cryptosporidium* species (*Cryptosporidium* sp. novel1 and *Cryptosporidium* sp. novel2) were present in the investigated wild rodents. Meanwhile, 5 known *E. bieneusi* genotypes (XJP-II, EbpC, EbpA, D, and NCF7) and 11 novel *E. bieneusi* genotypes (ZJR1 to ZJR7, GXM1, HLJC1, HLJC2, and SDR1) were also observed. This is the first report for existence of *E. bieneusi* and *Cryptosporidium* spp. in wild rodents in Shanxi, Guangxi, Zhejiang, and Shandong, China. The present study also demonstrated the existence of *E. bieneusi* and *Cryptosporidium* spp. in *S. dauricus* worldwide for the first time. This study not only

OPEN ACCESS

Edited by:
Wei Cong,
Shandong University, Weihai, China

Reviewed by:
Wen-Bin Zheng,
Shanxi Agricultural University, China
Katarzyna Buńkowska-Gawlik,
University of Wrocław, Poland
Jianhai Yin,
National Institute of Parasitic Diseases, China
Majid Pirestani,
Tarbiat Modares University, Iran

***Correspondence:**
Yan-Chun Wang
381770722@qq.com
Quan Zhao
zhaoquan0825@163.com
He-Ting Sun
xiaofengsht@163.com

†These authors have contributed equally to this work

Specialty section:
This article was submitted to Clinical Microbiology, a section of the journal Frontiers in Cellular and Infection Microbiology

Received: *26 September 2021*
Accepted: *02 November 2021*
Published: *25 November 2021*

Citation:
Ni H-B, Sun Y-Z, Qin S-Y, Wang Y-C, Zhao Q, Sun Z-Y, Zhang M, Yang D, Feng Z-H, Guan Z-H, Qiu H-Y, Wang H-X, Xue N-Y and Sun H-T (2021) Molecular Detection of Cryptosporidium spp. and Enterocytozoon bieneusi Infection in Wild Rodents From Six Provinces in China. Front. Cell. Infect. Microbiol. 11:783508. doi: 10.3389/fcimb.2021.783508

provided the basic data for the distribution of *E. bieneusi* and *Cryptosporidium* genotypes/species, but also expanded the host range of the two parasites. Moreover, the zoonotic *E. bieneusi* and *Cryptosporidium* species/genotypes were identified in the present study, suggesting wild rodents are a potential source of human infections.

Keywords: *Cryptosporidium* spp., *Enterocytozoon bieneusi*, prevalence, genotyping, wild rats, China

INTRODUCTION

The rodents are one of the largest families of mammals. Wild rodents (e.g., wild rats) are the most widely distributed worldwide. They can shed many pathogens (e.g., *Enterocytozoon* (*E.*) *bieneusi* and *Cryptosporidium* spp.) into the environment due to living in an open environment, thus becoming potential sources for transmission of pathogens to other animals (Deng et al., 2016; García-Livia et al., 2020; Gui et al., 2020). In addition, the rodents have a closed relationship with humans. Thus, many pathogens, including *E. bieneusi* and *Cryptosporidium* spp., might be transmitted from rodents to humans. (García-Livia et al., 2020; Gui et al., 2020; Zhao et al., 2020).

E. bieneusi and *Cryptosporidium* spp. are the common zoonotic enteric pathogens responsible for a majority of parasitic diarrhea diseases worldwide (Qi et al., 2015; Zhang X. et al., 2018; Zhao et al., 2018; Wang S. N. et al., 2020). Both of them can infect humans and a wide variety of animals (e.g., rodents) (Wang et al., 2013; Zhao et al., 2018; Li and Xiao, 2020; Wang S. N. et al., 2020) mainly through water-borne and food-borne routes (Wang et al., 2013; Zhao et al., 2018). In general, healthy people infected with both pathogens are asymptomatic or manifest symptoms of self-limiting diarrhea. However, the infection of *E. bieneusi* and *Cryptosporidium* spp. in immunocompromised individuals may cause chronic or life-threatening diarrheas (Wang et al., 2013; Sutthikornchai et al., 2021). Owing to their significance in public health, *Cryptosporidium* spp. and *E. bieneusi* have been put into Category B Priority Pathogen list by the National Institute of Allergy and Infectious Diseases (NIAID) (NIAID, 2018). Moreover, *E. bieneusi* is also listed on the Environmental Protection Agency (EPA) microbial contaminant candidate list of concern for waterborne transmission (Didier et al., 2009).

E. bieneusi is consist of more than 500 genotypes, which are classified into 11 groups based on the sequences of the internal transcribed spacer (ITS) region of the rRNA gene (Santin, 2015; Zhang Y. et al., 2018; Zhao et al., 2018; Li W. et al., 2019; Wang S. N. et al., 2020; Abarca et al., 2021). Group 1, identified as zoonotic, is responsible for a vast majority of human infections (Wang S. N. et al., 2020). Groups 2-11 are mainly composed of host-specific or host-adapted genotypes (Guo et al., 2014; Wang S. N. et al., 2020). To date, a total of 36 ITS genotypes of *E. bieneusi* have been found in rodent species and 15 (Type IV, BEB6, EbpA, EbpC, C, D, H, CZ3, S6, Peru6, Nig7, Peru8, Peru11, Peru16, and PigITS5) were considered as zoonotic genotypes (Danišová et al., 2015; Cama et al., 2007; Sak et al., 2011; Guo et al., 2014; Perec-Matysiak et al., 2015; Qi et al., 2015; Roellig et al., 2015; Deng et al., 2016).

Cryptosporidium spp. contains more than 100 species/genotypes based on the sequence of the small subunit (SSU) rRNA gene (Feng et al., 2018; Holubová et al., 2019). To date, 38 of them have been identified in humans, whereas only *C. hominis* and *C. parvum* were frequently found in humans (Essid et al., 2018; Krumkamp et al., 2021), and the remaining genotypes/species were occasionally observed in humans. Rodents are one of the most important reservoirs of *Cryptosporidium* spp. More than 30 *Cryptosporidium* species/genotypes have been identified in rodent species (Zhang X. et al., 2018). Among them, at least ten *Cryptosporidium* species (including *C. parvum*, *C. andersoni*, *C. muris*, *C. wrairi*, *C. tyzzeri*, *C. scrofarum*, *C. ubiquitum*, *C. hominis*, *C. suis*, and *C. meleagridis*) and more than 20 *Cryptosporidium* genotypes, such as ground squirrel genotypes (I-III), rat genotypes (I-IV), deer mouse genotypes (I-IV), chipmunk genotypes II, vole genotype, and mouse genotypes (II, III), have been identified in humans (Bajer et al., 2002; Nakai et al., 2004; Feng et al., 2007; Foo et al., 2007; Kimura et al., 2007; Kváč et al., 2008; Lv et al., 2009; Paparini et al., 2012; Backhans et al., 2013; Murakoshi et al., 2013; Ng-Hublin et al., 2013; Song et al., 2015; Stenger B. et al., 2015; Stenger B. L. et al., 2015; Zhao et al., 2015; Gholipoury et al., 2016; Saki et al., 2016; Danišová et al., 2017; Wang S. N. et al., 2020).

In view of such severe situations, it is essential to investigate the prevalence of *E. bieneusi* and *Cryptosporidium* spp. in different rodent species and identify their species/genotypes. However, information regarding *Cryptosporidium* spp. infection in rodents was limited in China, which was only reported in *Microtus fuscus* (Qinghai vole) and *Ochotona curzoniae* (wild plateau pika) in Qinghai (Zhang X. et al., 2018), brown rats (*Rattus norvegicus*) in Heilongjiang (Li et al., 2016), bamboo rats in Sichuan (Liu et al., 2015), pet chinchillas in Beijing, Henan and Guizhou (Qi et al., 2015), commensal rodents in Henan and Fujian (Zhao et al., 2015), brown rats in Heilongjiang (Zhao et al., 2018), wild, laboratory, and pet rodents in Beijing, Henan, Fujian and Sichuan (Lv et al., 2009), bamboo rats in Guangdong, Hunan, Guangxi, Jiangxi and Hainan (Wei et al., 2019; Li et al., 2020a; Li et al., 2020b), Asian house rats, brown rats, Edward's long-tailed rats and muridae in Hainan (Zhao et al., 2019). In China, *E. bieneusi* in rodents has been only reported in Heilongjiang (Zhao et al., 2018), Beijing (Qi et al., 2015), Henan (Qi et al., 2015; Wang J. et al., 2020), Guizhou (Qi et al., 2015), Sichuan (Deng et al., 2016), Shandong (Wang J. et al., 2020), Guangdong (Wang et al., 2019), Hunan (Wang et al., 2019; Gui et al., 2020), Jiangxi (Wang et al., 2019), Chongqing (Wang et al., 2019), Guangxi (Wang et al., 2019), and Hainan (Zhao et al., 2020).

However, it is still not known whether *E. bieneusi* and *Cryptosporidium* spp. are carried by wild rodents in Shanxi,

Guangxi, Zhejiang, Shandong, and Inner Mongolia, China. Thus, the present study was performed to estimate the prevalence and genotypes of *E. bieneusi* and *Cryptosporidium* spp. in wild rodents by the molecular biological method.

MATERIALS AND METHODS

Specimen Collection

A total of 536 feces samples were collected from four rodent species from Daqing City in Heilongjiang (n = 41; 39 *S. dauricus*, 2 *R. norvegicus*), Taigu County in Shanxi (n = 53, *R. norvegicus*), Nanning City in Guangxi (n = 74, *M. musculus*), Weihai City in Shandong (n = 227, *R. norvegicus*), Jiaxing City in Zhejiang (n = 119, *R. norvegicus*) and Xilingol League in Inner Mongolia (n = 22, *L. brandti*), China from June 2017 to November 2020. These rodents were captured by trapping method. The rodents had been euthanized by CO2 inhalation, and then the fresh feces sample (approximately 500 mg) was collected directly from the intestinal and rectal content of each rodent, and then was placed into ice boxes and sent to the laboratory. Information regarding sampling time, region, and species was recorded. This study was approved by the Ethics Committee of Qingdao Agricultural University.

DNA Extraction and PCR Amplification

Genomic DNA was extracted from fecal sample of approximately 200 mg using the E.Z.N.A.® Stool DNA Kit (Omega Biotek Inc., Norcross, GA, USA) according to the manufacturer's instructions, and then was stored at -20°C prior to PCR. The prevalence and genotypes of *E. bieneusi* were identified by PCR amplification of the ITS gene according to the previous description (Zhao et al., 2018). *Cryptosporidium* spp. in the fecal samples was confirmed by PCR amplification of the SSU rRNA gene according to the previous report (Zhao et al., 2018). The positive and negative controls were included in each test. The secondary PCR products were observed using UV light after an electrophoretic analysis at a 1.5% agarose gel containing ethidium bromide.

Sequence and Phylogenetic Analyses

The positive PCR specimens were sent to Sangon Biotech Company (Shanghai, China) for sequencing. A new PCR product should be sequenced if previously produced sequences had single nucleotide substitutions, insertions or deletions. The nucleotide sequences were aligned and analyzed with reference sequences by using the Clustal X 1.83 program and Basic Local Alignment Search Tool (BLAST) (https://blast.ncbi.nlm.nih.gov/), in order to determine the species/genotypes of *Cryptosporidium* spp. and *E. bieneusi*. The phylogenetic trees were reconstructed with Mega 5.0 using neighbor-joining (NJ) method under Kimura 2-parameter model (1,000 replicates). All nucleotide sequences were deposited in GenBank with accession numbers MT647749 – MT647806 and OK117929 – OK117932 for *E. bieneusi*, and MT561508 – MT561533 for *Cryptosporidium* spp.

Statistical Analysis

The statistical analysis for the prevalence of *E. bieneusi* and *Cryptosporidium* in wild rodents from different region, season, sampling year, and species were performed by using $\chi 2$ test in SAS version 9.1 (SAS Institute, Cary, NC, USA). The results were considered to be statistically significant when $P < 0.05$. Odds ratios (ORs) and their 95% confidence intervals (95% CIs) were also calculated to compare the magnitude of various risk factors for *E. bieneusi* and *Cryptosporidium* prevalence.

RESULTS

Prevalence of *Cryptosporidium* spp. and *E. bieneusi*

In the present study, 18 out of 536 (3.4%) fecal samples were identified as *Cryptosporidium*-positive (**Table 1**). The prevalence rates of *Cryptosporidium* in different species of rodents were 15% (6/401) in *R. norvegicus*, 9.5% (7/74) in *M. musculus*, 12.8% (5/39) in *S. dauricus*, and 0% (0/22) in *L. brandti* (**Table 1**). Moreover, the prevalence of *Cryptosporidium* in different regions ranged from 0% in Inner Mongolia (0/22) and Shandong (0/227) to 12.2% in Heilongjiang (5/41) (**Table 1**). Furthermore, the prevalence in different collection years ranged from 0% to 12.8% (**Table 1**). The prevalence of *Cryptosporidium* in rodent feces collected in autumn (3.7%, 12/321) was slightly higher than that in summer (2.8%, 6/215) (**Table 1**).

Among 536 rodents, 62 samples (11.6%) were detected to be *E. bieneusi*-positive in three rodent species, with 13.3% (53/399) in *R. norvegicus*, 6.8% (5/74) in *M. musculus*, and 9.8% (4/41) in *S. dauricus* (**Table 2**). The highest prevalence of *E. bieneusi* was found in Shanxi (37.7%, 20/53), and followed by Zhejiang (24.4%, 29/119), Heilongjiang (9.8%, 4/41), Guangxi (6.8%, 5/74), and Shandong (1.4%, 4/227) (**Table 2**). The prevalence of *E. bieneusi* was 6.8% (5/74), 20.9%, (49/235) 9.8% (4/41), and 1.4% (4/227) in rodents collected in 2017, 2018, 2019, and 2020, respectively (**Table 2**). The prevalence of *E. bieneusi* in rodents was 22.8% in summer (49/215) and 4.0% in autumn (13/321), respectively (**Table 2**).

E. bieneusi and *Cryptosporidium* spp. coinfection was found in three wild rodents in this study. All of them were *R. norvegicus* collected in 2018. Two were collected from Zhejiang Province, and the remaining one was collected from Shanxi Province.

Distribution of *Cryptosporidium* spp. and *E. bieneusi*

Cryptosporidium sp. rat genotype II/III, *Cryptosporidium felis*, and *Cryptosporidium viatorum* were identified in the investigated rodents through the analysis of SSU rRNA gene of *Cryptosporidium*. Furthermore, two *Cryptosporidium* genotypes with uncertain species status were observed (**Figure 1** and **Table 1**). *Cryptosporidium* sp. novel1 and *C. felis* were found in *S. dauricus* in Heilongjiang. *C. viatorum* and *Cryptosporidium* sp. rat genotype II/III were only identified in *M. musculus* in Guangxi. *Cryptosporidium* sp. novel2 was found in three provinces Zhejiang (*R. norvegicus*), Shanxi (*R. norvegicus*), and Guangxi (*M. musculus*) (**Table 1**).

A total of 16 *E. bieneusi* genotypes were identified in this study, including 5 known genotypes (XJP-II, EbpC, EbpA, D, and NCF7) and 11 novel genotypes (ZIR1 to ZJR7, GXM1, HLJC1,

TABLE 1 | Prevalence, associated factors, and distribution of *Cryptosporidium* spp. in rodents.

	No. positive/No. tested	Prevalence (%, 95% CI)	Species/Genotype	OR (95% CI)	*P*
Area					0.37
Zhejiang	4/119	3.4% (0.1-6.6)	*Cryptosporidium* sp. novel2 (n=4)	0.25 (0.06-10.98)	
Heilongjiang	5/41	12.2% (1.7-22.7)	*Cryptosporidium felis* (n=1), *Cryptosporidium* sp. novel1 (n=4)	Reference	
Shanxi	2/53	3.8% (0.0-9.1)	*Cryptosporidium* sp. novel2 (n=2)	0.28 (0.52-21.54)	
Guangxi	7/74	9.5% (2.6-16.3)	*Cryptosporidium viatorum* (n=1), *Cryptosporidium* sp. rat genotype II/III (n=5), *Cryptosporidium* sp. novel2 (n=1)	0.75 (0.22-2.54)	
Inner Mongolia	0/22	0	–	–	
Shandong	0/227	0	–	–	
Rodent species					0.001
Rattus norvegicus	6/401	1.5% (0.3-2.7)	*Cryptosporidium* sp. novel2 (n=6)	0.10 (0.0.-0.36)	
Mus musculus	7/74	9.5% (2.6-16.3)	*Cryptosporidium viatorum* (n=1), *Cryptosporidium* sp. novel2 (n=1), *Cryptosporidium* sp. rat genotype II/III (n=5)	0.71 (0.21-2.41)	
Spermophilus dauricus	5/39	12.8% (1.8-23.8)	*Cryptosporidium felis* (n=1), *Cryptosporidium* sp. novel1 (n=4)	Reference	
Lasiopodomys brandti	0/22	0		–	
Sampling years					< 0.01
2017	7/74	9.5% (2.6-16.3)	*Cryptosporidium viatorum* (n=1), *Cryptosporidium* sp. rat genotype II/III (n=5), *Cryptosporidium* sp. novel2 (n=1)	Reference	
2018	6/196	3.1% (0.6-5.5)	*Cryptosporidium* sp. novel2 (n=6)	0.30 (0.10-0.93)	
2019	5/39	12.8% (1.8-23.8)	*Cryptosporidium felis* (n=1), *Cryptosporidium* sp. novel1 (n=4)	1.41 (0.42-4.77)	
2020	0/227	0		–	
Seasons					0.77
Summer (6-8 months)	6/215	2.8% (0.6-5.0)	*Cryptosporidium* sp. novel2 (n=6)	Reference	
Autumn (9-11 months)	12/321	3.7% (1.7-5.8)	*Cryptosporidium viatorum* (n=1), *Cryptosporidium felis* (n=1), *Cryptosporidium* sp. rat genotype II/III (n=5), *Cryptosporidium* sp. novel1 (n=4), *Cryptosporidium* sp. novel2 (n=1)	1.16 (0.43-3.14)	
Total	18/536	3.4% (1.8-4.9)	*Cryptosporidium viatorum* (n=1), *Cryptosporidium felis* (n=1), *Cryptosporidium* sp. rat genotype II/III (n=5), *Cryptosporidium* sp. novel1 (n=4), *Cryptosporidium* sp. novel2 (n=7)		

HLJC2, and SDR1) (**Figure 2** and **Table 2**). Among them, genotype D was found in *R. norvegicus* in Zhejiang, Shanxi, and Shandong. EbpA was only found in *R. norvegicus* in Zhejiang and Shanxi, whereas EbpC was identified in Zhejiang (*R. norvegicus*), Shanxi (*R. norvegicus*), and Heilongjiang (*S. dauricus*). Moreover, NCF2 (*R. norvegicus* in Shandong), XJP-II (*R. norvegicus* in Shanxi), ZIR1 to ZJR7 (*R. norvegicus* in Zhejiang), GXM1 (*M. musculus* in Guangxi), HLJC1 (*S. dauricus* in Heilongjiang), HLJC2 (*S. dauricus* in Heilongjiang), and SDR1 (*R. norvegicus* in Shandong) were only found in one province (**Table 2**).

Phylogenetic Relationships of *Cryptosporidium* spp. and *E. bieneusi*

The phylogenetic analysis of various *Cryptosporidium* species/genotypes showed two uncertain species status and three known species/genotypes (**Figure 1**). The sequences of *Cryptosporidium* sp. novel2, including seven *Cryptosporidium* spp. sequences (isolates 32, 44, 63, 67, 70, 155, and 245), were clustered with *Cryptosporidium* spp. sequences identified from environmental samples (**Figure 1**). Five sequences (isolates 202, 205, 211, 231, and 233) were clustered with *Cryptosporidium* sp. rat genotype II/III in a same clade (**Figure 1**). Sequences of isolates 251, 261, 263, and 265 (*Cryptosporidium* sp. novel1) were grouped into a novel separate clade (**Figure 1**). Sequences of isolates 270 and 200 were clustered with that of *C. felis* and *C. viatorum* in a same clade, respectively (**Figure 1**).

The Neighbor-Joining analysis for sequences of *E. bieneusi* species/genotypes obtained in this study revealed that 5 known genotypes and 11 novel genotypes (**Figure 2**). Fourteen genotypes (5 known genotypes and 9 novel genotypes) were

TABLE 2 | Prevalence, associated factors, and distribution of *E. bieneusi* in rodents.

	No. positive/No. tested	Prevalence (%, 95% CI)	Genotype	OR (95% CI)	*P*
Area					0.00
Zhejiang	29/119	24.4% (16.5-32.2)	D (n=6), EbpA (n=3), EbpC (n=12), ZJR1 (n=1), ZJR2 (n=1), ZJR3 (n=1), ZJR4 (n=1), ZJR5 (n=1), ZJR6 (n=1), ZJR7 (n=2)	4.47 (1.64-12.08)	
Heilongjiang	4/41	9.8% (0.3-19.2)	EbpC (n=1), HLJC1 (n=2), HLJC2 (n=1)	1.49 (0.38-5.90)	
Shanxi	20/53	37.7% (24.2-51.2)	EbpA (n=3), EbpC (n=7), D (n=9), XJP-II (n=1)	8.36 (2.89-24.24)	
Guangxi	5/74	6.8% (0.9-12.6)	GXM1 (n=5)	Reference	
Inner Mongolia	0/22	0	–	–	
Shandong	4/227	1.4% (0.0-2.9)	NCF2 (n=1), SDR1(n=1), D (n=2)	0.25 (0.07-0.95)	
Rodent species					0.48
Rattus norvegicus	53/399	13.3% (9.9-16.6)	EbpA (n=6), EbpC (n=19), D (n=17), ZJR1 (n=1), ZJR2 (n=1), ZJR3 (n=1), ZJR4 (n=1), ZJR5 (n=1), ZJR6 (n=1), ZJR7 (n=2), XJP-II (n=1), NCF2 (n=1), SDR1(n=1)	1.33 (0.46-3.90)	
Mus musculus	5/74	6.8% (0.9-12.6)	GXR1 (n=5)	0.63 (0.16-2.51)	
Spermophilus dauricus	4/41	9.8% (0.3-19.2)	EbpC (n=1) HLJC1 (n=2) HLJC2 (n=1)	Reference	
Lasiopodomys brandti	0/22	0	–	–	
Sampling years					0.00
2017	5/74	6.8% (0.9-12.6)	GXM1 (n=5)	Reference	
2018	49/235	20.9% (15.6-26.1)	EbpA (n=6), EbpC (n=19), D (n=15), ZJR1 (n=1), ZJR2 (n=1), ZJR3 (n=1), ZJR4 (n=1), ZJR5 (n=1), ZJR6 (n=1), ZJR7 (n=2), XJP-II (n=1)	4.60 (1.76-12.06)	
2019	4/41	9.8% (0.3-19.2)	EbpC (n=1), HLJC1 (n=2), HLJC2 (n=1)	1.58 (0.40-6.25)	
2020	4/227	1.4% (0.0-2.9)	D (n=2), NCF2 (n=1), SDR1 (n=1)	0.25 (0.07-0.95)	
Seasons					0.00
Summer (6-8 months)	49/215	22.8% (17.1-28.4)	EbpA (n=6), EbpC (n=19), D (n=15), ZJR1 (n=1), ZJR2 (n=1), ZJR3 (n=1), ZJR4 (n=1), ZJR5 (n=1), ZJR6 (n=1), ZJR7 (n=2), XJP-II (n=1)	Reference	
Autumn (9-11 months)	13/321	4.0% (1.9-6.2)	GXM1 (n=5), EbpC (n=1), HLJC1 (n=2), HLJC2 (n=1), D (n=2), NCF2 (n=1), SDR1(n=1)	0.12 (0.06-0.23)	
Total	62/536	11.6% (8.9-14.3)	EbpA (n=6), EbpC (n=20), D (n=17), XJP-II (n=1), NCF2 (n=1), ZJR1 (n=1), ZJR2 (n=1), ZJR3 (n=1), ZJR4 (n=1), ZJR5 (n=1), ZJR6 (n=1), ZJR7 (n=2), GXM1 (n=5), HLJC1 (n=2), HLJC2 (n=1), SDR1 (n=1)		

divided into Group 1, with ZJR7, SDR1, and D in 1a, EbpC, ZJR5, and ZJR1 in 1d, HLJC1, ZJR4, EbpA, XJP-II, and ZJR3 in 1e, NCF2 in 1b, GXM1 in 1i, and ZJR6 in 1j (**Figure 2**). Furthermore, HLJC2 was grouped in Group 2, and ZJR2 was classified into Group 10 (**Figure 2**).

DISCUSSION

In this study, the total prevalence of *Cryptosporidium* spp. was 3.4% (18/536) in four rodent species (*R. norvegicus*, *M. musculus*, *L. brandti*, and *S. dauricus*), which was consistent with previous reports showing the prevalence rates ranged from 0.8% to 80.0% in a variety of rat species (Feng, 2010; Mirzaghavami et al., 2016; Wei et al., 2019), e.g., 1.5-38.0% in brown rats, 8.0-31.4% in mice, and 0.8-73.0% in voles (Feng, 2010; Wei et al., 2019; Ježková et al., 2021). The present study found that the prevalence rates of *Cryptosporidium* spp. in *R. norvegicus*, *M. musculus*, *L. brandti*, and *S. dauricus* were 1.5% (6/401), 9.5% (7/74), 0% (0/22), and 12.8% (5/39), respectively with statistical significance ($P < 0.05$). There was a 0.10- (OR = 0.10, 95% CI 0.0-0.36) and 0.71- (OR = 0.71, 95% CI 0.21-2.41) fold increase of *Cryptosporidium* spp. infection risk in *R. norvegicus* (1.5%, 95% CI 0.3-2.7), *M. musculus* (9.5%, 95% CI 2.6-16.3) compared with that in *S. dauricus* (12.8%, 95% CI 1.8-23.8). Furthermore, the prevalence of *E. bieneusi* in rodents varied in different countries, e.g., 87.5% in Peru (Cama et al., 2007), 28.6-42.9% in Poland (Perec-Matysiak et al., 2015), 1.1% in Slovakia (Danišová et al., 2015), 20.0-100% in USA (Roellig et al., 2015). In the present study, the overall *E. bieneusi* prevalence was 11.6% (62/536), with 13.3% (53/399) in *R. norvegicus*, 6.8% (5/74) in *M. musculus*, 9.8% (4/41) in *S. dauricus*, and 0% (0/22) in *L. brandti*. In China, *E. bieneusi* infection has also been reported in many rodent species, such as Bamboo rat (5.1%, 22/435; 15.4%, 18/117) (Wang et al., 2019; Zhao et al., 2020), Brown rat (7.9%, 19/242; 14.3%, 8/58) (Zhao et al., 2018; Zhao et al., 2020), Chinchilla (3.6%, 5/140) (Qi et al., 2015), Indo-Chinese forest rat (9.3%, 5/54) (Zhao et al., 2020), Asiatic brush-tailed porcupine (7.5%, 7/93) (Zhao et al., 2020), Bower's white-toothed rat (31.6%, 37/117) (Zhao et al., 2020), Edward's long-tailed rat (7.9%, 3/38) (Zhao et al., 2020), Chipmunk (17.6%, 49/279 (Deng et al., 2018), Asian house rat (23.1%, 31/134) (Zhao et al., 2020), Chinese

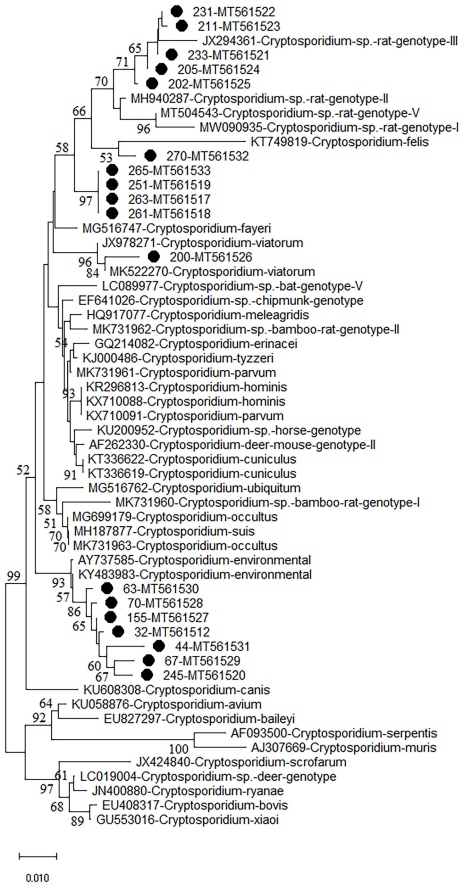

FIGURE 1 | Phylogenetic analyses of SSU rRNA gene of *Cryptosporidium* spp. using neighbor-joining (NJ) method (Kimura 2-parameter model, 1,000 replicates). Bootstrap values below 50% are not shown. *Cryptosporidium* isolates identified in the present study are pointed out by solid circles.

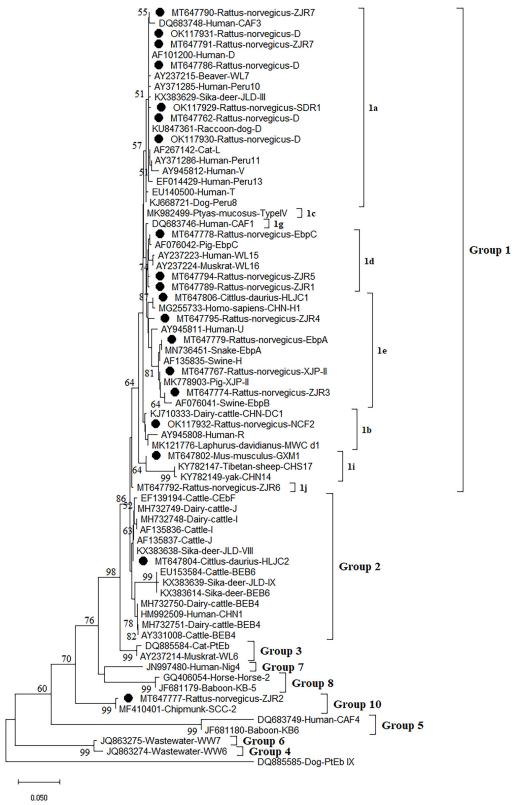

FIGURE 2 | Phylogenetic analyses of ITS gene of *Enterocytozoon bieneusi* using neighbor-joining (NJ) method (Kimura 2-parameter model, 1,000 replicates). Bootstrap values below 50% are not shown. *E. bieneusi* isolates identified in the present study are pointed out by solid circles.

white-bellied rat (18.2% 6/33) (Zhao et al., 2020), Lesser rice-feld rat (36.4%, 16/44) (Zhao et al., 2020). Coinfection (n = 3) of *E. bieneusi* and *Cryptosporidium* spp. was also found in the present study. Different susceptibility of different rodent species, different sampling time and sample size, animal age, and animal welfare could affect the prevalence of *Cryptosporidium* spp. and *E. bieneusi* in different rodent species in different regions.

Although *Cryptosporidium* spp. in rodent feces collected in summer (6/215, 2.8%, 95% CI 0.6-5.0) has a slightly lower prevalence than those collected in autumn (12/321, 3.7%, 95% CI 1.7-5.8), the difference was not significant statistically (P = 0.77) (**Table 1**). Moreover, the temperature and humidity in summer (49/215, 22.8%, 95% CI 17.1-28.4) may be more suitable for the survival of *E. bieneusi* oocysts than in autumn (13/321, 4.0%, 95% CI 1.9-6.2), the infection risk of *E. bieneusi* had 0.12-fold increase (OR = 0.12, 95% CI 0.06-0.23) in rodent feces collected in autumn (4.0%, 95% CI 1.9-6.2) than that in summer (22.8%, 95% CI 17.1-28.4) in the investigated rodents (**Table 2**). The investigated rodents were more active in the summer temperature, which might be the other reason for these rodents to be infection and transmission increase. Other ecological factors such as climate, food resources, breeding, physical activity, etc, which might affect the accuracy of prevalence of the two pathogens, should also be investigated in the further study.

More than 30 *Cryptosporidium* species/genotypes have been identified in rodents. However, only five species/genotypes were identified in this study, including *C. viatorum, C. felis, Cryptosporidium* sp. rat genotype II/III, *Cryptosporidium* sp. novel1, and *Cryptosporidium* sp. novel2. Among them, *Cryptosporidium* sp. rat genotype II/III, previously reported in rodents (García-Livia et al., 2020; Ježková et al., 2021), was also identified in this study, which was further confirmed that *Cryptosporidium* sp. rat genotype II/III was one of the prevalent *Cryptosporidium* genotypes in rodents. Moreover, two uncertain species of *Cryptosporidium* (*Cryptosporidium* sp. novel1 and novel2) were also identified in this study. *Cryptosporidium* sp. novel1 (isolates 251, 261, 263, and 265) was grouped into a new separate clade. *Cryptosporidium* sp. novel2 (isolates 32, 44, 63, 67, 70, 155, and 245), grouped with *Cryptosporidium* environmental. The results indicate two new genotypes/species that have clustered a branch in phylogenetic analysis with environmental isolates of *Cryptosporidium* spp.

One of the reasons that in environmental samples, it is difficult to determine the species and genotype is the simultaneous contamination of several species and genotypes in samples that after sequencing cannot detect a known species or genotype. Unfortunately, other genes such as COWP and HSP70 of the uncertain species have also not been successfully amplified. Thus, the investigation should be continue performed to further confirm whether presence of the two uncertain species of *Cryptosporidium* in wild rodents. *C. viatorum*, has been identified in humans (Insulander et al., 2013; Lebbad et al., 2013; Adamu et al., 2014; Ayinmode et al., 2014; De Lucio et al., 2016; Sanchez et al., 2017; Ukwah et al., 2017; Sannella et al., 2019). *C. viatorum* was first found in travellers who returned to the United Kingdom from the Indian subcontinent, with clinical signs of diarrhea, fever, headache, abdominal pain, nausea, vomiting, and marked weight loss (Elwin et al., 2012). So far, *C. viatorum* has been documented in the following countries: Bangladesh, Ethiopia, Barbados, Kenya, Colombia, Nigeria, Pakistan, Guatemala, India, and Nepal (Insulander et al., 2013; Lebbad et al., 2013; Adamu et al., 2014; Ayinmode et al., 2014; De Lucio et al., 2016; Sanchez et al., 2017; Ukwah et al., 2017; Sannella et al., 2019). Besides, *C. viatorum* was also found in China, such as Hainan Province (*Leopoldamys edwardsi*), Guangdong Province (*Berylms bowersi*), and Chongqing City (*Leopoldamys edwardsi*) in China, and in Australia (*Rattus lutreolus*) (Koehler et al., 2018; Chen et al., 2019; Zhao et al., 2019). C. felis has been widely reported in cats (Jiang et al., 2020), in addition to patients with HIV/AIDS in Peru, Ethiopia, Nigeria, Jamaica, and Portugal (Cama et al., 2003; Jiang et al., 2020). In this study, *C. viatorum* and *C. felis* were found in *M. musculus* and *S. dauricus*, which was worth for further research, e.g., whether wild rodents are potentially important reservoirs for *C. viatorum* and *C. felis* transmission to humans. More importantly, this is the first study showing existence of *Cryptosporidium* spp. in *S. dauricus*, which has expanded the host ranges of *Cryptosporidium*.

At present, more than 400 genotypes of *E. bieneusi* have been identified, most of which exhibit host specificity (Santín and Fayer, 2011; Wang S. N. et al., 2020). At least 48 genotypes of *E. bieneusi* infect both human and animals, bringing zoonoses risks (Li and Xiao, 2019). Through phylogenetic analysis, these genotypes were divided into at least 11 groups, e.g., Group 1 to Group 11 (Zhao et al., 2018; Wang S. N. et al., 2020). To date, some genotypes were found in rodents, of which 15 genotypes (CZ3, Peru6, BEB6, C, D, EbpA, EbpC, H, Peru8, Peru11, Peru16, PigITS5, S6, IV, and Nig7) were reported to infect human. In China, EbpA, EbpC, CHY1, N, D, Peru11, S7, SCC-2, PGP, Peru6, J, PigEBITS7, BR1 and BR2, Type IV, Peru8, ESH02, CHG5, HNR-I to HNR-VII, K, CQR-1, CQR-2, CQR-3, GDR-1, GDR-2, GDR-3. SCC-1, SCC-3, SCC-4, CHY1, Nig7 CHG9, ChG14, BEB6, CHG2, SC02, CE01 and CE02 genotypes were reported in rodents (Feng et al., 2009; Zhao et al., 2018; Wang et al., 2019; Li J. et al., 2020; Wang J. et al., 2020; Zhao et al., 2020). However, only 5 known genotypes (XJP-II, EbpC, EbpA, D, and NCF7) and 11 novel genotypes (ZIR1 to ZJR7, GXM1, HLJC1, HLJC2, and SDR1) were identified in the present study. Among them, 14 genotypes were clustered into a highly-supported monophyletic clade (Group 1), indicating that these genotypes are human-pathogenic types and may cause infection between humans and rodents, thus becoming a public health significance. This was the first record of *E. bieneusi* in *S. dauricus*. Eleven novel genotypes (ZIR1 to ZJR7, GXM1, HLJC1, HLJC2, and SDR1) were recorded in rodents for the first time. Of which, ZJR1, ZJR3, ZJR4, ZJR5, ZJR6, ZJR7, SDR1, HLJC1, and GXM1 were grouped into Group 1 (**Figure 2**), thus suggesting that rodents (*R. norvegicus*, *M. musculus*, and *S. dauricus*) may play an important role in the transmission of *E. bieneusi* between rodents and humans. Genotype XJP-II was previously found in pigs in Xinjiang (Li D. F. et al., 2019b), and NCF2 was also identified in farmed foxes (*Vulpes lagopus*) (Zhang et al., 2016; Ma et al., 2020) and raccoon dogs (*Nyctereutes procyonoides*) (Xu et al., 2016) in China, Kangaroo in Australia (Zhang Y. et al., 2018). Genotypes EbpC, EbpA, and D were frequently found in humans and a broad range of animals (Wang et al., 2013; Liu et al., 2017; Qi et al., 2018; Zhang X. X. et al., 2018; Zou et al., 2018; Wang H. et al., 2020; Wang Y. et al., 2020; Yu et al., 2020). The results showed that natural transmission of *E. bieneusi* among rodents, humans and many other animals may occur. More importantly, the three ITS genotypes were also found in water in China, which should be paid more attention to prevent the water-borne transmission of *E. bieneusi* (Hu et al., 2014).

Collectively, the present study firstly demonstrated that existence of *Cryptosporidium* spp. (3.4%, 18/536) and *E. bieneusi* (11.6%, 62/536) in rodents in Shanxi, Guangxi, and Zhejiang, China. Three known *Cryptosporidium* species/genotypes (*C. viatorum*, *C. felis*, and *Cryptosporidium* sp. rat genotype II/III), two uncertain *Cryptosporidium* species/genotypes (*Cryptosporidium* sp. novel1 and *Cryptosporidium* sp. novel2), 5 known *E. bieneusi* genotypes (XJP-II, EbpC, EbpA, D, and NCF7) and 11 novel *E. bieneusi* genotypes (ZJR1 to ZJR7, GXM1, HLJC1, HLJC2, and SDR1) were identified in the investigated rodents, suggesting rodents can act as a potential source of human and animal infections. *E. bieneusi* was more prevalent in *R. norvegicus*, whereas *Cryptosporidium* spp. was more frequently identified in *S. dauricus*. The present study also demonstrated that *S. dauricus* was the host of *E. bieneusi* and *Cryptosporidium* spp. for the first time. This study expanded the host range of these two parasites, which not only provided basic data for distribution of *E. bieneusi* and *Cryptosporidium* genotypes/species, but also provided foundation data for the prevention and control of *E. bieneusi* and *Cryptosporidium* spp. in China.

DATA AVAILABILITY STATEMENT

The datasets presented in this study can be found in online repositories. The names of the repository/repositories and accession number(s) can be found below: https://www.ncbi.

nlm.nih.gov/genbank/, MT647749-MT647806, OK117929-OK117932, MT561508-MT561533.

ETHICS STATEMENT

This study was approved by the Ethics Committee of Qingdao Agricultural University.

AUTHOR CONTRIBUTIONS

QZ, Y-CW, and H-TS conceived and designed the study and critically revised the manuscript. H-BN, S-YQ, DY, Z-HF, Z-HG, H-XW, H-YQ, and NX collected the samples. Z-YS, MZ, and Y-ZS performed the experiments. H-BN, Y-ZS, and S-YQ analyzed the data and drafted the manuscript. All authors contributed to the article and approved the submitted version.

FUNDING

This work was supported by the National Key R&D Program of China, the National Innovation and Entrepreneurship Training Program for College Students of Shandong Province (202110435018), the State Key Laboratory of Veterinary Etiological Biology, Lanzhou Veterinary Research Institute, Chinese Academy of Agricultural Sciences (SKLVEB2019KFKT012), the Wild Animal Disease Monitoring and Early Warning System Maintenance Project (2130211), and the Research Foundation for Distinguished Scholars of Qingdao Agricultural University (665-1120046).

REFERENCES

Abarca, N., Santín, M., Ortega, S., Maloney, J. G., George, N. S., Molokin, A., et al. (2021). Molecular Detection and Characterization of Blastocystis Sp. and *Enterocytozoon Bieneusi* in Cattle in Northern Spain. *Vet. Sci.* 8, 191. doi: 10.3390/vetsci8090191

Adamu, H., Petros, B., Zhang, G., Kassa, H., Amer, S., Ye, J., et al. (2014). Distribution and Clinical Manifestations of *Cryptosporidium* Species and Subtypes in HIV/AIDS Patients in Ethiopia. *PloS Negl. Trop. Dis.* 8 (4), e2831. doi: 10.1371/journal.pntd.0002831

Ayinmode, A. B., Zhang, H., Dada-Adegbola, H. O., and Xiao, L. (2014). *Cryptosporidium Hominis* Subtypes and *Enterocytozoon Bieneusi* Genotypes in HIV-Infected Persons in Ibadan, Nigeria. *Zoonoses Public Health* 61 (4), 297–303. doi: 10.1111/zph.12072

Backhans, A., Jacobson, M., Hansson, I., Lebbad, M., Lambertz, S. T., Gammelgård, E., et al. (2013). Occurrence of Pathogens in Wild Rodents Caught on Swedish Pig and Chicken Farms. *Epidemiol. Infect.* 141 (9), 1885–1891. doi: 10.1017/S0950268812002609

Bajer, A., Bednarska, M., Pawelczyk, A., Behnke, J. M., Gilbert, F. S., and Sinski, E. (2002). Prevalence and Abundance of *Cryptosporidium Parvum* and *Giardia* Spp. In Wild Rural Rodents From the Mazury Lake District Region of Poland. *Parasitology* 125 (Pt 1), 21–34. doi: 10.1017/s0031182002001865

Cama, V. A., Bern, C., Sulaiman, I. M., Gilman, R. H., Ticona, E., Vivar, A., et al. (2003). *Cryptosporidium* Species and Genotypes in HIV-Positive Patients in Lima, Peru. *J. Eukaryot Microbiol.* 50 (Suppl), 531–533. doi: 10.1111/j.1550-7408.2003.tb00620.x

Cama, V. A., Pearson, J., Cabrera, L., Pacheco, L., Gilman, R., Meyer, S., et al. (2007). Transmission of *Enterocytozoon Bieneusi* Between a Child and Guinea Pigs. *J. Clin. Microbiol.* 45 (8), 2708–2710. doi: 10.1128/JCM.00725-07

Chen, Y. W., Zheng, W. B., Zhang, N. Z., Gui, B. Z., Lv, Q. Y., Yan, J. Q., et al. (2019). Identification of *Cryptosporidium Viatorum* XVa Subtype Family in Two Wild Rat Species in China. *Parasit. Vectors* 12 (1), 502. doi: 10.1186/s13071-019-3763-6

Danišová, O., Valenčáková, A., Stanko, M., Luptáková, L., and Hasajová, A. (2015). First Report of *Enterocytozoon Bieneusi* and *Encephalitozoon Intestinalis* Infection of Wild Mice in Slovakia. *Ann. Agric. Environ. Med.* 22 (2), 251–252. doi: 10.5604/12321966.1152075

Danišová, O., Valenčáková, A., Stanko, M., Luptáková, L., Hatalová, E., and Čanády, A. (2017). Rodents as a Reservoir of Infection Caused by Multiple Zoonotic Species/Genotypes of C. Parvum, *C. Hominis*, *C. Suis*, *C. Scrofarum*, and the First Evidence of *Cryptosporidium Muskrat* Genotypes I and II of Rodents in Europe. *Acta Trop.* 172, 29–35. doi: 10.1016/j.actatropica.2017.04.013

De Lucio, A., Amor-Aramendia, A., Bailo, B., Saugar, J. M., Anegagrie, M., Arroyo, A., et al. (2016). Prevalence and Genetic Diversity of Giardia Duodenalis and *Cryptosporidium* Spp. Among School Children in a Rural Area of the Amhara Region, North-West Ethiopia. *PloS One* 11 (7), e0159992. doi: 10.1371/journal.pone.0159992

Deng, L., Li, W., Yu, X., Gong, C., Liu, X., Zhong, Z., et al. (2016). First Report of the Human-Pathogenic *Enterocytozoon Bieneusi* From Red-Bellied Tree Squirrels (*Callosciurus Erythraeus*) in Sichuan, China. *PloS One* 11 (9), e0163605. doi: 10.1371/journal.pone.0163605

Deng, L., Li, W., Zhong, Z., Chai, Y., Yang, L., Zheng, H., et al. (2018). Molecular Characterization and New Genotypes of *Enterocytozoon Bieneusi* in Pet Chipmunks (*Eutamias Asiaticus*) in Sichuan Province. *China BMC Microbiol.* 18 (1), 37. doi: 10.1186/s12866-018-1175-y

Didier, E. S., Weiss, L. M., Cali, A., and Marciano-Cabral, F. (2009). Overview of the Presentations on Microsporidia and Free-Living Amebae at the 10th International Workshops on Opportunistic Protists. *Eukaryot Cell.* 8 (4), 441–445. doi: 10.1128/EC.00302-08

Elwin, K., Hadfield, S. J., Robinson, G., Crouch, N. D., and Chalmers, R. M. (2012). *Cryptosporidium Viatorum* N. Sp. (Apicomplexa: *Cryptosporidiidae*) Among Travellers Returning to Great Britain From the Indian Subcontinen-2011. *Int. J. Parasitol.* 42 (7), 675–682. doi: 10.1016/j.ijpara.2012.04.016

Essid, R., Menotti, J., Hanen, C., Aoun, K., and Bouratbine, A. (2018). Genetic Diversity of *Cryptosporidium* Isolates From Human Populations in an Urban Area of Northern Tunisia. *Infect. Genet. Evol.* 58, 237–242. doi: 10.1016/j.meegid.2018.01.004

Feng, Y. (2010). *Cryptosporidium* in Wild Placental Mammals. *Exp. Parasitol.* 124 (1), 128–137. doi: 10.1016/j.exppara.2008.11.005

Feng, Y., Alderisio, K. A., Yang, W., Blancero, L. A., Kuhne, W. G., Nadareski, C. A., et al. (2007). *Cryptosporidium* Genotypes in Wildlife From a New York Watershed. *Appl. Environ. Microbiol.* 73 (20), 6475–6483. doi: 10.1128/AEM.01034-07

Feng, X., Reddy, V. K., Mayanja-Kizza, H., Weiss, L. M., Marton, L. J., and Tzipori, S. (2009). Therapeutic Evaluation of Polyamine Analogue Drug Candidates Against *Enterocytozoon Bieneusi* in a SCID Mouse Model. *Antimicrob. Agents Chemother.* 53 (6), 2417–2423. doi: 10.1128/AAC.01113-08

Feng, Y., Ryan, U. M., and Xiao, L. (2018). Genetic Diversity and Population Structure of *Cryptosporidium*. *Trends Parasitol.* 34 (11), 997–1011. doi: 10.1016/j.pt.2018.07.009

Foo, C., Farrell, J., Boxell, A., Robertson, I., and Ryan, U. M. (2007). Novel *Cryptosporidium* Genotype in Wild Australian Mice (*Mus Domesticus*). *Appl. Environ. Microbiol.* 73 (23), 7693–7696. doi: 10.1128/AEM.00848-07

García-Livia, K., Martín-Alonso, A., and Foronda, P. (2020). Diversity of *Cryptosporidium* Spp. In Wild Rodents From the Canary Islands, Spain. *Parasit. Vectors* 13 (1), 445. doi: 10.1186/s13071-020-04330-9

Gholipoury, M., Rezai, H. R., Namroodi, S., and Arab Khazaeli, F. (2016). Zoonotic and Non-Zoonotic Parasites of Wild Rodents in Turkman Sahra, Northeastern Iran. *Iran J. Parasitol.* 11 (3), 350–357.

Gui, B. Z., Zou, Y., Chen, Y. W., Li, F., Jin, Y. C., Liu, M. T., et al. (2020). Novel Genotypes and Multilocus Genotypes of *Enterocytozoon Bieneusi* in Two Wild

Rat Species in China: Potential for Zoonotic Transmission. *Parasitol. Res.* 119 (1), 283–290. doi: 10.1007/s00436-019-06491-8

Guo, Y., Alderisio, K. A., Yang, W., Cama, V., Feng, Y., and Xiao, L. (2014). Host Specificity and Source of *Enterocytozoon Bieneusi* Genotypes in a Drinking Source Watershed. *Appl. Environ. Microbiol.* 80 (1), 218–225. doi: 10.1128/AEM.02997-13

Holubová, N., Zikmundová, V., Limpouchová, Z., Sak, B., Konečný, R., Hlásková, L., et al. (2019). *Cryptosporidium Proventriculi* Sp. N. (Apicomplexa: *Cryptosporidiidae*) in Psittaciformes Birds. *Eur. J. Protistol.* 69, 70–87. doi: 10.1016/j.ejop.2019.03.001

Hu, Y., Feng, Y., Huang, C., and Xiao, L. (2014). Occurrence, Source, and Human Infection Potential of *Cryptosporidium* and *Enterocytozoon Bieneusi* in Drinking Source Water in Shanghai, China, During a Pig Carcass Disposal Incident. *Environ. Sci. Technol.* 48 (24), 14219–14227. doi: 10.1021/es504464t

Insulander, M., Silverlas, C., Lebbad, M., Karlsson, L., Mattsson, J. G., and Svenungsson, B. (2013). Molecular Epidemiology and Clinical Manifestations of Human Cryptosporidiosis in Sweden. *Epidemiol. Infect.* 141 (5), 1009–1020. doi: 10.1017/S0950268812001665

Ježková, J., Prediger, J., Holubová, N., Sak, B., Konečný, R., Feng, Y., et al. (2021). *Cryptosporidium Ratti* N. Sp. (Apicomplexa: Cryptosporidiidae) and Genetic Diversity of Cryptosporidium Spp. In Brown Rats (*Rattus Norvegicus*) in the Czech Republic. *Parasitology* 148 (1), 84–97. doi: 10.1017/S0031182020001833

Jiang, W., Roellig, D. M., Lebbad, M., Beser, J., Troell, K., Guo, Y., et al. (2020). Subtype Distribution of Zoonotic Pathogen *Cryptosporidium Felis* in Humans and Animals in Several Countries. *Emerg. Microbes Infect.* 9 (1), 2446–2454. doi: 10.1080/22221751.2020.1840312

Kimura, A., Edagawa, A., Okada, K., Takimoto, A., Yonesho, S., and Karanis, P. (2007). Detection and Genotyping of *Cryptosporidium* From Brown Rats (*Rattus Norvegicus*) Captured in an Urban Area of Japan. *Parasitol. Res.* 100 (6), 1417–1420. doi: 10.1007/s00436-007-0488-9

Koehler, A. V., Wang, T., Haydon, S. R., and Gasser, R. B. (2018). *Cryptosporidium Viatorum* From the Native Australian Swamp Rat *Rattus Lutreolus* - An Emerging Zoonotic Pathogen? *Int. J. Parasitol. Parasit. Wildl.* 7 (1), 18–26. doi: 10.1016/j.ijppaw.2018.01.004

Krumkamp, R., Aldrich, C., Maiga-Ascofare, O., Mbwana, J., Rakotozandrindrainy, N., Borrmann, S., et al. (2021). Transmission of *Cryptosporidium* Species Among Human and Animal Local Contact Networks in Sub-Saharan Africa: A Multicountry Study. *Clin. Infect. Dis.* 72 (8), 1358–1366. doi: 10.1093/cid/ciaa223

Kváč, M., Hofmannová, L., Bertolino, S., Wauters, L., Tosi, G., and Modrý, D. (2008). Natural Infection With Two Genotypes of *Cryptosporidium* in Red Squirrels (*Sciurus Vulgaris*) in Italy. *Folia Parasitol. (Praha)* 55 (2), 95–99. doi: 10.14411/fp.2008.012

Lebbad, M., Beser, J., Insulander, M., Karlsson, L., Mattsson, J. G., Svenungsson, B., et al. (2013). Unusual Cryptosporidiosis Cases in Swedish Patients: Extended Molecular Characterization of *Cryptosporidium Viatorum* and *Cryptosporidium Chipmunk* Genotype I. *Parasitology* 140 (14), 1735–1740. doi: 10.1017/S003118201300084X

Li, W., Feng, Y., and Santin, M. (2019). Host Specificity of *Enterocytozoon Bieneusi* and Public Health Implications. *Trends Parasitol.* 35, 436–451. doi: 10.1016/j.pt.2019.04.004

Li, J., Jiang, Y., Wang, W., Chao, L., Jia, Y., Yuan, Y., et al. (2020). Molecular Identification and Genotyping of *Enterocytozoon Bieneusi* in Experimental Rats in China. *Exp. Parasitol.* 210, 107850. doi: 10.1016/j.exppara.2020.107850

Li, Q., Li, L., Tao, W., Jiang, Y., Wan, Q., Lin, Y., et al. (2016). Molecular Investigation of *Cryptosporidium* in Small Caged Pets in Northeast China: Host Specificity and Zoonotic Implications. *Parasitol. Res.* 115 (7), 2905–2911. doi: 10.1007/s00436-016-5076-4

Liu, H., Jiang, Z., Yuan, Z., Yin, J., Wang, Z., Yu, B., et al. (2017). Infection by and Genotype Characteristics of *Enterocytozoon Bieneusi* in HIV/AIDS Patients From Guangxi Zhuang Autonomous Region, China. *BMC Infect. Dis.* 17 (1), 684. doi: 10.1186/s12879-017-2787-9

Liu, X., Zhou, X., Zhong, Z., Zuo, Z., Shi, J., Wang, Y., et al. (2015). Occurrence of Novel and Rare Subtype Families of *Cryptosporidium* in Bamboo Rats (*Rhizomys Sinensis*) in China. *Vet. Parasitol.* 207 (1-2), 144–148. doi: 10.1016/j.vetpar.2014.11.009

Li, W., and Xiao, L. (2019). Multilocus Sequence Typing and Population Genetic Analysis of *Enterocytozoon Bieneusi*: Host Specificity and Its Impacts on Public Pealth. *Front. Genet.* 10:307. doi: 10.3389/fgene.2019.00307

Li, W., and Xiao, L. (2020). Ecological and Public Health Significance of *Enterocytozoon Bieneusi*. *One Health* 12, 100209. doi: 10.1016/j.onehlt.2020.100209

Li, F., Zhang, Z., Hu, S., Zhao, W., Zhao, J., Kváč, M., et al. (2020b). Common Occurrence of Divergent *Cryptosporidium* Species and *Cryptosporidium Parvum* Subtypes in Farmed Bamboo Rats (*Rhizomys Sinensis*). *Parasit. Vectors* 13 (1), 149. doi: 10.1186/s13071-020-04021-5

Li, D. F., Zhang, Y., Jiang, Y. X., Xing, J. M., Tao, D. Y., Zhao, A. Y., et al. (2019). Genotyping and Zoonotic Potential of *Enterocytozoon Bieneusi* in Pigs in Xinjiang, China. *Front. Microbiol.* 10:2401. doi: 10.3389/fmicb.2019.02401

Li, F., Zhao, W., Zhang, C., Guo, Y., Li, N., Xiao, L., et al. (2020a). *Cryptosporidium* Species and C. Parvum Subtypes in Farmed Bamboo Rats. *Pathogens* 9 (12):1018. doi: 10.3390/pathogens9121018

Lv, C., Zhang, L., Wang, R., Jian, F., Zhang, S., Ning, C., et al. (2009). *Cryptosporidium* Spp. In Wild, Laboratory, and Pet Rodents in China: Prevalence and Molecular Characterization. *Appl. Environ. Microbiol.* 75 (24), 7692–7699. doi: 10.1128/AEM.01386-09

Ma, Y. Y., Zou, Y., Ma, Y. T., Nie, L. B., Xie, S. C., Cong, W., et al. (2020). Molecular Detection and Genotype Distribution of *Enterocytozoon Bieneusi* in Farmed Silver Foxes (*Vulpes Vulpes*) and Arctic Foxes (*Vulpes Lagopus*) in Shandong Province, Eastern China. *Parasitol. Res.* 119 (1), 321–326. doi: 10.1007/s00436-019-06538-w

Mirzaghavami, M., Sadraei, J., and Forouzandeh, M. (2016). Detection of *Cryptosporidium* Spp. In Free Ranging Animals of Tehran, Iran. *J. Parasit. Dis.* 40 (4), 1528–1531. doi: 10.1007/s12639-015-0720-y

Murakoshi, F., Fukuda, Y., Matsubara, R., Kato, Y., Sato, R., Sasaki, T., et al. (2013). Detection and Genotyping of *Cryptosporidium* Spp. In Large Japanese Field Mice, *Apodemus Speciosus*. *Vet. Parasitol.* 196 (1-2), 184–188. doi: 10.1016/j.vetpar.2013.02.011

Nakai, Y., Hikosaka, K., Sato, M., Sasaki, T., Kaneta, Y., and Okazaki, N. (2004). Detection of *Cryptosporidium Muris* Type Oocysts From Beef Cattle in a Farm and From Domestic and Wild Animals in and Around the Farm. *J. Vet. Med. Sci.* 66 (8), 983–984. doi: 10.1292/jvms.66.983

Ng-Hublin, J. S., Singleton, G. R., and Ryan, U. (2013). Molecular Characterization of *Cryptosporidium* Spp. From Wild Rats and Mice From Rural Communities in the Philippines. *Infect. Genet. Evol.* 16, 5–12. doi: 10.1016/j.meegid.2013.01.011

NIAID Emerging Infectious Diseases/Pathogens. Available at: https://www.niaid.nih.gov/research/emerging-infectious-diseases-pathogens (Accessed 7 May 2018).

Paparini, A., Jackson, B., Ward, S., Young, S., and Ryan, U. M. (2012). Multiple *Cryptosporidium* Genotypes Detected in Wild Black Rats (*Rattus Rattus*) From Northern Australia. *Exp. Parasitol.* 131 (4), 404–412. doi: 10.1016/j.exppara.2012.05.009

Perec-Matysiak, A., Buńkowska-Gawlik, K., Kváč, M., Sak, B., Hildebrand, J., and Leśniańska, K. (2015). Diversity of *Enterocytozoon Bieneusi* Genotypes Among Small Rodents in Southwestern Poland. *Vet. Parasitol.* 214 (3-4), 242–246. doi: 10.1016/j.vetpar.2015.10.018

Qi, M., Li, J., Zhao, A., Cui, Z., Wei, Z., Jing, B., et al. (2018). Host Specificity of *Enterocytozoon Bieneusi* Genotypes in Bactrian Camels (*Camelus Bactrianus*) in China. *Parasit. Vectors* 11 (1), 219. doi: 10.1186/s13071-018-2793-9

Qi, M., Luo, N., Wang, H., Yu, F., Wang, R., Huang, J., et al. (2015). Zoonotic *Cryptosporidium* Spp. And *Enterocytozoon Bieneusi* in Pet Chinchillas (*Chinchilla Lanigera*) in China. *Parasitol. Int.* 64 (5), 339–341. doi: 10.1016/j.parint.2015.05.007

Roellig, D. M., Salzer, J. S., Carroll, D. S., Ritter, J. M., Drew, C., Gallardo-Romero, N., et al. (2015). Identification of *Giardia Duodenalis* and *Enterocytozoon Bieneusi* in an Epizoological Investigation of a Laboratory Colony of Prairie Dogs, Cynomys Ludovicianus. *Vet. Parasitol.* 210 (1-2), 91–97. doi: 10.1016/j.vetpar.2015.03.022

Saki, J., Foroutan-Rad, M., and Asadpouri, R. (2016). Molecular Characterization of *Cryptosporidium* Spp. In Wild Rodents of Southwestern Iran Using 18S rRNA Gene Nested-PCR-RFLP and Sequencing Techniques. *J. Trop. Med.* 2016:6834206. doi: 10.1155/2016/6834206

Sak, B., Kváč, M., Květoňová, D., Albrecht, T., and Piálek, J. (2011). The First Report on Natural Enterocytozoon Bieneusi and *Encephalitozoon* Spp. Infections in Wild East-European House Mice (*Mus Musculus Musculus*) and West-European House Mice (*M. M. Domesticus*) in a Hybrid Zone Across the Czech Republic-Germany Border. *Vet. Parasitol.* 178 (3-4), 246–250. doi: 10.1016/j.vetpar.2010.12.044

Sanchez, A., Munoz, M., Gomez, N., Tabares, J., Segura, L., Salazar, A., et al. (2017). Molecular Epidemiology of *Giardia*, *Blastocystis* and *Cryptosporidium* Among Indigenous Children From the Colombian Amazon Basin. *Front. Microbiol.* 8, 248. doi: 10.3389/fmicb.2017.00248

Sannella, A. R., Suputtamongkol, Y., Wongsawat, E., and Caccio, S. M. (2019). A Retrospective Molecular Study of *Cryptosporidium* Species and Genotypes in HIV-Infected Patients From Thailand. *Parasit. Vectors* 12 (1), 91. doi: 10.1186/s13071-019-3348-4

Santin, M. (2015). "Enterocytozoon Bieneusi," in *Biology of Foodborne Parasites*. Eds. L. Xiao, U. Ryan and Y. Feng (Boca Raton, FL, USA: CRC Press), 149–174.

Santín, M., and Fayer, R. (2011). Microsporidiosis: *Enterocytozoon Bieneusi* in Domesticated and Wild Animals. *Res. Vet. Sci.* 90 (3), 363–371. doi: 10.1016/j.rvsc.2010.07.014

Song, J., Kim, C. Y., Chang, S. N., Abdelkader, T. S., Han, J., Kim, T. H., et al. (2015). Detection and Molecular Characterization of *Cryptosporidium* Spp. From Wild Rodents and Insectivores in South Korea. *Korean J. Parasitol.* 53 (6), 737–743. doi: 10.3347/kjp.2015.53.6.737

Stenger, B. L., Clark, M. E., Kváč, M., Khan, E., Giddings, C. W., Dyer, N. W., et al. (2015). Highly Divergent 18S rRNA Gene Paralogs in a *Cryptosporidium* Genotype From Eastern Chipmunks (*Tamias Striatus*). *Infect. Genet. Evol.* 32, 113–123. doi: 10.1016/j.meegid.2015.03.003

Stenger, B., Clark, M. E., Kváč, M., Khan, E., Giddings, C. W., Prediger, J., et al. (2015). North American Tree Squirrels and Ground Squirrels With Overlapping Ranges Host Different *Cryptosporidium* Species and Genotypes. *Infect. Genet. Evol.* 36, 287–293. doi: 10.1016/j.meegid.2015.10.002

Sutthikornchai, C., Popruk, S., Mahittikorn, A., Arthan, D., Soonthornworasiri, N., Paratthakonkun, C., et al. (2021). Molecular Detection of Cryptosporidium Spp., *Giardia Duodenalis*, and *Enterocytozoon Bieneusi* in School Children at the Thai-Myanmar Border. *Parasitol. Res.* 120 (8), 2887–2895. doi: 10.1007/s00436-021-07242-4

Ukwah, B. N., Ezeonu, I. M., Ezeonu, C. T., Roellig, D., and Xiao, L. (2017). Cryptosporidium Species and Subtypes in Diarrheal Children and HIV-Infected Persons in Ebonyi and Nsukka, Nigeria. *J. Infect. Dev. Ctries.* 11 (2), 173–179. doi: 10.3855/jidc.8034

Wang, H., Lin, X., Sun, Y., Qi, N., Lv, M., Xiao, W., et al. (2020). Occurrence, Risk Factors and Genotypes of *Enterocytozoon Bieneusi* in Dogs and Cats in Guangzhou, Southern China: High Genotype Diversity and Zoonotic Concern. *BMC Vet. Res.* 16 (1), 201. doi: 10.1186/s12917-020-02421-4

Wang, H., Liu, Q., Jiang, X., Zhang, Y., Zhao, A., Cui, Z., et al. (2019). Dominance of Zoonotic Genotype D of *Enterocytozoon Bieneusi* in Bamboo Rats (*Rhizomys Sinensis*). *Infect. Genet. Evol.* 73, 113–118. doi: 10.1016/j.meegid.2019.04.025

Wang, J., Lv, C., Zhao, D., Zhu, R., Li, C., and Qian, W. (2020). First Detection and Genotyping of *Enterocytozoon Bieneusi* in Pet Fancy Rats (*Rattus Norvegicus*) and Guinea Pigs (*Cavia Porcellus*) in China. *Parasite* 27, 21. doi: 10.1051/parasite/2020019

Wang, S. N., Sun, Y., Zhou, H. H., Lu, G., Qi, M., Liu, W. S., et al. (2020). Prevalence and Genotypic Identification of *Cryptosporidium* Spp. And *Enterocytozoon Bieneusi* in Captive Asiatic Black Bears (*Ursus Thibetanus*) in Heilongjiang and Fujian Provinces of China. *BMC Vet. Res.* 16 (1), 84. doi: 10.1186/s12917-020-02292-9

Wang, Y., Zhang, K., Zhang, Y., Wang, K., Gazizova, A., Wang, L., et al. (2020). First Detection of *Enterocytozoon Bieneusi* in Whooper Swans (*Cygnus Cygnus*) in China. *Parasit. Vectors* 13 (1), 5. doi: 10.1186/s13071-020-3884-y

Wang, L., Zhang, H., Zhao, X., Zhang, L., Zhang, G., Guo, M., et al. (2013). Zoonotic *Cryptosporidium* Species and *Enterocytozoon Bieneusi* Genotypes in HIV-Positive Patients on Antiretroviral Therapy. *J. Clin. Microbiol.* 51 (2), 557–563. doi: 10.1128/JCM.02758-12

Wei, Z., Liu, Q., Zhao, W., Jiang, X., Zhang, Y., Zhao, A., et al. (2019). Prevalence and Diversity of *Cryptosporidium* Spp. In Bamboo Rats (*Rhizomys Sinensis*) in South Central China. *Int. J. Parasitol. Parasit. Wildl.* 9, 312–316. doi: 10.1016/j.ijppaw.2019.06.010

Xu, C., Ma, X., Zhang, H., Zhang, X. X., Zhao, J. P., Ba, H. X., et al. (2016). Prevalence, Risk Factors and Molecular Characterization of *Enterocytozoon Bieneusi* in Raccoon Dogs (*Nyctereutes Procyonoides*) in Five Provinces of Northern China. *Acta Trop.* 161, 68–72. doi: 10.1016/j.actatropica.2016.05.015

Yu, F., Cao, Y., Wang, H., Liu, Q., Zhao, A., Qi, M., et al. (2020). Host-Adaptation of the Rare *Enterocytozoon Bieneusi* Genotype CHN4 in *Myocastor Coypus* (Rodentia: Echimyidae) in China. *Parasit. Vectors* 13 (1), 578. doi: 10.1186/s13071-020-04436-0

Zhang, X. X., Cong, W., Lou, Z. L., Ma, J. G., Zheng, W. B., Yao, Q. X., et al. (2016). Prevalence, Risk Factors and Multilocus Genotyping of *Enterocytozoon Bieneusi* in Farmed Foxes (*Vulpes Lagopus*), Northern China. *Parasit. Vectors* 9, 72. doi: 10.1186/s13071-016-1356-1

Zhang, X. X., Jiang, R. L., Ma, J. G., Xu, C., Zhao, Q., Hou, G., et al. (2018). *Enterocytozoon Bieneusi* in Minks (*Neovison Vison*) in Northern China: A Public Health Concern. *Front. Microbiol.* 9, 1221. doi: 10.3389/fmicb.2018.01221

Zhang, X., Jian, Y., Li, X., Ma, L., Karanis, G., and Karanis, P. (2018). The First Report of *Cryptosporidium* Spp. In Microtus Fuscus (*Qinghai Vole*) and Ochotona Curzoniae (*Wild Plateau Pika*) in the Qinghai-Tibetan Plateau Area, China. *Parasitol. Res.* 117 (5), 1401–1407. doi: 10.1007/s00436-018-5827-5

Zhang, Y., Koehler, A. V., Wang, T., Haydon, S. R., and Gasser, R. B. (2018). New Operational Taxonomic Units of *Enterocytozoon* in Three Marsupial Species. *Parasit. Vectors* 11 (1), 371. doi: 10.1186/s13071-018-2954-x

Zhao, W., Wang, J., Ren, G., Yang, Z., Yang, F., Zhang, W., et al. (2018). Molecular Characterizations of *Cryptosporidium* Spp. And *Enterocytozoon Bieneusi* in Brown Rats (*Rattus Norvegicus*) From Heilongjiang Province, China. *Parasit. Vectors* 11 (1), 313. doi: 10.1186/s13071-018-2892-7

Zhao, Z., Wang, R., Zhao, W., Qi, M., Zhao, J., Zhang, L., et al. (2015). Genotyping and Subtyping of *Giardia* and *Cryptosporidium* Isolates From Commensal Rodents in China. *Parasitology* 142 (6), 800–806. doi: 10.1017/S0031182014001929

Zhao, W., Zhou, H., Huang, Y., Xu, L., Rao, L., Wang, S., et al. (2019). *Cryptosporidium* Spp. In Wild Rats (*Rattus* Spp.) From the Hainan Province, China: Molecular Detection, Species/Genotype Identification and Implications for Public Health. *Int. J. Parasitol. Parasit. Wildl.* 9, 317–321. doi: 10.1016/j.ijppaw.2019.03.017

Zhao, W., Zhou, H., Yang, L., Ma, T., Zhou, J., Liu, H., et al. (2020). Prevalence, Genetic Diversity and Implications for Public Health of *Enterocytozoon Bieneusi* in Various Rodents From Hainan Province, China. *Parasit. Vectors* 13 (1), 438. doi: 10.1186/s13071-020-04314-9

Zou, Y., Hou, J. L., Li, F. C., Zou, F. C., Lin, R. Q., Ma, J. G., et al. (2018). Prevalence and Genotypes of *Enterocytozoon Bieneusi* in Pigs in Southern China. *Infect. Genet. Evol.* 66, 52–56. doi: 10.1016/j.meegid.2018.09.006

Conflict of Interest: Author Y-CW is employed by Veterinary Department, Muyuan Foods Co., Ltd.

The remaining authors declare that the research was conducted in the absence of any commercial or financial relationships that could be construed as a potential conflict of interest.

Publisher's Note: All claims expressed in this article are solely those of the authors and do not necessarily represent those of their affiliated organizations, or those of the publisher, the editors and the reviewers. Any product that may be evaluated in this article, or claim that may be made by its manufacturer, is not guaranteed or endorsed by the publisher.

frontiers in Cellular and Infection Microbiology

ORIGINAL RESEARCH
published: 26 November 2021
doi: 10.3389/fcimb.2021.788340

The Protective Role of TLR2 Mediates Impaired Autophagic Flux by Activating the mTOR Pathway During *Neospora caninum* Infection in Mice

Jielin Wang[1,2†], Xiaocen Wang[1†], Pengtao Gong[1†], Fu Ren[3], Xin Li[1], Nan Zhang[1], Xu Zhang[1], Xichen Zhang[1] and Jianhua Li[1*]*

[1] Key Laboratory of Zoonosis Research, Ministry of Education, College of Veterinary Medicine, Jilin University, Changchun, China, [2] Graduate College, Jinzhou Medical University, Jinzhou, China, [3] Department of Anatomy, Shenyang Medical College, Shenyang, China

OPEN ACCESS

Edited by:
Nian-Zhang Zhang,
Lanzhou Veterinary Research Institute (CAAS), China

Reviewed by:
Longxian Zhang,
Henan Agricultural University, China
Honglin Jia,
Harbin Veterinary Research Institute (CAAS), China

***Correspondence:**
Jianhua Li
jianhuali7207@163.com
Xichen Zhang
xczhang@jlu.edu.cn

[†]These authors have contributed equally to this work

Specialty section:
This article was submitted to Clinical Microbiology, a section of the journal Frontiers in Cellular and Infection Microbiology

Received: 02 October 2021
Accepted: 05 November 2021
Published: 26 November 2021

Citation:
Wang J, Wang X, Gong P, Ren F, Li X, Zhang N, Zhang X, Zhang X and Li J (2021) The Protective Role of TLR2 Mediates Impaired Autophagic Flux by Activating the mTOR Pathway During Neospora caninum Infection in Mice. Front. Cell. Infect. Microbiol. 11:788340. doi: 10.3389/fcimb.2021.788340

Autophagy has been shown to play an essential role in defending against intracellular bacteria, viruses, and parasites. Mounting evidence suggests that autophagy plays different roles in the infection process of different pathogens. Until now, there has been no conclusive evidence regarding whether host autophagy is involved in *Neospora caninum* infection. In the current study, we first monitored the activation of autophagy by *N. caninum*, which occurred mainly in the early stages of infection, and examined the role of host autophagy in *N. caninum* infection. Here, we presented evidence that *N. caninum* induced an increase in autophagic vesicles with double-membrane structures in macrophages at the early stage of infection. LC3-II expression peaked and decreased as infection continued. However, the expression of P62/SQSTM1 showed significant accumulation within 12 h of infection, indicating that autophagic flux was blocked. A tandem fluorescence protein mCherry-GFP-LC3 construct was used to corroborate the impaired autophagic flux. Subsequently, we found that *N. caninum* infection induced the activation of the TLR2–AKT–mTOR pathways. Further investigation revealed that TLR2–mTOR, accompanied by the blockade of autophagic flux, was responsible for impaired autophagy but was not associated with AKT. *In vitro* and *in vivo*, *N. caninum* replication was strongly blocked by the kinase inhibitor 3-methyladenine (3-MA, autophagy inhibitor). In contrast, rapamycin (Rapa, an autophagy inducer) was able to promote intracellular proliferation and reduce the survival rate of *N. caninum*-infected mice. On the other hand, the accumulation of autophagosomes facilitated the proliferation of *N. caninum*. Collectively, our findings suggest that activation of host autophagy facilitates *N. caninum* replication and may counteract the innate immune response of the host. In short, inhibition of the early stages of autophagy could potentially be a strategy for neosporosis control.

Keywords: *Neospora caninum*, autophagy, mTOR, TLR2, anti-infection, innate immune, parasite proliferation

INTRODUCTION

Neospora caninum (*N. caninum*), an intracellular protozoan parasite, is closely related to *Toxoplasma gondii* and causes abortion and reduced milk production in cattle, leading to financial losses worldwide (Reichel et al., 2013; Horcajo et al., 2016). Dogs (Langoni et al., 2013), cats (Silaghi et al., 2014), goats (Unzaga et al., 2014), and wild animals (Lempp et al., 2017) are all targets of *N. caninum* infection. Additionally, evidence indicates that *N. caninum* infections have been detected in humans (Lobato et al., 2006; Duarte et al., 2020).

Innate immune cells, such as macrophages, play a crucial role in controlling the initial parasite replication and pathogenesis of neosporosis, as these cells contribute to the first line of defense against intracellular infection. Upon *N. caninum* infection, various pattern recognition receptors (PRRs) of innate immune cells are activated, thus inducing a series of immune responses in the host (Yarovinsky et al., 2005; Mineo et al., 2010; Beiting et al., 2014; Davoli-Ferreira et al., 2016; Mansilla et al., 2016; da Silva et al., 2017; Wang et al., 2017). NF-κB, MAPK, and JAK/STAT signal pathways have been shown associated with infection (Jin et al., 2017; Nishikawa et al., 2018; Sharma et al., 2018). They influence the adaptive immune response by secreting many effector molecules including cytokines (Boucher et al., 2018; Jimenez-Pelayo et al., 2019; Miranda et al., 2019), controlling the proliferation and infection of *N. caninum*.

Autophagy is a protective mechanism that has evolved in eukaryotic organisms in response to environmental stress, achieving physiological homeostasis and internal environmental homeostasis through the degradation of intracellular components. It is a catabolic process that mainly includes initiation and formation of the autophagosome, docking and fusion with lysosomes, and subsequent degradation and reuse (Feng et al., 2014), which in brief, is manifested by increased LC3-II and degradation of p62/SQSTM1. It plays a key role not only in the growth and development of the organism but also in physiological and pathological processes such as immune defense. Autophagy has been proven to make an important contribution in defending against infection by microbial pathogens, including viruses, bacteria, and parasitic protozoa (Gomes and Dikic, 2014; Tao and Drexler, 2020). According to the mechanism of autophagy, invading pathogens are transported to the lysosome for degradation and elimination. In contrast, pathogens can also induce or disrupt host autophagy to promote intracellular survival and increased proliferation and thus promote intracellular infection.

The host–parasite relationship contributes to controlling infection (Kaye and Scott, 2011; Mukhopadhyay et al., 2020; Su et al., 2020). In parasitic infections, the complex immune system, acquired as a result of evolution, provides the most effective defense mechanism for the organism, which induces different effects, such as protecting the host, benefiting proliferation, or killing the parasite, while some immune responses will be harmful to the host.

Previous studies have shown that the autophagy pathway is conserved and essential in parasite infection. The autophagy pathway has a crucial role in *Trypanosoma cruzi* invasion (Romano et al., 2009) and provides protection against infection in mice (Casassa et al., 2019). During infection, *T. gondii* triggers the autophagic pathway in host cells which is beneficial to parasite recovery of host cell nutrients (Wang et al., 2009). The classical autophagy of the host is impaired by activating mTOR in the early stages of *Leishmania* infection, but at later stages of infection, autophagy is activated, which facilitates the survival of the parasite (Thomas et al., 2018).

In this study, we first addressed the key role of autophagy in the proliferation of *N. caninum in vivo* and in the pathogenesis of neosporosis *in vitro*. Furthermore, we found that *N. caninum* infection impairs TLR2–mTOR-dependent autophagy. Modulating autophagy in infected cells contributes to *N. caninum* proliferation and the development of neosporosis, meaning that rapamycin promotes severe infection, while 3-methyladenine (3-MA) has the opposite effect. This study provides a basis for exploring the pathogenesis of neosporosis and offers a new entry point for the prevention and control of neosporosis.

MATERIALS AND METHODS

Animals

C57BL/6 mice (female, 8–10 weeks old) were purchased from the Changsheng Experimental Animal Center (Changchun, China), and *TLR2*$^{-/-}$ mice were purchased from the Model Animal Research Center of Nanjing University (Nanjing, China). All mice were housed in the National Experimental Teaching Demonstration Center of Jilin University, the environment was free of specific pathogens, and food and water were sterilized for use.

Parasites, Cells, and Plasmids

Neospora caninum (*N. caninum*, *Nc*-1 isolate) and GFP-*Nc* were propagated in Vero (African green monkey kidney) in RPMI medium supplemented with 2% heat-inactivated fetal bovine serum (FBS). Then, 3–4 days after infection, monolayers of cells were scraped to harvest the tachyzoites, and cell suspensions were passed through a 27-gauge needle to lyse any remaining intact host cells. After centrifugation (2,000×*g*, 5 min), the tachyzoites were purified by density-gradient centrifugation on Percoll (Cornelissen et al., 1981). The pellet was collected and washed twice (2,000×*g*, 5 min) in PBS (pH 7.2). Tachyzoite density was measured using a hemocytometer to clarify the amount of parasite in the infection experiments. WT and *TLR2*$^{-/-}$ mice were injected intraperitoneally with 3 ml of 5% thioglycolate medium (BD Biosciences, New Zealand, USA) for 4 days, and the mice were humanely euthanized (Rutkowski et al., 2007) and sterilized with 75% alcohol. The cells were flushed with cold PBS, and peritoneal macrophages (PMs) were collected as previously described (Malvezi et al., 2014). The PMs were cultured in RPMI supplemented with 10% heat-inactivated fetal bovine serum. The culture medium was replaced after at least 12 h. RAW264.7 cells (American Type Culture Collection, Manassas, VA, USA), a mouse macrophage cell line, were routinely cultured in RPMI-1640 with 10% heat-inactivated FBS. The tandem fluorescent monomeric red

fluorescent protein mCherry-GFP-LC3 was maintained in the laboratory.

Transmission Electron Microscopy

In this assay, PMs in complete medium for 3 h were used as a negative control, and the PMs were challenged with *N. caninum* tachyzoites [multiplicity of infection (MOI) of 1:1] for 3 h. Cell samples were washed with PBS three times and centrifuged at 1,000×*g* for 10 min. Cells were collected at the bottom of 1.5 ml Eppendorf tubes. The cell pellets were fixed with 2.5% glutaraldehyde in PBS overnight at 4°C, postfixed in 1% OsO_4 for 2 h, dehydrated with a graded series of ethanol, and then embedded in epoxy resin. Then, ultrathin sections were prepared and stained with uranyl acetate and lead citrate as previously described (Risco et al., 2012). The examination of autophagosome-like vesicles was performed by transmission electron microscopy (TEM) (HITACHI, Japan).

Immunofluorescence

Confocal fluorescence microscopy was utilized to detect the expression of P62/SQSTM1 and the subcellular localization of NF-κB p65 in *N. caninum*-infected cells and measure the autophagic flux by mCherry-GFP-LC3. Cells were seeded in 22.1 mm dishes with coverslips. After infection, the coverslips were then washed three times with PBS, permeabilized with 0.25% Triton X-100 in PBS for 10 min, washed, and blocked in 3% BSA/PBS for 2 h at RT. After blocking, the samples were incubated with a 1:100 dilution of the antibodies overnight at 4°C, then washed and incubated with the suitable secondary antibody for 1 h at RT. The coverslips were stained with DAPI (Thermo Scientific) for 10 min before analysis on an Olympus FV1000 laser scanning confocal microscope (Japan). RAW264.7 cells were transfected with mCherry-GFP-LC3 when they grew to 60–70% confluence on coverslips, and after 24 h, they were infected with *N. caninum*. At 2 and 12 hpi, the cells were fixed and visualized by confocal microscopy.

Western Blotting Analysis

The cells were washed in cold PBS and lysed with RIPA lysis buffer (Solarbio, R0020, Beijing, China) plus 1 mM phenylmethylsulfonyl fluoride (Boster, AR1178, Beijing, China) on ice. Protein concentrations were measured using the BCA Protein Assay Kit (Thermo Scientific, Waltham, MA, USA). Protein samples were separated on SDS–polyacrylamide gels (8% or 12%). Following the transfer to polyvinylidene difluoride membranes (PVDF), the protein-immobilized PVDF membranes were incubated overnight at 4°C with primary antibodies against LC3B (L7543, Sigma), p62/SQSTM1 (ab109012, Abcam), β-actin (60008-1, Proteintech), and GAPDH (ab181602, Abcam) and antibodies against Akt (#4691), phospho-Akt (Ser473) (#9271), mTOR (#2983), phospho-mTOR (Ser2448) (#2971), TLR2 (#13744), phospho-p65 (#3033S), and phospho-IκBα (#2859s) purchased from Cell Signaling Technology, Inc. (Danvers, MA, USA). After incubation with HRP-conjugated secondary antibodies for 1 h, the membranes were visualized by an enhanced chemiluminescence (ECL) Western Blot Detection System (Clinx Science Instruments, Co., Ltd., Shanghai, China). The TLR2/TLR1 agonist Pam3CSK4 (10 μg/ml, InvivoGen) was used to stimulate macrophages as a positive control to detect TLR2 expression.

Stimulation and Experimental Design

To monitor the role of autophagy in the response to *N. caninum* infection in PMs, PMs were pretreated with rapamycin (AY-22989) (1 μM, S1039), 3-MA (10 mM, S2767), and bafilomycin A1 (Baf A1) (100 nM, S1413), which were purchased from Selleck Chemicals (Shanghai, China). To investigate the alteration of signaling pathways involved during *N. caninum* infection, PMs were pretreated with AKT inhibitor VIII (1.25 μM, S7776) and LY294002 (25 μM, S1105), which were purchased from Selleck Chemicals (Shanghai, China). The chemicals involved in the pretreatment experiments were removed prior to *N. caninum* stimulation, and the PMs were rinsed twice with sterile PBS.

Female C57BL/6 mice (8–10 weeks old) were randomized into seven groups (n = 8/each group), and 2×10^7 *N. caninum* tachyzoites or GFP-*Nc* were infected by the intraperitoneal route: i) PBS group, mice received the same volume of PBS alone; ii) rapamycin group (Rapa), mice received rapamycin; iii) 3-MA, mice received 3-methyladenine; iv) *Nc*, *N. caninum* infected alone; v) rapamycin + *Nc* (Rapa + *Nc*), *N. caninum*-infected mice received rapamycin; vi) 3-MA + *Nc*, *N. caninum* mice received 3-methyladenine; and vii) $TLR2^{-/-}$ + *Nc*, $TLR2^{-/-}$ mice infected by *N. caninum*. Rapamycin [1 mg/kg/day (Zhao et al., 2017)] or 3-MA [15 mg/kg/day (Carmignac et al., 2011)] was injected intraperitoneally 1 day after infection by *N. caninum*, and the dose was given once a day for 7 or 30 days.

Peritoneal exudate cells were prepared by a peritoneal wash with 1 ml of ice-cold PBS. CD11b+ cells were magnetically labeled with APC-labeled anti-mouse/human CD11b (BioLegend). After washing, the cells were analyzed in a FACSAria flow cytometer (BD Biosciences). A minimum of 300,000 events were acquired per sample, and the collected data were analyzed in FlowJo version 10.0 (Tree Star Inc.).

Assessment of Parasite Replication

Fluorescence microscopy observations and parasite-specific real-time quantitative PCR (qPCR) were employed to assess parasite replication.

PMs were challenged with *N. caninum* tachyzoites (MOI = parasite:cell; MOI = 1) for 24 h. When required, PMs were pretreated with Rapa and 3-MA for 2 h prior to *N. caninum* infection. At 24 h postinfection, samples were fixed in 4% paraformaldehyde for 20 min, permeabilized with PBS containing 0.25% Triton-X-100 for 10 min, blocked with PBS containing 3% bovine serum albumin (BSA) for 2 h, and washed three times for 5 min in PBS after each step. PMs were incubated with primary antibody against NcSAG1 (1:100) at 4°C overnight, washed three times with PBST, and then incubated with goat anti-rabbit fluorescein isothiocyanate (FITC)-conjugated secondary antibody (Proteintech) for 1 h at room temperature in the dark. F-actin and nuclei were stained with tetramethylrhodamine isothiocyanate (TRITC)-globulin (Yeasen, Shanghai, China) and 4′,6-diamidino-2-phenylindole (DAPI; Invitrogen, Carlsbad, CA, USA), respectively. The signals were detected using an Olympus FV1000 laser scanning confocal microscope (Japan). Infected cells were

observed, and at least 100 parasitic vacuoles were counted to determine the number of parasites in each experimental sample.

Parasite DNA was analyzed by qPCR as described previously to monitor parasite replication in cells (Collantes-Fernandez et al., 2002). In brief, DNA of infected cells was extracted according to the instructions of the Genomic DNA Extraction Kit (TIANGEN, Beijing, China). Total DNA (500 ng) from the samples was used as the template for qPCR analysis using the FastStart Universal SYBR Green Master template. A pair of specific primers for the Nc5 sequence of *N. caninum* (forward: 5′-ACTGGAGGCACGCTGAAC-3′, reverse: 5′-AACAATGCTTCGCAAGAGGAA-3′) was used to amplify a 76-bp DNA fragment. The number of parasites was determined by a standard curve method using DNA isolated from *N. caninum*.

Cell Viability Assay

Cell viability was measured by CCK-8 (Cell Counting Kit-8) after treatment. PMs were seeded at a density of 4×10^5 cells/well in 96-well plates. After at least 12 h, the medium was changed, and the cells were treated with various reagents according to the experimental design. After treatment, 10 μl of CCK-8 reagent was added to 100 μl of medium in each well and incubated at 37°C for 1 h. The absorbance was measured at 450 nm.

Statistical Analysis

Data are presented as the mean ± SEM. The significance of the variability between different treatment groups was analyzed by Student's *t*-test and one- or two-way analysis of variance (ANOVA) using GraphPad Prism software (version 6.0). Significance is shown by $^*P < 0.05$, $^{**}P < 0.01$, and $^{***}P < 0.001$.

RESULTS

Infection by *Neospora caninum* Enhances Autophagosome Formation in Macrophages

To investigate whether autophagy could be involved during infection, peritoneal macrophages were infected with *N. caninum* and the autophagy level was determined. Electron microscopic examination indicated that compared with the control group, there were more vesicles with bilayer membrane structures containing organelles and cytoplasmic components that appeared in macrophages at 3 h postinfection (MOI = 3) (**Figure 1A**). LC3 is one of the signature proteins of autophagy, and it has been shown that autophagy can lead to increased expression of LC3 (Mizushima et al., 2010). In the current study, Western blotting was employed to observe the expression of LC3-II at different time points within 24 h after *N. caninum* infection. Consistent with the TEM results, the expression of LC3-II in macrophages was increased by infection, but LC3-II accumulation did not show time dependency, and the highest expression was observed after 2 h of infection (**Figure 1B**). Furthermore, macrophages were infected by *N. caninum* at different infection doses (MOI = 1, 3, 5), and the results showed a consistent upregulation of LC3 expression for all groups (**Figure 1C**). To further illustrate the activation of autophagy by *N. caninum* infection, Baf A, a late-autophagy inhibitor, was utilized. We focused on the early stages of infection, approximately 2 h postinfection. Western blot results indicated that, compared with the Baf A-treated group, the Baf A and *N. caninum* cotreatment group showed upregulated expression of LC3 (**Figure 1D**). All of these results suggest that infection by

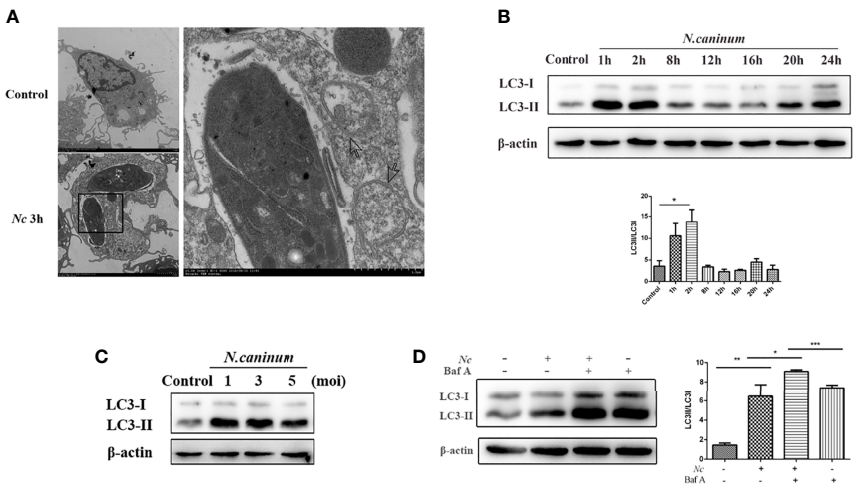

FIGURE 1 | Autophagosomes accumulate in *Neospora caninum*-infected macrophages. **(A)** Representative transmission electron microscopy images of the control and *Nc*-infected mouse macrophages at 3 h postinfection. Arrows indicate representative autophagosomes. **(B)** Peritoneal macrophages were infected with *N. caninum* tachyzoites (MOI = 3), and total protein was extracted after 0, 1, 2, 4, 8, 12, 16, 20, and 24 h. The expression of LC3 and the ratio of LC3-II to LC3-I were examined at the indicated times. **(C)** Infection at different *N. caninum* infection ratios (MOI = 1, 3, 5) with macrophages for 2 h. Upregulated LC3 expression was observed in each group. **(D)** Peritoneal macrophages were pretreated with or without bafilomycin A1 (Baf A1; 100 nM) for 4 h prior to infection with *N. caninum* tachyzoites (MOI = 3), and the expression of LC3 was determined 2 h later. $^*P < 0.05$, $^{**}P < 0.01$, $^{***}P < 0.001$ compared with the control groups. The data shown are representative of three independent experiments.

N. caninum in the early stages leads to an increase in autophagic structures in macrophages.

Autophagic Flux Is Suppressed During *Neospora caninum* Infection

The accumulation of autophagic structures caused by infection may be due to autophagy-induced or autophagy-prevented autophagic degradation (Mizushima et al., 2010; Klionsky et al., 2016); thus, the detection of autophagic flux is of critical importance (Zhang et al., 2013). SQSTM1, a cargo receptor protein, also known as p62, is a specific substrate for selective autophagy and an important component of the autophagosomal membrane. Western blotting was employed to examine the expression of p62/SQSTM1 at different time points within 24 h postinfection, and p62/SQSTM1 expression gradually increased, peaked at 12 h, and then decreased (**Figure 2A**). Furthermore, the cells were infected by *N. caninum* after Baf A and Rapa treatment, respectively. Rapa and *N. caninum* cotreatment stimulation decreased p62/SQSTM1 accumulation in macrophages compared with the *N. caninum*-infected group but displayed significantly higher expression than the Rapa group. In addition, pretreatment with Baf A resulted in more accumulation of *N. caninum*-induced p62/SQSTM1 compared with the *N. caninum*-infected group (**Figure 2B**). To test whether autophagic flux was blocked by infection, the tandem-tagged fluorescent reporter mCherry-GFP-LC3 was transfected into RAW264.7 cells and detected by fluorescence microscopy. The red signal of mCherry is responsible for demonstrating degradation, mainly because GFP fluorescence is less stable in the acidic environment of autophagic lysosomes and thus appears red. If colocalization appears yellow, it indicates impaired autophagic flux. The results showed that GFP puncta were increased by *N. caninum* at 12 h postinfection, and colocalization of red and green signals resulted in yellow puncta. However, the Rapa group showed red fluorescence because of the activated autophagy with complete autophagic flux. Taken together, these observations indicate that early infection by *N. caninum* can induce autophagy (**Figure 2C**). Autophagic flux was impaired with the *N. caninum* infection process.

AKT–mTOR Signaling Is Activated in Macrophages During *N. caninum* Infection

Autophagy is a complex physiological process, and a variety of signaling pathways are involved and contribute to the regulation of various processes of autophagy. The mTOR signaling pathway is important for regulating autophagy homeostasis. To characterize the effect of *N. caninum* infection on AKT and mTOR activation in macrophages, p-AKT and p-mTOR phosphorylation were examined using Western blotting. There was a significant time-dependent increase in the expression of p-AKT and p-mTOR in *N. caninum*-infected macrophages compared with the control group (**Figure 3A**). Combined with the previous experimental results (**Figures 1B**, **2A**), these results tentatively suggested that AKT–mTOR was possibly involved in *N. caninum*-induced inhibition of autophagy in the late stages of infection. For further validation, rapamycin (an inhibitor of mTOR), LY294002 (an inhibitor of PI3K), and Akt inhibitor VIII (an inhibitor of AKT) were used. The increased expression of p-mTOR and p-AKT induced by infection was significantly suppressed by coincubation with rapamycin (1 μM, 8 h). Not surprisingly, phosphorylation of mTOR was controlled by inhibition of PI3K and AKT (**Figure 3B**). Notably, rapamycin was the only treatment to reduce the expression of p62/SQSTM1 compared with the infection-only group (**Figure 3B**).

TLR2 Deficiency Results in Attenuated p62/SQSTM1 Accumulation and Restores Autophagic Flux by Regulating mTOR Signaling Pathways in *Neospora caninum* Infection

Previous studies have demonstrated that TLR2 signaling is essential to protect the host against infection by *N. caninum* (Mineo et al., 2010). To investigate the role of TLR2 in the impairment of autophagic flux induced by *N. caninum*, WT and *TLR2*$^{-/-}$ PMs were used. Stimulation of PMs with *N. caninum* caused activation of TLR2–NF-κB signaling pathways including increased TLR2, p-p65, and p-IκBα (**Figure 4A**). In addition, the nuclear translocation of NF-κB p65 confirmed that the activation of NF-κB was dependent on TLR2 (**Figure 4B**). p62/SQSTM1 degradation was impaired after *N. caninum* infection, while mTOR, which negatively regulates autophagy, was activated. It was interesting to note that the expression of p62/SQSTM1 was reduced in response to *N. caninum* in *TLR2*$^{-/-}$ compared with the WT, but there was no reduction in LC3-II expression (**Figure 4A**). We next detected p62/SQSTM1 puncta in both the WT and *TLR2*$^{-/-}$ groups after *N. caninum* infection. Consistent with our Western blotting data, fewer p62/SQSTM1 puncta were observed in *TLR2*$^{-/-}$ PMs infected with *N. caninum* than in WT PMs (**Figure 4C**). In addition, we found a significant downregulation of p-mTOR and p-AKT expression in *TLR2*$^{-/-}$ mice compared with WT mice (**Figure 4D**). The results suggested that the AKT–mTOR signaling pathway triggered by *N. caninum* was activated through TLR2. Together with the previous results showing that inhibition of mTOR by rapamycin reduced p62/SQSTM1 expression but AKT and PI3K inhibitors did not (**Figure 3B**), we demonstrate that TLR2 is involved in the mTOR-dependent inhibition of autophagic flux, which is meaningful for studying the relationship between autophagy and innate immunity in *N. caninum* infection.

TLR2 Deficiency Impairs Resistance to *N. caninum* Infection

Having observed that TLR2 is involved in the inhibition of autophagy in *N. caninum* infection, we decided to verify the anti-infection role of TLR2. The results showed that TLR2 deletion resulted in enhanced proliferation of *N. caninum* compared with infected WT cells (**Figure 5A**). Moreover, *TLR2*$^{-/-}$ mice were more susceptible to acute infection by *N. caninum* and showed increased mortality, but there were no obvious differences in weight loss between the *TLR2*$^{-/-}$ and WT groups (**Figures 5B, C**). Our results were in accordance with previous studies (Mineo et al., 2010; Zhang et al., 2021), suggesting that TLR2 contributed to the proliferation and resistance to infection in *N. caninum*.

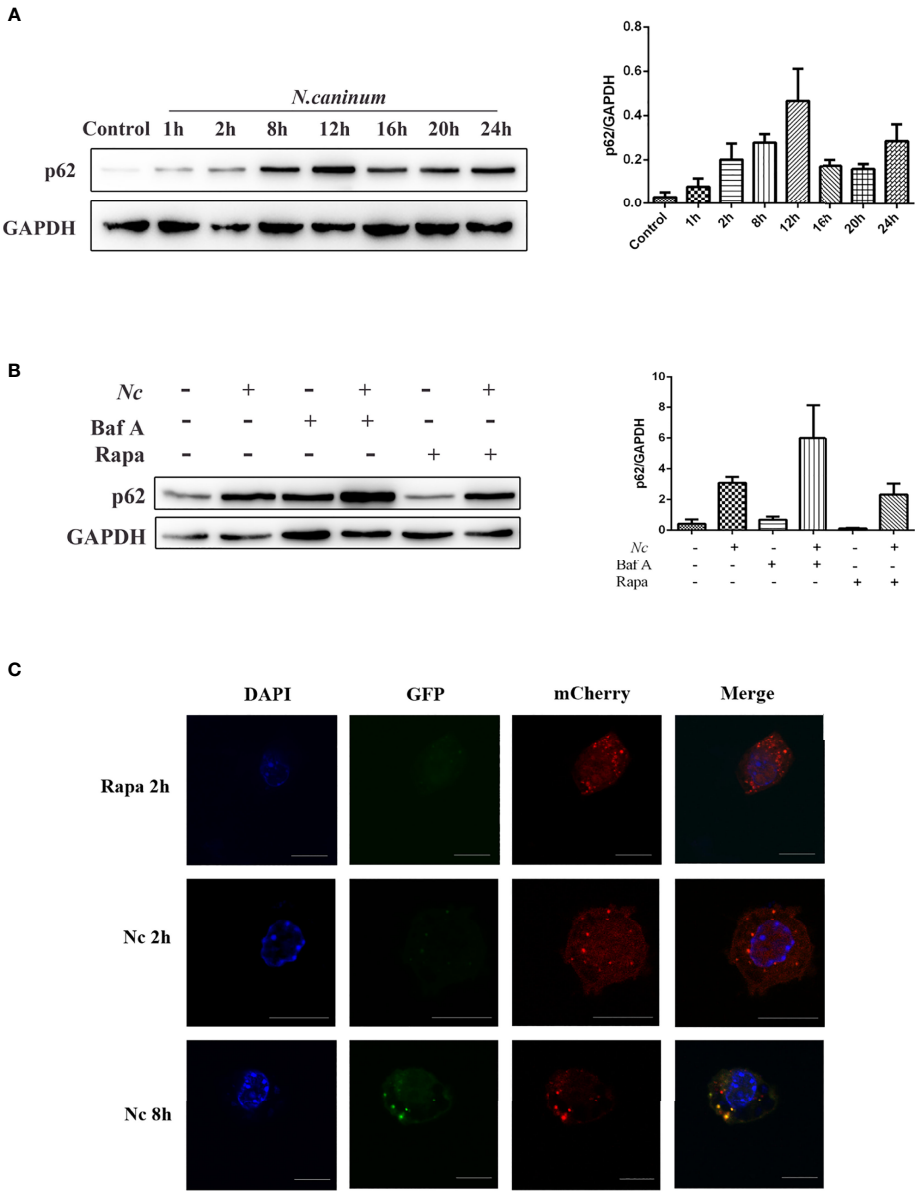

FIGURE 2 | *Neospora caninum* infection suppresses autophagic flux. The changes in p62 were determined by Western blot analysis. **(A)** Peritoneal macrophages were infected with *N. caninum* tachyzoites (MOI = 3), and total protein was extracted after 0, 1, 2, 4, 8, 12, 16, 20, and 24 h, respectively. **(B)** Peritoneal macrophages were pretreated with rapamycin (1 μM) or bafilomycin A (100 nM) for 1 and 4 h and then infected with *N. caninum* tachyzoites (MOI = 3:1, parasite: cell). **(C)** RAW264.7 cells were transfected with mCherry-GFP-LC3, and cells treated with 1 μM rapamycin for 2 h were used as the positive control for the induction of autophagy. At 2 and 12 h postinfection, the cells were fixed and assessed for GFP and mCherry fluorescence. Scale bars: 10 μm. One of the three experiments conducted is shown.

The Proliferation of *Neospora caninum* and Host Resistance Correlate With Autophagy Alterations Induced by Autophagy-Regulating Reagents

To evaluate the role of autophagy in the restriction of *N. caninum* replication in macrophages, parasite number in macrophages was quantified. WT PMs were pretreated with Rapa or 3-MA followed by stimulation with *N. caninum*, and then the proliferation of *N. caninum* was observed in comparison to the infection-only group. An intracellular replication assay was performed to assess the proliferation efficiency of the parasite. Twenty-four hours after infection, the number of tachyzoites in the parasitophorous was counted by fluorescence microscopy. The results showed that both the *Nc* group and Rapa + *Nc* group displayed similar replication dynamics, but the 3-MA-pretreated group exhibited a slight decrease in parasite burden (**Figures 5A, D, E**).

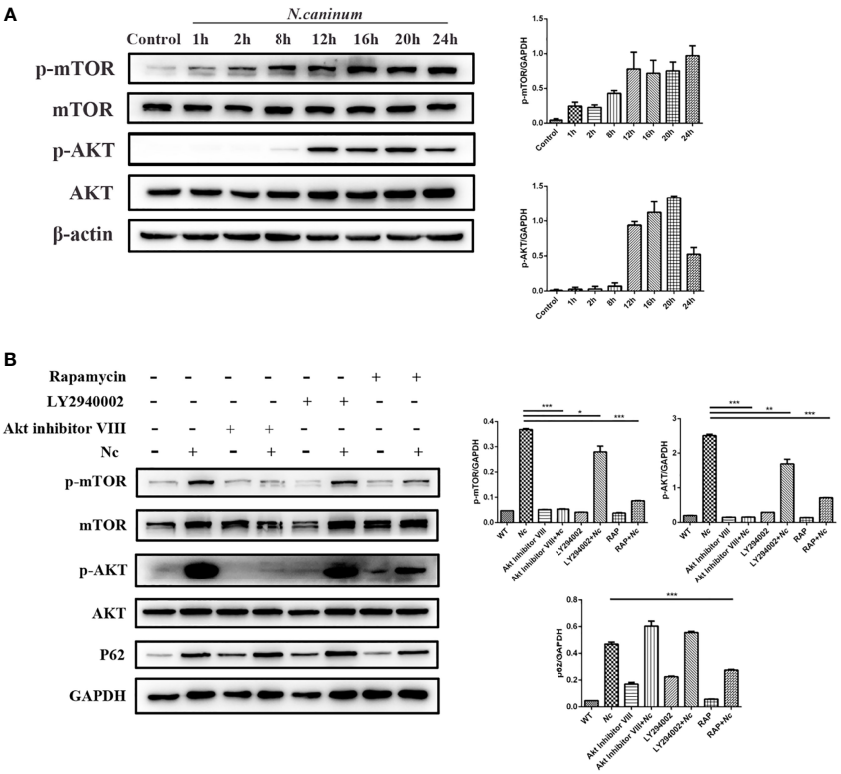

FIGURE 3 | The effect of *N. caninum* infection on the AKT/mTOR signaling pathway in macrophages. **(A)** Peritoneal macrophages were infected with *N. caninum* tachyzoites (MOI = 3), and total protein was extracted at the indicated times. The ratios of p-mTOR, mTOR, p-AKT, AKT, and β-actin were detected by Western blot analysis. **(B)** The ratios of p62, p-mTOR, mTOR, p-AKT, AKT, and GAPDH were detected by Western blot analysis of cell lysates from peritoneal macrophages pretreated with or without rapamycin (1 μM), LY294002 (25 μM), or AKT inhibitor VIII (1.25 μM) for 1 h prior to infection with *N. caninum* tachyzoites (MOI = 3). The data shown are representative of three independent experiments. Bar graphs are expressed as the mean ± SEM, $^{*}P < 0.05$; $^{**}P < 0.01$; $^{***}P < 0.001$.

To further explore the role of autophagy in *N. caninum* infection *in vivo*, mice were randomly divided into the control group (PBS, Rapa, 3-MA, $n = 8$) and infection group (*Nc*, Rapa + *Nc*, 3-MA + *Nc*, $n = 8$). Each treatment group was given the corresponding therapy. Weight, survival time, and parasite burdens were monitored.

During infection, reduced body weight of mice was observed in all infected groups, compared with the initial body weight. There was more pronounced body weight loss in the Rapa + *Nc* group than in the other infection groups. The other two infection groups shared similar levels of weight loss (**Figure 5C**). In addition, survival rates were consistent with *in vitro* infection results, with autophagy induced by Rapa causing earlier disease exacerbation and significantly decreased survival rates (**Figure 5B**). Unexpectedly, the 3-MA + *Nc* group shared similar survival rates to those of the *Nc*-infected only group, despite 3-MA reducing *N. caninum* replication in *in vitro* experiments. To investigate the role of autophagy against *N. caninum* infection, GFP-*Nc* was injected intraperitoneally. Seven days postinfection, the percentage of *N. caninum*-infected CD11b+ cells was assayed by flow cytometry of extruding cells from the peritoneal cavity at the site of initial infection. Not surprisingly, the Rapa + *Nc* group exhibited the most severe infection, while 3-MA was found to reduce the rate of *N. caninum* infection, compared with the infected-only group (**Figure 5F**). The results suggest that modification of autophagy by autophagy regulators leads to changes in *N. caninum* proliferation and host resistance.

Modulation of Autophagy Activity Does Not Affect Cell Viability

In this study, to investigate the effect of autophagy during *N. caninum* infection, we altered autophagy with specific drugs, including Rapa, 3-MA, and Baf A. The relationships of signaling pathways and their activation during *N. caninum* infection were studied by altering signaling pathways with appropriate inhibitors, including AKT VIII and LY294002. We found no significant changes in cell viability by the CCK-8 assay, which provides a basis for further exploration of the relationship between autophagy and *N. caninum* (**Figure 6**).

DISCUSSION

Autophagy is a conserved cellular physiological process that plays a fundamental role in cellular, tissue, and physiological homeostasis

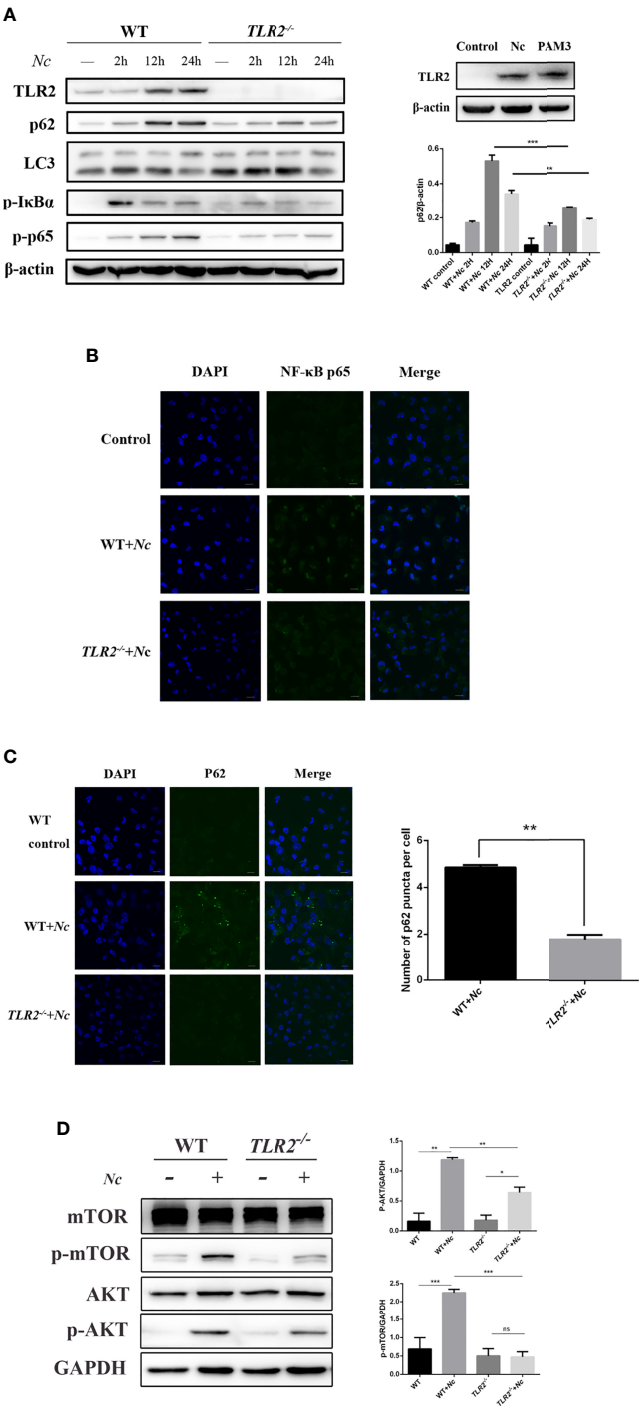

FIGURE 4 | Activation of the TLR2–NF-κB and mTOR signaling pathways by *N. caninum* infection impairs autophagy in mouse peritoneal macrophages (PMs). **(A)** Western blot analysis of TLR2, p62, LC3, p-IκBα, p-p65, and β-actin in macrophages from WT and *TLR2*$^{-/-}$ mice infected with *N. caninum* (MOI = 3) for 2, 12, and 24 h. Macrophages were treated with Pam3CSK4 (10 μg/ml) as a positive control. The rate of p62/β-actin was shown. **(B)** Confocal microscopy was used to detect the translocation of NF-κB from the cytoplasm to the nucleus in both WT and *TLR2*$^{-/-}$ mouse peritoneal macrophages. Scale bars: 10 μm. **(C)** Eight hours postinfection with *N. caninum* (MOI = 3), the accumulation of p62/SQSTM1 was examined by confocal microscopy in both the WT and *TLR2*$^{-/-}$ groups. Quantitative analysis of the number of p62 puncta. The graph represents the average data of at least 100 cells in each experimental group in three independent experiments. Scale bars: 10 μm. **(D)** WT and *TLR2*$^{-/-}$ mouse PMs were infected with *N. caninum* (MOI = 3) for 8 h and then immunoblotted for whole-cell lysis analysis of p-mTOR and p-AKT protein expression. The phosphorylated mTOR and AKT amounts were quantified by densitometric analysis. The data are expressed as the mean ± SEM from three separate experiments. *$P < 0.05$; **$P < 0.01$; ***$P < 0.001$; ns indicates not significant.

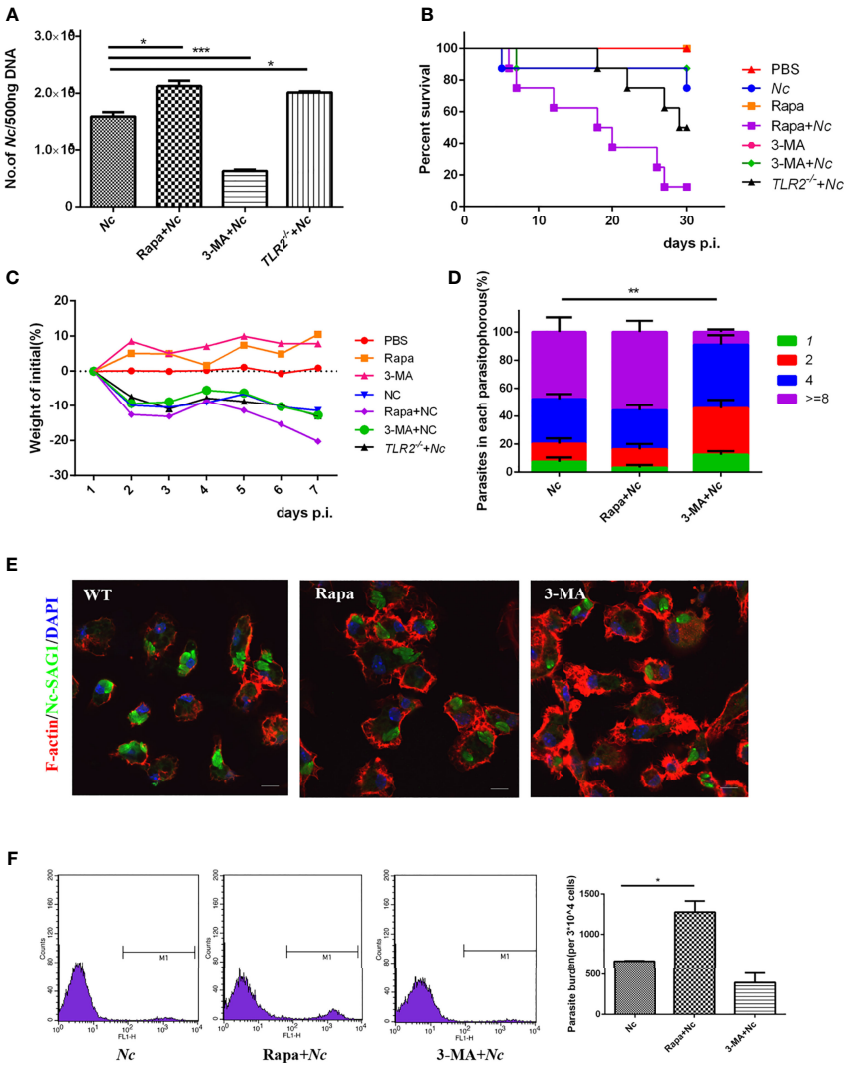

FIGURE 5 | Roles of autophagy in host resistance to *N. caninum* infection. PMs were infected with *N. caninum* at MOI of 1 in the presence or absence of rapamycin (1 μM) or 3-methyladenine (3-MA) (2.5 mM) for 24 h. **(A)** The number of parasites in each group was detected by quantitative PCR. Female C57BL/6 mice were infected with 2×10^7 *N. caninum* tachyzoites in the absence or presence of either Rapa or 3-MA and were monitored daily. **(B)** Survival of mice was monitored for 30 days. **(C)** Weight of mice was recorded daily within 7 days of infection. **(D)** Quantification of parasites in vacuoles in each group was monitored by fluorescence microscopy. **(E)** PMs were stained with polyclonal antisera against NcSAG1 and used to visualize *N. caninum*, and confocal microscopy was used to observe them. **(F)** Female C57BL/6 mice were intraperitoneally injected with 2×10^7 of GFP-*Nc*; rapamycin (1 mg/kg/day) or 3-MA (15 mg/kg/day) was injected intraperitoneally 1 day after infection. Seven days later, peritoneal exudate cells were detected by flow cytometry. The data are expressed as the mean ± SEM from three separate experiments, *$P < 0.05$; **$P < 0.01$; ***$P < 0.001$.

through the lysosomal degradation pathway (Mizushima and Komatsu, 2011). In immune cells, autophagy also exhibits extraordinary immune functions in the fight against pathogenic microorganisms, in addition to its essential functions. Prior studies have noted the importance of autophagy in the process of infection by various microorganisms, such as bacteria, viruses, and parasites. Those include *Mycobacterium tuberculosis* (Gutierrez et al., 2004), *Listeria monocytogenes* (Py et al., 2007), and *Salmonella* (Nagy et al., 2019), whose intracellular proliferation is controlled by autophagy. Human immunodeficiency virus 1 (HIV-1) (Marin et al., 2003) and hepatitis C virus (Ait-Goughoulte et al., 2008) are also subject to autophagic degradation. However, the proliferation of protozoan parasites is affected by host cell autophagy, such as *T. gondii* (Wang et al., 2009) and *Leishmania* (Thomas et al., 2018).

Little to no research has attempted to assess the role played by autophagy in *N. caninum* infection. In this study, we demonstrated the accumulation of autophagosomes and increased levels of p62/SQSTM1 in *N. caninum*-infected cells. Additionally, failure of autophagosome–lysosome fusion was detected, which implied impaired autophagy. These results suggest that the activated autophagy mechanism triggered by

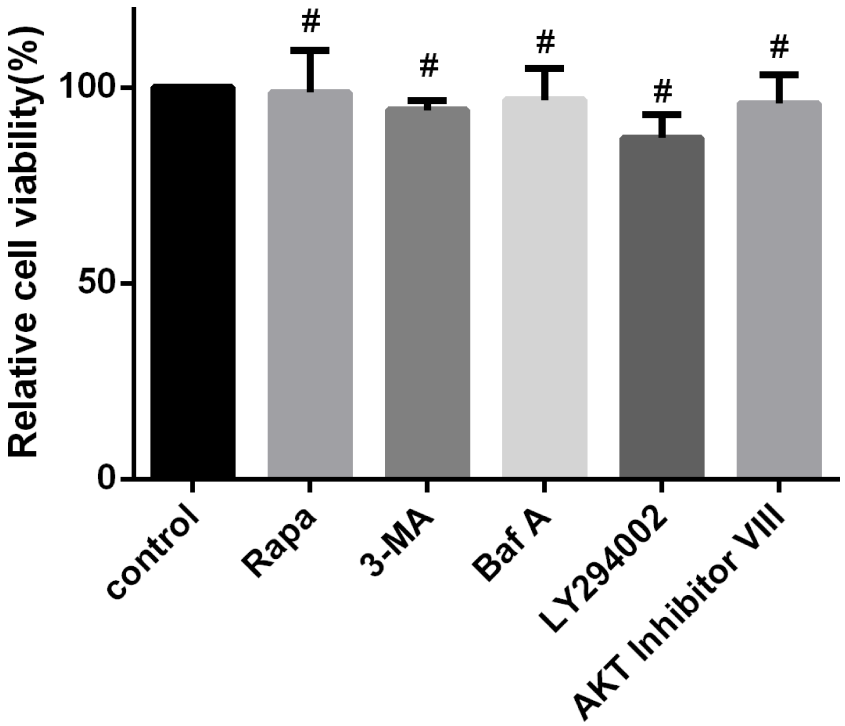

FIGURE 6 | Regulation of autophagy and upstream signaling pathways does not affect cell viability. PMs were treated separately with rapamycin (1 μM), 3-MA (2.5 mM) for 24 h, Baf A (100 nM) for 4 h, LY294002 (25 μM), and AKT inhibitor VIII (1.25 μM) for 1 h. Cell viability was measured using a Cell Counting Kit-8 (CCK-8) assay. Data are shown as the mean ± SEM for three independent experiments. $^{\#}P > 0.05$.

N. caninum at the early stage of infection is incomplete, and autophagosomes do not efficiently fuse with lysosomes.

Various proteins are involved in the autophagy process. p62/SQSTM1, a well-studied autophagy receptor and substrate, interacts with Atg8 family members such as LC3 and ubiquitin and is conjugated to autophagosome membranes. This constitutes a mechanism of autophagic degradation for the delivery of selective autophagic cargo. The classical autophagic process includes the appearance of autophagosomes, fusion with lysosomes forming autolysosomes, and further degradation of autolysosomes, which, in brief, manifests as an increased LC3-II and the degradation of p62/SQSTM1. Moreover, p62/SQSTM1 performs other functions in addition to participating in autophagy. In particular, the interaction of p62/SQSTM1 with a number of signaling molecules increases its complexity as a reporter of autophagic flux. Even so, the detection of p62/SQSTM1 degradation is still an effective method that reflects the level of autophagic flux (Pankiv et al., 2007; Zheng et al., 2016). In the present work, with infection progression, we observed an accumulation of p62/SQSTM1 in macrophages within 12 h postinfection by *N. caninum*, which implied an impaired autophagic flux. In addition, we employed mCherry-GFP-LC3 to observe autophagic flux, which confirmed the impairment of autophagic flux presumed by p62/SQSTM1 accumulation. Of note, some other species were found to activate host autophagy, consistent with our current results. *Staphylococcus aureus*-infected bovine macrophages activate autophagy and increase LC3 expression at different times, accompanied by the accumulation of p62/SQSTM1 (Cai et al., 2020). Acting as a viral restriction factor, p62/SQSTM1 restricts dengue virus replication during infection (Metz et al., 2015). In addition, p62/SQSTM1 accumulates on PVs during *T. gondii* infection of human cells, and parasite growth is stunted in vacuoles positive for p62/SQSTM1 (Selleck et al., 2015). *N. caninum* triggered a large amount of p62/SQSTM1 in infected cells, and given this, we hypothesized that it should play a role in the anti-infection processes of *N. caninum*, which requires further investigation.

mTOR is considered a major negative regulator of autophagy, and the detailed mechanisms of its action have been intensively investigated (Jung et al., 2009; Kim et al., 2011). Few studies have focused on the effects of *N. caninum* infection on the host mTOR signaling pathway. A previous study showed that compared with *T. gondii* infection, the mTOR signaling pathway is not significantly enriched during *N. caninum* infection (Al-Bajalan et al., 2017). The inconsistent results are most likely due to distinct host cells, rather than macrophages, and a previous study targeted HFF cells.

The PI3K–Akt–mTOR pathway regulates a variety of cellular processes (Heras-Sandoval et al., 2014; Zabala-Letona et al., 2017), and autophagy is one of the most critical regulatory pathways, performing mainly negative regulation. Pretreatment

of macrophages with a PI3K inhibitor (LY290042), AKT inhibitors (AKT VIII), and mTOR inhibitors (rapamycin) demonstrated that *N. caninum* infection activated the PI3K–Akt–mTOR signaling pathway. Contrary to expectations, this study did not find a significant difference in the inhibitor group in terms of p62/SQSTM1 expression, except for rapamycin, compared with the infection alone group. This possibly indicates that PI3K and AKT are not associated with *N. caninum*-induced inhibition of autophagic flux.

Although *N. caninum* activates AKT–mTOR and these signaling molecules have been reported to exert an inhibitory effect on autophagy, autophagosome formation was not blocked by *N. caninum* infection in macrophages. These findings prove that increased autophagosome structures are detectable in infected macrophages with increased levels of LC3-II in the early postinfection stage. It has been shown that *T. gondii* blocks autophagy through AKT signaling, but it has also been shown that autophagy can be utilized as an additional source of nutrition (Wang et al., 2009). Both starvation and drug-mediated (rapamycin and chloroquine) manipulation of autophagy influence the growth and survival of *Plasmodium* (Prado et al., 2015). The distinction between selective autophagy and canonical autophagy is believed to explain the opposite viewpoint. While parasites control selective autophagy to avoid elimination, canonical autophagy appears to be utilized by pathogens (Prado et al., 2015). The accumulation of autophagic vesicles due to autophagic flux damage is conducive to pathogen survival. As another example, autophagosomes are triggered by influenza A virus (IAV) but fail to form autophagolysosomes, which benefits the accumulation of viral elements (Liu et al., 2016). Treatment with 3-MA or knockdown of ATG5 and Beclin1 inhibits the early phases of autophagy, leading to impaired EBV replication (Granato et al., 2014). However, since the outbreak of autophagic vesicles occurs at the early stage of infection, and the first round of proliferation cannot be completed within a short period of time, it was not directly observed. It is only presumed that the formation of autophagosomes facilitates the growth of *N. caninum* in the early postinfection stage.

TLR2, a pattern recognition receptor, generally known as a sensor of bacterial lipoproteins, also senses molecular patterns from viruses and parasites (Oliveira-Nascimento et al., 2012). When TLR2 is activated, it recruits adaptor molecules to the intracellular Toll/interleukin-1 receptor (TIR) domain and ultimately activates NF-κB to regulate the expression of inflammation-associated genes (Oliveira-Nascimento et al., 2012). Previous studies found that TLR2 was upregulated when exposed to extracellular vesicles, soluble antigens, and glycosylphosphatidylinositols (GPIs) from *N. caninum* or parasite infection and regulated the secretion of a variety of cytokines (Mineo et al., 2010; Li et al., 2018; Debare et al., 2019). Whether TLR2 is engaged in the autophagy process during *N. caninum* infection in host cells has never been investigated. Our study showed that *N. caninum* infection increased the expression of the autophagic adaptor proteins p62/SQSTM1 and LC3-II in macrophages and triggered the TLR2–NF-κB signaling pathway. Studies on the relationship between p62/SQSTM1 and the NF-κB signaling pathway found that p62/SQSTM1 is involved in the regulation of NF-κB signaling (Pan et al., 2014); in turn, activation of NF-κB induces the expression of p62 (Yang et al., 2017), which forms a positive feedback loop. In this study, we observed a downregulation of p62/SQSTM1 expression in *TLR2*$^{-/-}$ PMs by *N. caninum* infection, accompanied by a downregulation of p-p65 expression and diminished p65 nuclear translocation. We speculate that the accumulation of p62/SQSTM1 in PMs by *N. caninum* may play a regulatory role in the activation of NF-κB, but the mechanisms of interaction need further investigation. Additionally, as a TLR2 ligand, the GPI anchor of *N. caninum* may also be involved in the autophagic process, which needs more supporting evidence.

To further elucidate the role of TLR2 in impaired autophagy by infection, we applied TLR2-deficient macrophages to observe the potential interaction between TLR2 and the AKT/mTOR pathway. AKT/mTOR expression was detected in both the WT and *TLR2*$^{-/-}$ groups. The results indicate that TLR2 deficiency downregulated both the expression and phosphorylation of AKT/mTOR. As previously mentioned, mTOR primarily plays a central negative regulatory role in autophagy. In our study, the phosphorylation of mTOR was positively correlated with TLR2, indicating an interaction between TLR2 and the mTOR pathway in the modulation of autophagy during *N. caninum* infection.

To gain insight into the role of autophagy in *N. caninum* infection, autophagy modulators were used to investigate the effect of autophagy on parasite proliferation as well as the resistance against infection. Autophagy inducers (rapamycin, mTOR inhibitor) and early autophagy inhibitors (3-MA, PI3K inhibitor) were employed. Parasite intracellular proliferation, percentage of infection at the initial location of the infection, and survival rate in the experimentally infected murine model were examined. Our data showed that *N.* caninum proliferation was promoted by rapamycin treatment in an autophagy-dependent manner and subsequently experienced rapid health deterioration and plummeting survival rates. Treatment with the early autophagy inhibitor 3-MA controlled the proliferation of *N. caninum*, although there was no significant difference in survival rate between the coadministration of the 3-MA group and the *N. caninum*-infected group, which may be attributable to the complex physiological environments. Similar findings have been observed in the study of many other pathogenic microorganisms, such as *T. cruzi* (Romano et al., 2009), *Plasmodium* (Thieleke-Matos et al., 2016), mouse hepatitis virus (Prentice et al., 2004), and duck Tembusu virus (Hu et al., 2020). The results indicate that the formation of early autophagosomes has a facilitative effect on *N. caninum* proliferation; in contrast, the activation of autophagy rather than exerting an anti-infection effect promotes *N. caninum* infection. These findings illustrate that modulation of host cell autophagy functions in the *in vivo* resistance to *N. caninum* infection, particularly in activating autophagy. Activated autophagy promotes the development of infection. Combined with infection-induced impairment of autophagy, we hypothesize that this is an anti-infective mechanism, although

the early formation of autophagosomes is utilized by *N. caninum* to facilitate its proliferation.

In conclusion, we reported that the initial phase of autophagy triggered by *N. caninum* infection presented increased autophagosomes, especially in the early stages of infection. However, as the infection progressed, there was impaired autophagic flux. The autophagy involved in *N. caninum* infection is associated with the modulation of TLR2–mTOR signaling. Most unexpectedly, rapamycin, as an autophagic agonist, promoted the proliferation and infection of *N. caninum*. Taken together, the evidence suggests that *N. caninum* employs host autophagy machinery to facilitate proliferation and infection. Thus, the noted impairment of autophagic flux in macrophages triggered by *N. caninum* is beneficial to the resistance against *N. caninum* infection. Although the mechanism needs to be further elucidated in detail, our findings provide important evidence for understanding the role of autophagy in *N. caninum* infection and the underlying mechanisms.

DATA AVAILABILITY STATEMENT

The original contributions presented in the study are included in the article. Further inquiries can be directed to the corresponding authors.

ETHICS STATEMENT

The animal study was reviewed and approved by the Animal Welfare and Research Ethics Committee at Jilin University.

AUTHOR CONTRIBUTIONS

JW, XW, PG, XCZ, and JL drafted the main manuscript and performed the data analysis. JW, PG, NZ, XZ, and XW planned and performed the experiments. JW, XCZ, and JL were responsible for the experimental design. JW, XL, NZ, XZ, FR, and JL were responsible for guiding and supporting the experiments and revising the manuscript. All authors contributed to the article and approved the submitted version.

FUNDING

Project support was provided by the State Key Laboratory of Veterinary Etiological Biology, Lanzhou Veterinary Research Institute, Chinese Academy of Agricultural Sciences (grant no. SKLVEB2019KFKT006); National Natural Science Foundation of China (grant no. 31902296); and National Key Basic Research Program (973 program) of China (grant no. 2015CB150300).

REFERENCES

Ait-Goughoulte, M., Kanda, T., Meyer, K., Ryerse, J. S., Ray, R. B., and Ray, R. (2008). Hepatitis C Virus Genotype 1a Growth and Induction of Autophagy. *J. Virol.* 82 (5), 2241–2249. doi: 10.1128/JVI.02093-07

Al-Bajalan, M. M. M., Xia, D., Armstrong, S., Randle, N., and Wastling, J. M. (2017). Toxoplasma Gondii and *Neospora Caninum* Induce Different Host Cell Responses at Proteome-Wide Phosphorylation Events; a Step Forward for Uncovering the Biological Differences Between These Closely Related Parasites. *Parasitol. Res.* 116 (10), 2707–2719. doi: 10.1007/s00436-017-5579-7

Beiting, D. P., Peixoto, L., Akopyants, N. S., Beverley, S. M., Wherry, E. J., Christian, D. A., et al. (2014). Differential Induction of TLR3-Dependent Innate Immune Signaling by Closely Related Parasite Species. *PloS One* 9 (2), e88398. doi: 10.1371/journal.pone.0088398

Boucher, E., Marin, M., Holani, R., Young-Speirs, M., Moore, D. M., and Cobo, E. R. (2018). Characteristic Pro-Inflammatory Cytokines and Host Defence Cathelicidin Peptide Produced by Human Monocyte-Derived Macrophages Infected With Neospora Caninum. *Parasitology* 145 (7), 871–884. doi: 10.1017/S0031182017002104

Cai, J., Li, J., Zhou, Y., Wang, J., Li, J., Cui, L., et al. (2020). *Staphylococcus Aureus* Facilitates Its Survival in Bovine Macrophages by Blocking Autophagic Flux. *J. Cell Mol. Med.* 24 (6), 3460–3468. doi: 10.1111/jcmm.15027

Carmignac, V., Svensson, M., Korner, Z., Elowsson, L., Matsumura, C., Gawlik, K. I., et al. (2011). Autophagy Is Increased in Laminin Alpha2 Chain-Deficient Muscle and Its Inhibition Improves Muscle Morphology in a Mouse Model of MDC1A. *Hum. Mol. Genet.* 20 (24), 4891–4902. doi: 10.1093/hmg/ddr427

Casassa, A. F., Vanrell, M. C., Colombo, M. I., Gottlieb, R. A., and Romano, P. S. (2019). Autophagy Plays a Protective Role Against Trypanosoma Cruzi Infection in Mice. *Virulence* 10 (1), 151–165. doi: 10.1080/21505594.2019.1584027

Collantes-Fernandez, E., Zaballos, A., Alvarez-Garcia, G., and Ortega-Mora, L. M. (2002). Quantitative Detection of Neospora Caninum in Bovine Aborted Fetuses and Experimentally Infected Mice by Real-Time PCR. *J. Clin. Microbiol.* 40 (4), 1194–1198. doi: 10.1128/JCM.40.4.1194-1198.2002

Cornelissen, A. W., Overdulve, J. P., and Hoenderboom, J. M. (1981). Separation of Isospora (*Toxoplasma*) Gondii Cysts and Cystozoites From Mouse Brain Tissue by Continuous Density-Gradient Centrifugation. *Parasitology* 83 (Pt 1), 103–108. doi: 10.1017/s0031182000050071

da Silva, M. V., Ferreira Franca, F. B., Mota, C. M., de Macedo Junior, A. G., Ramos, E. L., Santiago, F. M., et al. (2017). Dectin-1 Compromises Innate Responses and Host Resistance Against Neospora Caninum Infection. *Front. Immunol.* 8, 245. doi: 10.3389/fimmu.2017.00245

Davoli-Ferreira, M., Fonseca, D. M., Mota, C. M., Dias, M. S., Lima-Junior, D. S., da Silva, M. V., et al. (2016). Nucleotide-Binding Oligomerization Domain-Containing Protein 2 Prompts Potent Inflammatory Stimuli During Neospora Caninum Infection. *Sci. Rep.* 6, 29289. doi: 10.1038/srep29289

Debare, H., Schmidt, J., Moire, N., Ducournau, C., Acosta Paguay, Y. D., Schwarz, R. T., et al. (2019). *In Vitro* Cellular Responses to Neospora Caninum Glycosylphosphatidylinositols Depend on the Host Origin of Antigen Presenting Cells. *Cytokine* 119, 119–128. doi: 10.1016/j.cyto.2019.03.014

Duarte, P. O., Oshiro, L. M., Zimmermann, N. P., Csordas, B. G., Dourado, D. M., Barros, J. C., et al. (2020). Serological and Molecular Detection of Neospora Caninum and *Toxoplasma Gondii* in Human Umbilical Cord Blood and Placental Tissue Samples. *Sci. Rep.* 10 (1), 9043. doi: 10.1038/s41598-020-65991-1

Feng, Y., He, D., Yao, Z., and Klionsky, D. J. (2014). The Machinery of Macroautophagy. *Cell Res.* 24 (1), 24–41. doi: 10.1038/cr.2013.168

Gomes, L. C., and Dikic, I. (2014). Autophagy in Antimicrobial Immunity. *Mol. Cell* 54 (2), 224–233. doi: 10.1016/j.molcel.2014.03.009

Granato, M., Santarelli, R., Farina, A., Gonnella, R., Lotti, L. V., Faggioni, A., et al. (2014). Epstein-Barr Virus Blocks the Autophagic Flux and Appropriates the Autophagic Machinery to Enhance Viral Replication. *J. Virol.* 88 (21), 12715–12726. doi: 10.1128/JVI.02199-14

Gutierrez, M. G., Master, S. S., Singh, S. B., Taylor, G. A., Colombo, M. I., and Deretic, V. (2004). Autophagy Is a Defense Mechanism Inhibiting BCG and Mycobacterium Tuberculosis Survival in Infected Macrophages. *Cell* 119 (6), 753–766. doi: 10.1016/j.cell.2004.11.038

Heras-Sandoval, D., Perez-Rojas, J. M., Hernandez-Damian, J., and Pedraza-Chaverri, J. (2014). The Role of PI3K/AKT/mTOR Pathway in the Modulation of Autophagy and the Clearance of Protein Aggregates in Neurodegeneration. *Cell Signal* 26 (12), 2694–2701. doi: 10.1016/j.cellsig.2014.08.019

Horcajo, P., Regidor-Cerrillo, J., Aguado-Martinez, A., Hemphill, A., and Ortega-Mora, L. M. (2016). Vaccines for Bovine Neosporosis: Current Status and Key Aspects for Development. *Parasite Immunol.* 38 (12), 709–723. doi: 10.1111/pim.12342

Hu, Z., Pan, Y., Cheng, A., Zhang, X., Wang, M., Chen, S., et al. (2020). Autophagy Is a Potential Therapeutic Target Against Duck Tembusu Virus Infection *In Vivo*. *Front. Cell Infect. Microbiol.* 10, 155. doi: 10.3389/fcimb.2020.00155

Jimenez-Pelayo, L., Garcia-Sanchez, M., Regidor-Cerrillo, J., Horcajo, P., Collantes-Fernandez, E., Gomez-Bautista, M., et al. (2019). Immune Response Profile of Caruncular and Trophoblast Cell Lines Infected by High- (Nc-Spain7) and Low-Virulence (Nc-Spain1H) Isolates of Neospora Caninum. *Parasit. Vectors* 12 (1), 218. doi: 10.1186/s13071-019-3466-z

Jin, X., Gong, P., Zhang, X., Li, G., Zhu, T., Zhang, M., et al. (2017). Activation of ERK Signaling *via* TLR11 Induces IL-12p40 Production in Peritoneal Macrophages Challenged by *Neospora Caninum*. *Front. Microbiol.* 8, 1393. doi: 10.3389/fmicb.2017.01393

Jung, C. H., Jun, C. B., Ro, S. H., Kim, Y. M., Otto, N. M., Cao, J., et al. (2009). ULK-Atg13-FIP200 Complexes Mediate mTOR Signaling to the Autophagy Machinery. *Mol. Biol. Cell* 20 (7), 1992–2003. doi: 10.1091/mbc.E08-12-1249

Kaye, P., and Scott, P. (2011). Leishmaniasis: Complexity at the Host-Pathogen Interface. *Nat. Rev. Microbiol.* 9 (8), 604–615. doi: 10.1038/nrmicro2608

Kim, J., Kundu, M., Viollet, B., and Guan, K. L. (2011). AMPK and mTOR Regulate Autophagy Through Direct Phosphorylation of Ulk1. *Nat. Cell Biol.* 13 (2), 132–141. doi: 10.1038/ncb2152

Klionsky, D. J., Abdelmohsen, K., Abe, A., Abedin, M. J., Abeliovich, H., Acevedo Arozena, A., et al. (2016). Guidelines for the Use and Interpretation of Assays for Monitoring Autophagy (3rd Edition). *Autophagy* 12 (1), 1–222. doi: 10.1080/15548627.2015.1100356

Langoni, H., Fornazari, F., da Silva, R. C., Monti, E. T., and Villa, F. B. (2013). Prevalence of Antibodies Against Toxoplasma Gondii and Neospora Caninum in Dogs. *Braz. J. Microbiol.* 44 (4), 1327–1330. doi: 10.1590/s1517-83822013000400043

Lempp, C., Jungwirth, N., Grilo, M. L., Reckendorf, A., Ulrich, A., van Neer, A., et al. (2017). Pathological Findings in the Red Fox (Vulpes Vulpes), Stone Marten (Martes Foina) and Raccoon Dog (Nyctereutes Procyonoides), With Special Emphasis on Infectious and Zoonotic Agents in Northern Germany. *PloS One* 12 (4), e0175469. doi: 10.1371/journal.pone.0175469

Li, S., Gong, P., Tai, L., Li, X., Wang, X., Zhao, C., et al. (2018). Extracellular Vesicles Secreted by Neospora Caninum Are Recognized by Toll-Like Receptor 2 and Modulate Host Cell Innate Immunity Through the MAPK Signaling Pathway. *Front. Immunol.* 9, 1633. doi: 10.3389/fimmu.2018.01633

Liu, G., Zhong, M., Guo, C., Komatsu, M., Xu, J., Wang, Y., et al. (2016). Autophagy Is Involved in Regulating Influenza A Virus RNA and Protein Synthesis Associated With Both Modulation of Hsp90 Induction and mTOR/P70s6k Signaling Pathway. *Int. J. Biochem. Cell Biol.* 72, 100–108. doi: 10.1016/j.biocel.2016.01.012

Lobato, J., Silva, D. A., Mineo, T. W., Amaral, J. D., Segundo, G. R., Costa-Cruz, J. M., et al. (2006). Detection of Immunoglobulin G Antibodies to Neospora Caninum in Humans: High Seropositivity Rates in Patients Who Are Infected by Human Immunodeficiency Virus or Have Neurological Disorders. *Clin. Vaccine Immunol.* 13 (1), 84–89. doi: 10.1128/CVI.13.1.84-89.2006

Malvezi, A. D., da Silva, R. V., Panis, C., Yamauchi, L. M., Lovo-Martins, M. I., Zanluqui, N. G., et al. (2014). Aspirin Modulates Innate Inflammatory Response and Inhibits the Entry of Trypanosoma Cruzi in Mouse Peritoneal Macrophages. *Mediators Inflamm* 2014, 580919. doi: 10.1155/2014/580919

Mansilla, F. C., Quintana, M. E., Langellotti, C., Wilda, M., Martinez, A., Fonzo, A., et al. (2016). Immunization With Neospora Caninum Profilin Induces Limited Protection and a Regulatory T-Cell Response in Mice. *Exp. Parasitol* 160, 1–10. doi: 10.1016/j.exppara.2015.10.008

Marin, M., Rose, K. M., Kozak, S. L., and Kabat, D. (2003). HIV-1 Vif Protein Binds the Editing Enzyme APOBEC3G and Induces Its Degradation. *Nat. Med.* 9 (11), 1398–1403. doi: 10.1038/nm946

Metz, P., Chiramel, A., Chatel-Chaix, L., Alvisi, G., Bankhead, P., Mora-Rodriguez, R., et al. (2015). Dengue Virus Inhibition of Autophagic Flux and Dependency of Viral Replication on Proteasomal Degradation of the Autophagy Receptor P62. *J. Virol.* 89 (15), 8026–8041. doi: 10.1128/JVI.00787-15

Mineo, T. W., Oliveira, C. J., Gutierrez, F. R., and Silva, J. S. (2010). Recognition by Toll-Like Receptor 2 Induces Antigen-Presenting Cell Activation and Th1 Programming During Infection by Neospora Caninum. *Immunol. Cell Biol.* 88 (8), 825–833. doi: 10.1038/icb.2010.52

Miranda, V. D. S., Franca, F. B. F., da Costa, M. S., Silva, V. R. S., Mota, C. M., Barros, P., et al. (2019). Toll-Like Receptor 3-TRIF Pathway Activation by Neospora Caninum RNA Enhances Infection Control in Mice. *Infect. Immun.* 87 (4), e00739–18. doi: 10.1128/IAI.00739-18

Mizushima, N., and Komatsu, M. (2011). Autophagy: Renovation of Cells and Tissues. *Cell* 147 (4), 728–741. doi: 10.1016/j.cell.2011.10.026

Mizushima, N., Yoshimori, T., and Levine, B. (2010). Methods in Mammalian Autophagy Research. *Cell* 140 (3), 313–326. doi: 10.1016/j.cell.2010.01.028

Mukhopadhyay, D., Arranz-Solis, D., and Saeij, J. P. J. (2020). Influence of the Host and Parasite Strain on the Immune Response During Toxoplasma Infection. *Front. Cell Infect. Microbiol.* 10, 580425. doi: 10.3389/fcimb.2020.580425

Nagy, T. A., Quintana, J. L. J., Reens, A. L., Crooks, A. L., and Detweiler, C. S. (2019). Autophagy Induction by a Small Molecule Inhibits Salmonella Survival in Macrophages and Mice. *Antimicrob. Agents Chemother* 63 (12), e01536–19. doi: 10.1128/AAC.01536-19

Nishikawa, Y., Shimoda, N., Fereig, R. M., Moritaka, T., Umeda, K., Nishimura, M., et al. (2018). *Neospora Caninum* Dense Granule Protein 7 Regulates the Pathogenesis of Neosporosis by Modulating Host Immune Response. *Appl. Environ. Microbiol.* 84 (18), e01350–18. doi: 10.1128/AEM.01350-18

Oliveira-Nascimento, L., Massari, P., and Wetzler, L. M. (2012). The Role of TLR2 in Infection and Immunity. *Front. Immunol.* 3, 79. doi: 10.3389/fimmu.2012.00079

Pankiv, S., Clausen, T. H., Lamark, T., Brech, A., Bruun, J. A., Outzen, H., et al. (2007). P62/SQSTM1 Binds Directly to Atg8/LC3 to Facilitate Degradation of Ubiquitinated Protein Aggregates by Autophagy. *J. Biol. Chem.* 282 (33), 24131–24145. doi: 10.1074/jbc.M702824200

Pan, H., Zhang, Y., Luo, Z., Li, P., Liu, L., Wang, C., et al. (2014). Autophagy Mediates Avian Influenza H5N1 Pseudotyped Particle-Induced Lung Inflammation Through NF-kappaB and P38 MAPK Signaling Pathways. *Am. J. Physiol. Lung Cell Mol. Physiol.* 306 (2), L183–L195. doi: 10.1152/ajplung.00147.2013

Prado, M., Eickel, N., De Niz, M., Heitmann, A., Agop-Nersesian, C., Wacker, R., et al. (2015). Long-Term Live Imaging Reveals Cytosolic Immune Responses of Host Hepatocytes Against Plasmodium Infection and Parasite Escape Mechanisms. *Autophagy* 11 (9), 1561–1579. doi: 10.1080/15548627.2015.1067361

Prentice, E., Jerome, W. G., Yoshimori, T., Mizushima, N., and Denison, M. R. (2004). Coronavirus Replication Complex Formation Utilizes Components of Cellular Autophagy. *J. Biol. Chem.* 279 (11), 10136–10141. doi: 10.1074/jbc.M306124200

Py, B. F., Lipinski, M. M., and Yuan, J. (2007). Autophagy Limits Listeria Monocytogenes Intracellular Growth in the Early Phase of Primary Infection. *Autophagy* 3 (2), 117–125. doi: 10.4161/auto.3618

Reichel, M. P., Alejandra Ayanegui-Alcerreca, M., Gondim, L. F., and Ellis, J. T. (2013). What Is the Global Economic Impact of Neospora Caninum in Cattle - The Billion Dollar Question. *Int. J. Parasitol* 43 (2), 133–142. doi: 10.1016/j.ijpara.2012.10.022

Risco, C., Sanmartin-Conesa, E., Tzeng, W. P., Frey, T. K., Seybold, V., and de Groot, R. J. (2012). Specific, Sensitive, High-Resolution Detection of Protein Molecules in Eukaryotic Cells Using Metal-Tagging Transmission Electron Microscopy. *Structure* 20 (5), 759–766. doi: 10.1016/j.str.2012.04.001

Romano, P. S., Arboit, M. A., Vazquez, C. L., and Colombo, M. I. (2009). The Autophagic Pathway Is a Key Component in the Lysosomal Dependent Entry of Trypanosoma Cruzi Into the Host Cell. *Autophagy* 5 (1), 6–18. doi: 10.4161/auto.5.1.7160

Rutkowski, M. R., McNamee, L. A., and Harmsen, A. G. (2007). Neutrophils and Inducible Nitric-Oxide Synthase Are Critical for Early Resistance to the Establishment of Tritrichomonas Foetus Infection. *J. Parasitol* 93 (3), 562–574. doi: 10.1645/GE-976R.1

Selleck, E. M., Orchard, R. C., Lassen, K. G., Beatty, W. L., Xavier, R. J., Levine, B., et al. (2015). A Noncanonical Autophagy Pathway Restricts Toxoplasma Gondii Growth in a Strain-Specific Manner in IFN-Gamma-Activated Human Cells. *mBio* 6 (5), e01157–e01115. doi: 10.1128/mBio.01157-15

Sharma, P., Hartley, C. S., Haque, M., Coffey, T. J., Egan, S. A., and Flynn, R. J. (2018). Bovine Neonatal Monocytes Display Phenotypic Differences Compared With Adults After Challenge With the Infectious Abortifacient Agent Neospora Caninum. *Front. Immunol.* 9, 3011. doi: 10.3389/fimmu.2018.03011

Silaghi, C., Knaus, M., Rapti, D., Kusi, I., Shukullari, E., Hamel, D., et al. (2014). Survey of Toxoplasma Gondii and *Neospora Caninum*, Haemotropic Mycoplasmas and Other Arthropod-Borne Pathogens in Cats From Albania. *Parasit. Vectors* 7, 62. doi: 10.1186/1756-3305-7-62

Su, X. Z., Zhang, C., and Joy, D. A. (2020). Host-Malaria Parasite Interactions and Impacts on Mutual Evolution. *Front. Cell Infect. Microbiol.* 10, 587933. doi: 10.3389/fcimb.2020.587933

Tao, S., and Drexler, I. (2020). Targeting Autophagy in Innate Immune Cells: Angel or Demon During Infection and Vaccination? *Front. Immunol.* 11, 460. doi: 10.3389/fimmu.2020.00460

Thieleke-Matos, C., Lopes da Silva, M., Cabrita-Santos, L., Portal, M. D., Rodrigues, I. P., Zuzarte-Luis, V., et al. (2016). Host Cell Autophagy Contributes to Plasmodium Liver Development. *Cell Microbiol.* 18 (3), 437–450. doi: 10.1111/cmi.12524

Thomas, S. A., Nandan, D., Kass, J., and Reiner, N. E. (2018). Countervailing, Time-Dependent Effects on Host Autophagy Promotes Intracellular Survival of Leishmania. *J. Biol. Chem.* 293 (7), 2617–2630. doi: 10.1074/jbc.M117.808675

Unzaga, J. M., More, G., Bacigalupe, D., Rambeaud, M., Pardini, L., Dellarupe, A., et al. (2014). *Toxoplasma Gondii* and Neospora Caninum Infections in Goat Abortions From Argentina. *Parasitol Int.* 63 (6), 865–867. doi: 10.1016/j.parint.2014.07.009

Wang, X., Gong, P., Zhang, X., Wang, J., Tai, L., Wang, X., et al. (2017). NLRP3 Inflammasome Activation in Murine Macrophages Caused by Neospora Caninum Infection. *Parasit Vectors* 10 (1), 266. doi: 10.1186/s13071-017-2197-2

Wang, Y., Weiss, L. M., and Orlofsky, A. (2009). Host Cell Autophagy Is Induced by Toxoplasma Gondii and Contributes to Parasite Growth. *J. Biol. Chem.* 284 (3), 1694–1701. doi: 10.1074/jbc.M807890200

Yang, S., Qiang, L., Sample, A., Shah, P., and He, Y. Y. (2017). NF-kappaB Signaling Activation Induced by Chloroquine Requires Autophagosome, P62 Protein, and C-Jun N-Terminal Kinase (JNK) Signaling and Promotes Tumor Cell Resistance. *J. Biol. Chem.* 292 (8), 3379–3388. doi: 10.1074/jbc.M116.756536

Yarovinsky, F., Zhang, D., Andersen, J. F., Bannenberg, G. L., Serhan, C. N., Hayden, M. S., et al. (2005). TLR11 Activation of Dendritic Cells by a Protozoan Profilin-Like Protein. *Science* 308 (5728), 1626–1629. doi: 10.1126/science.1109893

Zabala-Letona, A., Arruabarrena-Aristorena, A., Martin-Martin, N., Fernandez-Ruiz, S., Sutherland, J. D., Clasquin, M., et al. (2017). Mtorc1-Dependent AMD1 Regulation Sustains Polyamine Metabolism in Prostate Cancer. *Nature* 547 (7661), 109–113. doi: 10.1038/nature22964

Zhang, X. J., Chen, S., Huang, K. X., and Le, W. D. (2013). Why Should Autophagic Flux be Assessed? *Acta Pharmacol. Sin.* 34 (5), 595–599. doi: 10.1038/aps.2012.184

Zhang, X., Li, X., Gong, P., Wang, X., Zhang, N., Chen, M., et al. (2021). Host Defense Against Neospora Caninum Infection *via* IL-12p40 Production Through TLR2/TLR3-AKT-ERK Signaling Pathway in C57BL/6 Mice. *Mol. Immunol.* 139, 140–152. doi: 10.1016/j.molimm.2021.08.019

Zhao, D., Wang, W., Wang, H., Peng, H., Liu, X., Guo, W., et al. (2017). PKD Knockdown Inhibits Pressure Overload-Induced Cardiac Hypertrophy by Promoting Autophagy *via* AKT/mTOR Pathway. *Int. J. Biol. Sci.* 13 (3), 276–285. doi: 10.7150/ijbs.17617

Zheng, K., Li, Y., Wang, S., Wang, X., Liao, C., Hu, X., et al. (2016). Inhibition of Autophagosome-Lysosome Fusion by Ginsenoside Ro *via* the ESR2-NCF1-ROS Pathway Sensitizes Esophageal Cancer Cells to 5-Fluorouracil-Induced Cell Death *via* the CHEK1-Mediated DNA Damage Checkpoint. *Autophagy* 12 (9), 1593–1613. doi: 10.1080/15548627.2016.1192751

Conflict of Interest: The authors declare that the research was conducted in the absence of any commercial or financial relationships that could be construed as a potential conflict of interest.

Publisher's Note: All claims expressed in this article are solely those of the authors and do not necessarily represent those of their affiliated organizations, or those of the publisher, the editors and the reviewers. Any product that may be evaluated in this article, or claim that may be made by its manufacturer, is not guaranteed or endorsed by the publisher.

frontiers in Cellular and Infection Microbiology

ORIGINAL RESEARCH
published: 02 December 2021
doi: 10.3389/fcimb.2021.783662

Integrative Transcriptomics and Proteomics Analyses to Reveal the Developmental Regulation of *Metorchis orientalis*: A Neglected Trematode With Potential Carcinogenic Implications

*Jun-Feng Gao†, Qing-Bo Lv†, Rui-Feng Mao, Yun-Yi Sun, Ying-Yu Chen, Yang-Yuan Qiu, Qiao-Cheng Chang and Chun-Ren Wang**

College of Animal Science and Veterinary Medicine, Heilongjiang Bayi Agricultural University, Daqing, China

OPEN ACCESS

Edited by:
Nian-Zhang Zhang, Lanzhou Veterinary Research Institute (CAAS), China

Reviewed by:
Guangyou Yang, Sichuan Agricultural University, China
Xue Bai, Jilin University, China

***Correspondence:**
Chun-Ren Wang
chunrenwang@sohu.com

†These authors have contributed equally to this work and share first authorship

Specialty section:
This article was submitted to Clinical Microbiology, a section of the journal Frontiers in Cellular and Infection Microbiology

Received: *26 September 2021*
Accepted: *16 November 2021*
Published: *02 December 2021*

Citation:
Gao J-F, Lv Q-B, Mao R-F, Sun Y-Y, Chen Y-Y, Qiu Y-Y, Chang Q-C and Wang C-R (2021) Integrative Transcriptomics and Proteomics Analyses to Reveal the Developmental Regulation of Metorchis orientalis: A Neglected Trematode With Potential Carcinogenic Implications. Front. Cell. Infect. Microbiol. 11:783662. doi: 10.3389/fcimb.2021.783662

Metorchis orientalis is a neglected zoonotic parasite of the gallbladder and bile duct of poultry, mammals, and humans. It has been widely reported in Asian, including China, Japanese, and Korea, where it is a potential threat to public health. Despite its significance as an animal and human pathogen, there are few published transcriptomic and proteomics data available. Transcriptome Illumina RNA sequencing and label-free protein quantification were performed to compare the gene and protein expression of adult and metacercariae-stage *M. orientalis*, resulting in 100,234 unigenes and 3,530 proteins. Of these, 13,823 differentially expressed genes and 1,445 differentially expressed proteins were identified in adult versus metacercariae. In total, 570 genes were differentially expressed consistent with the mRNA and protein level in the adult versus metacercariae stage. Differential gene transcription analyses revealed 34,228 genes to be expressed in both stages, whereas 66,006 genes showed stage-specific expression. Compared with adults, the metacercariae stage was highly transcriptional. GO and KEGG analyses based on transcriptome and proteome revealed numerous up-regulated genes in adult *M. orientalis* related to microtubule-based processes, microtubule motor activity, and nucleocytoplasmic transport. The up-regulated genes in metacercariae *M. orientalis* were mainly related to transmembrane receptor protein serine/threonine kinase activity, transmembrane receptor protein serine/threonine kinase signaling pathway. Transcriptome and proteome comparative analyses showed numerous up-regulated genes in adult stage were mainly enriched in actin filament capping, spectrin, and glucose metabolic process, while up-regulated genes in metacercariae stage were mainly related to cilium assembly, cilium movement, and motile cilium. These results highlight changes in protein and gene functions during the development of metacercariae into adults, and provided evidence for the mechanisms involved in morphological and metabolic changes at both the protein and gene levels.

Interestingly, many genes had been proved associated with liver fibrosis and carcinogenic factors were identified highly expressed in adult *M. orientalis*, which suggests that *M. orientalis* is a neglected trematode with potential carcinogenic implications. These data provide attractive targets for the development of therapeutic or diagnostic interventions for controlling *M. orientalis*.

Keywords: *Metorchis orientalis*, transcriptome, proteome, adult stage, metacercariae stage, differentially expressed genes

INTRODUCTION

The Opisthorchiidae is a large family of trematodes causing diseases with significant socioeconomic impacts in humans and animals in Asia and Europe, with more than 10 million people affected and ~680 million people estimated to be at risk of infection (Saijuntha et al., 2021). Opisthorchiidae flukes inhabit the biliary tract of the host, causing chronic diseases, including cholangitis, cholecystitis, cholelithiasis, and cholangiocarcinoma. Despite their significance, many of them have been neglected in terms of research and their control. *Metorchis orientalis* is a freshwater fluke and one such neglected member of the Opisthorchiidae. It mainly inhabits the gallbladder and bile duct of poultry and mammals, including humans. *M. orientalis* is endemic predominantly in regions of Korea and China (Qiu et al., 2017; Zhan et al., 2017; Sohn et al., 2021), where it has a wide geographical distribution across 19 provinces in China, thus representing a significant socioeconomic burden (Gao et al., 2018).

The life cycle of *M. orientalis* is very similar to that of *Clonorchis sinensis*. It includes two intermediate aquatic hosts (aquatic snails and freshwater fish) and a definitive host (piscivorous poultry and mammals). The first intermediate host (aquatic snail) is infected *via* consumption of embryonated eggs released with the feces of the definitive host. After asexual development in the snails, the cercarial stage is released and swims in search of its second intermediate hosts (freshwater fish). It then penetrates the skin of the fish and encysts as a metacercariae. Metacercariae are the infective stage of the fluke and its definitive hosts (poultry and mammals) become infected *via* the consumption of raw or undercooked infected freshwater fish. The metacercariae excyst in the duodenum and migrate into the bile duct, where they develop into adult flukes. The eggs are released *via* bile fluid into the intestine and expelled from the host *via* its feces into an aquatic environment, thus completing the life cycle (Zhang et al., 1985). No commercial vaccines against *M. orientalis* are currently available, therefore, treatment of metorchiasis relies predominantly on anthelmintic treatment with praziquantel (http://www.waterpathogens.org/book/liver-flukes), hosts can be reinfected because of a lack of acquired immunity in endemic regions. Thus, new methods of controlling metorchiasis in livestock and for the treatment of drug-resistant disease in humans are urgently needed.

Recent advances in various high-throughput omics technologies has allowed for the identification of key biomolecules crucial to the processes of parasitic transmission, and the identification of novel drug and/or vaccine targets. Numerous omics data are available for socioeconomically important fluke species, such as the transcriptomes conjunction with the sequencing and assembly of their genomes of *Schistosoma japonicum*, has generated a comprehensive picture of transcriptional and genomic diversity, then combination with the omics technologies to extend large-scale screens of the transcriptome and proteome of *Schistosoma japonicum* (Liu et al., 2006; Hokke et al., 2007). The multiple omics strategy also was applied to analyses in different development stages within parasite, to elucidate host responses that mirror the stage of infection and the developmental changes that occur within the migrating parasite, it gave great hope that effective rational strategies for vaccine and drug target identification were achievable.

Systematic comparisons across parasite developmental stages and related parasites have offered insights into parasite biology, while an 'immuno-omic approach' has leveraged this information to allow the identification of potential vaccine and diagnostic candidates (Bennuru et al., 2016). Thus, the current study carried out a combined transcriptomic and proteomic analyses of *M. orientalis* metacercariae and adults. The resulting data will provide attractive targets for the development of new therapeutic or diagnostic interventions for controlling the development and reproduction of *M. orientalis*.

MATERIALS AND METHODS

Parasite Samples

Metacercariae of *M. orientalis* were isolated from infected *Pseudorasbora parva* from the Wuyuer river basin (47.53°N, 124.44°E), Heilongjiang Province, China. Sheldrakes were orally infection with 100 metacercariae isolated from *P. parva* and then euthanized 6 weeks later. Adult *M. orientalis* were obtained from the liver and gallbladder of the ducks. These organs were thoroughly washed in sterile saline solution and frozen in liquid nitrogen until use. The metacercariae and adults were identified to the species level according to existing keys and descriptions (Sohn, 2009), immediately frozen in liquid nitrogen, and stored at -80°C until use.

RNA Isolation and Illumina Sequencing

Total RNA was extracted using TRIzol reagent (Invitrogen Life Technologies, Carlsbad, CA, USA) according to the manufacturer's protocol in three biological replicates of each *M. orientalis* development stage (pool of adults comprising of n = 50 and pool

of metacercariae comprising n = 2000). Total RNA of *M. orientalis* adults or metacercariae was stored at -80°C until use. Library construction was performed according to the Illumina sample preparation for RNA-sequencing (RNA-seq) protocol. Brifely, The Oligo (dT) was used to isolate poly (A) mRNA from total RNA. Then the mRNA is fragmented into short fragments by mixing with fragmentation buffer. The cDNA was synthesized using the mRNA fragments as templates. Short fragments were purified and dissolved with EB buffer for end reparation and then connected with adapters. The suitable fragments are selected for the PCR amplification as templates. During the quality control steps, Agilent 2100 Bioanaylzer and Qubit® RNA Assay Kit in Qubit® 2.0 Flurometer (Life Technologies, CA, USA) were used in quantification and qualification. Sequencing of the library preparations was performed by an Illumina Hiseq X Ten platform to obtain paired-end reads.

Transcriptome Assemble and Bioinformatic Analyses

Raw reads were subjected to quality control to obtain clean reads by removing reads with adaptors, reads containing > 10% 'N' residues, and low-quality reads containing > 50% bases. Clean reads were assembled into unigenes base on the default settings of the Trinity program (Grabherr et al., 2011). Unigene sequences were aligned with the NCBI non-redundant nucleotide (NT) database (Liu et al., 2016) by BLASTn (Zhang et al., 2017), and aligned with the NCBI non-redundant protein (NR) database (Liu et al., 2016), Swiss protein (Swiss-Prot) database (Liu et al., 2016), Cluster of Orthologous Groups of proteins (COG) database (Liu et al., 2016) and Kyoto Encyclopedia of genes and genomes (KEGG) database (Liu et al., 2016) by BLASTx (Zhang et al., 2017) to assign the predicted function. Hmmscan version 3.3.2 (Finn et al., 2011) was employed to match the established HMM model of protein structure domain among the Pfam database (Zhang et al., 2017). ESTScan version 3.0.3 (Iseli et al., 1999) was employed to predict protein coding sequences (CDS) with default setting. Blast2GO (Götz et al., 2008) was employed to classify unigenes to Interpro and Gene Ontology (GO) terms including molecular function, biological processes, and cellular components (Conesa et al., 2005) and analyzed the distribution of *M. orientalis* gene functions at the macro-level. The clean reads were deposited in the Sequence Read Archive database of NCBI (accession no. PRJNA474572), with sra run accessions numbers SRR7410653 and SRR7410652 for adult and metacercaria *M. orientalis*, respectively. The assembled cDNA sequences were deposited in the Transcriptome Shotgun Assembly (TSA) database of GenBank (accession no. GGVK00000000).

Identification of Genes Differentially Expressed Between Adult and Metacercariae *M. orientalis*

Unigene expression was calculated based on the Fragments Per kb per Million reads (FPKM) method (Mortazavi et al., 2008). The FPKM values were used directly used to compare the differences in gene expression levels between the two developmental stages. The Benjamini-Hochberg procedure is used to perform multiple corrections to *p*-values and generate false discovery rate (FDR) values. Differentially expressed genes (DEGs) were identified with an adjusted FDR < 0.005 found by DESeq2 version 1.34.0 (Love et al., 2014).

Quantitative Real-Time PCR Validation

Partial of total RNA same as transcriptome sequencing were used for quantitative real-time PCR (qRT-PCR) validation. Primers designed according to the Illumina sequencing data are listed in **Table S1**. CDNA was synthesized from total RNA using the reverse transcription kit (Takara, Dalian, China) following the manufacturer's instructions. Thermocycling conditions were: 40 cycles each with 95°C for 10 s for denaturation, 60°C for 20 s for annealing, and 72°C for 30 s for extension, performed in StepOne Plus Real-Time PCR System (Applied Biosystems, Foster City, CA, USA) with SYBR Green Pre-mix Ex Taq (Takara, Dalian, China) in triplicate. Relative gene expression was calculated using the $2^{-\Delta\Delta Ct}$ method with β-actin (GenBank no. EU109284) as the internal control. The correlation coefficients between the transcriptome and qRT-PCR values were calculated.

Protein Preparation and Digestion

Each *M. orientalis* development stage of total proteins (pool of adults comprising of n = 50 and pool of metacercariae comprising n = 2000) were extracted using protein lysis buffer (7 M urea, pH 8.0) in three biological replicates, and were lysed by sonication on ice (2/3 s, 5 min) using a high-intensity ultrasonic processor (Scientz Biotechnology Co. LTD, Ningbo, China).

The lysate was centrifuged at 20,000 × g for 20 min at 4°C in order to remove debris. After centrifugation, the supernatant was treated with 10 mM dithiothreitol for 60 min at 37°C. Then, the samples were alkylated with 55 mM iodoacetamide, protected from light for 45 min at room temperature. The concentration of protein was quantified using the BCA protein assay kit (Pierce, Rockford, IL, USA). For each sample approximately 10 μg of protein was subjected to 12.5% sodium dodecyl sulfate-polyacrylamide gel electrophoresis (SDS-PAGE) to assess protein integrity.

The protein samples for 50 μg were diluted with 30 mM HEPES until the concentration of urea becomes < 2 M. Trypsin was added into each sample at an enzyme to protein ratio of 1:50 and the samples were further digested overnight at 37°C. Enzymatic digestion was terminated by adding 0.5% (v/v) formic acid. Finally, peptides of each sample were desalted and concentrated using Sep-Pack C_{18} Cartridges (Waters, Worcester, MA, USA).

HPLC and LC-MS/MS

All samples filtering experiment were separated by an HPLC system (Easy-nanoLC, Thermo Scientific, Chelmsford, MA, USA) connected to an orbitrap fusion mass spectrometer (Thermo Scientific, Chelmsford, MA, USA). Peptides were resuspended with phase A [2% acetonitrile (ACN), 0.1% formic acid (FA)] and centrifuged at 12,000× *g* for 10 min. The supernatant was loaded on the trap column to be enriched

and desalted. Then, the peptides were separated at a flow rate of 300 nL/min on a 15 cm analytical column (Beijing Qinglian Biotech, China, 150 μm ×150 mm, 100A°, 1.9 μm) connected to the trap column. The linear gradient of LC was set at 3% buffer B (95% ACN, 0.1% FA) (from 0 to 5 min), 8–28% buffer B (from 5 to 107 min), and finally a hold at 28–80% buffer B (from 107 to 120 min).

Peptides were ionized by a nano-electrospray ion source and then identified by the orbitrap fusion mass spectrometer (Thermal Scientific, Chelmsford, MA, USA) in the mode of DDA (data-dependent acquisition). The scan of first-grade MS ranged from 350 to 1550 m/z at a resolution of 120,000 and an automatic gain control (AGC) target of 2×10^6. The scan of second-grade MS was initiated as 100 m/z at a resolution of 30,000 with a dynamic exclusive time of 30 ms and an AGC target of 5×10^4. The mode of second-grade MS spectra was high-energy collisional dissociation, and inject ions for all available parallelizable time.

Protein Quantification and Bioinformatic Analyses

Raw mass spectra were searched against *M. orientalis* transcriptome database in present study, and protein identification was performed using MaxQuant version 1.5.3.30 (Wiśniewski et al., 2009). The search parameters were set as follows: first and main search peptide tolerances of 20 ppm and 6 ppm, respectively, precursor ion mass tolerances of 20 ppm, a maximum of two missed trypsin cleavage sites, fixed cysteine carbamidomethylation, and variable methionine oxidation. Then, the acetylated sites were filtrated at the level of site decoy fraction ≤ 1% to obtain the significant modification. The *p*-value for identification and quantification of proteins was set as $p \leq 0.05$ and acetylated proteins with a fold-change of two were deemed as differentially expressed proteins (DEPs). Protein annotation used BLASTP on the UniProt database (Wang et al., 2011) with default parameters. GO enrichment analysis was used to determine whether the identified proteins were enriched in certain functional groups, as compared with the uniprot *Clonorchis sinensis* dataset (Wang et al., 2011), and Fisher's exact test was used for the analysis. Next, the identified proteins were blasted against the kyoto encyclopedia of genes and genomes (KEGG) (Wang et al., 2011) for orthology identification of the corresponding genes, and subsequently mapped to metabolic and regulatory pathways in KEGG. The proteomic data were deposited in the iProX platform (http://www.iprox.org) with the project no. IPX0003502000.

Parallel Reaction Monitoring Validation

Partial of total proteins same as proteome sequencing were used for further targeted quantification by Parallel Reaction Monitoring (PRM) by Beijing QLBio Biotechnology Co. (China). Briefly, An AQUA stable-isotope peptide as an internal standard reference was spiked in with each sample. Digested peptides were desalted on C_{18} stage tips prior to reversed phase chromatography on an Easy-nanoLC system (Thermal Scientific, Chelmsford, MA, USA). One hour liquid chromatography at a flow rate of 300 nL/min was used with the following gradients: 3 to 28% buffer B in 107min and 28 to 80% buffer B in 3 min. PRM analyses was performed using an orbitrap fusion mass spectrometer (Thermal Scientific, Chelmsford, MA, USA). Optimal collision energy, charge state, and retention time for the most significantly regulated peptides were generated experimentally using unique peptides of high intensity and confidence for each target protein. The mass spectrometer was operated in position ion mode with the following parameters: the full scan was collected with a resolution of 120,000 at 200m/z, the AGC target was 2×10^6 and the maximum injection time was at 100 ms. All PRM data analyses and data integration were performed using Skyline version 3.5.0 (MacLean et al., 2010). Three replicates were included for each sample in the PRM-MS analyses. Relative peptide quantification was calculated by dividing the peptide peak area. A two-tailed Student's t-test was used to estimate the significance of the difference in relative peptide abundance between *M. orientalis* adults and metacercariae.

Conjoint Analyses of Transcriptome and Proteome

In order to examine the detail post-translational regulation between transcriptome and proteome in adult and metacercaria *M. orientalis*, the fold changes of mRNA and protein were compared. In briefly, the fold changes were got in mRNA and protein level separately between adult stage and metacercariae-stage *M. orientalis*. And then, fold change ratio was calculated (As the following formula).

$$\text{Fold change ratio} = \frac{\text{Fold change(Protein)}}{\text{Fold change(mRNA)}}$$

We propose for most genes, the fold changes of mRNA and protein are similar. In order to get those genes with significant different fold change, significance A were calculate using MaxQuant version 1.5.3.30 (Wiśniewski et al., 2009), and those genes with the p value less than 0.05 and fold change ratio greater than 2 or less than 2 were consider as the significance up or down genes.

The statistical analyses involved in this study was implemented on R 4.0.3 platform (https://www.r-project.org/). Visualization of graphics were built in GraphPad Prism 8.0 (GraphPad Software, La Jolla, CA, USA) and R environment using the ggplot2 version 3.3.5 and ggpubr version 0.4.0 by online website https://github.com/kassambara/ggpubr/.

RESULTS

Overview of Transcriptomic Analyses and Quantitative Proteomics

A total of 47,396,124 and 51,014,100 clean reads were obtained from *M. orientalis* adults and metacercariae, respectively. The average ratio of clean reads to raw reads was 94.43% (**Table S2**). A total of 254,543 (>200 nt) transcripts were produced by the Trinity program for all samples. The N50 size was 1,002

nucleotide base pairs, which is shorter than other helminth transcriptomes (Liu et al., 2016; Zhang et al., 2017). Removing the redundancy resulted in 100,234 unigenes based on at least 0.3 FPKM in all samples. Functional annotation of the 100,234 unigenes data set was carried out using seven in public databases (Nr, Nt, Pfam, COG, Swiss-Prot, KEGG, and GO), resulting in 58.27% (n = 58,402) of the data set being annotated in at least one database (**Table 1**). Using a cut-off FDR of < 0.005 and a twofold change identified 13,823 DEGs in adult versus metacercariae, of which 4,773 were upregulated and 9,050 were downregulated (**Table S3**; **Figure 1A**).

In total, 21,604 peptides, 10,704 unique peptides, and 3,530 proteins were determined *via* proteomic analyses (**Table S4**). In terms of protein mass distribution, most proteins (73.5%) had molecular weights ranging from 10 to 70 ku, 12.1% of proteins had a molecular weight > 100 ku. Using KEGG and GO database annotations, 45.98% of proteins (1,623/3,530) were annotated to 1,036 GO terms and 67.56% proteins (2,385/3,530) were

TABLE 1 | Bioinformatics annotation of transcriptome unigenes and proteome proteins.

Bioinformatics annotations of unigenes	Number of Unigenes	Percentage (%)	Number of Protein	Percentage (%)
Annotated in NR	52,144	52.02	–	–
Annotated in NT	25,397	25.34	–	–
Annotated in KO	16,834	16.79	1,623	45.98
Annotated in SwissProt	30,959	30.89	–	–
Annotated in PFAM	35,949	35.87	–	–
Annotated in GO	36,042	35.96	2,385	67.56
Annotated in KOG	20,732	20.68	–	–
Annotated in all Databases	3,163	3.16	–	–
Annotated in at least one Database	58,401	58.26	–	–
Total Unigenes/Proteins	100,234	100	3,530	100

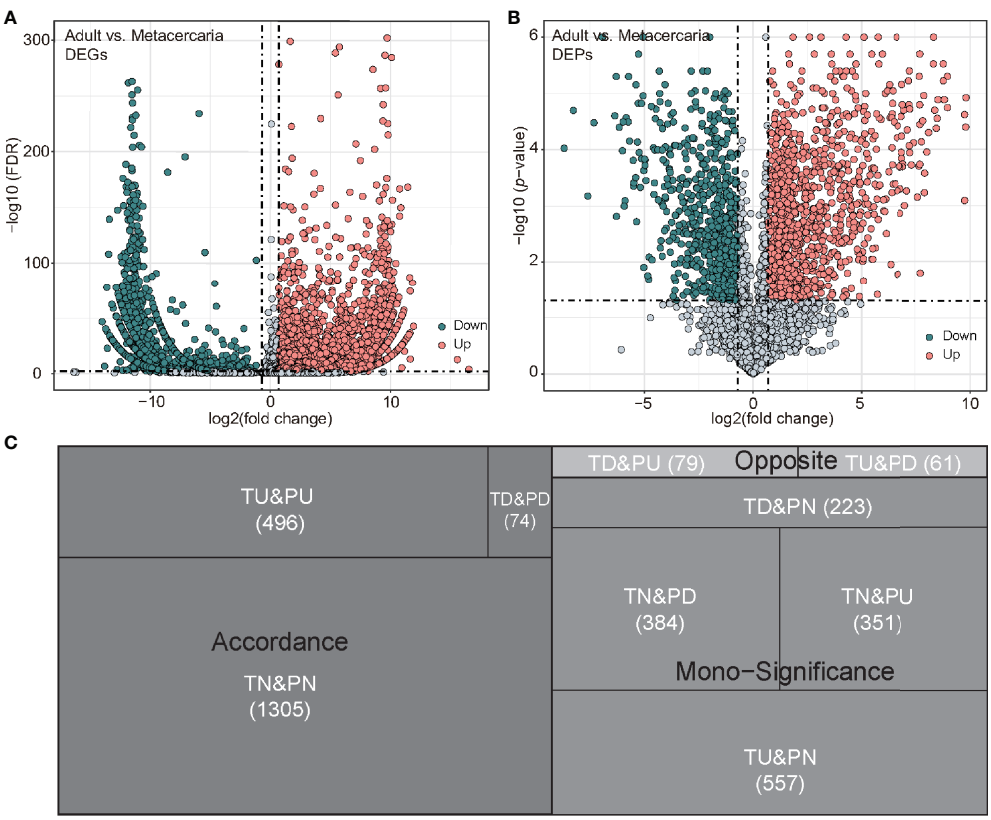

FIGURE 1 | Differentially expressed genes (DEGs) and differentially expressed proteins (DEPs) between adult stage and metacercariae stage. **(A, B)** presented DEGs and DEPs volcanoes, respectively. The differential expression cut-off of mRNA was FDR < 0.005 and 2-fold change, while the differential expression cut-off of protein was *p*-value <0.05 and 2-fold change. **(C)** The tree diagram shows the results of mRNA and protein co-expression. TU, TD and TN represent up-regulated, down-regulated and unchanged mRNA, respectively. PU, PD and PN represent up-regulated, down-regulated and unchanged protein, respectively.

annotated to 1,140 KEGG pathways (**Table 1**). Using a twofold change and p-value < 0.05 as a threshold resulted in 1,445 DEPs detected by the proteomic analyses (adult versus metacercariae), among which 519 proteins were up-regulated and 926 proteins were down-regulated (**Table S5**; **Figure 1B**).

By comparing the RNA-seq data with the proteomic data, all proteins were matched to the corresponding unigenes. Of these, 2,225 genes, including 780 DEGs and 1445 DEPs displayed differential expression at either the mRNA or protein levels between adult stage and metacercariae-stage *M. orientalis*. Of these, 496 genes were consistently upregulated between the adult stage and metacercariae stage, and 74 genes were consistently downregulated between the adult stage and metacercariae stage (**Table 2**; **Figure 1C**). However, 1,655 genes showed inconsistent expression at the mRNA and protein levels between the adult stage and metacercariae stage, which might result from post-translational regulation or modifications.

TABLE 2 | Combined analyses of transcriptome and proteome data.

Classification	Transcriptomic/Proteomic	Adult versus Metacercariae
Accordance	Invariant/Invariant	1305
	Up/Up	496
	Down/Down	74
Mono-Significance	Down/Invariant	223
	Up/Invariant	557
	Invariant/Down	384
	Invariant/Up	351
Opposite	Up/Down	61
	Down/Up	79

Transcriptomic Analyses of Adult and Metacercariae Stages of *M. orientalis*

Analyses of gene sharing between the adult stage and metacercariae-stage *M. orientalis* revealed 34,228 unigenes to be co-expressed by adults and metacercariae, whereas most (n = 66,006) exhibited stage-specific expression (adult = 25,426; metacercariae = 40,850) (**Figure 2A**). This suggested that the transcriptome level during the metacercariae stage is high, which might be related to the infection ability of metacercariae. There were 1,272 terms common to both adults and metacercariae. Only 81 GO terms were unique to the adults, compared with 998 GO terms in the metacercariae. The unique GO terms in the adults included GO:0044163, GO:0075521, and GO:0071479, involving host cytoskeleton, microtubule-dependent intracellular transport of viral material towards nucleus, and cellular response to ionizing radiation. Specific GO entries in the metacercariae included GO:0004664, GO:0004298, GO:0005839,

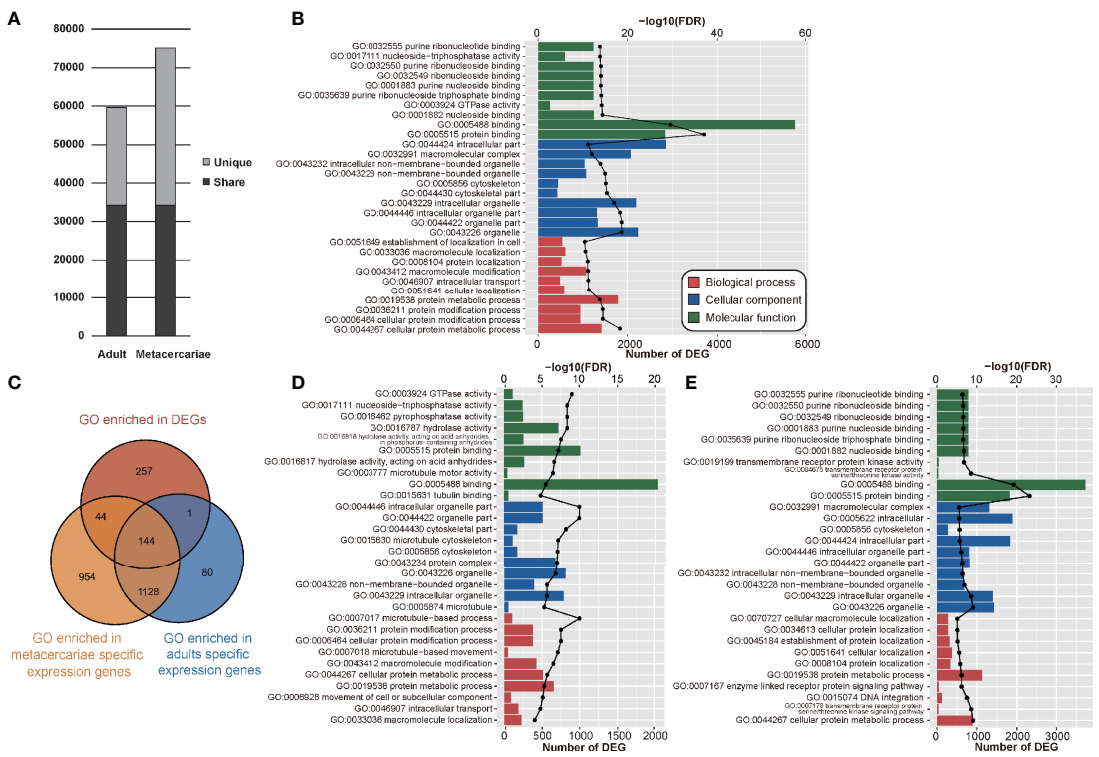

FIGURE 2 | The results of transcriptome analyses between adult stage and metacercariae stage. **(A)** The bar chart shows the number and sharing of genes expressed in adult stage and metacercariae stage. **(B)** Demonstrated the gene ontology (GO) assigned to the DEGs. **(C)** Demonstrated the relationship between the enrichment function and stage-specific genes. **(D)** Enrichment of up-regulated and down-regulated DEGs (adult versus metacercariae) in GO function. **(E)** Enrichment of down-regulated DEGs (adult vs metacercariae) in GO function.

and GO:0051603. These functions involved prephenate dehydratase activity, threonine-type endopeptidase activity, proteasome core complex, and proteolysis involved in cellular protein catabolism.

GO analyses were performed on DEGs and all DEGs were assigned to 4,389 GO terms, of which 446 GO terms were significantly enriched ($p < 0.05$). We focused on these enriched functions. In terms of biological processes, 267 GO terms were associated with these DEGs, most of which were involved in cellular protein metabolic process, cellular protein modification process, protein modification process. In terms of the cellular component, 77 GO terms were associated with these DEGs and were mainly involved in organelle, organelle part, and intracellular organelle part. By contrast, 102 molecular function GO terms were associated with these DEGs, including protein binding, binding, nucleoside binding, GTPase activity, and purine ribonucleoside triphosphate binding (**Figure 2B**; **Table S6**). In addition, nucleocytoplasmic transport (GO:0006913) was the only function that was significantly enriched among the genes unique to adults. By contrast, 44 GO terms were significantly enriched that involved genes unique to metacercariae (**Figure 2C**).

The up- and down-regulated genes were further analyzed to better understand the DEGs between adult and metacercariae-stage *M. orientalis*. All the upregulated genes were assigned to 139 GO terms (**Table S7**). Among these, up-regulated genes were uniquely enriched in 64 GO functions, mainly related to microtubules, and were significantly enriched in functions such as microtubule-based processes, microtubule-based movement, microtubule motor activity, and tubulin binding (**Figure 2D**). In addition, numerous up-regulated genes were enriched in GO functions of catalytic activity, hydrolase activity, and catalytic complexes. By contrast, down-regulated genes were assigned to 234 GO terms, of which 159 were uniquely enriched, including transmembrane receptor protein serine/threonine kinase activity, transmembrane receptor protein serine/threonine kinase signaling pathway, DNA integration, transmembrane receptor protein kinase activity, and enzyme linked receptor protein signaling pathway (**Figure 2E**). In addition, numerous down-regulated genes were concentrated in primary metabolic processes, cellular metabolic processes, macromolecule metabolic processes, and cellular macromolecule metabolic processes. Interestingly, a few genes participated in a variety of negatively regulated functions, such as neuropeptide hormone activity, negative regulation of proteasomal protein catabolic processes, and negative regulation of mitotic nuclear division.

KEGG pathway enrichment analyses of DEGs showed that 215 up-regulated DEGs were significantly enriched in 35 pathways ($p < 0.05$) (**Figure 3A**; **Table S8**). Consistent with the GO analyses, up-regulated genes were enriched in a variety of pathways related to reproduction, substance metabolism, and biosynthesis, such as oocyte meiosis (ko04114), glycolysis/gluconeogenesis (ko00010), pyrimidine metabolism (ko00240), nitrogen metabolism (ko00910), N-glycan biosynthesis (ko00510), purine metabolism (ko00230), starch and sucrose metabolism (ko00500) and arginine biosynthesis (ko00220). Similarly, various up-regulated genes participated in pathways related to genetic information processing, suggesting vigorous reproductive behavior during the adult stage. Of note, up-regulated genes were significantly enriched in the ko05130 pathway, which is mainly involved in the encoding of ACTB_G1 (Actin beta/Gamma 1), a protein with a key role in adult motion. In addition, these genes were enriched in the p53 signaling pathway (ko04115), which is highly associated with cancers and mainly regulates the apoptosis and senescence of cells. Interestingly, genes that were highly expressed in adults were also involved in butirosin and neomycin biosynthesis (ko00524), thyroid hormone synthesis (ko04918), inflammatory mediator regulation of TRP channels (ko04750), and drug metabolism - cytochrome P450 (ko00982). These findings could provide clues to the mechanisms by which the parasites fight bacteria and immune evasion.

Of the down-regulated DEGs, 261 were significantly enriched in 26 pathways ($p < 0.05$) (**Figure 3B**). Most of these genes expressed in metacercariae were involved in various biological cycles and some metabolic processes, such as the citrate cycle (TCA cycle) (ko00020), oxidative phosphorylation (ko00190), pyruvate metabolism (ko00620), and one-carbon pool by folate (ko00670). In addition, many hyperexpressed genes in metacercariae were enriched in the AMPK signaling pathway (ko04152), a fuel sensor and regulator that promotes ATP-producing and inhibits ATP-consuming pathways in various tissues. This suggests that the parasite regulates its energy use during the metacercariae stage when food intake is not possible. Interestingly, the overexpressed metacercariae genes were also involved in a variety of disease-related pathways, such as herpes simplex infection (ko05168), epithelial cell signaling in *Helicobacter pylori* infection (ko05120), bacterial invasion of epithelial cells (ko05100), non-alcoholic fatty liver disease (NAFLD) (ko04932), viral carcinogenesis (ko05203), and salmonella infection (ko05132). These findings could provide clues to a potential association between the *M. orientalis* metacercariae and these diseases.

Validation of RNA-Seq Profiles by qRT-PCR

To validate the transcriptome data, eight genes (three up-regulated and five down-regulated in adult stage versus metacercariae stage) were selected randomly among the DEGs, and their expression levels were verified by qRT-PCR (**Figure S1**). The results showed that DEGs of phosphoglycerate mutase, translation initiation factor 3 subunit B, and cathepsin F precursor were up-regulated in the adult stage versus metacercariae stage, whereas cytoplasmic 1, serpin, glutamine synthetase, elongation factor 1-gamma, and lactate dehydrogenase were up-regulated in metacercariae stage versus adult *M. orientalis*, which showed a similar expression trend to the transcriptome analysis, providing evidence on the reliability of the transcriptome sequencing results.

Proteomic Analyses of Adult and Metacercariae-Stage *M. orientalis*

GO analyses were performed on DEPs, and all DEPs were assigned to 630 GO functions. Among these, there were 218,

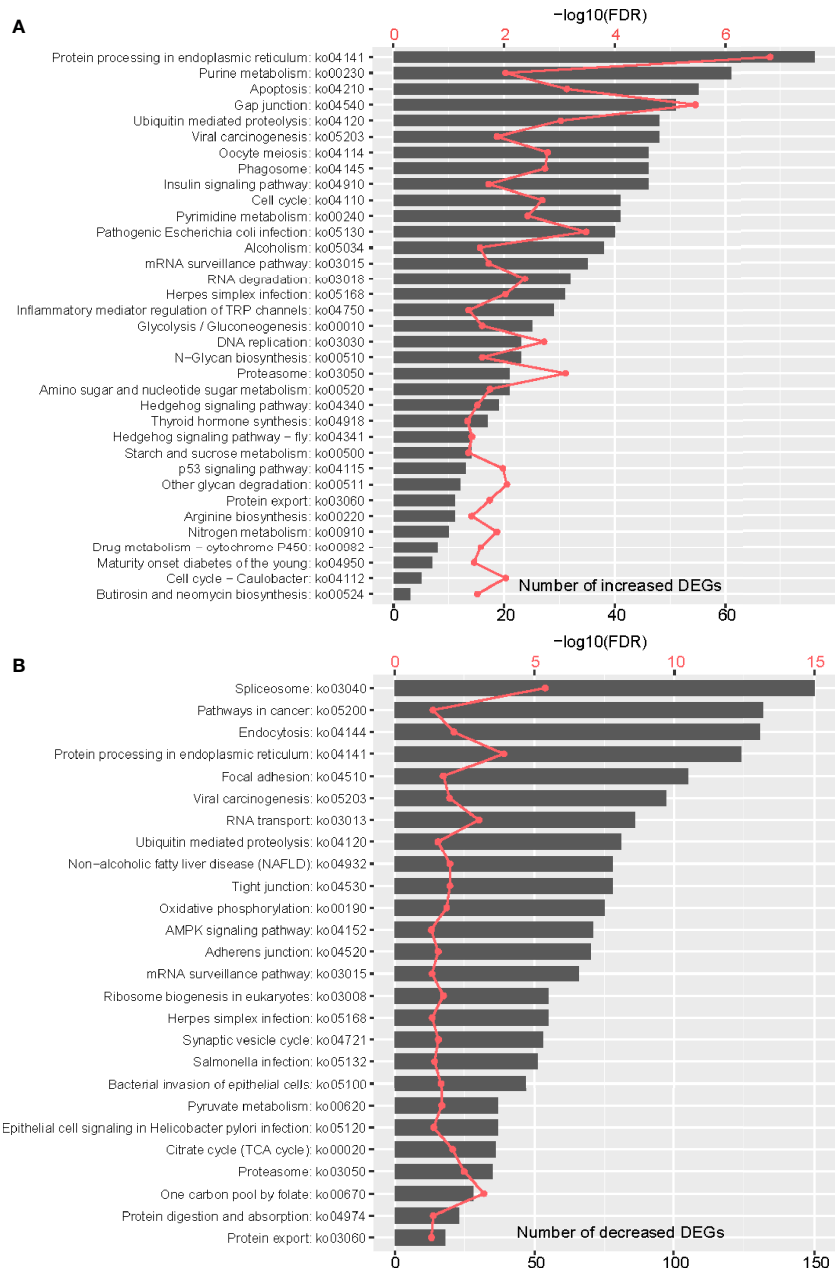

FIGURE 3 | Functional analyses of DEGs between adult stage and metacercariae stage. **(A)** showed the enrichment of DEGs in GO function, and **(B)** showed the enrichment of DEGs in KEGG function. Only results with FDR < 0.05 are shown.

101, and 311 GO terms for biological processes, cellular components and molecular functions, respectively (**Figure 4A**). Enrichment analyses showed that only protein folding (GO:0006457) was significantly enriched (FDR < 0.05) (**Figure 4B**; **Table S9**). The DEPs up- and down-regulated between the adult and metacercariae *M. orientalis* were then analyzed. In terms of biological processes, up-regulated proteins were significantly enriched in protein folding, microtubule-based processes and translation, whereas down-regulated proteins were significantly enriched in carbohydrate metabolic processes, TCA cycle, and the pentose-phosphate shunt (**Figure 4C**). In terms of cellular components, up-regulated proteins were significantly enriched in microtubules and ribosomes, whereas down-regulated proteins were significantly enriched in extracellular space, integral membrane components, and synaptic vesicles. In terms of molecular functions, up-regulated proteins were significantly concentrated in the unfold protein binding, structural dynamics of ribosomes, protein kinase activity, and

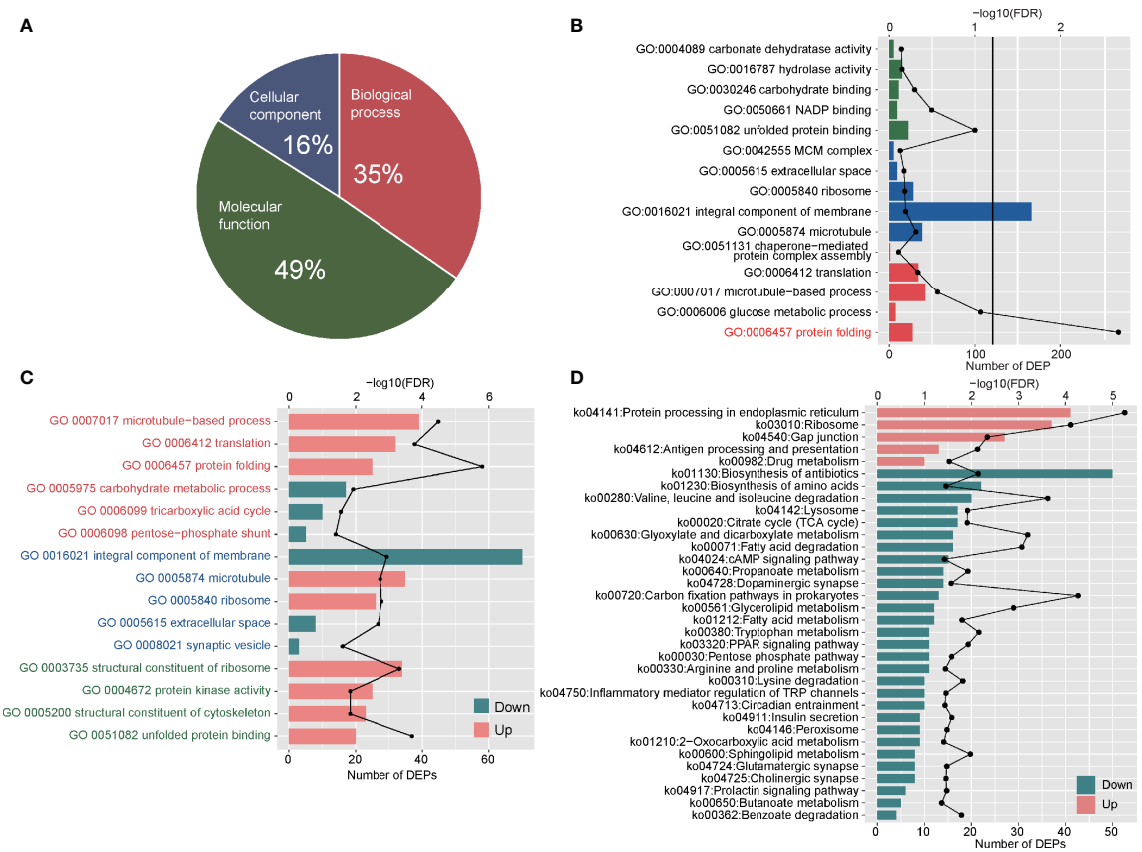

FIGURE 4 | Functional analyses of DEPs between adult stage and metacercariae stage. **(A)** Demonstrated the classification of DEPs by cellular component, biological process and molecular function. **(B)** The DEPs enriched in GO function. The red font indicates the significant enrichment function. **(C)** The increased and decreased DEPs enriched in GO function. The red font represents biological process classification, the blue font represents cellular component classification, and the green font represents molecular function classification. **(D)** The up-regulated DEPs and down-regulated DEPs enriched pathways in KEGG function. The discount graph represents the -log10 value of FDR and only shows the results of FDR < 0.05.

structural constituents of cytoskeleton categories, whereas down-regulated proteins were assigned to 205 GO terms (**Figure 4C**), however, no protein were enriched for any function.

KEGG pathway enrichment analyses were performed for DEPs, and all DEPs were assigned to 335 KEGG pathways (**Table S10**). These proteins were significantly enriched in glutathione metabolism (ko00480) and glycerolipid metabolism (ko00561). Up-regulated and down-regulated proteins enrichment analyses showed that a total of 388 up-regulated DEPs were involved in 294 KEGG pathways, and 265 down-regulated DEPs were involved in 304 pathways. The up-regulated proteins were significantly enriched in protein processing in endoplasmic reticulum, ribosomes, gap junctions, antigen processing and presentation, and drug metabolism (**Figure 4D**). By contrast, the down-regulated proteins were significantly enriched in 29 pathways, among which numerous proteins were enriched in the biosynthesis of antibiotics, biosynthesis of amino acids, valine, leucine and isoleucine degradation pathways (**Figure 4D**). In addition, a few down-regulated proteins were enriched in inflammatory mediator regulation of TRP channels, PPAR signaling pathways, and cAMP signaling pathways.

Verification of DEPs by PRM

PRM is an ion monitoring technology based on high resolution and high precision mass spectrometry, and can selectively detect target proteins and peptides, such as post-translational modifications peptides. To confirm DEPs in label-free analyses between adult stage and metacercariae-stage *M. orientalis*, eight significant DEPs were selected randomly for PRM analyses. The results showed the similar expression trends for the label-free proteomics data and PRM data (**Table 3**), verifying the accuracy and reliability of the proteome analyses.

Combined Transcriptome and Proteome Functional Analyses

In order to examine the detail post-translational regulation between transcriptome and proteome in adult and metacercaria *M. orientalis*, the significance up or down genes were calculated by significance A method (**Table S11**). Further analyses of the significance up or down genes were conducted through GO and KEGG pathways. Analyses of potential translation regulation were performed to obtain possible up-regulation and down-regulation results. Among 669

TABLE 3 | Confirmation of DEPs detected in label-free analyses using PRM assay.

Accession	Description	Labelfree Ratio (Ma versus Mm)	PRM Ratio (Ma versus Mm)
Cluster-2852.76449.orf1	saposin	0.42	0.43
Cluster-2852.68591.orf1	tegument antigen	0.78	0.43
Cluster-2852.68242.orf1	cathepsin F	118.36	55.80
Cluster-2852.85169.orf1	glutathione transferase	102.19	51.20
Cluster-2852.88752.orf1	acetylcholinesterase	0.02	0.09
Cluster-2852.60070.orf1	major egg antigen	50.98	10.94
Cluster-2852.68699.orf1	protein kinase A	46.96	10.15
Cluster-2852.53609.orf1	calreticulin	35.27	11.93

up-regulated genes, 230, 213, and 364 genes were assigned to biological processes, cellular components and molecular functions, respectively (**Figure 5A**; **Table S12**). These up-regulated genes were associated with actin filament capping, spectrin, glucose metabolic processes, arginine metabolic processes, structural constituents of cytoskeleton, myosin complexes and ATP binding (**Figure 5B**). In addition, some up-regulated genes were enriched in urea cycle, glucose metabolic processes, aromatic amino acid family metabolic processes, TCA cycle, and glycolytic processes (**Table S13**). This suggested that energy metabolism activities increased during metacercariae development. In addition, these up-regulated genes were also involved in the phagosome, spliceosome, and PPAR signaling and Hippo signaling pathways. Interestingly, many of the up-regulated genes were also involved in a variety of disease processes, such as hypertrophic cardiomyopathy (HCM), dilated cardiomyopathy (DCM), *Vibrio cholerae* infection, and viral myocarditis. Among 235 down-regulated genes, 53, 55, and 83 genes were assigned to biological processes, cellular components, and molecular

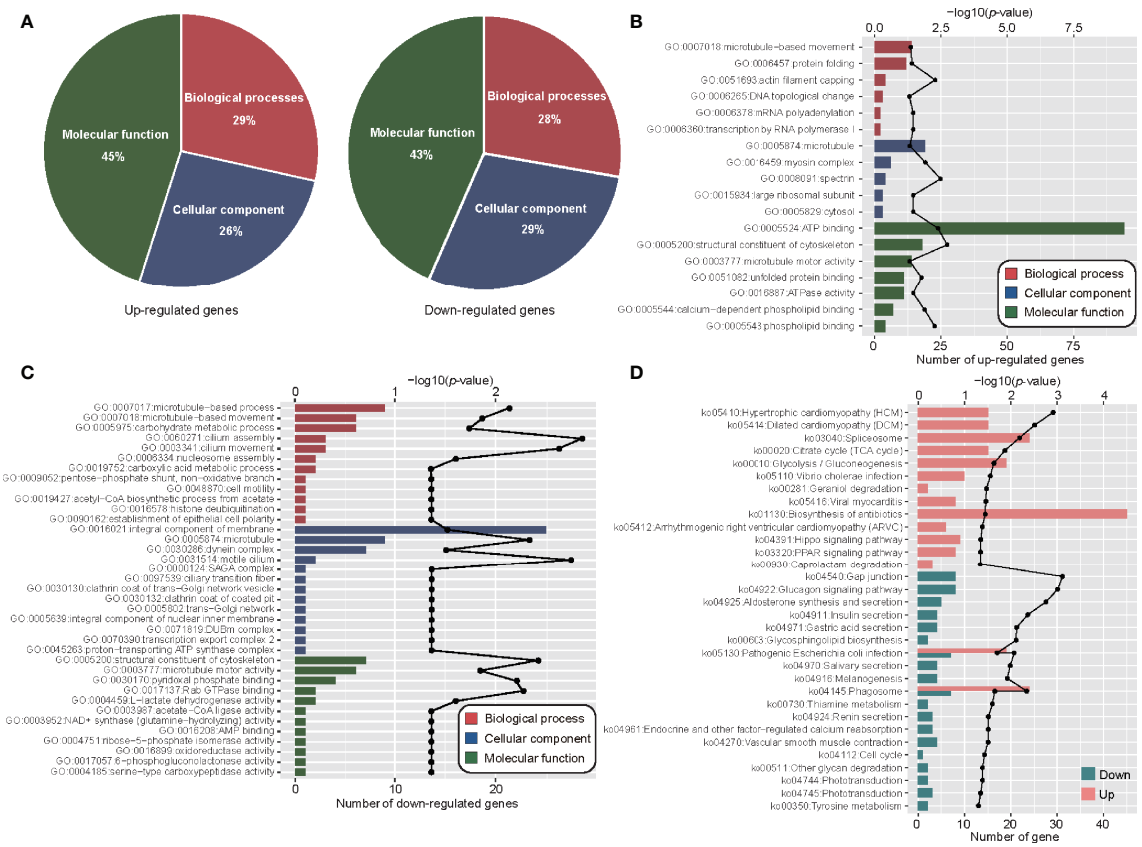

FIGURE 5 | Functional analyses combined transcriptome and proteome. **(A)** The pie plot shows the classification of co-up-regulated and co-down-regulated mRNA and proteins in GO function. **(B)** Co-up-regulated gene enrichment of GO function. **(C)** Co-down-regulated gene enriched GO function. **(D)** KEGG enriched function of genes with consistent mRNA and protein expression levels. The discount graph represents the -log10 value of *p*-value and only shows the results of *p*-value < 0.05.

functions, respectively. These decreased genes were associated with cilium assembly and movement, motile cilia, microtubule pyridoxal phosphate binding, and Rab GTPase binding (**Figure 5C**). Some down-regulated genes were also enriched in gap junctions, glucagon signaling pathway, aldosterone synthesis and secretion, insulin secretion, and other pathways (**Figure 5D**). These results suggest that although gene and protein expression levels were not always consistent, there was a high degree of consistency between the functions of DEGs and DEPs in the different stages of *M. orientalis*.

DISCUSSION

The liver fluke *M. orientalis* is an economically important pathogen of livestock worldwide, as well as being an important neglected zoonosis. Metorchiasis control is reliant on the use of drugs, particularly praziquantel, which is effective against multiple parasite stages (http://www.waterpathogens.org/book/liver-flukes). However, the spread of parasites resistant to praziquantel has intensified the pursuit for novel control strategies (Fairweather et al., 2020). Emerging omic technologies are helping advance our understanding of parasite biology, specifically the molecules that act at the host-parasite interface and are central to infection, virulence and long-term survival within the host (Prasopdee et al., 2019). To better understand the biology of *M. orientalis*, transcripts from the adult stage were sequenced by next-generation sequencing in a previous study (Gao et al., 2018). Although this published data set provided significant insights into the transcriptome of *M. orientalis*, only the adult stage was represented, and this initial study performed a qualitative exploration of the transcriptome, quantitative assessment of transcription during the life-cycle of this parasite was not possible at the time of study. To overcome these limitations for *M. orientalis*, a next-generation sequencing platform and proteomics were used to develop a global view of the transcriptomes of adult and metacercariae stages of *M. orientalis* in the present study.

In total, 13,823 distinct genes and 1,445 proteins were found to be differentially expressed between adult and metacercariae *M. orientalis*, which is significantly higher than that found for *C.sinensis, O. felineus, and O. viverrini* (Jex et al., 2012; Huang et al., 2013; Pomaznoy et al., 2016). Although some genes involved in basal and energy metabolisms were abundantly expressed in both stages of *M. orientalis*, some genes showed differential expression because of the different biological characteristics of the two developmental stages. Adult worms produce abundant eggs daily, thus the transcriptome profile is tightly linked with egg production. In the current study, many reproduction-associated proteins, such as vitelline B precursor protein and egg protein, were highly expressed at both the transcription and translation levels in the adult stage. Tyrosinase has a key role in the formation of eggshell, which originates from the vitelline cells inside the vitellaria. In the current study, tyrosinase was highly expressed in the adult stage, a result that was consistent with a previous report (Anderson et al., 2015). In addition, because adults *M. orientalis* inhabit the bile duct of their definitive host, and biliary duct cells are frequently exposed to liver-derived endogenous and exogenous toxins, carcinogens, drugs, and their metabolites (xenobiotics), the flukes have evolved an antioxidant system to protects its cells against such compounds. For example, glutathione-S-transferases can protect the parasite by reducing lipid hydroperoxides, as well as detoxifying xenobiotic substrates *via* glutathione conjugation.

In metacercariae stage, because the parasite remains dormant and maintains a low metabolic ratee, some ribosomal proteins, such as elongation factor 2 and structural housekeeping genes, such as Heat shock proteins 70, were transcribed at a higher rate in this stage. Such structural housekeeping genes can maintain the most basic life characteristics and consume the least amount of energy until it is engulfed by its definitive host (Pomaznoy et al., 2016). The metacercariae experience a significant thermal change when they move from their intermediate host (freshwater fish) to the stomach of the definitive host (poultry or mammals), thus, the high transcription of the heat shock proteins might be related to their response to thermal-induced stresses (Abou-El-Naga, 2020). Moreover, cysteine protease was also highly transcribed in metacercariae, and is an essential enzyme involved in initiating excystation (Yoo et al., 2011).

C. sinensis and *O. viverrini* have been assessed as carcinogenic biological agents to humans by the Agency for Research on Cancer, and *O. felineus* has also been reported to be associated with the development of cholangiocarcinoma by comparing previously reported molecular targets (Pomaznoy et al., 2016; Prueksapanich et al., 2018). However, as a member of the Opisthorchiidae, little is known about the carcinogenicity of *M. orientalis*. The pathways of pathogenesis of opisthorchiasis-associated cholangiocarcinoma are thought to be multifactorial, including mechanical damage, inflammation-induced immunopathology, and direct effects of fluke-secreted growth factors (Pakharukova and Mordvinov, 2016). Cathepsin F and granulins are considered as the crucial carcinogenic factors secreted by flukes (Pomaznoy et al., 2016). Cathepsin F is a cysteine protease family, which can induce inflammation and promote malignancy. The fluke secretes several cathepsin F cysteine proteases into the bile duct that could induce or contribute to the pathologies associated with hepatobiliary abnormalities (Pinlaor et al., 2009). Granulins are growth factors that can be secreted into the bile ducts, they have mitogenic properties that drive cell proliferation, creating a tumorigenic environment (Arunsan et al., 2020). In the present study, cathepsin F and granulins were found most highly expressed in *M. orientalis* (mainly in the adult stage), which is consistent with previous reports (Pomaznoy et al., 2016; Young et al., 2021). This suggests that *M. orientalis* is a neglected trematode with potential carcinogenic implications, although further research is needed.

Based on the KEGG pathway, the most enriched pathway terms between adult stage and metacercariae *M. orientalis* included protein processing in endoplasmic reticulum (200 genes; 45 proteins), spliceosome (200 genes; 15 proteins), and proteasome (56 genes; 5 proteins), indicating the involvement of active metabolic processes in the development of *M. orientalis* metacercariae to adults. Interestingly, signaling pathways

associated with "liver fibrosis" were also identified, namely the TGF-β signaling pathway (44 genes; two proteins). Similar to *O. felineus* and *C. sinensis*, *M. orientalis* can caused liver fibrosis during chronic infection (Wang et al., 2020). Previous studies showed that liver fibrosis was orchestrated by a complex network of signaling pathways involved in regulating the deposition of extracellular matrix (Yan et al., 2015). Among these signaling pathways, the TGF-β signaling pathway has been shown to have an important role in the development of liver fibrosis caused by parasitic infection (Gao et al., 2018). TGF-β is a major pro-fibrotic cytokine, with a crucial role in orchestrating fibrogenesis. TGF-β1 triggers its downstream signaling pathway meditated by TGF-β type I (TGFβRI) and type II receptors (TGFβRII), causing Smad2 and Smad3 phosphorylation. Phosphorylated Smad2 and Smad3 rapidly combine with Smad4 and subsequently migrates to the nucleus, leading to mass of fibrotic genes expression (Hata and Chen, 2016; Hu et al., 2018). Meanwile, the TGF-β signaling pathway has also been related to egg-laying behavior in *Fasciola gigantica* (Zhang et al., 2017). Thus, these data provide attractive targets for the development of new therapeutic or diagnostic interventions for controlling the development and the reproductive process of *M. orientalis*.

CONCLUSION

The present study revealed a transcriptome and proteome data set for adult stage and metacercariae-stage *M. orientalis* that significant expands the currently gene repertoire of this parasitic trematode. The characterization of these transcriptome and proteome data has implications for an improved understanding of the biology of *M. orientalis*, and will facilitate the development of intervention agents for this and other pathogenic flukes of human and animal health significance.

DATA AVAILABILITY STATEMENT

The datasets presented in this study can be found in online repositories. The names of the repository/repositories and accession number(s) can be found in the article/**Supplementary Material**.

ETHICS STATEMENT

The animal study was reviewed and approved by the National Institute of Animal Health Animal Care and Use Committee of the Heilongjiang Bayi Agricultural University.

AUTHOR CONTRIBUTIONS

C-RW designed the project and experiments. J-FG analyzed the data and writing original manuscript. Q-BL writing, reviewing and editing manuscript. R-FM and Y-YS validation the data. Y-YC and Y-YQ conducted the experiments. Q-CC analyses and interpretation of data. All authors contributed to the article and approved the submitted version.

FUNDING

This work was supported by National Natural Science Foundation of China (31972703; 32172886), Natural Science Foundation of Heilongjiang Province (LH2021C071), Heilongjiang Provincial Postdoctoral Science Foundation (LBH-Z19191) and Heilongjiang Bayi Agricultural University Support Program for San Heng San Zong (TDJH202002).

ACKNOWLEDGMENTS

We thank Beijing QLBio biotechnology Co., Ltd. for providing technical support and International Science Editing (http://www.internationalscienceediting.com) for editing this manuscript.

SUPPLEMENTARY MATERIAL

The Supplementary Material for this article can be found online at: https://www.frontiersin.org/articles/10.3389/fcimb.2021.783662/full#supplementary-material

Supplementary Figure 1 | Validation of RNA-seq profiles by quantitative real-time PCR.

REFERENCES

Abou-El-Naga, I. F. (2020). Heat Shock Protein 70 (Hsp70) in Schistosoma Mansoni and its Role in Decreased Adult Worm Sensitivity to Praziquantel. *Parasitology.* 147, 634–642. doi: 10.1017/S0031182020000347

Anderson, L., Amaral, M. S., Beckedorff, F., Silva, L. F., Dazzani, B., Oliveira, K. C., et al. (2015). *Schistosoma Mansoni* Egg, Adult Male and Female Comparative Gene Expression Analysis and Identification of Novel Genes by RNA-Seq. *PloS Negl. Trop. Dis.* 9, e0004334. doi: 10.1371/journal.pntd.0004334

Arunsan, P., Chaidee, A., Cochran, C. J., Mann, V. H., Tanno, T., Kumkhaek, C., et al. (2020). Liver Fluke Granulin Promotes Extracellular Vesicle-Mediated Crosstalk and Cellular Microenvironment Conducive to Cholangiocarcinoma. *Neoplasia.* 22, 203–216. doi: 10.1016/j.neo.2020.02.004

Bennuru, S., Cotton, J. A., Ribeiro, J. M., Grote, A., Harsha, B., Holroyd, N., et al. (2016). Stage-Specific Transcriptome and Proteome Analyses of the Filarial Parasite Onchocerca Volvulus and Its Wolbachia Endosymbiont. *mBio* 7, e02028–e02016. doi: 10.1128/mBio.02028–16

Conesa, A., Götz, S., García-Gómez, J. M., Terol, J., Talón, M., and Robles, M. (2005). Blast2GO: A Universal Tool for Annotation, Visualization and Analysis in Functional Genomics Research. *Bioinformatics* 21, 3674–3676. doi: 10.1093/bioinformatics/bti610

Grabherr, M. G., Haas,B. J., Yassour,M., Levin,J. Z., Thompson,D. A., Amit,I., et al. (2011). Fulllength Transcriptome Assembly From RNA-Seq Data Without a Reference Genome. *Nat. Biotechnol.* 29, 644–652. doi: 10.1038/nbt.1883

Fairweather, I., Brennan, G. P., Hanna, R. E. B., Robinson, M. W., and Skuce, P. J. (2020). Drug Resistance in Liver Flukes. *Int. J. Parasitol. Drugs Drug Resist.* 12, 39–59. doi: 10.1016/j.ijpddr.2019.11.003

Finn, R. D., Clements, J., and Eddy, S. R. (2011). HMMER Web Server: Interactive Sequence Similarity Searching. *Nucleic. Acids Res.* 39, W29–W37. doi: 10.1093/nar/gkr367

Gao, J. F., Gao, Y., Qiu, J. H., Chang, Q. C., Zhang, Y., Fang, M., et al. (2018). *De Novo* Assembly and Functional Annotations of the Transcriptome of Metorchis Orientalis (Trematoda: Opisthorchiidae). *Exp. Parasitol.* 184, 90–96. doi: 10.1016/j.exppara.2017.12.001

Götz, S., García-Gómez, J. M., Terol, J., Williams, T. D., Nagaraj, S. H., Nueda, M. J., et al. (2008). High-Throughput Functional Annotation and Data Mining With the Blast2GO Suite. *Nucleic. Acids Res.* 36, 3420–3435. doi: 10.1093/nar/gkn176

Jex,A. R., Young,N. D., Sripa,J., Hall, R. S., Scheerlinck, J. P., Laha, T., et al. (2012). Molecular Changes in Opisthorchis Viverrini (Southeast Asian Liver Fluke) During the Transition From the Juvenile to the Adult Stage. *PloS Negl. Trop. Dis.* 6, e1916. doi: 10.1371/journal.pntd.0001916

Hata, A., and Chen, Y. G. (2016). TGF-β Signaling From Receptors to Smads. *Cold Spring Harb. Perspect. Biol.* 8:a022061. doi: 10.1101/cshperspect.a022061

Hokke, C. H., Fitzpatrick, J. M., and Hoffmann, K. F. (2007). Integrating Transcriptome, Proteome and Glycome Analyses of *Schistosoma* Biology. *Trends Parasitol.* 23, 165–174. doi: 10.1016/j.pt.2007.02.007

Huang, Y., Chen, W., Wang, X. Y., Liu, H. L., Chen, Y. Y., Guo, L., et al. (2013). The Carcinogenic Liver Fluke, Clonorchis Sinensis: New Assembly, Reannotation and Analysis of the Genome and Characterization of Tissue Transcriptomes. *PloS One* 8, e54732. doi: 10.1371/journal.pone.0054732

Hu, H. H., Chen, D. Q., Wang, Y. N., Feng, Y. L., Cao, G., Vaziri, N. D., et al. (2018). New Insights Into TGF-β/Smad Signaling in Tissue Fibrosis. *Chem. Biol. Interact.* 292, 76–83. doi: 10.1016/j.cbi.2018.07.008

Iseli, C., Jongeneel, C. V., and Bucher, P. (1999). ESTScan: A Program for Detecting, Evaluating, and Reconstructing Potential Coding Regions in EST Sequences. *Proc. Int. Conf. Intell. Syst. Mol. Biol.* 138–148.

Liu, F., Lu, J., Hu, W., Wang, S. Y., Cui, S. J., Chi, M., et al. (2006). New Perspectives on Host-Parasite Interplay by Comparative Transcriptomic and Proteomic Analyses of Schistosoma Japonicum. *PloS Pathog.* 2, e29. doi: 10.1371/journal.ppat.0020029

Liu, G. H., Xu, M. J., Song, H. Q., Wang, C. R., and Zhu, X. Q. (2016). *De Novo* Assembly and Characterization of the Transcriptome of the Pancreatic Fluke *Eurytrema Pancreaticum* (Trematoda: Dicrocoeliidae) Using Illumina Paired-End Sequencing. *Gene* 576, 333–338. doi: 10.1016/j.gene.2015.10.045

Love, M. I., Huber, W., and Anders, S. (2014). Moderated Estimation of Fold Change and Dispersion for RNA-Seq Data With Deseq2. *Genome Biol.* 15:550. doi: 10.1186/s13059-014-0550-8

MacLean, B., Tomazela, D. M., Shulman, N., Chambers, M., Finney, G. L., Frewen, B., et al. (2010). Skyline: An Open Source Document Editor for Creating and Analyzing Targeted Proteomics Experiments. *Bioinformatics* 26, 966–968. doi: 10.1093/bioinformatics/btq054

Mortazavi, A., Williams, B. A., McCue, K., Schaeffer, L., and Wold, B. (2008). Mapping and Quantifying Mammalian Transcriptomes by RNA-Seq. *Nat. Methods* 5, 621–628. doi: 10.1038/nmeth.1226

Pakharukova, M. Y., and Mordvinov, V. A. (2016). The Liver Fluke *Opisthorchis Felineus*: Biology, Epidemiology and Carcinogenic Potential. *Trans. R. Soc Trop. Med. Hyg.* 110, 28–36. doi: 10.1093/trstmh/trv085

Pinlaor, P., Kaewpitoon, N., Laha, T., Sripa, B., Kaewkes, S., Morales, M. E., et al. (2009). Cathepsin F Cysteine Protease of the Human Liver Fluke, Opisthorchis Viverrini. *PloS Negl. Trop. Dis.* 3, e398. doi: 10.1371/journal.pntd.0000398

Pomaznoy, M. Y., Logacheva, M. D., Young, N. D., Penin, A. A., Ershov, N. I., Katokhin, A. V., et al. (2016). Whole Transcriptome Profiling of Adult and Infective Stages of the Trematode Opisthorchis Felineus. *Parasitol. Int.* 65, 12–19. doi: 10.1016/j.parint.2015.09.002

Prasopdee, S., Thitapakorn, V., Sathavornmanee, T., and Tesana, S. (2019). A Comprehensive Review of Omics and Host-Parasite Interplays Studies, Towards Control of Opisthorchis Viverrini Infection for Prevention of Cholangiocarcinoma. *Acta Trop.* 196, 76–82. doi: 10.1016/j.actatropica.2019.05.011

Prueksapanich, P., Piyachaturawat, P., Aumpansub, P., Ridtitid, W., Chaiteerakij, R., and Rerknimitr, R. (2018). Liver Fluke-Associated Biliary Tract Cancer. *Gut Liver* 12, 236–245. doi: 10.5009/gnl17102

Qiu, J. H., Zhang, Y., Zhang, X. X., Gao, Y., Li, Q., Chang, Q. C., et al. (2017). Metacercaria Infection Status of Fishborne Zoonotic Trematodes, Except for Clonorchis Sinensis in Fish From the Heilongjiang Province, China. *Foodborne Pathog. Dis.* 14 (8), 440–446. doi: 10.1089/fpd.2016.2249

Saijuntha, W., Sithithaworn, P., Petney, T. N., and Andrews, R. H. (2021). Foodborne Zoonotic Parasites of the Family Opisthorchiidae. *Res. Vet. Sci.* 135, 404–411. doi: 10.1016/j.rvsc.2020.10.024

Sohn, W. M. (2009). Fish-Borne Zoonotic Trematode Metacercariae in the Republic of Korea. *Korean J. Parasitol.* 47, S103–S113. doi: 10.3347/kjp.2009.47.S.S103

Sohn, W. M., Na, B. K., Cho, S. H., Lee, H. I., Ju, J. W., Lee, M. R., et al. (2021). Survey of Zoonotic Trematode Metacercariae in Fish From Irrigation Canal of Togyo-Jeosuji (Reservoir) in Cheorwon-Gun, Gangwon-Do, Republic of Korea. *Korean J. Parasitol.* 59, 427–432. doi: 10.3347/kjp.2021.59.4.427

Wang, X., Chen, W., Huang, Y., Sun, J., Men, J., Liu, H., et al. (2011). The Draft Genome of the Carcinogenic Human Liver Fluke Clonorchis Sinensis. *Genome Biol.* 12, R107. doi: 10.1186/gb-2011-12-10-r107

Wang, Y. R., Li, X., Sun, Q. S., Gong, P. T., Zhang, N., Zhang, X. C., et al. (2020). First Case Report of Metorchis Orientalis From Black Swan. *Int. J. Parasitol. Parasites. Wildl.* 13, 7–12. doi: 10.1016/j.ijppaw.2020.07.011

Wiśniewski, J. R., Zougman, A., Nagaraj, N., and Mann, M. (2009). Universal Sample Preparation Method for Proteome Analysis. *Nat. Methods* 6, 359–362. doi: 10.1038/nmeth.1322

Yan, C., Wang, L., Li, B., Zhang, B. B., Zhang, B., Wang, Y. H., et al. (2015). The Expression Dynamics of Transforming Growth Factor-β/Smad Signaling in the Liver Fibrosis Experimentally Caused by *Clonorchis sinensis Parasites Vectors.* 8, 70. doi: 10.1186/s13071–015–0675–y

Yoo, W. G., Kim, D. W., Ju, J. W., Cho, P. Y., Kim, T. I., Cho, S. H., et al. (2011). Developmental Transcriptomic Features of the Carcinogenic Liver Fluke, Clonorchis sinensis. *PloS Negl. Trop. Dis.* 5, e1208. doi: 10.1371/journal.pntd.0001208

Young, N. D., Stroehlein, A. J., Kinkar, L., Wang, T., Sohn, W. M., Chang, B. C. H., et al. (2021). High-Quality Reference Genome for. *Clonorchis sinensis. Genomics* 113, 1605–1615. doi: 10.1016/j.ygeno.2021.03.001

Zhang, X. X., Cong, W., Elsheikha, H. M., Liu, G. H., Ma, J. G., Huang, W. Y., et al. (2017). *De Novo* Transcriptome Sequencing and Analysis of the Juvenile and Adult Stages of Fasciola Gigantica. *Infect. Genet. Evol.* 51, 33–40. doi: 10.1016/j.meegid.2017.03.007

Zhang, Y. J., Tang, Z. Z., and Tang, C. T. (1985). Studies on the Life Histories of Three Species of Heterophyid Trematodes and *Metorchis Orientalis* Tanabe 1921. *Ji Sheng Chong Xue Yu Ji Sheng Chong Bing Za Zhi* 3, 12–16. (in Chinese).

Zhan, X., Li, C., Wu, H., Sun, E., and Zhu, Y. (2017). Investigation on the Endemic Characteristics of Metorchis Orientalis in Huainan Area, China. *Nutr. Hosp.* 34, 675–679. doi: 10.20960/nh.1333

Conflict of Interest: The authors declare that the research was conducted in the absence of any commercial or financial relationships that could be construed as a potential conflict of interest.

Publisher's Note: All claims expressed in this article are solely those of the authors and do not necessarily represent those of their affiliated organizations, or those of the publisher, the editors and the reviewers. Any product that may be evaluated in this article, or claim that may be made by its manufacturer, is not guaranteed or endorsed by the publisher.

frontiers in Cellular and Infection Microbiology

ORIGINAL RESEARCH
published: 16 December 2021
doi: 10.3389/fcimb.2021.787635

Enhancing Immune Responses to a DNA Vaccine Encoding *Toxoplasma gondii* GRA7 Using Calcium Phosphate Nanoparticles as an Adjuvant

Hong-Chao Sun[1], *Jing Huang*[2], *Yuan Fu*[1], *Li-Li Hao*[3], *Xin Liu*[3] *and Tuan-Yuan Shi*[1]*

[1] Department of Animal Parasitology, Institute of Animal Husbandry and Veterinary Medicine, Zhejiang Academy of Agricultural Science, Hangzhou, China, [2] Department of Animal Epidemic Surveillance, Zhejiang Provincial Animal Disease Prevention and Control Center, Hangzhou, China, [3] College of Life Science and Technology, Southwest Minzu University, Chengdu, China

OPEN ACCESS

Edited by:
Xiao-Xuan Zhang,
Qingdao Agricultural University, China

Reviewed by:
Jin Lei Wang,
Lanzhou Veterinary Research Institute (CAAS), China
Si-Yang Huang,
Yangzhou University, China
Na Yang,
Shenyang Agricultural University, China

***Correspondence:**
Tuan-Yuan Shi
lstone2008@126.com

Specialty section:
This article was submitted to Clinical Microbiology, a section of the journal Frontiers in Cellular and Infection Microbiology

Received: 01 October 2021
Accepted: 08 November 2021
Published: 16 December 2021

Citation:
Sun H-C, Huang J, Fu Y, Hao L-L, Liu X and Shi T-Y (2021) Enhancing Immune Responses to a DNA Vaccine Encoding Toxoplasma gondii GRA7 Using Calcium Phosphate Nanoparticles as an Adjuvant. Front. Cell. Infect. Microbiol. 11:787635. doi: 10.3389/fcimb.2021.787635

Toxoplasma gondii infects almost all warm-blooded animals, including humans. DNA vaccines are an effective strategy against *T. gondii* infection, but these vaccines have often been poorly immunogenic due to the poor distribution of plasmids or degradation by lysosomes. It is necessary to evaluate the antigen delivery system for optimal vaccination strategy. Nanoparticles (NPs) have been shown to modulate and enhance the cellular humoral immune response. Here, we studied the immunological properties of calcium phosphate nanoparticles (CaPNs) as nanoadjuvants to enhance the protective effect of *T. gondii* dense granule protein (GRA7). BALB/c mice were injected three times and then challenged with *T. gondii* RH strain tachyzoites. Mice vaccinated with GRA7-pEGFP-C2+ nano-adjuvant (CaPNs) showed a strong cellular immune response, as monitored by elevated levels of anti-*T. gondii*-specific immunoglobulin G (IgG), a higher IgG2a-to-IgG1 ratio, elevated interleukin (IL)-12 and interferon (IFN)-γ production, and low IL-4 levels. We found that a significantly higher level of splenocyte proliferation was induced by GRA7-pEGFP-C2+nano-adjuvant (CaPNs) immunization, and a significantly prolonged survival time and decreased parasite burden were observed in vaccine-immunized mice. These data indicated that CaPN-based immunization with *T. gondii* GRA7 is a promising approach to improve vaccination.

Keywords: *Toxoplasma gondii*, DNA vaccine, dense granule protein 7 (GRA7), calcium phosphate nanoparticles (CaPNs), immune response

INTRODUCTION

Toxoplasma gondii, the causative agent of toxoplasmosis (Kato, 2018), is an Apicomplexa phylum parasite with a broad host range and worldwide distribution. *T. gondii* can infect almost all homeothermic animals including humans (Prandovszky et al., 2018; Coutermarsh-Ott, 2019). Although most infections are asymptomatic, the pathogen can cause severe disease manifestations

and even death in immunocompromised individuals and significant economic losses to the livestock industry (Wang et al., 2017). *T. gondii* infection is acquired by consumption of raw or undercooked meat containing tissue cysts and food or water contaminated with oocysts shed from cats (Mévélec et al., 2020). Currently, there are no effective vaccines against toxoplasmosis, and treatment relies on the use of drug therapies. However, all treatments affect only tachyzoites and are ineffective against *T. gondii* cysts in tissues. Furthermore, antiparasitic drugs cause serious adverse side effects and produce drug-resistant parasite strains (Dunay et al., 2018). Therefore, a safe and effective vaccine formulation that prevents *T. gondii* infection is needed. Many antigens have been identified as vaccine candidates in the last few years (Zhang et al., 2013; Zhang et al., 2015; Montazeri et al., 2017; Wang et al., 2019). The cellular immune response plays a major role in controlling both acute and chronic *T. gondii* infection. Interleukin (IL)-12 is generated by innate immune cells to protect against *T. gondii* infection and is essential for the regulation of interferon gamma (IFN-γ) (Aliberti, 2005). Among the vaccine candidates, dense granule protein (GRA7) induces a strong antibody response during acute infection (Quan et al., 2012) and strong humoral and cellular immunity responses against *T. gondii* infection (Verhelst et al., 2011; Selseleh et al., 2012); therefore, GRA7 is an attractive vaccine candidate against *T. gondii*.

In recent years, DNA vaccines, such as GRA4 (Zhang et al., 2007), ROP29 (Lu et al., 2018), and GRA2 (Ching et al., 2016), have been of great interest in immunization against *T. gondii* infection. Although DNA vaccines produced a better immune response, these vaccines have often been poorly immunogenic, and it is critical to optimize the pathways of delivery for an optimal vaccination strategy (Min et al., 2012). Nanoparticles (NPs) as vaccine adjuvants have been shown to enhance humoral and immune responses, and the use of novel NP technologies can induce $CD8^+$ T-cell immunity responses (Wilson et al., 2015). Calcium phosphate nanoparticles (CaPNs) and aluminum hydroxide (alum) have been used as vaccine adjuvants (effective antigen delivery systems) for many years and have several advantages, such as biocompatibility, safety, effective delivery of antigens to specific locations, and robust humoral and cellular responses (Lin et al., 2017).

In this study, a DNA vaccine using *T. gondii* GRA7 was designed and encapsulated in CaPNs, which has never been previously evaluated to our knowledge. The objective of this study was to assess the immunogenic and protective efficacy of the GRA7-pEGFP-C2+nano-adjuvant (CaPNs) vaccine.

MATERIALS AND METHODS

Mice and Parasites

BALB/c mice aged between 6 and 8 weeks were purchased from the Laboratory Animal Centre of Zhejiang Academy of Agricultural Sciences. All the mice were maintained under specific pathogen-free standard conditions with stable temperature (24°C ± 1°C), 50% ± 10% humidity, and a 12/12-h light–dark cycle; food and water were supplied *ad libitum*. All experiments were approved by the Animal Ethics Committee of Zhejiang Academy of Agricultural Sciences. BALB/c mice were used for the vaccination study, and Vero cells were used for maintenance and proliferation of *T. gondii* RH strain tachyzoites.

Preparation of *Toxoplasma gondii* Antigen (*Toxoplasma* lysate antigen)

Toxoplasma lysate antigen (TLA) was obtained as previously described (Holec-Gasior et al., 2010). Briefly, 10^7 tachyzoites were collected from Vero cells, washed three times with sterile phosphate buffered saline (PBS), and then centrifuged at 1,000 rpm for 10 min. The tachyzoites were disrupted using 10 freezing cycles at -80°C and thawing at 37°C. Then, the supernatant with TLA was collected, its concentration was measured using a bicinchoninic acid (BCA) Protein Assay Kit (Sangon Biotech, Shanghai, China), and it was stored at -80°C until use.

Plasmid Preparation

A total of 10^7 *T. gondii* tachyzoites were collected, and total RNA was extracted using TRIzol reagent according to the manufacturer's instructions and then reverse transcribed into cDNA using the First Strand cDNA Synthesis Kit. The whole Coding sequence (CDS) of GRA7 was amplified from cDNA using PCR with primers containing *EcoRI* and *BamHI* restriction sites (underlined), 5′-gaattcATGGCCCGACACGCAATT-3′ (forward) and 5′-ggatccCTGGCGGGCATCCTCCCCATCTT-3′ (reverse). PCR amplification was performed as follows: 95°C for 5 min, followed by 35 cycles of 95°C for 30 s, 55°C for 30 s, and 72°C for 1 min, with a final extension time of 72°C for 10 min. The PCR product was detected by 1.5% agarose gel electrophoresis, the target band was purified and cloned into the pMD-19T vector, and the clone was sequenced by Sangon Biotech Company (Shanghai). The correct GRA7-pMD-19T sequence was cloned into the eukaryotic expression plasmid pEGFP-C2 using *EcoRI* and *BamHI* restriction enzymes. The recombinant plasmid GRA7-pEGFP-C2 was extracted using a Plasmid Purification Kit (Solarbio, China, Beijing), and its concentration was measured using a NanoDrop2000 Ultra Micro Spectrophotometer. Then, the preparation plasmid was stored at -20°C until use.

Recombinant Plasmid Expression in Vero Cells

Vero cells were cultured in Dulbecco's modified Eagle's medium (DMEM) with 100 μg/ml streptomycin/penicillin and 10% fetal bovine serum (FBS) at 37°C and 5% CO_2. Vero cells were cultivated in six-well plates with cell slides before transfection, and then the recombinant plasmid GRA7-pEGFP-C2 (4 μg) or the empty plasmid (pEGFP-C2) was transfected into Vero cells using 10 μl LipoFiterTM Liposomal Transfection Reagent (Hanbio Biotechnology, Shanghai, China). After inoculation for 48 h, the cell climbing tablets were removed from the six-well plates and washed with 0.1 M PBS three times and then fixed in 4% paraformaldehyde for 15–20 min. Fifty microliters of 2-(4-amidinophenyl)-6-indolecarbamidine dihydrochloride (DAPI;

Beyotime, Shanghai, China) was added to the climbing tablets and incubated for 5 min. Finally, the expression of GRA7 in Vero cells was observed using a laser confocal microscope.

GRA7 protein expression from the Vero cells was analyzed by Western blot as follows. Vero cells transfected with GRA7-pEGFP-C2 and pEGFP-C2 were collected, and protein was isolated with radioimmunoprecipitation assay (RIPA) lysis buffer containing 1 mM phenyl-methanesulfonyl fluoride (PMSF; Beyotime Biotechnology, China), then the lysis solution was centrifuged at 12,000 rpm for 10 min at 4°C. Next, the protein was separated by sodium dodecyl sulfate-polyacrylamide gel electrophoresis (SDS-PAGE) and transferred onto a polyvinylidene fluoride (PVDF) membrane by electric transfer instrument (Bio-Rad, America). The membrane was sealed overnight at 4°C with 5% skimmed milk after washing three times with PBS with 0.05% Tween-20 (PBST), then coated with anti-*T. gondii* tachyzoite antigen mouse sera (diluted 1:1,000), followed by incubation for 2 h with a horseradish peroxidase (HRP)-labeled goat anti-mouse IgG antibody (Solarbio, China). Finally, the bands were detected using enhanced chemiluminescence (ECL; Thermo, America).

Nanoparticle Synthesis and Calcium Phosphate Nanoparticle-Coated DNA Vaccine

CaPNs were prepared as previously described (He et al., 2000). Briefly, 12.5 mM dibasic sodium phosphate, 12.5 mM calcium chloride, and 15.6 mM sodium citrate were mixed together slowly and stirred for 48 h. After sonication for 30 min, a dynamic light-scattering instrument (Anton Paar Litesizer 500) and transmission electron microscope were used to determine the average size distribution, and the particle morphology was observed by scanning electron microscopy (SEM). Subsequently, a GRA7 DNA vaccine coated with CaPNs was prepared by vortexing mixtures of GRA7-pEGFP-C2 and CaPNs for 60 min, with 100 μg plasmid plus 100 μg NPs. The particles were isolated by ultracentrifugation at 66,000 g for 30 min, the supernatant was collected, the particles were redispersed in 1 ml sterile ultrapure water, and the uncoated plasmid was removed by this purification method. Afterward, the concentration of the GRA7-pEGFP-C2 plasmid in the supernatant or in the particles was analyzed using a NanoDrop2000 Ultra Micro Spectrophotometer. The loading efficiency (LE) was determined using the following equation:

$$LE\,\% = (\text{Total amount of plasmid} - \text{free plasmid}) / \text{Total amount of plasmid} \times 100.$$

A sample with non–loaded CaPNs was applied as a negative blank .

Immunization and Challenge

A total of five groups of female BALB/c mice (13 mice/group) were used for the immunization experiment, and these mice were injected three times with 100 μl of the purified GRA7-pEGFP-C2 plasmid DNA dissolved in 100 μl sterile 0.1 M PBS, empty vector (pEGFP-C2), or GRA7-pEGFP-C2+nano-adjuvant (CaPNs). At the same time, two control groups (PBS and CaPNs) were designed. For the second and third inoculations, mice were boosted using the same protocol on days 14 and 28. Tail blood was collected from each mouse on days 0, 14, 28, 42, and 63, and sera were obtained and stored at -20°C until use.

Two weeks after the last immunization, 10 mice from each group were intraperitoneally injected with *T. gondii* RH strain tachyzoites (1×10^4/each) as previously described (Han et al., 2017; Song et al., 2020). The status of infected mice was monitored every day, and the survival rate was recorded.

Determination of Immunoglobulin G Titer and Subclasses

To investigate the humoral immune response induced in all immunized mice, total immunoglobulin G (IgG), IgG1, and IgG2 were measured using enzyme-linked immunosorbent assays (ELISAs) according to the manufacturer's instructions (MultiSciences, Hangzhou, China). Briefly, 96-well microplates were coated with 100 μl/well of TLA (20 μg/ml) (Ahmadpour et al., 2017; Roozbehani et al., 2018). The microplates were blocked with 100 μl 5% skimmed milk in PBST for 2 h after overnight coating. Then, 100 μl of mouse serum (diluted 1:100 in 1% skimmed milk) was added to each well and incubated for 1 h at 37°C. After washing three times with PBST, the wells were incubated with HRP-conjugated anti-mouse IgG (diluted 1:2,000 in 1% skimmed milk), IgG1 (1:2,000), and IgG2a (1:2,000) for 40 min at 37°C. After five times of washing, a Tetramethylbenzidine (TMB) substrate solution was added and incubated for 15 min at 37°C and then was stopped by the addition of 2 M H_2SO_4. Finally, optical density (OD) values were measured at 450 nm. All samples were run in triplicate.

Lymphocyte Proliferation Assay and Cytokine Assay

Two weeks after the last immunization, three mice from each group were euthanized, and splenocytes were collected and treated with red blood cell lysate and then cultured in a 96-well plate (1×10^5 cells/well) in DMEM (100 μg/ml streptomycin/penicillin and 10% FBS). Thereafter, the cells were stimulated with 10 μg/ml TLA or 7.5 μg/ml concanavalin A (ConA) (positive control). As a negative control, media alone were added. The plates were incubated at 37°C in 5% CO_2 for 72 h, after which Cell Counting Kit (CCK)-8 solution was added (50 μl/well) and cultured for 4 h. Proliferative activity was evaluated by measuring the OD values at 450 nm using an ELISA reader. The splenocyte stimulation index (SI) was calculated as the ratio of the average absorbance of the TLA-treated samples to the average absorbance of the negative groups. All samples were run in triplicate.

Splenocytes were collected as mentioned above and cultured in 96-well microtiter plates. The supernatants were harvested and assayed for IL-4 at 24 h, IL-10 at 72 h, and IL-12 and interferon gamma (IFN-γ) at 96 h using ELISA kits according to the manufacturer's instructions.

Determination of Parasite Burden

In order to evaluate tissue parasite burden, the heart, liver, spleen, and lung from three mice (each group) were removed.

We collected the tissues using sterile scissors, and the tissues were divided into masses of equal quality (1 mg). Genomic DNA was extracted using the genomic DNA extraction kit (TIANGEN, Beijing, China) according to the manufacturer's instructions. Afterward, the parasite burdens were determined by quantitative real-time PCR using the repeated element (RE) primers (forward, 5-AGGGACAGAAGTCGAAGGGG-3; reverse, 5- GCAGCCAA GCCGGAAACATC-3) (Roozbehani et al., 2018). The final volume of the Q-PCR reaction was 20 μl containing 10 μl SYBR green master mix (TAKARA, Japan), 0.5 μl forward primer (10 pmol), 0.5 μl reverse primer (10 pmol), 1 μl DNA template, 8 μl RNase-free water. The amplification steps were an initial denaturation at 95°C for 10 min, and amplification consisted of 40 cycles of denaturation at 95°C for 15 s, annealing at 60°C for 30 s, and amplification at 72°C for 30 s. Melting curve analysis was performed to verify the specific amplification of the correct sequence. The standard curve was determined by the known concentration of the *T. gondii* RH tachyzoites DNA. The number of parasites in the samples was calculated from the threshold cycle (Ct) value according to the standard curve ($Y = -3.48X + 32.326$; $R^2 = 0.987$). The results were based on three independent experiments.

Statistical Analysis

All statistical analyses were performed using GraphPad Prism Version 5. Antibody production and cytokine levels were analyzed using one-way ANOVA. Tukey's Student range test was used when a significant difference appeared. *P* value of <0.05 was considered a significant difference.

RESULTS

Expression of the Recombinant Plasmid

The expression and localization of GRA7 in Vero cells and cells transfected with pEGFP-C2 were analyzed using laser confocal microscopy (**Figures 1A, B**). Green fluorescence was observed in the GRA7-pEGFP-C2 (**Figures 1A1, A2**)- and pEGFP-C2-transfected groups (**Figures 1B1, B2**). A2 and B2 showed the single cell transfected with GRA7-pEGFP-C2 and pEGFP-C2 and A3 and B3 exhibited the cells transfected with GRA7-pEGFP-C2 pEGFP-C2 (**Figures 1A3, B3**), which were detected under white light, whereas no fluorescence was observed in the untransfected cells. GRA7 protein expression in the transfected Vero cells was determined by Western blot analysis; as shown in **Figure 1C**, a specific band was detected in lysates of the GRA7-pEGFP-C2-transfected cells, whereas the negative control cells showed no bands. These results indicated that the GRA7-pEGFP-C2 recombinant plasmid was successfully transfected and expressed in Vero cells.

Synthesis of Calcium Phosphate Nanoparticles and Preparation of Nanoparticle-Coated DNA Vaccines

The average NP diameter was 47.28 nm, and the diffusion coefficient was approximately 4, indicating acceptable monodispersity (**Figures 2A, B**); a consistent size was observed by transmission electron microscopy (TEM) (**Figure 2C**). The morphology of adjuvant (CaPNs) NPs was analyzed by SEM, showing that most of them were circular in shape with a smooth surface (**Figure 2D**).

Humoral Immune Responses Induced by Vaccination

To determine the *T. gondii*-specific antibody response, sera from all vaccinated mice were collected, and the total IgG and IgG subclasses (IgG1 and IgG2a) were analyzed by ELISA. High levels of IgG were observed in the serum of the vaccine-immunized groups (GRA7-pEGFP-C2+nano-adjuvant, GRA7-pEGFP-C2) ($P < 0.01$); however, no significant difference was observed between these two vaccine groups ($P > 0.05$) (**Figure 3A**). IgG1 in the immunization groups was also significantly elevated compared to that in the control groups (**Figure 3B**) ($P < 0.05$ for both vaccine groups). The GRA7-pEGFP-C2+nanoadjuvant (CaPN) group exhibited a higher level of IgG2a (**Figure 3C**) ($P < 0.01$), and higher levels of IgG2a were also observed in GRA7-pEGFP-C2-immunized mice ($P < 0.05$) than that in the control groups. Meanwhile, the levels of IgG2a were significantly higher than IgG1 in the vaccine groups ($P < 0.05$, compared to control groups), and the ratios of IgG2a/IgG1 were higher in mice immunized with GRA7-pEGFP-C2+nano-adjuvant (CaPNs) compared to those immunized with GRA7-pEGFP-C2 alone ($P < 0.05$) (**Figure 3D**). Taken together, these results showed that a Th1-type immune response was elicited in response to nanoadjuvant vaccine immunization.

Cellular Immune Responses

Splenocytes were collected from immunized and control groups (5 weeks after the last immunization) to analyze their proliferation, and the cells were treated with TLA and ConA. As shown in **Figure 4**, a significantly higher lymphocyte proliferation SI was obtained in the GRA7-pEGFP-C2+nano-adjuvant (CaPNs) and GRA7-pEGFP-C2 groups compared to the control groups ($P < 0.05$). In addition, the GRA7-pEGFP-C2 +nano-adjuvant (CaPNs) group induced an almost 2-fold higher level of lymphocyte proliferation than the GRA7-pEGFP-C2 immunization group ($P < 0.05$).

Cytokine Responses

To further explore T-cell responses to vaccination, splenocytes were collected 63 days after immunization, and supernatants were harvested to evaluate the expression of cytokines, including IL-12, IFN-γ, IL-4, and IL-10 (**Figure 5**). Compared with the control groups, the IL-12 level of mice vaccinated with GRA7-pEGFP-C2+nano-adjuvant (CaPNs) was statistically higher ($P < 0.01$) (**Figure 5A**). Moreover, the production of IFN-γ was significantly higher in the GRA7-pEGFP-C2+nano-adjuvant (CaPNs) group than that in the control groups ($P < 0.01$), and GRA7-pEGFP-C2-treated mice displayed higher levels of IFN-γ ($P < 0.05$) (**Figure 5B**). In contrast, IL-4 and IL-10 levels showed no statistically significant differences in any of the groups compared to the control groups ($P > 0.05$) (**Figures 5C, D**). These results confirmed that immunization with GRA7-pEGFP-

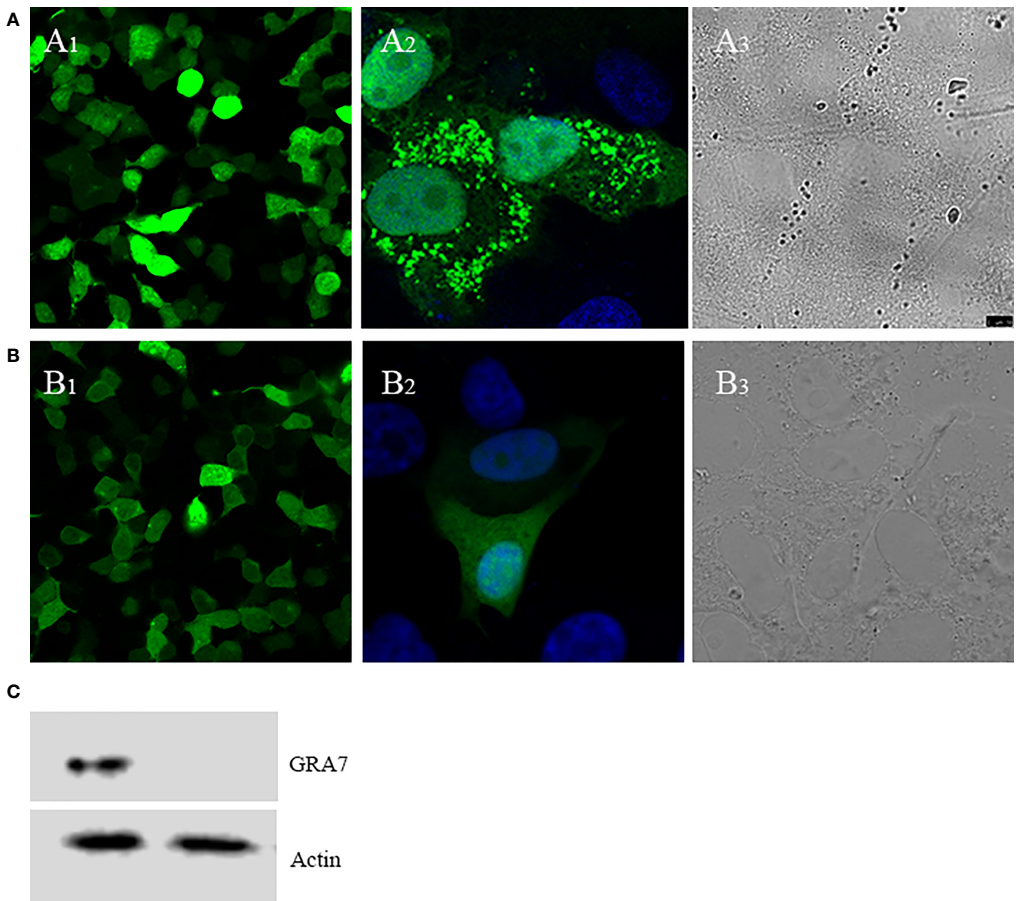

FIGURE 1 | Direct fluorescence detection of the GRA7-EGFP-C2 fusion protein in transfected Vero cells. **(A)** Cells transfected with GRA7-pEGFP-C2 were detected under blue light **(A1)**; the localization of GRA7 in Vero cells was observed under blue light **(A2)** and white light **(A3)**. **(B)** Cells transfected with pEGFP-C2 were detected under blue light **(B1)**; single cells transfected with pEGFP-C2 were observed under blue light **(B2)** and white light **(B3)**. **(C)** Western blot analysis of GRA7 protein recognized by anti-*Toxoplasma gondii* mouse sera.

C2+nano-adjuvant (CaPNs) or GRA7-pEGFP-C2 promoted a Th1-type immune response.

Protection From the Recombinant DNA Vaccine

To evaluate protective efficacy, mice from all groups were intraperitoneally challenged with 10^4 tachyzoites of the *T. gondii* RH strains 5 weeks after the final vaccination, and the survival time was recorded. As shown in **Figure 6**, mice in the control groups all died within 4 days ($P > 0.05$), while the survival times of mice immunized with GRA7-pEGFP-C2+nano-adjuvant (CaPNs) (extending survival time to the 14th day) were significantly longer by comparison ($P < 0.05$); however, no significant difference was observed between the GRA7-pEGFP-C2+nano-adjuvant (CaPNs) and GRA7-pEGFP-C2 groups.

Parasite Burden

Three mice from each group were randomly selected after death to determine the parasite burden in tissues of *T. gondii*-infected mice in the heart, liver, spleen, and lung. SYBR-green real-time PCR was used to quantify parasite loads. As shown in **Figure 7**, all tissues examined were *T. gondii* infection positive, but the vaccine immunization groups exhibited lower parasite loads than the control groups. Mice immunized with GRA7-pEGFP-C2 +nano-adjuvant (CaPNs) or GRA7-pEGFP-C2 exhibited significantly reduced parasite loads in the liver, spleen, and lung ($P < 0.001$) (**Figures 7B–D**), and the average parasite loads in the heart (GRA7-pEGFP-C2+nano-adjuvant group) were reduced by 3.15-fold ($P < 0.05$) compared with the control groups (**Figure 7A**). GRA7-pEGFP-C2+nano-adjuvant (CaPNs)-immunized mice showed decreased parasite loads compared to the GRA7 pEGFP-C2-immunized group in the spleen and lung ($P < 0.05$), and no significant differences were found in the control groups ($P > 0.05$).

DISCUSSION

DNA vaccines have been considered an effective approach for inducing protection against challenge infections, with the ability

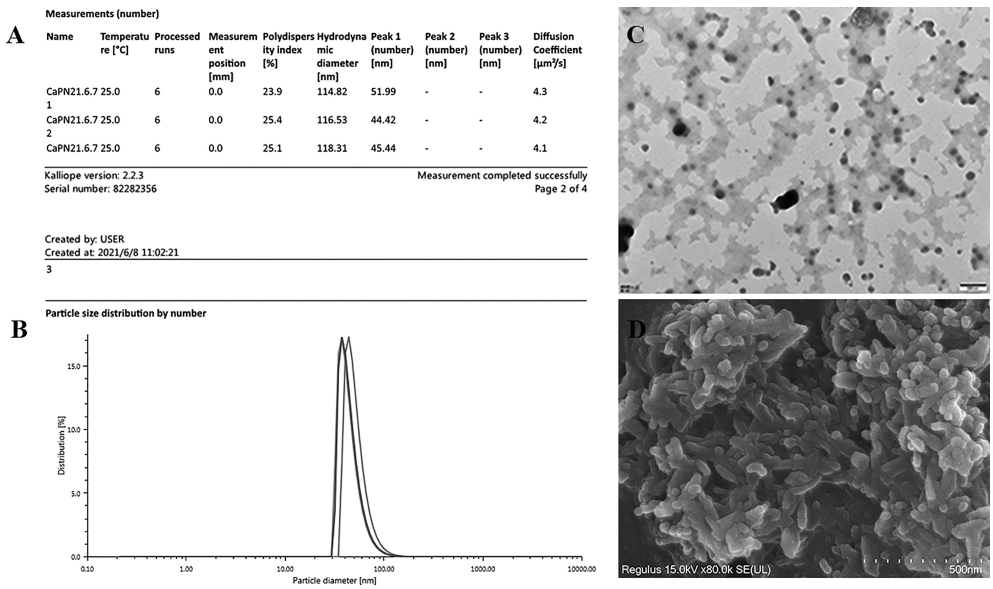

FIGURE 2 | Characterization of calcium phosphate nanoparticles (CaPNs). **(A)** Morphology was observed using scanning electron microscopy (SEM). **(B)** Nanoparticle size and distribution were observed using transmission electron microscopy (TEM). **(C)** Nanoparticle size and diffusion coefficient were analyzed using an Anton Paar Litesizer 500. **(D)** Particle size distribution by number is shown.

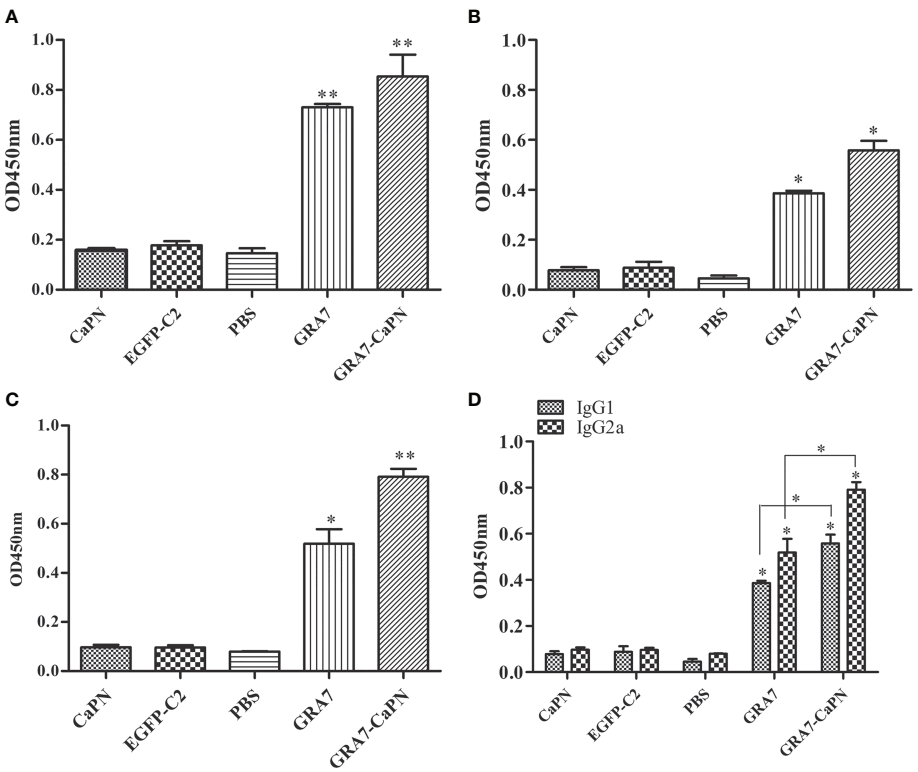

FIGURE 3 | Specific immunoglobulin G (IgG) and IgG isotype analysis. **(A)** Total IgG. **(B)** IgG1. **(C)** IgG2a. **(D)** Levels of IgG1 and IgG2a. Results are represented as the means of OD 450 nm ± SD. *$P < 0.05$, ** $P < 0.01$. The labels "GRA7" and "GRA7-CaPN" in **Figures 3**–**7** were the abbreviations of "GRA7- pEGFP-C2" and "GRA7- pEGFP-C2-CaPNs".

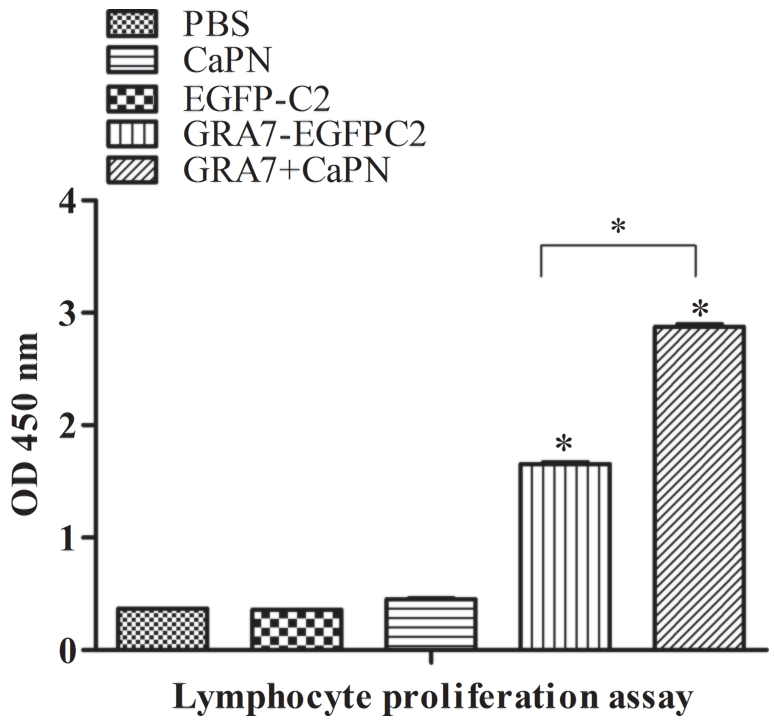

FIGURE 4 | Splenocyte proliferation response in BALB/c mice. Splenocytes from immunized mice and non-immunized mice were collected 63 days after immunization, and the proliferation response was analyzed by Cell Counting Kit (CCK)-8 assay. The data are shown as the means ± *SD* of three independent experiments. *$P < 0.05$.

to simultaneously elicit both humoral and cellular immune responses (Matowicka-Karna et al., 2009; Wang et al., 2011). DNA vaccines have many advantages, such as the ease of constructing recombinant plasmids and native protein structures, ensuring appropriate processing and immune presentation (Li and Petrovsky, 2016). Although DNA vaccines can trigger an immune response, these vaccines have often been poorly immunogenic due to various factors, such as poor distribution of plasmids (Verma and Khanna, 2013; Zhang et al., 2013), inefficient expression, or rapid degradation by lysosomes and DNase. To improve DNA vaccine immunogenicity, novel adjuvants have been explored (Petrovsky and Aguilar, 2004). NPs are promising adjuvants that can deliver antigens to certain cells (Van Riet et al., 2014) and trigger an immune response to vaccine antigens (De Koker et al., 2011; Kasturi et al., 2011). Many studies have shown that NPs can modulate cellular and humoral immune responses, such as poly (gamma-glutamic acid) NPs (Okamoto et al., 2009), novel core–shell nanospheres and microspheres (Caputo et al., 2009), new cationic NPs (Debin et al., 2002), and CaPNs (Ahmadpour et al., 2017). A specific anti-*T. gondii* antibody response contributes to killing engulfed parasites (Xu et al., 2014), and several adjuvants have been used to enhance immune responses against *T. gondii* infection. CaPNs are known to be biocompatible and non-cytotoxic and can be efficient adjuvant materials for antigen delivery systems (Zhang et al., 2012). The Ca^{2+} and $PO4^{3-}$ ions can participate in the normal metabolism of organisms (Wang et al., 2020). CaPNs loaded with different types of nucleotide chains have been widely used as nano-platforms for gene, drug, and vaccine delivery systems (Zhou et al., 2017; HeBe et al., 2019). Calcium is highly effective in condensing DNA because a small hydrodynamic radius prompts a high charge-to-surface area (Kulkarni et al., 2006). Calcium phosphate (CAP) has a proper adjuvant potential in enhancing immune responses against different infectious illnesses (Lin et al., 2017). Previous study has shown that CaPNs were a potent antigen delivery system to immunize brucellosis compared with aluminum hydroxide (AH) and chitosan (CS) NPs (Abkar et al., 2019).

The size and morphology of CaPs greatly affect their transfection efficiency (Neumann et al., 2009), their ability to bind to specific cell membrane receptors, their trafficking inside the cells, and their intracellular flow (Jiang et al., 2008; Liu et al., 2011). All particles used in vaccine formulations typically have comparable size (Pedraza et al., 2008), and the mechanism by which NPs (20–200 nm in diameter) are taken up is typically endocytosis; larger particles (0.5–5 μm) are taken up by micropinocytosis, while particles above 0.5 μm are thought to be taken up by phagocytosis (Xiang et al., 2006). The average diameter of CaPNs in our study was 47.28 nm (**Figure 2A**), which was suitable for delivery of DNA into cells through endocytosis and thereby enhanced the immune response.

In the present study, mice injected with the GRA7-pEGFP-C2+nano-adjuvant (CaPNs) vaccine developed a significant level

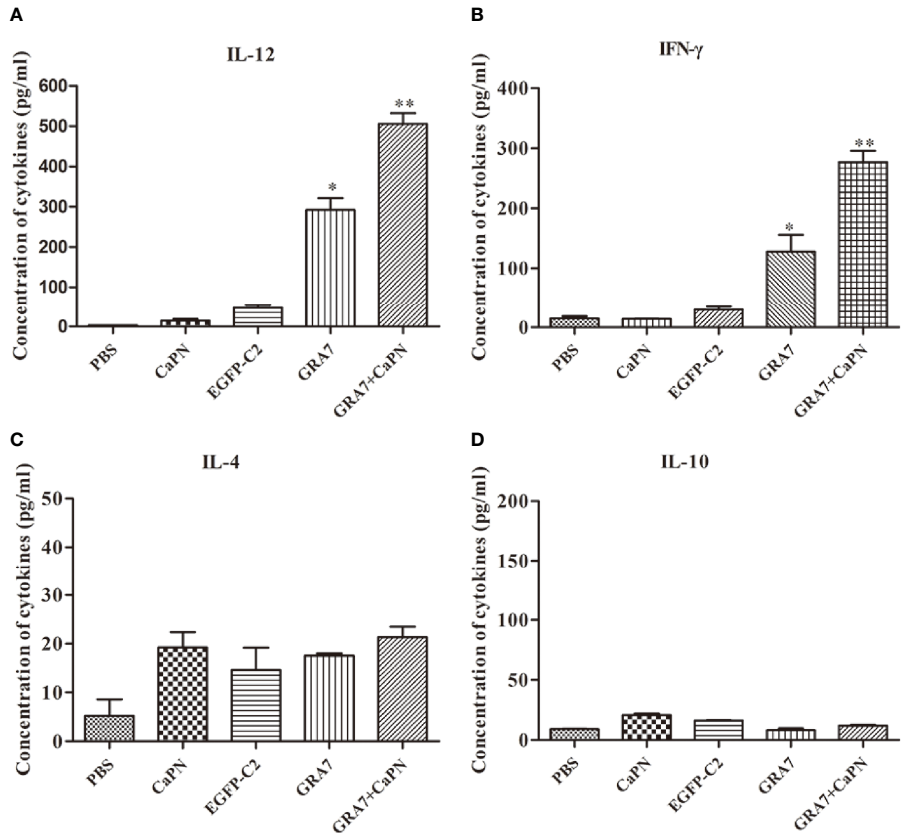

FIGURE 5 | Levels of cytokines produced by splenocyte culture supernatants. **(A)** Production of interleukin (IL)-12 collected from splenocyte supernatants after culture for 96 h. **(B)** Detection of interferon (IFN)-γ collected from splenocyte supernatants. **(C)** Production of IL-4 after culture for 24 h. **(D)** Production of IL-10 after culture for 72 h. *$P < 0.05$, ** $P < 0.01$.

of *T. gondii*–specific total IgG and a higher IgG2a-to-IgG1 ratio. Elevated IgG2a is an indicator of a Th1-based immune response, while IgG1 indicates the development of a Th2 immune response. These results were confirmed by the results of the cytokine assay conducted on spleen cell culture supernatants, in which the expression levels of IL-12 and IFN-γ (Th1-type cytokine) in mice immunized with GRA7-pEGFP-C2+nano-adjuvant (CaPNs) ($P < 0.01$) or GRA7-pEGFP-C2 ($P < 0.05$) were significantly higher than those in the control mice (**Figure 5**), while mice in the GRA7-pEGFP-C2+nano-adjuvant injection group produced higher IFN-γ levels than those in the GRA7-pEGFP-C2 immunization group. We suggest that the presence of CaPNs as a nano-adjuvant within pcGRA7 provided an immunogenic antigen and induced a high antibody response. IL-12 leads to the release of IFN-γ and induces the differentiation of Th1 T lymphocyte response to control *T. gondii* infection; disruption of IL-12 expression promoted *T. gondii* growth and dissemination because of diminishing Th1 immune responses (Morgado et al., 2014). The Th2-type cytokines, IL-4 and IL-10, were not induced by immunization with the vaccine ($P > 0.05$). IL-4 is vital for inhibiting severe immunopathology during both the acute and chronic phases of *T. gondii* infection (Denkers and Gazzinelli, 1998), and IL-4 is generally antagonistic to IFN-γ and plays important roles in early *T. gondii* infection (Hunter and Sibley, 2012). Elevated IFN-γ production and low IL-4 levels were also detected in mice injected with the ROP18 multi-epitope DNA vaccine plus the IL-12 plasmid as a genetic adjuvant, and coadministration of pcIL-12 with multi-epitope ROP8 enhanced the levels of IgG antibody and the IgG2a-to-IgG1 ratio (Foroutan et al., 2020). The use of a genetic adjuvant successfully enhanced the protection level. As mice immunized with the ROP13-GRA14-alum nano-adjuvant exhibited significant production of IL-4 and IgG1, the Th2 immune response was developed by immunization with a DNA vaccine coated with alum nano-adjuvant (Pagheh et al., 2021). Mouse priming with GRA1 DNA vaccine-loaded chitosan particles resulted in high anti-GRA1 antibodies and a higher IgG2a/IgG1 ratio (Bivas-Benita et al., 2003).

Specific T-lymphocyte activation ($CD4^+$ and $CD8^+$ T cells) may play an important role in controlling *T. gondii* infection. $CD8^+$ T cells are specialized cytotoxic T lymphocytes that mediate lysis of *T. gondii* through the production of IFN-γ (Dupont et al., 2012); in other words, IFN-γ promotes the acquired cell-mediated immune response by directly acting on $CD8^+$ T cells (Grover et al., 2012). In the present study, we found

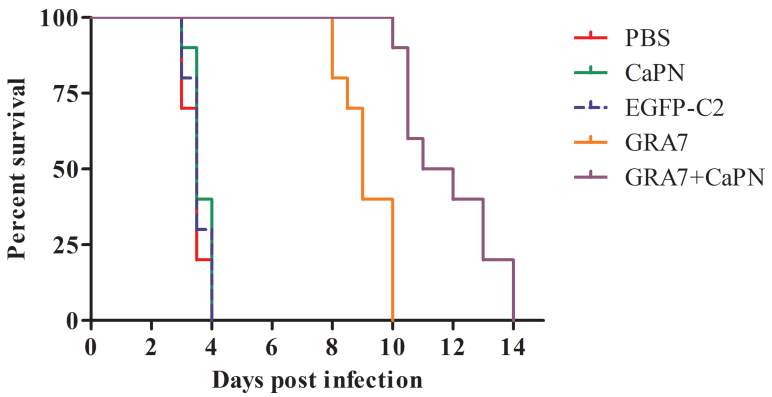

FIGURE 6 | Survival time of BALB/c mice after challenge with *Toxoplasma gondii* tachyzoites. Each group contained 10 mice, and survival was significantly higher in the GRA7-pEGFP-C2+nano-adjuvant (CaPNs)–immunized mice than that in control mice.

that a significantly higher level of splenocyte proliferation was induced by GRA7-pEGFP-C2+nano-adjuvant (CaPNs) immunization (**Figure 4**), which indicated that an activated cellular immune response was induced in the vaccine immunization group and that increased proliferation of lymphocytes was induced by coating with CaPNs compared to mice immunized with GRA7 alone ($P < 0.05$). A vigorous lymphocyte proliferation effect was observed in mice immunized with pcGRA14+rGRA14-CaPNs compared to mice immunized with GRA14 alone, indicating that enhancement of humoral and cellular immune responses and the protective effects were induced by CaPNs (Pagheh et al., 2019).

No effective vaccine has been shown to completely protect against infection by the *T. gondii* RH strain (Johnson et al., 2004), so the survival rates of immunized mice challenged with a lethal dose (1×10^4) of tachyzoites were analyzed in the present study. The findings indicated that mice immunized with GRA7-pEGFP-C2+nano-adjuvant (CaPNs) or GRA7-pEGFP-C2

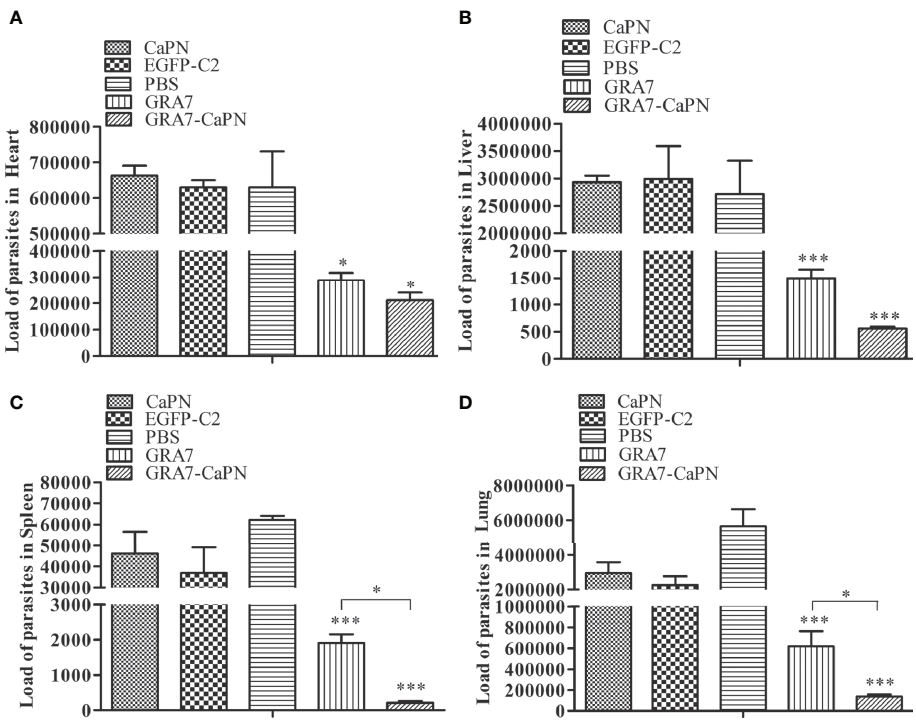

FIGURE 7 | Parasite burden in heart, liver, spleen, and lung tissues in the vaccine and control groups. **(A)** Parasite burden in the heart. **(B)** Parasite burden in the liver. **(C)** Parasite burden in the spleen. **(D)** Parasite burden in the lung. The data are shown as means ± *SD* for three experiments. *$P < 0.05$, *** $P < 0.001$.

vaccine exhibited extended survival time compared to control groups. Control mice all died within 4 days, while those immunized with GRA7-pEGFP-C2+nano-adjuvant (CaPNs) survived for significantly longer, indicating that GRA7 induces partially effective protection in mice against acute *T. gondii* infection and that CaPNs increase protection against *T. gondii* infection, in agreement with the research by Pagheh et al. (2019). In another study, *T. gondii* nucleoside triphosphate hydrolase-II (NTPase-II) coated with lipid NPs showed an increased protective effect against *T. gondii* RH strain (1×10^3) infection, and a significantly prolonged survival time was observed compared to immunization with the NTPase-II vaccine alone (Luo et al., 2017). Various studies have analyzed the presence of *T. gondii* in different tissues of vaccine-injected mice or non-vaccine immunization groups by qualitative PCR to evaluate the protective effect against *T. gondii* infection (Lu et al., 2017; Alizadeh et al., 2019). We investigated the parasite load in the present study. The parasite load in the GRA7-pEGFP-C2 immunization group was significantly decreased compared to that in the control groups and was particularly low in GRA7-pEGFP-C2+nano-adjuvant (CaPNs)-immunized mice (**Figure 7**). GRA7-pEGFP-C2+nano-adjuvant (CaPNs)-immunized mice displayed decreased parasite loads compared to those in the GRA7-pEGFP-C2-immunized group in the spleen and lung ($P < 0.05$).

In conclusion, in the work presented herein, we presented a nano-particulate vaccine, GRA7-pEGFP-C2+nano-adjuvant (CaPNs). *T. gondii* GRA7 coated with CaPNs induced a significant level of *T. gondii*–specific total IgG and a higher IgG2a-to-IgG1 ratio. CaPNs enhanced splenocyte proliferation, elevated IL-12 and IFN-γ production, and decreased IL-4 levels in mice injected with the GRA7-pEGFP-C2+nano-adjuvant (CaPNs) vaccine. GRA7-CaPN-immunized mice exhibited markedly longer survival times and decreased parasite loads compared to mice immunized with GRA7 alone. Taken together, these results indicated that CaPN-based immunization with *T. gondii* GRA7 represents a promising approach for improving vaccination.

DATA AVAILABILITY STATEMENT

The original contributions presented in the study are included in the article/supplementary material. Further inquiries can be directed to the corresponding author.

ETHICS STATEMENT

The animal study was reviewed and approved by the Animal Ethics Committee of Zhejiang Academy of Agricultural Sciences.

AUTHOR CONTRIBUTIONS

H-CS and T-YS conceived and supported the study. H-CS wrote the article. JH and YF performed the experiments. L-LH and XL analyzed the data. All authors contributed to the article and approved the submitted version.

FUNDING

This work was supported by the National Natural Science Foundation of China (31802183), Zhejiang Province "Sannongliufang" Science and Technology Cooperation Project (Grant No. 2020SNLF007), and the National Natural Science Foundation of China (32072883).

REFERENCES

Abkar, M., Alamian, S., and Sattarahmady, N. (2019). A Comparison Between Adjuvant and Delivering Functions of Calcium Phosphate, Aluminum Hydroxide and Chitosan Nanoparticles, Using a Model Protein of Brucella Melitensis Omp31. *Immunol. Lett.* 207, 28–35. doi: 10.1016/j.imlet.2019.01.010

Ahmadpour, E., Sarvi, S., Hashemi Soteh, M. B., Sharif, M., Rahimi, M. T., Valadan, R., et al. (2017). Enhancing Immune Responses to a DNA Vaccine Encoding *Toxoplasma Gondii* GRA14 by Calcium Phosphate Nanoparticles as an Adjuvant. *Immunol. Lett.* 185, 40–47. doi: 10.1016/j.imlet.2017.03.006

Aliberti, J. (2005). Host Persistence: Exploitation of Anti-Inflammatory Pathways by *Toxoplasma Gondii*. *Nat. Rev. Immunol.* 5, 162–170. doi: 10.1038/nri1547

Alizadeh, P., Ahmadpour, E., Daryani, A., Kazemi, T., Spotin, A., Mahami-Oskouei, M., et al. (2019). IL-17 and IL-22 Elicited by a DNA Vaccine Encoding ROP13 Associated With Protection Against *Toxoplasma Gondii* in BALB/C Mice. *J. Cell Physiol.* 234, 10782–10788. doi: 10.1002/jcp.27747

Bivas-Benita, M., Laloup, M., Versteyhe, S., Dewit, J., De Braekeleer, J., Fau - Jongert, E., et al. (2003). Generation of *Toxoplasma Gondii* GRA1 Protein and DNA Vaccine Loaded Chitosan Particles: Preparation, Characterization, and Preliminary *In Vivo* Studies. *Int. J. Pharm.* 266, 17–27. doi: 10.1016/S0378-5173(03)00377-6

Caputo, A., Castaldello, A., Brocca-Cofano, E., Voltan, R., Bortolazzi, F., Altavilla, G., et al. (2009). Induction of Humoral and Enhanced Cellular Immune Responses by Novel Core-Shell Nanosphere- and Microsphere-Based Vaccine Formulations Following Systemic and Mucosal Administration. *Vaccine* 27, 3605–3615. doi: 10.1016/j.vaccine.2009.03.047

Ching, X. T., Fong, M. Y., and Lau, Y. L. (2016). Evaluation of Immunoprotection Conferred by the Subunit Vaccines of GRA2 and GRA5 Against Acute Toxoplasmosis in BALB/C Mice. *Front. Microbiol.* 7, 609. doi: 10.3389/fmicb.2016.00609

Coutermarsh-Ott, S. (2019). Toxoplasma Gondii as a Model of *In Vivo* Host-Parasite Interactions. *Methods Mol. Biol.* 1960, 237–247. doi: 10.1007/978-1-4939-9167-9_21

Debin, A., Kravtzoff, R., Santiago, J. V., Cazales, L., Sperandio, S., Melber, K., et al. (2002). Intranasal Immunization With Recombinant Antigens Associated With New Cationic Particles Induces Strong Mucosal as Well as Systemic Antibody and CTL Responses. *Vaccine* 20, 2752–2763. Fau. doi: 10.1016/S0264-410X(02)00191-3

De Koker, S., Lambrecht, B., Willart, M. A., van, K. Y., Grooten, J., Vervaet, C., et al. (2011). Designing Polymeric Particles for Antigen Delivery. *Chem. Soc. Rev.* 40, 320–339. doi: 10.1039/B914943K

Denkers, E. Y., and Gazzinelli, R. T. (1998). Regulation and Function of T-Cell-Mediated Immunity During *Toxoplasma Gondii* Infection. *Clin. Microbiol. Rev.* 11, 569–588. doi: 10.1128/CMR.11.4.569

Dunay, I. R., Gajurel, K., Dhakal, R., Liesenfeld, O., and Montoya, J. G. (2018). Treatment of Toxoplasmosis: Historical Perspective, Animal Models, and Current Clinical Practice. *Clin. Microbiol. Rev.* 31 (4), e00057–e00017. doi: 10.1128/CMR.00057-17

Dupont, C. D., Christian, D., and Hunter, C. A. (2012). Immune Response and Immunopathology During Toxoplasmosis. *Semin. Immunopathol.* 34, 793–813. doi: 10.1007/s00281-012-0339-3

Foroutan, M., Barati, M., and Ghaffarifar, F. (2020). Enhancing Immune Responses by a Novel Multi-Epitope ROP8 DNA Vaccine Plus Interleukin-12 Plasmid as a Genetic Adjuvant Against Acute *Toxoplasma Gondii* Infection in BALB/C Mice. *Microb. Pathog.* 147, 5. doi: 10.1016/j.micpath.2020.104435

Grover, H. S., Blanchard, N., Gonzalez, F., Chan, S., Robey, E. A., Shastri, N., et al. (2012). The *Toxoplasma Gondii* Peptide AS15 Elicits CD4 T Cells That Can Control Parasite Burden. *Infect. Immun.* 80, 3279–3288. doi: 10.1128/IAI.00425-12

Han, Y., Zhou, A., Lu, G., Zhao, G., Wang, L., Guo, J., et al. (2017). Protection *via* a ROM4 DNA Vaccine and Peptide Against *Toxoplasma Gondii* in BALB/C Mice. *BMC Infect. Dis.* 17, 016–2104. doi: 10.1186/s12879-016-2104-z

HeBe, C., Kollenda, S., Rotan, O., Pastille, E., Adamczyk, A., Wenzek, C., et al. (2019). A Tumor-Peptide-Based Nanoparticle Vaccine Elicits Efficient Tumor Growth Control in Antitumor Immunotherapy. *Mol. Cancer Ther.* 18, 1069–1080. doi: 10.1158/1535-7163.MCT-18-0764

He, Q., Mitchell, A., Johnson, S. L., Wagner-Bartak, C., Morcol, T., and Bell, S. J. (2000). Calcium Phosphate Nanoparticle Adjuvant. *Clin. Diagn. Lab. Immunol.* 7, 899–903. doi: 10.1128/CDLI.7.6.899-903.2000

Holec-Gasior, L., Kur, J., Hiszczyńska-Sawicka, E., Drapała, D., Dominiak-Górski, B., Pejsak, Z., et al. (2010). Application of Recombinant Antigens in Serodiagnosis of Swine Toxoplasmosis and Prevalence of *Toxoplasma Gondii* Infection Among Pigs in Poland. *Pol. J. Vet. Sci.* 13, 457–464. doi: 10.1590/S0100-736X2010000100015

Hunter, C. A., and Sibley, L. D. (2012). Modulation of Innate Immunity by *Toxoplasma Gondii* Virulence Effectors. *Nat. Rev. Microbiol.* 10, 766–778. doi: 10.1038/nrmicro2858

Jiang, W., Kim, B. Y. S., Rutka, J. T., and Chan, W. C. W. (2008). Nanoparticle-Mediated Cellular Response Is Size-Dependent. *Nat. Nanotechnol* 3, 145–150. doi: 10.1038/nnano.2008.30

Johnson, L. L., Lanthier, P., Hoffman, J., and Chen, W. X. (2004). Vaccination Protects B Cell-Deficient Mice Against an Oral Challenge With Mildly Virulent *Toxoplasma Gondii*. *Vaccine* 22, 4054–4061. doi: 10.1016/j.vaccine.2004.03.056

Kasturi, S. P., Skountzou, I., Albrecht, R. A., Koutsonanos, D., Tang, H., Nakaya, H. I., et al. (2011). Programming the Magnitude and Persistence of Antibody Responses With Innate Immunity. *Nature* 470, 543–547. doi: 10.1038/nature09737

Kato, K. (2018). How Does *Toxoplama Gondii* Invade Host Cells? *J. Vet Med. Sci.* 80, 1702–1706. doi: 10.1292/jvms.18-0344

Kulkarni, V. I., Shenoy, V. S., Shamsunder, S., Dodiya, S. S., Rajyaguru, T. H., and Murthy, R. R. (2006). Role of Calcium in Gene Delivery. *Expert Opin. Drug Deliv.* 3, 235–245. doi: 10.1517/17425247.3.2.235

Lin, Y., Wang, X., Huang, X., Zhang, J., Xia, N., and Zhao, Q. (2017). Calcium Phosphate Nanoparticles as a New Generation Vaccine Adjuvant. *Expert Rev. Vaccines* 16, 895–906. doi: 10.1080/14760584.2017.1355733

Li, L., and Petrovsky, N. (2016). Molecular Mechanisms for Enhanced DNA Vaccine Immunogenicity. *Expert Rev. Vaccines* 15, 313–329. doi: 10.1586/14760584.2016.1124762

Liu, Y., Wang, T., He, F. L., Liu, Q., Zhang, D. X., Xiang, S. L., et al. (2011). An Efficient Calcium Phosphate Nanoparticle-Based Nonviral Vector for Gene Delivery. *Int. J. Nanomed* 6, 721–727. doi: 10.2147/IJN.S17096

Luo, F., Zheng, L., Hu, Y., Liu, S., Wang, Y., Xiong, Z., et al. (2017). Induction of Protective Immunity Against *Toxoplasma Gondii* in Mice by Nucleoside Triphosphate Hydrolase-II (Ntpase-II) Self-Amplifying RNA Vaccine Encapsulated in Lipid Nanoparticle (LNP). *Front. Microbiol.* 8, 605. doi: 10.3389/fmicb.2017.00605

Lu, G., Zhou, J., Zhao, Y. H., and Wang, L. (2018). DNA Vaccine ROP29 From *Toxoplasma Gondii* Containing R848 Enhances Protective Immunity in Mice. *Parasite Immunol.* 40, 12578. doi: 10.1111/pim.12578

Lu, G., Zhou, J., Zhou, A., Han, Y., Guo, J., Song, P., et al. (2017). SAG5B and SAG5C Combined Vaccine Protects Mice Against *Toxoplasma Gondii* Infection. *Parasitol Int.* 66, 596–602. doi: 10.1016/j.parint.2017.06.002

Matowicka-Karna, J., Dymicka-Piekarska, V., and Kemona, H. (2009). Does *Toxoplasma Gondii* Infection Affect the Levels of Ige and Cytokines (IL-5, IL-6, IL-10, IL-12, and TNF-Alpha)? *Clin. Dev. Immunol.* 374696, 25. doi: 10.1155/2009/374696

Mévélec, M. N., Lakhrif, Z., and Dimier-Poisson, I. (2020). Key Limitations and New Insights Into the *Toxoplasma Gondii* Parasite Stage Switching for Future Vaccine Development in Human, Livestock, and Cats. *Front. Cell Infect. Microbiol.* 10, 607198. doi: 10.3389/fcimb.2020.607198

Min, J., Qu, D., Li, C., Song, X. L., Zhao, Q. L., Li, X. A., et al. (2012). Enhancement of Protective Immune Responses Induced by *Toxoplasma Gondii* Dense Granule Antigen 7 (GRA7) Against Toxoplasmosis in Mice Using a Prime-Boost Vaccination Strategy. *Vaccine* 30, 5631–5636. doi: 10.1016/j.vaccine.2012.06.081

Montazeri, M., Sharif, M., Sarvi, S., Mehrzadi, S., Ahmadpour, E., and Daryani, A. (2017). A Systematic Review of *In Vitro* and *In Vivo* Activities of Anti-*Toxoplasma* Drugs and Compounds, (2006-2016). *Front. Microbiol.* 8, 25. doi: 10.3389/fmicb.2017.00025

Morgado, P., Sudarshana, D. M., Gov, L., Harker, K. S., Lam, T., Casali, P., et al. (2014). Type II *Toxoplasma Gondii* Induction of CD40 on Infected Macrophages Enhances Interleukin-12 Responses. *Infect. Immun.* 82, 4047–4055. doi: 10.1128/IAI.01615-14

Neumann, S., Kovtun, A., Dietzel, I. ,. D., Epple, M., and Heumann, R. (2009). The Use of Size-Defined DNA-Functionalized Calcium Phosphate Nanoparticles to Minimise Intracellular Calcium Disturbance During Transfection. *Biomaterials* 30, 6794–6802. doi: 10.1016/j.biomaterials.2009.08.043

Okamoto, S., Matsuura, M., Akagi, T., Akashi, M., Tanimoto, T., Ishikawa, T., et al. (2009). Poly(Gamma-Glutamic Acid) Nano-Particles Combined With Mucosal Influenza Virus Hemagglutinin Vaccine Protects Against Influenza Virus Infection in Mice. *Vaccine* 27, 5896–5905. doi: 10.1016/j.vaccine.2009.07.037

Pagheh, A. S., Daryani, A., Alizadeh, P., Hassannia, H., Rodrigues Oliveira, S. M., Kazemi, T., et al. (2021). Protective Effect of a DNA Vaccine Cocktail Encoding ROP13 and GRA14 With Alum Nano-Adjuvant Against *Toxoplasma Gondii* Infection in Mice. *Int. J. Biochem. Cell Biol.* 132, 7. doi: 10.1016/j.biocel.2021.105920

Pagheh, A. S., Sarvi, S., Gholami, S., Asgarian-Omran, H., Valadan, R., Hassannia, H., et al. (2019). Protective Efficacy Induced by DNA Prime and Recombinant Protein Boost Vaccination With *Toxoplasma Gondii* GRA14 in Mice. *Microb. Pathog.* 134, 15. doi: 10.1016/j.micpath.2019.103601

Pedraza, C. E., Bassett, D. C., McKee, M. D., Nelea, V., Gbureck, U., and Barralet, J. E. (2008). The Importance of Particle Size and DNA Condensation Salt for Calcium Phosphate Nanoparticle Transfection. *Biomaterials* 29, 3384–3392. doi: 10.1016/j.biomaterials.2008.04.043

Petrovsky, N., and Aguilar, J. C. (2004). Vaccine Adjuvants: Current State and Future Trends. *Immunol. Cell Biol.* 82, 488–496. doi: 10.1111/j.0818-9641.2004.01272.x

Prandovszky, E., Li, Y., Sabunciyan, S., Steinfeldt, C. B., Avalos, L. N., Gressitt, K. L., et al. (2018). *Toxoplasma Gondii*-Induced Long-Term Changes in the Upper Intestinal Microflora During the Chronic Stage of Infection. *Scientifica* 2018, 1–11. doi: 10.1155/2018/2308619

Quan, J. H., Chu, J. Q., Ismail, H. A. H. A., Zhou, W., Jo, E. K., Cha, G. H., et al. (2012). Induction of Protective Immune Responses by a Multiantigenic DNA Vaccine Encoding GRA7 and ROP1 of *Toxoplasma Gondii*. *Clin. Vaccine Immunol.* 19, 666–674. doi: 10.1128/CVI.05385-11

Roozbehani, M., Falak, R., Mohammadi, M., Hemphill, A., Razmjou, E., Meamar, A. R., et al. (2018). Characterization of a Multi-Epitope Peptide With Selective MHC-Binding Capabilities Encapsulated in PLGA Nanoparticles as a Novel Vaccine Candidate Against *Toxoplasma Gondii* Infection. *Vaccine* 36, 6124–6132. doi: 10.1016/j.vaccine.2018.08.068

Selseleh, M., Keshavarz, H., Mohebali, M., Shojaee, S., Shojaee, S., Selseleh, M., et al. (2012). Production and Evaluation of *Toxoplasma Gondii* Recombinant GRA7 for Serodiagnosis of Human Infections. *Korean J. Parasitol* 50, 233–238. doi: 10.3347/kjp.2012.50.3.233

Song, P. X., Yao, S. H., Yao, Y., Zhou, J., Li, Q. F., Cao, Y. H., et al. (2020). Epitope Analysis and Efficacy Evaluation of Phosphatase 2c (PP2C) DNA Vaccine Against *Toxoplasma Gondii* Infection. *J. Parasitol.* 106, 513. doi: 10.1645/18-210

Van Riet, E., Ainai, A., Suzuki, T., Kersten, G., and Hasegawa, H. (2014). Combatting Infectious Diseases; Nanotechnology as a Platform for Rational Vaccine Design. *Adv. Drug Deliv. Rev.* 74, 28–34. doi: 10.1016/j.addr.2014.05.011

Verhelst, D., De, C. S., Dorny, P., Melkebeek, V., Goddeeris, B., Cox, E., et al (2011). Ifn-γ Expression and Infectivity of *Toxoplasma* Infected Tissues Are

Associated With an Antibody Response Against GRA7 in Experimentally Infected Pigs. *Vet. Parasitol* 179, 14–21. doi: 10.1016/j.vetpar.2011.02.015

Verma, R., and Khanna, P. (2013). Development of *Toxoplasma Gondii* Vaccine: A Global Challenge. *Hum. Vaccin Immunother.* 9, 291–293. doi: 10.4161/hv.22474

Wang, Z. D., Wang, S. C., Liu, H. H., Ma, H. Y., Li, Z. Y., Wei, F., et al. (2017). Prevalence and Burden of *Toxoplasma Gondii* Infection in HIV-Infected People: A Systematic Review and Meta-Analysis. *Lancet HIV* 4, e177–e188. doi: 10.1016/S2352-3018(17)30005-X

Wang, Y. H., Wang, M., Wang, G. X., Pang, A., Fu, B. Q., Yin, H., et al. (2011). Increased Survival Time in Mice Vaccinated With a Branched Lysine Multiple Antigenic Peptide Containing B- and T-Cell Epitopes From T. *gondii Antigens Vaccine* 29, 8619–8623. doi: 10.1016/j.vaccine.2011.09.016

Wang, M., Zhang, M., Fu, L., Lin, J., Zhou, X., Zhou, P., et al. (2020). Liver-Targeted Delivery of TSG-6 by Calcium Phosphate Nanoparticles for the Management of Liver Fibrosis. *Theranostics* 10, 36–49. doi: 10.7150/thno.37301

Wang, J. L., Zhang, N. Z., Li, T. T., He, J. J., Elsheikha, H. M., and Zhu, X. Q. (2019). Advances in the Development of Anti-*Toxoplasma Gondii* Vaccines: Challenges, Opportunities, and Perspectives. *Trends Parasitol* 35, 239–253. doi: 10.1016/j.pt.2019.01.005

Wilson, K. L., Xiang, S. D., and Plebanski, M. (2015). Montanide, Poly I:C and Nanoparticle Based Vaccines Promote Differential Suppressor and Effector Cell Expansion: A Study of Induction of CD8 T Cells to a Minimal *Plasmodium Berghei* Epitope. *Front. Microbiol.* 6. doi: 10.3389/fmicb.2015.00029

Xiang, S. D., Scholzen, A., Minigo, G., David, C., Apostolopoulos, V., Mottram, P. L., et al. (2006). Pathogen Recognition and Development of Particulate Vaccines: Does Size Matter? *Methods* 40, 1–9. doi: 10.1016/j.ymeth.2006.05.016

Xu, Y., Zhang, N. Z., Tan, Q. D., Chen, J., Lu, J., Xu, Q. M., et al. (2014). Evaluation of Immuno-Efficacy of a Novel DNA Vaccine Encoding *Toxoplasma Gondii* Rhoptry Protein 38 (Tgrop38) Against Chronic Toxoplasmosis in a Murine Model. *BMC Infect. Dis.* 14, 1471–2334. doi: 10.1186/1471-2334-14-525

Zhang, N. Z., Chen, J., Wang, M., Petersen, E., and Zhu, X. Q. (2013). Vaccines Against *Toxoplasma Gondii*: New Developments and Perspectives. *Expert Rev. Vaccines* 12, 1287–1299. doi: 10.1586/14760584.2013.844652

Zhang, G., Huong, V. T., Battur, B., Zhou, J., Zhang, H., Liao, M., et al. (2007). A Heterologous Prime-Boost Vaccination Regime Using DNA and a Vaccinia Virus, Both Expressing GRA4, Induced Protective Immunity Against *Toxoplasma Gondii* Infection in Mice. *Parasitology* 134, 1339–1346. doi: 10.1017/S0031182007002892

Zhang, M., Lin, W., Lin, B., Huang, Y., Lin, H. X., and Qul, J. (2012). Facile Preparation of Calcium Phosphate Nanoparticles for Sirna Delivery: Effect of Synthesis Conditions on Physicochemical and Biological Properties. *J. Nanosci Nanotechnol* 12, 9029–9036. doi: 10.1166/jnn.2012.6783

Zhang, N. Z., Wang, M., Xu, Y., Petersen, E., and Zhu, X. Q. (2015). Recent Advances in Developing Vaccines Against *Toxoplasma Gondii*: An Update. *Expert Rev. Vaccines* 14, 1609–1621. doi: 10.1586/14760584.2015.1098539

Zhou, Z., Li, H., Wang, K., Guo, Q., Li, C., Jiang, H., et al. (2017). Bioreducible Cross-Linked Hyaluronic Acid/Calcium Phosphate Hybrid Nanoparticles for Specific Delivery of Sirna in Melanoma Tumor Therapy. *ACS Appl. Mater Interfaces* 9, 14576–14589. doi: 10.1021/acsami.6b15347

Conflict of Interest: The authors declare that the research was conducted in the absence of any commercial or financial relationships that could be construed as a potential conflict of interest.

Publisher's Note: All claims expressed in this article are solely those of the authors and do not necessarily represent those of their affiliated organizations, or those of the publisher, the editors and the reviewers. Any product that may be evaluated in this article, or claim that may be made by its manufacturer, is not guaranteed or endorsed by the publisher.

frontiers in Cellular and Infection Microbiology

ORIGINAL RESEARCH
published: 05 January 2022
doi: 10.3389/fcimb.2021.793571

Characterization of the Pathology, Biochemistry, and Immune Response in Kunming (KM) Mice Following *Fasciola gigantica* Infection

Xuefang Mei[1,2], *Yaoyao Zhang*[2], *Chenyu Quan*[3], *Yiying Liang*[2], *Weiyi Huang*[2*] and *Wei Shi*[4*]

[1] Xinxiang Key Laboratory of Pathogenic Biology, Department of Pathogenic Biology, School of Basic Medical Sciences, Xinxiang Medical University, Xinxiang, China, [2] School of Animal Science and Technology, Guangxi University, Nanning, China, [3] Guangxi Key Laboratory of Veterinary Biotechnology, Guangxi Veterinary Research Institute, Nanning, China, [4] School of Preclinical Medicine, Guangxi Medical University, Nanning, China

As a putative model of *Fasciola gigantica* infection, detailed data in Kunming (KM) mice infected with *F. gigantica* are lacking. In this study, KM mice were orally infected with 15 metacercaria for 8 weeks. Macroscopic and microscopic changes, serum biochemistry, cytokine responses, and changes in parasite-specific immunoglobulin G (IgG) antibody levels were monitored at 1, 3, 5, 7, and 8 weeks post-infection (wpi), respectively. The serum levels of aspartate aminotransferase (AST) and alanine aminotransferase (ALT) increased after infection, while that of albumin (ALB) decreased, which was positively correlated with the degree of liver damage. Between 5 and 7 wpi, the mice showed symptoms of anemia and weight loss, possibly caused by the decrease of alkaline phosphatase (ALP). Moreover, the changing tendencies of the levels of globulin (GLB) and parasite-specific IgG antibody were similar, suggesting a potential correlation between GLB production and adaptive immune response in the host. Coordinated variations in interferon gamma (IFN-γ) and interleukin 4 (IL-4) indicated a mixed T helper 1 (Th1)/Th2 cellular immune response. Furthermore, the serum IgG antibody increased after infection and peaked at 5 wpi, and it was positively correlated with the average parasite burdens. The worms collected from mice were approximately 1 cm in length at 8 wpi, their digestive and reproductive systems were well developed, and no eggs were found in the uterus. To the best of our knowledge, this is the first report describing detailed histological, biochemical, and immunological indices in KM mice infected with *F. gigantica*, which provides basic information on KM mice against infection with *F. gigantica.*

Keywords: *Fasciola gigantica*, mice, pathology, immunology, biochemical indices

OPEN ACCESS

Edited by:
Ehsan Ahmadpour,
Tabriz University of Medical Sciences, Iran

Reviewed by:
Bahador Sarkari (Shahriari),
Shiraz University of Medical Sciences, Iran
Rui-Si Hu,
University of Electronic Science and Technology of China, China
Wen-Bin Zheng,
Shanxi Agricultural University, China
Panat Anuracpreeda,
Mahidol University, Thailand

***Correspondence:**
Weiyi Huang
wyhuang@gxu.edu.cn
Wei Shi
shiwei2012@hotmail.com

Specialty section:
This article was submitted to Clinical Microbiology, a section of the journal Frontiers in Cellular and Infection Microbiology

Received: *12 October 2021*
Accepted: *01 December 2021*
Published: *05 January 2022*

Citation:
Mei X, Zhang Y, Quan C, Liang Y, Huang W and Shi W (2022) Characterization of the Pathology, Biochemistry, and Immune Response in Kunming (KM) Mice Following Fasciola gigantica Infection. Front. Cell. Infect. Microbiol. 11:793571. doi: 10.3389/fcimb.2021.793571

INTRODUCTION

Fasciolosis is a globally distributed foodborne, zoonotic parasitic disease caused by *Fasciola hepatica* or *Fasciola gigantica* (Ahasan et al., 2016; Cabada et al., 2016). The life cycle of *Fasciola* includes the following stages: egg, miracidium, sporocyst, redia, cercaria, metacercaria, excystic juvenile, and adult parasite (Saba and Korkmaz, 2005; Mcmanus and Dalton, 2007). The egg, miracidium, sporocyst, redia, cercaria, and metacercaria stages occur in microorganisms that are usually detected with a microscope. The larval stage requires a molluscan intermediate host such as freshwater snails, while in the adult stage, the parasite lives on the terminal mammalian host (Roy and Reddy, 1969; Halton and Johnston, 1983). Ruminants, including sheep and cattle, are the natural hosts of *Fasciola*. Yet, these animal models are not suitable for research purposes due to the high cost of maintenance (experimental site, food, and shelter) and the complexity of the experimental protocols, which can seriously hinder experimentation in this field.

Small laboratory animals such as rabbits, mice, and rats are common animal models used to study *F. hepatica* infection. However, different animal models show varied susceptibilities to *Fasciola* (Dixon, 1964; Sewell, 1966; Reddington et al., 1986). Different parasite burdens, even within the same host species, can cause diverse pathological changes, immune responses, and parasite recovery rates (Kendall and Parfitt, 1962; Boray, 1967).

Murine models, such as mice and rats, are easy to handle and are not too costly to maintain. Therefore, using a murine laboratory model for experiments of *F. gigantica* infection may largely overcome the limitations of using large animals. BALB/c mice, Kunming (KM) mice, C57BL/6 mice, and Swiss mice are widely used models for biological and biomedical research. However, comparative studies have confirmed that the conditions of pathogen infection could differ when using different mouse strains (Jussi et al., 2005; Ley et al., 2005). In China, KM mice are the most productive and the most preferably used mouse strain for laboratory research purposes, including vaccine or drug studies (Liu et al., 2004; Zhang et al., 2007; Yuan et al., 2011). These mice are the outbred offspring of Swiss mice that have been bred into different inbred lines in different regions. Their advantages compared to Swiss mice include disease resistance, adaptability, high reproductive rate, and high survival rate (Shang et al., 2009). These advantages make them ideal animal models for artificial infection with *F. gigantica*.

Previous studies have shown that small laboratory animals may be potentially used for early infection studies (particularly the migrating larvae stage) of larger helminthic parasites (Mango et al., 1972; Dawkins and Grove, 1982; Kozek and Marroquin, 1982; Eriksen et al., 1987). The migrating larvae stage is considered as the best time to eliminate liver flukes (Kaplan and Ray, 2001). However, data on the immunology, biochemistry, and pathology of early infection of *F. gigantica* in KM mice are still lacking. In addition, there are no existing data that can serve as guidelines as to what can be expected during infection, which are all critical for further investigation when using this animal as a model and for the comparison of this model to other animal models, as well as for any downstream research on vaccine and therapeutic reagent development.

In this study, we investigated the dynamic changes in the pathology, serum biochemistry, and T helper 1 (Th1)/Th2 immune responses in KM mice infected with *F. gigantica* metacercaria during the early infection stage. The connection between macroscopic and microscopic changes was also investigated. These data may further explain the relationship between the parasite and the host.

MATERIALS AND METHODS

Preparation of *F. gigantica* Metacercaria

F. gigantica metacercaria was prepared as previously described (Anuracpreeda et al., 2009). Briefly, the parasite eggs were obtained from the gall bladder of infected water buffalo from a local slaughterhouse using the nylon mesh elutriation method. The eggs were washed and then incubated in a 28°C incubator for approximately 12–14 days. The hatched miracidia were isolated and used to infect naive freshwater snails (*Galba pervia*) locally collected from ditches and water tunnels bordering paddy fields, with a parasite load of two miracidia per snail in the tanks. Plastic films were cut into small pieces and placed over the water surface to collect the metacercaria. After approximately 35 days, the metacercaria attached to the films were collected, rinsed, counted, and stored in sterilized water at 4°C until further use.

Animals, Experimental Infection, and Sampling

Six-week-old female KM mice (SPF grade, 20–25 g body weight) were provided by the Experimental Animal Center of Guangxi Medical University. In order to explore the appropriate number of metacercaria infections, the infection cycle, and the development of *F. gigantica* during infection, 144 KM mice were divided into four groups. Each group was infected with 5, 15, 30, and 50 metacercariae by oral gavage. From 1 to 9 weeks post-infection (wpi), the clinical symptoms and the number of deaths were recorded, and fecal eggs were monitored. Four mice from each group were sacrificed and dissected every week, after which worms were collected and analyzed. Another four mice served as uninfected controls for observation of the clinical symptoms from 1 to 9 wpi.

Sixty KM mice were randomly assigned into the infection group (40 animals) and the control group (20 animals). Mice in the infected group received 15 metacercaria (the dose of infection was based on the screening results) in 0.5 ml sterilized water by oral gavage, while mice in the control group were orally administered an equal volume of water. Four mice from each group were euthanized at 1, 3, 5, 7, and 8 wpi. Blood was collected by retro-orbital bleeding for serum separation before the mice were sacrificed. The livers were then harvested and analyzed by histopathology. Commercial feed and sterilized water were provided *ad libitum* for all animals during the

study period. All mice were examined weekly to monitor signs of infection.

Gross Examination, Parasite Burdens, and Macroscopic Liver Lesion

All mice were sacrificed and examined for gross pathological lesions. Successful infection by *F. gigantica* was confirmed by the observation of typical pathological lesions. The organs and tissues (including subcutaneous tissue, brain, heart, lung, stomach, liver, gallbladder, intestine, and urinary bladder) were individually separated, and visible parasites were examined by the naked eye so as not to miss any possible ectopic parasitism of liver flukes. In order to facilitate statistical analysis of the correlation between lesions and the various biochemical and immunological indices, the severity of liver lesions was scored (from 0 to 5 points) according to the criteria of Lvova et al. (2012) and Raadsma et al. (2007), with minor modifications: 0 point, no obvious tissue necrosis or liver nodules; 1 point, mild liver necrosis or the presence of nodules, with lesions occupying <5% of the surface of the liver; 2 points, damaged liver area <15%; 3 points, liver damage or nodule area of <30%; 4 points, severe liver injury or liver nodules, with lesion area <50%; and 5 points, extensive liver necrosis, present in >50% of the liver surface.

Histopathological Evaluation

The liver tissue was preserved in Bouin's fixative for 2 days, after which it was dehydrated, rinsed in xylene, and embedded in paraffin. Three-micrometer ultrathin sections of the paraffin-embedded tissue were mounted onto glass slides and stained with hematoxylin and eosin (H&E) dye. The samples were then sealed and the stained tissue sections were microscopically examined at ×400 magnification and imaged using a Zeiss Axio Imager manual upright research microscope (HITACHI, Tokyo, Japan).

Measurements of Biochemical Indices and Cytokines

To evaluate the liver function, several enzymes in the serum were examined. Sera from all mice were separated from whole coagulated blood by centrifugation. Subsequently, routine biochemical indices, including aspartate aminotransferase (AST), alanine aminotransferase (ALT), alkaline phosphatase (ALP), albumin (ALB), and globulin (GLB), were determined using commercial diagnostic kits (Nanjing Jiancheng Bioengineering Institute, Jiangsu, China) and an automatic biochemical analyzer (HITACHI, Tokyo, Japan). The serum levels of the circulating cytokines interferon gamma (IFN-γ) and interleukin 4 (IL-4) were measured using commercial enzyme-linked immunosorbent assay (ELISA) kits (Cloud-Clone Corp., Houston, TX, USA) following the manufacturer's instructions.

Detection of *F. gigantica*-Specific IgG Antibody

ELISA was performed to assess the dynamics of antibody titer against *F. gigantica* infection according to the protocol of Ridi et al. (2007). Briefly, *F. gigantica* excretory/secretory products (FgESPs) were prepared following the previously described procedure (Ridi et al., 2007). Flat-bottom 96-well microtiter plates (Jet Biofil, Guangzhou, China) were coated with 0.25 mg/well of laboratory-made FgESPs in carbonate–bicarbonate buffer, pH 9.6, overnight at 4°C. The tested serum was diluted 1:200 with PBST [0.05 M phosphate-buffered saline containing 0.05% (*v*/*v*) Tween 20], followed by incubation for 1 h at 37°C. All experiments were performed in duplicate. All wells were washed with PBST four times and incubated for another 1 h at 37°C with 1:20,000-diluted goat anti-mouse immunoglobulin G (IgG) (CWBIO, Beijing, China). After washing with PBST four times, bound antibodies were detected by adding 100 μl/well of tetramethylbenzidine (CWBIO, Beijing, China) for 20 min at 37°C. Absorbance was measured at 450 nm on a microplate reader (iMarkTM Microplate Reader, Bio-Rad, Hercules, CA, USA).

Statistical Analysis

Statistical analysis and graphing were performed using GraphPad Prism version 6.02 (GraphPad Software Inc., La Jolla, CA, USA). The levels of all biochemical indices, cytokines, and IgG antibody titers were compared at different time points after infection using one-way analysis of variance (ANOVA) with *post-hoc* least significant difference (LSD) *t*-tests. Pearson's correlation coefficient (*r* value) was used to assess the correlation between the average parasite burdens, liver lesion scores, and the serum levels of specific IgG antibodies, biochemical indices, and cytokines in a pairwise fashion followed by a two-tailed *post-hoc* test and presented as a *p*-value. All data shown represent the mean ± SEM. The level of significance for all analyses was evaluated with a confidence interval >95% ($p < 0.05$).

RESULTS

Screening of Metacercariae Number Infected in Mice

The number of deaths in each group were recorded, including weekly dissection and sudden death (**Figure 1**). Uninfected mice had normal hair, breathing, and feeding during the experiment. Mice infected with 30 and 50 metacercariae showed symptoms of depression, anemia, and abdominal edema at 4 wpi. The longest survival times were 58 and 44 days, respectively. Mice infected with five metacercariae were healthy; only one mouse died after 52 days. No abnormalities were observed in the tissues or organs, and no worm was found at 9 wpi, suggesting that infection of mice with five metacercariae had a low success rate. The disease process of the mice infected with 15 metacercariae was relatively mild, and the worms were collected at all tested time points, except at 1 wpi.

The worms collected from mice were milky white, with a body length of about 0.5 mm at 1 wpi, and intestinal branches were visible under an optical microscope. From 5 weeks after infection, worms were found in the bile ducts of mice; the digestive and reproductive systems of the worms were well developed, and no eggs were found in the uterus. Between 1

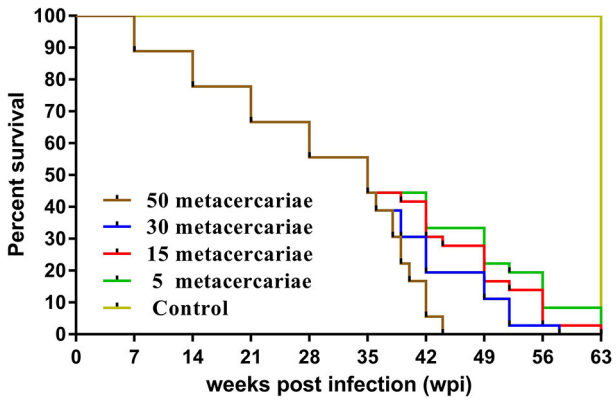

FIGURE 1 | Survival curve of mice. *Green*, *red*, *blue*, and *brown lines* indicate mice infected with 5, 15, 30, and 50 metacercariae, respectively. The *yellow line* represents uninfected mice.

and 7 wpi, the length of the worms rapidly increased from <1 mm to about 1 cm. No significant changes in body size and development were observed in the time that followed (**Figure 2**). Therefore, 15 doses of metacercariae were selected as the appropriate dose of infection in KM mice in this study, and the infection period the ranged from 0 to 8 weeks, which was suitable for the study of the juvenile stage of *F. gigantica*.

Average Parasite Burdens and Macroscopic Liver Lesion Scores

F. gigantica was recovered at different time points, except for 1 wpi, and the worm burden reached a peak at 5 wpi, when an average of 2.5 parasites per mice was recovered (**Table 1**). Histopathological evaluation was individually scored (**Table 2**), and the most severe liver lesions were observed at 7 wpi, suggesting that the severity of pathology was time-dependent.

Gross Lesion and Histopathology

Visual examination of control KM mice showed that the liver was dark red and had an overall smooth surface (**Figure 3A**). About 1 week after infection, white spots or streaks of blood became visible on the surface (**Figure 3B**), after which the liver damage gradually worsened. During the late stages of infection (7 wpi), cellulose exudate, connective tissue hyperplasia, and abscesses were observed on the surface (**Figure 3C**). In more severe cases, holes could be observed on the surface and a cellulose-like exudate was visible on the liver serosa. In addition, the texture of the liver appeared tough, and the lobes were no longer clearly defined (**Figure 3D**).

H&E staining showed that the lobule structure in the control group liver was intact, the hepatocytes were neatly arranged, and the hepatic cord contained radially arranged cells (**Figure 4**). At 1 wpi, the arrangement of hepatocytes became disordered. At 3 wpi, the hepatocytes showed necrosis and disintegration. At 5 wpi, the liver tissue structure was further destroyed, and red blood cells, eosinophils, and lymphocytes significantly increased in the sinusoids. At 7 wpi, multiple focal areas of necrosis could be observed in hepatic structures, while necrosis and structural disintegration, hepatocyte atrophy, and fibroblast proliferation in the portal area were observed in the liver. At 8 wpi, the central vein was filled with red blood cells; some of the red blood cells collapsed, while connective tissues increased in the portal area and a great amount of inflammatory cell infiltration was observed.

Biochemical Response

Compared with the control group, the serum ALT and AST levels in the experimental group increased at 3 wpi ($p < 0.01$), reaching a peak at 7 wpi. The ALP level significantly increased at 3 wpi ($p < 0.01$) and significantly decreased from 5 to 7 wpi ($p < 0.01$). At 8 wpi, the ALP level increased compared to the levels observed in the control group ($p > 0.05$).

The level of ALB was lower than that of the control group, showing a downward trend and reaching its lowest value at 7 wpi ($p < 0.01$). The GLB level began to increase at 5 wpi ($p < 0.01$). Between 5 and 8 wpi, the ratio of ALB to GLB (A/G) was significantly lower when compared to that in the control group ($p < 0.01$; **Figure 5**).

Th1/Th2 Immune Response

The level of serum IFN-γ significantly increased at 1 wpi ($p < 0.001$) and remained relatively high, reaching a peak at 7 wpi ($p < 0.0001$), whereas serum IL-4 concentration was elevated from 3 to 5 wpi ($p < 0.05$, $p < 0.0001$; **Figure 6**).

Antibody Titers

Serum specific IgG antibody levels were significantly increased at 3 wpi ($p < 0.001$) and peaked at 5 wpi ($p < 0.0001$). The levels subsequently decreased until the last time point in the experiment (**Figure 7**).

Correlation Analysis

The correlation analysis showed that the serum IgG antibody level was positively correlated with the average parasite burdens

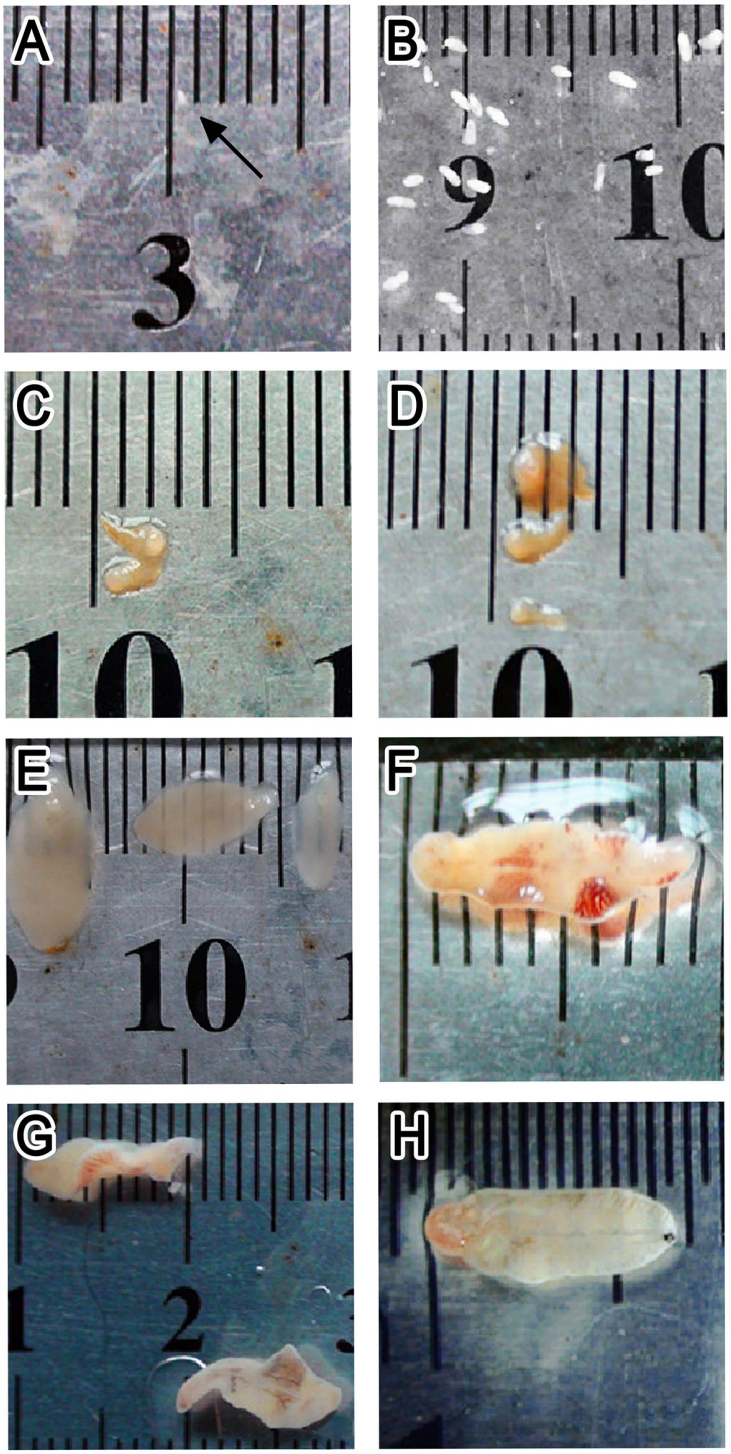

FIGURE 2 | Worms collected from Kunming (KM) mice at different infection stages. **(A–H)** Worms at 1, 2, 3, 4, 5, 6, 7, and 9 weeks post-infection, respectively.

between 1 and 8 wpi in the infected mice (**Figure 8**). A possible linear correlation was observed between the macroscopic liver examination scores and the serum levels of IFN-γ, AST, ALT, ALB, and GLB; however, these were not statistically significant ($p > 0.05$; figure not shown). Considering the excessive inflammation and lesion, the data acquired from 8 wpi may not consistently reflect the tendency of each tested indicator. After excluding the 8-wpi data from all tests, significant linear

TABLE 1 | Average parasite burdens of Kunming (KM) mice infected with *Fasciola gigantica* metacercariae.

Week post-infection (wpi)	1	3	5	7	8
Average number of parasites recovered	0	0.5	2.5	1.75	1.5

correlations were found between the serum levels of AST, ALT, and ALB and liver lesions between 1 and 7 wpi ($p < 0.05$; **Figure 9**).

DISCUSSION

This is the first study evaluating KM mice as a small laboratory infection model for examination of early infection (1–8 wpi) with *F. gigantica*. In this study, we investigated the macroscopic and microscopic changes in infected KM mice, including pathological changes and histopathology in the liver. We also determined and analyzed the dynamic level changes of biochemical indices, parasite-specific IgG antibody, and major Th1/Th2 cytokines in mouse serum. As an essential prerequisite, *F. gigantica* infection was successfully established in KM mice, mainly confirmed by the recovery of parasites at the end. No worm was recovered from infected individuals at 1 wpi. This may be because the size of juveniles at this stage was too small to be seen by the naked eye. Although invisible, this does not entirely mean that the parasites were not present in the tissues.

Serum levels of AST, ALT, ALP, ALB, and GLB can be used as indicators of liver damage (Kolodziejczyk et al., 2005; Kamel et al., 2015; Gattani et al., 2018). AST and ALT are used to evaluate hepatic parenchymal cell injury and are more sensitive than other serum enzymes (Mahmoud et al., 2002; Myers et al., 2003; Pierr et al., 2012; Beek et al., 2013). Elevated ALP levels are common in hepatobiliary diseases and provide important hints about primary biliary cirrhosis (Kaplan and Righetti, 1970; Thapa and Walia, 2007; Lindor et al., 2009). The liver is the largest and one of the most important organs of the immune system. Once the immune cells in the liver are activated, the amount of GLB secreted in the liver increases. Low ALB and high immunoglobulin are commonly seen in fasciolosis (Ulger et al., 2014; Ibrahim, 2017). Previous data suggested that the levels of AST and ALT increased after infection with *Fasciola* in cattle (Edith et al., 2010; Gattani et al., 2018), sheep (Ahmed et al., 2006; Solanki et al., 2017), rats (Kolodziejczyk et al., 2005), and humans (Arslan et al., 2012; Kamel et al., 2015), which is consistent with the results of the current study. Gattani et al. (2018) found that the levels of ALP were elevated in the serum of cattle naturally infected with *F. hepatica.* Moreover, Galtier et al. (2011) showed that rats infected with *F. hepatica* had elevated ALP during the entire chronic phase (when the parasite enters the bile duct). However, the results of our study showed that the levels of ALP significantly decreased at 5 wpi, coinciding with a period of high death rate, which may be related to the anemia and malnutrition observed in mice during this period. Anemia, low ALB, eosinophilia, and subacute and chronic infections characterized by severe weight loss, low ALB, and high GLB are the main clinical features of human fasciolosis (Ibrahim, 2017). A survey in Turkey (Veli et al., 2014) showed that the low ALB presented as one of the symptoms in 44% of *F. hepatica*-infected cases. The results of our study showed that the ALB level exhibited a downward trend and was lower than that of the control group, indicating that, once KM mice were infected with *F. gigantica*, ALB synthesis was reduced due to liver damage. The level of GLB was consistent with the trend of specific IgG antibody levels, meaning that the change in the level of GLB was possible due to the immune responses by mechanical damage and repeated stimulation of the host liver by *Fasciola*-associated proteins.

Due to the diversities in body size and pathogenicity, *F. gigantica* and *F. hepatica* generate different types of cellular immunity when infecting different hosts. For example, cellular immune response shifting from Th0 to Th2 is a characteristic immunological process in cattle infected with *F. hepatica* (Oldham and Williams, 1985). Furthermore, buffaloes infected with *F. gigantica* mainly display a Th0-like immune response (which should now be described as a mixed Th1/Th2 immune response due to the co-upregulation of both serum Th1 and Th2 cytokines observed) (Zhang et al., 2006). In this study, the murine immune response was characterized by a mixed Th1/Th2 response, sharing similar immune response characteristics of large animals. In cattle and buffaloes infected with high parasitic loads (1,000 metacercaria), the levels of IFN-γ in the host sera did not significantly change before and after infection, indicating that these two hosts lack an effective mechanism for killing early larvae (Estes et al., 1994; Hansen et al., 1999; Molina, 2005). In our KM mice, IFN-γ increased at 1 wpi and decreased

TABLE 2 | Macroscopic liver lesion scores of Kunming (KM) mice infected with *Fasciola gigantica* metacercariae.

Week post-infection (wpi)	Animal 1	Animal 2	Animal 3	Animal 4
1	0	0	0	0
3	1	0	1	0
5	1	2	1	1
7	4	2	3	2
8	2	2	4	2

A score of 0 indicates no signs of tissue necrosis or liver nodules, a score of 1 indicates mild hepatic necrosis or nodules that are limited to <5% of the liver surface area, 2 indicates liver damage due to damage occupying <15% of the liver surface area, 3 indicates that moderate liver damage is present and nodules are limited to <30% of the liver surface area, 4 represents liver damage and nodules occupying <50% of the liver surface area, and a score of 5 represents extensive liver necrosis and >50% of the liver surface area occupied by liver nodules.

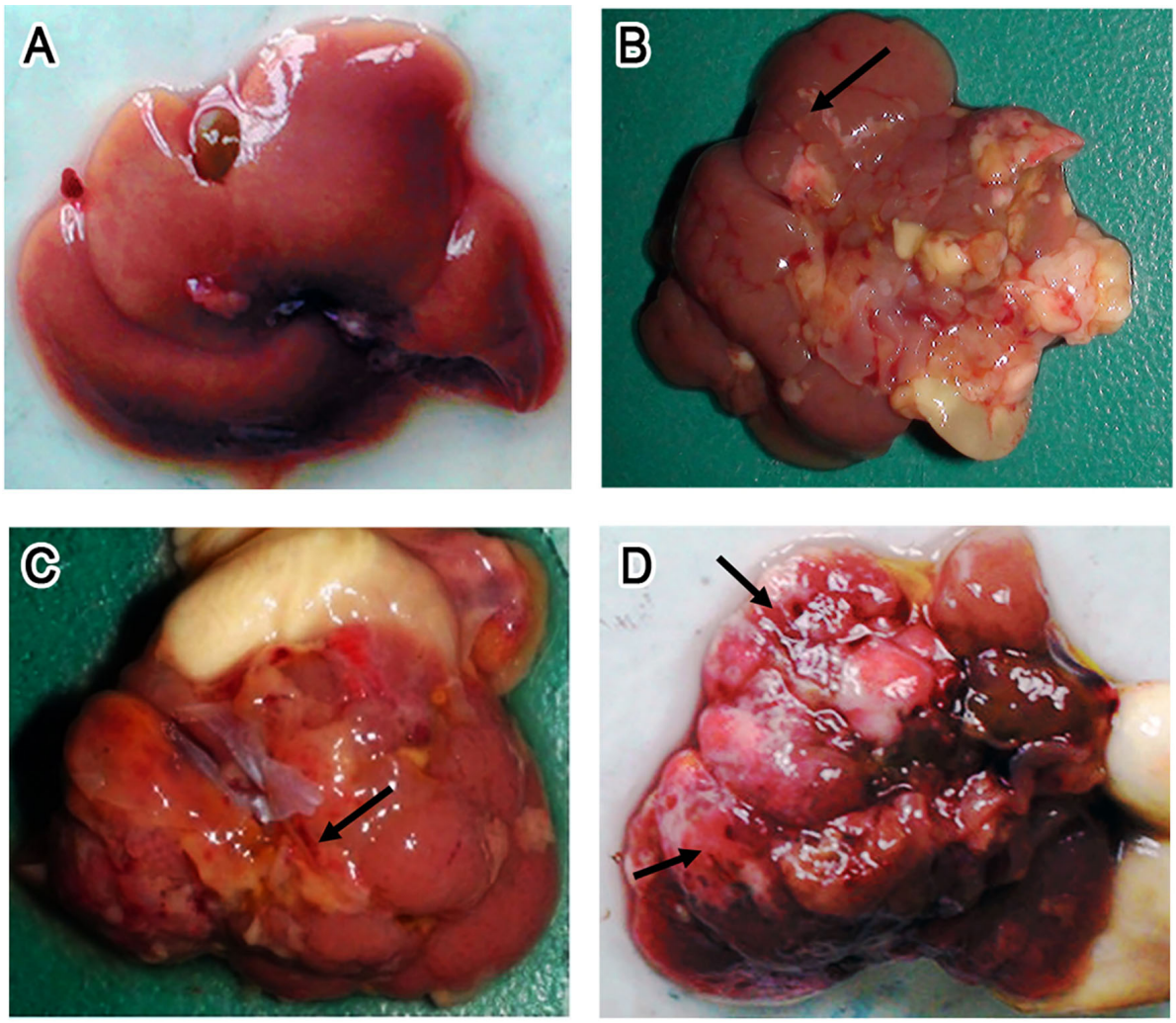

FIGURE 3 | Gross lesion of the liver. **(A–D)** Photographs of livers isolated from uninfected control Kunming (KM) mice **(A)** and mice infected with 15 *Fasciola gigantica* metacercaria at 7 days post-infection (dpi) **(B)** or 49 dpi **(C, D)**. *Black arrows* point to regions with bleeding, while *blue arrows* point to a typical lesion, i.e., gray–white nodules or pyogenic foci in the liver.

after reaching a peak at 7 wpi. The specific IgG antibody level reached a peak at 5 wpi and then decreased, while the average parasite burdens were highest at 5 wpi. We infer that a persistent Th1-type inflammatory response in KM mice infected with *F. gigantica* has a deadly effect on the larvae, resulting in the death of a certain percentage of the parasites and a decrease in the total amount of specific IgG antibodies produced. Together with data from large animals (which have a bigger worm burden) and KM mice (which have a lower worm burden), our data suggested that the relatively low worm burden may mainly be due to the early Th1 response characterized by the rapidly increased serum IFN-γ and IgG levels in KM mice. In addition, as we observed in all tested animal models in previous studies, flukes of *Fasciola* spp. could reach over 1 cm in length within 8 weeks in the host (Valero et al., 1998). Obviously, the small size of the bile duct, gallbladder, and hepatic parenchyma might physically (but not immunologically) limit the fast growth and migration of worms inside the hepatobiliary system in mice, unlike that in large animal hosts. This may also be another possible reason for the early clearance of most newly excysted juveniles (NEJs), as well as for the low worm burden after infection of KM mice with *F. gigantica*.

We also observed that the change of serum IL-4 in mice was similar to that of IFN-γ; still, the increase of IL-4 was observed later than that of IFN-γ and remained high for a shorter period than IFN-γ, which is very similar to the immunological response observed in buffalo infected with *F. gigantica* (Shi et al., 2017; Zhang et al., 2017). IL-4 is an important cytokine benefiting liver flukes that contributes to the inhibition of the host Th1-type pro-inflammatory response and is essential for the parasites to achieve immune evasion during the early stage of infection (Cervi et al., 2001). A transient increase of IL-4 from 3 to 5

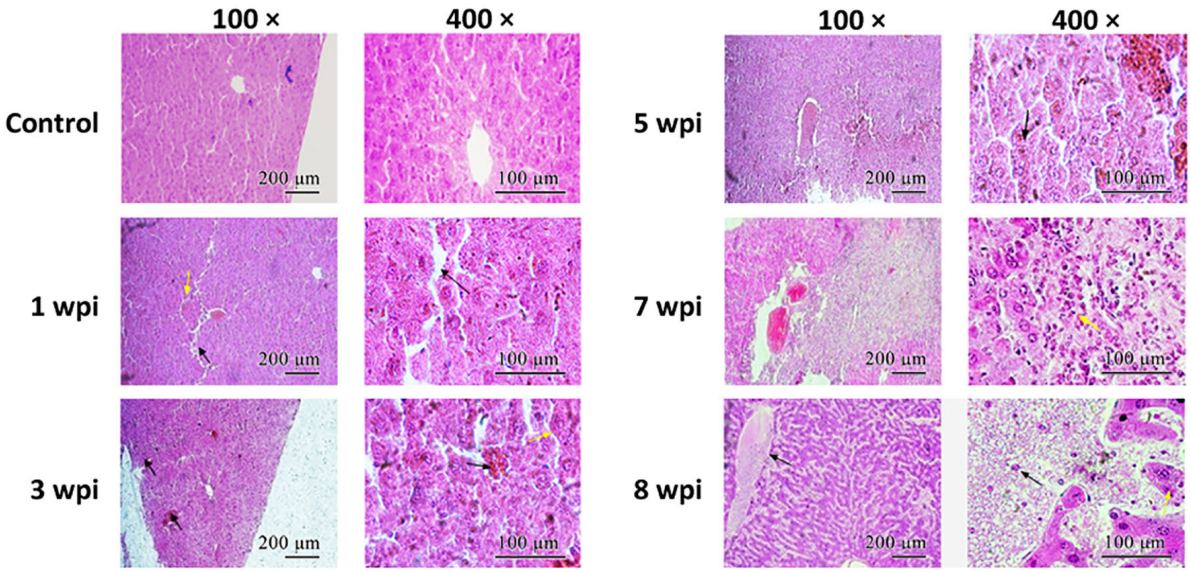

FIGURE 4 | Histopathological characteristics of the liver. The tissue sections were stained with hematoxylin–eosin. *Arrows* indicate the corresponding morphological features described in the article. *Scale bars*: *left panel*, 200 μm; *right panel*, 100 μm.

wpi may contribute to the rapid development and migration of *F. gigantica* at this stage and may have a role in maintaining immunosuppression and promoting tissue fibrosis and repair. Focal fibrosis forms external physical barriers that block the impairment of liver tissues and the access of immune cells to the parasites, thereby creating a protective environment benefiting parasite development (Mendes et al., 2012; Mendes et al., 2013; Shi et al., 2017; Zhang et al., 2017). The production of IL-4 induced by *F. gigantica* infection could promote tissue repair and further liver fibrosis. However, KM mice may not be able to repair the severe liver damage observed, which may lead to more acute symptoms rather than more moderate chronic symptoms during infection. This is evidenced by the occurrence of the first death of infected individuals at 8 wpi, which showed extremely severe liver tissue pathology. We suggest that the main reason for the death could be excessive inflammation and lesion, which gradually increased from 1 to 7 wpi. Similar studies on other animal models (for example, buffalo and sheep) have shown a direct connection between liver damage and parasite burden, as well as infection period in any animal model (Kendall and Parfitt, 1962; Boray, 1967; Prasitirat et al., 1996). Thus, it is clear that the deficiency of tissue repair during longer infection is responsible for the overall damage of the liver in KM mice.

Different infection dosages of parasites may also influence the type of host immune response. O'Neill et al. (2000) found that infection with five *F. hepatica* metacercaria induced a strong Th2 immune response in BALB/c and 129Sv/Ev mice and a mixed Th1/Th2 immune response in C57BL/6 mice. However, infection with 15 *F. hepatica* metacercaria caused the immune response of C57BL/6 mice, making them more Th2-dominant. This is likely closely related to the degree of host organ damage and tissue repair caused by different parasitic burdens. In our study, KM mice infected with 15 metacercaria showed a mixed Th1/Th2 immune response; however, the dynamic changes in cytokine levels during infection with different parasitic burdens must be further confirmed (Machicado et al., 2016).

Detection of serum antibodies using ELISA is the most popular technique for fasciolosis diagnosis (Castro et al., 2000; Reichel, 2002; Molloy et al., 2005; Ridi et al., 2007). Previous studies have shown that parasite-specific serum antibodies in sheep infected with *F. gigantica* increased at 2–4 wpi (Guobadia and Fagbemi, 1995; Phiri et al., 2006; Ridi et al., 2007), while the antibody titers increased at 4 wpi after *F. hepatica* infection (Santiago and Hillyer, 1988). The parasite recovery rate from sheep infected with *F. hepatica* was significantly higher than that from sheep infected with *F. gigantica* (Zhang et al., 2004; Zhang et al., 2005). The delay in antibody production, which prevents the host immune system from completely killing the smaller and more vulnerable larvae during the early stages of infection, is a major factor in the susceptibility of sheep to *F. hepatica* infection. In this study, the level of specific IgG antibody in the serum of mice infected with 15 of *F. gigantica* metacercaria was not significantly changed at 1 wpi, but increased starting at 3 wpi and then remained high until death. This is similar to what has been observed in other susceptible animals (Guobadia and Fagbemi, 1995; Phiri et al., 2006; Ridi et al., 2007), indicating that the production of specific antibodies can be induced at 2–3 wpi in hosts and that the antibody concentration can be maintained until the adult stage (although the experimental host in our case was unable to achieve chronic infection).

Based on the dynamics of various biochemical indices and cytokines, we found that some of these indicators could be associated with the course of progressive host liver disease. Therefore, we further analyzed the correlation between liver

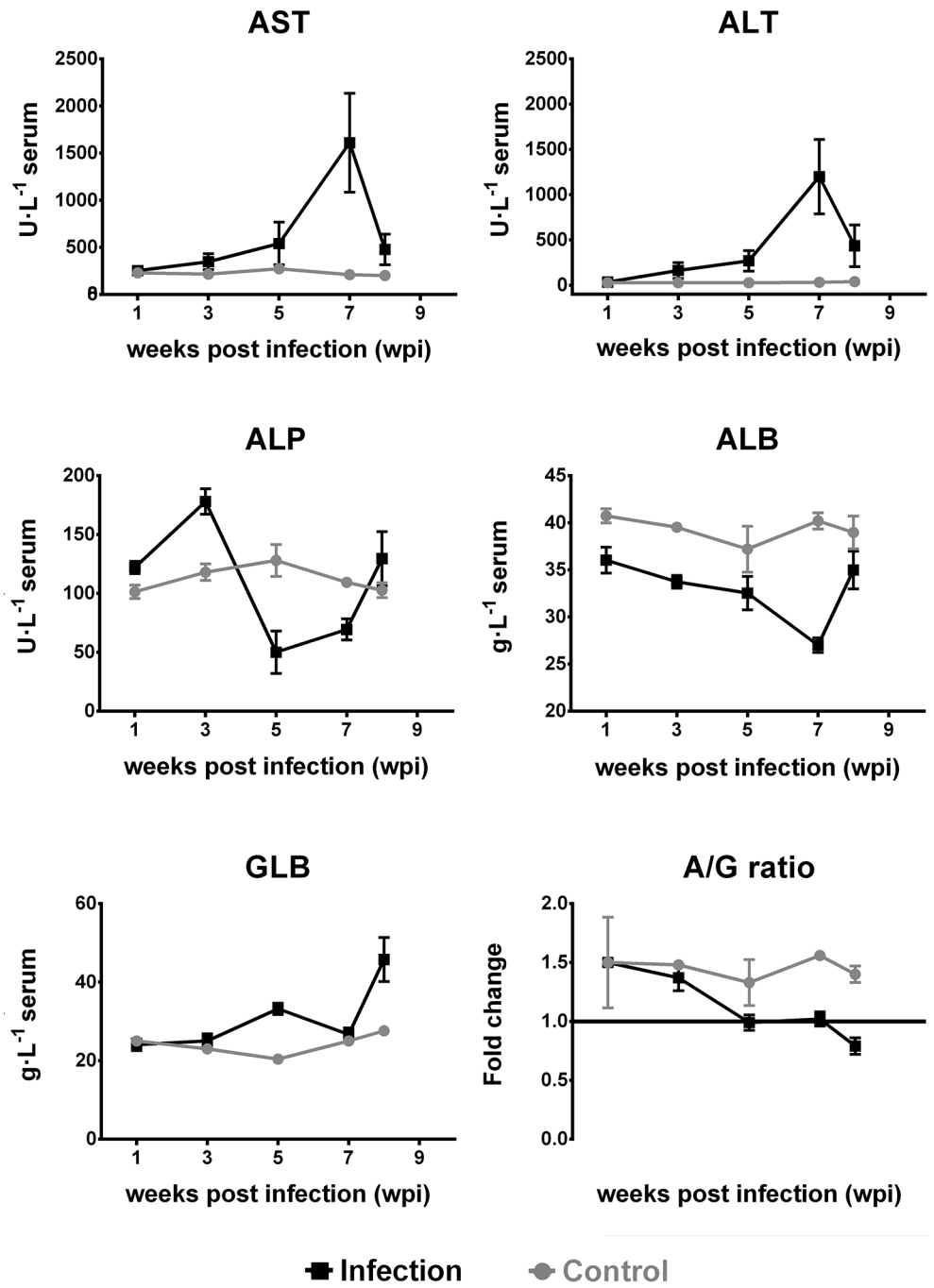

FIGURE 5 | Dynamic changes in serum alanine aminotransferase (ALT), aspartate aminotransferase (AST), alkaline phosphatase (ALP), albumin (ALB), and globulin (GLB) levels and the ratio of ALB to GLB (*A/G*) in Kunming (KM) mice infected with *Fasciola gigantica*. The *X*-axis represents weeks post-infection (wpi) and the *Y*-axis represents the biochemical indices or the fold change of the level of ALB level relative to that of GLB. *Red lines* show the trends of the tested biochemical indices in *F. gigantica*-infected mice, while *blue lines* show the trends of the uninfected control mice. The mean values of the biochemical indices from three independent experiments are also plotted.

lesions and these indicators. Our analysis showed that the liver lesion scores in KM mice were likely to have a linear correlation with IFN-γ, AST, ALT, ALB, and GLB between 1 and 8 wpi; however, the correlation was not statistically significant ($p > 0.05$; figure not shown). In cases where most biochemical and immunological indices were suddenly downregulated at 8 wpi, we assumed that the destruction of liver structures led to a significant decrease in the number of secretory cells. Therefore,

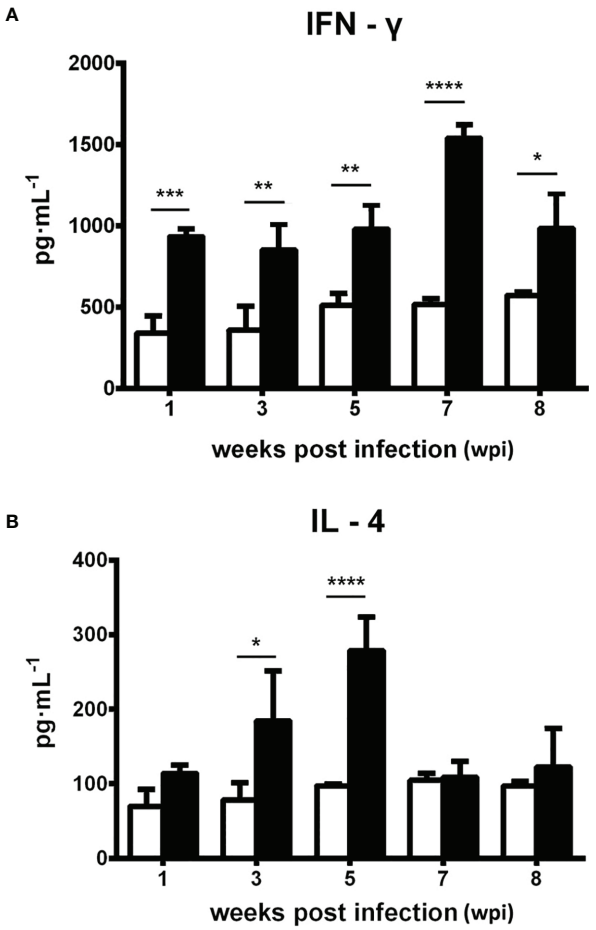

FIGURE 6 | Dynamic changes of the serum cytokines IFN-γ and IL-4 in Kunming (KM) mice infected with *Fasciola gigantica* compared with uninfected control mice. The mean ± SE values of three independent experiments are shown. The *X*-axis represents weeks post-infection (wpi) and the *Y*-axis represents the production of serum cytokine measured by commercial ELISA kits. Significant differences of each time point compared with the control: $^{*}p < 0.05$; $^{**}p < 0.01$; $^{***}p < 0.001$; $^{****}p < 0.0001$ (analyzed by one-way ANOVA, *post-hoc* LSD test).

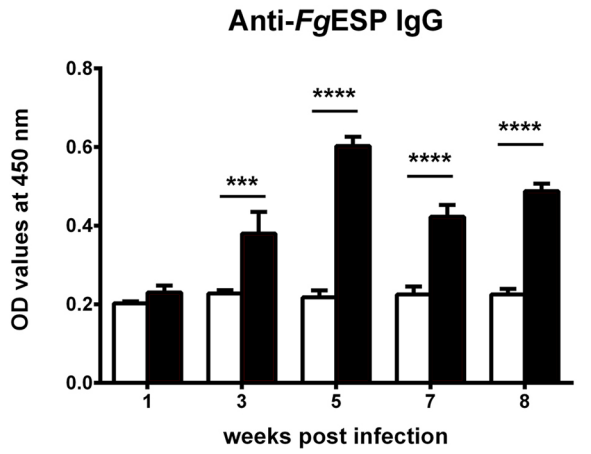

FIGURE 7 | Dynamic changes of serum antibodies in Kunming (KM) mice infected with *Fasciola gigantica* measured using an excretory/secretory product of *F. gigantica* (FgESP)-based direct ELISA method. The *X*-axis represents weeks post-infection (wpi) and the *Y*-axis represents the optical density (OD) values of the antibody titers relative to the uninfected control. *Columns* show the means and *error bars* show SEMs. Significant differences of each time point compared with control: $^{***}p < 0.001$; $^{****}p < 0.0001$ (analyzed by one-way ANOVA, *post-hoc* LSD test).

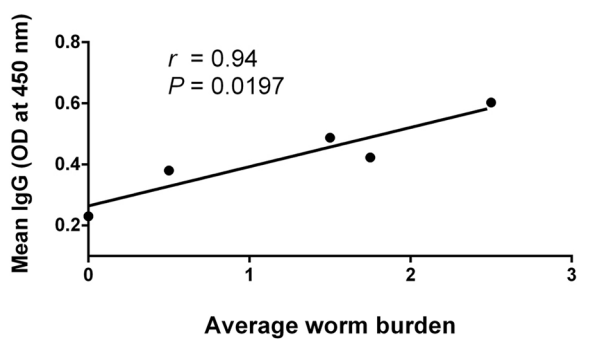

FIGURE 8 | Pearson's correlation analysis between average worm burdens and *Fasciola gigantica*-specific IgG. Positive correlation between the average worm burdens of infected mice and *F. gigantica*-specific IgG mean levels [optical density (OD) value at 450 nm absorption] at 1–8 wpi of infection based on a Pearson's linear regression analysis by pairwise comparison. The *solid line* comes from the best-fit linear regression model with a slope of 0.1284, a *Y*-intercept of 0.2640, and a *X*-intercept of –2.055 ($r = 0.569$, $p < 0.05$).

the 8-wpi data were intentionally excluded from the correlation analysis, and we found that AST, ALT, and ALB did have a significant linear correlation with liver lesions within 1–7 wpi ($p < 0.05$; **Figure 7**), which again confirmed that AST, ALT, and ALB are reliable and convincing biochemical markers for evaluating the degree of liver injury and the prognosis of hosts from fasciolosis (Edith et al., 2010; El-Boshy et al., 2015), contrary to other indicators. Nevertheless, the lack of correlation between the liver damage scores and the tested serum cytokines suggested that the inflammation balance may not be the major or only influencing factor deciding the degree of liver damage. Herein, our correlation analysis denoted that the continuously intensifying liver damage, but without an effective IL-4-dependent repair mechanism (Minutti et al., 2017; Gieseck III et al., 2018), could be responsible for the liver disease progression of fascioliasis until the final death of the infected mice at 8 wpi.

CONCLUSIONS

This preliminarily study explored the pathology, biochemistry, and immune responses after early infection of *F. gigantica* in KM mice, characterized as severe and rapid hepatitis. The results of

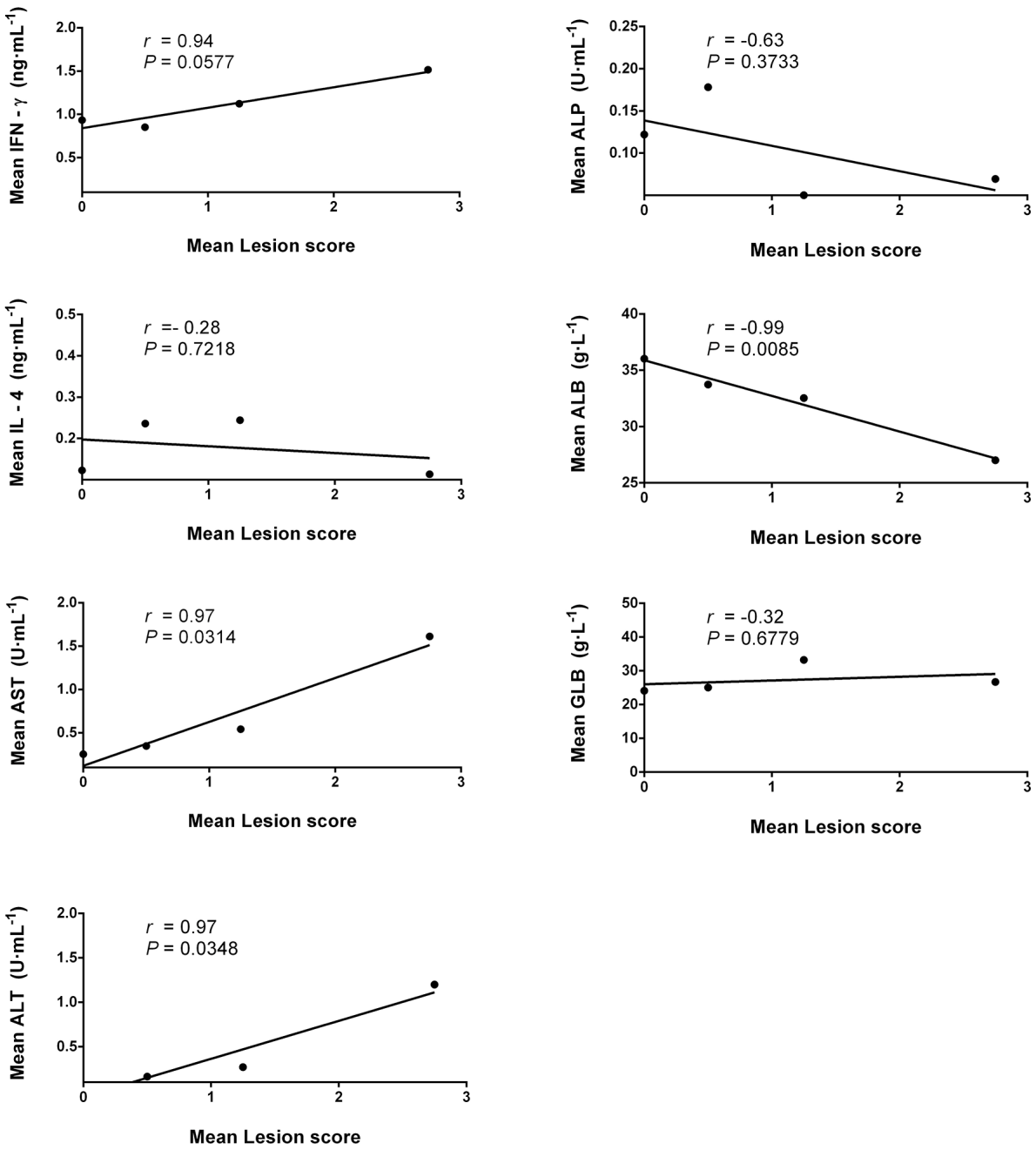

FIGURE 9 | Pearson's correlation analysis for the mean liver lesion scores of infected mice against the mean values of the serum biochemical indices (AST, ALT, ALP, ALB, and GLB) and serum cytokines (IFN-γ and IL-4) for 1–7 weeks post-infection (wpi) by pairwise comparison. The *solid lines* are from the best-fit linear regression model and illustrate positive ($r > 0$) or negative ($r < 0$) correlation, while $p < 0.05$ represents statistically significant differences. *AST*, aspartate aminotransferase; *ALT*, alanine aminotransferase; *ALP*, alkaline phosphatase; *ALB*, albumin; *GLB*, globulin.

this study will provide a basis for studying the small laboratory animal model of *F. gigantica*. Moreover, measurement of the levels of AST, ALT, and ALB combined with the parasite-specific antibody titer in the serum samples using ELISA can be applied in clinical diagnosis to effectively determine the pathogenic course of *F. gigantica* infection. Understanding of the immunological and biochemical information on KM mice during *F. gigantica* early infection provides an important theoretical framework for further comparative studies on other laboratory animal species (including other mouse genotypes) and may help elucidate the etiology underlying human and animal fascioliasis.

DATA AVAILABILITY STATEMENT

The original contributions presented in the study are included in the article/Supplementary Material. Further inquiries can be directed to the corresponding author.

ETHICS STATEMENT

All the animals were housed in an environment with a temperature of 22 ± 1°C, relative humidity of 50 ± 1%, and a light/dark cycle of 12/12 hr. All experimental protocols and methods were approved by the Ethics Committee of the College of Animal Science and Technology, Guangxi University. Animals used in this study were handled in accordance with good animal practices, as required by the Animal Ethics Procedures and Guidelines of the People's Republic of China.

AUTHOR CONTRIBUTIONS

XM, WS, YZ, and WH designed the study and critically revised the paper. XM, WS, YZ, CQ, and YL prepared the experimental samples and performed the experimental procedures. XM, YZ, and WS analyzed the results. XM, WS, and CQ contributed to the writing of the manuscript. All authors contributed to the article and approved the final version.

FUNDING

This study was financially supported by the Doctoral Scientific Research Activation Foundation of Xinxiang Medical University (grant no. XYBSKYZZ202140) and the National Natural Science Foundation of China (grant no. 31760728).

REFERENCES

Ahasan, S. A., Valero, M. A., Chowdhury, E. H., Islam, M. T., Islam, M. R., Hussain Mondal, M. M., et al. (2016). CIAS Detection of Fasciola Hepatica / F. Gigantica Intermediate Forms in Bovines From Bangladesh. *Acta Parasitol* 61 (2), 267–277. doi: 10.1515/ap-2016-0037

Ahmed, I. M., Ambali, G. A., and Baba, S. S. (2006). Haematological and Biochemical Responses of Balami Sheep to Experimental *Fasciola Gigantica* Infection. *Int. J. Food Agric. Environ.* 4 (2), 71–74.

Anuracpreeda, P., Wanichanon, C., and Sobhon, P. (2009). *Fasciola Gigantica*: Immunolocalization of 28.5 Kda Antigen in the Tegument of Metacercaria and Juvenile Fluke. *Exp. Parasitol* 122 (2), 75–83. doi: 10.1016/j.exppara.2009.03.007

Arslan, F., Batirel, A., and Samasti, M. (2012). Fascioliasis: 3 Cases With Three Different Clinical Presentations. *Turkish J. Gastroenterol. Off. J. Turkish Soc. Gastroenterol.* 23 (3), 267–271. doi: 10.4318/tjg.2012.0388

Beek, J. H., Moor, M. H., Geus, E. J., Lubke, G. H., Vink, J. M., Willemsen, G., et al. (2013). The Genetic Architecture of Liver Enzyme Levels: GGT, ALT and AST. *Behav. Genet.* 43 (3), 329–339. doi: 10.1007/s10519-013-9593-y

Boray, J. C. (1967). Studies on Experimental Infections With *Fasciola Hepatica*, With Particular Reference to Acute Fascioliasis in Sheep. *Ann. Trop. Med. Parasitol.* 61 (4), 439–450. doi: 10.1080/00034983.1967.11686513

Cabada, M. M., Lopez, M., Cruz, M., Delgado, J. R., Hill, V., and White, A. C. (2016). Treatment Failure After Multiple Courses of Triclabendazole Among Patients With Fascioliasis in Cusco, Peru: A Case Series. *PloS Neglect. Trop. Dis.* 10 (1), e0004361. doi: 10.1371/journal.pntd.0004361

Castro, E., Freyre, A., and Hernández, Z. (2000). Serological Responses of Cattle After Treatment and During Natural Re-Infection With *Fasciola Hepatica*, as Measured With a Dot-ELISA System. *Vet. Parasitol* 90 (3), 201–208. doi: 10.1016/S0304-4017(00)00228-4

Cervi, L., Cejas, H., and Masih, D. T. (2001). Cytokines Involved in the Immunosuppressor Period in Experimental Fasciolosis in Rats. *Int. J. Parasitol.* 31 (13), 1467–1473. doi: 10.1016/S0020-7519(01)00275-2

Dawkins, H. J., and Grove, D. I. (1982). Attempts to Establish Infections With *Strongyloides Stercoralis* in Mice and Other Laboratory Animals. *J. Helminthol.* 56 (1), 23–26. doi: 10.1017/S0022149X00034957

Dixon, K. E. (1964). The Relative Suitability of Sheep and Cattle as Hosts for the Liver Fluke, *Fasciola Hepatica* L. *J. Helminthol.* 38 (3-4), 203–212. doi: 10.1017/S0022149X00033782

Edith, R., Godara, R., Sharma, R. L., and Thilagar, M. B. (2010). Serum Enzyme and Hematological Profile of *Fasciola Gigantica* Immunized and Experimentally Infected Riverine Buffaloes. *Parasitol. Res.* 106 (4), 947–956. doi: 10.1007/s00436-010-1741-1

El-Boshy, M. E., Husien, S. H., Fatma, M. A., Engy, F. R., and Osama, A. M. (2015). Comparative Studies on Triclabendazole and Mirazid in Guinea Pigs Experimentally Infected With Fasciola Gigantica. *J. Bioanal. Biomed.* 7 (1), 13–17. doi: 10.4172/1948-593X.1000117

Eriksen, L., Rygaard, J., Brünner, N., Graem, N., and Spang-Thomsen, M. (1987). "Effect of Anthelmintic Treatment With Levamisole Chloride and Ivermectin on Migrating Ascaris Suum Larvae in Thymus-Bearing and Thymus-Deficient Mice," in *Immune-Deficient Animals* (Copenhagen, Denmark: Karger Publishers), 129–130.

Estes, D. M., Closser, N. M., and Allen, G. K. (1994). IFN-Gamma Stimulates IgG2 Production From Bovine B Cells Costimulated With Anti-μ and Mitogen. *Cell. Immunol.* 154 (2), 287–295. doi: 10.1006/cimm.1994.1078

Galtier, P., Battaglia, A., More, J., and Franc, M. (2011). Impairment of Drug Metabolism by the Liver in Experimental Fascioliasis in the Rat. *J. Pharm. Pharmacol.* 35, 729–733. doi: 10.1111/j.2042-7158.1983.tb02879.x

Gattani, A., Kumar, A., Singh, G. D., Tiwary, R., Kumar, A., Das, A. K., et al. (2018). Hematobiochemical Alteration in Naturally Infected Cattle With *Fasciola* Under Tropical Region. *J. Vet. Sci. Technol.* 4, 20–23.

Gieseck, R. L.III, Wilson, M. S., and Wynn, T. A. (2018). Type 2 Immunity in Tissue Repair and Fibrosis. *Nat. Rev. Immunol.* 18 (1), 62–76. doi: 10.1038/nri.2017.90

Guobadia, E. E., and Fagbemi, B. O. (1995). Time-Course Analysis of Antibody Response by EITB and ELISA Before and After Chemotherapy in Sheep Infected With Fasciola Gigantica. *Vet. Parasitol* 58 (3), 247–253. doi: 10.1016/0304-4017(94)00721-N

Halton, D. W., and Johnston, B. R. (1983). Development *In Vitro* of the Metacercaria of *Bucephaloides Gracilescens* (Trematoda: *Bucephalidae*). *Int. J. Parasitol.* 13 (2), 157–164. doi: 10.1016/0020-7519(83)90006-1

Hansen, D. S., Clery, D. G., Estuningsih, S. E., Widjajanti, S., Partoutomo, S., and Spithill, T. W. (1999). Immune Responses in Indonesian Thin Tail and Merino Sheep During a Primary Infection With *Fasciola Gigantica*: Lack of a Specific IgG 2 Antibody Response Is Associated With Increased Resistance to Infection in Indonesian Sheep. *Int. J. Parasitol.* 29 (7), 1027–1035. doi: 10.1016/S0020-7519(99)00038-7

Ibrahim, N. (2017). Fascioliasis: Systematic Review. *Adv. Biol. Res.* 11 (5), 278–285. doi: 10.5829/idosi.abr.2017.278.285

Jussi, V., Erkki, E., and Paavo, T. (2005). Comparison of Cellular Fatty Acid Profiles of the Microbiota in Different Gut Regions of BALB/c and C57BL/6J Mice. *Antonie Van Leeuwenhoek* 88 (1), 67–74. doi: 10.1007/s10482-004-7837-9

Kamel, H. H., Sarhan, R. M., and Saad, G. A. (2015). Biochemical Assessment of Oxidative Status Versus Liver Enzymes in Patients With Chronic Fascioliasis. *J. Parasitic Dis.* 39 (4), 628–633. doi: 10.1007/s12639-014-0431-9

Kaplan, R. M., and Ray, M. (2001). *Fasciola Hepatica*: A Review of the Economic Impact in Cattle and Considerations for Control. *Vet. Ther.* 2 (1), 40–50. doi: 10.1172/JCI106260

Kaplan, M. M., and Righetti, A. (1970). Induction of Rat Liver Alkaline Phosphatase: The Mechanism of the Serum Elevation in Bile Duct Obstruction. *J. Clin. Invest.* 49 (3), 508–516. doi: 10.1172/JCI106260

Kendall, S. B., and Parfitt, J. W. (1962). The Chemotherapy of Fascioliasis. *Br. Vet. J.* 118, 1–4.1. doi: 10.1016/S0007-1935(17)43251-9

Kolodziejczyk, L., Siemieniuk, E., and Skrzydlewska, E. (2005). Antioxidant Potential of Rat Liver in Experimental Infection With *Fasciola Hepatica*. *Parasitol. Res.* 96 (6), 367–372. doi: 10.1007/s00436-005-1377-8

Kozek, W. J., and Marroquin, H. F. (1982). Attempts to Establish *Onchocerca Volvulus* Infection in Primates and Small Laboratory Animals. *Acta Tropica* 39 (4), 317–324.

Ley, R. E., Bäckhed, F., Turnbaugh, P., Lozupone, C. A., Knight, R. D., and Gordon, J. I. (2005). Obesity Alters Gut Microbial Ecology. *Proc. Natl. Acad.* 102 (31), 11070–11075. doi: 10.1073/pnas.0504978102

Lindor, K. D., Gershwin, M. E., Poupon, R., Kaplan, M., Bergasa, N. V., and Heathcote, E. J. (2009). Primary Biliary Cirrhosis. *Hepatology* 50 (1), 291–308. doi: 10.1002/hep.22906

Liu, J. M., Cai, X. Z., Lin, J. J., Fu, Z. Q., Yang, G. Z., Shi, F. H., et al. (2004). Gene Cloning, Expression and Vaccine Testing of *Schistosoma Japonicum* SjFABP. *Parasite Immunol.* 26 (8-9), 351–358. doi: 10.1111/j.0141-9838.2004.00720.x

Lvova, M. N., Tangkawattana, S., Balthaisong, S., Katokhin, A. V., Mordvinov, V. A., and Sripa, B. (2012). Comparative Histopathology of *Opisthorchis Felineus* and *Opisthorchis Viverrini* in a Hamster Model: An Implication of High Pathogenicity of the European Liver Fluke. *Parasitol. Int.* 61 (1), 167–172. doi: 10.1016/j.parint.2011.08.005

Machicado, C., Machicado, J. D., Maco, V., Terashima, A., and Marcos, L. A. (2016). Association of *Fasciola Hepatica* Infection With Liver Fibrosis, Cirrhosis, and Cancer: A Systematic Review. *PloS Negl. Trop. Dis.* 10, e0004962. doi: 10.1371/journal.pntd.0004962

Mahmoud, R. M., Elabhar,, and Saleh, S. H. (2002). The Effect of Nigella Sativa Oil Against the Liver Damage Induced by *Schistosoma Mansoni* Infection in Mice. *J. Ethnopharmacol.* 79, 1–11. doi: 10.1016/S0378-8741(01)00310-5

Mango, A. M., Mango, C. K., and Esamal, D. (1972). A Preliminary Note on the Susceptibility, Prepatency and Recovery of *Fasciola Gigantica* in Small Laboratory Animals. *J. Helminthol.* 46 (4), 381–386. doi: 10.1017/S0022149X00023385

Mcmanus, D., and Dalton, J. (2007). Vaccines Against the Zoonotic Trematodes *Schistosoma Japonicum*, *Fasciola Hepatica* and Fasciola Gigantica. *Parasitology* 133 (S2), 43–61. doi: 10.1017/S0031182006001806

Mendes, E. A., Mendes, T. A., Santos, S. L., Menezes-Souza, D., Bartholomeu, D. C., Martins, I. V. F., et al. (2013). Expression of IL-4, IL-10 and IFN-γ in the Liver Tissue of Cattle That Are Naturally Infected With *Fasciola Hepatica*. *Vet. Parasitol.* 195 (1-2), 177–182. doi: 10.1016/j.vetpar.2013.03.035

Mendes, E. A., Vasconcelos, A. C., and Lima, W. (2012). Histopathology of *Fasciola Hepatica* Infection in Meriones Unguiculatus. *Rev. Patologia Trop.* 41 (1), 55–62. doi: 10.5216/rpt.v41i1.17747

Minutti, C. M., Jackson-Jones, L. H., García-Fojeda, B., Knipper, J. A., Sutherland, T. E., Logan, N., et al. (2017). Local Amplifiers of IL-4rα–Mediated Macrophage Activation Promote Repair in Lung and Liver. *Science* 356 (6342), 1076–1080. doi: 10.1126/science.aaj2067

Molina, E. C. (2005). Serum Interferon-Gamma and Interleukins-6 and -8 During Infection With *Fasciola Gigantica* in Cattle and Buffaloes. *J. Vet. Sci.* 6 (2), 135–139. doi: 10.4142/jvs.2005.6.2.135

Molloy, J. B., Anderson, G. R., Fletcher, T. I., Landmann, J., and Knight, B. C. (2005). Evaluation of a Commercially Available Enzyme-Linked Immunosorbent Assay for Detecting Antibodies to Fasciola Hepatica and *Fasciola Gigantica* in Cattle, Sheep and Buffaloes in Australia. *Vet. Parasitol.* 130 (3-4), 207–212. doi: 10.1016/j.vetpar.2005.02.010

Myers, R. P., Tainturier, M. H., Ratziu, V., Piton, A., Thibault, V., Imbert-Bismut, F., et al. (2003). Prediction of Liver Histological Lesions With Biochemical Markers in Patients With Chronic Hepatitis B. *J. Hepatol.* 39 (2), 222–230. doi: 10.1016/S0168-8278(03)00171-5

O'Neill, S. M., Brady, M. T., Callanan, J. J., Mulcahy, G., Joyce, P., Mills, K. H., et al. (2000). *Fasciola Hepatica* Infection Downregulates Th1 Responses in Mice. *Parasite Immunol.* 22 (3), 147–155. doi: 10.1046/j.1365-3024.2000.00290.x

Oldham, G., and Williams, L. (1985). Cell Mediated Immunity to Liver Fluke Antigens During Experimental *Fasciola Hepatica* Infection of Cattle. *Parasite Immunol.* 7 (5), 503–516. doi: 10.1111/j. 1365-3024.1985. tb00095.x

Phiri, I. K., Phiri, A. M., and Harrison, L. J. S. (2006). Serum Antibody Isotype Responses of Fasciola -Infected Sheep and Cattle to Excretory and Secretory Products of Fasciola Species. *Vet. Parasitol.* 141 (3-4), 234–242. doi: 10.1016/j.vetpar.2006.05.019

Pierr, B., Christine, P., Nicolas, V., Jean-Luc, B., Arnaud, B., Valerie, P., et al. (2012). Histopathological Algorithm and Scoring System for Evaluation of Liver Lesions in Morbidly Obese Patients. *Hepatology* 56 (5), 1751–1759. doi: 10.1002/hep.25889

Prasitirat, P., Thammasart, S., Chompoochan, T., Nithiuthai, S., and Noriyuki, T. (1996). Dynamics of Antibody Titres and Faecal Egg Output in Cattle and Buffalo Following Infection With 500 and 1000 *Fasciola Gigantica* Metacercariae. *Wetchasan Sattawaphaet* 26, 85–97.

Raadsma, H. W., Kingsford, N. M., Suharyanta,, Spithill, T. W., and Piedrafita, D. (2007). Host Responses During Experimental Infection With Fasciola Gigantica or *Fasciola Hepatica* in Merino Sheep: I. Comparative Immunological and Plasma Biochemical Changes During Early Infection. *Vet. Parasitol.* 143 (3-4), 275–286. doi: 10.1016/j.vetpar.2006.09.008

Reddington, J. J., Leid, R. W., and Wescott, R. B. (1986). The Susceptibility of the Goat to *Fasciola Hepatica* Infections. *Vet. Parasitol.* 19, 145–150. doi: 10.1016/0304-4017(86)90042-7

Reichel, M. P. (2002). Performance Characteristics of an Enzyme-Linked Immunosorbent Assay for the Detection of Liver Fluke (*Fasciola Hepatica*) Infection in Sheep and Cattle. *Vet. Parasitol.* 107 (1-2), 65–72. doi: 10.1016/S0304-4017(02)00095-X

Ridi, R. E., Salah, M., Wagih, A., William, H., Tallima, H., Shafie, M. H. E., et al. (2007). *Fasciola Gigantica* Excretory–Secretory Products for Immunodiagnosis and Prevention of Sheep Fasciolosis. *Vet. Parasitol.* 149 (3-4), 219–228. doi: 10.1016/j.vetpar.2007.08.024

Roy, R. M., and Reddy, N. R. (1969). Studies on the Activity of Nitroxynil Against *Fasciola Gigantica* in Naturally Infected Buffaloes, Cattle and Sheep. *Vet. Rec.* 85 (4), 85–87. doi: 10.1136/vr.85.4.85

Saba, R., and Korkmaz, M. (2005). Human Fascioliasis. *Clin. Microbiol. Newslett.* 27 (4), 27–34. doi: 10.1016/S0196-4399(05)80004-2

Santiago, N., and Hillyer, G. V. (1988). Antibody Profiles by EITB and ELISA of Cattle and Sheep Infected With Fasciola Hepatica. *J. Parasitol.* 74 (5), 810–818. doi: 10.2307/3282259

Sewell, M. M. (1966). The Pathogenesis O Fascioliasis. *Vet. Rec.* 78 (3), 98–105. doi: 10.1136/vr.78.3.98

Shang, H., Wei, H. B., Xu, P., and Huang, H. (2009). Microsatellite Analysis in Two Populations of Kunming Mice. *Lab. Anim.* 43 (1), 34–40. doi: 10.1258/la.2008.008098

Shi, W., Wei, Z. Y., Elsheikha, H. M., Zhang, F. K., Sheng, Z. A., Lu, K. J., et al. (2017). Dynamic Expression of Cytokine and Transcription Factor Genes During Experimental *Fasciola Gigantica* Infection in Buffaloes. *Parasites Vectors* 10 (1), 602–613. doi: 10.1186/s13071-017-2538-1

Solanki, S., Shrivastav, C., and Gaherwal, S. (2017). Studies on Biochemical Alteration in *Fasciola Hepatica* Infected *Capra Hircus* (Goats). *J. Zoological And Biosci. Res.* 3 (3), 1–10.

Thapa, B. R., and Walia, A. (2007). Liver Function Tests and Their Interpretation. *Indian J. Pediatr.* 74 (7), 663–671. doi: 10.1007/s12098-007-0118-7

Ulger, B. V., Kapan, M., Boyuk, A., Uslukaya, O., Oguz, A., Bozdag, Z., et al. (2014). *Fasciola Hepatica* Infection at a University Clinic in Turkey. *J. Infect. Develop. Countries* 8 (11), 1451–1455. doi: 10.3855/jidc.5124

Valero, M. A., Marcos, M. D., Fons, R., and Mas-Coma, S. (1998). *Fasciola Hepatica* Development in the Experimentally Infected Black Rat Rattus Rattus. *Parasitol Res.* 84 (3), 188–194. doi: 10.1007/s004360050381

Veli, U. B., Murat, K., Abdullah, B., Omer, U., Abdullah, O., and Zubeyir, B. (2014) Fasciola Hepatica Infection at a University Clinic in Turkey. *J. Infect. Dev. Ctries.* 8, 1451–1455. doi: 10.3855/jidc.5124

Yuan, Z. G., Zhang, X. X., Lin, R. Q., Petersen, E., He, S. Y., Yu, M., et al. (2011). Protective Effect Against Toxoplasmosis in Mice Induced by DNA Immunization With Gene Encoding *Toxoplasma Gondii* ROP18. *Vaccine* 29 (38), 6614–6619. doi: 10.1016/j.vaccine.2011.06.110

Zhang, H., Cheng, C., Zheng, M., Chen, J. L., Meng, M. J., Zhao, Z. Z., et al. (2007). Enhancement of Immunity to an *Escherichia Coli* Vaccine in Mice Orally Inoculated With a Fusion Gene Encoding Porcine Interleukin 4 and 6. *Vaccine* 25 (41), 7094–7101. doi: 10.1016/j.vaccine.2007.07.050

Zhang, F. K., Guo, A. J., Hou, J. L., Sun, M. M., Sheng, Z. A., Zhang, X. X., et al. (2017). Serum Levels of Cytokines in Water Buffaloes Experimentally Infected With Fasciola Gigantica. *Vet. Parasitol.* 244, 97–101. doi: 10.1016/j.vetpar.2017.07.028

Zhang, W. Y., Moreau, E., Hope, J. C., Howard, C. J., Huang, W. Y., and Chauvin, A. (2005). *Fasciola Hepatica* and *Fasciola Gigantica*: Comparison of Cellular Response to Experimental Infection in Sheep. *Exp. Parasitol.* 111 (3), 154–159. doi: 10.1016/j.exppara.2005.06.005

Zhang, W., Moreau, E., Huang, W., and Chauvin, A. (2004). Comparison of Humoral Response in Sheep to *Fasciola Hepatica* and *Fasciola Gigantica* Experimental Infection. *Parasite Journal la Societe Francaise Parasitol.* 11 (2), 153–159. doi: 10.1051/parasite/2004112153

Zhang, W. Y., Moreau, E., Yang, B. Z., Li, Z. Q., Hope, J. C., Howard, C. J., et al. (2006). Humoral and Cellular Immune Responses to *Fasciola Gigantica* Experimental Infection in Buffaloes. *Res. Vet. Sci.* 80 (3), 299–307. doi: 10.1016/j.rvsc.2005.07.003

Conflict of Interest: The authors declare that the research was conducted in the absence of any commercial or financial relationships that could be construed as a potential conflict of interest.

Publisher's Note: All claims expressed in this article are solely those of the authors and do not necessarily represent those of their affiliated organizations, or those of the publisher, the editors and the reviewers. Any product that may be evaluated in this article, or claim that may be made by its manufacturer, is not guaranteed or endorsed by the publisher.

frontiers in Cellular and Infection Microbiology

ORIGINAL RESEARCH
published: 02 March 2022
doi: 10.3389/fcimb.2022.806085

Prevalence of *Eimeria* Spp. Among Goats in China: A Systematic Review and Meta-Analysis

Nai-Chao Diao[1†], Bo Zhao[2†], Yu Chen[3†], Qi Wang[2], Zi-Yang Chen[2], Yang Yang[1], Yu-Han Sun[1], Jun-Feng Shi[2], Jian-Ming Li[1], Kun Shi[1], Qing-Long Gong[2*] and Rui Du[1*]*

[1] College of Chinese Medicine Materials, Jilin Agricultural University, Changchun City, China, [2] College of Animal Science and Technology, Jilin Agricultural University, Changchun City, China, [3] College of Animal Science and Veterinary Medicine, Heilongjiang Bayi Agricultural University, Daqing City, China

Eimeria spp. infection can cause weight loss in goats, and severe cases can lead to the death of lambs, resulting in economic losses to the goat industry. To explore the pooled prevalence of *Eimeria* spp. in goats in China, we obtained 70 related publications from five databases and conducted a meta-analysis. In China, the combined prevalence of *Eimeria* spp. in goats was 78.7% (95% confidence interval (CI): 68.15–87.67). Among them, the most serious infections occurred in Northeast China (88.0%, 95% CI: 83.54–91.86). The main *Eimeria* species were *E. alijevi* (43.7%, 95% CI: 29.53–58.45), *E. arloingi* (49.7%, 95% CI: 34.83–64.49), *E. christenseni* (41.2%, 95% CI: 27.07–56.16), and *E. ninakohlyakimovae* (35.9%, 95% CI: 21.02–52.31). In the sampling year subgroup, 2006 or later presented a lower prevalence (75.3%, 95%CI: 58.72–88.72). In terms of age, the point estimate for young goats (≤ 1 year) was higher (89.9%, 95% CI: 80.82–96.48). The Float (NaCl) method showed the lowest prevalence of *Eimeria* spp. in goats (75.9%, 95%CI: 62.00–87.46). In the season subgroup, the highest prevalence was in summer (81.5%, 95%CI: 49.62–99.18). Female goats presented a higher prevalence of *Eimeria* spp. infection than male goats (70.7%, 95%CI: 27.90–98.96). The prevalence was lower in the intensive feeding model (77.4%, 95%CI: 66.56–86.67) and higher in free feeding goats (79.4%, 95%CI: 66.46–89.92). In addition, we also analyzed the potential relationship between geographical factors and the prevalence of *Eimeria* spp. infection in goats in China. Our findings suggested that *Eimeria* spp. infection in goats is widespread in China. Despite the overall downward trend, this infection cannot be ignored. We recommend that breeders use anticoccidial drugs to prevent and treat this disease, while improving the feeding conditions and managemental practices to reduce the economic losses caused by *Eimeria* infection to the goat industry.

Keywords: goat, *Eimeria*, prevalence, China, meta-analysis

OPEN ACCESS

Edited by:
Wei Cong,
Shandong University, China

Reviewed by:
Idrees Mehraj Allaie,
Sher-e-Kashmir University of Agricultural Sciences and Technology of Kashmir, India
Kangkang Zhang,
Northeast Normal University, China
Aoqiang Li,
Northeast Normal University, China

***Correspondence:**
Kun Shi
sk1981521@126.com
Qing-Long Gong
gongqinglong1001@163.com
Rui Du
durui197101@sina.com

†These authors have contributed equally to this work

Specialty section:
This article was submitted to Clinical Microbiology, a section of the journal Frontiers in Cellular and Infection Microbiology

Received: *31 October 2021*
Accepted: *14 February 2022*
Published: *02 March 2022*

Citation:
Diao N-C, Zhao B, Chen Y, Wang Q, Chen Z-Y, Yang Y, Sun Y-H, Shi J-F, Li J-M, Shi K, Gong Q-L and Du R (2022) Prevalence of Eimeria Spp. Among Goats in China: A Systematic Review and Meta-Analysis. Front. Cell. Infect. Microbiol. 12:806085. doi: 10.3389/fcimb.2022.806085

INTRODUCTION

In ruminants, coccidiosis is a parasitic disease caused by the *Eimeria* spp., which has a significant economic impact (Taylor et al., 2016; Keeton and Navarre, 2018; Bangoura and Bardsley, 2020). *Eimeria* spp. is distributed globally, and the infection rates can reach more than 90% in some areas (Cavalcante et al., 2012; Mohamaden et al., 2018; Juszczak et al., 2019). The main clinical feature of coccidiosis is diarrhea. Under conditions that promote *Eimeria* development, the accompanying clinical symptoms include low feed conversion rate, weight loss, and lethargy (Foreyt, 1990).

Eimeria has a high degree of host specificity, with different species of *Eimeria* in goats and sheep, among which 13 species of *Eimeria* are currently recognized to infect goats (Lotze et al., 1961; Bangoura and Bardsley, 2020). Among the 13 species of *Eimeria*, *E. ninakohlyakimovae* and *E. arloingi* are considered to be more pathogenic.

China is one of the most important agricultural countries in the world, and since the late, 1980s, China has become the country with the largest number of goats (Liu et al., 2018; Wang et al., 2020). Goat meat and mutton production reached 4.68 million tons in, 2017 (Liu et al., 2018). *Eimeria* spp. infection affects the health of goats, thereby affecting their production profits. Consequently, we conducted a systematic review and meta-analysis of the prevalence of *Eimeria* spp. in goats in China, taking into account sampling year, age, species, detection methods, feeding model, season, presence of diarrhea, regions, and quality level, to determine the factors which affect *Eimeria* prevalence in goats. Furthermore, geographical factors (longitude, latitude, and altitude) and climatic factors (annual temperature, maximum and minimum temperature, rainfall, and humidity) were analyzed in our meta-analysis, which might be potential factors influencing *Eimeria* infection in goats. Exploration of the prevalence and geographical distribution of *Eimeria* in goats in China along with the identification of the predisposing factors might highlight weak points and accelerate the future eradication of *Eimeria*.

MATERIAL AND METHODS

Search Strategy

Our research was performed according to the Preferred Reporting Items for Systematic Review and Meta-Analysis (PRISMA) protocols (**Table S1**) (Moher et al., 2015). To obtain the maximum number of publications, we searched in five databases (China national knowledge internet (CNKI), VIP databases, Wan Fang databases, PubMed, and ScienceDirect). In PubMed, we used the MeSH index to determine the following subject terms: "Goats", "*Eimeria*", "China". In MeSH Terms, the free words obtained by goats were: "Goat", "Capra" and "Capras". The free words obtained by *Eimeria* were: "*Eimerias*", "Coccidia" and "Coccidias". China's free words were: "People's Republic of China", "Mainland China", "Manchuria", "Sinkiang", and "Inner Mongolia". We used the "OR" combination between subject words and free words. Finally, the search formula we established was as follows: ("Eimeria"[Mesh] OR Eimerias OR Coccidia OR Coccidias) AND ("Goats"[Mesh] OR Goat OR Capra OR Capras) AND ("China"[Mesh] OR People's Republic of China OR Mainland China OR Manchuria OR Sinkiang OR Inner Mongolia). In ScienceDirect, we searched using the keywords "Goats", "*Eimeria*" and "China", and the title, abstract, and keywords must include "China". In the three Chinese database (CNKI, VIP and WanFang), the search query we chose was "Goat" and "*Eimeria*" in Chinese, and synonym expansion and fuzzy search were enabled. We conducted a final search on October 9, 2021.

Inclusion and Exclusion Criteria

The literature information was processed using EndNote X9.3.2 for summarization (Wang et al., 2021). After excluding duplicate articles, three systematically trained researchers reviewed the titles and abstracts of all the articles and conducted the preliminary screening. To ensure the quality of the included articles, we have established the following inclusion criteria, based on the premise that full text and original research could be obtained:

(1) The study purpose was to examine the prevalence of *Eimeria* among goats in China;
(2) The study was published in English or Chinese;
(3) One sample was taken from each goat (not mixed samples);

The exclusion criteria comprised:

(1) Articles with incorrect data;
(2) Articles reporting the same data;
(3) Review articles;
(4) Articles dealing with other parasitic disease prevalence surveys;
(5) Articles reporting data for other hosts.

Data Extraction

All the articles were distributed to three trained reviewers (BZ, ZYC, and YY) for review. The extracted data included: First author, publication year, sampling year, geographical factors of sampling location (latitude and longitude, rainfall, annual average temperature, annual minimum temperature, annual maximum temperature), detection method, sex, age, breeding method, and season. In the process of selecting the articles, we neither contacted the authors of the articles to obtain more research information, nor included unpublished data (**Table S2**). Any doubts and uncertainties about the data of the included articles were processed uniformly after evaluation by the major reviewer (QLG, the methodology provider for this meta-analysis).

Quality Assessment

The quality of the included articles was evaluated by means of scoring (Guyatt et al., 2008; Gong et al., 2021). The specific method was as follows: Each of the below mentioned five points was counted as one point: (1) Whether there is a sampling time, (2) whether the sampling method is described in detail,

(3) whether random sampling was used, (4) whether there was a detection method, and (5) whether it included 3 subgroups or more. According to the score of each article, it was assigned to the corresponding level. There were three levels: 0–1 point, 2–3 points and 4–5 points (**Table S3**). The data gleaned from the included studies were summarized and edited using Microsoft Excel (version 16.32; Microsoft Corp., Redmond, WA, USA).

Statistical Analysis

We used the "meta" package in the R software to perform this meta-analysis ("R core team, version 4.0.0; "R: A language and environment for statistical computing", R core team, 2018) (Wang, 2018). According to the description of the conversion rate in a previous study, we used the Freeman-Tukey double arcsine transformation (named "PFT" in the meta package) to perform conversion to conform to the normal distribution (**Table 1** and **Table S4**) (Li et al., 2020). The combined estimates included in the study were described using forest plots. The heterogeneity in the prevalence meta-analysis is usually very large, therefore, we made a judgment in advance and used a random-effect model to analyze the overall prevalence (including subgroups). For the differences caused by the heterogeneity of the included studies, Cochran's Q statistics and Higgin's statistics were used for evaluation. In the funnel diagram, the symmetry of the figure was judged subjectively. If the dots in the funnel plot were symmetrically distributed on both sides of the symmetry line, there was no publication bias, if they were asymmetric, there was a publication bias in the included studies. At the same time, we used sensitivity analysis and trimming and filling analysis to evaluate the reliability of the articles and used Egger's test and funnel plots to estimate the heterogeneity in the included studies (Li et al., 2020; Gong et al., 2021).

To track the potential sources of heterogeneity in our study, we performed subgroup analysis and univariate meta-regression (Wang et al., 2017). The potential factors included geographical area (Central China, Eastern China, Northern China, Northeastern China, Northwestern China, Southern China, and Southwestern China); sampling year (before, 2006 and, 2006 or later); detection method (Float (NaCl), Float ($C_{12}H_{22}O_{11}$), and others); feeding model (free range vs. intensive); age (≤1 year and > 1 year); sex (male and female); season (spring, summer, autumn, and winter), score level (2–3 points vs. others). We further extracted geographical factors based on the sampling location using data obtained from the National Meteorological Information Center of China Meteorological Administration for subgroup analysis and univariate meta-regression to track the source of heterogeneity. We inquired about the latitude, longitude, precipitation, annual average temperature, annual average humidity and altitude of each sample source, and divided each factor into different intervals, including latitude (20–30°, 30–35°, 35–40°, and 40–50°), longitude (80–105°, 105–110°, 110–120°, 120–125°), precipitation (0–400 mm, 400–800 mm, and 800–2000 mm), annual average temperature (-5–10°C, 10–15°C, and 15–20° C), annual average humidity (30–60%, 60–70%, 70–80%, and 80–100%), and altitude (4–100 m, 100–1500 m, and, 1500–5000 m). Our meta-analysis was not registered in the Cochrane database. The code in R software for this study is provided in **Table S5**.

RESULTS

Study Characteristics

According to our inclusion criteria, 985 articles were collected from five databases, and 70 studies were finally included to build this meta-analysis (**Figure 1**). A total of 40 studies scored 4–5 points, 25 studies scored 2–3 points, and only 5 studies scored 0–1 point (**Tables S2**, **S3**).

Pooled Estimates and Heterogeneity Analyses

The forest plots showed there was a high heterogeneity in the included studies (I^2 = 99.7%, P < 0.01; **Figure 2**). In the funnel plot, we observed asymmetry, which indicated that there was a publication bias in our meta-analysis (**Figure 3**). The Egger's test showed the same result as the funnel chart (P < 0.05; **Figure S1**, **Table S6**). The trim and fill analysis showed that the number of added studies was 33, indicating that there was publication bias or small sample bias in our included studies (**Figure S2**). Sensitivity analysis verified the reliability of the results, and excluding any one study had little effect on the overall quality of the meta-analysis (**Figure 4**). We also provided the funnel plot for each subgroup to determine whether there was a publication bias or small-sample bias (**Figures S3**–**S10**).

Meta-Analysis

In the 70 selected studies, the pooled prevalence of *Eimeria* spp. infection of goats in China was 78.7% (95% CI: 68.15–87.67; 15,635/27,388) (**Table 2**). In terms of regions, the highest prevalence was in the Northeast (88.0%, 95% CI: 83.54–91.86; 216/246), and the lowest prevalence was in Central China (70.9%, 95% CI: 50.57–

TABLE 1 | Normal distribution test for the normal rate and the different conversion of the normal rate.

Conversion form	*W*	*P*
PRAW	0.81473	6.021e-08
PLN	0.5427	1.968e-13
PLOGIT	NaN	NA
PAS	0.89765	3.134e-05
PFT	0.88739	1.275e-05

"PRAW", original rate; "PLN", logarithmic conversion; "PLOGIT", logit transformation; "PAS", arcsine transformation; "PFT", double-arcsine transformation, NA, No answer; NaN, Not a number.

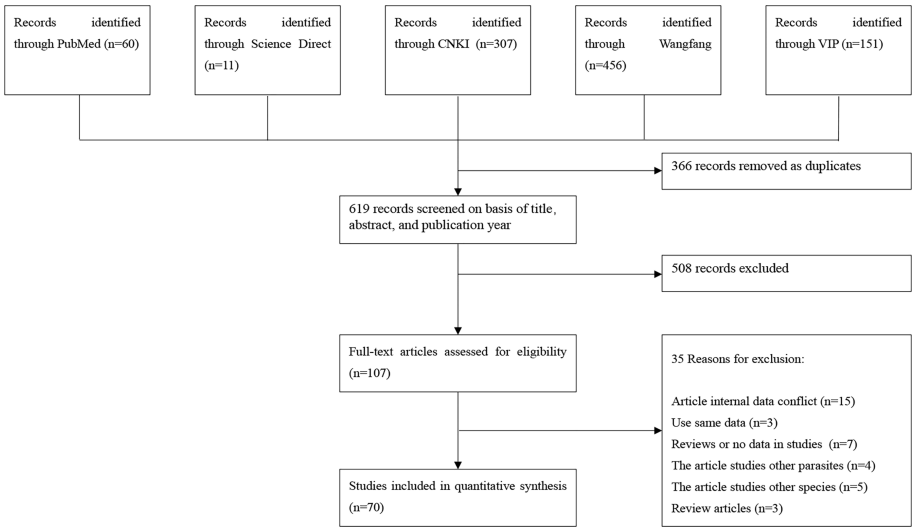

FIGURE 1 | Flow diagram of eligible studies for searching and selecting.

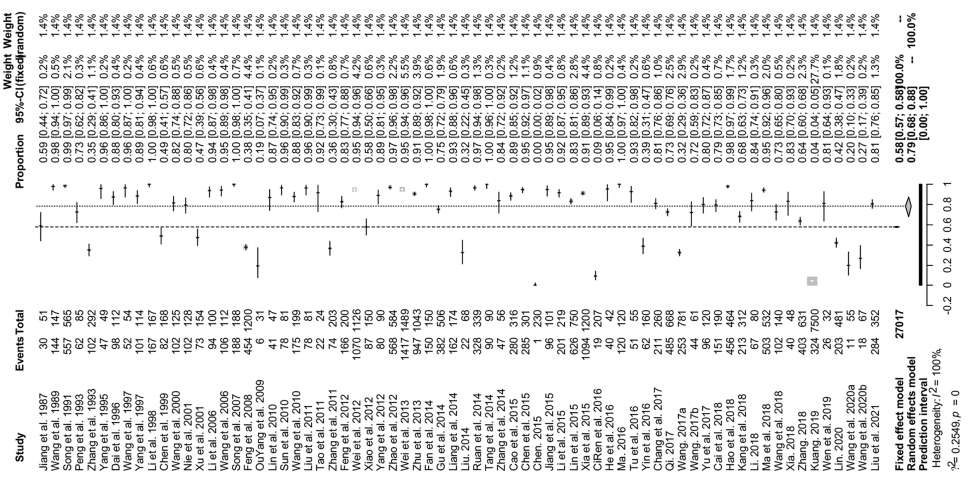

FIGURE 2 | Forest plot of prevalence of *Eimeria* spp. in goats amongst studies conducted in China. The length of the horizontal line represents the 95% CI; the diamond represents the summarized effect.

87.63; 2,559/3,255). At the provincial level, except for Zhejiang (26.9%, 95% CI: 16.85–38.19; 18/67), in the other provinces, the prevalence was above 50% (**Figure 5** and **Table 3**). In the sampling year subgroup, we found that the prevalence of *Eimeria* spp. in goats in China showed a downward trend. In terms of age, the estimated prevalence of goats ≤ 1 year old (89.9%, 95%CI: 80.82–96.48; 3,153/3,677) was higher than that at > 1 year (82.2%; 95% CI: 73.97–89.15; 3,689/4,357). In the sex subgroup, male goats (70.7%, 95%CI: 27.9–98.96, 120/211) had a lower *Eimeria* spp. prevalence than female (89.9%, 95%CI: 70.86–99.78, 800/897). The estimated pooled prevalence of *Eimeria* spp. detected using the Float (NaCl) method was 75.9% (95% CI: 62.00–87.46; 8,220/18,613), which was lower than that using the Float ($C_{12}H_{22}O_{11}$) method (85.7%; 95% CI: 75.25–93.67; 5,867/7,016). Among seasons *Eimeria* spp. were more prevalent in summer (81.5%, 95%CI: 46.52–99.73; 1,625/3,648). In the feeding model subgroup, the estimated prevalence among free range goats (79.4%, 95%CI: 66.46–89.92; 2,295/2,940) was higher than in intensively farmed goats (77.4%, 95%CI: 66.56–86.67, 6,326/8,521) (**Table 2**). The articles which got 2–3 score level (69.0%, 95%CI: 57.46–79.55; 3,682/5,980) have reached the lowest prevalence among the three score levels.

Twelve species of *Eimeria* were found in goats of China. Among them, *E. arloingi* had the highest prevalence (49.7%, 95% CI: 34.83–64.49; 2,417/5,595) (**Table 4**). On the basis of our

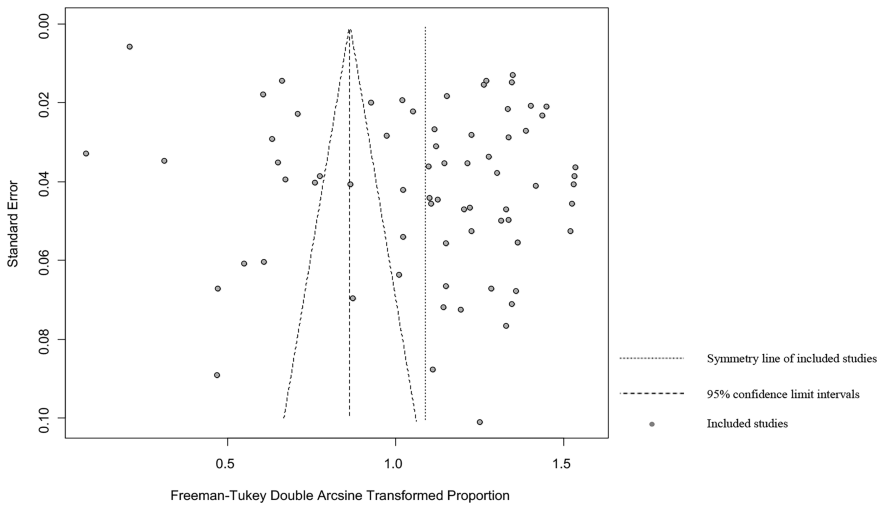

FIGURE 3 | Funnel plot with pseudo 95% confidence interval limits for the examination of publication bias.

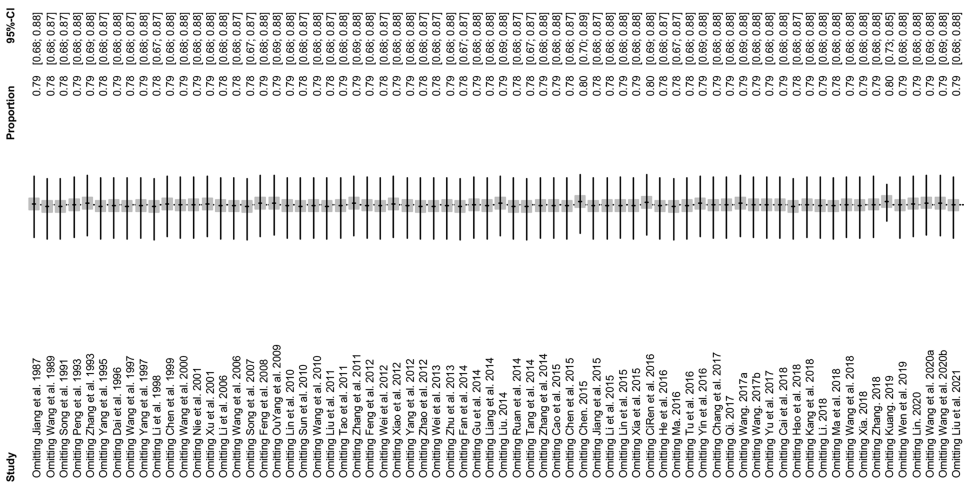

FIGURE 4 | Sensitivity analysis. After removing one study at a time, the remaining studies were re-combined using a random-effects model to verify the impact of a single study on the overall results.

calculated prevalence of *Eimeria* spp. in goats in China, we used data from, 2018 data of the *Chinese Animal Husbandry and Veterinary Yearbook* report to calculate that there were 108,792,519 (94,277,634–121,233,849) cases of *Eimeria* infection in goats in China (**Table S7**).

We also conducted a subgroup analysis of geographical factors. The prevalence was highest when the longitude is 80–105° (84.6%, 95%CI: 74.84–92.34; 2,270/2,519), and the same was true for latitudes 30–35° (80.5%, 95%CI: 68.94–90.00, 4,554/6,437), precipitation > 800–2000 mm (79.8%, 95%CI: 64.86–91.47; 3,827/3,094), the annual average temperature -5–10°(84.8%, 95%CI: 78.36–90.29; 2,088/2,385), humidity 80–100% (95.7%, 95%CI: 93.14–97.72; 629/663), and altitude above, 1500–5000 m (81.2%, 95%CI: 72.23–88.79; 2,600/2,325) (**Table 5**).

DISCUSSION

Coccidiosis caused by *Eimeria* spp. is one of the most common intestinal diseases in goats (Ruiz et al., 2006). Whether there is a clinical infection, or the goat is in a subclinical state, it will cause economic losses (Zhao et al., 2012; Keeton and Navarre, 2018). Therefore, we conducted a meta-analysis of *Eimeria* spp. infection of goats in China. In, 2006, the China's Ministry of Agriculture issued

TABLE 2 | Pooled prevalence of *Eimeria* spp. infection in goats in China.

		No. studies	No. examined	No. positive	% (95% CI*)	Heterogeneity	*P*-value	Univariate meta-regression		
						χ^2		I^2 (%)	*P*-value	Coefficient (95% CI)
Region*									0.584	-0.099 (-0.455 to 0.256)
	Central China	9	3255	2559	70.9% (50.57-87.63)	1066.20	< 0.01	99.2%		Reference
	Eastern China	24	4935	3384	79.8% (69.78-88.21)	1331.54	< 0.01	98.3%		
	Northern China	5	1081	777	78.4% (57.25-93.78)	175.84	< 0.01	97.7%		
	Northeastern China	2	246	216	88.0% (83.54-91.86)	0.06	0.81	0.00%		
	Northwestern China	12	2985	1996	80.7% (59.36-95.42)	1562.79	0.00	99.3%		
	Southern China	1	61	44	72.1% (60.13-82.75)	0.00	–	–		
	Southwestern China	21	12714	4727	78.4% (50.75-96.62)	14870.98	0.00	99.9%		
Sampling year									0.508	0.105 (-0.206 to 0.416)
	Before, 2006	16	2794	2238	83.9% (70.48-93.84)	910.51	< 0.01	98.4%		Reference
	2006 or later	38	20728	10823	75.3% (58.72-88.72)	21371.00	0.00	99.8%		
Detection methods*									0.343	-0.129 (-0.396 to 0.138)
	Float (NaCl)	50	19189	8774	75.9% (62.00-87.46)	18390.77	0.00	99.7%	Reference	
	Float ($C_{12}H_{22}O_{11}$)	14	7016	5867	85.7% (75.25-93.67)	1537.52	< 0.01	98.2%		
	Others	2	218	197	87.7% (27.78-100.00)	68.59	< 0.01	98.5%		
Feeding model									0.829	0.022 (-0.180 to 0.225)
	Free range	16	2940	2295	79.4% (66.46-89.92)	884.77	< 0.01	98.3%	Reference	
	Intensive	33	8521	6326	77.4% (66.56-86.67)	3966.04	0.00	99.2%		
Age									0.165	-0.111 (-0.268 to 0.046)
	> 1 year	23	4357	3689	82.2% (73.97-89.15)	800.04	< 0.01	97.3%		
	≤ 1 year	23	3677	3153	89.9% (80.82-96.48)	1240.90	< 0.01	98.2		Reference
Sex									0.258	-0.246 (-0.672 to 0.180)
	Female	6	897	800	89.9% (70.86-99.78)	168.80	< 0.01	97.0%		
	Male	4	211	120	70.7% (27.90- 98.96)	115.08	< 0.01	97.4%	Reference	
Season*									0.324	0.181 (-0.178 to 0.541)
	Spring	12	3116	791	60.5% (32.14-85.58)	1946.74	0.00	99.4%		
	Summer	10	3648	1625	81.5% (46.52-99.73)	3687.38	0.00	99.8%		Reference
	Autumn	10	4297	1580	70.5% (41.19-92.73)	2929.92	0.00	99.7%		
	Winter	5	2210	284	67.8% (8.79- 100.00)	1322.86	< 0.01	99.7%		
Score level									0.188	-0.170 (-0.424 to 0.083)
	4–5	40	20130	10805	82.9% (67.49-94.10)	22252.61	0.00	99.8%		
	2–3	25	5980	3682	69.0% (57.46-79.55)	1991.91	0.00	98.8%	Reference	
	0–1	5	907	829	88.8% (80.67-94.99)	30.53	< 0.01	86.9%		
Total		70	27017	15316	78.7% (68.15-87.67)	25056.86	0.00	99.7%		

CI, Confidence interval;*
NA, not applicable;*
Region: Northern China: Beijing; Northwestern China: Shanxi, Gansu, Inner Mongolia, Shaanxi, Qinghai; Southwestern China: Chongqing, Guizhou, Sichuan, Tibet, Yunnan; Northeastern China: Heilongjiang; Central China: Henan; Eastern China: Fujian, Jiangsu, Anhui, Zhejiang, Shandong; Southern China: Hubei, Guangxi.*
Detection methods: Float (NaCl): Saturated Salt Water Floatation Method; Float ($C_{12}H_{22}O_{11}$): Saturated Sucrose Solution Floatation Method; Others: Stauer's Method, Saturated Magnesium Sulfate Solution as Test Tube Floatation Method.*
Season: Spring: Mar to May; Summer: Jun to Aug; Autumn: Sep to Nov; Winter: Dec to Feb.*

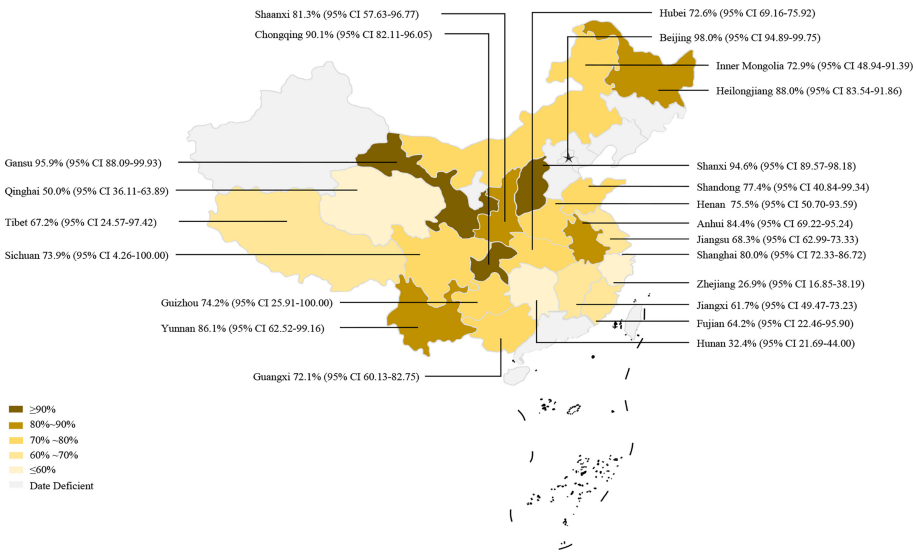

FIGURE 5 | Map of *Eimeria* spp. in goats amongst studies conducted in China.

the "Parasitic Disease Control Plan (2006–2016)", which was subsequently extended to, 2021, in order to further strengthen the prevention and control of parasites. Therefore, we used, 2006 as the boundary to analyze the changes in point estimates of Chinese goat coccidiosis. We found that the point estimate of goat coccidiosis in, 2006 or latter decreased. Before, 2006, the main goal of Chinese animal husbandry was to increase production rapidly and optimize the industrial structure (Wang, 2015), thus ignoring the environmental pollution caused by the wastewater and feces from goat breeding farms. The implementation of disease control policies has brought positive results due to changes in managemental aspects leading to a decline in the prevalence of goat coccidiosis. Notably, the differences between year subgroups were not significant. This might have been because we only had 2,794 samples prior to, 2006. Therefore, further studies are needed to demonstrate whether there is a downward trend in goat coccidiosis or not.

In China, goat coccidiosis is widespread, and infections were found in all areas. According to the analysis of the geographical subgroups, we found the highest point estimates was in Northwestern China, and the sampling locations were in the range 80–110° longitude (n = 10) and range 30–40° latitude (n = 8). Goats are economically significant animals in arid and semi-arid regions like Northwestern China because of their high adaptability (Abo-Shehada and Abo-Farieha, 2003; Chen, 2011). Our research showed that the prevalence of *Eimeria* spp. varies with precipitation levels. *Eimeria* spp. infection was more prevalent in places with moderate temperature and humidity (Mai et al., 2009; Keeton and Navarre, 2018). This point is consistent with the result in the season subgroup: *Eimeria* spp. prevalence in summer and autumn, with more rainfall, was higher than that in spring and winter, with less rainfall. Interestingly, in the temperature subgroup, the prevalence of *Eimeria* spp. infection in goats in China correlated negatively with temperature within a certain temperature range, although the difference was not significant. Infection by *Eimeria* spp. is considered to have no obvious seasonality (Hao, 2017). According to our results, we doubt whether there are more complex and hard-to-find connections between the *Eimeria* infection and seasons or not. At the same time, we found that many studies did not provide details of the sampling month, which also had a certain impact on our analysis of the seasons. When investigating goat coccidiosis, researchers should clarify the sampling month, because such details will help to analyze the effect of season and other climatic factors on goat coccidiosis. Notably, the results of both the altitude and humidity subgroups were generally high as most of the studies were before, 2006. This is consistent with the results of our research in the sampling year subgroup. However, in some areas, we only obtained a small number of studies, which might not reflect the true prevalence (Northeastern China = 2, Southern China = 1). This might also be one of the reasons for the insignificant differences.

For farmers who raise goats, high prevalence and highly pathogenic coccidia species will cause huge economic losses. According to our results, the prevalence of *E. alijevi*, *E. arloingi* and *E. christenseni*, were above 40%, and the prevalence of *E. caprina*, *E. hirci* and *E. ninakohlyakimovae* were all over 30%. Previous researches pointed out that when *E. ninakohlyakimovae* and *E. arloingi* are the main infective species, the fatality rate can reach 30% (Koudela and Boková, 1998). Moreover, we tried to conduct a subgroup analysis on the medication; however, no studies mentioned this information; therefore, we could not quantify it as a covariate for meta-analysis, although we believe that the correct use of anti-coccidial drugs might inhibit coccidiosis (Peek and Landman, 2003; Dang et al., 2019; Liu, 2019).

In the feeding model subgroup, the prevalence of infection in both feeding subgroups was close to 80%. A few weeks after

TABLE 3 | Pooled prevalence of *Eimeria* spp. by provincial in China.

Province	No. studies	Region	No. tested	No. positive	% Prevalence	% (95% CI)
Anhui	11	East China	1977	1261	83.0%	64.96-95.53
Beijing	1	North China	147	144	98.0%	94.89-99.75
Chongqing	4	Southwest China	660	600	90.1%	82.11-96.05
Fujian	2	East China	1231	829	64.2%	22.46-95.90
Gansu	1	Northwest China	49	47	95.9%	88.09-99.93
Guangxi	1	South China	61	44	72.1%	60.13-82.75
Guizhou	5	Southwest China	1341	1009	74.2%	25.91-100.00
Heilongjiang	2	Northeast China	246	216	88.0%	83.54-91.86
Henan	7	Central China	2519	2052	75.5%	50.70-93.59
Hubei	1	Central China	668	485	72.6%	69.16-75.92
Hunan	1	Central China	68	22	32.4%	21.69-44.00
Inner Mongolia	3	North China	822	527	72.9%	48.94-91.39
Jiangsu	7	East China	720	534	68.3%	62.99-73.33
Jiangxi	1	East China	312	213	61.7%	49.47-73.23
Qinghai	1	Northwest China	50	25	50.0%	36.11-63.89
Shaanxi	10	Northwest China	2886	1924	81.3%	57.63-96.77
Shandong	3	East China	137	114	77.4%	40.84-99.34
Shanghai	1	East China	120	96	80.0%	72.33-86.72
Shanxi	1	North China	112	106	94.6%	89.57-98.18
Sichuan	4	Southwest China	8121	923	73.9%	4.26-100.00
Tibet	4	Southwest China	1715	1364	67.2%	24.57-97.42
Yunnan	4	Southwest China	877	831	86.1%	62.52-99.16
Zhejiang	1	East China	67	18	26.9%	16.85-38.19
Total	76		24906	13384	77.2%	66.62-86.27

TABLE 4 | Estimates of *Eimeria* spp. prevalence in goats in China.

	No.studies	No. tested	No. positive	Prevalence of infection
E. alijevi	16	5365	1791	43.7% (29.53-58.45)
E. apsheronica	12	4463	276	9.71% (5.21-15.35)
E. arloingi	17	5595	2417	49.7% (34.83-64.49)
E. caprina	16	5365	1505	36.6% (21.18-53.44)
E. caprovina	8	3883	400	12.1% (4.92-21.6)
E. christenseni	18	5984	2003	41.2% (27.07-56.16)
E. hirci	13	4896	1515	37.8% (22.95-53.88)
E. jolchijevi	14	4976	847	16.3% (8.09-26.49)
E. kocharli	2	1749	99	6.9% (3.01-12.16)
E. ninakohlyakimovae	12	3937	731	35.9% (21.02-52.31)
E. pallida	3	1803	160	13.6% (0.00-57.71)
E. punctata	5	2397	48	3.0% (0.40-7.34)

newborn goats are infected, they can excrete millions of oocysts from their feces (Abo-Shehada and Abo-Farieha, 2003). When the oocysts are discharged into the farm with feces, the infection pressure caused by closed enclosure feeding is higher than that of grazing (Long and Joyner, 1984). We recommend that breeding farms should keep the breeding environment clean. Moreover, some disinfectants have important anticoccidial activity against oocysts and sporozoites of *Eimeria*, which is one of the key steps to control coccidiosis (López et al., 2019). Therefore, cleaning the feeding house with disinfectants might play an important role in the control of goat coccidiosis. However, the difference between subgroups was not significant, and further research is needed on the relationship between feeding methods and goat coccidiosis.

In the age subgroup, goats less than 1 year old had a higher prevalence, which might have been caused by resistance to *Eimeria* infection in adult animals that have been exposed to *Eimeria* previously (Carrau et al., 2018). *Eimeria* spp. has important economic significance for juvenile animals (Bawm et al., 2020). In juvenile animals, the occurrence of diarrhea can inhibit weight gain during the growth period (Daugschies and Najdrowski, 2005). Therefore, regarding coccidiosis, we suggest that more attention should be paid to younger animals. Furthermore, when adult animals are in a subclinical state, they can act as carriers of *Eimeria*, thus causing more goats to be infected (Carrau et al., 2016). Breeders should optimize the population structure and try to breed in groups, which might reduce the infection rate of *Eimeria* spp. In our study, female goats had a higher *Eimeria* infection prevalence than male goats. It might be explained that goat kids ingest oocysts attached to the udders of their dams finally lead to clinical signs (Kanyari, 1993). The kids then start excreting oocysts in feces from the second to the fourth weeks onwards and if these goat kids are kept with their mothers, the infection pressure can

TABLE 5 | Subgroup analysis of the prevalence of *Eimeria* spp. according to geographic location and climatic variables.

		No. studies	No. examined	No. positive	% (95% CI*)	Heterogeneity	*P*-value	Univariate meta-regression		
						χ^2		I^2 (%)	*P*-value	Coefficient (95% CI)
Latitude									0.523	-0.057 (-0.121 to 0.234)
	20–30°	20	4,954	3,891	76.1% (61.25–88.32)	2329.12	0.00	99.2		
	30–35°	28	6347	4554	80.5% (68.94–90.00)	2901.06	0.00	99.1	Reference	
	35–40°	11	2,774	1,645	76.5% (59.07–90.28)	795.66	<0.01	98.7		
	40–50°	2	250	197	68.2% (21.29–99.19)	40.18	<0.01	97.5		
Longitude									0.533	0.071 (-0.152 to 0.294)
	80–105°	10	2,519	2,270	84.6% (74.84–92.34)	258.58	<0.01	96.5	Reference	
	105–110°	22	5,404	3,766	79.7% (64.91–91.31)	3009.06	0.00	99.3		
	110–120°	26	5196	3597	77.4% (66.03–87.06)	2011.65	0.00	98.8		
	120–125°	5	578	454	75.2% (55.63–90.63)	98.02	<0.01	95.9		
Precipitation (mm)									0.474	-0.088 (-0.330 to 0.154)
	0–400	10	3,131	2,131	71.4% (49.37–89.09)	1257.90	<0.01	99.3	Reference	
	400–800	14	2742	2205	77.8% (65.09–88.40)	669.85	<0.01	98.1		
	800-2000	21	3827	3094	79.8% (64.86–91.47)	2143.59	0.00	99.1		
Temperature (°C)									0.277	0.128 (-0.103 to 0.360)
	-5–10	12	2,385	2,088	84.8% (78.36–90.29)	133.05	<0.01	91.7	Reference	
	10–15	11	2134	1538	72.0% (44.08–93.08)	1654.60	0.00	99.4		
	15–20	23	5181	3804	75.0% (61.20–86.55)	2374.38	0.00	99.1		
Humidity (%)									0.139	0.303 (-0.098 to 0.705)
	30–60	12	3,658	3,214	82.6% (72.24–90.96)	546.34	<0.01	98.0		
	60–70	17	1,948	1,494	76.1% (62.91–0.87)	609.19	<0.01	97.4		
	70–80	19	3431	2093	76.7% (58.87–90.70)	2271.35	0.00	99.2		
	80–100%	3	663	629	95.7% (93.14-97.72)	2.51	0.29	20.2	Reference	
Altitude (m)									0.817	-0.020 (-0.186 to 0.146)
	4–100	26	3441	2391	79.2% (67.46–88.92)	1484.36	<0.01	98.3		
	100–1500	30	7636	5,371	77.7% (65.64–87.73)	3878.01	0.00	99.3	Reference	
	1500–5000	9	2,600	2325	81.2% (72.23–88.79)	179.51	<0.01	95.5		

CI, Confidence interval;*
NA, Not applicable.*

be high both in female goats and the kids (Ruiz and Molina, 2020).

Most of the 70 included studies used the saturated sodium chloride solution floating method [Float (NaCl), n = 50, and Float ($C_{12}H_{22}O_{11}$), n = 14]. These are all traditional parasitic disease diagnosis methods that test for *Eimeria* oocysts. There were no significant differences between these methods in the reported prevalence. Our meta-regression analysis here suggested that detection methods were unlikely to be a significant source of heterogeneity in this analysis. There were only 5 studies with a score of 0–1, but 25 with a score of 2–3. Further research revealed that they did not clarify whether the sampling was random or not and the sampling method was not detailed, which caused them to lose some points. In addition, some risk factors were lacking that could not be analyzed, such as diarrhea. When investigating the prevalence of goat coccidiosis, researchers should collect and present more information.

This study had three limitations. First, before determining the search style, we tried different search styles in order to obtain a more comprehensive range of articles, however, there may be some omissions. Second, the number of studies from Southern and Northeastern China were few, which might have affected the analyses of the results from these regions. Third, the lack of some information (for example, whether the goats had diarrhea or not) will also affect the analysis results. However, we believe that this meta-analysis can reflect the true prevalence of *Eimeria* spp. infection in goats in China.

CONCLUSION

Our analysis showed that the *Eimeria* spp. infection in goats is common in China. Most breeders do not pay attention to coccidiosis, resulting in a high overall prevalence. We suggest the development of different control strategies according to the geographical conditions of different regions. To further explore the susceptibility factors of goat coccidiosis, it is necessary to carry out epidemiological investigations in more areas and in detail.

DATA AVAILABILITY STATEMENT

The original contributions presented in the study are included in the article/**Supplementary Material**. Further inquiries can be directed to the corresponding authors.

AUTHOR CONTRIBUTIONS

RD and KS contributed to conception and design of this analysis. Q-LG provided the methodology. BZ, Z-YC, and YY collected

the data and built the database. QW and Q-LG analyzed the results. N-CD prepared the manuscript. YC and J-ML revised the manuscript. All authors contributed to the article and approved the submitted version.

ACKNOWLEDGMENTS

We thank the scientists and personnel of the College of Animal Science and Technology, Jilin Agricultural University and the College of Chinese Medicine Materials, Jilin Agricultural University, and the College of Animal Science and Veterinary Medicine, Heilongjiang Bayi Agricultural University, for their collaboration.

SUPPLEMENTARY MATERIAL

The Supplementary Material for this article can be found online at: https://www.frontiersin.org/articles/10.3389/fcimb.2022.806085/full#supplementary-material

REFERENCES

Abo-Shehada, M. N., and Abo-Farieha, H. A. (2003). Prevalence of *Eimeria* Species Among Goats in Northern Jordan. *Small Ruminant Res.* 49, 109–113. doi: 10.1016/S0921-4488(03)00078-6

Bangoura, B., and Bardsley, K. D. (2020). Ruminant Coccidiosis. *Vet. Clin. North Am. Food Anim. Pract.* 36, 187–203. doi: 10.1016/j.cvfa.2019.12.006

Bawm, S., Win, T. Z. B., Win, S. Y., Htun, L. L., Nakao, R., and Katakura, K. (2020). First Detection of *Eimeria* Species in Myanmar Domestic Goats With Both Microscopic and Molecular Methods. *Parasite* 27, 38. doi: 10.1051/parasite/2020037

Carrau, T., Silva, L. M. R., Pérez, D., Failing, K., Martínez-Carrasco, C., Macías, J., et al. (2018). Associated Risk Factors Influencing Ovine *Eimeria* Infections in Southern Spain. *Vet. Parasitol* 263, 54–58. doi: 10.1016/j.vetpar.2018.10.004

Carrau, T., Silva, L. M., Pérez, D., Ruiz de Ybáñez, R., Taubert, A., and Hermosilla, C. (2016). First Description of an *In Vitro* Culture System for *Eimeria Ovinoidalis* Macromeront Formation in Primary Host Endothelial Cells. *Parasitol Int.* 65, 516–519. doi: 10.1016/j.parint.2016.05.003

Cavalcante, A. C. R., Teixeira, M., Monteiro, J. P., and Lopes, C. W. G. (2012). Eimeria Species in Dairy Goats in Brazil. *Vet. Parasitol* 183, 356–358. doi: 10.1016/j.vetpar.2011.07.043

Chen, C. (2011). Retrospect and Prospect of China's Animal Husbandry Development Since the New Century. *Agr Outlook* 7, 39–42. doi: 10.3969/j.issn.1673-3908.2011.06.011

Dang, R. Y., Wang, B., Wang, X. L., and Song, J. K. (2019). Diagnosis and Treatment of Coccidiosis in Lambs in a Sheep Farm in Shaanxi Province. *Heilongjiang Anim. Sci. Vet. Med.* 12, 95–96. doi: 10.13881/j.cnki.hljxmsy.2018.07.0449

Daugschies, A., and Najdrowski, M. (2005). Eimeriosis in Cattle: Current Understanding. *J. Vet. Med. B Infect. Dis. Vet. Public Health* 52, 417–427. doi: 10.1111/j.1439-0450.2005.00894.x

Foreyt, W. J. (1990). Coccidiosis and Cryptosporidiosis in Sheep and Goats. *Vet. Clin. North Am. Food Anim. Pract.* 6, 655–670. doi: 10.1016/s0749-0720(15)30838-0

Gong, Q. L., Chen, Y., Tian, T., Wen, X., Li, D., Song, Y. H., et al. (2021). Prevalence of Bovine Tuberculosis in Dairy Cattle in China During 2010-2019: A Systematic Review and Meta-Analysis. *PLoS Negl. Trop. Dis.* 15, e0009502. doi: 10.1371/journal.pntd.0009502

Gong, Q. L., Zhao, W. X., Wang, Y. C., Zong, Y., Wang, Q., Yang, Y., et al. (2021). Prevalence of Coccidia in Domestic Pigs in China Between 1980 and 2019: A Systematic Review and Meta-Analysis. *Parasit Vectors* 14, 248. doi: 10.1186/s13071-021-04611-x

Guyatt, G. H., Oxman, A. D., Vist, G. E., Kunz, R., Falck-Ytter, Y., Alonso-Coello, P., et al. (2008). GRADE: An Emerging Consensus on Rating Quality of Evidence and Strength of Recommendations. *BMJ* 336, 924–926. doi: 10.1136/bmj.39489.470347.AD

Hao, G. Y. (2017). Advances in Coccidiosis of Goats and Sheep. *Chin. J. Vet. Sci.* 37, 577–584. doi: 10.16303/j.cnki.1005-4545.2017.03.36

Juszczak, M., Sadowska, N., and Udała, J. (2019). Parasites of the Digestive Tract of Sheep and Goats From Organic Farms in Western Pomerania, Poland. *Ann. Parasitol* 65, 245–250. doi: 10.17420/ap6503.206

Kanyari, P. W. N. (1993). The Relationship Between Coccidial and Helminth Infections in Sheep and Goats in Kenya. *Vet. Parasitol* 51, 137–141. doi: 10.1016/0304-4017(93)90204-z

Keeton, S. T. N., and Navarre, C. B. (2018). Coccidiosis in Large and Small Ruminants. *Vet. Clin. North Am. Food Anim. Pract.* 34, 201–208. doi: 10.1016/j.cvfa.2017.10.009

Koudela, B., and Boková, A. (1998). Coccidiosis in Goats in the Czech Republic. *Vet. Parasitol* 76, 261–267. doi: 10.1016/s0304-4017(97)00147-7

Li, X., Ni, H. B., Ren, W. X., Jiang, J., Gong, Q. L., Zhang, X. X., et al. (2020). Seroprevalence of *Toxoplasma Gondii* in Horses: A Global Systematic Review and Meta-Analysis. *Acta Trop.* 201, 105222. doi: 10.1016/j.actatropica.2019.105222

Liu, Z. P. (2019). Causes and Control Measures of Goat Coccidiosis. *Chin. J. Anim. Husb Vet. Med.* 12, 88.

Liu, E. M., Lu, Z. K., and Le, X. P. (2018). Reflections on the Current Situation and Future Development of Ovis Husbandry in China. *Chin. Anim. Husb* 9, 34–35.

Long, P. L., and Joyner, L. P. (1984). Problems in the Identification of Species of Eimeria. *J. Protozool.* 31, 535–541. doi: 10.1111/j.1550-7408.1984.tb05498.x

López, A. M., Muñoz, M. C., Molina, J. M., Hermosilla, C., Taubert, A., Zárate, R., et al. (2019). Anticoccidial Efficacy of Canary Rue (*Ruta Pinnata*) Extracts Against the Caprine Apicomplexan Eimeria Ninakohlyakimovae. *J. Anim. Sci.* 97, 101–110. doi: 10.1093/jas/sky389

Lotze, J. C., Leek, R. G., Shalkop, W. T., and Behin, R. (1961). Coccidial Parasites in the "Wrong Host" Animal. *J. Parasitol.* 47, 34.

Mai, K., Sharman, P. A., Walker, R. A., Katrib, M., Souza, D. D., McConville, M. J., et al. (2009). Oocyst Wall Formation and Composition in Coccidian Parasites. *Mem Inst Oswaldo Cruz* 104, 281–289. doi: 10.1590/s0074-02762009000200022

Mohamaden, W. I., Sallam, N. H., and Abouelhassan, E. M. (2018). Prevalence of Eimeria Species Among Sheep and Goats in Suez Governorate, Egypt. *Int. J. Vet. Sci. Med.* 18, 65–72. doi: 10.1016/j.ijvsm.2018.02.004

Moher, D., Shamseer, L., Clarke, M., Ghersi, D., Liberati, A., Petticrew, M., et al. (2015). Preferred Reporting Items for Systematic Review and Meta-Analysis Protocols (PRISMA-P) 2015. *Statement* Syst. 4, 1 doi: 10.1186/2046-4053-4-1

Peek, H. W., and Landman, W. J. (2003). Resistance to Anticoccidial Drugs of Dutch Avian *Eimeria* Spp. Field Isolates Originating From 1996, 1999 and 2001. *Avian Pathol.* 32, 391–401. doi: 10.1080/0307945031000121149

Ruiz, A., González, J. F., Rodríguez, E., Martín, S., Hernández, Y. I., Almeida, R., et al. (2006). Influence of Climatic and Management Factors on *Eimeria* Infections in Goats From Semi-Arid Zones. *J. Vet. Med. B Infect. Dis. Vet. Public Health* 53, 399–402. doi: 10.1111/j.1439-0450.2006.00985.x

Ruiz, A., and Molina, J. M. (2020). "Coccidiosis in Goat (Capra Hircus)", in *Coccidiosis in Livestock, Poultry, Companion Animals, and Humans*. Ed. J. P. Dubey (Boca Raton, FL: CRC Press), 112.

Taylor, M. A., Coop, R. L., and Wall, R. L. (2016). *Veterinary Parasitology. 4th edition* (Ames (IA: Wiley Blackwell).

Wang, Z. L. (2015). Review and Prospect of the Development of Animal Husbandry in China. *Vet. Orientation* 1, 8–10.

Wang, N. (2018). *How to Conduct a Meta-Analysis of Proportions in R: A Comprehensive Tutorial*. John Jay College of Criminal Justice, CUNY: Preprint on ResearchGate. doi: 10.13140/RG.2.2.27199.00161

Wang, W., Gong, Q. L., Zeng, A., Li, M. H., Zhao, Q., and Ni, H. B. (2021). Prevalence of Cryptosporidium in Pigs in China: A Systematic Review and Meta-Analysis. *Transbound Emerg. Dis.* 68, 1400–1413. doi: 10.1111/tbed.13806

Wang, Z. D., Wang, S. C., Liu, H. H., Ma, H. Y., Li, Z. Y., Wei, F., et al. (2017). Prevalence and Burden of *Toxoplasma Gondii* Infection in HIV-Infected People: A Systematic Review and Meta-Analysis. *Lancet HIV* 4, e177–e188. doi: 10.1016/S2352-3018(17)30005-X

Wang, R. J., Wang, Z. Y., Zhang, Y. J., and Su, R. (2020). Analysis on Key Factors Restricting Sustainable Development of Goat Industry. *J. Domest Anim. Ecol.* 41, 77–81. doi: 10.3969/j.issn.1673-1182.2020.02.014

Zhao, G. H., Lei, L. H., Shang, C. C., Gao, M., Zhao, Y. Q., Chen, C. X., et al. (2012). High Prevalence of *Eimeria* Infection in Dairy Goats in Shaanxi Province, Northwestern China. *Trop. Anim. Health Prod* 44, 943–946. doi: 10.1007/s11250-011-9997-8

Conflict of Interest: The authors declare that the research was conducted in the absence of any commercial or financial relationships that could be construed as a potential conflict of interest.

Publisher's Note: All claims expressed in this article are solely those of the authors and do not necessarily represent those of their affiliated organizations, or those of the publisher, the editors and the reviewers. Any product that may be evaluated in this article, or claim that may be made by its manufacturer, is not guaranteed or endorsed by the publisher.

Advantages of publishing in Frontiers

OPEN ACCESS
Articles are free to read for greatest visibility and readership

FAST PUBLICATION
Around 90 days from submission to decision

HIGH QUALITY PEER-REVIEW
Rigorous, collaborative, and constructive peer-review

TRANSPARENT PEER-REVIEW
Editors and reviewers acknowledged by name on published articles

Frontiers
Avenue du Tribunal-Fédéral 34
1005 Lausanne | Switzerland

Visit us: www.frontiersin.org
Contact us: frontiersin.org/about/contact

REPRODUCIBILITY OF RESEARCH
Support open data and methods to enhance research reproducibility

DIGITAL PUBLISHING
Articles designed for optimal readership across devices

FOLLOW US
@frontiersin

IMPACT METRICS
Advanced article metrics track visibility across digital media

EXTENSIVE PROMOTION
Marketing and promotion of impactful research

LOOP RESEARCH NETWORK
Our network increases your article's readership